



NBS SPECIAL PUBLICATION 470

U.S. DEPARTMENT OF COMMERCE / National Bureau of Standards

WIND AND SEISMIC EFFECTS

Proceedings of the
Seventh Joint UJNR
Panel Conference

NATIONAL BUREAU OF STANDARDS

The National Bureau of Standards¹ was established by an act of Congress March 3, 1901. The Bureau's overall goal is to strengthen and advance the Nation's science and technology and facilitate their effective application for public benefit. To this end, the Bureau conducts research and provides: (1) a basis for the Nation's physical measurement system, (2) scientific and technological services for industry and government, (3) a technical basis for equity in trade, and (4) technical services to promote public safety. The Bureau consists of the Institute for Basic Standards, the Institute for Materials Research, the Institute for Applied Technology, the Institute for Computer Sciences and Technology, the Office for Information Programs, and the Office of Experimental Technology Incentives Program.

THE INSTITUTE FOR BASIC STANDARDS provides the central basis within the United States of a complete and consistent system of physical measurement; coordinates that system with measurement systems of other nations; and furnishes essential services leading to accurate and uniform physical measurements throughout the Nation's scientific community, industry, and commerce. The Institute consists of the Office of Measurement Services, and the following center and divisions:

Applied Mathematics — Electricity — Mechanics — Heat — Optical Physics — Center for Radiation Research — Laboratory Astrophysics² — Cryogenics² — Electromagnetics² — Time and Frequency².

THE INSTITUTE FOR MATERIALS RESEARCH conducts materials research leading to improved methods of measurement, standards, and data on the properties of well-characterized materials needed by industry, commerce, educational institutions, and Government; provides advisory and research services to other Government agencies; and develops, produces, and distributes standard reference materials. The Institute consists of the Office of Standard Reference Materials, the Office of Air and Water Measurement, and the following divisions:

Analytical Chemistry — Polymers — Metallurgy — Inorganic Materials — Reactor Radiation — Physical Chemistry.

THE INSTITUTE FOR APPLIED TECHNOLOGY provides technical services developing and promoting the use of available technology; cooperates with public and private organizations in developing technological standards, codes, and test methods; and provides technical advice services, and information to Government agencies and the public. The Institute consists of the following divisions and centers:

Standards Application and Analysis — Electronic Technology — Center for Consumer Product Technology: Product Systems Analysis; Product Engineering — Center for Building Technology: Structures, Materials, and Safety; Building Environment; Technical Evaluation and Application — Center for Fire Research: Fire Science; Fire Safety Engineering.

THE INSTITUTE FOR COMPUTER SCIENCES AND TECHNOLOGY conducts research and provides technical services designed to aid Government agencies in improving cost effectiveness in the conduct of their programs through the selection, acquisition, and effective utilization of automatic data processing equipment; and serves as the principal focus within the executive branch for the development of Federal standards for automatic data processing equipment, techniques, and computer languages. The Institute consist of the following divisions:

Computer Services — Systems and Software — Computer Systems Engineering — Information Technology.

THE OFFICE OF EXPERIMENTAL TECHNOLOGY INCENTIVES PROGRAM seeks to affect public policy and process to facilitate technological change in the private sector by examining and experimenting with Government policies and practices in order to identify and remove Government-related barriers and to correct inherent market imperfections that impede the innovation process.

THE OFFICE FOR INFORMATION PROGRAMS promotes optimum dissemination and accessibility of scientific information generated within NBS; promotes the development of the National Standard Reference Data System and a system of information analysis centers dealing with the broader aspects of the National Measurement System; provides appropriate services to ensure that the NBS staff has optimum accessibility to the scientific information of the world. The Office consists of the following organizational units:

Office of Standard Reference Data — Office of Information Activities — Office of Technical Publications — Library — Office of International Standards — Office of International Relations.

¹ Headquarters and Laboratories at Gaithersburg, Maryland, unless otherwise noted; mailing address Washington, D.C. 20234.

² Located at Boulder, Colorado 80302.

18 1977

acc.

C

0

57

470

57

2

WIND AND SEISMIC EFFECTS

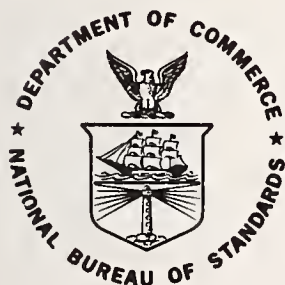
special publication, no. 470

Proceedings of the Seventh Joint
Panel Conference of the U.S.-Japan
Cooperative Program in
Natural Resources

May 20-23, 1975
Tokyo, Japan

H.S. Lew, Editor

Center for Building Technology
Institute for Applied Technology
National Bureau of Standards
Washington, D.C. 20234



U.S. DEPARTMENT OF COMMERCE, Juanita M. Kreps, Secretary

Dr. Betsy Ancker-Johnson, Assistant Secretary for Science and Technology

U.S. NATIONAL BUREAU OF STANDARDS, Ernest Ambler, Acting Director

Issued April 1977

Library of Congress Cataloging in Publication Data

United States-Japan Cooperative Program in Natural Resources.

Panel on Wind and Seismic Effects. Wind and seismic effects.

(National Bureau of Standards special publication ; 470)

Supt. of Docs. no.: C13.10:470

1. Wind-pressure--Congresses. 2. Earthquakes and building--
Congresses. I. Lew, Hai Sang. II. Title. III. Series: United States.
National Bureau of Standards. Special publication ; 470.

QC100U57 no. 470 [TA654.5] 602'.1s [624'.176] 77-608015

National Bureau of Standards Special Publication 470

Nat. Bur. Stand. (U.S.), Spec. Publ. 470, 513 pages (Apr. 1977)

CODEN: XNBSAV

U.S. GOVERNMENT PRINTING OFFICE

WASHINGTON: 1977

For sale by the Superintendent of Documents, U.S. Government Printing Office, Washington, D.C. 20402
(Order by SD Catalog No. C13.10:470). Stock No. 003-003-01762-1 Price \$5.60.
(Add 25 percent additional for other than U.S. mailing)

PREFACE

The Seventh Joint Meeting of the U.S. - Japan Panel on Wind and Seismic Effects was held in Tokyo, Japan on May 20-23, 1975. This panel is one of the twenty panels in the U.S. Japan Cooperative Program in Natural Resources (UJNR). The UJNR was established in 1964 by the U.S. - Japan Cabinet-level Committee on Trade and Economic Affairs. The purpose of the UJNR is to exchange scientific and technological information which will be mutually beneficial to the economics and welfare of both countries. Accordingly, the purpose of the annual joint meeting of this panel is to exchange technical information on the latest research and development activities within governmental agencies of both countries in the area of wind and seismic effects.

The proceedings include the program, the formal resolutions, and the technical papers presented at the Joint Meeting. The papers were presented in the respective language of each country. The texts of the papers, all of which were prepared in English, have been edited. The illustrations were reproduced from the working documents used at the Joint Meeting. The formal resolutions were drafted at the closing session of the Joint Meeting and adopted unanimously by the panels of both countries.

Pages of the technical papers are numbered with a prefix corresponding to the Theme number. The texts are consecutively numbered in each theme.

H. S. Lew, Secretary
U.S. Panel on Wind and
Seismic Effects

SI Conversion Units

In view of present accepted practice in this technological area, U.S. customary units of measurements have been used throughout this report. It should be noted that the U.S. is a signatory to the General Conference on Weights and Measures which gave official status to the metric SI system of units in 1960. Conversion factors for units in this report are:

	<u>Customary Unit</u>	<u>International (SI), UNIT</u>	<u>Conversion Approximate</u>
<u>Length</u>	inch (in)	meter (m) ^a	1 in=0.0254m*
	foot (ft)	meter (m)	1 ft=0.3048m*
<u>Force</u>	pound (lbf)	newton (N)	1 lbf=4.448N
	kilogram (kgf)	newton (N)	1 kgf=9.807N
<u>Pressure</u>	pound per square		
<u>Stress</u>	inch (psi)	newton/meter ²	1 psi=6895N/m ²
	Kip per square		
	inch (ksi)	newton/meter ²	1 ksi=5895x10 ⁶ N/m ²
<u>Energy</u>	inch-pound (in-lbf)	joule (J)	1 in-lbf=0.1130 J
	foot-pound (ft-lbf)	joule (J)	1 ft-lbf=1.3558 J
<u>Torque</u> or	pound-inch	newton-meter (N-m)	1 lbf-in=0.1130 N-m
	pound-foot (lbf-ft)	newton-meter (N-m)	1 lbf-ft=1.3558 N-m
<u>Bending</u> <u>Moment</u>			
<u>Weight</u> or	pound (lbf)	kilogram (kg)	1 lb=0.4536 kg
<u>Mass</u>			
<u>Unit Weight</u>	pound per cubic foot (pcf)	kilogram per cubic meter (kg/m ³)	1 pcf=16.018 kg/m ³
<u>Velocity</u>	foot per second (ft/sec)	meter per second (m/s)	1 fps=0.3048 m/s
<u>Acceleration</u>	foot per second per second (ft/sec ²)	meter per second per second (m/s ²)	1 ft/sec ² =0.3048 m/s ²

^a Meter may be subdivided. A centimeter (cm) is 1/100 m and a millimeter (mm) is 1/1000 m.

* Exact

CONTENTS

Preface.	iii
SI Conversion.	iv
Abstract	vii
Program of the Joint Meeting	ix
Opening Session.	ix
List of Members.	xiii
Formal Resolutions	xvii
Themes and Technical Papers.	I-1
 THEME I: CHARACTERISTICS OF STRONG WIND	
Present Status of Wind Characteristics	
Kiyonide Takeuchi	I-1
A Re-examination of Hurricane Camille	
Arnold R. Hull.	I-18
Fire-Tornadoes and Its Maximum Wind Speed	
S. Soma and K. Suda	I-28
A Research Project on the Wind Flow Around Tall Buildings	
Tatsuo Murota and Kiyoshi Nakano.	I-42
 THEME II: RESPONSE OF FULL-SCALE STRUCTURES TO WIND ACTION	
Wind Engineering Research Program Supported by the National Science Foundation	
Michael P. Gaus	II-1
Study of the Wind Pressure and the Response of Roof Corners	
Tatsuo Murota and Mitsuo Makahara	II-11
On the Wind Response of the Kanmon Bridge	
T. Okubo, N. Narita, and K. Yokoyama.	II-20
Luling, Louisiana Cable-Stayed Bridge Wind Tunnel Section Model Tests	
Richard H. Gade, Walter Podolny, Jr. and Harold R. Bosch.	II-47
 THEME III: GEOLOGICAL DISTRIBUTION OF SEISMIC ACTIVITY	
Regional Distribution of Earthquake Risk in Japan	
S. Hattori, Y. Kitagawa and T. Santo.	III-1
Quantification of Seismicity	
Teutomu Terashima and Tetsuo Santo.	III-18
 THEME IV: MAINTENANCE OF STRONG MOTION ACCELEROGRAPHS AND DATA PROCESSING	
Maintenance of the Strong Motion Accelerograph and Data Processing of Records Obtained	
Eiichi Kuribayashi, Hajime Tsuchida and Makoto Watabe	IV-1
The United States Strong-Motion Network: Field Operation	
Richard P. Maley.	IV-35
Strong-Motion Data Management	
Christopher Rojahn.	IV-53

THEME V: STRONG EARTHQUAKE MOTIONS AND GROUND FAILURES

Brief Review on Liquefaction During Earthquakes in Japan Eiichi Kuribayashi and Fumio Tatsuoka	V-1
Vibration Test on Settlement of Submerged Sand Layer K. Sawada and Y. Koga	V-16

THEME VI: RESPONSE OF HYDRAULIC AND BUILDING STRUCTURES TO SEISMIC FORCES

Study on Earthquake Response of Structures by Considering Non-Deterministic Variables Yutaka Yamazaki and Yasunori Koizume.	VI-1
Least Weight Structures for Threshold Frequencies R.D. McConnell.	VI-22
Ductile Shear Walls in Earthquake-Resistant Multistory Buildings Mark Fintel	VI-33
Surveillance of Corps of Engineers Structures in Earthquake-prone Area Keith O. O'Donnell.	VI-47
School and Hospital Construction in California John F. Meehan.	VI-64
Improved Earthquake Resistive Design and Construction of Single Family Residential Dwellings G. Robert Fuller.	VI-74

THEME VII: ASEISMIC CONSIDERATIONS FOR VESSELS

Dynamic Tests of Structures for Oil Tanks and Nuclear Power Plants Seiichi Inaba	VII-1
Sheet Pile Foundation and its Structural Characteristics against Horizontal Loads Kenji Kawakami, Tadyoshi Okubo, Keiichi Komada and Michio Okahara	VII-7

THEME VIII: RECENT REVISIONS OF DESIGN STANDARDS ON WIND AND SEISMIC EFFECTS

A Review on Specifications of Earthquake Resistant Design for Highway Bridges - 1971 Kenji Kawakami, Eiichi Kuribayashi, Toshio Iwasaki and Yutaku Iida.	VIII-1
Specifications for Earthquake Resistant Design of the Honshu-Shikoku Bridges (JSCE 1974) Ishio Kawasaki and Eiichi Kuribayashi	VIII-31
Recent Revision of Design Standards on Seismic Effect for Port and Harbour Structures Satoshi Hayashi, Hajime Tsuchida and Setsuo Noda.	VIII-42
JSCE Specifications for Earthquake Resistant Design of Submerged Tunnels (1975) Eiichi Kuribayashi and Hajime Tsuchida.	VIII-56

THEME IX: JOINT RESEARCH PROGRAM UTILIZING LARGE SCALE TESTING FACILITIES

Joint Research Program Utilizing the Large Scale Testing Facilities (Free Discussion) Makoto Watabe, Masaya Hirose and Shinsuke Nakata	IX-1
Earthquake Disaster Mitigation: A Joint Research Approach Charles T. Theil.	IX-6

THEME X: TECHNOLOGICAL ASSISTANCE TO DEVELOPING COUNTRIES

High Wind Study in the Philippines

Noel J. Raufaste. X-1

Survey on Seismology and Earthquake Engineering in India, Iran and Turkey

Makoto Watabe, Hideo Tokuhiko and Masakazu Shinozuka. X-12

ABSTRACT

The Seventh Joint Meeting of the U.S. - Japan Panel on Wind and Seismic Effects was held in Tokyo, Japan on May 20-23, 1975. The proceedings of the Joint Meeting include the program, the formal resolutions, and the technical papers. The subject matter covered in the papers includes characteristics of strong wind; response of full-scale structures to wind action; geological distribution of seismic activity; maintenance of strong motion accelerographes and data processing; strong earthquake motions and ground failures; response of hydraulic and building structures to seismic forces; aseismic considerations for vessels; recent revisions of design standards on wind and seismic effects; joint research program utilizing large scale testing facilities; and technological assistance to developing countries.

Key Words: Accelerograph; bridges; buildings; codes; disaster; dynamic analysis; earthquakes; ground failures; hydraulic structures; seismicity; soils; standards; storage tanks; structural response; winds.

SEVENTH JOINT MEETING
PROGRAM OF THE
U.S. - JAPAN PANEL ON WIND AND SEISMIC EFFECTS
May 20-23, 1975
at
Tokyo, Japan

TUESDAY - May 20

Opening Ceremony (Room HANA NO MA, 6F, Zenkyoren Building)

9:30 A.M. Call to order by Mr. Hiroshi Yoshimura, Head, Planning Division,
Public Works Research Institute

Remarks by Mr. Mitsuo Kikuchi, Engineer General, Ministry of Construction

Remarks by Mr. William W. Henoch, Acting Counselor for Scientific and
Technological Affairs, U.S. Embassy

Remarks by Mr. Saburo Ueda, Chief, International Division Promotion Bureau,
Science and Technology Agency

Remarks by Mr. Kenji Kawakami, Director, Public Works Research Institute,
Ministry of Construction

Remarks by Dr. E.O. Pfrang, Chief, Structures, Materials & Life Safety
Division Center for Building Technology, IAT, National Bureau of Standards

Introduction of United States Panel Members by U.S. Chairman and Japan
Panel Members by Japanese Chairman

Election of Conference Chairman

Adoption of Agenda

11:00 A.M. Explanation of the 1974 Off Izu-Peninsula Earthquake

11:30 A.M. Lunch

THEME III: Geological Distribution of Seismic Activity

11:00 P.M. Regional Distribution of Earthquake Risk in Japan
S. Hattoru, Y. Kitagawa and T. Scuto

1:25 P.M. Quantification of Seismicity
Tsutomii Terashima, Tetsuo Santo

1:50 P.M. Discussion

2:10 P.M. Recess

THEME IV: Maintenance of Strong Motion
Accelerographs and Data Processing

2:25 P.M. Maintenance of the Strong Motion Accelerograph and Data Processing of Records
Obtained
Eiichi Kuribayashi, Hagime Tsuchida and Makoto Watabe

2:50 P.M. The United States Strong-Motion Network: Field Operation
Richard P. Maley

3:15 P.M. Strong-Motion Data Management
Christopher Rojahn: presented by R. Maley

3:40 P.M. Discussion

Courtesy Call (at the office of the Minister of Construction)

4:45 P.M. Courtesy call to Mr. T. Kariya, Minister of Construction

Reception (at the Rose-Room 6F, in Zenkyoren Building)

6:00 P.M. Reception to be hosted by Mr. M. Kikuchi, Engineering General

8:00 P.M. Ministry of Construction

WEDNESDAY - May 21

THEME V: Strong Earthquake Motions
and Ground Failures

9:00 A.M. Brief Review on Liquefaction During Earthquakes in Japan
Eiichi Kuribayashi and Fumiotatsuoka

9:25 A.M. Vibration Test on Settlement of Submerged Sand Layer
S. Sawada and Y. Koga

9:50 A.M. Discussion

10:50 A.M. Recess

THEME VI: Response of Hydraulic and Building
Structures to Seismic Forces

10:25 A.M. Study on Earthquake Response of Structures by Considering Non-Deterministic
Variables
Yutaki Yamazaki and Yasunori Koizumi

10:50 A.M. Least Weight Structures for Threshold Frequencies
Richard D. McConnell

11:15 A.M. Ductile Shear Walls in Earthquake-Resistant Multistory Buildings
Mark Fintel

11:40 A.M. Discussion

12:00 P.M. Lunch

1:30 P.M. Surveillance of Corps of Engineers Structures in Earthquake-prone Area
Keith O. O'Donnell

1:55 P.M. School and Hospital Construction in California
John F. Meehan; presented by E.O. Pfrang

2:20 P.M. Improved Earthquake Resistive Design and Construction of Single Family
Residential Dwelling
G. Robert Fuller

2:45 P.M. Discussion

3:05 P.M. Recess

THEME VII: Recent Revisions of Design Standards
on Wind and Seismic Effects

- 3:20 P.M. A Review on Specifications of Earthquake Resistant Design for Highway Bridges - 1971
- 3:45 P.M. Specifications for Earthquake Resistant Design of the Honshu-Shikoku Bridge (JSCE-1974)
Ishio Kawasaki and Etichi Kuribayashi
- 4:10 P.M. Discussion
- 4:30 P.M. Recent Revision of Design Standards on Seismic Effect for Port and Harbour Structures
Sagoshi Hayashi, Hajime Tsuchida and Setsuo Noda
- 4:55 P.M. JSCE Specifications for Earthquake Resistant Design of Submerged Tunnels (1975)
Eiichi Kuribayashi and Hajime Tsuchida
- 5:20 P.M. Discussion

THURSDAY - May 22

THEME I: Characteristics of Strong Wind

- 9:00 A.M. Present Status of Wind Characteristics in Japan
Kiyohide Takeuchi
- 9:25 A.M. A Reexamination of Hurricane Camille
Arnold R. Hull
- 9:50 A.M. Discussion
- 10:10 A.M. Recess
- 10:25 A.M. Fire-Tornadoes and its Maximum Wind Speed
S. Soma and K. Suda
- 10:50 A.M. High Wind Study in the Philippines
Noel Raufaste

THEME II: Response of Full Scale Structures
To Wind Action

- 11:15 A.M. Wind Engineering Research Program Supported by the National Science Foundation
Michael P. Gaus; presented by E.O. Pfrang
- 11:40 A.M. Discussion
- 12:00 P.M. Lunch
- 1:30 P.M. A Research Project on the Wind Flow Around Tall Buildings
Tatsuo Murota and Kyoshi Nakano
- 1:55 P.M. Study of the Wind Pressure and the Response of Flat Roof Corners
Tatsuo Murato
- 2:20 P.M. Luling Louisiana Cable-stayed Bridge Wind Tunnel Section Model Tests
Richard H. Gade; presented by J. Cooper
Walter Podoling, Jr. and Harold R. Busch

2:45 P.M. Discussion

3:05 P.M. Recess

3:20 P.M. On the Wind Response of the Kanmon Bridge
T. Okubo, N. Narita and K. Yokoyama

3:45 P.M. Newport, Rhode Island Suspension Bridge; Hurricane "Doria" Wind Spectra
Richard H. Gade; presented by J. Cooper

4:10 P.M. Discussion

THEME VII: A Seismic Considerations for Vessels

4:30 P.M. Dynamic Tests of Structures for Oil Tanks and Nuclear Power Plants
Seiichi Inaba

4:55 P.M. Sheet Pile Foundation and its Structural Characteristic against
Horizontal Loads
Kenji Kawakami, Tadyoshi Okubo, Keiichi Komada and Michio Okahara

5:20 P.M. Discussion

FRIDAY - May 23

THEME IX: Joint Research Program Utilizing Large
Scale Testing Facilities

9:00 A.M. Joint Research Program Utilizing the Large Scale Testing Facilities
(Free Discussion)
Makota Watabe, Masaya Hirose and Shinsuke Nakata

9:25 A.M. Disaster Mitigation: A Joint Approach
Charles T. Thiel; presented by E.O. Pfrang

THEME X: Technological Assistance to Developing Countries

9:50 A.M. Survey on Seismology and Earthquake Engineering in India, Iran and Turkey
Makoto Watabe, Hideo Tokuhito and Masekazu Shinozuka

10:15 A.M. Discussion

10:35 A.M. Recess

10:55 A.M. Explanation of Oita Earthquake

12:00 P.M. Lunch

1:30 P.M. Free Discussion

2:00 P.M. Closing Session

3:28 P.M. Lv. Tokyo

U. S. PANEL ON WIND AND SEISMIC EFFECTS
MEMBERSHIP LIST
APRIL 1975

Dr. Edward O. Pfrang, Chairman
Chief, Structures, Materials and
Safety Division
Center for Building Technology, IAT
National Bureau of Standards
Room B368, Bldg. 226
Washington, D.C. 20234
(301) 921-2196

Dr. S. T. Algermissen, Member
Seismicity and Risk Analysis Branch
USGS, R10X4, RB3, Rm. A434
Boulder, Colorado 80302
(303) 234-4014

Dr. Robert D. Borchardt, Member
USGA
National Center for Earthquake Research
345 Middlefield Road
Menlo Park, California 94025
(415) 323-8111

Dr. George Ericksen, Member
USGS
12201 Sunrise Valley Drive
Reston, Virginia 22092
(703) 860-6553

Dr. Michael P. Gaus, Member
Head, Engineering Mechanics Section
Engineering Division
National Science Foundation
1800 G. Street, N.W.
Washington, D.C. 20550
(202) 632- 5787

Dr. R. Cecil Gentry, Member
Director, National Hurricane Research
Laboratory
NOAA
P. O. Box 8265, University of Miami Branch
Coral Gables, Florida 33124
(305) 350-4150

Mr. Sigmund Gerber, Member
Director for Construction Standards and
Design for Installation and Logistics
Office of the Secretary of Defense
Room 3E763, The Pentagon
Washington, D.C. 20301
(202) 695-2713

Mr. Jack Healy, Member
Chief, Material Systems and Science Division
Department of the Army
Construction Engineering Research Labs.
P. O. Box 4005
Champaign, Illinois 61820
(217) 352-6416 (FTS only)
(217) 352-6511 (commercial)

Mr. Arnold R. Hull, Member
Associate Director for Climatology
NOAA-EDS
Washington, D.C. 20235
(202) 634-7319

Dr. William B. Joyner, Member
USGS
Office of Earthquake Research
345 Middlefield Road
Menlo Park, California 94025
(415) 323-8111 x2754

Mr. John W. Kaufman, Member
Chief, Atmospheric Dynamics Branch
Aerospace Environment Division
National Aeronautics & Space Administration
Marshall Space Flight Center, Alabama 35812
(205) 453-3103

Mr. James Lefter, Member
Director, Civil Engineering Service
Office of Construction
Veterans Administration
Lafayette Building, Room 507
811 Vermont Avenue, N.W.
Washington, D.C. 20420
(202) 389-2864

Dr. R.B. Matthiesen, Member
Chief, Seismic Engineering Branch
USGS
390 Main Street, Room 7067
San Francisco, California 94105
(415) 556-7768

Mr. Keith O. O'Donnell, Member
Assistant Chief, Structural Branch
Engineering Division, Civil Works
Directorate
Forrestal Building, ATTN: DAEN-CWE-D
Washington, D.C. 20314
(202) OX3-7311

Mr. Larry F. Rousch, Member
Public Building Service
General Services Administration
18th & F Streets, N.W.
Washington, D.C. 20405

Dr. Charles Scheffey, Member
Acting Associate Administrator
Federal Highway Administration
Washington, D.C. 20590
(202) 426-2943

Dr. Warren A. Shaw, Member
Head, Civil Engineering Department
Civil Engineering Laboratory
Naval Construction Battalion Center
Port Hueneme, California 93043
(805) 982-5407

Mr. Lawrence C. Shao, Member
Directorate of Licensing
U.S. Atomic Energy Commission
Washington, D.C. 20545
(201) 973-7808

Dr. Charles T. Thiel, Member
Program Manager, Earthquake Engineering
Division of Advanced Technology Applications
National Science Foundation
Washington, D.C. 20550
(202) 632-0648

Mr. William J. Werner, Member
Division of Building Technology and Safety
Department of Housing and Urban Development
Room 4120
451 7 Street, S.W.
Washington, D.C. 20410
(202) 755-5574

ALTERNATES

Dr. H.S. Lew, Secretary and Alternate
Structures, Materials and Life Safety
Division
Center for Building Technology, IAT
National Bureau of Standards
Washington, D.C. 20234
(301) 921-3851

Dr. Richard D. McConnell, Alternate
Veterans Administration
Office of Construction
Washington, D.C. 20420

Dr. John B. Scalzi, Alternate
Division of Advanced Technology and
Applications
National Science Foundation
Washington, D.C. 20550
(202) 632-5970

Mr. F.J. Tamanini, Alternate
Chief, Structures, and Applied Mechanics
Division
HRS-10
Federal Highway Administration
U.S. Department of Transportation
Washington, D.C. 20550
(703) 557-5287

MEMBERSHIP LIST

Japan Panel

Mr. Kenji Kawakami, Chairman
Director, Public Works Research Institute
Ministry of Construction
2-28-32 Honkomagome, Bunkyo-ku, Tokyo

Dr. Satoshi Hayashi
Head, Structure Division
Port and Harbor Research Institute,
Ministry of Transport
3-1-1 Nagase, Yokosuka-shi, Kanagawa-ken

Mr. Seiichi Inaba
Chief, Earthquake Engineering Laboratory
National Research Center for Disaster
Prevention
Science and Technology Agency
4489 Kurihara Aza, Sakuramura,
Niihari-gun, Ibaragi-ken

Dr. Yasunori Koizumi
Director, Building Research Institute
Ministry of Construction
3-28-8 Hyakunin-cho, Shinjuku-ku, Tokyo

Mr. Keiichi Komada
Chief, Founding Engineering Section
Structure and Bridge Division, Chiba Branch
Public Works Research Institute,
Ministry of Construction
4-12-52 Anagawa, Chiba-shi, Chiba-ken

Mr. Eiichi Kuribayashi
Chief, Earthquake Engineering Section
Structure and Bridge Division, Chiba Branch
Public Works Research Institute, Ministry
of Construction
4-12-52 Anagawa, Chiba-shi, Chiba-ken

Mr. Tatsuo Murota
Senior Research Officer, Third Research
Division
Building Research Institute
Ministry of Construction
3-28-8 Hyakunin-cho, Shinjuku-ku, Tokyo

Dr. Kiyoshi Nakano
Head, Structural Division, Building
Research Institute
Ministry of Construction
3-28-8 Hyakunin-cho, Shinjuku-ku, Tokyo

Mr. Nobuyuki Narita
Chief, Structure Section
Structure and Bridge Division,
Chiba Branch
Public Works Research Institute,
Ministry of Construction
4-12-52 Anagawa, Chiba-shi, Chiba-ken

Dr. Tadayoshi Okubo
Head, Structure and Bridge Division,
Chiba Branch
Public Works Research Institute,
Ministry of Construction
4-12-52 Anagawa, Chiba-shi, Chiba-ken

Dr. Tetsuo Santo
Head, International Institute of Seismology
and Earthquake Engineering
Building Research Institute, Ministry of
Construction
3-28-8 Hyakunin-cho, Shinjuku-ku, Tokyo

Mr. Kenkichi Sawada
Chief, Soil Dynamics Section
Construction Method and Equipment Division
Chiba Branch
Public Works Research Institute, Ministry
of Construction
4-12-52 Anagawa, Chiba-shi, Chiba-ken

Dr. Seiji Soma
Chief, First Research Section
Physical Meteorology Laboratory
Meteorological Research Institute
Japan Meteorological Agency, Ministry of
Transport
4-35-8 Kita, Koenji, Suginami-ku, Tokyo

Dr. Ken Suda
Director, Meteorological Research Institute
Japan Meteorological Agency, Ministry of
Transport
4-35-8 Kita, Koenji, Suginami-ku, Tokyo

Mr. Akira Suwa
Head, Seismological Laboratory
Meteorological Research Institute
Japan Meteorological Agency, Ministry of
Transport
4-35-8 Kita, Koenji, Suginami-ku, Tokyo

Dr. Kiyohide Takeuchi
Head, Applied Meteorological Laboratory
Meteorological Research Institute
Japan Meteorological Agency, Ministry of
Transport
4-35-8 Kita Koenji, Suginami-ku, Tokyo
,

Mr. Hajime Tsuchida
Chief, Earthquake Resistant Structures
Laboratory
Structure Division
Port and Harbor Research Institute,
Ministry of Transportation
3-1-1 Ngase, Yokosuka-shi, Kanagawa-ken

Dr. Makoto Watabe
Chief, International Institute of Seismology
and Earthquake Engineering
Building Research Institute,
Ministry of Construction
3-28-8 Hyakunin-cho, Shinjuku-ku, Tokyo

Secretary-General

Mr. Hiroshi Yoshimura
Head, Planning Division
Public Works Research Institute
Ministry of Construction
2-28-32 Honkomagome, Bunkyo-ku, Tokyo

RESOLUTIONS OF SEVENTH JOINT MEETING
U.S.-JAPAN PANEL ON WIND AND SEISMIC EFFECTS
U.J.N.R.
May 20 - 23, 1975

The following resolutions for future U.S.-Japan activities of the Joint Panel on Wind and Seismic Effects are hereby proposed:

1. The Seventh Joint Meeting of U.S.-Japan Panel on Wind and Seismic Effects, U.J.N.R. Program, was extremely fruitful to both countries. Considering the importance of the technical information exchanged between the two delegations, it is considered essential that the joint program be continued
2. Due to the continuous nature of the research programs reported, it is recommended that dissemination of technical reports and state-of-art reports be encouraged on a continual basis during the coming year
3. In accordance with the resolutions of the Sixth Joint Panel Meeting, the proceedings of the Joint Meeting should be published for the benefit of other scientific representatives in each country as soon as possible
4. Efforts should be made to exchange, on a timely basis, list of significant strong-motion earthquake and high speed wind recorded data. Clearly defined good quality digitizable record copies are needed and a procedure for exchanging records should be established. Records should also include the characteristics of instruments needed for all processing and analytical procedures
5. Attempts should be made to solicit papers from other official governmental offices and private technical organizations involved in wind and seismic research. Papers written by non-panel members may be synopsized in state-of-art reports
6. Promote the exchange of technological information, concerning strong winds and earthquakes, with developing countries
7. Cooperative research programs including exchange of personnel and equipment should be undertaken by both governments to address the following problems of mutual interest:
 - a) Strong-motion instrumentation arrays, at selected sites throughout the world,
 - b) Large-scale testing programs,
 - c) Repair and retrofit of existing structures, ie; buildings, bridges, dams, etc
 - d) Structural performance evaluation,
 - e) Land use programs for controlling natural hazard effects,
 - f) Disaster prevention methods for lifeline systems.
8. It is suggested that all future papers incorporate the SI Metric System for units of measurement, contained within parenthesis
9. Future reports should consider an overview of codes and problems of implementation associated with "nonstructural" and "operational" requirements and subsequently should be exchanged

10. More exposure and exchange of innovative techniques for improved seismic design spectra is considered highly important
11. The date and location for the 8th Joint Panel Meeting on Wind and Seismic Effects will be Spring 1976 in Washington, D.C., U.S.A. The specific date, inspection sites and field trips will be determined by the U.S. Panel with approval by the Japanese Panel.

A formal expression of appreciation is hereby presented by the U.S. Panel members to the Japanese delegation for the excellent arrangements, technical exchange and magnificent hospitality received at this Seventh Joint Panel Meeting in Tokyo, May 1975.

PRESENT STATUS OF WIND CHARACTERISTICS IN JAPAN

by

Kiyohide Takeuchi
Applied Meteorology Laboratory
Meteorological Research Institute

ABSTRACT

The present status of a study on the wind characteristics in Japan is given herein. Observational studies constructed from a tower and an array of towers are described in addition to results obtained from tethered balloons.

The observations obtained from towers in Tokushima Pref. and analysis of the data, which were made by Shiotani (1972 and 1974), are detailed and unique. Also other observations from towers located at Tarama Island, Okinawa Pref. are being conducted by Mitsuta (1974). Detailed analysis of these observations are also presented.

Finally some model experiments on the local wind, using a tunnel, are also presented.

Key Words: Field Measurements; Model; Towers; Wind; Wind Observation; Wind Tunnel.

Introduction

The behavior of wind has been under constant study in Japan, and is one of the most fundamental subjects in meteorology. Meteorological disasters in Japan are caused mainly by the wind and rain, as induced by typhoons, cyclones and monsoons.

Tall buildings and structures as well as long suspension bridges have recently been constructed in Japan. Accordingly detailed information of the wind characteristics is required for their proper design and for maintenance after construction.

However, air pollution caused by various industries and cars has become a serious problem in Japan. Since the wind in the atmospheric boundary layer plays an essential role in the dispersion of pollutants, a study of the wind, especially the local wind in the industrial and urban areas is quite urgent.

Since the interaction between the air and the earth surface is an essential problem in meteorology, a study on the wind fluctuation near the surface has been intensively conducted.

The characteristics of the wind has been investigated in Japan through observations conducted on field towers and through wind tunnel experiments in the laboratory.

Observations made in the field were conducted on single towers and tower arrays in order to obtain more detailed information on the time and space characteristics of the wind. In addition to using tethered balloons, pilot balloons, low altitude radiosondes, low altitude rawin sondes and aircraft were often used for observing the local wind.

The present status of the study on wind characteristics is described in detail herein.

Observation from a Single Tower

Observation from a Tower Near the Mouth of River Naka

In order to obtain data required for the design of a long suspension bridge, since 1964 Shiotani (1975) has studied wind characteristics from a tower located near the mouth of River Naka, Tokushima Pref. This meteorological tower, 150m in height, is located approximately 150m away from the beach (see Fig. 1). The base of the tower is on a low sand dune covered with pine trees, a few meters in height, but in north north-west direction, a marsh extends a distance of 400m. The land surrounding the tower, which is 1 km from the coast, is under cultivation with intermittent farm houses, trees and small hills.

This meteorological tower is a guyed mast made of steel pipe. The Aerovane-type anemometers were installed 3 m apart from the center of the tower at 15.8, 30.8, 50.8, 80.8, 110.8 and 150.8 m above the ground. The mean wind speed was continuously recorded during a minute period, at each anemometer level. Instantaneous wind speeds and wind directions were measured at any three levels with pen-writing recorders when the wind speed became high. In addition, measurement of the vertical direction of the wind was made with two bidirectional vanes. Temperature differences between 150 and 30 m, and 80 and 30 m were measured with bead-thermistors thermometers.

The wind behavior during a 15 min interval were recorded every 2.5 s when wind speeds were under 25 m/s, and every 2.0 s when wind speed were over 25 m/s. From these data mean wind speed U , turbulent velocity σ_u (i.e., r.m.s. of the longitudinal wind fluctuation),

auto correlation, power spectrum $S(n)$ (n : frequency), and other statistical quantities were obtained. Analyses of these data 197 recordings indicated that the range of wind speeds was between 20 and 30 m/s, and only 13 data had wind speeds higher than 30 m/s.

Since the characteristics of the high wind are determined mainly by the surface roughness, the wind data has, therefore, divided into three groups. The first group had a wind direction 1 (E-ES) - the wind from the sea after passing 150-300 m over the land. The second, Direction 2 (SSE-WSW) had the wind passing more than 2 km over the delta of River Naka, which is modified from the sea wind. The third group, Direction 3 (WNW-NNW) has a wind parallel to the coastal line (see Fig. 1). The results from these classifications are as follows;

(a) Velocity Fluctuation and Their Magnitudes

The frequency distribution of the fluctuating wind velocities can be expressed approximately by Gaussian distribution. The intensity of turbulence (σ_u/U) of the wind in Direction 2 is higher than that from the other two directions, and it is recognized that the turbulent intensity increases with increasing roughness.

The intensity of turbulence of the wind at 30.8 m is much higher than that at the other heights. This means that the rough ground coverage, in the close proximity to the tower, greatly disturbs the wind in the lowest region. The turbulent intensities of the wind in the range between 50.8 m and 150.8 m are nearly the same in Directions 1 and 3, and they decrease with increasing heights. However, they are approximately constant with those heights in Direction 2. In order to examine the vertical distribution of wind turbulent velocities, their ratios to those recorded at 80.8 m, i.e. $\sigma_u/\sigma_u(80)$, were studied. These results indicate that they are nearly constant with height in Direction 2, while they decrease with power exponents -0.10 and -0.16 in Directions 1 and 3, respectively.

(b) Power Spectrum

The relationship between the logarithmic spectrum $nS(n)$ and the logarithm of the wave number $\log(n/U)$, was examined. It was noted that of the 261 recordings, 139 recordings had single peak spectrum $nS(n)$. These single-peak spectra were then used for further analyses. The shapes of the spectra are quite varied, therefore, the whole spectra cannot be represented by a single curve.

The wave number $(n/U)_m$, corresponding to the maximum value of $nS(n)$, is generally independent of the wind speed and wind direction. Therefore, the height distribution of $(n/U)_m$ averaged at each height, was found that the wave number of the spectrum peak decreases slightly with increasing height.

Examination of the similarity theory, however, suggests that $nS(n)$ can be expressed by the factor nz/U , therefore, examination of collected data results in the following empirical formula;

$$(nz/U)_m = 0.0018 z^{0.82}$$

This indicated that the spectrum peak shifts slightly to a low-frequency with an increase in height, for a height range between 50.8 m and 150.8 m. However, the accuracy of the formula is not so restrictive such that $(n/U)_m$ can be considered constant with height.

The friction velocity u_* can be estimated from the high-frequency part of the spectrum. The mean value of σ_u/u_* can then be evaluated, giving 2.4 for the case of Direction 2. However, u_* can also be estimated from the logarithmic law of the mean wind speed, which gives a value for the same direction, equal to 2.1.

(c) Correlation Coefficient Between Two Heights

An example of the correlation coefficient $R(z_2, z_1, \tau)$ with time lag τ between the two heights z_2 and z_1 ($z_2 > z_1$), is shown in Fig. 2. It should be noted that the maximum correlation does not occur when $\tau = 0$, but occurs when the wind record of the upper layer is delayed. This means that the phase of the wind gusts advances when in the upper air layer. Now, using Taylor's hypothesis, the space correlation is as shown in Fig. 3. Examination of this Figure shows that the scale of the turbulence becomes larger, and the phase advances during an increase in air layer height.

The vertical correlation coefficient $R(z_2, z_1)$ appears to be independent of the wind direction and wind speed. Therefore, the correlation coefficient will depend not only on the height difference $(z_2 - z_1)$, but on the actual heights z_2 and z_1 . Examination of the correlation coefficients between two points which have the same height differences indicates that the largest value in the case where the two points are in the highest air layer, which means the scale of turbulence increases upward. The correlation coefficient is empirically formulated as follows:

$$R(z_2, z_1) = \exp[-0.85(z_2^{1/3} - z_1^{1/3})]$$

The coherence function $\gamma(z_2, z_1, n)$ between the two heights z_2 and z_1 can now be calculated. The coherence is found empirically and is expressed as:

$$[\gamma(z_2, z_1, n)]^{1/2} = \exp[-kn(z_2 - z_1)/U_{10}]$$

Because the correlation coefficient between the two heights depends on the height difference, k should be a function of two heights. Also, it has been formed that k increase as the wind speed increases and the height of the air layer decreases.

Observation at the NHK Kawaguchi Tower

Many observations of the atmospheric boundary layer have been made by using broadcasting towers in or near the city. For example, Soma (1964) has analyzed the data obtained at the Tokyo Tower and has studied the turbulent structure of high wind over the urban area.

Since air pollution has recently become a serious problem in the urban area, various meteorological observations have often been made. The following will describe such observations taken at the NHK Broadcasting tower near Tokyo.

In 1971 and 1972, Yokoyama and his collaborators installed sonic anemometer-thermometers, to measure the wind fluctuations which are closely associated with diffusion of pollutants (see Mitsuta, 1966 for the sonic anemometer-thermometer). The heights of the anemometers used were 10, 45, 90, 180 and 313 m, respectively. The tower is located in a suburban residential area where the ground is rather flat. Measured signals were recorded by long-time magnetic tape recorders and the play-back signals were processed by an analogue-digital converter and a computer. Various statistical quantities, such as turbulent velocity and momentum flux, were then analyzed. The analyses of these quantities, indicate the following;

(a) Magnitude of Vertical Fluctuation

For a constant flux layer (i.e., layer up to about 50 m above the ground) it is well known that the magnitude of vertical fluctuation σ_w is related to the friction velocity u_* as follows;

$$\sigma_w = Au_* \phi_w(z/L)$$

The term ϕ_w is a universal function of the stability a/L (L : Monin-Obukhov stability length) and A is constant. In the constant flux layer, the friction velocity u_* is obtained from the vertical distribution of the mean wind speed and also from the covariance of wind fluctuation. In a layer higher than the constant flux layer, the equation mentioned above does apply. However, when the local friction velocity obtained from the covariance (i.e., $u_* = \overline{-u'w'}^{1/2}$) is used, the equation applies in the higher layer. The relation between σ_w/u_* and the stability z/L is then studied and ϕ_w is determined as a function of the stability.

(b) Stability and Relation between σ_w and U

In many cases at height of 45 m, the magnitude of vertical fluctuation is proportional to the mean velocity U . At a height of 313 m, however, it seems that there exists a linear relation only over the certain value which might be determined by the stability as shown in Fig. 4.

Observations at the Tower in Okinawa and Iwo-Jima

Kinase et al. (1972) have made wind observations by using the OHK TV-Tower in Okinawa (165 m high above the ground) and Loran Tower in Iwo-Jima (410 m high). Aerovane-type anemometers were installed at 6 levels at the OHK TV-Tower and at 8 levels at the Loran Tower. Since there existed strong electromagnetic fields, special attention was given in the installation of the anemometers at both towers.

(a) Vertical Distribution of Mean Wind Speed

The data obtained at the Loran Tower during Typhoon No. 7017 shows that the power index is approximately equal to 0.12 although the wind was not very strong. Similar

power index values were obtained from the other winds. The wind profile at OHK TV-Tower is not represented by a single straight line in a logarithmic chart and during certain runs, the power index is 0.47 in the upper part of the profile and 0.22 in the lower region.

(b) Intensity of Turbulence

Examples of the intensity of the turbulence σ_u/U obtained at the OHK TV-Tower and the Tower Loran are shown in Fig. 5. The turbulence intensity decreases with increasing height and also mean wind speed at the OHK TV-Tower but the data shows a different tendency at the Loran Tower.

(c) Gust Factor

The Gust factor u_m/U (u_m : maximum wind speed) obtained at both towers is depicted in Fig. 6. The factor varies between 1.2 and 1.6, and seems to decrease with increasing height and mean wind speed.

Observation at an Array of Towers

Observation at Tarama Island, Okinawa

In order to obtain data on high winds, which are required for the economic design of towers for large power transmission lines, a number of observing poles were installed at Tarama Island in Okinawa (Mitsuta, 1974). The island is elliptic (about 4 km x 5 km), and has a flat surface as shown in Fig. 7. Most of the island, ground is level and is around 10 m high above m.s.l. Okinawa, as is well known, is often subjected to typhoons, which is why Tarama Island has been chosen as an observation site.

The observation site as shown in Fig. 7, is near the southwestern coast. The observation facility consists of an array of 27 observing poles, installed with 39 anemometers and an instrumentation house. The configuration of the array is shown in Fig. 8. Twenty-five poles are distributed with equal separation of 30 m on a straight line of 720 m in length. The height of the poles are 15 m except one which is 50 m in height and is located in the center of the array. Two 15 m poles are placed 90 m away from the center in the direction perpendicular to the base line three-cup anemometers and Aerovantype anemometers are attached to the poles as shown in Fig. 8. The system is started when the monitoring anemometer output exceeds a preset wind speed. The wind observation was initiated in the middle of 1972 and has continued since that time.

(a) Correlation Coefficient

The wind, whose direction is perpendicular to the base line, is selected and read out every 1.5 s for 12 min. Examples of auto and cross correlation coefficient for the same run are shown in Figs. 9 and 10, in which the wind comes from an inland direction. The dots in Fig. 10 show the correlations of all possible combinations from the observing points, and the solid lines show the average values. The average integral scale of the turbulence, in the longitudinal direction, is about 120 m and in the lateral direction is about 20 m.

(b) Gust Factor

The Gust factor, as a function of both gust duration and its lateral scale at the height of 15 m was obtained from the data. Figs. 11 and 12 show an example of the two

dimensional gust factors for the same run. Variations of space averaged gust factors, with an averaging time, are shown in Fig. 11 and show the power law approximation. Fig. 12 shows the time averaged gust factors as a function of average time, which also shows the power law approximation.

Observation and further analysis are now being conducted, and more detailed results are expected in the near future.

Observation at Satoura, Tokushima Pref.

Five towers were placed along a line parallel to the coastal line, which runs from SSE to NNE, at Satoura of Naruto City, Tokushima Pref. (Shiotani, 1969), for the same purpose as described in Section 2.1. The towers were located at 12, 35, 80 and 190 m from the south end. They are 40 m in height and were installed with Aerovane-type anemometers. The observations were initiated in 1966, with readings taken every 1 s for 10-13 min.

(a) Correlation Coefficient and Scale

The cross correlation coefficient of the longitudinal wind at the points separated by η in the lateral direction, is denoted as $R_{uu}(\eta, \tau)$, where τ is time lag. The data shown as open circles in Fig. 13, is the parameters $R_{uu}(\eta)$, which is defined as $R_{uu}(\eta, 0)$. In the lateral direction the integral scale of the turbulence is about 50 m representing the wind from the sea, and is about 65 m for the wind from the land. The integral scale is somewhat larger for the wind from the land than from the sea, at a height of 40 m.

The auto correlation coefficient, $R_{uu}(\xi)$ where ξ is the downwind distance in the longitudinal direction, can be estimated from the auto correlation coefficient by use of Taylor's hypothesis. The results are $R_{uu}(\xi) = R_{uu}(\tau)$ where $\xi = U\tau$, where the parameters $R_{uu}(\xi)$ is shown in Fig. 13. The longitudinal scale of the turbulence can then be estimated using this data. The scale thus obtained using a constant height is 204 m for the wind from the sea and 154 m for the wind from the land. The turbulence becomes greater for the wind from the sea, which is opposite to the result in the lateral direction. The scale of the turbulence in the longitudinal direction is 3 to 4 times as large as that in the lateral direction.

(b) Space Correlation Coefficient

Using Taylor's hypothesis, the spatial pattern of the space correlation coefficient $R_{uu}(\xi, \eta)$ can be estimated. An example of the pattern is shown in Fig. 14.

Field Observation by Other Methods

In connection with air pollution, as mentioned previously, extensive observations have been made in industrial and urban areas. In addition to making observations using towers, other techniques have been employed.

One such method utilizes a special radiosonde attached to a tethered balloon and can measure turbulent winds (Yokoyama, 1969). A low altitude radiosonde has recently been developed for observing the wind, temperature and pressure in the layer up to 2000 m. These instruments and the low altitude radiosonde are often used for observing the wind over the urban area (Takeuchi, 1975). Data thus obtained are of great use in classifying

local wind.

Additional papers concerning the turbulent wind over the urban area have been published, by Nakano et al., 1974 and Hanafusa et al., 1974.

Wind Tunnel Experiment

In order to clarify the characteristics of local wind, many tests have been conducted in a wind tunnel, but few papers have been published.

Kamei et al. (1974) conducted wind tunnels experiments in order to study local wind induced by tall buildings, and also recommended some practical methods to estimate the high wind region.

Suda et al. (1974), presented a paper on model experiments concerned with the study of local winds induced by a small island. This study will be a great help in the design of long span suspension bridges.

In order to simulate the atmospheric boundary layer in the laboratory, Sato et al. (1974) developed a velocity-distribution generator by introducing a variable resistance in the wind tunnel. This device consists of a series of sliding plates, and should be of great use in studying the local wind in detail.

Concluding Remarks

A survey of recent work on the characteristics and structure of the wind in Japan is given relative to the author's interests. Thus, other important studies are not included herein. This survey indicated that further research studies on the structure of turbulent wind, should be conducted.

Data should be accumulated by various methods (e.g., tower, tethered balloon and any radiosonde) at different locations i.e. urban areas and coastal areas. The structure of local wind should also be clarified in relation to the synoptic meteorology and topography.

References

1. Hanafusa, T. and S. Soma, 1974: On the Characteristics of Atmospheric Turbulence Above the Urban Area. Proc. of the Third Symposium on Wind Effects on Structures in Japan, 63-70. (in Japanese with English abstract).
2. Kamei, I. and E. Maruta, 1974: The Wind Tunnel Test on High Wind Region Induced With Tall Building. Proc. of the Third Symposium on Wind Effects on Structures in Japan, 115-122. (in Japanese with English abstract).
3. Kinase, T., N. Toyama and S. Ito, 1972: On the Structure of Strong Wind for Constructing 600 m Tower. Meteorological Material for Tower Construction (Japan Meteorological Agency), No. 4, 22-43. (in Japanese).
4. Mitsuta, Y., 1966: Sonic Anemometer-Thermometer for General Use. J. Meteor. Soc. Japan, 44, 12-24.
5. Mitsuta, Y., 1974: Preliminary Results of Typhoon Wind Observation at Tarama Island, Okinawa. Paper presented at US-Japan Research Seminar on Wind Effects on Structures, Kyoto, Sept. 9 - 13, 1974.
6. Nakano, M., K. Takeuchi, Y. Mitsuta and T. Hanafusa, 1974: On the Characteristics of Atmospheric Turbulence Above the Urban Area. Meteor. Research Note, No. 119, 133-141 (in Japanese).
7. Sato, H., Y. Onda and T. Saito, 1974: Laboratory Simulation of Atmospheric Turbulence: Generation of Arbitrary Velocity Distribution and Model Experiment of Flow Around Mt. Fuji. Advances in Geophysics, 18B, 241 - 251.
8. Shiotanti, M., 1969: Structures of Gusts in High Winds (Interim report, Part 3). Nihon Univ. at Narashino. 118 pp. (in Japanese with English abstract).
9. Shiotani, M., 1975: Turbulence Measurements at the Sea Coast During High Winds. J. Meteor. Soc. Japan, 53. (to be published)
10. Soma, S., 1964: Turbulent Structures in Strong Winds. J. Meteor. Soc. Japan, 42, 372 - 396. (in Japanese with English abstract).
11. Suda, K., S. Soma and K. Takeuchi, 1974: Wind Tunnel Experiments for Studying a Local Wind. Paper presented at the Sixth Joint Meeting of US-Japan Panel on the Wind and Seismic Effects, Washington, D.C., May 15-17, 1974.
12. Takeuchi, K., 1975: Observation of Local Wind. J. Appl. Phys. Japan. (to be published)
13. Yokoyama, O., 1969: Measurement of Wind Fluctuations by a Vane Mounted on the Captive Balloon Cable. J. Meteor. Soc. Japan, 47, 159-166.
14. Yodoyama, O., 1971: An Experimental Study on the Structure of Turbulence in the Lowest 500 m of the Atmosphere and Diffusion in it. Report of National Research Institute for Pollution and Resources. No. 2.
15. Yokoyama, O., 1972: The structure of the Planetary Boundary Layer Obtained by Measurements, Tenki (meteor. Soc. Japan), 19, 654-659. (in Japanese).

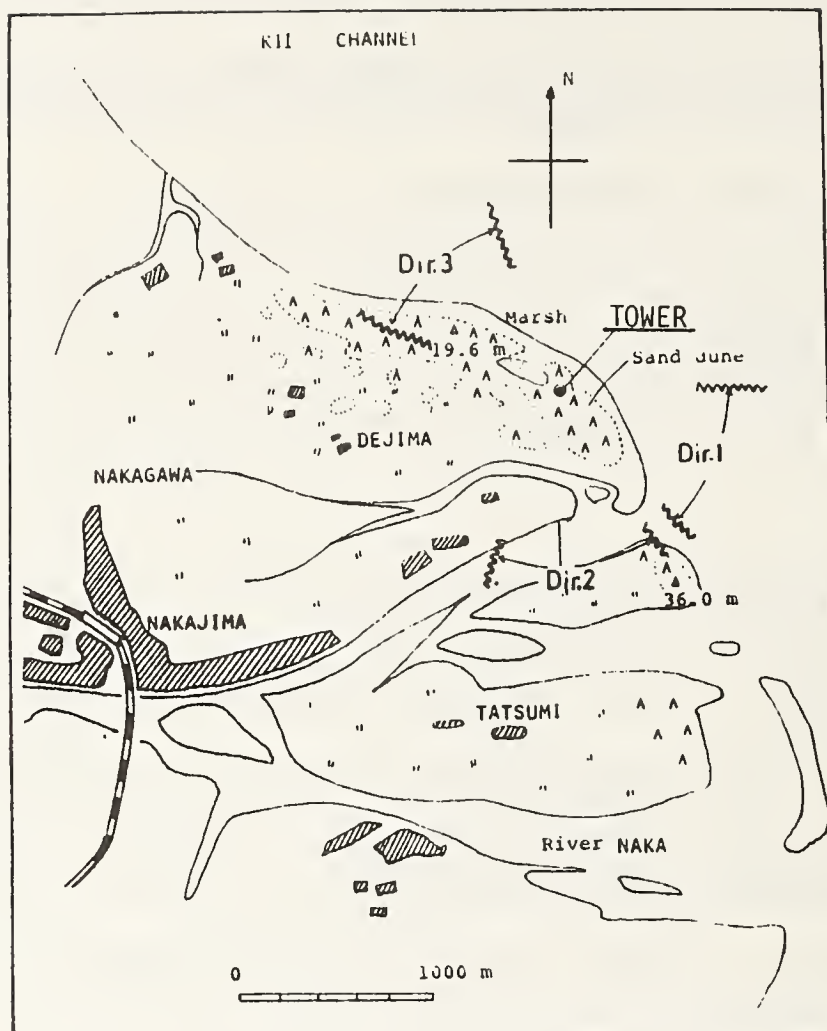


Fig.1 Topography around the meteorological tower by the mouth of River Naka (shiotani,1975)

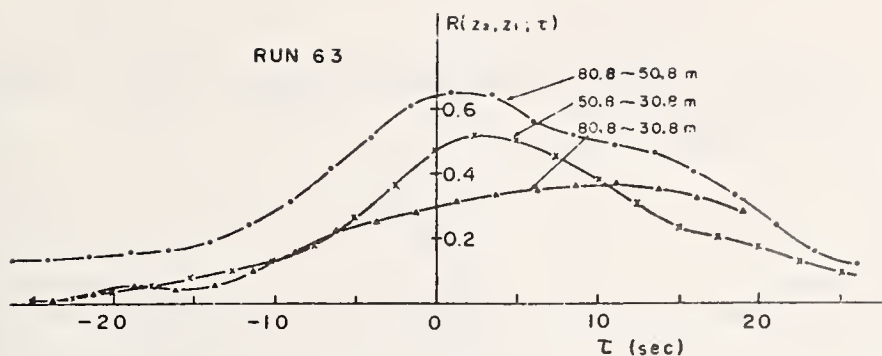


Fig.2 Cross correlation coefficients between two heights (Shiotani,1975)

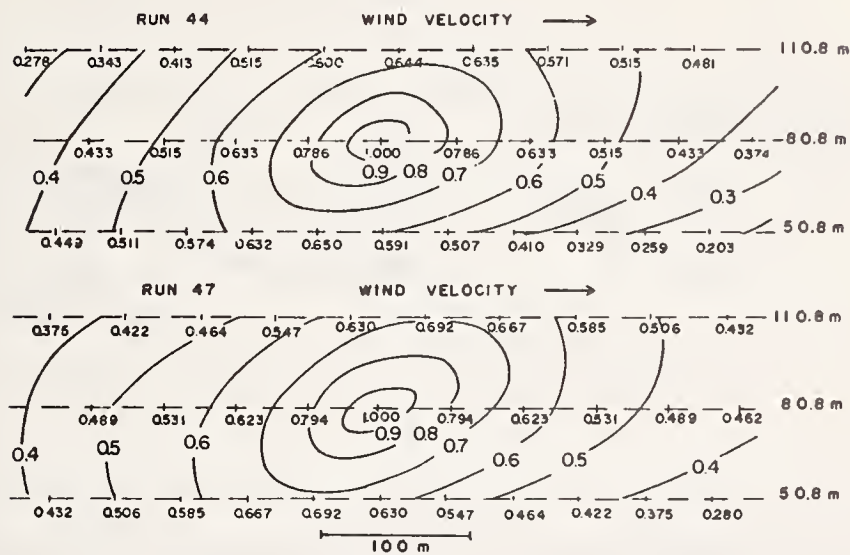


Fig.3 Isopleth of correlation coefficients in a vertical plane parallel to mean wind velocity (Shiotani,1975)

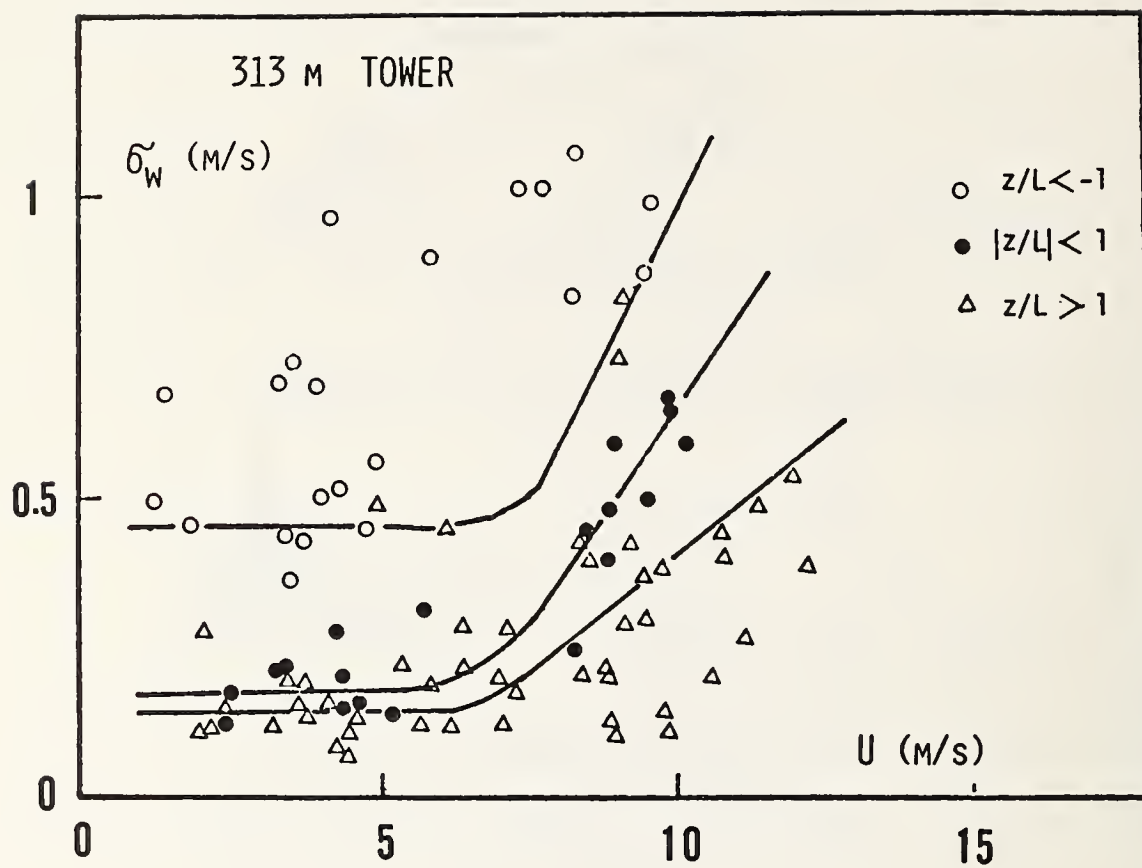


Fig.4 Stability dependency of relation between σ_w and U (yokoyama,1972)

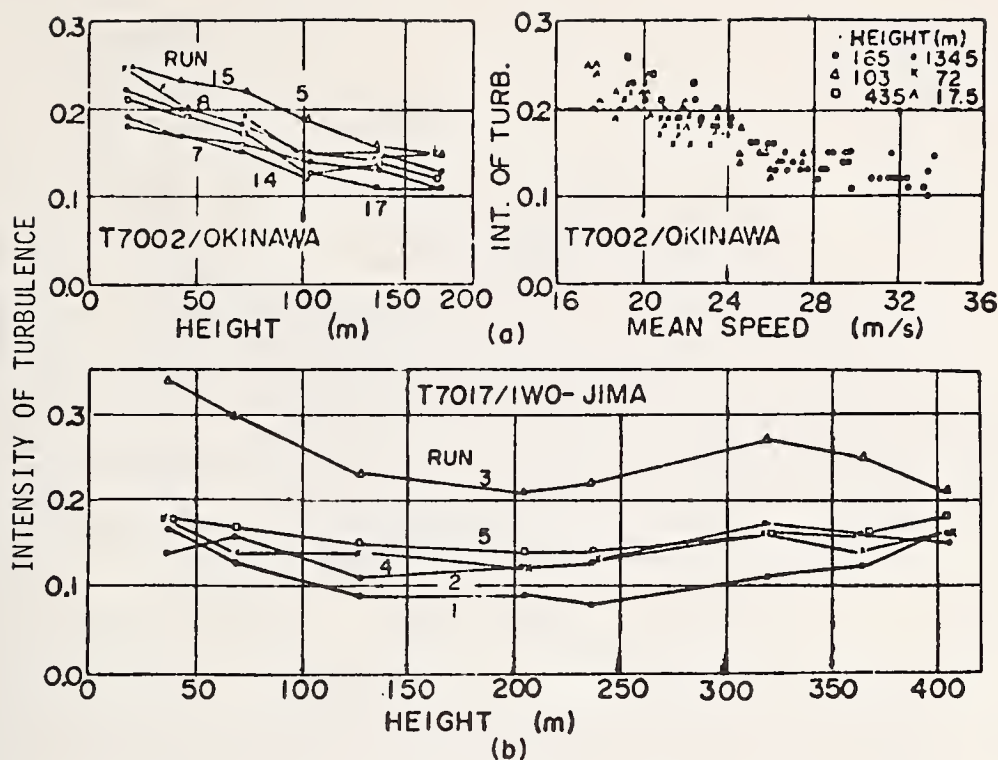


Fig.5 Intensity of turbulence: (a) Okinawa,(b) Iwo-Jima (Kinase et al.,1972)

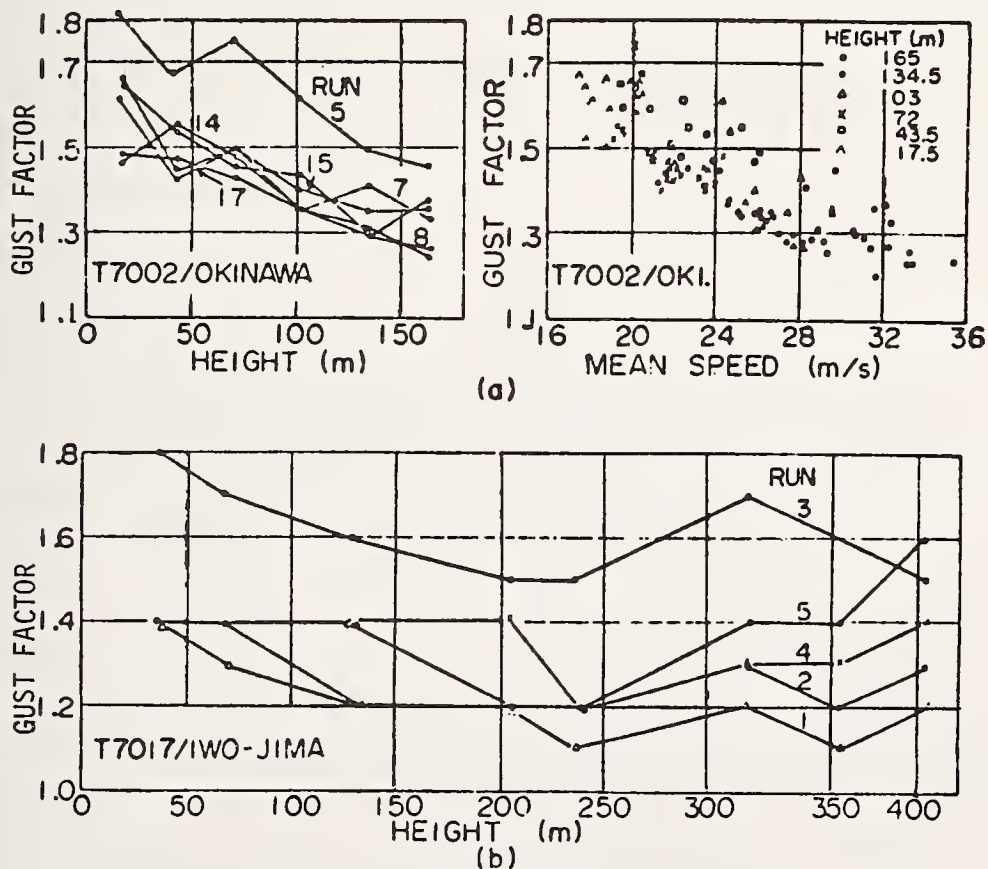


Fig.6 Gust factor: (a) Okinawa,(b) Iwo-Jima (Kinase et al.,1972)

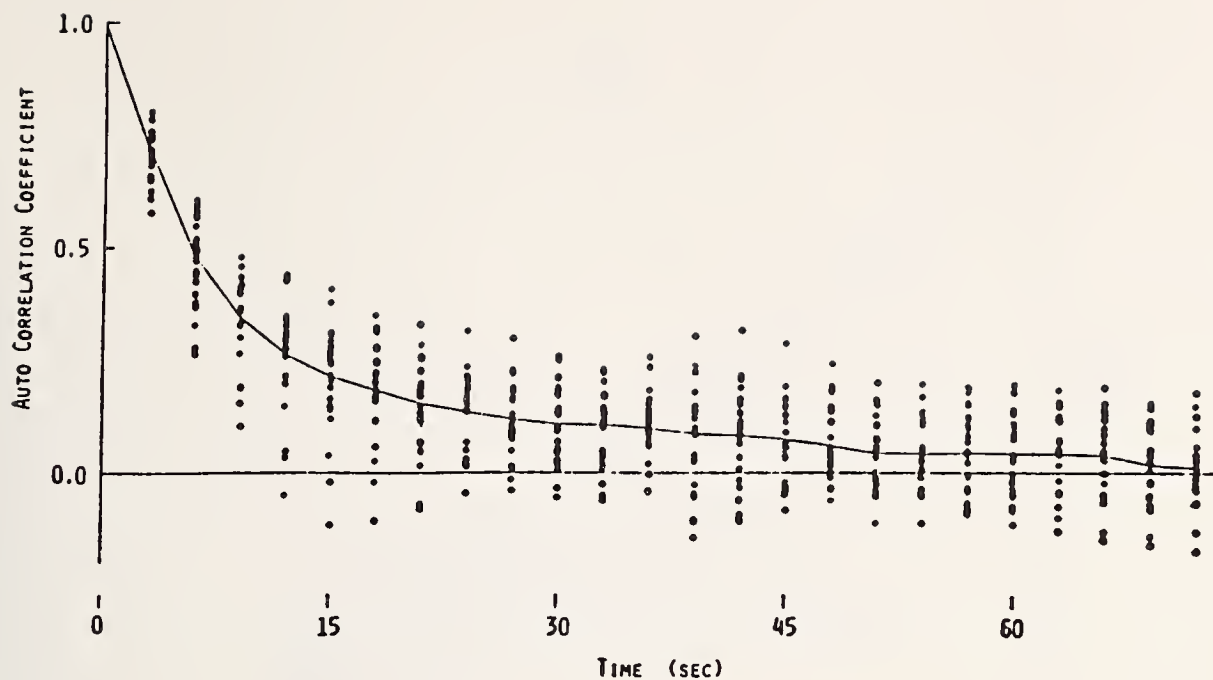


Fig.9 Auto-correlation coefficient of wind velocity whose direction is perpendicular to the base line (Mitsuta,1974)

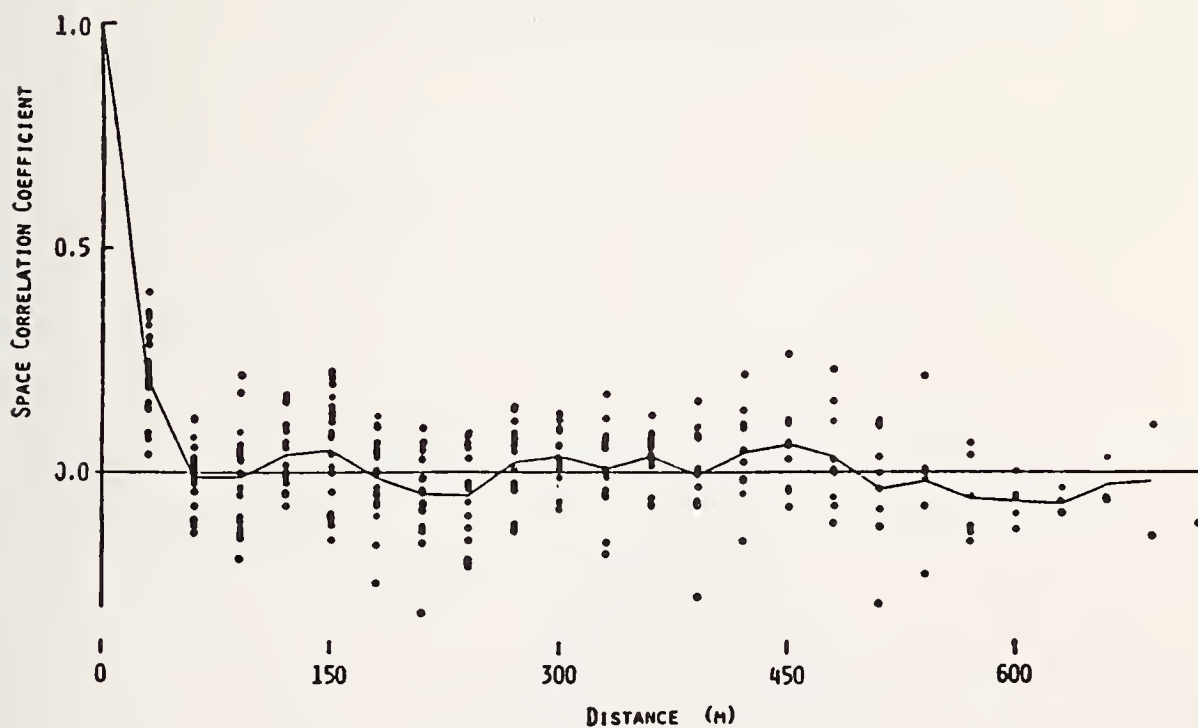


Fig.10 Same as Fig.9 but space correlation coefficient

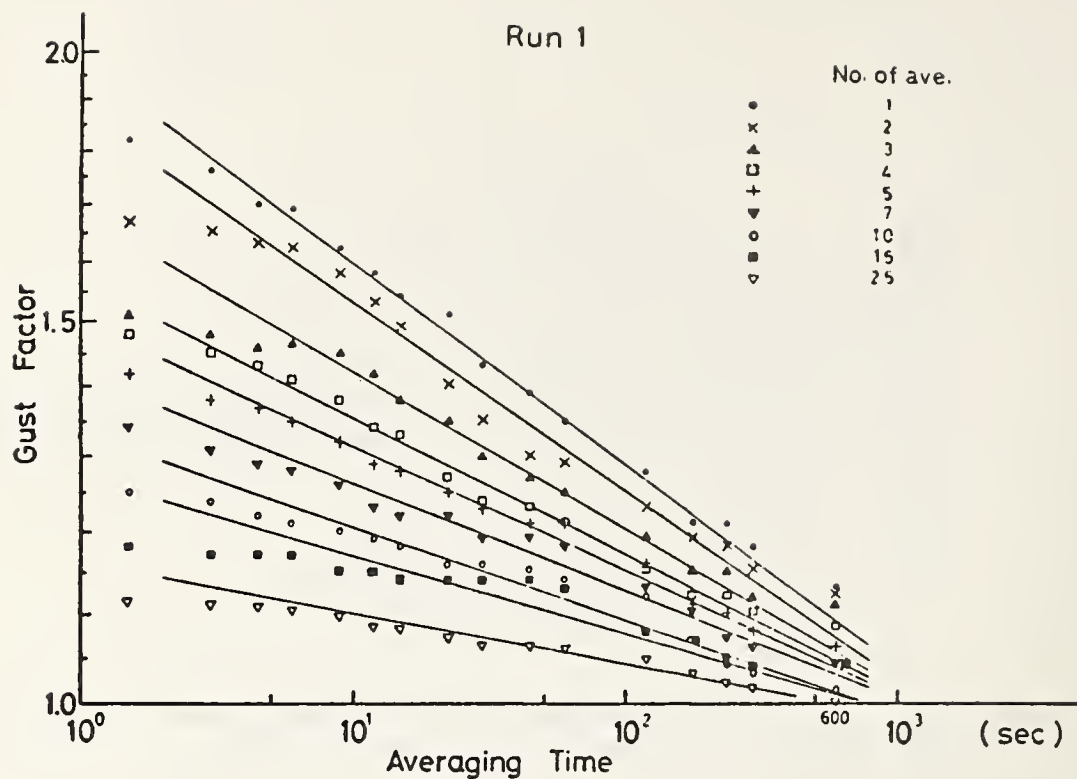


Fig.11 Space averaged gust factors as a function of averaging time (Mitsuta,1974)

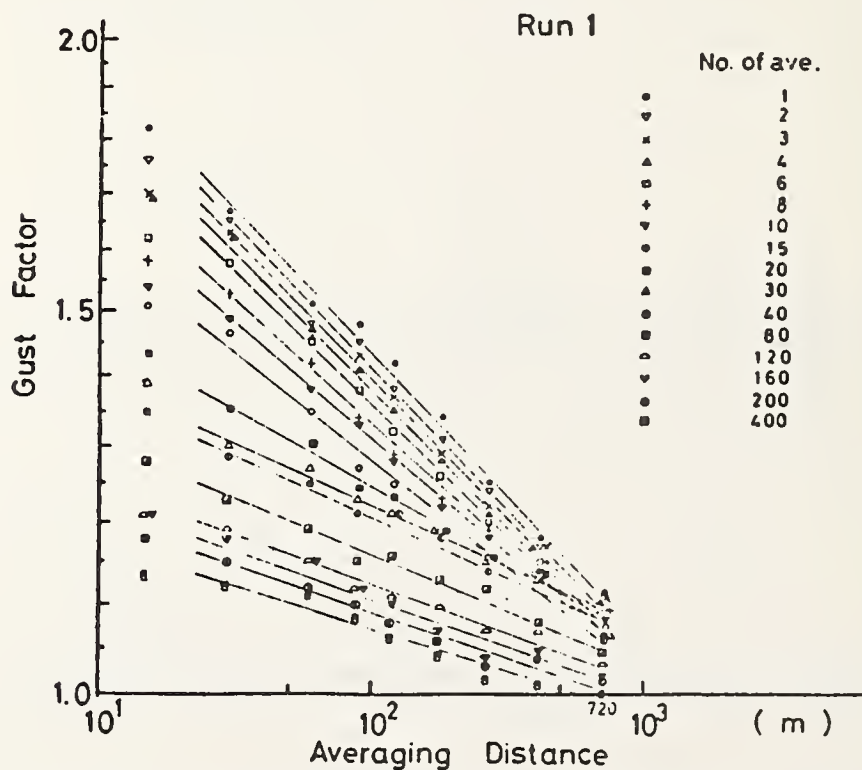


Fig.12 Time averaged gust factors as a function of averaging distance in lateral direction (Mitsuta,1974)

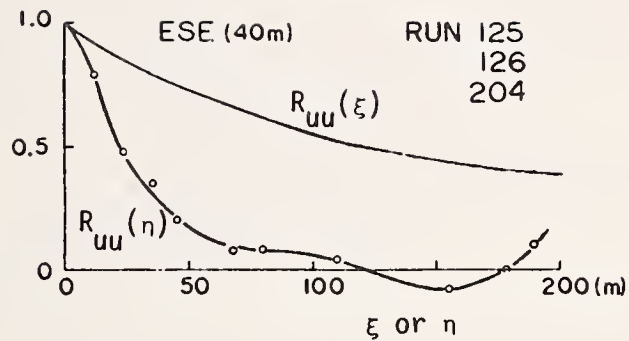


Fig.13 Averaged cross-correlation coefficients as a function of lateral distance (open circle) and averaged auto-correlation coefficients as a function of downwind distance (Shiotani,1969)

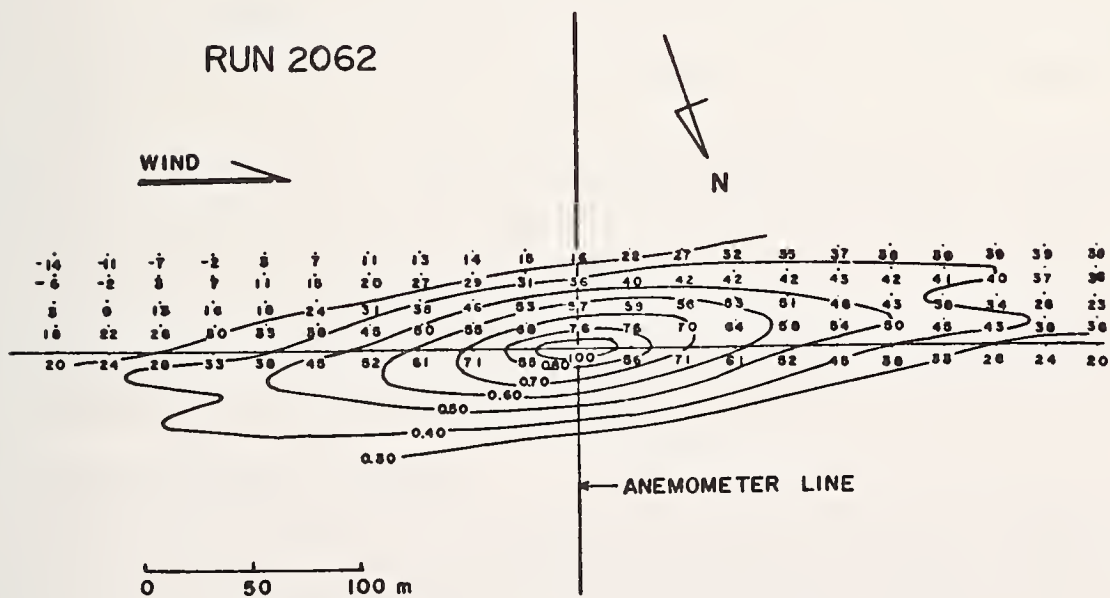


Fig.14 Spatial pattern of correlation coefficients (Shiotani,1969)

A REEXAMINATION OF HURRICANE CAMILLE

by

Arnold R. Hull
Environmental Data Service
National Oceanic and Atmospheric Administration
U.S. Department of Commerce

ABSTRACT

Newly available oceanographic and meteorological data on major storms and hurricanes striking the Gulf of Mexico during a 31-month period provided by eight petroleum firms present an opportunity to reexamine and reevaluate Hurricane Camille, one of the most severe and destructive storms ever to strike the Gulf. (Maximum wave heights of 72 feet were recorded as the eye of the hurricane passed within 15 miles of one measurement station.) The new data on Camille comprise one of the most comprehensive sets of oceanographic and meteorological information available for such an extreme weather event and should prove invaluable in basic research and offshore engineering applications. With increasing availability of this type of information likely as the Nation develops its offshore energy resources, questions arise as to what procedures should be followed to access, disseminate, and use these data most effectively and what contributions this important new data source may make to current knowledge of extreme storm events and their effects on engineering structures. The data available for Camille are examined to provide tentative answers to these questions.

Key Words: Hurricane; Storm Surge; Tropical Storms; Wind; Wind Data; Wind Speed.

Introduction

The Shell Oil Company of Houston, Texas, acting on behalf of eight petroleum firms, recently donated oceanographic and meteorological data on major storms and hurricanes striking the Gulf of Mexico from October 1968 to November 1971 to the Environmental Data Service of the U.S. Department of Commerce's National Oceanic and Atmospheric Administration. These data include information on Hurricane Camille, one of the most intense and destructive tropical storms ever to hit the United States mainland. Camille killed 256 people and caused property damage of about \$1.42 billion along the Mississippi/Louisiana Gulf Coast and in Virginia (flooding). [2]*

The data were collected at a cost exceeding one million dollars in a cooperative effort called the Oceanographic Data Gathering Program.

Data on wave height, wind speed and direction, and barometric pressure were recorded at six offshore drilling and production platforms spaced along 260 miles of the Louisiana coastline. These six locations are shown in figure 1.

Wind and Wave Instrumentation

The wind and wave sensors used were Baylor Model 9737 Wave Measuring Systems (rugged construction, non-fouling, with a long record of reliable performance) and Bendix Model 120 Aerovanes, which measure wind speed through the rotation of a propeller which drives a DC generator. The wave-measuring instruments give a continuous analog output, with a resolution of 0.1% of full-scale accuracy and a linearity of 1.0% of full scale. The wind speed threshold is 3 mph, with an accuracy of $\pm 3/4$ mph from 3 to 45 mph, and ± 3 mph from 45 to 300 mph. The direction sensors are servo-transmitters driving servo-receivers which rotate potentiometers. The overall accuracy of wind direction is $\pm 5^\circ$, with a 10° deadband at north. [4]

Data Collected

The total data collection comprises 252 analog magnetic tapes. Additionally, 170 strip charts of varying quality and usefulness were recovered. When estimated by sensor, data were gathered for waves approximately 70% of the time; for wind speed 61% of the time; and for wind direction 55% of the time. In general, the quality of the data recorded on the magnetic tapes is good. The accuracy of the data gathered by each sensor must be considered individually, but the accuracy for all data is generally within $\pm 5\%$ of the value.

Data Previously Available on Camille

In severe storm situations it is difficult to obtain reliable wind speed measurements, and Hurricane Camille was no exception. Of data previously available, approximately six wind speed observation records could be considered reasonably reliable. Two of the most useful in establishing the general level of the wind were the observations taken at Keesler Air Force Base and a record from Transworld Drilling Company's Rig 50.

* Figures in brackets refer to the references listed at the end of this report.

A reproduction of the Transworld record [1] is given in figure 2. It shows a maximum wind speed of 172 mph at the 100 ft. level. When reduced to the 30-ft. level using the 1/7 power law, the resulting peak gust is 144 mph.

Earlier wave data from the storm area are limited to a total of 14 observations from ships close enough to Camille to record winds of 35 knots or more. [5]

The most complete information previously available on Hurricane Camille concerns storm surge and is based on charts prepared by the U.S. Geological Survey (figure 3).

New Camille Data

Camille was spawned by a tropical wave that moved off the African coast on August 5, 1969. It was tracked across the Atlantic to the western tip of Cuba by the evening of August 15, entered the Gulf of Mexico with a central pressure of 908 millibars, and early on August 17 was located 250 miles south of Mobile, Alabama.

Camille's storm track (figure 1) was such that the storm passed between Stations 1 and 2 of the Ocean Data Gathering Program, with the center passing about 14 miles west-southwest of Station 1 at 1730 CDT on August 17, 1969, and about 48 miles east-northeast of Station 2 at 1645 CDT on August 17. [3] Station 1 gathered complete wave data until 1600 CDT on August 17, when the wave sensor broke loose subsea, twisted, and shorted out against the platform. Wind data continued to be gathered until 1620 CDT August 17 when salt water shorted out the power system. Subsequent to the loss of power to the station, the Bendix Aerovane came apart leaving only the center section assembly attached to the tower.

Twenty foot waves were first recorded at Station 1 at about 0500 CDT August 17, 1969, marking the beginning of the storm at that station. Due to power failure, which occurred at 1620 CDT August 17, 1969, the end of the storm at Station 1 could not be determined. Significant wave and wind characteristics during the period from 1330 to 2230 CDT on August 17 at platforms 1 and 2 appear in Table 1.

Wave data have been analyzed for one-half hour intervals during periods of the storm, and the wave spectrum for Station 1 for the period 1545 to 1615 CDT August 17, 1969, appears as figure 4. At that time, Camille was located about 24 miles south-southwest of the station, and station weather conditions are thought to have been very close to their maximum values. The significant wave height was calculated from each wave spectra and figure 5 shows the significant wave heights versus time for Stations 1 through 3. The maximum wave height recorded during the same interval (1545 to 1615 CDT) was 72 ft.

Significance of the New Data

Using the extreme value distributions of wind speed and significant wave heights for extratropical storms available from Ocean Station Vessel data, H.C.S. Thom [6] developed a technique to derive an extreme wave height distribution in any extratropical area of the deep oceans. With new data such as that for Hurricane Camille, where the relationship of wave scale to wind scale can be determined, a similar technique might be developed for tropical areas. And such data are likely to become increasingly available as the United States and other nations expand their offshore energy exploration and drilling activities.

Recognizing the importance of wind, wave, and storm surge information to structural design along coastal areas and to offshore facilities such as nuclear powerplants, drilling rigs, and supertanker terminals, it is imperative that immediate attention be given to assessing specific requirements for such information in our coastal zone areas. The increasing number of offshore platforms that will soon be erected in coastal waters offers us the opportunity to develop onsite observation networks capable of obtaining the optimum wind and wave information needed to give us a better understanding of the internal structure of hurricanes and tropical storms. Such onsite data collection will provide at least semipermanent sources of detailed "point" observations, as opposed to current random ship observations summarized over one degree squares (or even larger areas) because of the lack of fixed observation platforms.

Such long-term "point" records are critical to the development of accurate detailed environmental data statistics needed for the design, construction, and operation of both offshore and onshore facilities in the coastal area.

References

1. DeAngelis, R. M. and E. R. Nelson. Hurricane Camille-August 5-22, Climatological Data, National Summary, Vol. 20, No. 8, ESSA, Washington, 1969.
2. Dijkers, R. D., R. D. Marshall, and H. C. S. Thom. Hurricane Camille-August 1969, NBS Technical Note 569, NBS Washington, 1971.
3. Hamilton, R. C. and D. B. Steere. Ocean Data Gathering Program Report No. 2, Covering Hurricane Camille, Baylor Company, Houston, 1969.
4. Hamilton, R. C. and E. G. Ward. Ocean Data Gathering Program - Quality and Reduction of Data, 6th Annual Offshore Technology Conference, Paper No. 2108-A, Houston, 1974.
5. Selected Gale Observations, Mariners Weather Log, Vol. 14, No. 1, Essa, Washington, 1970.
6. Thom, H. C. S. Extreme Wave Height Distributions over the Oceans, Environmental Data Service, NOAA, 1972 (an unpublished report).

TABLE 1

SIGNIFICANT WAVE AND WEATHER CHARACTERISTICS

Station	Significant Wave Height (Ft.)	Significant Wave Period (Sec.)	Maximum Wave Height (Ft.)	Period of Maximum Wave (Sec.)	Maximum Wave of (Ft.)	Maximum 2-Minute Wind (MPH)	Average Wind (MPH)	Direction of Aver. Wind	Maximum Gust (MPH)
	<u>1330-1400 CDT August 17, 1969</u>								
No. 2	26.7	13.3	49.6	11.0	21.0	15	44	N	80
	<u>1400-1430 CDT August 17, 1969</u>								
No. 1	36.1	12.4	45.0	10.5	16.0	30	66	ENE	104
No. 2	30.5	12.2	39.0	11.5	20.0	12	34	N	70
	<u>1545-1615 CDT August 17, 1969</u>								
No. 1	43.2	11.5	72.0	13.0	18.0	42	90	ENE	119
	<u>1800-1830 CDT August 17, 1969</u>								
No. 2	--	--	--	--	--	44	76	NWS	114
	<u>2200-2230 CDT August 17, 1969</u>								
No. 2	--	--	--	--	--	52	66	WSW	74

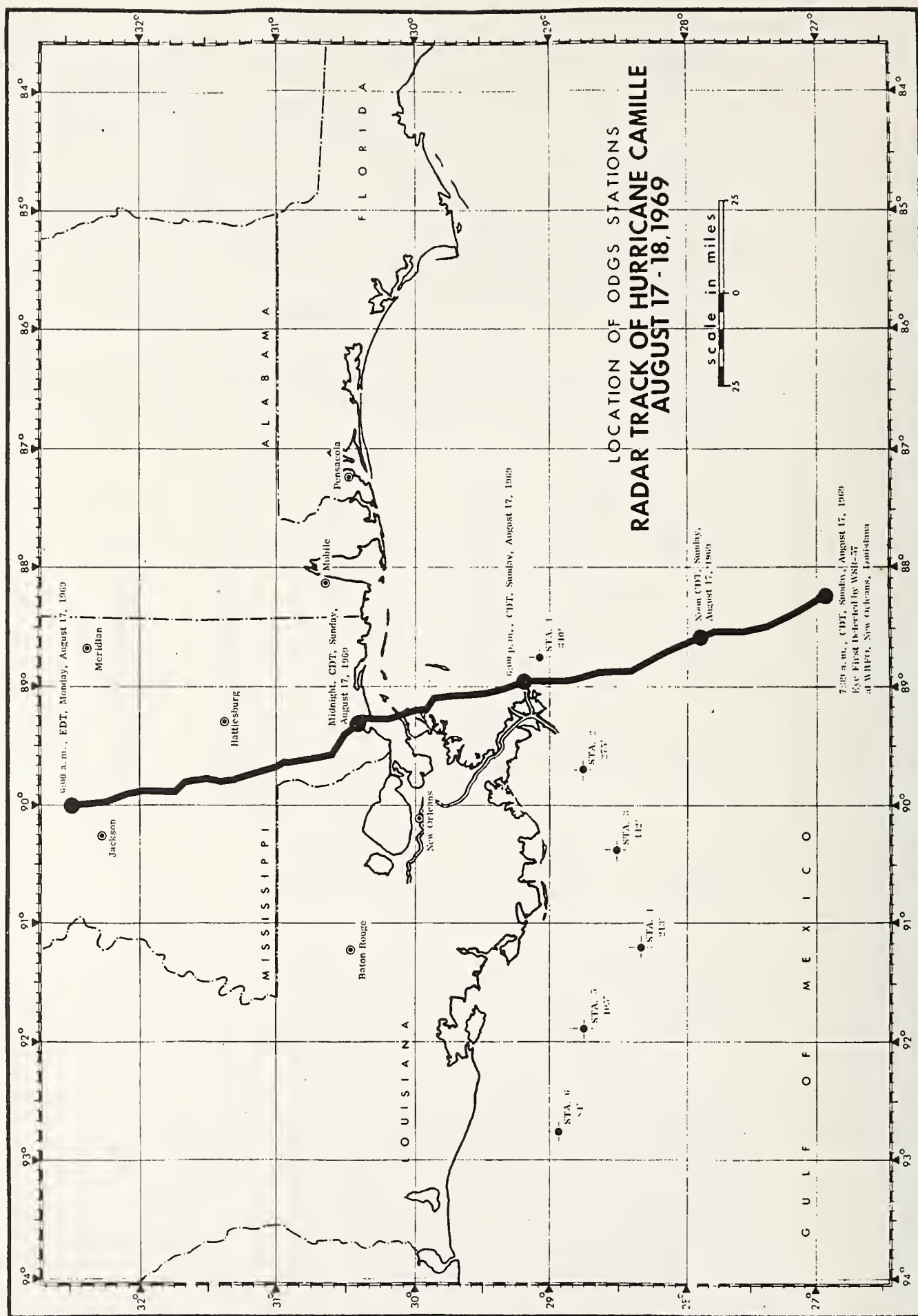


Figure 1

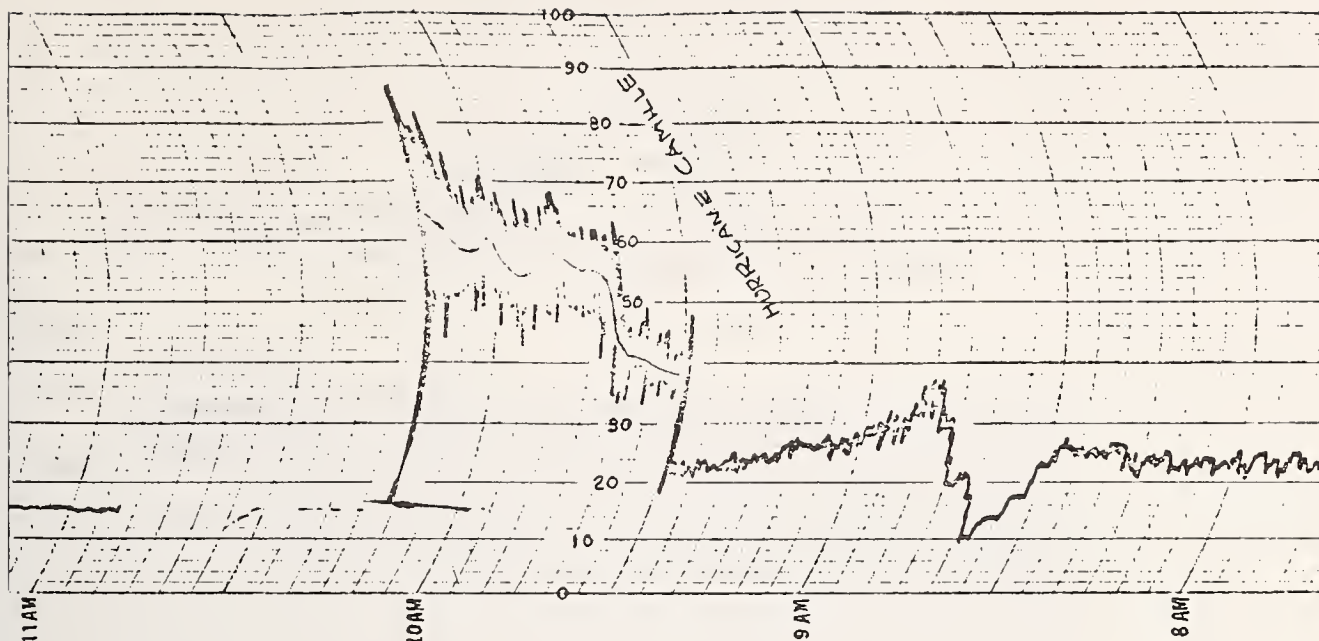


Figure 2. This wind chart from Transworld Drilling Company's Rig 50 was set on double scale, and the recorder was left running after the crew evacuated.

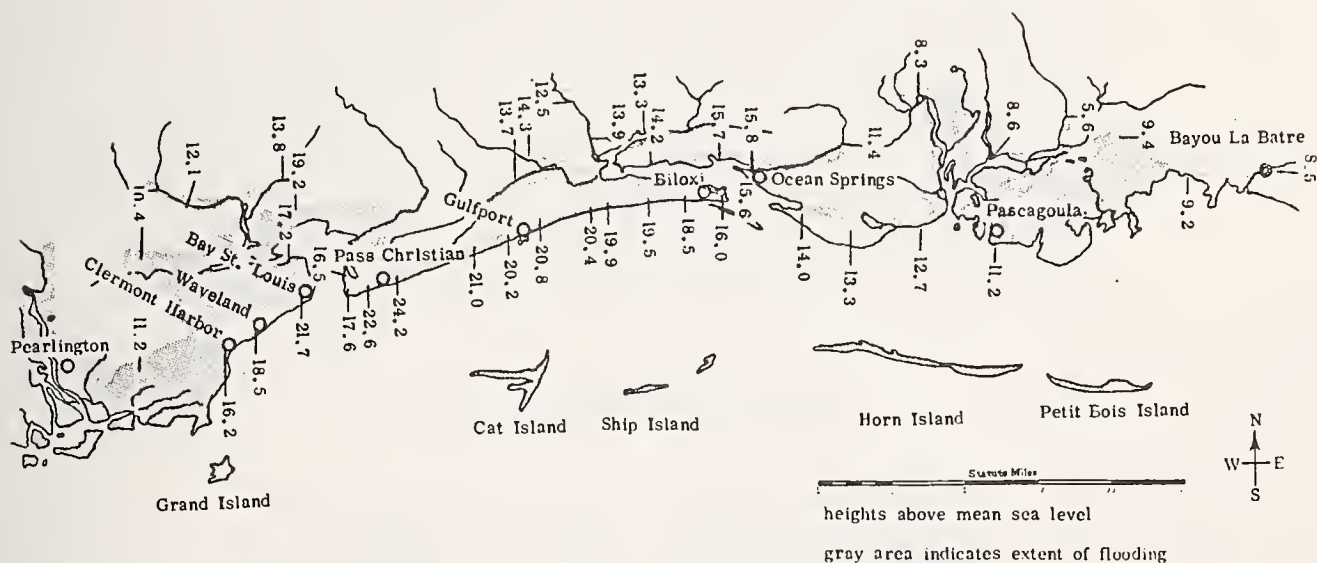


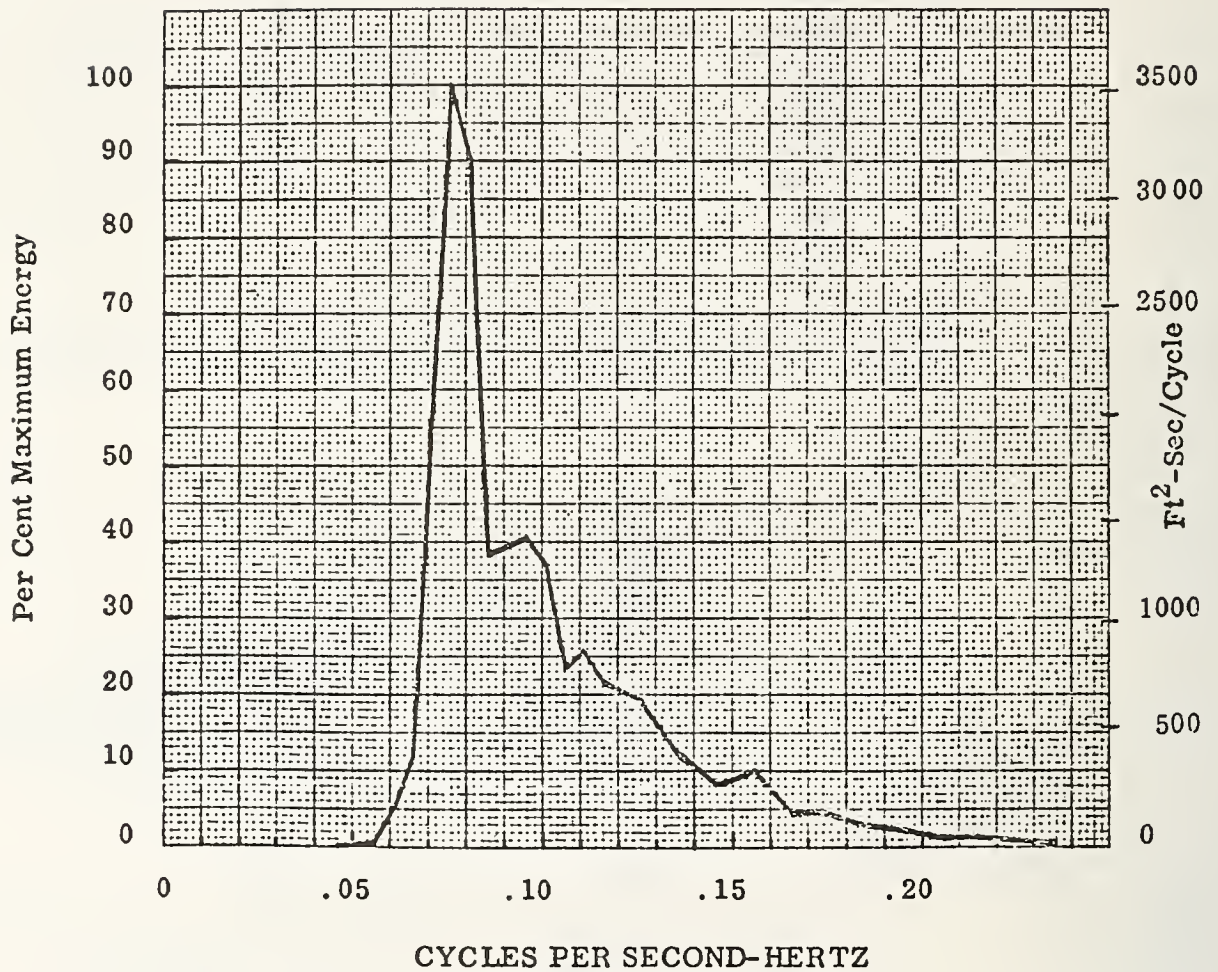
Figure 3. These are the results of the storm surge generated by Hurricane Camille on the Gulf Coast from the Pearl River to Bayou La Batre; based on charts prepared by the U.S. Geological Survey.

WAVE POWER SPECTRAL DENSITY-LINEAR

Data Tape 115

Location SP 62 A

Time 1545-1615 CDT August 17, 1969



Area under curve,	$M_0 =$	<u>116.82</u>	ft. ²
R. M. S. wave height,	$\sqrt{M_0} =$	<u>10.8</u>	ft.
Significant wave height,	$4\sqrt{M_0} =$	<u>43.2</u>	ft.
Period of Max. Energy	$=$	<u>13.2</u>	sec.

Figure 4

SIGNIFICANT WAVE HEIGHT VS. TIME

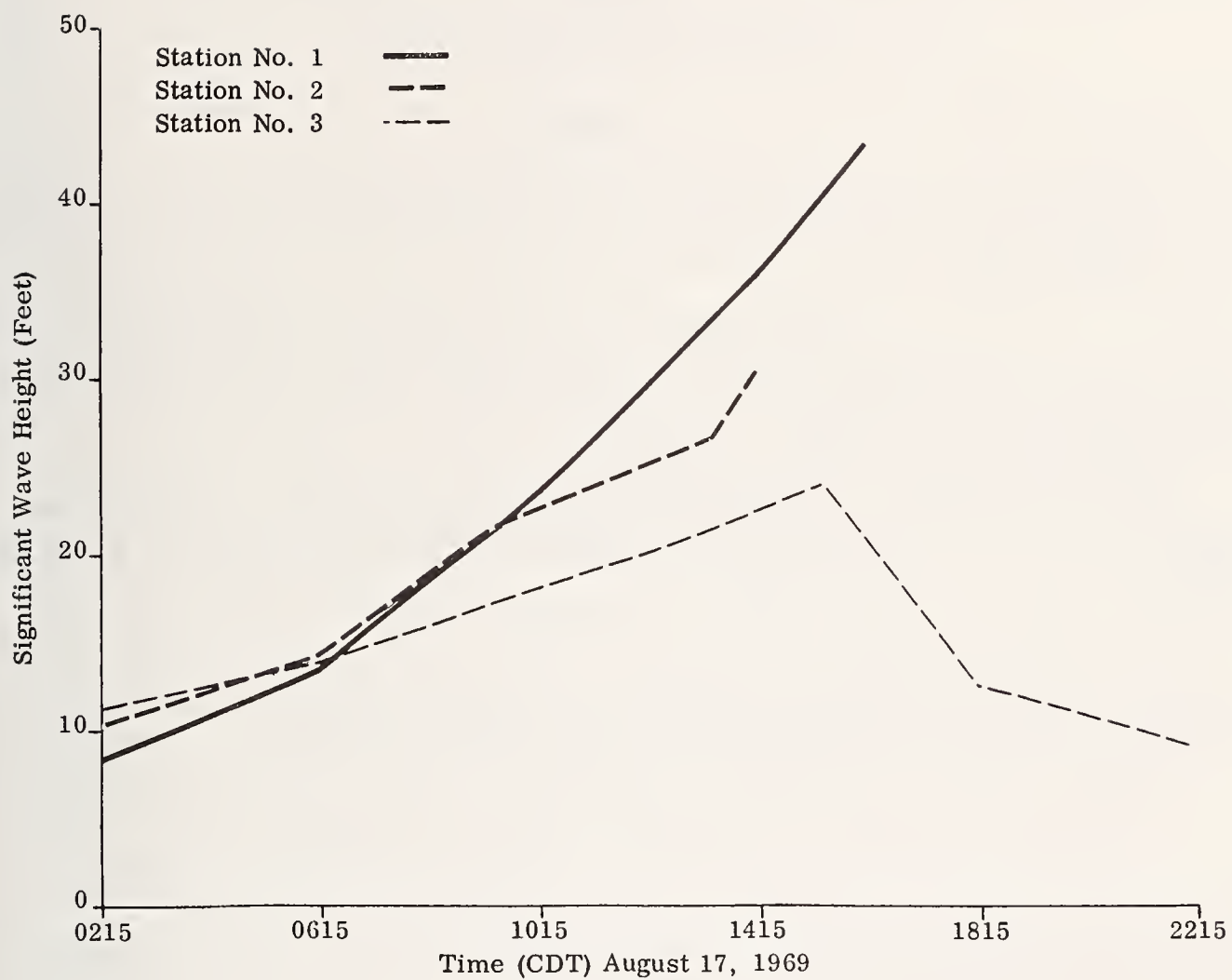


Figure 5

FIRE TORNADO AND ITS MAXIMUM WIND-SPEED

by

S. Soma
Physical Meteorology Laboratory
Meteorological Research Institute

and

K. Suda
Director
Meteorological Research Institute

ABSTRACT

Very few studies have been conducted on fire tornadoes, owing to its rare occurrence. However, in Japan, much public attention has been directed to this phenomenon in view of the fact that catastrophic damage has been caused by two fire tornadoes. One such tornado developed during the Great Kanto Earthquake in 1923 and another at Wakayama City in 1945. The cause of such catastrophic damage, due to these fire tornadoes is two-fold. One is the formation of a tornado, in burning of the urban area, and the other is the peculiar feature that the tornado is accompanied by strong winds.

In the present report, the characteristics of the fire tornadoes, which have been experienced in Japan are reported and the estimated maximum wind speed in the tornadoes are given.

Key Words: Fires; Fire Tornadoes; Tornadoes; Tornado Model; Wind Speed.

Introduction

Only a very few studies have been made on the fire tornadoes because of the rarity of the phenomenon and accordingly, many problems related to it are left unsolved. However, in Japan, much public attention has been directed to this phenomenon in view of the catastrophic events that occurred during the Great Kanto Earthquake in 1923, which killed 38,000 people. The formation of this fire tornado was then attributed to the passage of a cold front and this view has been maintained for about fifty years without any reexamination by scientists. However, a survey of studies made in various countries and the detailed analysis of weather data at the time of the formation of the tornado, revealed that the fire tornado was due mainly to the conflagration caused by the earthquake.

In Japan, two well known fire tornadoes have caused many casualties: one is related to the Great Kanto Earthquake in 1923 and the other to the great fire of Wakayama in 1945. The causes of the catastrophic damage are: (1) formation of the tornado in the burning of the urban area and (2) peculiar feature of the tornado accompanied by extremely strong wind. In the present report the formation and characteristics of the above two tornadoes, in Japan, are described.

1. Process Leading to the Formation of Fire Tornado in Tokyo.

(i) The Old Site for the Clothing Depot just before the Formation of the Fire Tornado

In the City of Tokyo, in 1923, there was a vacant area of 70,000 square meters wide along the River Sumida, which had once been the site for the Clothing Depot of the Imperial Army and then transferred to the Tokyo City for construction of a park. This vacant area popularly called "The Old Site for the Clothing Depot" (to be abbreviated OSCD) was located in downtown Tokyo which was crowded with wooden houses. Following the great shock of September 1, 1923, fire spread all over this area and refugees from the fire advanced toward the vacant ground of the OSCD voluntarily or led by policemen. As a result, a little after 3 p.m. on Sept. 1, the ground was crowded with more than 40,000 refugees. People there, free from fear, were eating food or making a bed for the night and nobody expected the formation of a fire tornado.

(ii) Spread of Fire Around the OSCD.

Examination of the spread of the fire, on the basis of a map of the burnt area prepared by Prof. S. Nakamura of Tokyo University, reveals that about 3:30 to 4:00 p.m. on Sept. 1, 1923, when the fire tornado formed, the entire Tokyo City had not been on fire. Around the OSCD along the River Sumida, however, a vast urban area of 3,000 meters long in North-South and 1,600 meters wide in East-West had already been on fire except the OSCD. In other words, the OSCD was then surrounded by a burning area several times larger than itself and was crowded with 40 thousand refugees.

(iii) Strike of the Fire Tornado

A refugee who barely survived the disaster of OSCD and witnessed the strike of fire tornado reports the following: The tornado attacked OSCD with a deafening roar and scattered fire-flakes on the heads of the refugees. Clothes and household goods, brought by the refugees caught fire at once and the fire, fanned by strong wind, spread all over the OSCD. The tornado raged for only about 20 minutes but it took

38,000 lives in a quick moment.

2. Characteristic Feature of the Fire Tornado

(i) Shape of the Fire Tornado

Based on old literature, a study was made on the shape of the OSCD fire tornado in order to see whether it was like the funnel of a natural tornado hanging down from the mother cloud.

There were at least two thousand people who barely survived the rage of the strong wind and flame in OSCD. They must have had a chance to witness the fire tornado by their own eyes. Furthermore, there must be many people who could see the tornado from the opposite bank of River Sumida, even if they were frightened by the earthquake. As the river is only 150 meters wide, it must well be possible to observe the tornado across the river. But, only very few of the old literature includes a description of the shape of fire tornado, as quoted below.

"About 3:30 p.m. I saw the smoke gathering and towering high up in the sky"--witness of Mr. K. Kondo. "About 3:30 p.m. a strong crack was heard from the northern direction. With the intensification of the sound, some attributed it to approaching tsunami while others to ignition of explosives but nothing definite was known. Then I saw deep black smoke flowing in a whirl as big as a hill presenting a horrible sight."--witness of Mr. K. Kawanabe who observed the fire tornado from the Ekoin ground located 700 m to the south of OSCD.

These witnesses may perhaps suggest the presence of a whirling fire tornado but nothing definite is known about its shape.

(ii) Wind Speed Associated With the Fire Tornado

The order of magnitude of the wind speed, associated with the fire tornado, is a matter of meteorological interest but anemometric observation is never possible in view of the condition of the tornado formation. In the case of the OSCD fire tornado, some refugees testified that persons and carts were picked up by the strong wind, but it is difficult to estimate the wind speed from the testimony alone. Fortunately, photographic plates showing the wind damage on trees were found in the Report of the Great Kanto Earthquake and we could estimate the maximum wind speed associated with the fire tornado. Plate 1 (a), which is reproduced from the above report, shows that the trunk of a tree, about 30 cm in diameter, was broken by the wind. A picture of the wind damage of trees, quite similar to the above, was taken during the tornado which formed in July, 1971 in the suburbs of Omiya City, Saitama Prefecture (Plate 1 (b)). According to K. Watanabe of the Meteorological Research Institute (1971), the intensity of this tornado is estimated to rank among Class F3 of Fujita Scale, which ranges from 70.4 to 92.5 m/sec. Considering the similarity of wind damage of trees in both cases and referring to the statements of witnesses quoted above, we may suppose that the fire tornado of OSCD was accompanied by strong winds of the same order of magnitude.

(iii) Direction of the movement of the OSCD fire tornado

Examining the reports on the Great Kanto Earthquake, we found that unexpectedly many people stated the direction of the fire tornado. However, many have mistaken the direction of the wind, for the direction of the tornado motion. Dr. S. Fujiwara (1924) made a comparative study of their reports and estimated the track of the tornado wind system as follows:

"Judging from the above circumstances, the fire tornado that brought about the disaster in OSCD would have formed at the southern border of Kitabanbacho, passed nearby Umayabashi Bridge, moved along the River Sumida up to Mr. Yasuda's mansion in Yokoamicho, turned eastward, merged with other tornadoes at Ishiharcho and then moved back to OSCD from the northeast." If we trace the motion of the tornado based on Dr. Fujiwhara's analysis, the tornado seems to have advanced from northeast to southeast. No natural tornado ever observed in Japan moved in such a direction. Furthermore, the direction of motion of the OSCD tornado was exactly opposite to the direction of the prevailing wind.

(iv) Clouds in the Case of the Great Earthquake

In the old data log of the Central Meteorological Observatory in Tokyo, Cb cloud of 3/10 in amount, is recorded for 4 p.m. of September 1. It is almost certain that this cloud was then overhead of the OSCD. The statement in the Report of Great Kanto Earthquake "As it began to rain, we made preparation to protect us from it with sliding doors and straw mats." supports this fact. The cloud, which is recorded in the data log of the Observatory simply as Cb, seems to have been unusual enough in shape to attract public attention and is mentioned in many statements in the Report of the Earthquake. From these, Prof. T. Terada's statement depicting the cloud condition is quoted below:

"About 3:30 p.m. on September 1, I stood in the verandah of my house at Komagome-Akebonocho, looking at a remarkable cumulus cloud towering up in the sky in the southeast. Surface appearance of the cloud was characteristically different from the average, i.e., protuberances on the surface were fine and well-defined reminding me of the texture of the volcanic smoke photographed during the recent eruption of Mt. Sakurajima. The towering of the cumulus cloud in the blue sky presented an unprecedented spectacle."

This cumulus cloud may be identified with the cloud that covered the OSCD since it was observed by Prof. Terada from Komagome Akebonocho in the southeastern direction.

A picture of cumulonimbus taken by Mitso Harada was found in the Report of the Earthquake (Plate 2). It is not clear whether this was the cloud covering OSCD, but its unusual shape is exactly the same as depicted by Prof. Terada. Although the formation of the cloud may partly be due to the favorable synoptic condition such as the presence of subtropical air mass and front, its direct cause will more properly be attributed to the energy of instability created in the stratification of the atmosphere by the extensive fire.

3. Examples of Fire Tornadoes

In the history of disasters in foreign countries violent fire tornadoes, that have burnt to death tens of thousand people have been recorded. However, smaller ones have been recorded, and formed in olden times as well as in recent years. One such example of a foreign fire tornado is given herein;

In June, 1961, a French cloud physicist J. Dessens conducted an experiment by making artificial cumulus clouds on the plateau of the Pyrenees. He placed forty-eight kerosene burners in an area of 125 x 125 km wide and made lit all of them at once. Then, quite unexpectedly, a fire tornado formed in the lee of the experiment area and developed to a size of 10 meters in diameter and 200 meters in height in a distance of 525 meters leeward from the origin of the fire (Plate 3-(a)). Careful observations revealed that, following the first tornado, a number of others formed in succession.

In May, 1965, in the port of Muroran, a Norwegian mammoth tanker (56,000 t) cracked in a wharf. A large hole was then made on the side of the ship and petroleum gushed out and caught fire. In this case too, a remarkable fire tornado formed in the lee of the large fire. (Plate 4)

On the occasion of the Nankai Earthquake (magnitude 8.1) in December, 1946, a large fire broke out in Shingu City, Wakayama Prefecture, and burnt down 2,612 houses, destroying 25% of the entire urban area. On this occasion, a fire tornado is reported to have formed in the river beach, in which citizens took refuge. This tornado was not large, but was accompanied by a strong wind which blew up a mat of 22 Kg in weight into the sky.

4. Fire Tornado in the Great Fire of Wakayama City

(i) Formation of the Fire Tornado

A fire tornado, much larger than those mentioned above, formed in association with the great fire of Wakayama City in July, 1945, which destroyed 68% of the urban area. On this occasion, a violent fire tornado formed in vacant area of the old prefectural offices, and burnt to death 748 people. Although the number of victims was far less than that of the catastrophic OSCD tornado, it corresponds to more than 60% of the total loss of lives due to the fire, showing the violence of fire tornado.

Now, several statements on the formation of the tornado in Wakayama are quoted from old reports. "Thirty to forty minutes after the outbreak of the great fire, violent fire tornadoes formed in several places in the city. The largest one among them originated in a street with a tramway 200m away to the south of the old city office ground and moved northward. The incandescent flame of the fire tornado streamed horizontally as if it were blown by bellows. Pine trees planted along the moat were torn away. An automobile flew over the bank and jumped into the moat; red hot zinc sheets and big logs were uplifted to a height of 20 - 30 meters."

Aside from the above, another fire tornado formed at night on the same day over a spot, 1500 meters away from the old prefectural office ground. "In the Naval timber yard there was hundreds of thousands of feet of timber stored. This timber caught fire and were uplifted by the tornado presenting a spectacle of countless burning chopsticks flying high in to the sky to a great astonishment of the refugees around Tsukiji Bridge.

"According to the observations, taken by Wakayama Weather Station, east-northeasterly winds of 2.5 m/s was blowing just before the outbreak of the fire. Examining the weather charts, six hours prior to the fire, we find that fine weather prevailed all around Wakayama City without any indication of front or other weather systems, that would lead to the formation of a tornado.

(ii) Estimation of Maximum Wind Speed

It is not easy to estimate exactly what the maximum wind speed was in association with the fire tornado of Wakayama City. However, let us try to make a rough estimate using recent studies on Tornadoes.

To begin with, the estimation of the damage of the pine trees planted along the avenue, wind speed of about 40 m/s were required to break the pine trees. However, from the expression that "pine trees--were broken" and that "big logs were lifted up to the height of 20-30 meters", the maximum wind speed would probably have exceeded 50 m/s.

Next, turning to the wind estimation by examining the damage of automobiles, we refer to the record of the tornado that struck Toyohashi City, Aichi Prefecture in December, 1969. As this tornado passed right across damage, not only to the buildings of the drive-in and its annex but also to the cars parked therein. Some of the cars were reported to have blown a distance of some tens of meters. Ishizaki and others (1970) made an estimation of the maximum wind speed accompanying the tornado based on the damage caused on buildings and concluded that the speed was in the range from 63 to 119 m/s (Fig. 1). If the estimation is applicable to the damage caused on cars by the fire tornado of Wakayama, it will be possible to rank the intensity of the tornado on a scale of F2, which corresponds to wind speeds ranging from 50.4 to 70.3 m/s.

For the wind speed of the fire tornado, which lifted up numerous timbers at the Naval timber yard in Wakayama, we shall only make an estimate of the speed of the up-draft. If we suppose that the diameter of the timber lifted up by the wind to be 20 cm, density of the timber to be 0.5 gr/cm^3 and the drag coefficient (C_D) of a cylinder to be 1.0, then we get 35 m/s as the speed of the upward current that will hold the timber from falling down. As for the horizontal wind speed, we have at present no means to estimate its value.

5. Experimental Study

Although a considerable number of fire tornadoes have been observed, the mechanism of their formation has not been made. It is difficult to clarify the mechanism through the study of weather data and other materials in the formative stage of the tornado because of the peculiarity of the condition during the formation of the tornado. Therefore, an experimental study of fire tornadoes was made. These experiments, which are incomplete and have yielded only qualitative results, will now be outlined.

(i) Experimental Apparatus

The apparatus used in the experiment consisted of a circular metal base, 2 meters in diameter simulating the ground surface and a wind generator that can provide any wind distribution in either the horizontal and vertical directions (Plate 5). Attached to

bottom of the metal base, is a tank of 2 meters in diameter which was filled with water. The water temperature was controlled in order to give instability to the stratification of the air above the base. The wind generator has 15 wind ducts arranged in three rows and five lines, each of which is equipped with a fan and can produce any desired wind speed.

(a) The formation of a fire tornado is developed by placing on the metal base a circular burning plate, which simulates in the simplest way the burning urban area. The burning disc, 600 mm in diameter and 10 mm thick, is made from glass-wool soaked with methyl alcohol.

Raising the temperature of the surface of the base by 20°C above the room temperature and, at the same time, giving an appropriate wind speed, a fire tornado of Dessens type was formed as shown in Plate 3 (b).

(b) Considering the fact that, in the formation of the OSCD tornado, the OSCD ground was surrounded by a burning urban area, an experiment was conducted using a burning plate similar to the burning area in shape. In the same manner as described previously, the temperature of the surface of the metal base was raised by 20°C above the room temperature. Then, after giving appropriate wind speed and horizontal wind shear, formation of a remarkable vortex column like a whirl-wind was observed at the spot surrounded the burning area (Plate 6 and Fig. 2). Although this experiment simplifies the natural wind condition, it seems to give essentially the model of the OSCD fire tornado.

If the temperature of the metal base is lowered to decrease the instability of air stratification, the formation of the vortex column like tornado becomes rare. However, even if the metal base is not heated, vortex columns are formed sporadically at the same spot, after applying an appropriate wind speed and wind shear.

6. Characteristic Feature of the Earthquake Fire

Our investigation of the fire tornadoes in the OSCD and the Wakayama prefectural office ground revealed that the presence of an extensive burning area seems to be the decisive factor in the formation of fire tornadoes. However, not all of the large fires recorded in the history are accompanied by fire tornadoes. Although further investigation is required for the final solution of this problem, it is highly probable that there are at least two kinds of fire tornadoes, one favorable for the formation of a fire and the other not.

Examining materials of past large fires, it was found that in most cases strong wind played an important part in the extensive spread of the fire. For example, in the instance of the great fire of Hakodate City, Hokkaido, which destroyed the major part of the city on March 21, 1934, the maximum wind speed of 22 m/s was observed. Among the Three Great Fires of Edo (old Tokyo), which are well known in the modern history of Japan, at least two were due to strong wind. A common feature of these is that the fire originated from one source and spread to an extensive area fanned by a strong wind; the burned area extends in a strip (Fig. 3). However, fires due to earthquake show a burn as an area with quite a

different shape. In this case, there are numerous fire sources and the fire breaks out all at once over an extensive area. In the case of the great fire of Wakayama, which was not due to an earthquake, the shape of burned area indicates the same process. Therefore, it can be concluded that there are two kinds of great fires, one of which fire breaks out from one source and fanned by strong wind, and then extends along a strip. The other fire starts burning all at once from numerous sources. Generally in the formation of fire tornadoes, the latter is more favorable.

In describing the experimental study on fire tornadoes, we have stated that a vortex column like fire tornado was formed providing an appropriate wind speed was given. Namely, in our experiment, the vortex column did not form in a weak wind or a strong wind, but did form if a wind speed around 1 m/s was provided. As a matter of fact, both of the fire tornadoes of OSCD and of Wakayama prefectural office ground formed in relatively weak wind with a speed of 4 - 5 m/s for the former and 2 - 3 m/s for the latter. Thus the wind speeds of such range seem to be appropriate for the formation of fire tornadoes.

Conclusions

Fire tornadoes of OSCD and Wakayama prefectural office ground, which caused catastrophies were studied relative to their cause formation, their characteristic features and their relation to the damage induced. As a result, it was found that the main cause of their formation was the extensive fire that was initiated from numerous sources, the peculiar shape of the burning area, an appropriate wind speed and the unstable stratification of the atmosphere. Furthermore, it was revealed that fire tornadoes are accompanied by very strong winds reaching speeds of 70.4 - 92.5 m/s for OSCD tornado and 50.4 - 70.3 m/s for Wakayama prefectural office ground.

The major characteristic of fire tornadoes is the updrift and induced fire-flakes, thus spreading the burnt area. In addition, the fire tornado fans the fire with violent wind that surpasses the storm in typhoon.

In the report of the OSCD fire tornado, the following statements are found. "Fire crept about over the ground. People fell down breathing in the flame." "He survived the fire without getting burnt but, a few days later, died complaining of a pain in his breast". There are a few other statements with the same implication. According to "The Fire" compiled by Dr. K. Nakata (1969), the lung may be burnt by breathing in fire which can be fatal to life. At first difficult breathing occurs due to the break of pulmonary capillaries, then emphysema of lungs. Patients, if they survive this stage, they are generally doomed to death suffering from bacterial pneumonia.

In the case of the OSCD fire tornado, an exceedingly strong wind in the open area made the fales creep about the ground and consequently many people would probably have breathed in hot air. Recently, if the fire of tall buildings, many people have been reported to have been suffocated to death by breathing in smoke. In the case of fire tornadoes, however, the process leading to death is somewhat different.

References

1. Central Meteorological Observatory (1924): Report of the Great Kanto Earthquake (Meteorological Part, in Japanese), pp. 1 - 161.
2. Dessens, J. (1962): Man-made Tornadoes, Nature, Jan. 6, Vol. 193, pp. 13-14.
3. Isizaki, H. et al (1970): Investigation on Tornado and its damage which struck the city of Toyohashi, Dec. 7, 1969, WDD Technical Note No. 5, by Grant in-Aid for Fundamental Scientific Research from the Ministry of Education, (1)-96100.
4. Lee, S.L. (1972): Fire Research, Applied Mechnaics Review, May, Vol. 25, No. 25, pp. 503-509.
5. Nakata, K. (1969): The Fire, Kyoritsu Publishing Co. (in Japanese), pp. 629.
6. Disaster Science Research Society (1956): Great Fires in Japan, Gihodo Book Co. (in Japanese), pp. 13.
7. Terada, T. (1925): On the tornado of September 1 - 2, 1923, Report of EArthquake Disaster Prevention Society, No. 100 (in Japanese), pp. 185-227.
8. City Office of Wakayama (1956): History of War Damage of Wakayama City (in Japanese) pp. 30-40.

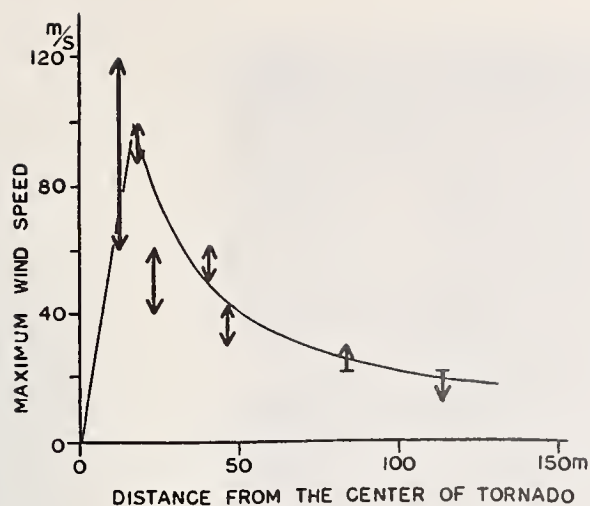


Fig. 1:

Maximum wind speed estimated from the damages of structures (Toyohashi Tornado December 7, 1969).

(by H. Ishizaki)

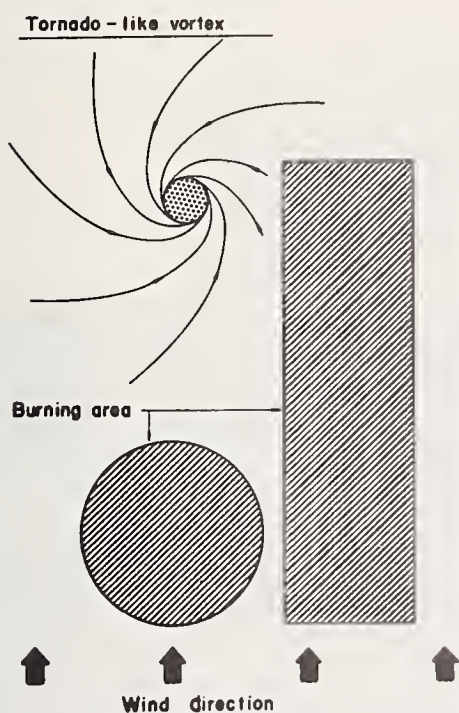


Fig. 2:

Relative position of vortex column and burning areas in the case when the most remarkable vortex column was generated.

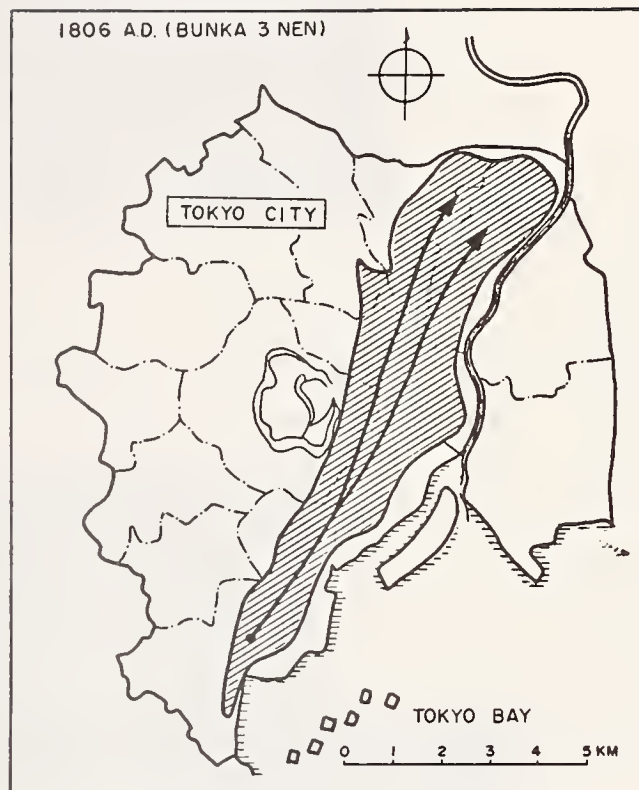


Fig. 3:

An example of the greatest fire in Tokugawa Era; the fire broke out at one point and spread lee-ward in a long and narrow strip fanned by high wind.



Plate 1 (a):

A tree torn off by the fire-tornado. This was taken at the former site of the Army Clothing Depot immediately after the Great Kanto Earthquake.

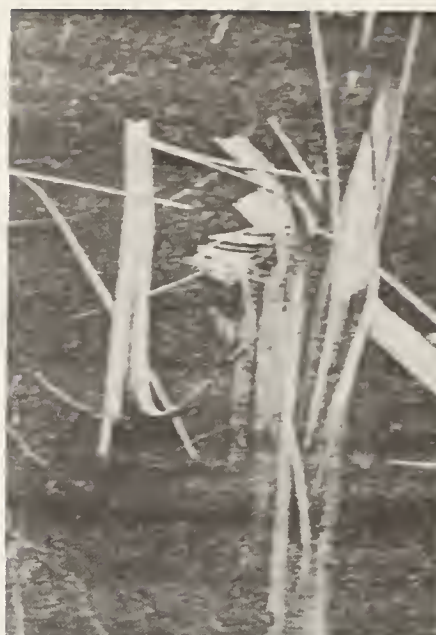


Plate 1 (b):

A tree torn off by the meteorological tornado. This was taken at the suburbs of Omiya City, near Tokyo on 7th July, 1971.



Plate 2: Gigantic cumulonimbus in the sky over Tokyo after the Great Kanto Earthquake (taken by M. Harada). The former site of the Army Clothing Depot seems to have been covered by such a cumulonimbus at the time of fire-tornado occurrence.

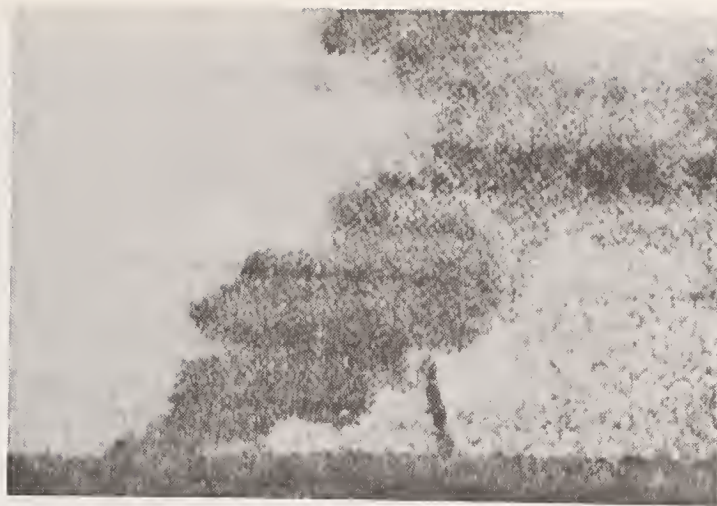


Plate 3 (a): A fire-tornado which formed accidentally in the lee of a large scale fire plume (by J. Dessens, 1961).

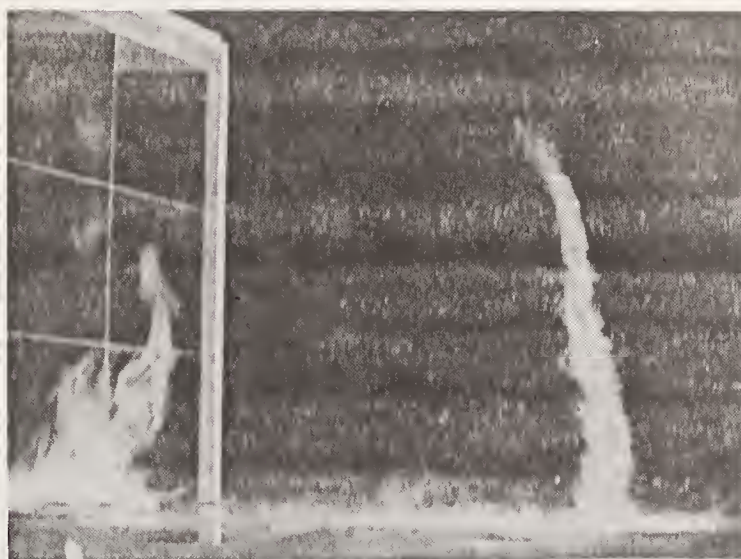


Plate 3 (b):
Vortex column like a fire-tornado in laboratory (by S. Soma, 1973).



Plate 4: Fire-tornado which formed on the leeside of a burning tanker (56,000 t) in Muroran Port in Hokkaido, 1965. (Provided by Hokkaido Newspaper)



Plate 5: Apparatus for the experimental study of fire-tornado. Vortex column like fire-tornado is made on the copper disk.



Plate 6:

Vortex column like fire-tornado
obtained by the burning area
model. Vortex column can be
seen on upper left. (Picture
taken from the above.)

A RESEARCH PROJECT ON THE WIND FLOW
AROUND TALL BUILDINGS

by

Tatsuo Murota
Senior Research Officer
3rd Research Division
Building Research Institute
Ministry of Construction

and

Kiyoshi Nakano
Head
Senior Research Officer
3rd Research Division
Building Research Institute
Ministry of Construction

ABSTRACT

The problem of wind effects, produced by the construction of tall buildings, is analyzed. A research project designed to obtain information about this problem and to study the counterpart for the prevention of high winds around tall buildings, has been initiated. Some preliminary observations are described herein.

Key Words: Building; Wind; Wind Effects; Wind Loads; Wind Observation; Wind Speed.

Introduction

During the past 10 years in Japan, the number of tall buildings which have been constructed has increased dramatically. Many of these buildings have been constructed in the central part of large cities, and sometimes produce high wind speeds near the ground surface in pedestrian areas. Previously tall buildings were constructed in low building areas. After construction, alterations have occurred between the owner of the tall building and nearby habitants about the change of wind environment. It is difficult, however, to find a solution to the problem, because quantitative data concerning the modification of air flow and the frequency of occurrence of high winds is too scarce.

The Ministry of Construction, therefore, initiated a research project to obtain information about this phenomenon and to obtain a guidance on this wind problem.

In the followings, after discussion of the problem concerning this phenomenon, an outline of this research and some preliminary results of wind observations are described.

Wind Surrounding Tall Buildings

The problems due to the wind caused by the modification of airflow surrounding tall buildings can be divided into two categories: 1) the change of the environment, and 2) the increase in damage to the structures surrounding the tall buildings.

The former is concerned with two kinds of phenomena; a) an increase of the frequency of occurrence of high winds and b) an increase of frequency of occurrence of calm conditions. The "high wind" condition is a wind which has a speed which becomes annoying to people, which is generally 5 m/s or greater. These "high winds", cause difficulty in walking, increase heating consumption in winter, create difficulties in opening of doors, cause disturbance in rooms when windows are open, and impede plant growth. The occurrence of the high winds increase the frequency of calm conditions, and thus, the complaints of sultriness during the summer.

The change in the environment is the most serious problem, because this is related to calm wind which occurs very frequently. These winds are affected by the air's thermal stratification (vertical temperature gradient) in addition to the large-scale weather condition, and thus, makes it very difficult to estimate the change in the environment.

The second wind problem, the increase in damage to structures, is related to higher winds such as those caused by typhoons. In general, buildings exposed to such high winds will be subjected to some damage risk. However, buildings standing near tall buildings may be exposed to the additional increase of wind speed caused by the modification of air flow, thus increasing the risk of damage.

In order to solve these problems the following information needs to be collected;

Change of Environment

- (1) Distribution of wind speed around tall buildings in relation to the air's thermal stratification.
- (2) Frequency of occurrence of each pattern of wind speed distribution.
- (3) Criteria of allowable change of environment stipulating the correlation of wind speed and frequency of occurrence.

Increase of Damage

- (1) Distribution of wind speed around tall buildings
- (2) Distribution of turbulence

Description of the Research Project

The Building Research Institute has instituted a research project relative to this problem since 1975. The purpose of this project is to provide informations stated above and solutions to eliminate the high wind speeds. The following studies are part of this project;

- (1) Wind observation around tall buildings

High winds around tall buildings have been observed at several tall buildings sites in Japan. The periods of these observations, however, were for only a few hours, and thus the data obtained are not reliable in order to understand the quantitative nature of winds around these tall buildings. Therefore, continual wind observations around and in the vicinity of a few tall buildings will be conducted during the next several years.

- (2) Field investigation of the influence of the wind in the environment

In the vicinity and around many tall buildings, the intensity and spatial distribution of the change of wind will be studied. The relation between the dimension or shape of tall buildings and the change of wind on the environment will be analyzed.

- (3) Study of wind through wind tunnel test

If a reliable similarity law is available, wind tunnel tests are quite effective in evaluating the wind distribution. However, such a similarity law is not known at present and therefore the possibility of such a law will be studied in this project by comparing ad hoc testing methods with full-scale measurements.

- (4) Development of methods to reduce high winds

Windbreaks and shelterbelts have been utilized in agriculture areas in order to reduce surface wind speed and to obtain the resulting micro-climatic change in plant growth. In this project such applications will be examined relative to winds on buildings.

Preliminary Results

The Building Research Institute has conducted wind observations in 1974 at two 14-story building sites.

- (1) Wind observations at Tokorozawa City

Tokorozawa New Town is a housing area developed in the outskirt of Tokorozawa City. Three 14-story apartments are arranged in a line running from west to east in the center of this New Town. Surrounding the three tall buildings is a five story apartment and one and two story houses. Wind observations were made at 3 levels of two observation points as shown in Fig. 1. Between these two points a wind-shelter fence of 4 m in height and 40 m in length were arranged from south to north.

Wind data collected at the Tokorozawa Fire Station, which is located 3 km from the New Town, were used as the reference location. The height of the anemometer at the reference point, is 9 m above the ground.

Fig. 2 shows the frequency of occurrence of wind speeds at points P_1 to P_6 in the New Town compared with that at the reference point. According to this figure, at P_1 , P_2 , P_3 and P_6 the frequency of occurrence of the calm wind is 10% below 2 m/s. However, the frequency of occurrence of the higher winds is several percents higher at every wind speed. The frequency of occurrence at points P_4 and P_5 is quite different from other points and is similar to that at the Fire Station. This is probably due to the shelter effect of the fence.

Fig. 3 shows the relationship between the ratio of the wind speeds at points P_1 to P_6 to the reference wind speeds, when the reference wind direction is N, NNW and NW. The values of the wind speed ratio R is greatly scattered at the lower reference wind speeds, but the scatter becomes less with increasing reference wind speeds. The maximum value of R is greater than 3 and is observed at reference wind speed of 2 m/s. At the higher reference wind speeds the value of R approach unity.

(2) Wind observation at Koto-ku, Tokyo

The other location where preliminary wind observations were conducted was at Koto-ku, Tokyo. At this location there are eight-fourteen story apartment buildings which were constructed in 1975 as shown in Fig. 4. Wind observations were made in 1974, when the apartments No. 4, 5 and 6 were under construction and they were only two storied buildings at the end of the year. The average wind speeds were continually observed at 6 points as shown in Fig. 4 and at a height of 5 m above the ground. The wind data collected at a wind tower (54m high above the ground) of the Japan Meteorological Agency, which is located 7 km from the observation site and was used as a reference.

Fig. 5 shown the relationship between the reference wind speed and the wind speed ratio R (wind speeds at points P_1 to P_6 to reference wind speed), when the reference wind direction was NW. As shown in this figure, there is a tendency for the R value to scatter and is similar to that in Tokorozawa areas with the mean value of R differing greatly from point to point.

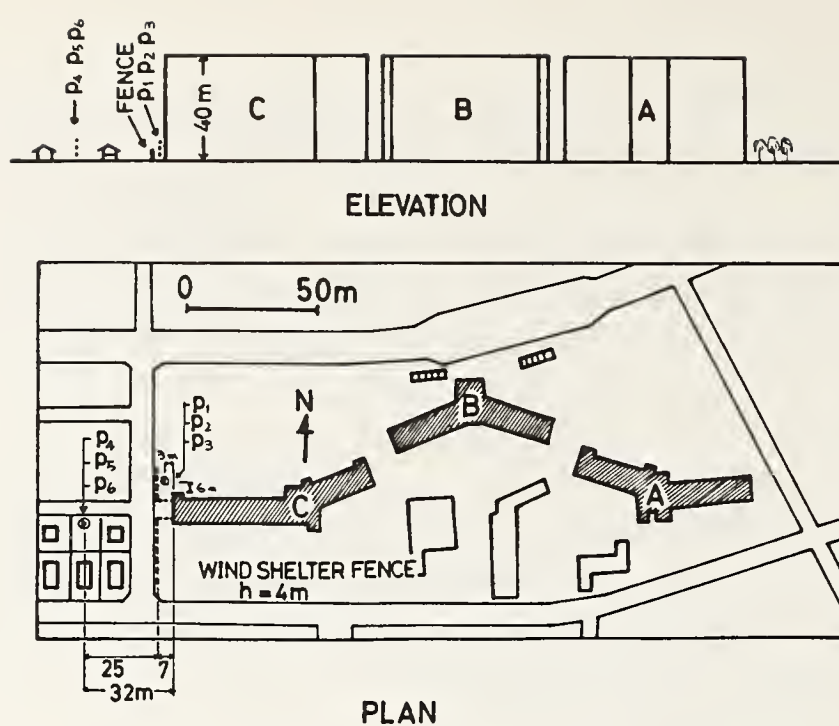
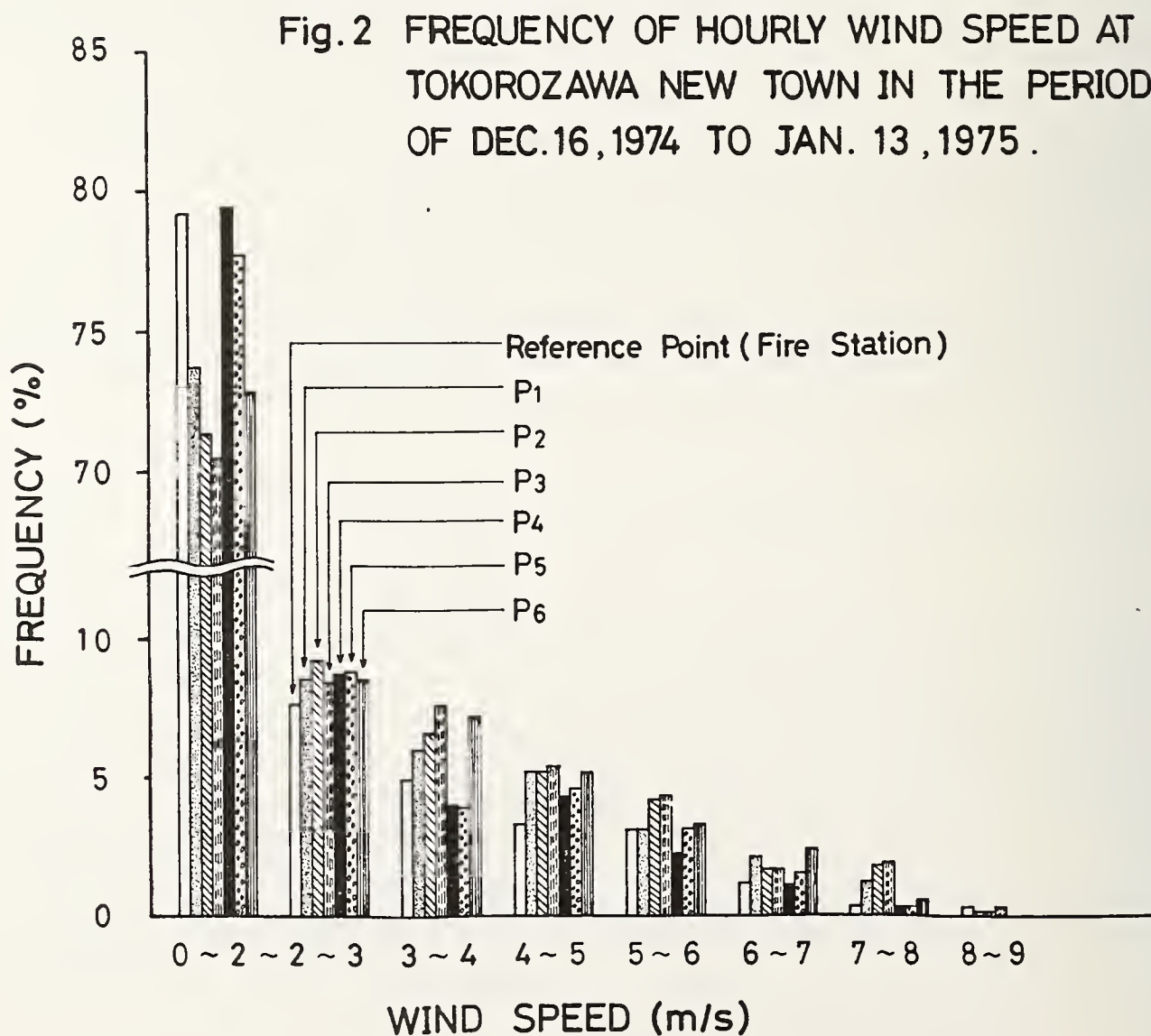


Fig.1 ARRANGEMENT OF WIND OBSERVATION POINTS
P₁~P₆. HEIGHTS OF P₁ TO P₆ ARE 2,4,6,2,4.5
AND 7m, RESPECTIVELY.



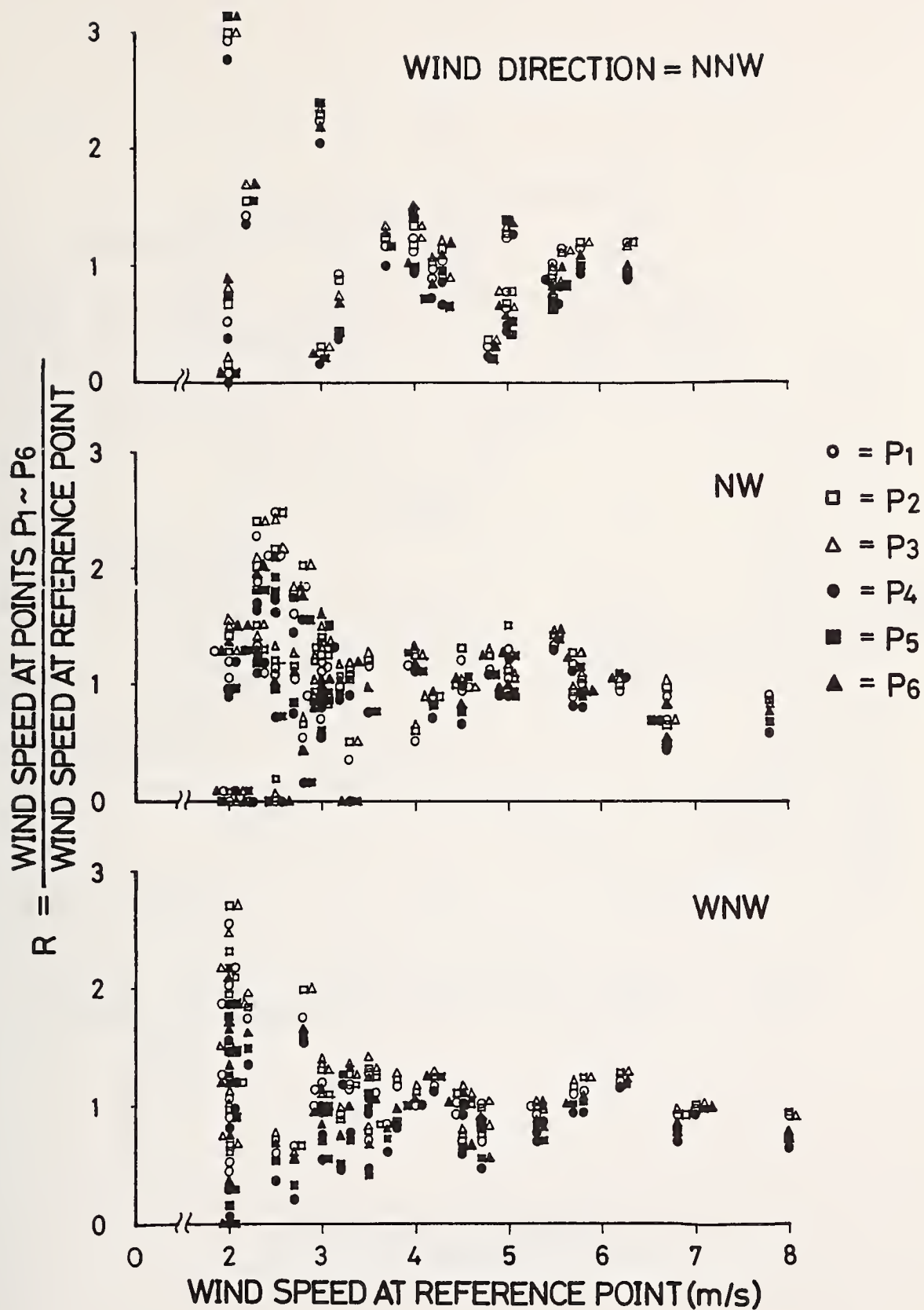


Fig. 3 RELATION BETWEEN THE WIND SPEED RATIO R AND THE WIND SPEED AT REFERENCE POINT

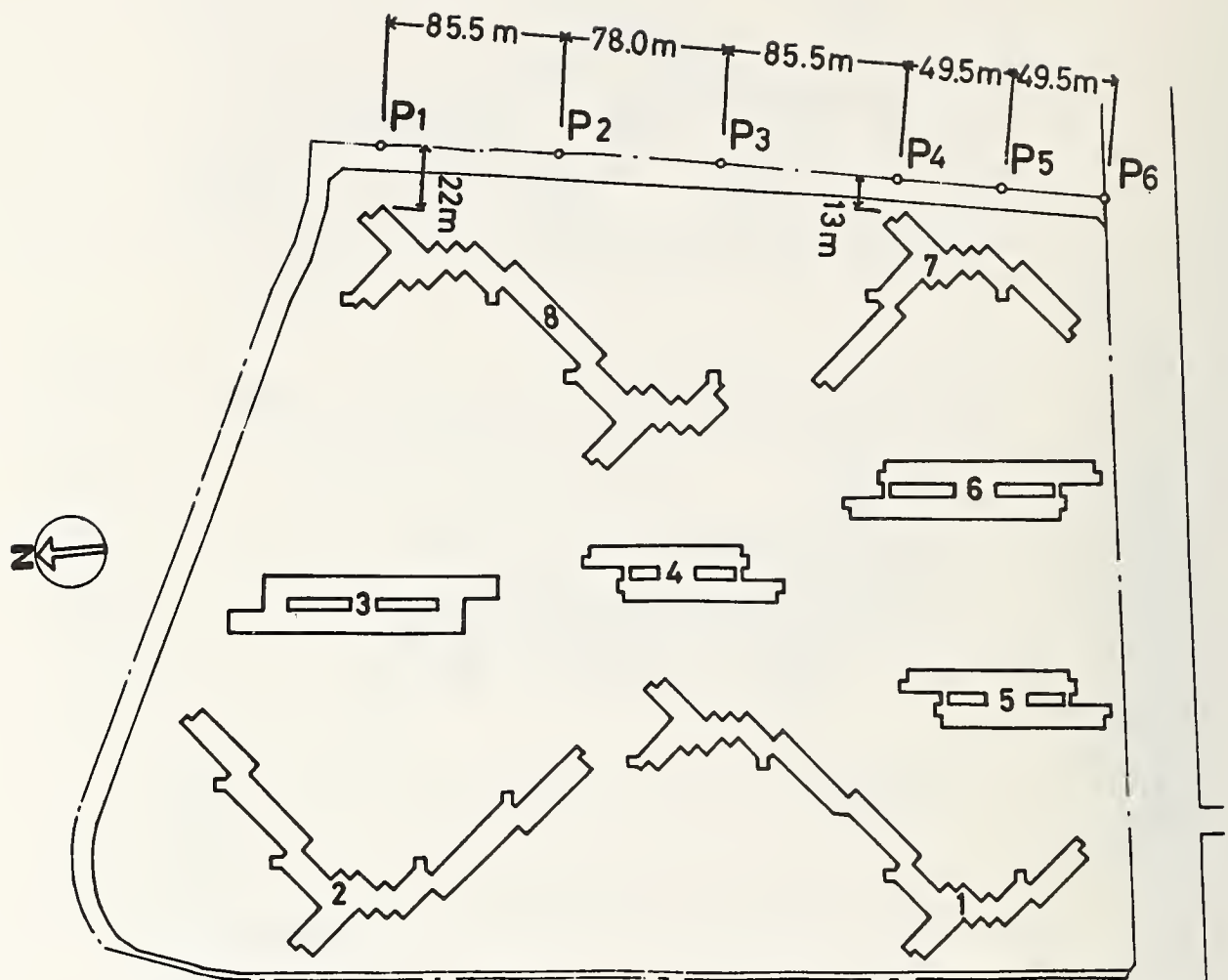


Fig.4 LAYOUT OF WIND OBSERVATION POINTS

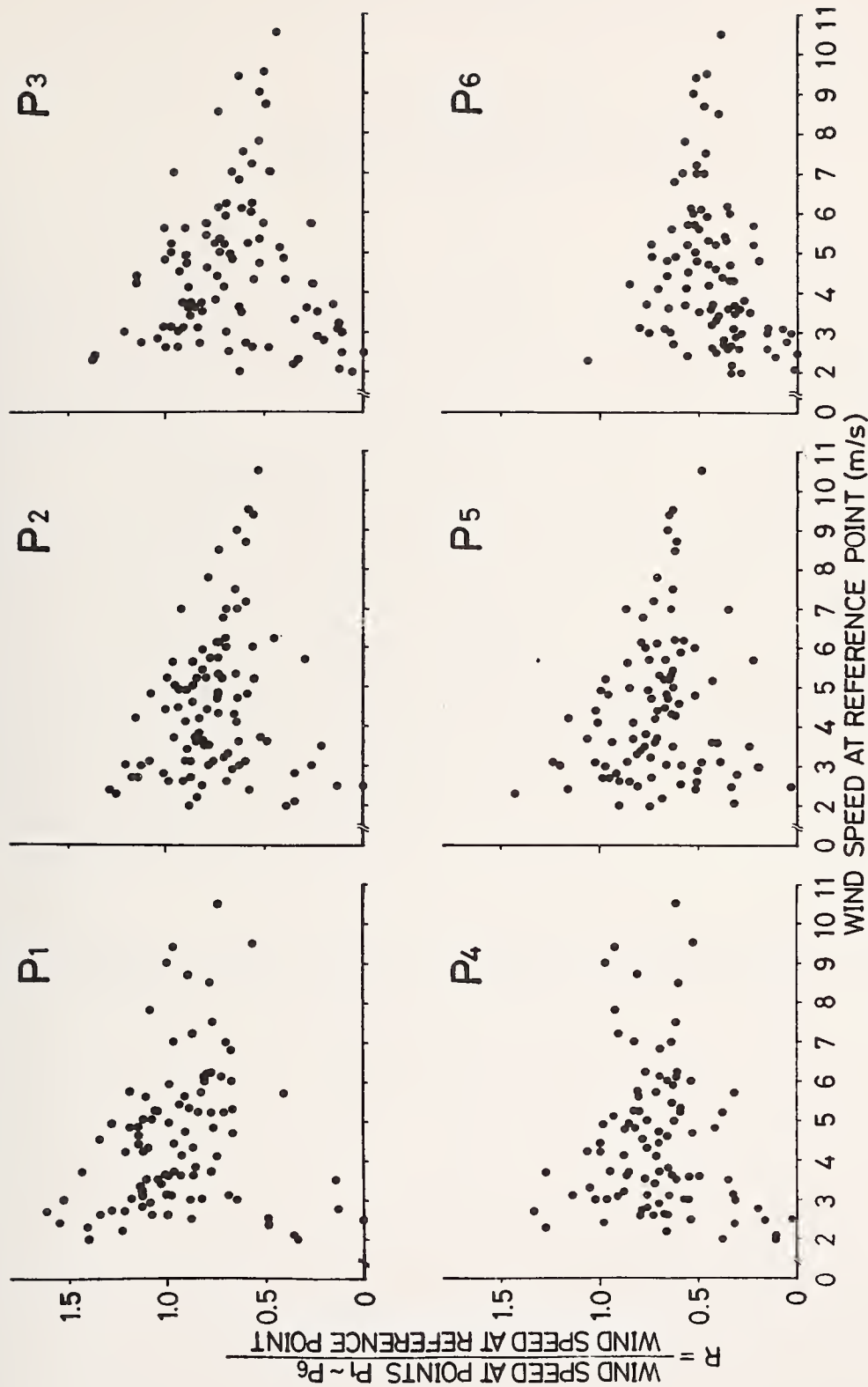


Fig.5 RELATION BETWEEN THE WIND SPEED RATIO R
AND THE WIND SPEED AT REFERENCE POINT

WIND ENGINEERING RESEARCH PROGRAM
SUPPORTED BY
THE NATIONAL SCIENCE FOUNDATION

by

Michael P. Gaus
Head
Engineering Mechanics Section, NSF
Washington, D.C.

ABSTRACT

The National Science Foundation is an Agency of the Federal Government established in 1950 to advance scientific and technical progress in the United States. The Foundation fulfills this responsibility primarily by sponsoring scientific research, encouraging and supporting improvements in science education, and fostering scientific information exchange. NSF does not itself conduct research or carry out education projects.

Operating under this charter the Foundation supports a substantial amount of research in Wind and Seismic effects. The Division of Engineering has for the past years had an organized area activity in Wind Engineering Research. The primary emphasis of this research has been toward developing a better understanding of the structure and flow of the earth's boundary layer to develop new knowledge and techniques for predicting and coping with the interaction between the boundary layer wind and man-made or natural objects and to develop methods to assess or predict environmental effects related to wind flow. Almost all of the current research programs being supported are at academic institutions. A summary of these current research projects is given herein.

Key Words: Education; Research; Research Programs; Wind Engineering; Wind Studies.

Introduction

For purposes of classification, Wind Engineering research is divided into 16 categories. These categories are shown in Fig. 1. Primary emphasis during the early years of the program has been in categories 1 thru 10 and in category 16.

Of special interest during the last year has been the beginning of operations of the Wind Engineering Research Council which was funded during FY 1974. Objectives and organization of the Council are shown in Figures 2, 3, 4, 5 and 6. The Council has already been active in promoting interchange between wind engineering researchers and anticipates organizing a series of workshops in the future to assess important problems and opportunities for wind engineering research.

Also made available during the last year is the first issue of the Wind Engineering Digest. The Wind Engineering Digest is a survey of current projects in various aspects of wind engineering research. The digest is intended to alert investigators to research in progress. The original intention was to include in the first volume only research projects in the U.S.A. However, because of international interest, it was decided to include international projects for which questionnaires were received. The cover and index of the WERD Digest are shown in Fig's. 7 and 8.

Activities of the Committee on Natural Disasters of the National Academy of Engineering have continued to be supported. The wind related activities are twofold. One is to send investigation teams to sites of natural disasters (such as tornadoes or cyclones) to collect data on damage and effects which may latter be used to reconstruct damage mechanisms, velocities, missile densities, and so forth. Much of this information is of a perishable nature and may be obliterated by rescue and clean-up operations. This information is then made available to researchers who might wish to do in-depth studies on the effects of such storms. Several teams were dispatched during the last year to document damage due to tornadoes. The second wind related activity is to prepare a comprehensive report on Wind Engineering research. This report would be similar to the 1969 report on Earthquake Engineering Research prepared under the auspices of the same committee which at that time was operating under the title "Committee on Earthquake Engineering Research." The title page is shown in Fig. 9. (not submitted for publication).

During FY 1975 a total of 19 research projects were funded. This is in addition to projects funded in previous years, but still in progress due to multiple year funding periods. A list of all projects currently in progress would be rather voluminous, therefore a complete listing of such projects in progress, describing FY 1975 research grants, may be obtained from NSF. Total dollar support for Wind Engineering research during the last five years is shown in Fig. 10.

WIND ENGINEERING

- 1) Structure of Wind
 - a) Boundary-layer-vertical (50 to 100 meter region) and horizontal profiles, turbulence intensities
 - b) Extremes and durations
 - c) Effects of Moisture content - rain, snow, hail
- 2) Wind-Wave Effects
 - a) Wave generation
 - b) Open sea structures - floating platforms, ships
 - c) Off-shore structures
 - d) Coastal structures
 - e) Harbors, estuaries, inlets
- 3) Effects on Urban Areas
 - a) Characteristics of Wind build-up areas
 - b) Influence of tall structures
 - c) Transport and entrainment of pollutants
 - d) V/STOL airports and heliports
 - e) Micro-thermal phenomena
- 4) Wind Loading on Structures
 - a) Drag, vortex shedding and separation
 - b) Dynamic response and stochastic analysis
 - c) Numerical algorithms and computer software
 - d) Loads on cladding and glass
 - e) Static vs. statistical approach
 - f) Permeability effects
- 5) Severe Storms
 - a) Thunderstorms
 - b) Hurricanes - wind velocities, wind-water interactions
 - c) Tornadoes - wind and pressure distributions
 - d) Local phenomena
 - e) Prediction capabilities
- 6) Design for Hurricanes and Tornadoes
 - a) Critical structures - nuclear reactor, etc.
 - b) Standard structures - controlled-sequence failure to protect life
 - c) Missile damage
 - d) Economic considerations
- 7) Full-Scale Testing
 - a) Instrumentation development
 - b) Urban and rural profiles for engineering applications
 - c) Structure testing - fixed and portable structures, bridges, cooling towers, tall stacks, tall buildings
- 8) Model Testing
 - a) Special wind tunnel facilities
 - b) Model scaling and dynamic similitude
 - c) Structure testing - fixed and portable structures, bridges, cooling towers and tall stacks
 - d) Effects of clustering and wake interaction

- 9) Environmental Factors
 - a) Effects of structure on surroundings - entrapment of pollutants, stability of vehicles and pedestrians
 - b) Effects on environmental control systems
- 10) Psycho-Physical Factors
 - a) Perception levels for motion in various structures
 - b) Motion tolerance
 - c) Psychological response to drift
- 11) Legal Factors
 - a) Pollution problems
 - b) Buffeting of downstream structures, etc.
 - c) Missile damage caused by other structures
 - d) Structural damage
 - e) Occupancy discomfort
 - f) Insurance rates
- 12) Special Problems
 - a) Moisture penetration of buildings
 - b) Wind zoning for cities
 - c) Building code requirements
- 13) Wind Considerations in Urban Planning
- 14) Building Codes and Regulations
- 15) Socio-Economic Effects
- 16) International Cooperation

Fig. 2

Wind
Engineering
Research
Council

An organization for coordinating
research activity and disseminating information
on Wind Engineering problems

Fig. 3

PURPOSE

The Wind Engineering Research Council was formed to provide a mechanism for the free exchange of information on research plans, priorities, and programs; and to assist in the coordination of research efforts in wind engineering.

The primary objectives of the Wind Engineering Research Council are:

- To stimulate the initiation of, and provide the coordination, of research efforts in wind engineering.
- Implement the dissemination and exchange of information between research workers in the various disciplines of wind engineering.
- Delineate problems that most urgently need research.
- Establish a National Wind Engineering Information Center consisting of a library of publications and research reports.
- Provide advice to government agencies and other interested parties on wind research efforts and problems.

Fig. 4

ACTIVITIES

The Council organizes periodic national meetings of research investigators in Wind Engineering. These meetings consist of reports on current research and discussions in or by working sub-groups on directions for future research. The proceedings of these national meetings are published and sent to those individuals and organizations on the WERC mailing list. In addition, a quarterly newsletter reporting on activities and forthcoming events in Wind Engineering is mailed to all interested parties.

The activities of WERC are supported by a grant from the National Science Foundation.

MEMBERSHIP

Because of the nature of the organization there is no formal membership classification for participants in WERC activities. The "membership" of the Council consists of all persons and organizations, on the WERC mailing list, having an active interest in one of the areas of Wind Engineering. Interested parties may be included on the WERC mailing list by submitting their name, organization, and address to:

Dr. Richard A. Parmelee, Executive Secretary
Wind Engineering Research Council
Department of Civil Engineering
Northwestern University
Evanston, Illinois 60201

Phone: (312) 492-3172

Fig. 5

WIND ENGINEERING

Recognizing that the effects of wind on the works of man result in extensive damage and unacceptable loss of life, the Wind Engineering Research Council was formed to encourage and coordinate research on winds and wind effects, and to disseminate information. WERC is especially concerned with the following aspects of the wind engineering problem.

BOUNDARY-LAYER WINDS

- Distribution of mean air speeds
- Distribution of mean temperature
- Turbulence characteristics
- Orographic effects
- Urban effects
- Joint probability of air velocity, temperature and humidity

SEVERE STORMS

- Thunderstorms
- Hurricanes
- Tornadoes
- Extratropical cyclones
- Downslope winds
- Post-disaster inspections
- Extreme wind statistics

WIND LOADING ON STRUCTURES

- Mean and dynamic responses
- Vortex-shedding excitation and galloping
- Loading on cladding and glass
- Effects of architectural details
- Stochastic analysis
- Impact of wind-driven missiles
- Building code requirements

PSYCHO-PHYSICAL FACTORS

- Preception thresholds of motion
- Tolerance for vibratory motion
- Wind criteria for pedestrian safety and comfort

EFFECTS ON URBAN AREAS

- Transport, entrainment and entrapment of pollutant
- Stability of vehicles and pedestrians
- Location of V/STOL airports and heliports
- Location of industrial and power plants
- Wind zoning for cities
- Micro-thermal characteristics

FULL-SCALE MEASUREMENTS

- Instrumentation development
- Meteorological variables
- Pollutant concentrations
- Wind pressures on building surfaces
- Structural responses

MODEL TESTS

- Wind-tunnel facilities
- Model-prototype similitude
- Blockage effects
- Wind characteristics for complex geometry
- Structural responses
- Building surface pressures
- Diffusion of stack and automobile exhausts

SPECIAL PROBLEMS

- Agricultural aerodynamics
- Air-sea interactions
- Wind-induced noise
- Wind power generation

Fig. 6

WERC ADVISORY COUNCIL

The affairs of the Council are handled by an Advisory Committee which consists of the following members:

EXECUTIVE BOARD

Chairman

Jack E. Cermak
Colorado State University

1st Vice-Chairman

Leslie E. Robertson
Skilling, Helle, Christiansen, Robertson

2nd Vice-Chairman

Anatol Roshko
California Institute of Technology

Executive Secretary

Richard A. Parmelee
Northwestern University

ADVISORY COMMITTEE

Arthur N. L. Chiu
University of Hawaii

Alan G. Davenport
University of Western Ontario

Joseph H. Golden
National Severe Storms Laboratory

Robert J. Hansen
Massachusetts Institute of Technology

George W. Housner
California Institute of Technology

Kishor C. Mehta
Texas Tech University

Nathan M. Newmark
University of Illinois

Hans A. Panofsky
Pennsylvania State University

George W. Reynolds
Woodward-ENVICON Inc.

Robert H. Scanlan
Princeton University

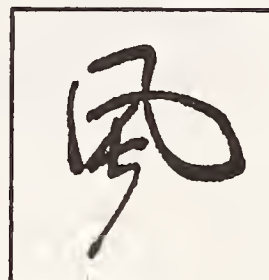
Anshel J. Schiff
Purdue University

H. C. S. Thom
Consulting Meteorologist

Fig. 7

Wind Engineering Research Digest

Volume I - 1974



Sponsored through Grant GK-38047
National Science Foundation

Conducted in Cooperation with the
Wind Engineering Research Council

University of Hawaii
Honolulu, Hawaii

TABLE OF CONTENTS

PREFACE

1. Structure of Wind
2. Wind-Wave Effects
3. Effects on Urban Areas
4. Wind Loading on Structures
5. Severe Storms
6. Design for Hurricanes and Tornadoes
7. Full-Scale Testing
8. Model Testing
9. Environmental Factors
10. Psycho-Physical Factors
11. Legal Factors
12. Special Problems
13. Wind Considerations in Urban Planning
14. Building Codes and Regulations
15. Socio-Economic Effects
16. International Cooperation
17. Wind Energy Conversion System

AUTHOR INDEX

INSTITUTION/AGENCY INDEX

TABLE 1 - Projects Reported and Sponsors

TABLE 2 - Sponsors of U.S. Projects

ADDRESSES OF PRINCIPAL INVESTIGATORS

NSF WIND ENGINEERING EXPENDITURES

FY 1971	\$ 136,300
FY 1972	630,900
FY 1973	1,013,200
FY 1974	772,800
FY 1975	\$1,222,800

STUDY OF THE WIND PRESSURE AND THE RESPONSE OF ROOF CORNERS

by

Tatsuo Murota
Senior Research Officer
3rd Research Division
Building Research Institute
Ministry of Construction

and

Mitsuo Nakahara
Senior Research Officer
3rd Research Division
Building Research Institute
Ministry of Construction

ABSTRACT

In 1972, a number of prefabricated dwellings in the Nagoya district, Japan, suffered damage from high winds caused by Typhoon No. 7220. Much of the damage to the dwellings caused by this typhoon was the removal of the flat roofs of the buildings. It is known that the corners of flat roofs, when subjected to high winds have high suctions with periodic fluctuating force components. The cause of this type of damage has created a need for studying the dynamic effect of wind pressure on roof corners. Such a study has been conducted since 1973 by the Building Research Institute. The results of the 1974 field observations, by the BRI, will be given herein.

Key Words: Buildings; Dynamic Effects; High Winds; Roofs; Typhoon; Wind Pressure.

Full-Scale Measurement of Wind Pressure

A two-story dwelling, shown in Fig. 1, was used to measure wind pressures on roof corners. The locations of the pressure measurements were arranged on the roof of the 2nd story as shown in Fig. 2.

Typical power spectra of the wind pressure fluctuations, at several pressure measurement locations, are shown in Figs. 3 and 4.

Fig. 3 shows the power spectra at the north west corner of the roof during a 11 m/s wind from NE-E direction. At the NE-1 location, the energy power distribution occurs in all frequency ranges and, therefore, the pressure fluctuation is considered to be random. However, at locations NE-2 and NE-3, two predominant frequency components are observed at values of 0.4 and 0.72 H_z . At location NE-2, the energy peaks are observed at 1.9, 2.2 and 2.8 H_z , and at location NE-4 only a line power is observed at 2.65 H_z .

The reduced frequencies are given by;

$$f = \frac{nD}{V}$$

where n = frequency, D = characteristic length, and V = wind velocity.

Using the predominant frequencies of 0.4 and 0.72 H_z at locations NE-2 and 3, the reduced frequencies are 0.17 and 0.13, respectively, where the characteristic lengths D are taken as $2h$ (h = height of the wind story roof from the 1st roof) and $2l$ (l = projected length of the eave), respectively. These values of reduced frequencies are approximately the same as those obtained on square cylinders during wind tunnel tests, and it is considered that these predominant frequency components are caused by the vortex formation near the roof corner.

The physical meaning of the predominant frequency of 2.65 H_z at location NE-4 has not been determined and will require future studies.

At locating NE-5 and 6, the energy peaks, as shown in Fig. 4, are also observed to have the same frequencies as those at locations NE-2 and 3 as shown in Fig. 3. Consider, for example, point NE-1 shown in Fig. 4, which has a peak frequency of 1.6 H_z . Suppose that D is 2 times the projected length of the curve, the reduced frequency becomes 0.18. The power spectrum for point NE-7 has the same feature as that for point NE-4 as shown in Fig. 3.

Model Test on the Response of Roof Corners

A small model of a roof corner was set on a building 60 m high above the ground and the vertical displacements of the roof corner was observed for 0° to 30° roof slopes, as shown in Fig. 5. The model was set at a position where the wind direction was constant and the vertical wind component was very small.

The results from these observations are as follows;

- a) The mean displacement changed with roof slope: that is the direction of the mean response was downward for 0° to 10° and upward for 15° to 30° as shown in Fig. 6.

- b) The root mean square values of the displacement σ_y , was independent of the roof slope. Assuming that the maximum response Y_{\max} and the mean response Y_{mean} is given by;

$$Y_{\max} = Y_{\text{mean}} \left(1 + \frac{k \cdot \sigma_y}{Y_{\text{mean}}} \right)$$

the constant k equals 3 to 4, in the range of roof slope 0° to 30° as shown in Fig. 7.

- c) Fig. 8a to e shows the power spectra of the displacement for the roof slope 0° to 10° . In these figures the energy peaks are observed at the fundamental frequency of this model roof. However, when the roof slope is in the range of 15° to 30° , these peaks are not observed, as shown in Fig. 8f to h.

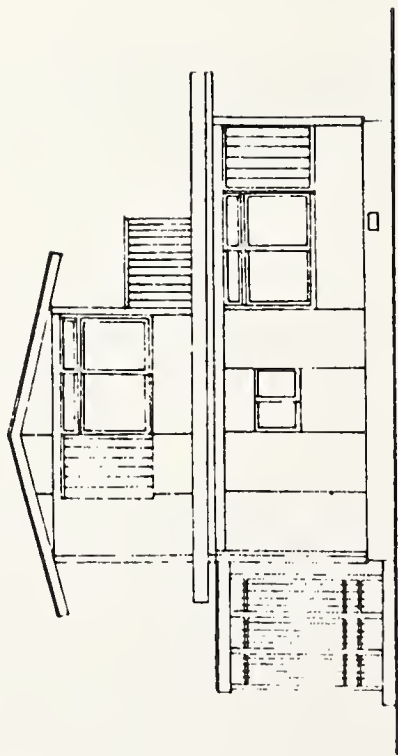
Conclusion

The following phenomena has been observed from the measurement of wind pressure and the response of the roof corners.

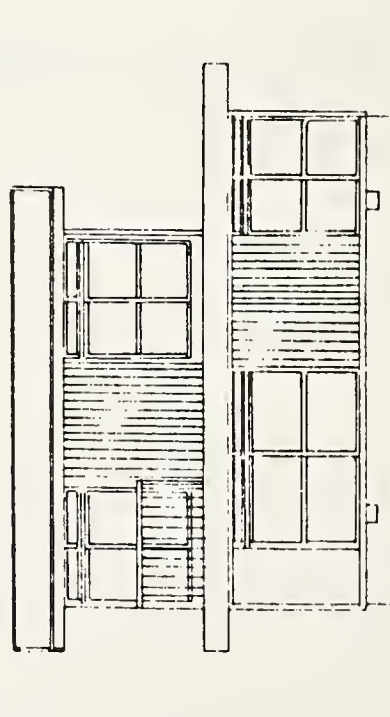
- 1) The predominant frequency components were observed during the wind pressure fluctuation at the roof corners.
- 2) The values of the reduced frequency of these predominant components were nearly equal to those recorded on square cylinders' during wind tunnel tests and these components are considered to be caused by the vortex formation.
- 3) The response of roof corners in the wind, from the diagonal direction, changes its feature discontinuously for a slope angle of 10° to 15° .

Acknowledgment

This study was conducted at the Building Center of Japan in 1974. The authors wish to express their thanks to the chairman, Dr. Isamu Kamli and the other members of the Task Committee on this study organized in BCJ.



WEST ELEV. 1/100



SOUTH ELEV. 1/100

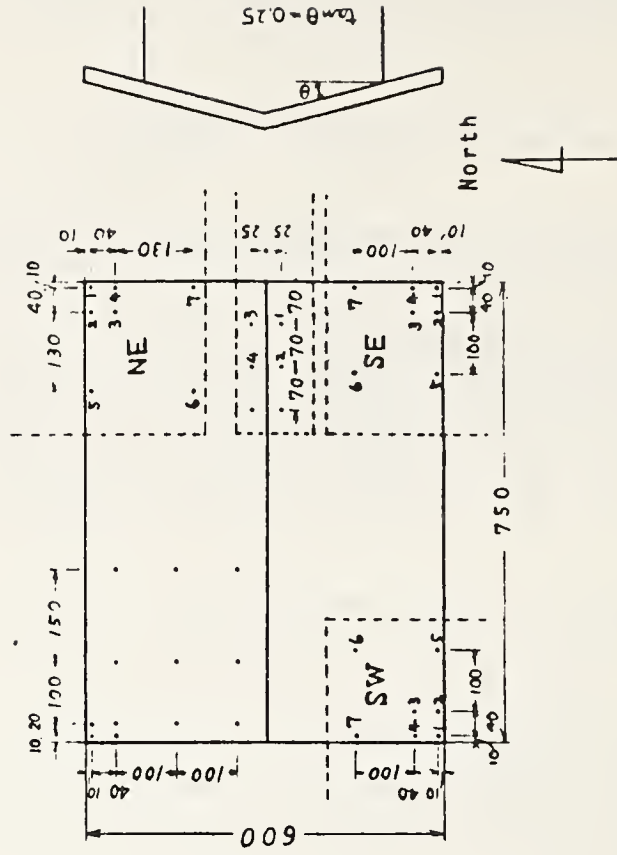


Fig.2 Arrangement of pressure holes on the roof (Unit in cm)

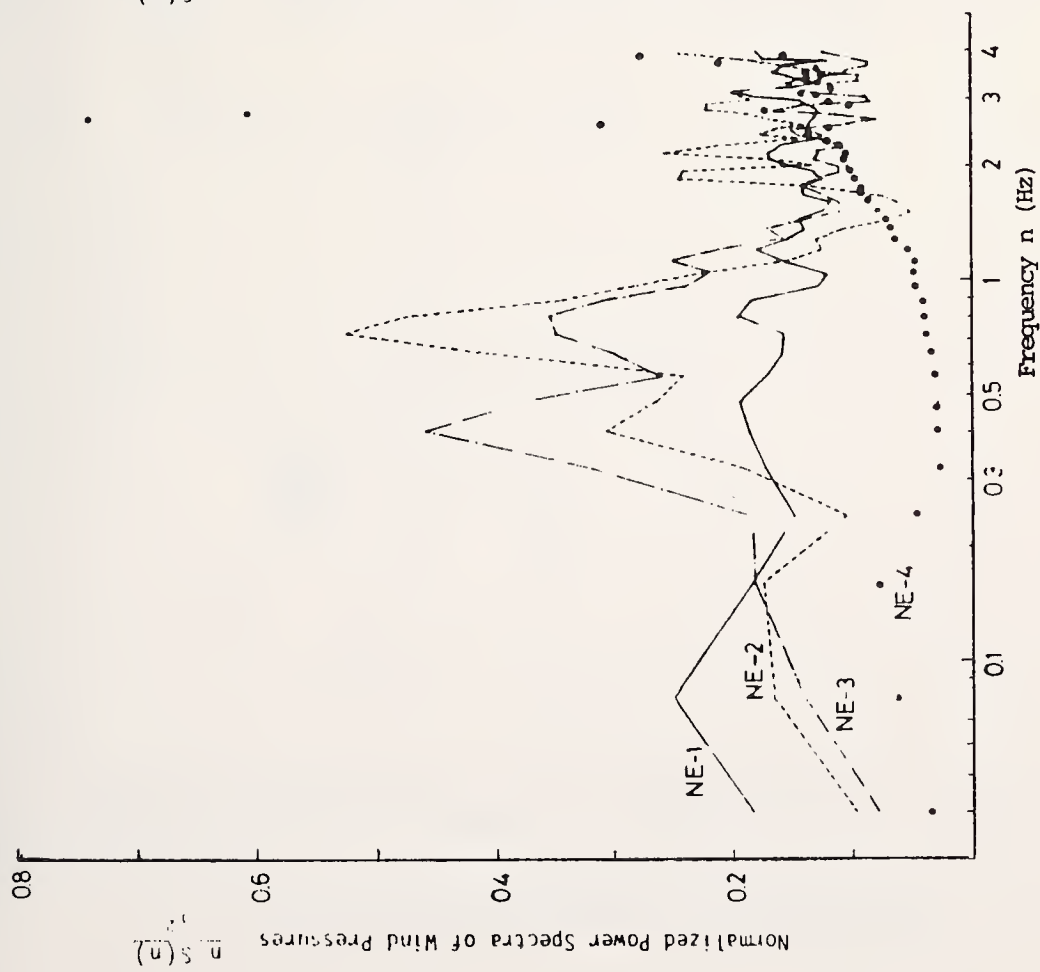


Fig.3 Power spectra of wind pressures.
(Wind dir.:NE-E, Wind speed:11.0m/s)

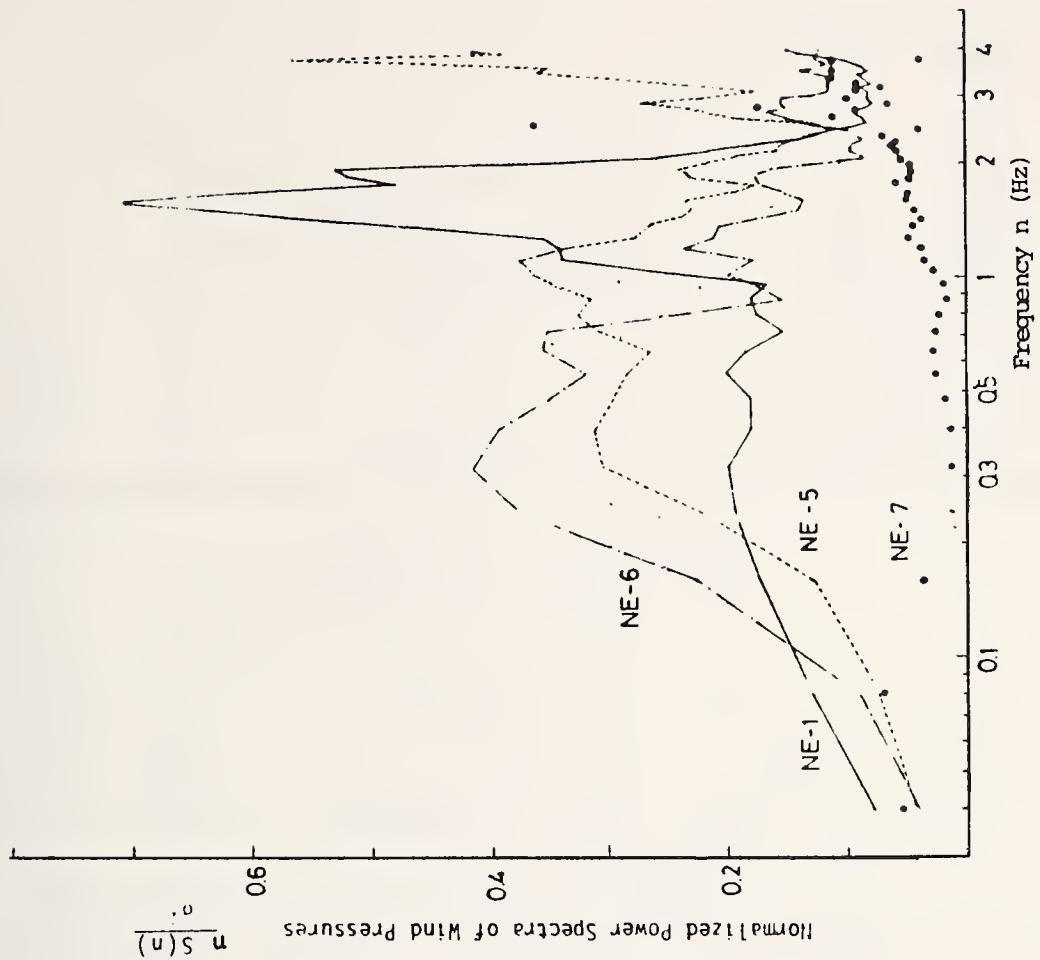


Fig.4 Power spectra of wind pressures.
(Wind dir.:E, Wind speed:10.5m/s)

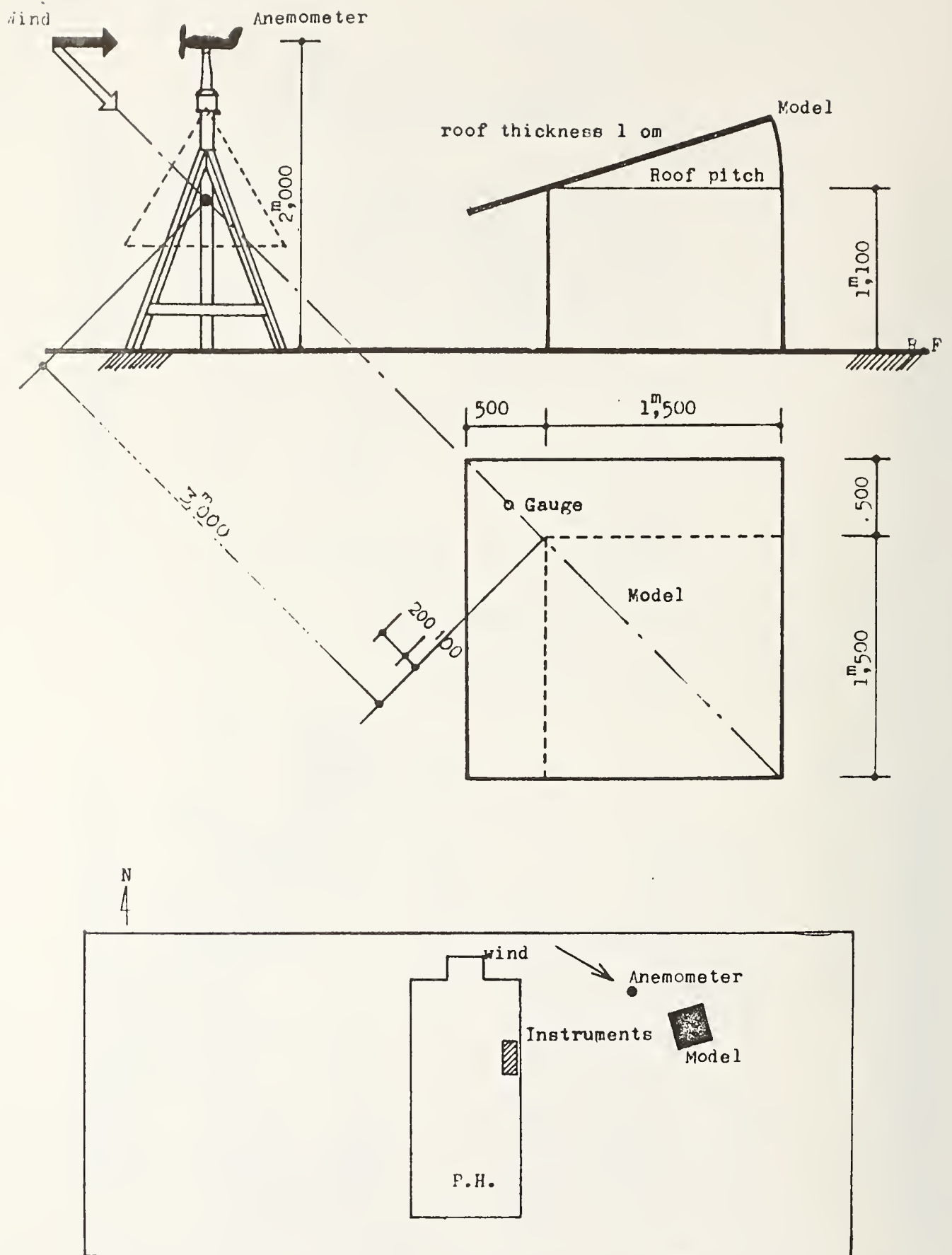


Fig.5 Plan and elevation of the roof-corner model.
Arrangement of the model on a building.

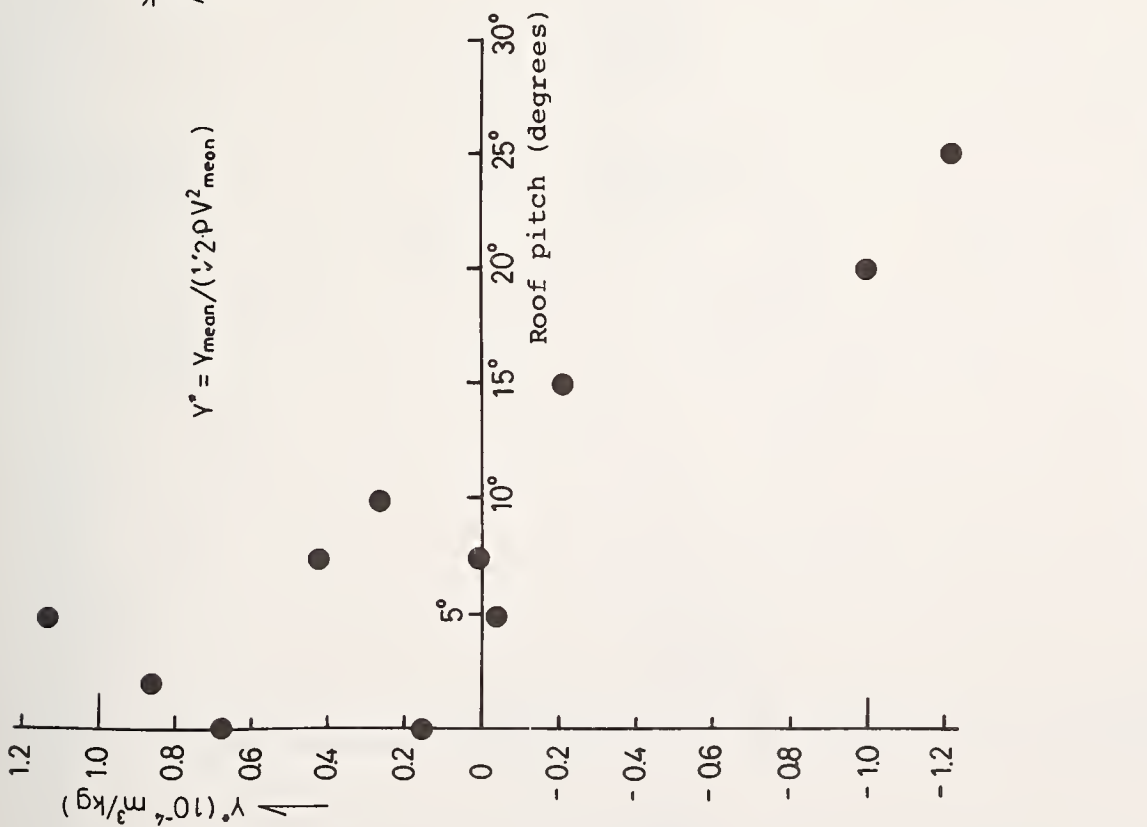


Fig. 6 Mean displacement

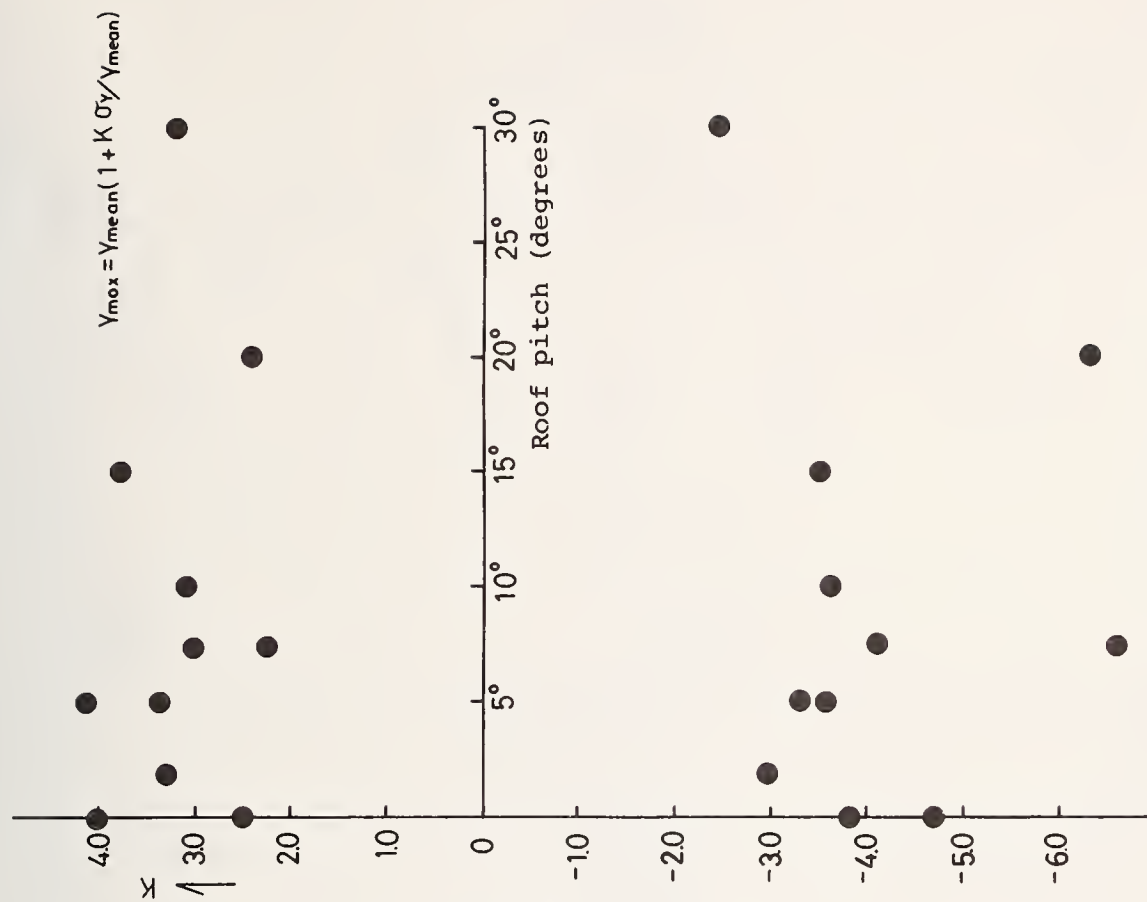


Fig. 7 Maximum deviation

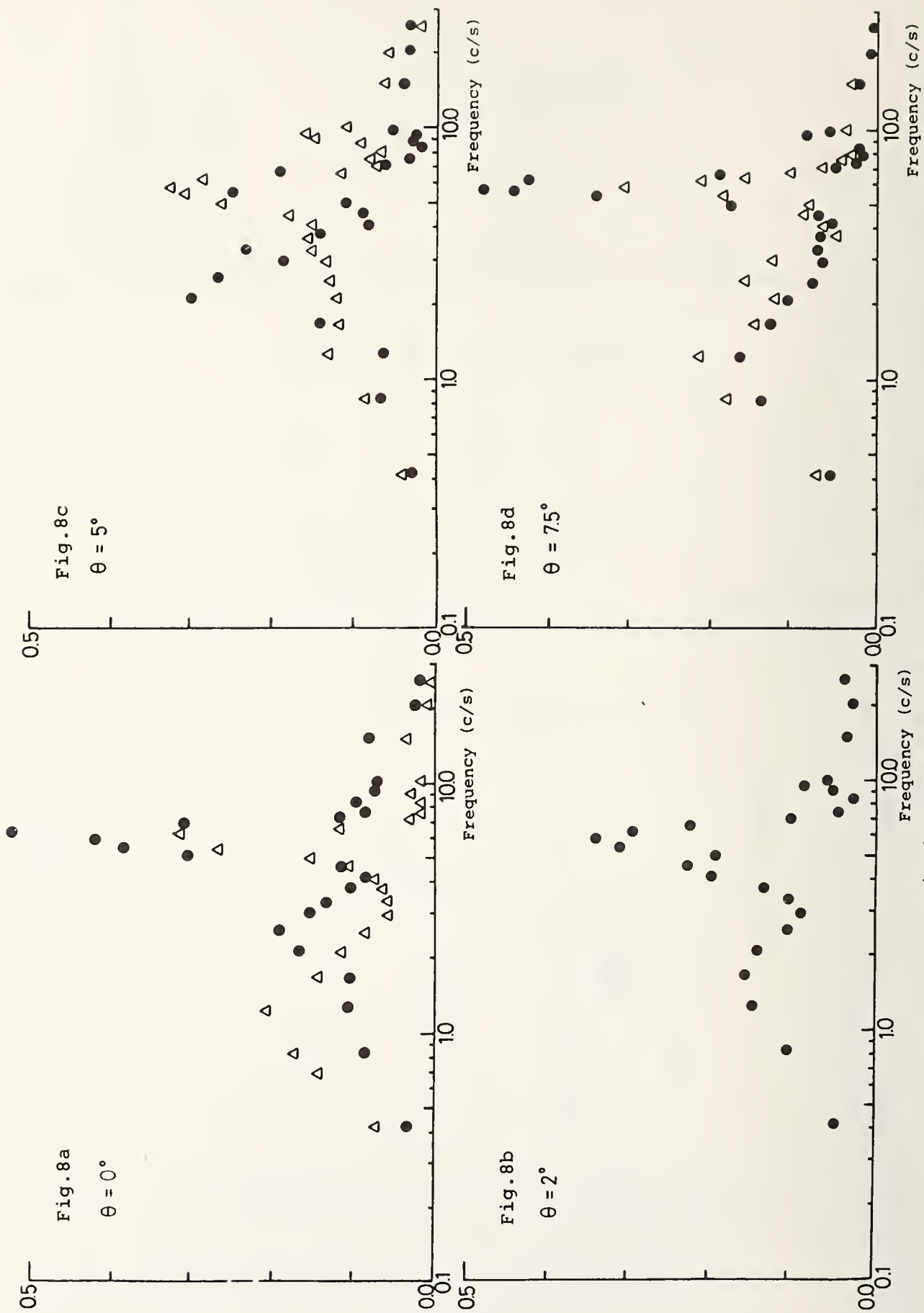


Fig. 8 Power spectra of displacement

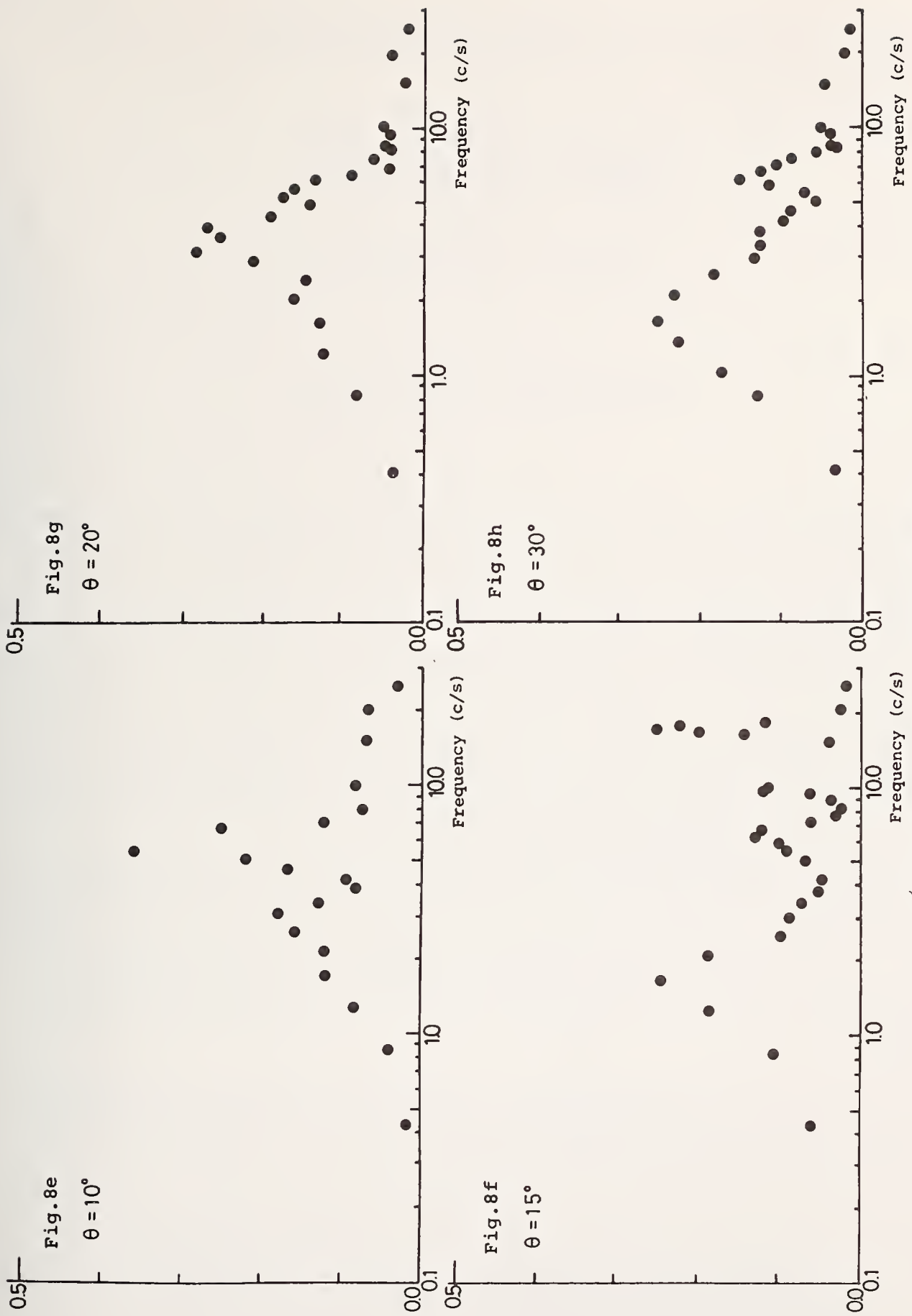


Fig. 8 Power spectra of displacement

ON THE WIND RESPONSE OF THE KANMON BRIDGE

by

T. Okubo
Head, Structure and Bridge Division
Public Works Research Institute
Ministry of Construciton Japan

N. Narita
Chief, Structure Section
Public Works Research Institute

and

K. Yokoyama
Research Engineer, Structure Section
Public Works Research Institute

ABSTRACT

The resistance against wind of a long-span suspension bridges is one of the important design problems because this type of bridge is flexible and sensitive to wind action. The Kanmon Bridge, opened to the public in November 1973, is a typical long-span suspension bridge in Japan. The design of this bridge against wind initiated during the early design phases and its stability against wind was confirmed through wind tunnel experiments on section models. However, confirmation between theory and model tests can only be confirmed by considering field studies and the resulting data. Such studies can reconfirm the bridge safety when the bridge behavior is examined under strong wind conditions. Considering these thoughts, a long-term observation plan system was established on the Kanmon Bridge, with actual observations initiated in April 1974.

In this paper, the research plan for the long-term observation system is reviewed. Then, the characteristics of the approaching wind and the response of the suspended structure are presented. A comparison is then made between observed and theoretical wind gust responses. The results show that the observed response is less than the theoretical response and thus shows the need for accumulation of data which can improve analytical techniques.

Key Words: Bridges; Displacements; field Tests; Winds; Wind Measurements; Wind Speed.

Introduction

Wind effects on a structure are generally classified into two categories, static and dynamic effects. Generally in suspension bridge design only the mean drag component is considered as design wind load. The design wind load is generally of minor importance for short span bridges, but is important in long span bridges, because the cross-sectional area of the principal members in long-span bridges are governed by wind load.

In addition, there is a possibility that suspension bridges or cable-stayed girder bridges will demonstrate aerodynamic instability such as flutter or vortex-excited oscillations as a result of the dynamic effect of the wind. Therefore, design information and girders are required to account for this effect in the design procedure.

Then, during the preliminary design of the Kanmon Bridge, a comprehensive survey was conducted. The basic wind speed (expected wind speed averaged over ten minutes at a height of ten meters above sea level) for determining the design wind speed was selected based on both the expected return wind speed at the construction site and the wind distribution estimated from the wind tunnel experiment on a topographical model. The cross sectional configuration of the suspended structure was selected from section model tests under laminar flow, which showed sufficient stability against the wind.

In addition to the Kanmon Bridge, several other long span bridges such as the Wakato Bridge and the Onomichi Bridge have been constructed in Japan. The construction of these bridges were made possible by the results obtained during the Honshu-Shikoku Bridge Project study.

The first wind resistant design criteria, for the Proposed Honshu-Shikoku Bridge was developed in 1967. The revised slope of this design criteria was initiated in 1972 in conjunction with a field study. An analytical method based on statistical concepts for buffeting the problem of suspension bridges was subsequently adopted.

The design specifications for the Proposed Honshu-Shikoku Bridge (1975) provides for a design wind speed (V_D) and a design wind load (P_D) which are computed by the following equations:

$$\text{for horizontal line-like structure: } V_D = v_1 \cdot v_2 \cdot V_{10}$$

$$\text{for vertical line-like structure: } V_D = v_1 \cdot v_3 \cdot V_{10}$$

$$\text{for horizontal line-like structure: } P_D = 1/2 \rho V_D^2 C_D \cdot A_n \cdot v_4$$

$$\text{for vertical line-like structure: } P_D = 1/2 \rho V_D^2 C_D \cdot A_n \cdot v_5$$

where,

V_{10} : basic wind speed (m/sec)

v_1 : wind speed modification factor for the elevation of the structure

v_2 : wind speed modification factor for horizontal length of the structure

v_3 : wind speed modification factor for vertical length of the structure

ρ : air density ($\text{Kg} \cdot \text{sec}^2 \cdot \text{m}^{-4}$)

C_D : drag coefficient

A_n : exposed area for unit length of the structure (m^2/m)

V_4 : wind load modification factor for horizontal length of the structure

V_5 : wind load modification factor for vertical length of the structure.

The fundamental concept used in this design criteria is to determine the wind speed modification factors and the wind load modification factors such that the magnitude of the lateral bending moment of the stiffening trusses caused by the natural wind is equal to that induced by a uniform wind. Thus analytical method is based primarily on the statistical concepts proposed by A.G. Davenport in 1962. However only a few suspension bridges have shown lateral vibrations during stormy winds, thus this infrequency has been introduced in the analytical process. In order to further substantiate these assumptions field observations on full scale structures and wind tunnel tests on section models, have been conducted. A long-term observation system was then installed on the Kanmon Bridge, in order to collect useful data and thus confirm the design adequacy of the bridge and enhance the design philosophy of the proposed Honshu-Shikoku Bridges.

The Kanmon Bridge and its Aerodynamic Characteristics

The Kanmon Bridge, which was constructed over the Kanmon Straits and forms the Kanmon Highway connects Shimonoseki City in Honshu and the Moji District of Kitakyushu City. This is the largest suspension bridge in Japan, and has a center span length of 712 meters with equal side spans of 178 meters in length. The suspended structure carries six traffic lanes and consists of stiffened trusses, nine meters deep spaced at 29 meters. The clear height is 61 meters above sea level at the center span. The cross-sectional shape of the stiffening girder was selected through wind tunnel tests. The elevation of the upper chord of the stiffening truss is nearly equal to that of the road surface, with three lanes at the edge and central part of the road deck, constructed of open grid. These constitute a positive characteristic of the bridge relative to wind stability.

The location, general view and fundamental dimension of the bridge are shown in Figs. 1 and 2 and Table 1.

The wind speed survey and the wind tunnel model tests, were conducted in relation to the wind resistant design. In the former, the vertical profile of the mean wind speed, and the vertical inclination of wind were investigated. Also studied in detail was the relationship between the wind direction and the wind convergence as the topographical conditions of the construction site was modified. As a consequence of this study, the wind distribution was determined and the basic wind speed was fixed at 35.5 m/sec, which then gave a design wind speed as 53.5 m/sec for the stiffening girder. In the latter, the mean wind force and wind stability of the suspended structure were then examined. Two types of stiffening girder were proposed for the suspended structure namely, the box-stiffened girder and the truss-stiffened girder. After prudent comparison of the wind stability for both systems, the truss-stiffened suspended structure was adopted. The wind stability, of the final design structure, is given in Fig. 3 and indicates the relationship between the angle of

attack and the critical wind speed for the torsional flutter. The occurrence of the restricted oscillation was anticipated by the wind tunnel test on a main tower model under construction, and the oscillation was suppressed by a special energy absorption device. The design wind load for a suspended structure and the main tower was determined in accordance with wind tunnel test results.

After completion of the actual bridge structure a field vibration test was conducted by use of twin exciters and heavy trucks. The natural frequencies and the damping characteristics obtained from the test are given in Table 2. The observed frequencies are about four percent less than those calculated, which suggests that the critical wind speed should be decreased by the same percent. Though the observed damping capacity was smaller than that expected, it does not appear necessary to modify the critical wind speed by the magnitude, because the observed amplitude of the oscillation was small compared to the expected value.

Long-term Observation System

An instrumentation and data-recording system, designed to monitor and record wind speed and direction as well as earthquake tremor and to indicate their effect on the structure, has been provided by the Japan Highway Corporation. The location of these instruments are shown in Fig. 4 and Table 3. The characteristic features of the system are (i) a large number of instruments are provided, (ii) the system is immediately available to record and monitor, and (iii) a digital signal is used in the transmission, in order to increase the accuracy.

(1) Transducers

(a) Propeller type anemometer: Four anemometers were positioned on the top of poles located on the bridge deck, and used for observing the horizontal distribution of the wind. One anemometer was installed at the top of the main tower and used as reference.

(b) Sonic anemometer: One set of three-component sonic anemometers was located at the mid-point of the main span and used for observing the wind inclination angle.

(c) Servo-type accelerometer: Servo-type accelerometers of high fidelity were positioned at the mid and quarter points of the center span. One element measured the horizontal component and the other two elements the vertical component, at each point.

(d) Displacementmeter: Using an optical device, both horizontal and vertical motions of the stiffening structure were detected.

(e) Others: Transducers used for earthquake detection were placed on the structure, but are not described herein.

(2) Data transmission system

The output data are digitized by Analog-to-Digital convertors near the transducers and are transmitted 1.5 kilo-meters to the data processing system located in the administration office.

(3) Data processing system

A data processing system equipped a mini-computer ordinarily performs the monitoring and records the data. When the wind speed exceeds a preset level, the acquisition system automatically starts and the data is stored on magnetic tapes.

Observed Data and Discussion

Wind Characteristics

The observation system was set into operation in April 1974. As strong typhoons have not been in the area thus far, only a few recordings at low wind conditions were obtained. Wind characteristics have been examined in order to compare the real wind distribution with that expected. Fig. 5 indicated a trace of the wind speed and the direction, at four stations. From this information statistical data such as mean wind speed and standard deviation are calculated as shown in Fig. 6 which gives the variation of the wind with time. A set of power spectral density is given in Fig. 7, from which the characteristic features of the approaching wind is:

(1) The turbulence intensity, gust factor and power spectral density of the wind agree well with those obtained previously in the past, with a noticeable effect of wind convergence.

(2) The horizontal distribution of the wind speed was observed on the deck and is almost uniform, with a small deviation of 1 m/sec. The mean wind direction is nearly equal for each station. However, instantaneous wind speeds and directions fluctuate so violently, that cross-correlation of the wind speed rapidly decreases with an increase in the distance between stations. According to the cross-correlation coefficient of wind speed as shown in Fig. 8, the wind speed has a strong correlation with the anemometers set at 20 meters apart, but has a weak correlation for those meters which are 180 meters apart.

(3) According to the topographical model tests, the vertical inclination of the wind at the straits varies with the principal wind direction. For instance, the S-W wind, which comes from Mt. Hinoyama (EL. 268 m), has an angle of inclination of 3 degrees at the Shimonoseki side, with the N-E wind showing a negative angle on that side. The recordings of the sonic anemometers at the east side of the bridge deck showed a positive angle for both the E-SSW wind and the E-NNE wind.

Response of the Stiffening Girder

In order to better understand the behavior of the suspended structure when subjected to wind, a motion picture was made by a computer output microfilming system. This motion picture showed that the bridge vibrated randomly in vertical bending, torsional, and lateral bending modes with the vertical bending mode being dominant. Fig. 9(1) through Fig. 9(5) shows the power spectral density of the acceleration for each mode, and Fig. 9(6) and Fig. 9(7) displacement mode. In Fig. 9(1) and Fig. 9(2) the natural frequencies are indicated, which were obtained by forced vibration test. These frequencies coincide with the peak frequencies of the power spectral density curve. However, the peak frequencies of the lateral bending vibrations are smaller than the calculated frequencies using the Ellis' method. It was determined, from the acceleration record, that the response vibra-

tion of the suspended structure is random in character and the lowest mode of either symmetry or antisymmetry is dominant. According to the power spectral density of the displacement the contribution of the higher mode of vibration is smaller than the lower mode of vibration. It may be said that the vibration with the lowest mode is important not only for the flutter phenomena but for the gust response problem.

Wind Speed and Structural Response

In Fig. 10 and Fig. 11 the original trace of the wind speed and the structural response is given. The structure starts to vibrate at a wind threshold level during the combined vertical and lateral bending mode and is random rather than sinusoidal. The magnitude of the vibration seems to depend on the wind speed level rather than on the wind turbulence level, and with an increase in the wind speed the lowest mode of the vibration becomes dominant.

Fig. 11(1) shows experimental and analytical mean and the standard deviation of the lateral displacement at midpoint of the center span in relation to the transverse component of the mean wind. The analytical method that was used is the same as reported at the last Joint Meeting. According to Fig. 11, the observed values coincide qualitatively with the theoretical value but the observed magnitudes are smaller in comparison to the theoretical values. This indicates the necessity to reexamine the wind characteristics (spatial distribution, power spectral density of wind), structural characteristics (natural frequency, damping capacity) and the aerodynamic response characteristics (aerodynamic admittance, aerodynamic damping).

Concluding Remarks

The main part of this work has been concerned with the examination of data collected by a long-term observation system, in which only a few samples of data have been obtained. The primary analysis of this minimum data indicates the following;

(1) The observed wind characteristics (power spectral density of wind speed, turbulent intensity, and gust factor) are similar to those observed previously. The horizontal distribution of the wind speed and the direction is nearly uniform, however, the wind convergence at the straits has not been confirmed. The wind inclination data shows that reverse characteristics in comparison with wind tunnel experiments, thus indicating a detailed survey is necessary.

(2) During the field studies no information of the flutter problem was obtained. However, some response characteristics of the suspended structure, against natural wind, were obtained. It was found that the structure vibrates randomly and that the higher mode components as well as lower mode ones are included in the power spectral density of acceleration but the lowest mode is dominant in displacement.

(3) The observed vibrational displacement shows the same tendency when compared to the calculated values based on Davenport's method, but does not agree quantitatively.

Acknowledgment

The authors are indebted to Mr. M. Hurumichi of Japan Highway Corporation who assisted during the field work. The authors also wish to thank Mr. M. Katsuragi and Mr. K. Nomura of the Structure Section P.W.R.I. for use of the computer program.

References

1. Meteorological Agency, Ministry of Construction: Investigation into the Second Kanmon Road, March 1967
2. Soma, S.: Wind Tunnel Test of Air-stream at Kanmon Straits, November, 1967
3. P.W.R.I.: An Investigation for Design and Construction of the Kanmon Bridge, March 1973, P.W.R.I. Tech. Note
4. P.W.R.I.: Report of Vibration Test on the Kanmon Bridge, March, 1974, P.W.R.I. Tech. Note.
5. Narita, N. and Yokoyama, K.: On the Gust Response of Long-span Suspension Bridge (Progress Report), May, 1974, Sixth Joint Meeting, UJNR, Washington, D.C.

Table-1 Dimension

Item	Unit	Center span	Side span
Span length	m	712.0	178.0
Effective span length	m	703.5	167.75
Sag	m	64.0	3.906
Height of truss	m	9.0	
Distance of main truss	m	29.0	
Panel length of stiffening girder	m	10.35	
Panel length of lateral member	m	20.7	
Dead load (whole structure)	t/m/br.	24.172	25.946
" (cable)	t/m/br.	4.378	
Cross sectional area (cable)	m ² /br.	0.559	
" (chord member)	m ²	0.0380	0.0320
" (diagonal member)	m ²	0.0185	
" (lateral member)	m ²	0.0232	
Young's modulus of cable	t/m ²	2.0x10 ⁷	
Moment of inertia of area of truss	m ⁴	2.916	
Polar moment of inertia (cables included)	t·m·sec ² /m/br.	276.60	

Table-2 Natural frequencies and damping capacity of the Kanmon Bridge

Mode of vibration	Symmetry	Order	Natural frequency (Hz)			Logarithmic decrement (Mean, Standard deviation)
			Theoretical (A)	Observed (B)	(B)/(A)	
Vertical bending	Symmetric	1	0.200	0.212	1.06	0.015 ~ 0.037 (0.031, 0.005)
		2	0.270	0.298	1.10	0.013 ~ 0.028 (0.018, 0.003)
		3	0.429	-	-	—
		4	0.528	0.570	1.08	0.008 ~ 0.011 (0.009, 0.001)
		5	0.914	0.918	1.00	0.007 ~ 0.011 (0.009, 0.001)
	Anti-symmetric	1	0.152	0.180	1.18	0.039 ~ 0.062 (0.050, 0.009)
		2	0.375	-	-	—
		3	0.705	0.740	1.05	0.010 ~ 0.023 (0.013, 0.003)
Torsional	Symmetric	1	0.384	0.387	1.01	0.009 ~ 0.016 (0.013, 0.001)
		2	0.766	0.717	0.94	0.008 ~ 0.019 (0.013, 0.003)
	Anti-symmetric	1	0.492	0.472	0.96	0.013 ~ 0.025 (0.016, 0.003)

Table-3 Instruments for long term observation system at Kanmon Bridge

Observation item	Measuring point	Maximum measuring range	Instruments	Number of instruments	Number of elements		Rate of sampling (freq./sec)
					per M.P.	Total	
Acceleration	Ground	±500 gal	Submerged accelerometer	3	3	9	100
	Abutment	±500	Electro-magnetic accelerometer	4	1	4	50
	Pier	±500		8	1	8	
	Tower	±500		4	1	4	
	Stiffening frame	±200	Servo-accelerometer	6	1	6	25
Displacement	Stiffening frame	Horizontal ±2 m Vertical ±2 m	XY-Analyser	1	3	3	25
		Longitudinal ±25 cm	Differential transducer	1	1	1	25
Wind speed	Stiffening frame	Horizontal 60 m/sec Vertical ±10 m/sec	Supersonic anemometer	1	3	3	25
Wind direction		Horizontal 60 m/sec 540°	Propellar type anemomer	3	2	6	25
Wind speed		Horizontal 60 m/sec		1	2	2	25
Wind direction	Top of Shimono-seki tower	540°					

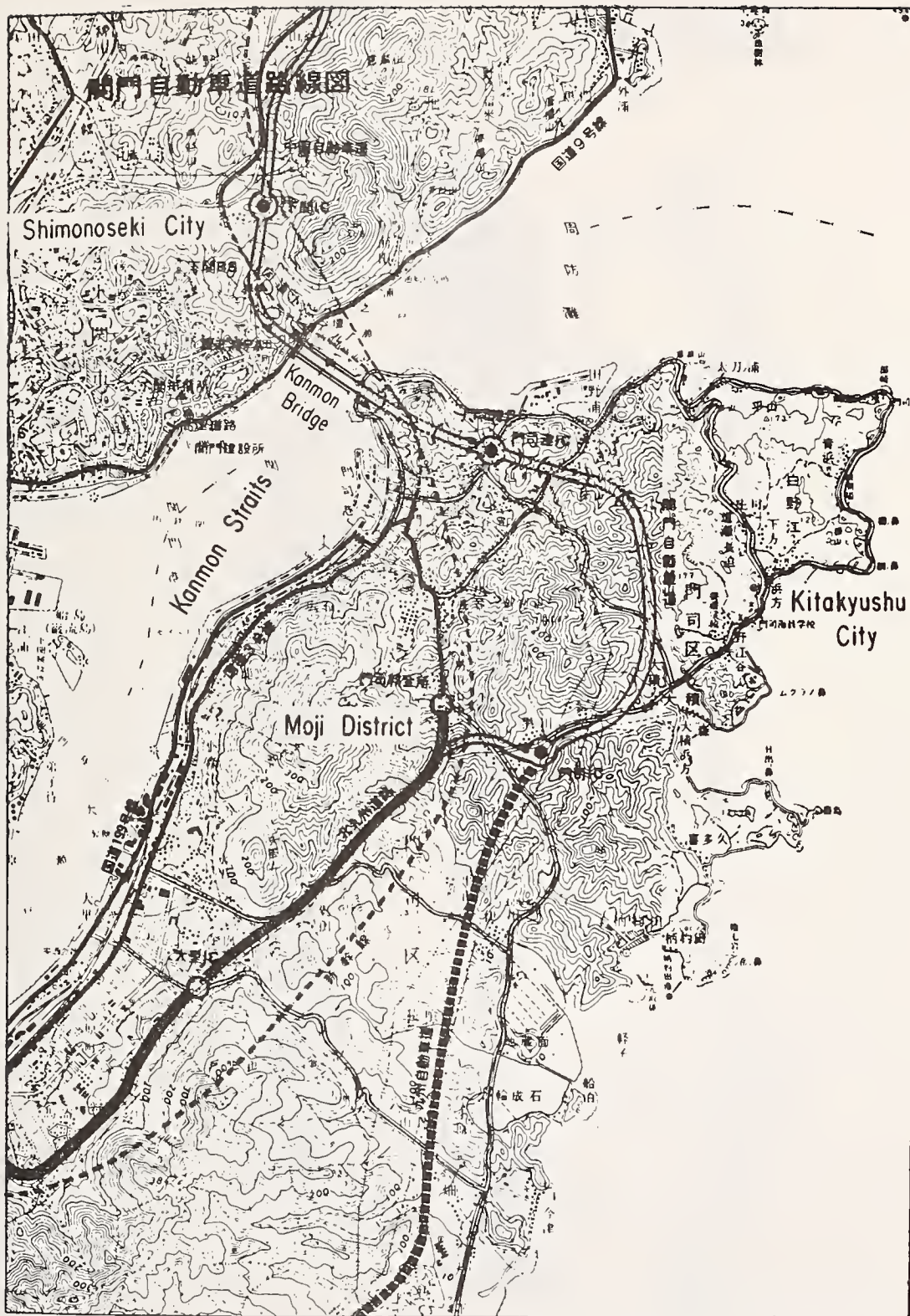


Fig.-1 Map of the Kanmon Straits



Fig.-2 General view of the Kanmon Bridge

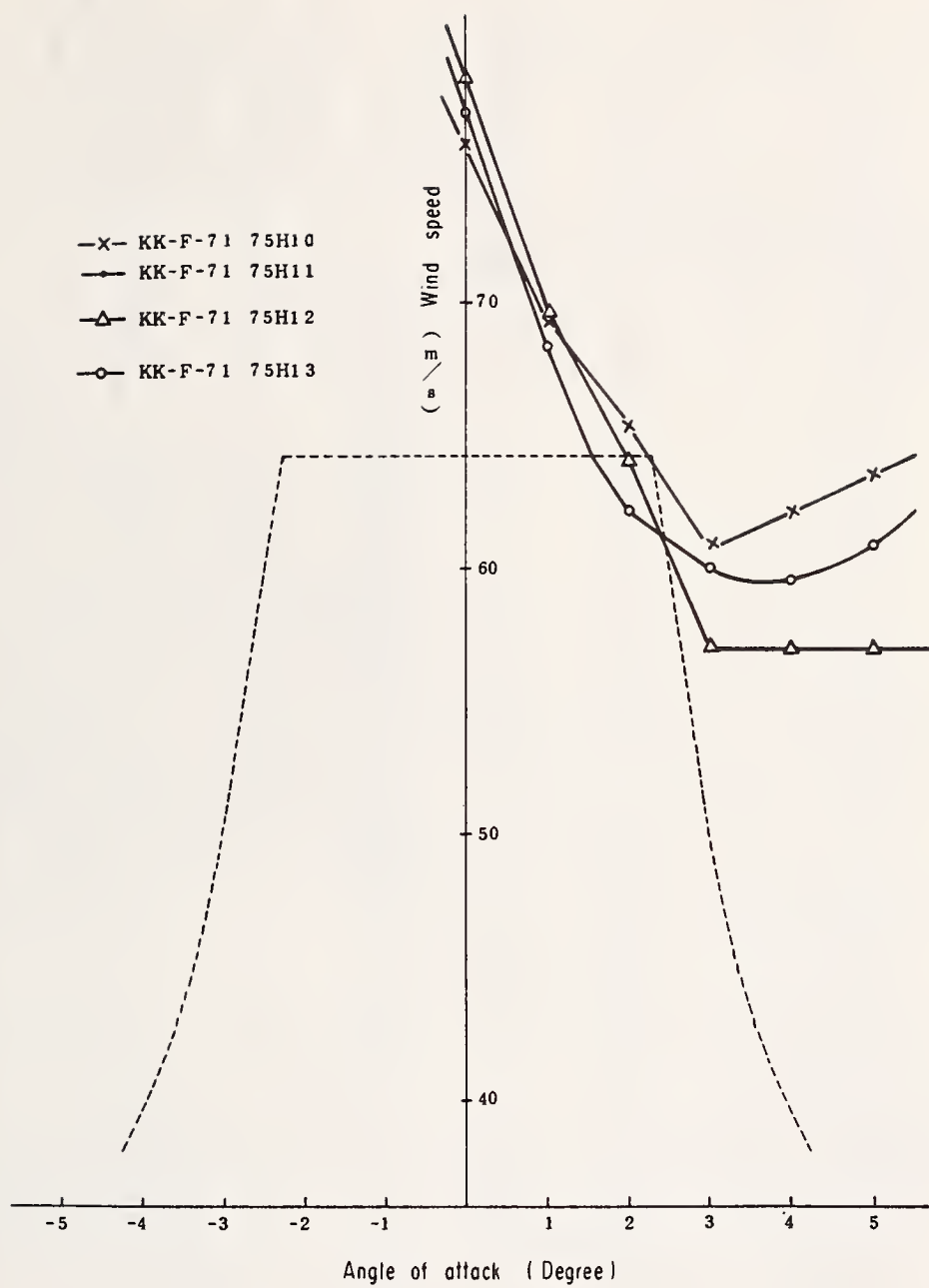


Fig.-3 The aerodynamic characteristics of the Kanmon Bridge

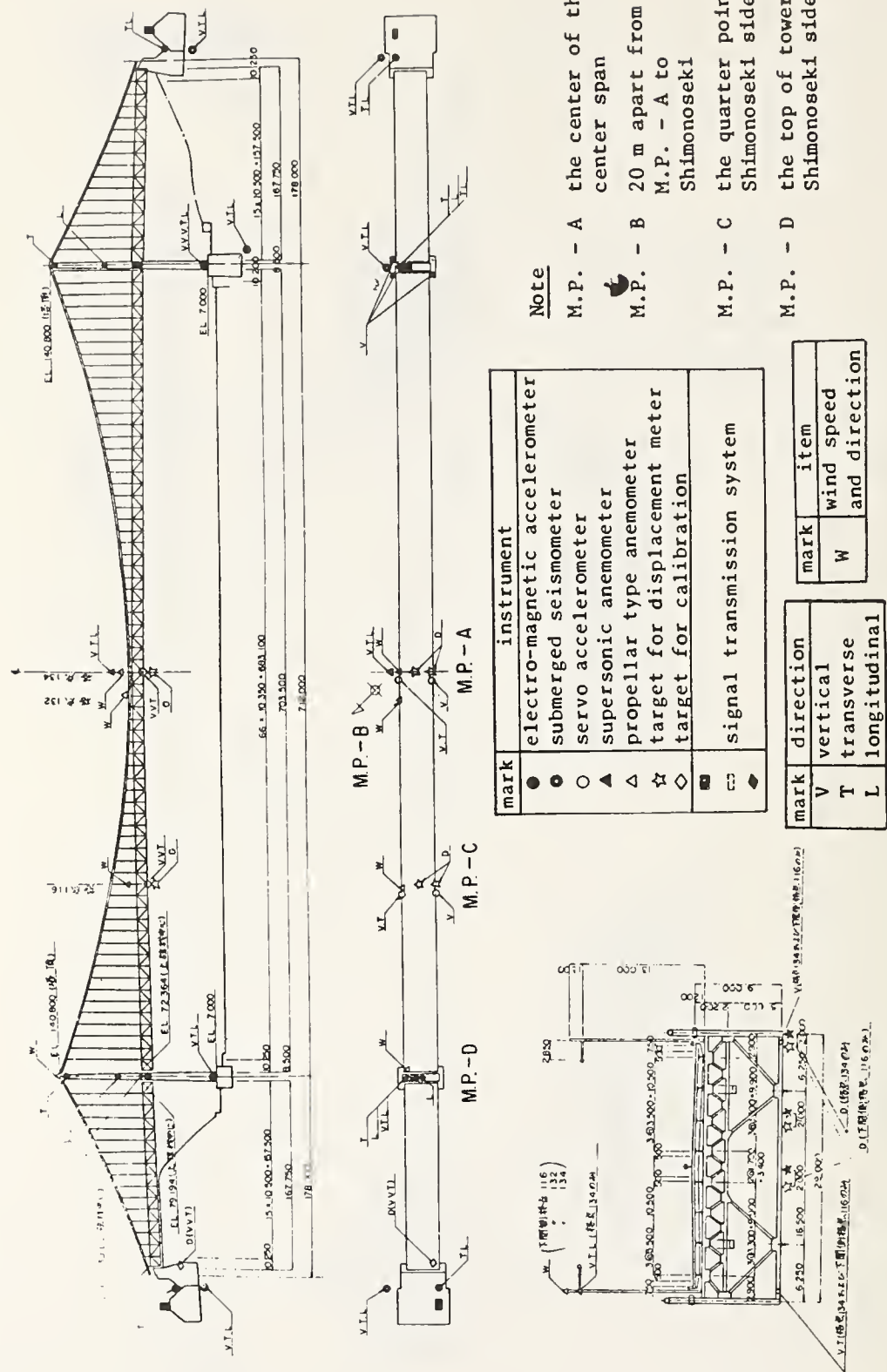


Fig.-4 Long term observation system of the Kammon Bridge

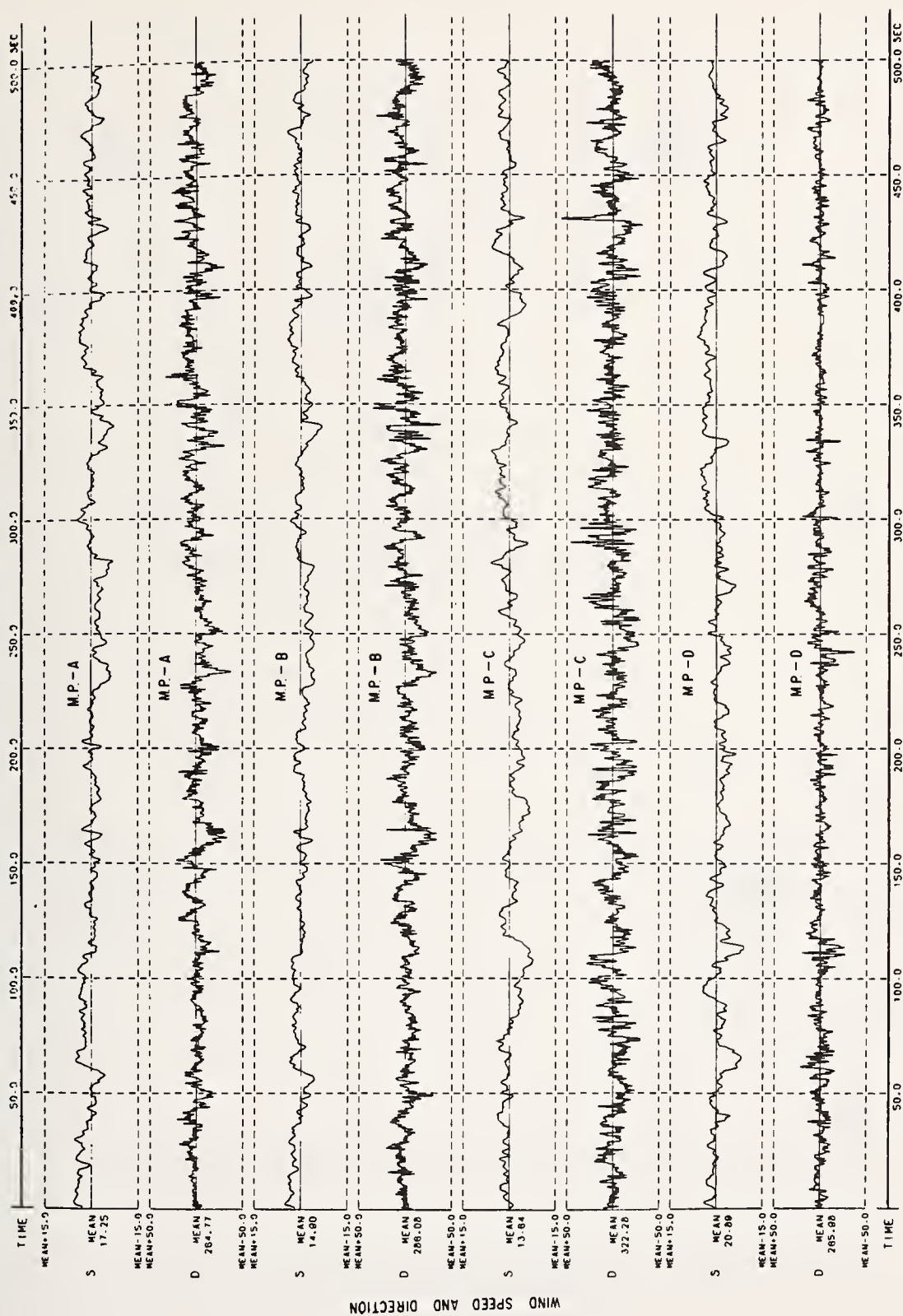


Fig.-5 Record of wind (8:50:00 18 Nov. 1974)

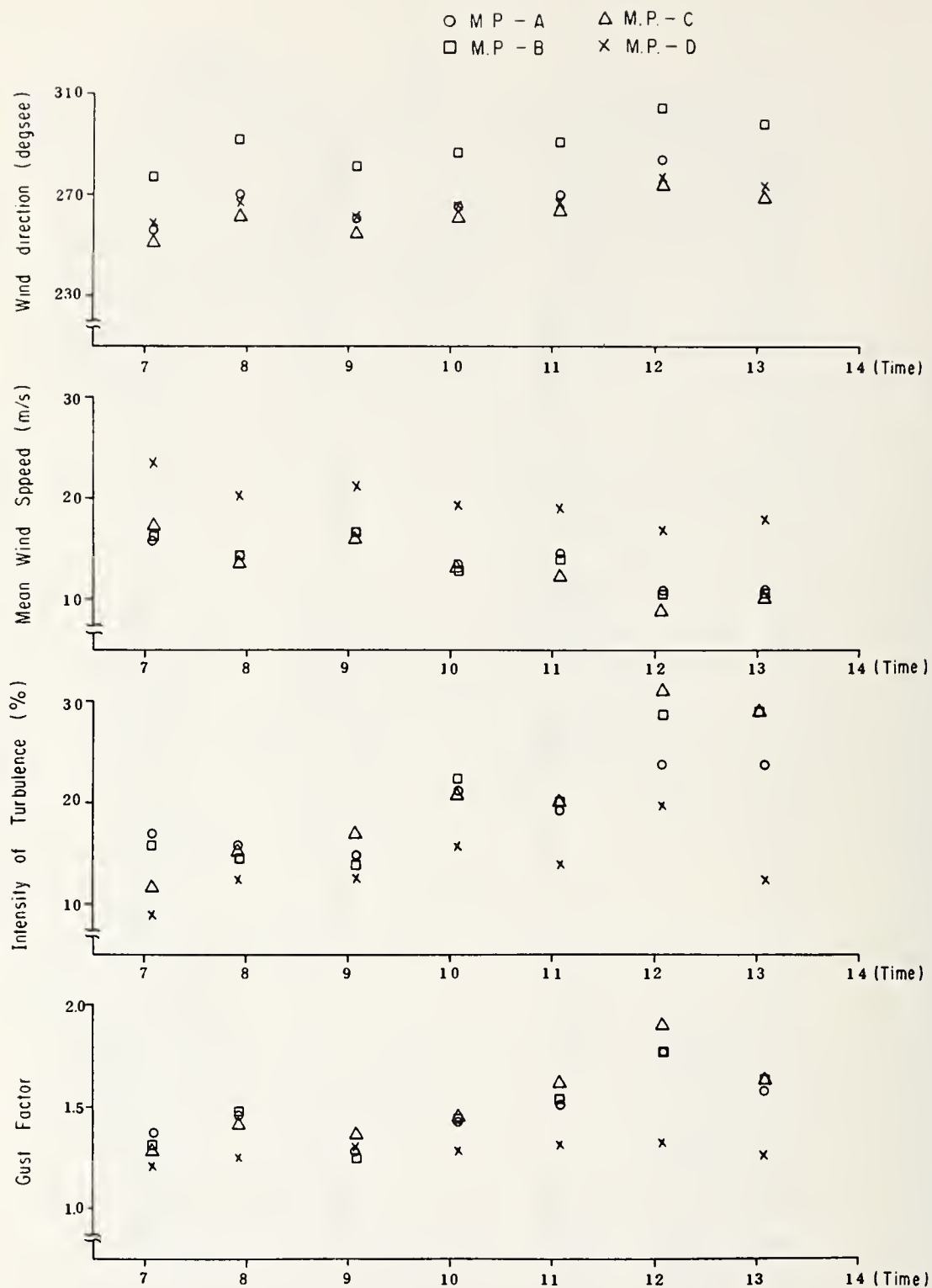


Fig.-6 The variation of wind characteristics with time (18 Nov. 1974)

POWER SPECTRUM OF WIND
1974.11.18
8:50:00
DT=200MS
N=2500
CH 23

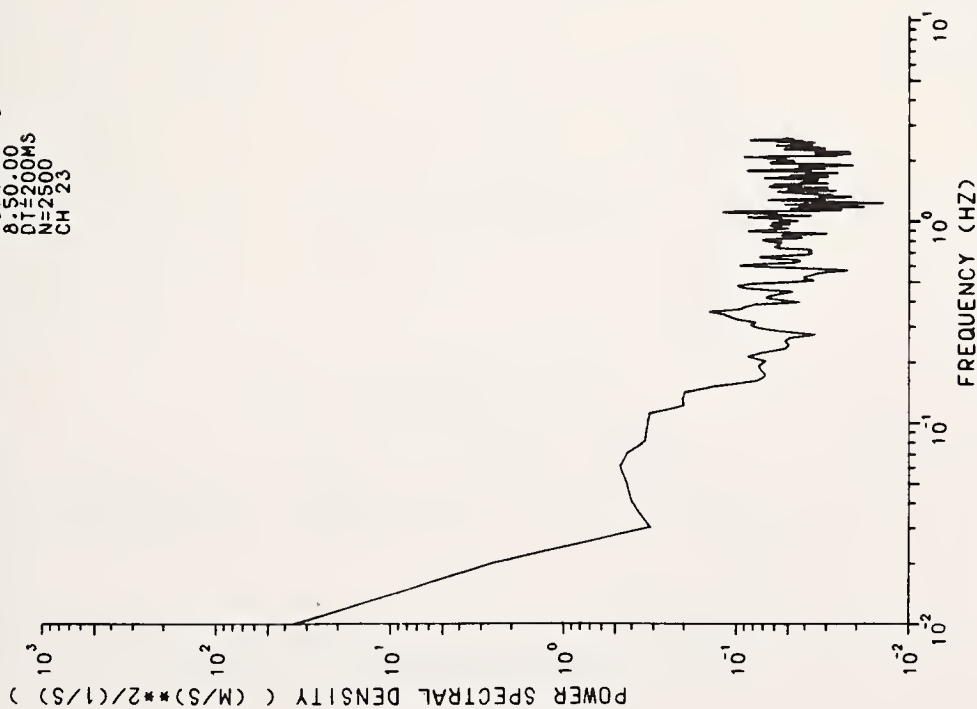


Fig.-7 (2) Power spectrum of Wind
(M.P.-A, Vertical)

POWER SPECTRUM OF WIND
1974.11.18
8:50:00
DT=200MS
N=2500
CH 15

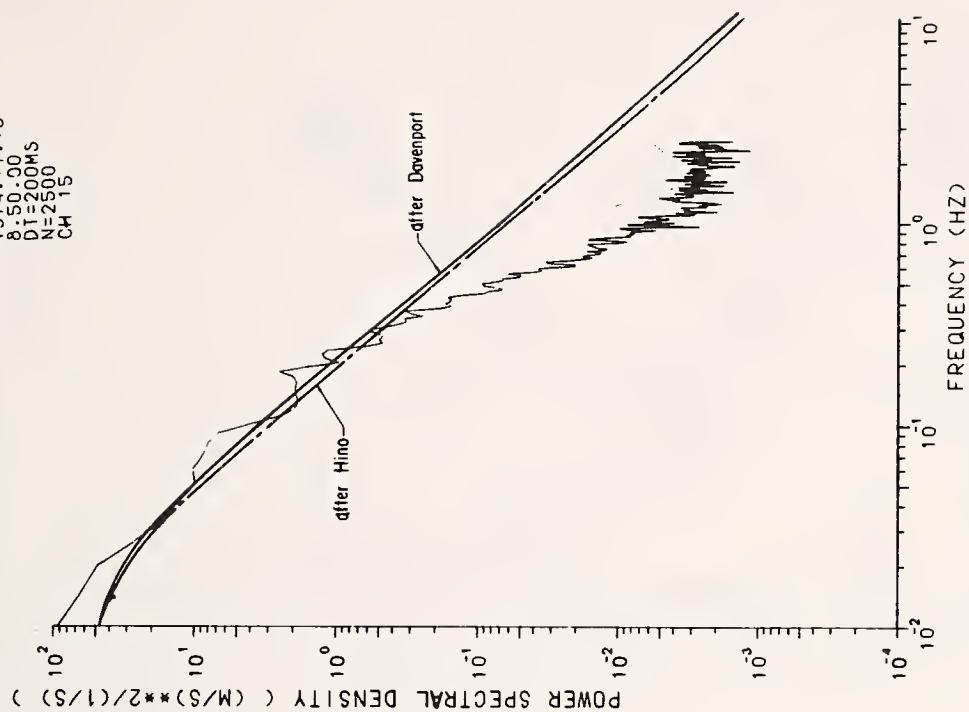


Fig.-7 (1) Power spectrum of Wind (M.P.-A)

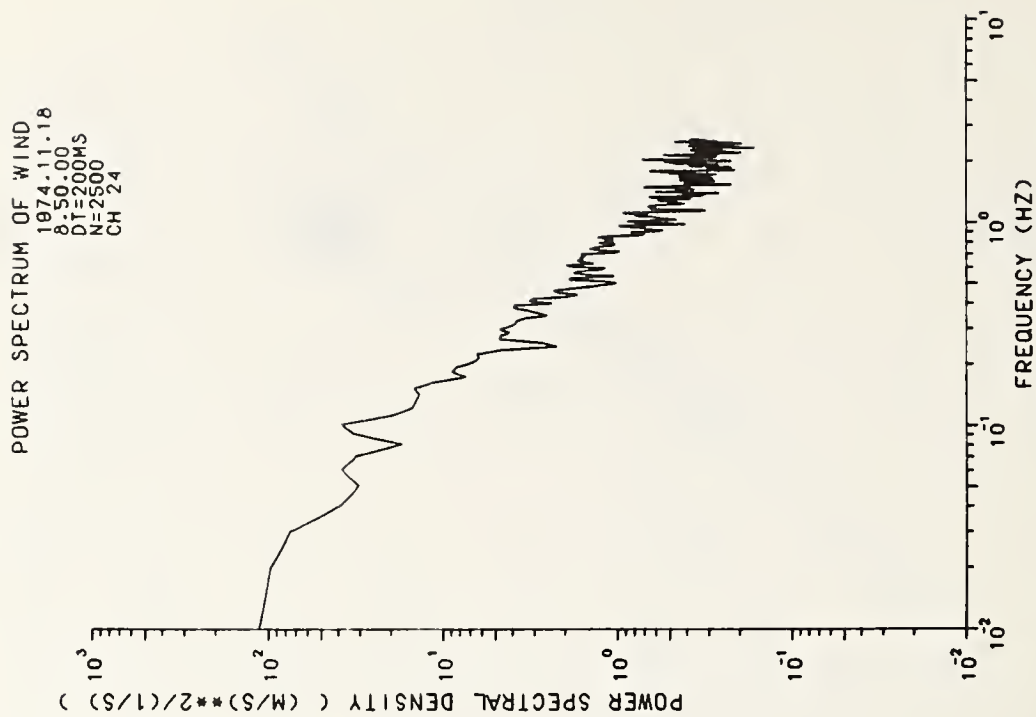


Fig.-7(3) Power spectrum of Wind
(M.P.-A, Horizontal)

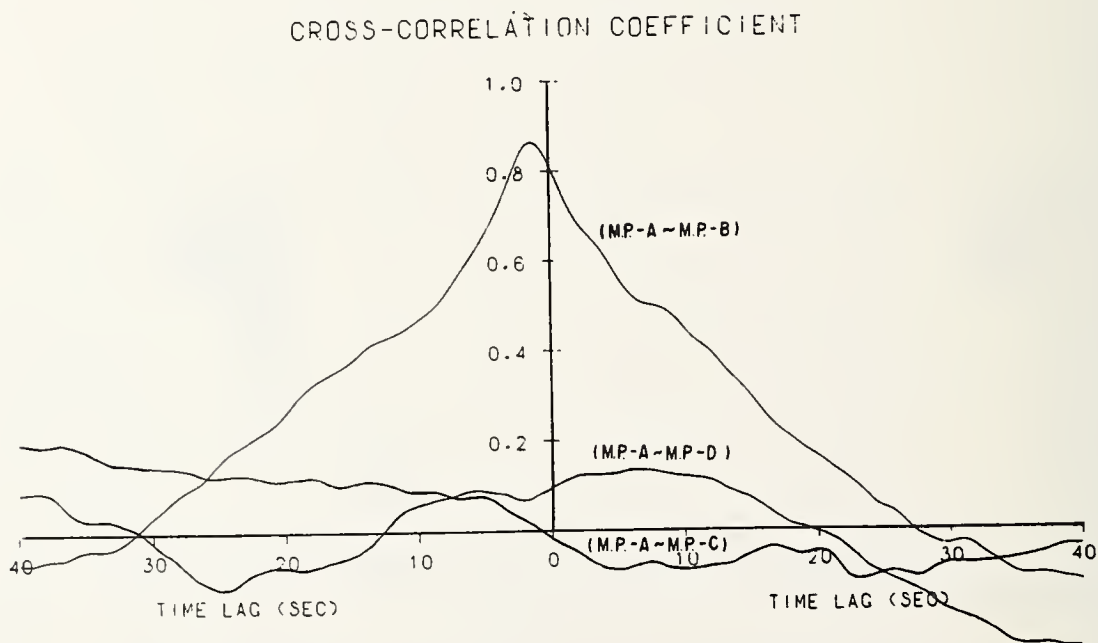


Fig.-8 Cross-correlation coefficient

P.S.D
($\frac{\text{rad}}{\text{sec}^2}$)²
 $\times 10^{-7}$

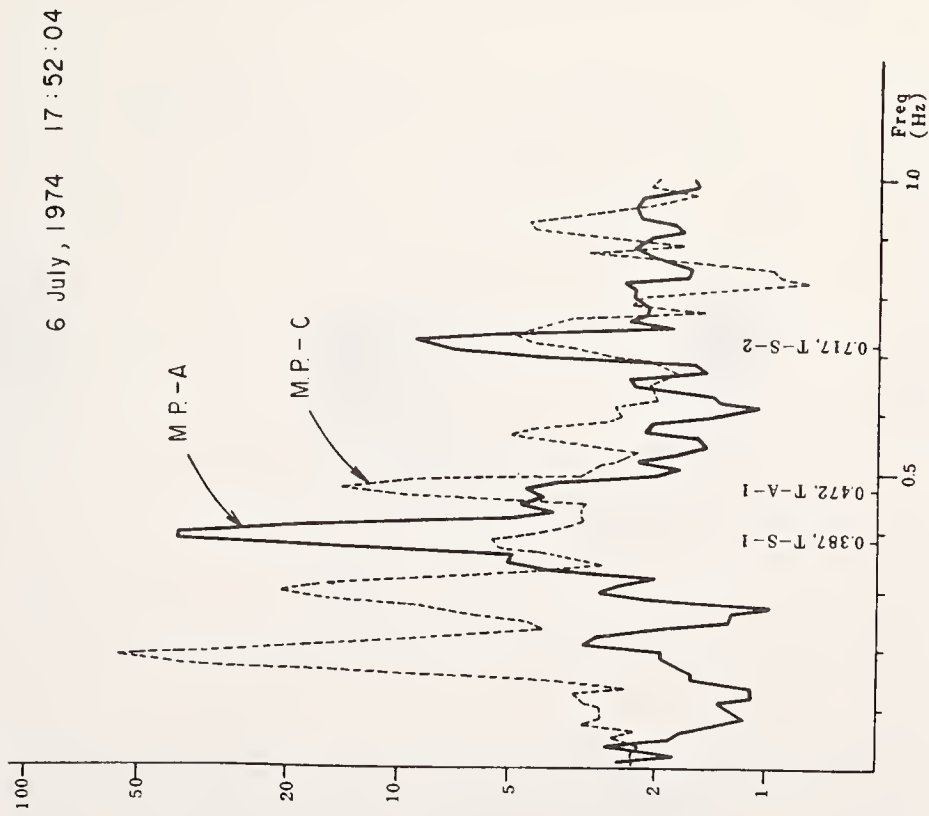


Fig.-9(2) Power spectrum of Response
(Torsional Vibration)

P.S.D
($\frac{\text{rad}}{\text{sec}^2}$)²
 $\times 10^{-7}$

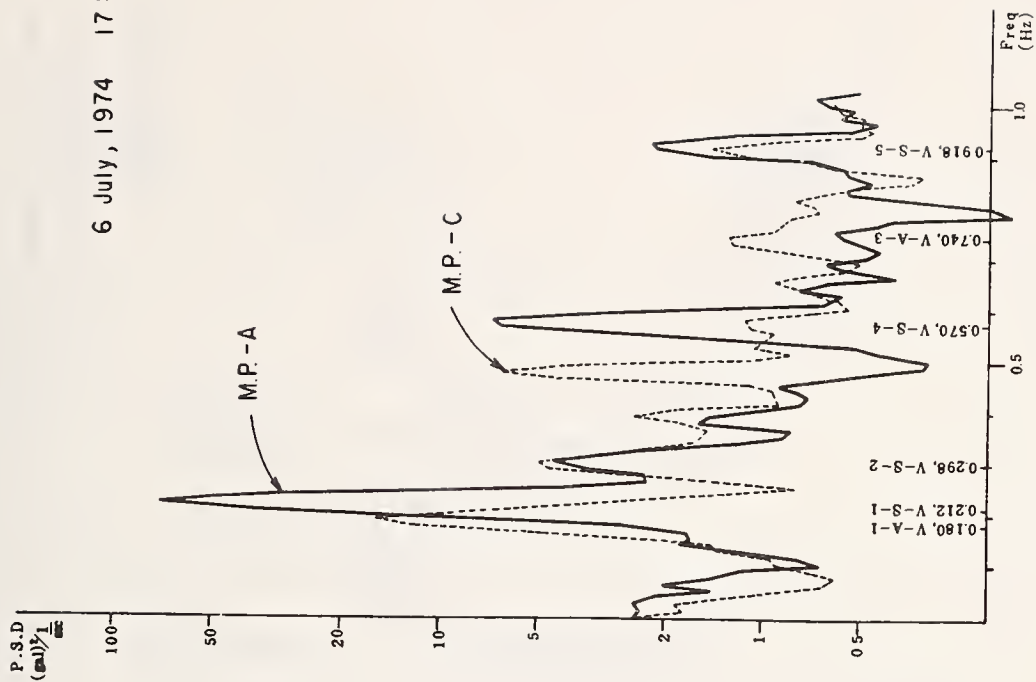


Fig.-9(1) Power spectrum of Response
(Vertical bending Vibration)

6 July, 1974 17:52:04

6 July, 1974 17:52:04

POWER SPECTRUM OF RESPONSE

1974.11.18
8:50.00
DT=200MS
N=2500
CH 9

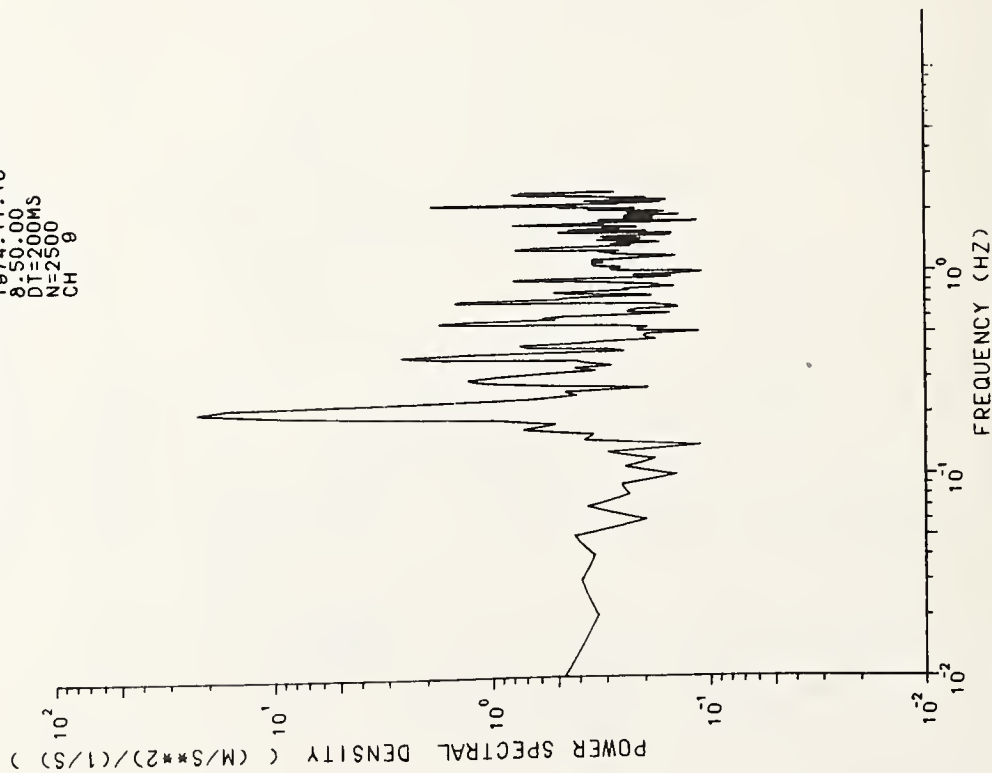


Fig.-9(4) Power spectrum of Response
(M.P.-A, Vertical)

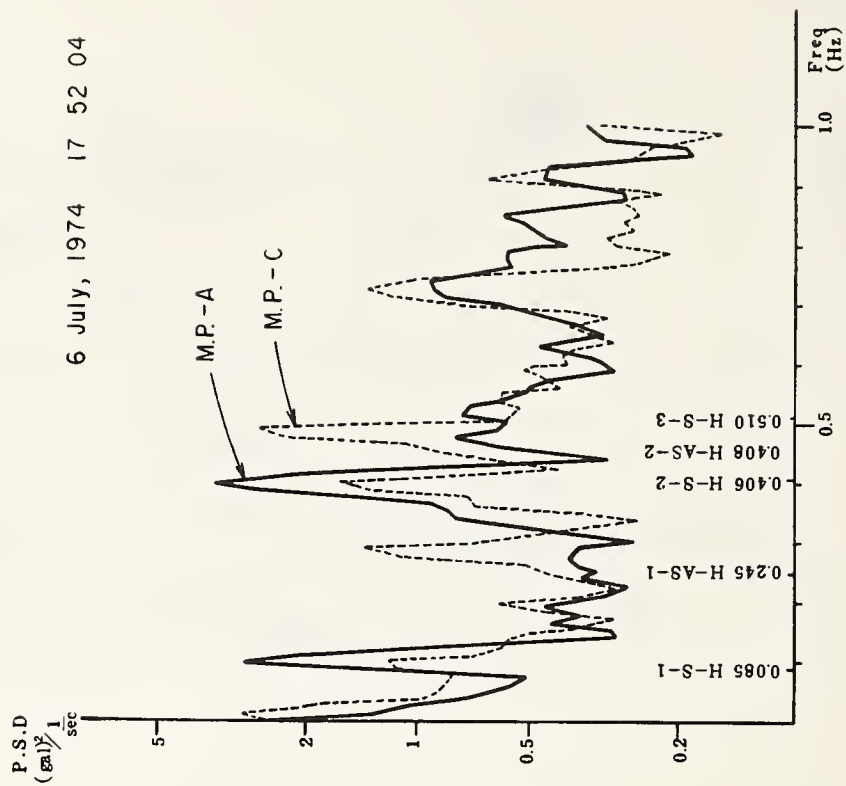


Fig.-9(3) Power spectrum of Response
(Horizontal bending Vibration)

POWER SPECTRUM OF RESPONSE
1974.11.18
8.50.00
DT=200MS
N=2500
CH 26

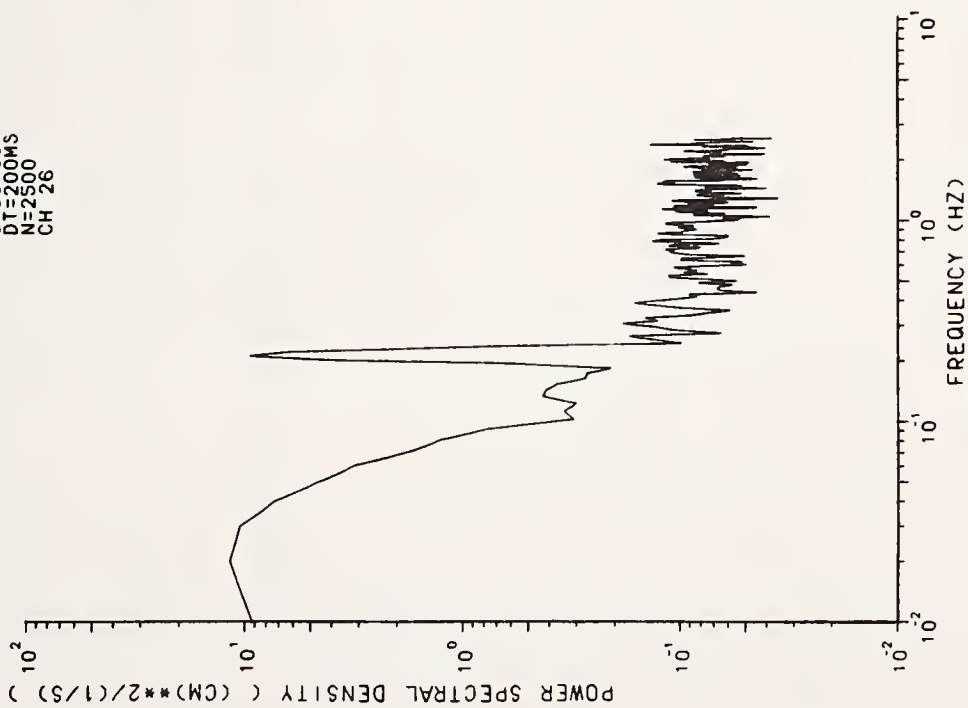


Fig.-9(6) Power spectrum of Response
(M.P.-A, Vertical)

POWER SPECTRUM OF RESPONSE
1974.11.18
8.50.00
DT=200MS
N=2500
CH 11

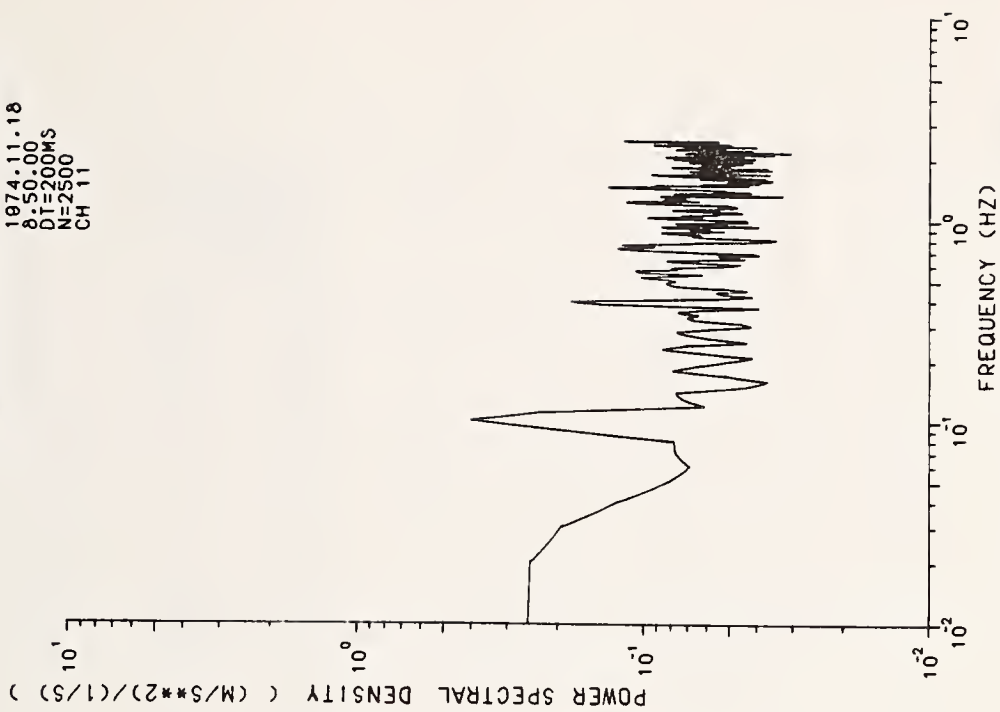


Fig.-9(5) Power spectrum of Response
(M.P.-A, Horizontal)

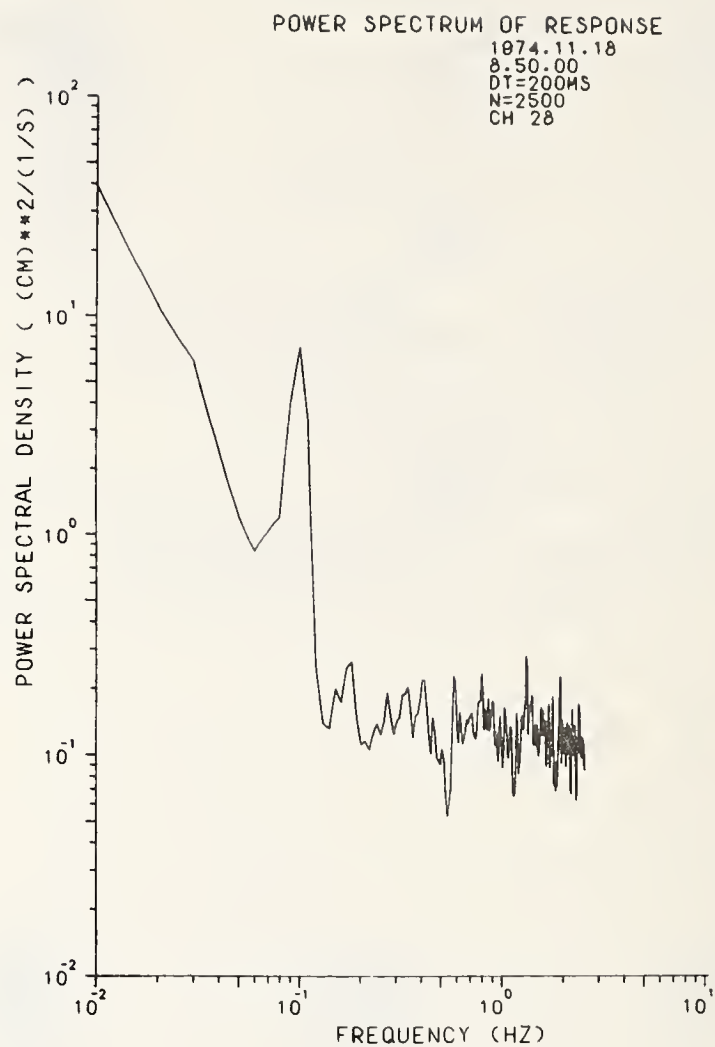


Fig.-9(7) Power spectrum of Response
(M.P.-A. Horizontal)

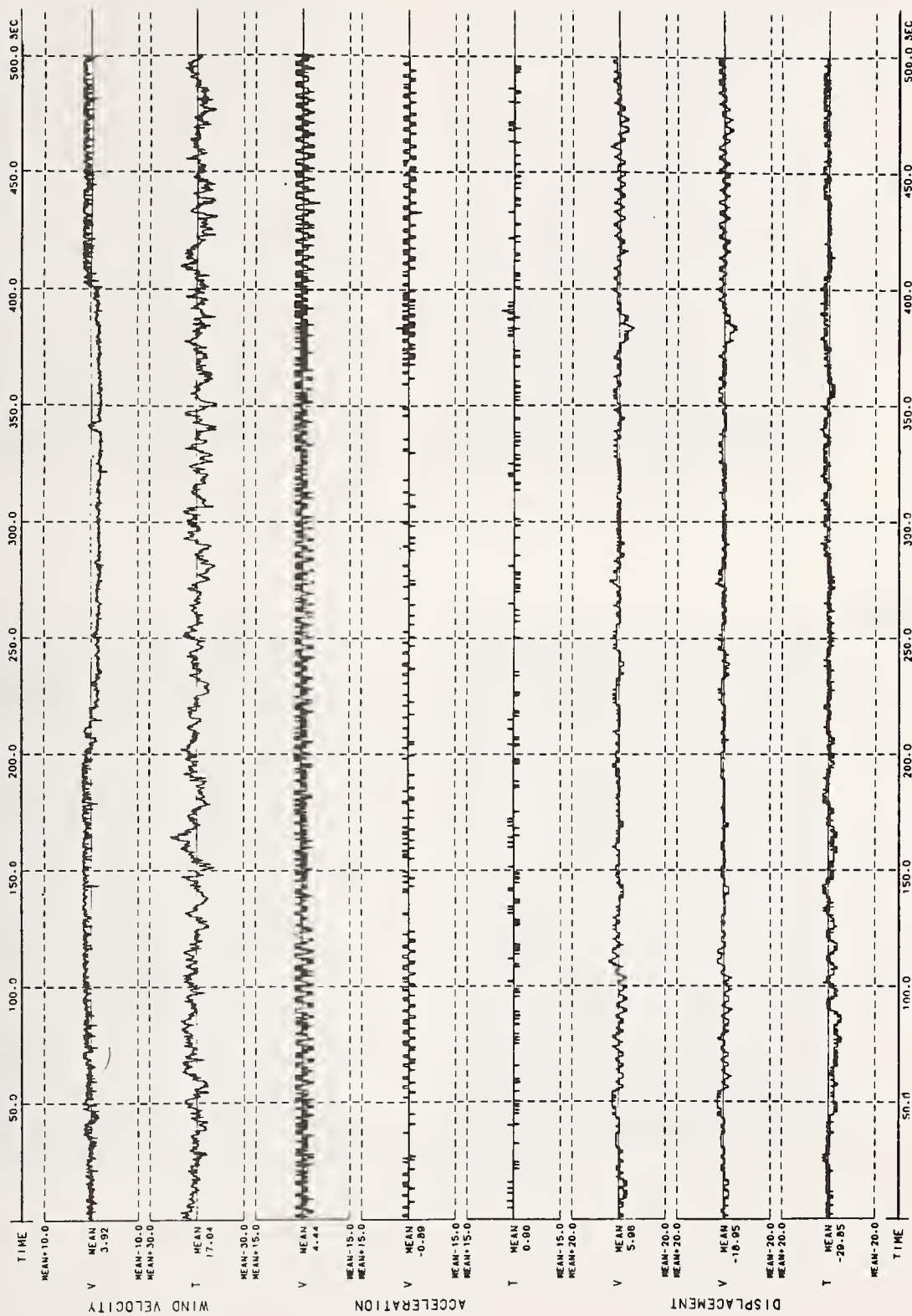


Fig. 10 Record of Wind and Response (8:50:00 18 Nov. 1974, M.P.-A)

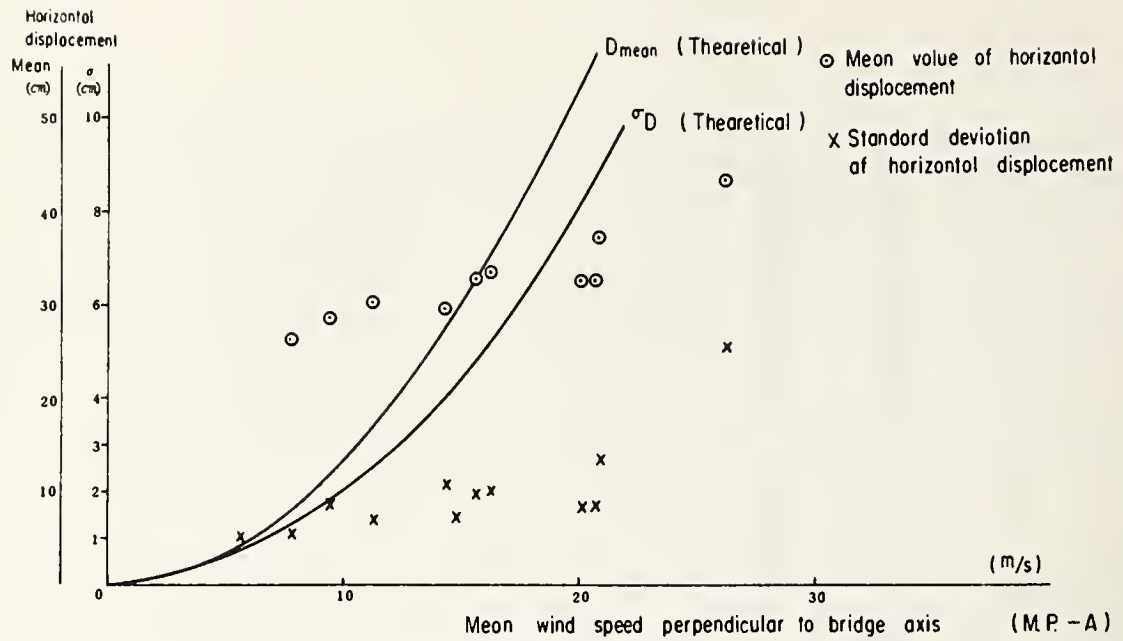


Fig. 11(1) Wind speed v.s. Horizontal displacement

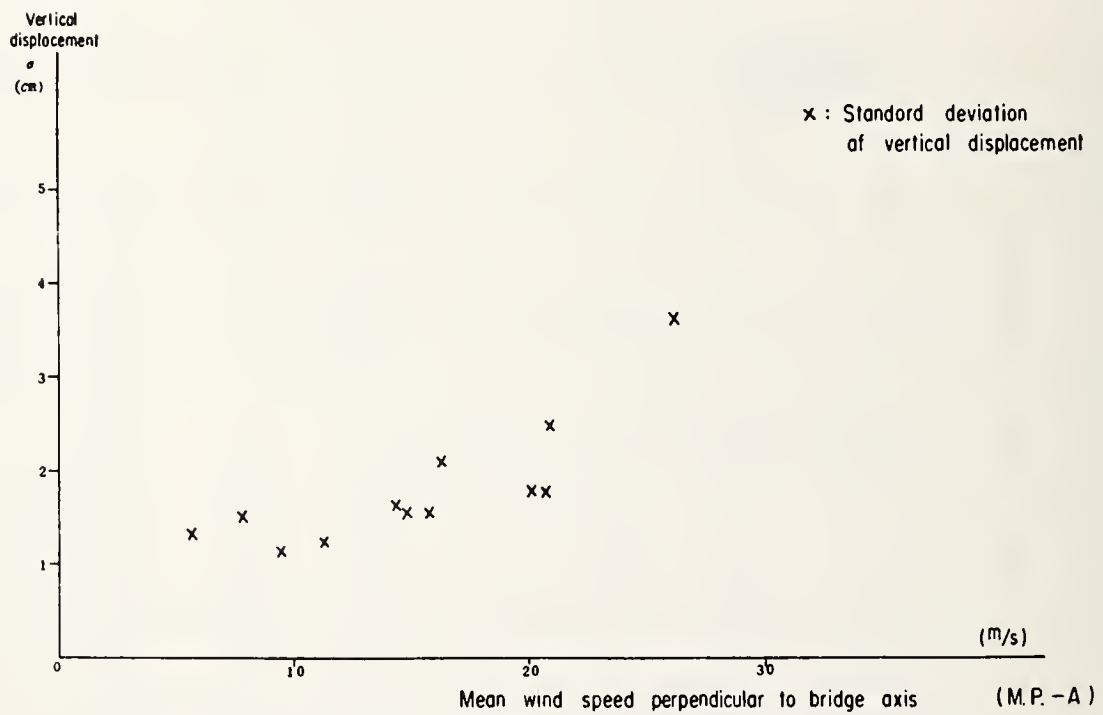


Fig. 11(2) Wind speed v.s. Vertical displacement



Photo.-2 Servo-accelerometer
(M.P.-A, V-component)



Photo.-4 X-Y Analyzer
(Anchor at Shimonoseki side)



Photo.-1 Propellar type anemometer and
supersonic anemometer
(M.P.-A)



Photo.-3 Electro-magnetic accelerometer
(the tower at Shimonoseki side)

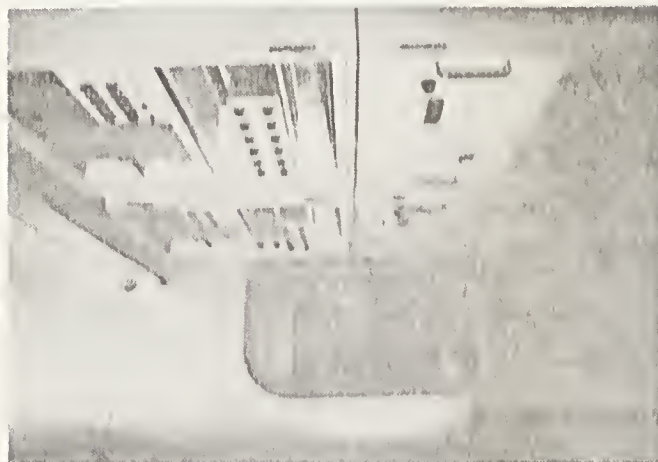


Photo.-6 Data Transmission system



Photo.-5 Transducers
(the tower of Shimonoseki side)

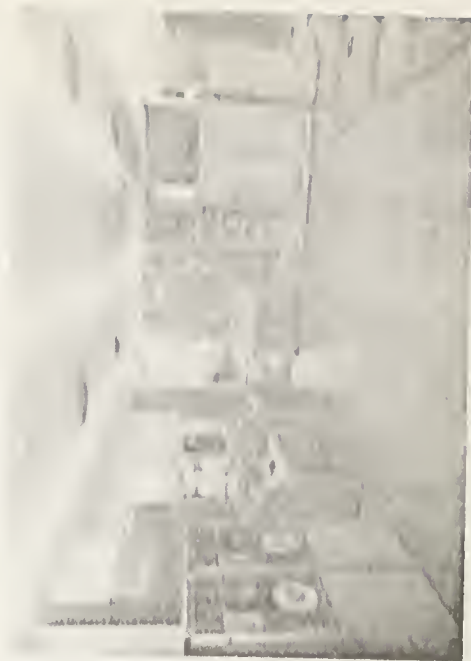


Photo.-7 Data processing system

LULING, LOUISIANA CABLE-STAYED BRIDGE
WIND TUNNEL SECTION MODEL TESTS

by

Richard H. Gade
Research General Engineer
Office of Research

and

Walter Podolny, Jr.
Structural Engineer
Office of Engineering

and

Harold R. Bosch
Structural Research Engineer
Office of Research

Federal Highway Administration
Washington, D. C.

ABSTRACT

Results of wind tunnel section model tests of five orthotropic superstructure configurations for the Luling, Louisiana, Cable-stayed bridge are presented.

The 1,235-foot (376.4 meters) long main span crossing of the Mississippi River is designed for 150 miles per hour (67 meters per second) hurricane wind velocity.

The section models, 1/60 scale, are tested at six wind angles: -4° , -2° , 0° , 2° , 4° , and 6° . Flutter coefficients are plotted for all tests.

The tests show freedom from flutter at the design wind speed. Vortex excitation, vertical and torsional, is exhibited.

Testing is performed in smooth flow conditions at the Fairbank Highway Research Station of the Federal Highway Administration, utilizing the George S. Vincent Wind Tunnel.

Key Words: Bridge, cabled stayed, wind tunnel, models, displacements, flutter, wind angles.

Introduction

Recent bridge structures have increased dimensions and flexibility and decreased dead weight and damping characteristics. Reduction of dead weight produces a magnification of wind effects relative to the inertia of the structure. Increased flexibility decreases the natural frequency of vibration. Modern fabrication techniques have decreased the structure's ability to absorb energy by sliding friction between component parts and thus less energy is required to initiate and maintain vibration. As a result, recent structures are becoming more sensitive to not only static wind effects but dynamic ones as well. Some existing and relatively recent structures have been so affected by wind oscillations that they have required reinforcement or modification by fairing.

The assessment of dynamic deflections and oscillations of long-span bridges due to wind action usually resorts to a wind tunnel model test. This is particularly so for the traditional truss stiffened suspension bridge. The cable-stayed box-girder bridge which is currently receiving popularity by designers in the United States is subject, fundamentally, to the same wind excitation mechanism as the traditional suspension bridge. The inherent general increase in stiffness of the cable-stayed box-girder does place it in a different realm of response.

This paper will present data gathered from model studies conducted by the Federal Highway Administration (FHWA) on the Luling, Louisiana cable-stayed bridge.

Wind Force and Angle of Attack

Wind force on an object is normally not in line with the direction of the wind. In conventional aerodynamic analysis, i.e., airfoil design, wind force is divided into two components: drag and lift, parallel and perpendicular to the wind direction. This same convention may be applied to a bridge deck wherein the resultant wind is oriented to the structure by the angle of attack α , positive when striking the section from the underside. It is convenient in considering wind effects on bridge structures to consider lift being perpendicular to the normal cross-section position of the bridge deck.

In the evaluation of wind forces on a structure there is a concern for the determination of the possible direction of critical wind velocity. In plan it is generally assumed that the critical wind direction is perpendicular to the longitudinal axis of the bridge. An obvious question arises as to what maximum value of the angle of attack, α , should be considered on the deck cross-section. The angle of attack is a function of wind velocity and site conditions. Preliminary data for the relationship between maximum observed angle of attack and wind velocity obtained by the FHWA at the Newport, Rhode Island Suspension Bridge over Narragansett Bay (Fig. 1) provided measurements of the mean vertical wind angle for a range of wind speed recorded for Hurricane "Doria". From these curves it can be seen that the angle of attack decreases with increasing wind speed, thus, at lower wind speeds the structure must be stable for larger values of angle of attack. The curves shown in Fig. 1 may serve as a guide but may not necessarily be applicable to other sites and possibly may impose unnecessary constraints to the analysis.

Luling Bridge

Wind tunnel tests are being conducted on 1:60 scale section models for the proposed bridge deck superstructure cross-section shapes of the Luling, Louisiana, cable-stayed bridge over the Mississippi River. These tests, still in progress, are being conducted at the FHWA's Fairbank Highway Research Station, McLean, Virginia, using the low speed, smooth flow, 6 ft. by 6 ft. open jet, George S. Vincent Memorial Wind Tunnel facility.

The experimental procedure, Fig. 2, suspends the essentially rigid model by four equal springs at each corner of the end supporting brackets. End plates are employed so that the air flow near the end of the model is two-dimensional. The models, five feet in span, are scaled by the Froude Number Criteria for mass property and vertical natural frequency. Due to practical limitations of simulating the relatively high prototype torsional characteristics, values of polar mass moment of inertia and torsional natural frequency do not achieve Froude Scaling.

The behavior of damped spring-mass systems is dependent on the value of the damping coefficient. A specific value of structural damping for a proposed bridge structure (which for practical purposes is impossible to obtain) is difficult to assign, and consequently, so is the value for a model system. The section model testing is, therefore, treated as a method of extracting aerodynamic information which can be used analytically with any selected value (or values) of prototype structural damping. Thereby, the need for adjusting the model system to a specific value of structural damping is avoided. The tests are conducted with the values of mechanical damping exhibited by the freely oscillating model.

Seven superstructure configurations are considered, all having a center line median barrier. A typical section model of the double trapezoidal box-girder design with an orthotropic deck is indicated in Fig. 3. The same section model modified by a slanted, non-structural, fascia plate is shown in Fig. 4. Initial wind tunnel tests suggested that this "faired" cross-section would exhibit a marked improvement in aerodynamic response. A section model of a multi-cell steel box-girder of a "streamlined" cross-section is shown in Fig. 5.

The aerodynamic information obtained from the section model tests is in the form of flutter derivatives, following the procedure and linearized treatment of Scanlan and Tomko.² The mathematical model for lift and torsional moment are indicated in Eq. (1).

$$\begin{aligned} m \left[\ddot{h} + 2\zeta_{\omega} \dot{h} + \omega_h^2 h \right] &= \left(\frac{1}{2} \rho v^2 \right) (2B) \left[KH_1^* \frac{h}{v} + KH_2^* \frac{B\dot{\alpha}}{v} + K^2 H_3^* \alpha \right] \\ I_p \left[\ddot{\alpha} + 2\zeta_{\omega_{\alpha}} \dot{\alpha} + \omega_{\alpha}^2 \alpha \right] &= \left(\frac{1}{2} \rho v^2 \right) (2B^2) \left[KA_1^* \frac{h}{v} + KA_2^* \frac{B\dot{\alpha}}{v} + K^2 A_3^* \alpha \right] \end{aligned} \quad (1)$$

where α	=	angular displacement
B	=	deck width
H_i^*, A_i^*	=	nondimensional coefficients dependent upon K ($i=1,2,3$)
ζ_h, ζ_α	=	damping ratios respectively in vertical and torsional motions of the free bridge
ω_h, ω_α	=	corresponding natural frequencies
m, I_P	=	mass and mass moment of inertia of the deck per unit span, referred to the elastic axis
h	=	vertical displacement
ρ	=	air density
v	=	wind velocity
K	=	$B\omega/v$ or "reduced frequency"
ω	=	circular frequency of oscillatory motion

The Luling Bridge models exhibited uncoupled response motion, therefore, only the H_1^* , A_2^* and A_3^* stability derivatives are applicable. H_1^* is the function for aerodynamic damping of vertical oscillation, A_2^* is indicative of torsional aerodynamic damping and A_3^* is the measure of change in torsional frequency between aerodynamic damping and mechanical damping.

Six wind angles varying from -4° to $+6^\circ$ and increments of equivalent prototype wind speed to 160 mph were investigated. The experimental values for the respective derivatives are plotted as functions of reduced velocity (v/NB) which may be considered as a non-dimensional frequency.

An example of the test results are shown in Fig's. 6 through 8 for H_1^* , A_2^* and A_3^* . The test results illustrated are for model C-2C-A at zero wind angle.

All model shapes showed freedom from self-excited, divergent, vertical flutter oscillation. Torsional flutter occurred at wind speeds well above the design value of 150 mph, or at unlikely wind angles. However, all models responded, variously, to vortex shedding response. This is an amplitude limited response whereby the periodic shedding of vortices in the wake of the structure is resonant with the vertical and/or torsional modes of the structural system. This amplitude limited oscillation can be an unacceptable characteristic of the design when it occurs at moderate wind speeds and the resulting acceleration of the oscillating structure is disturbing to the user.

A small scale (1:150) sectional representation of the cross-section scheme C-2C was placed in an air flow containing smoke filaments for purposes of flow visualization. Flow separation tripped by the leading parapet railing, and again by the median barrier is illustrated in Fig. 9(a). Fig's. 9(b) and (c) capture the trailing vortex.

An estimate of the prototype response to vortex shedding is provided by data from the model tests. As suggested by Scanlan³, the analytical model for the homogeneous self-excited condition of "flutter methodology" is modified by providing a special periodic forcing function applicable at the Strouhal or vortex exciting condition. For the case of purely vertical response motion, the test observations provide a derivative, H_0^* , characterizing the decay from an amplitude greater than resonance to the steady-state resonant

amplitude, and a dynamic lift coefficient C_{LO} , Eq. (2). With these coefficients, and a selected value of prototype damping, a conservative estimate of prototype behavior can be calculated, when 100% lateral coherence of vortex exciting wind flow is assumed.

$$m \ddot{h} + 2\zeta_h \omega_h \dot{h} + \omega_h^2 h = \left(\frac{1}{2} \rho v^2\right) (2B) \quad KH_{OV}^* \frac{h}{v} + C_{LO} \sin \omega_s t \quad (2)$$

A summary of the test results for three comparative models is shown in Fig's. 10 through 12. The oscillating response characteristics of the section shape, referred to equivalent prototype wind speed, and for wind angles of attack are plotted. The shaded bands show the "locking in" range of wind speed over which vortex excitation takes place. The natural wind angle boundaries are for the Severn Bridge reference data, and for the recorded data on the Newport, Rhode Island suspension bridge.

For the same sections, an estimation of the double amplitude response of the prototype structure to vortex induced oscillations have been calculated and plotted in Fig's. 13 through 15. The ordinate scale is critical damping ratio. The abscissa scale is feet of double amplitude at center of span with associated value of root mean square g's of acceleration.

Closure

As a result of innovations in structure concepts, sophisticated structural analysis, materials, fabrication and erection procedures, recent bridge structures are becoming more sensitive to not only static wind effects, but dynamic ones as well. As a consequence, wind forces have taken on an increased importance and significance and can be a major problem in cable-supported bridge systems; serious consideration of these forces is required by the designer.

While most problems of bridge stability resulting from wind forces are recognized, the acquisition of data for new designs in the wind tunnel is mandatory to produce adequate wind stability information to enhance their design. At the present time there is no purely analytical methodology to preclude wind tunnel testing.

Data has been presented on current or on-going studies of the aerodynamics of selected structures. The method employed of extracting the aerodynamic derivative data from test results places no A Priori restriction on the frequencies, damping value, or inertias employed in the section model although it is suggested that highly unlikely values not be used.

It is important to note that while the validation of stability of the completed structure (for expected wind speeds at the site) is mandatory, it does not necessarily imply the most critical stability condition of the structure. A more dangerous condition may be during erection when full connection of the joints may not have been established and thus full stiffness of the structure is not achieved, the frequencies are lower than in the final state and the ratio of torsional frequency to flexural frequency approaches unity. The use of welded components in towers has contributed to the susceptibility of tower vibration during erection.

Component parts of the structure are also in themselves susceptible to wind excitation. The cables of cable-stay bridges, the hangers of suspension bridges and arch bridges, and the towers of suspension and cable-stay bridges have been known to present problems, usually from vortex excited vibrations.

Consideration as to an acceptable level of motion falls into two categories: 1) structurally damaging motion and 2) human response motion. The first relates to violent motion that may be catastrophic and/or motion that over a period of time may lead to fatigue related failures. The second relates to motion that may not be structurally damaging but may be objectionable from the stand point of user acceptance, i.e., vibration that is noticeable to pedestrians or occupants of standing or moving vehicles.

A great amount of research needs to be expended to study the stability of bridges of new designs, to develop criteria to rectify existing bridges that are or may become troublesome from a wind stability point of view, and to develop adequate procedures such that designers can produce stable designs at the conception of a bridge or at least to minimize the probability of unsteadiness.

A necessary prerequisite to any attempt at developing design criteria and/or predictive techniques that will produce a reasonable confidence level of aerodynamic stability for various cross-sections in use or contemplated and the accommodation of the vagaries of the natural wind will require extensive additional field and laboratory work.

References

1. Roberts, G., "Severn Bridge - Design and Contract Arrangements," Proc. of the Inst. Civ. Engrs., Vol. 41, September 1958.
2. Scanlan, R. H. and Tomko, J. J., "Airfoil and Bridge Deck Flutter Derivatives," Journal of the Engineering Mechanics Division, ASCE, Vol. 97 No. EM 6, December, 1971.
3. Scanlan, R. H., "Vortex-Shedding Response," Private Communication, R. Scanlan to R. Gade, 1974.
4. Wardlaw, R. L., "A Review of the Aerodynamics of Bridge Road Decks and the Role of Wind Tunnel Investigation," U. S. Department of Transportation, Federal Highway Administration, Report No. FHWA-RD-73-76.
5. Bosch, Harold R. and Gade, Richard H., "Wind Tunnel Section Model Tests, Luling, Louisiana, Cable-Stayed Bridge," Interim Report, Federal Highway Administration, Washington, D.C., April 1, 1975.

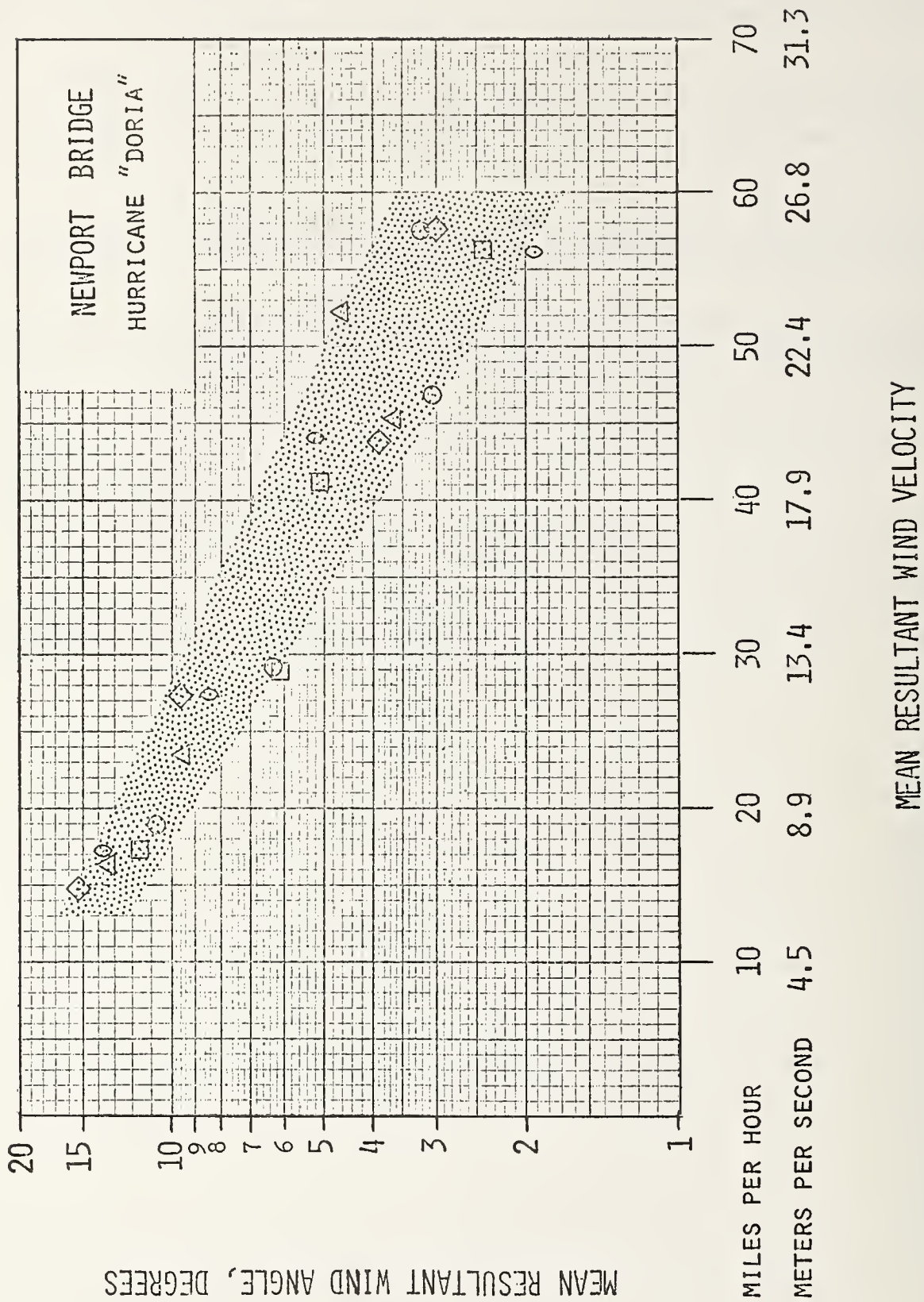


Fig. 1

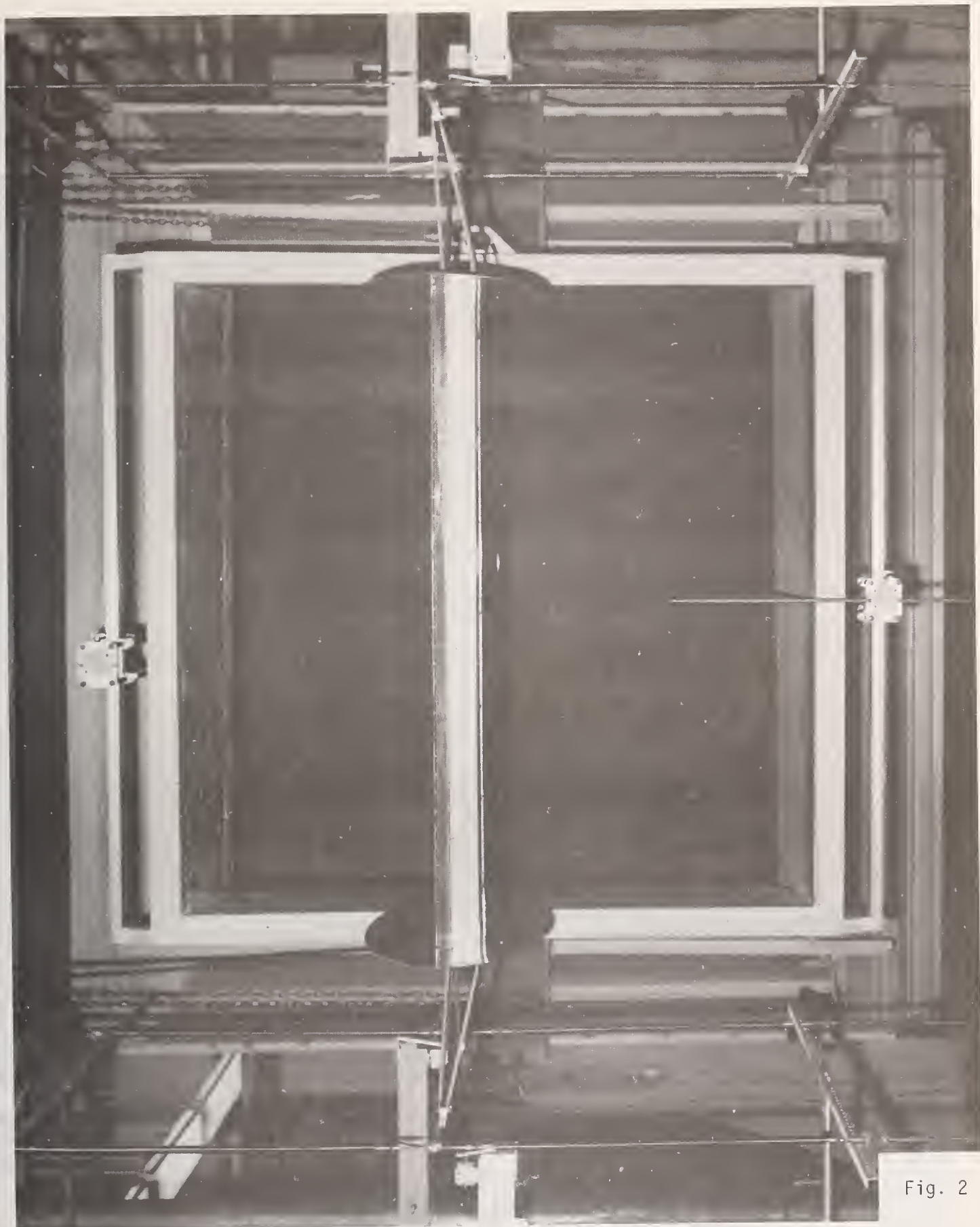
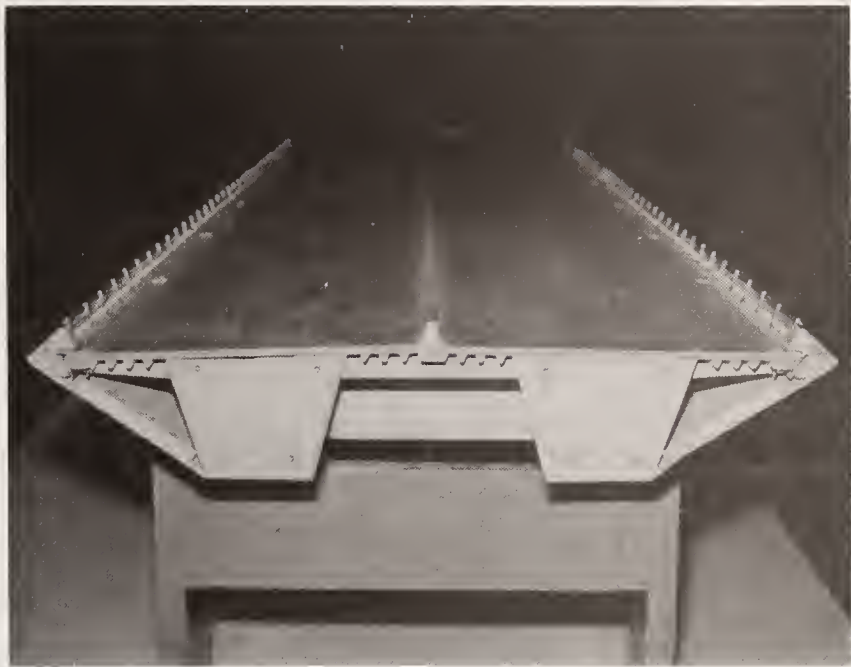


Fig. 2



Fig. 3



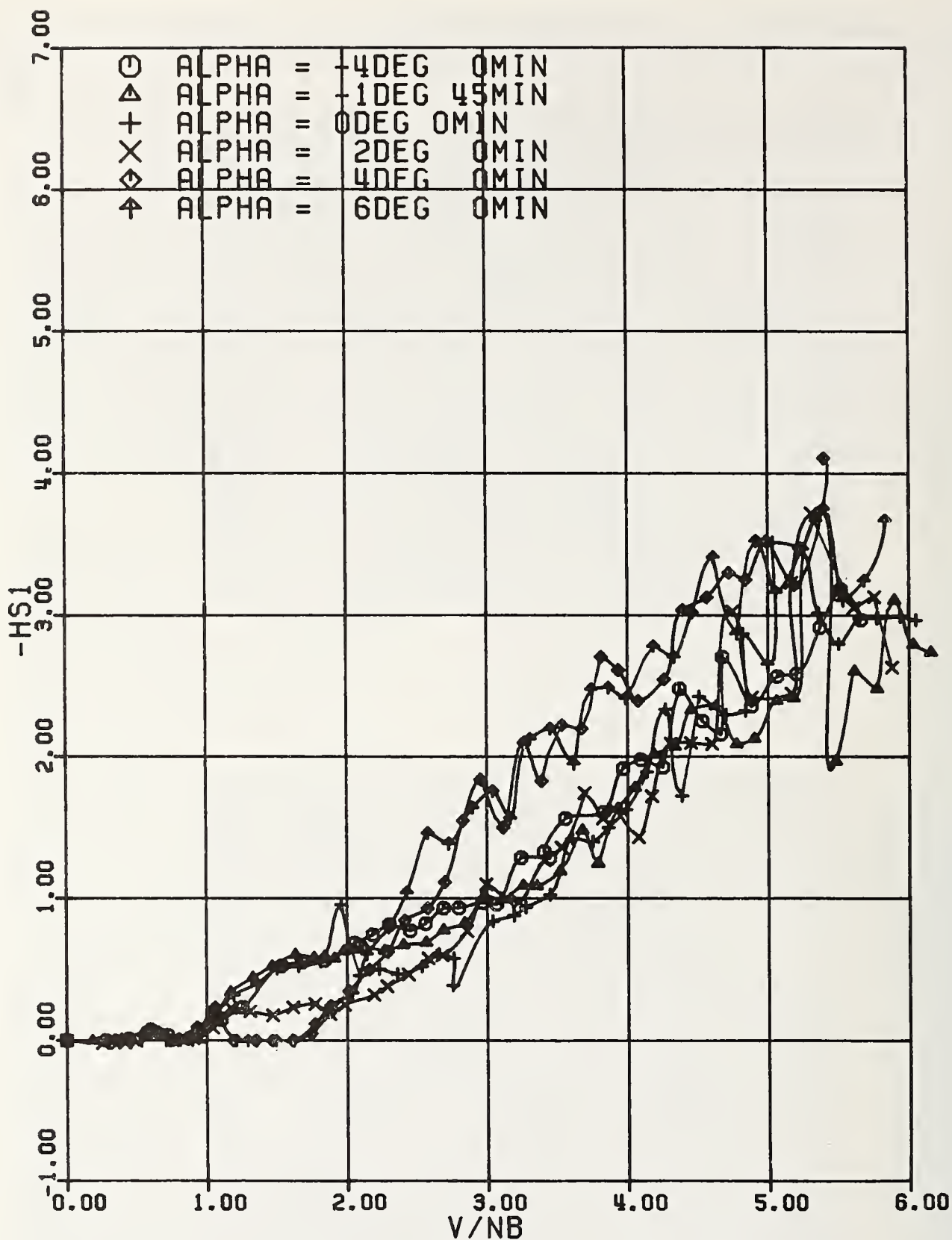
Luling Bridge Section Model C-2C-A

Fig. 4



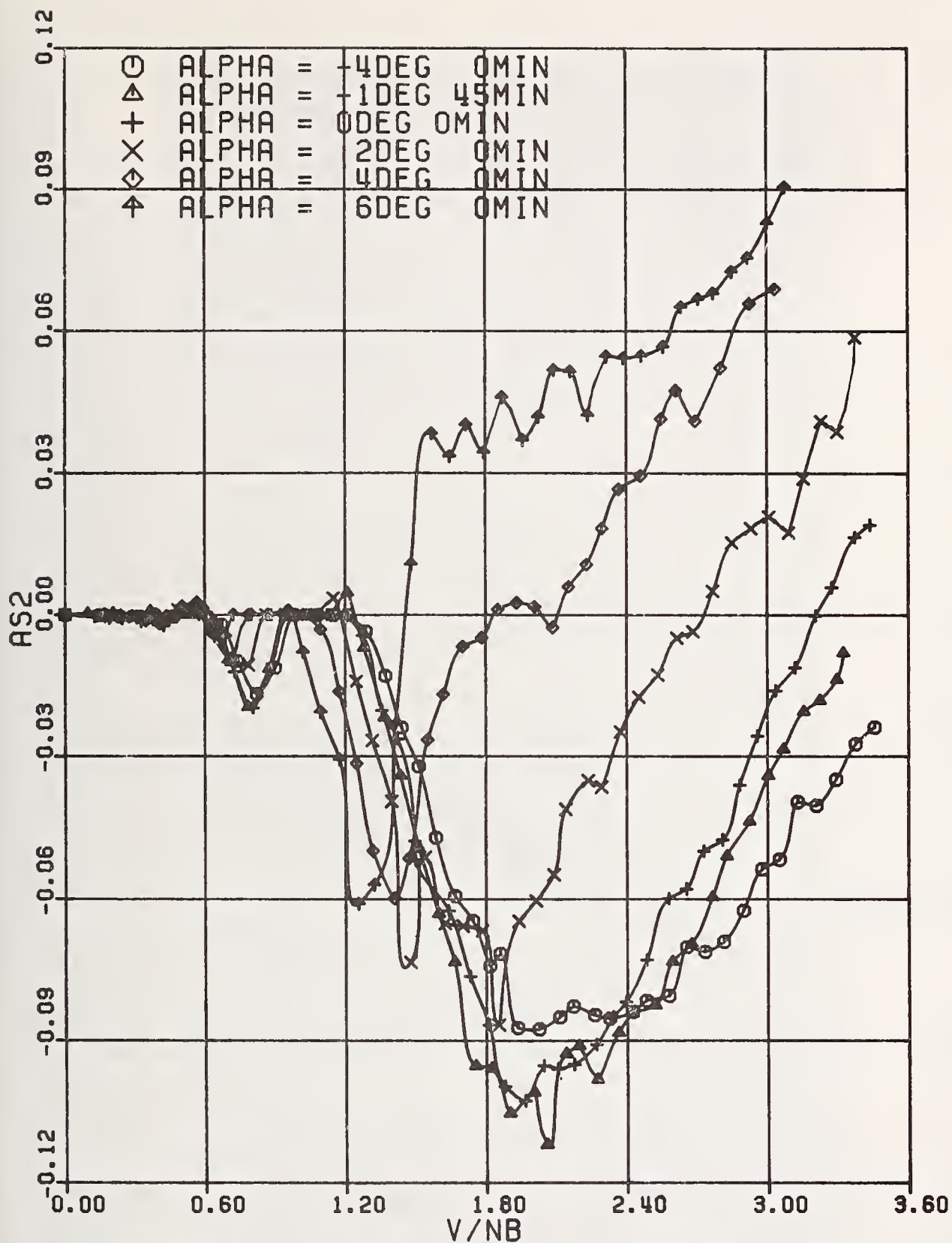
Luling Bridge Section Model C-6-C-B

Fig. 5



EXPERIMENTAL RESULTS FOR HS1
LULING LOUISIANA CABLE-STAYED BRIDGE
MODEL C-2C-A

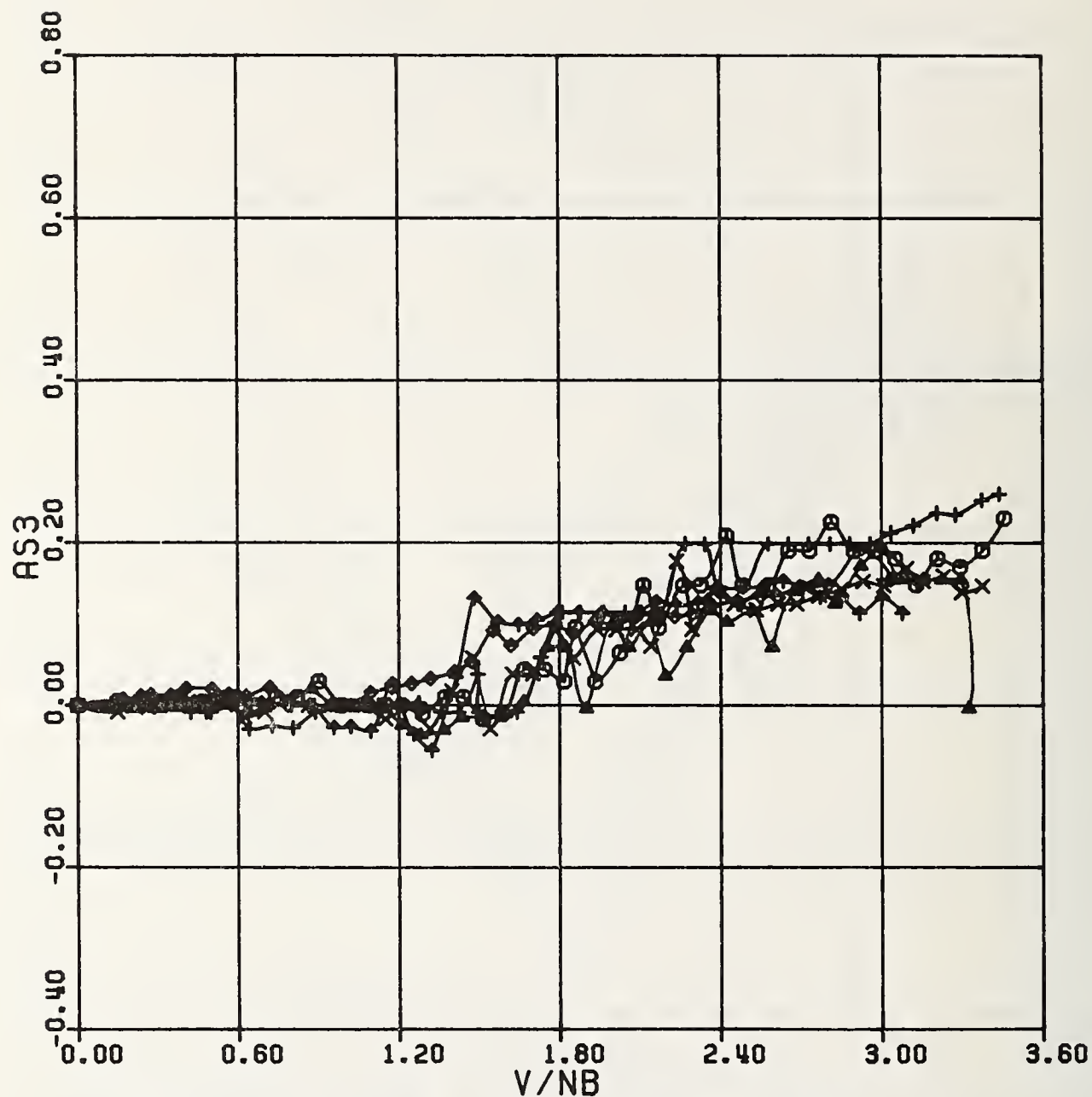
Fig. 6



EXPERIMENTAL RESULTS FOR AS2
 LULING LOUISIANA CABLE-STAYED BRIDGE
 MODEL C-2C-A

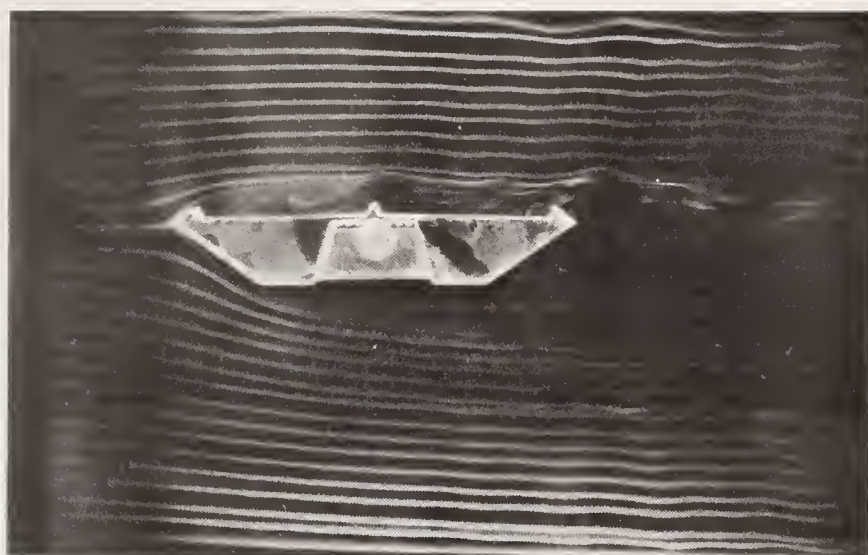
Fig. 7

○ ALPHA = -4DEG 0MIN
 △ ALPHA = -1DEG 45MIN
 + ALPHA = 0DEG 0MIN
 × ALPHA = 2DEG 0MIN
 ◇ ALPHA = 4DEG 0MIN
 † ALPHA = 6DEG 0MIN

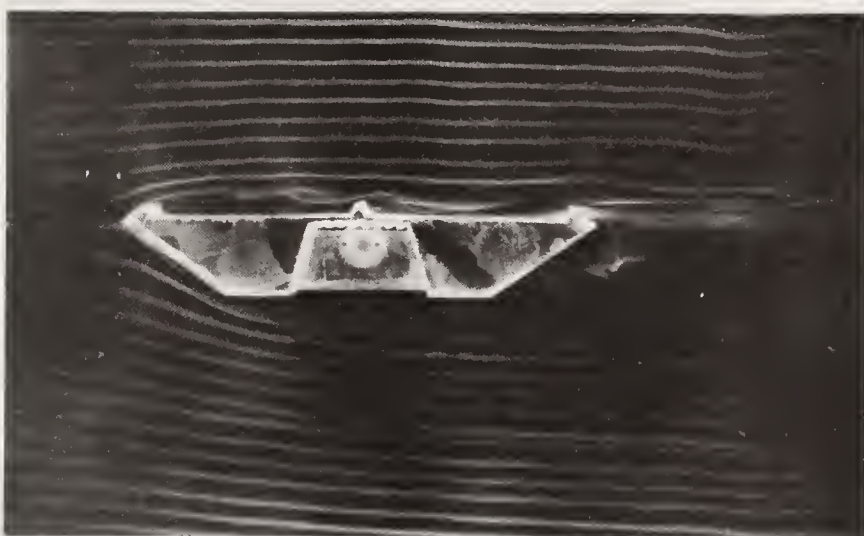


EXPERIMENTAL RESULTS FOR AS3
 LULING LOUISIANA CABLE-STAYED BRIDGE
 MODEL C-2C-A

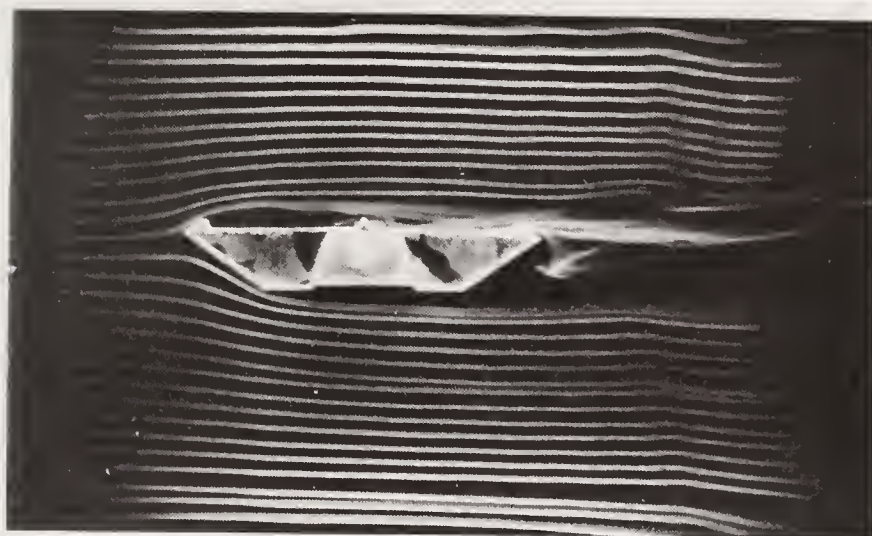
Fig. 8



(a)



(b)



(c)

SMOKE FLOW VISUALIZATION MODEL

Fig. 9

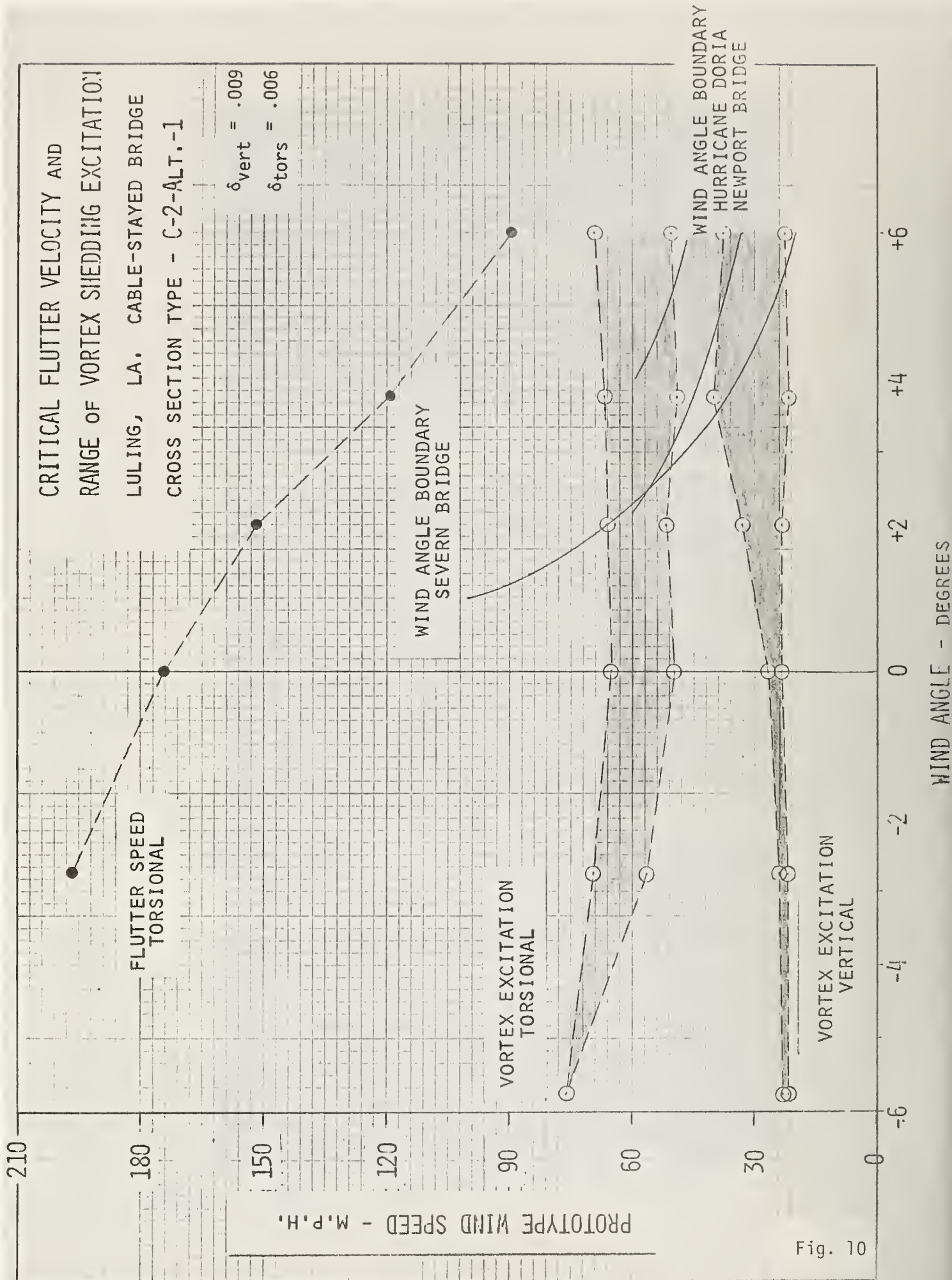


Fig. 10

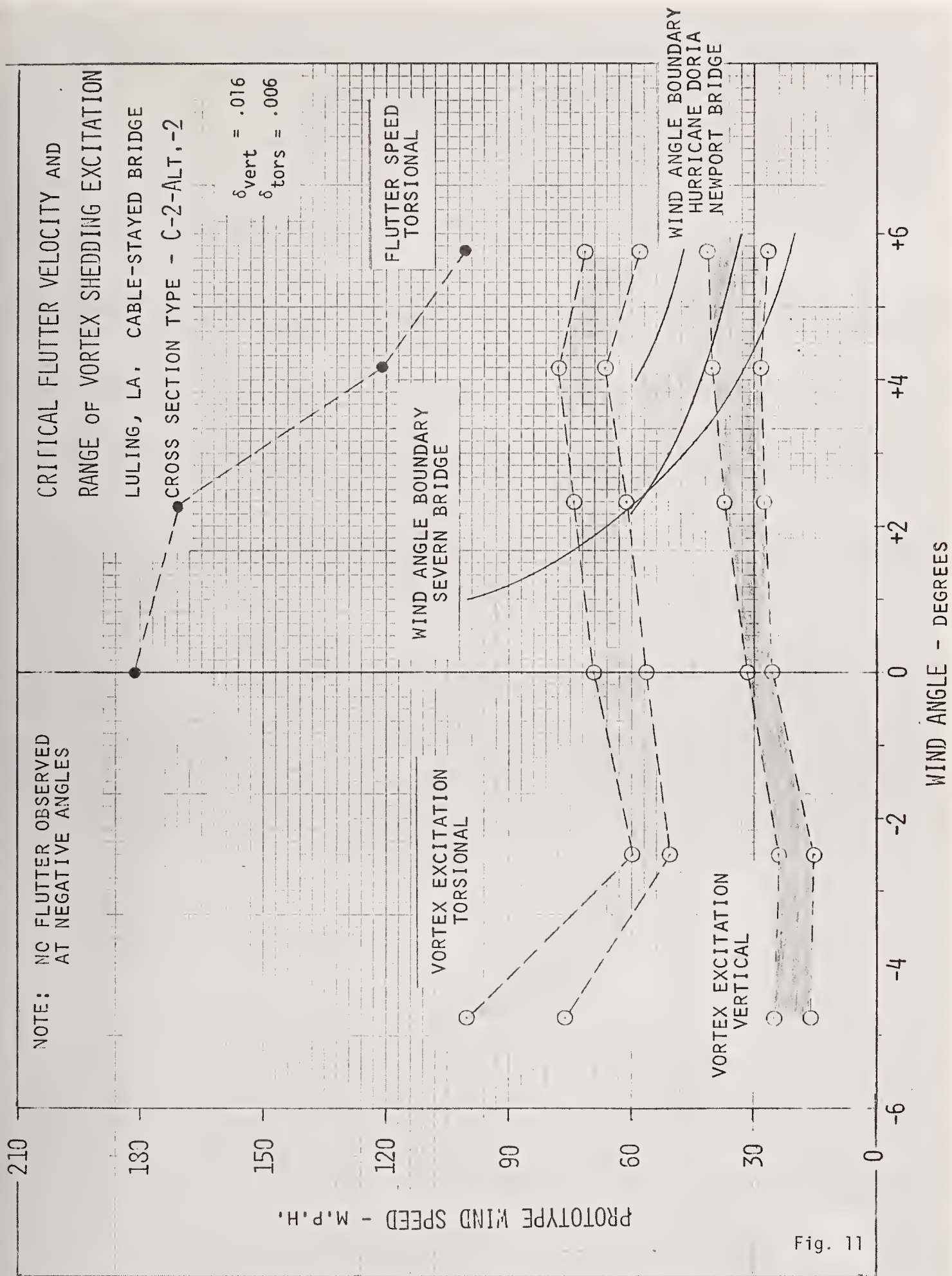


Fig. 11

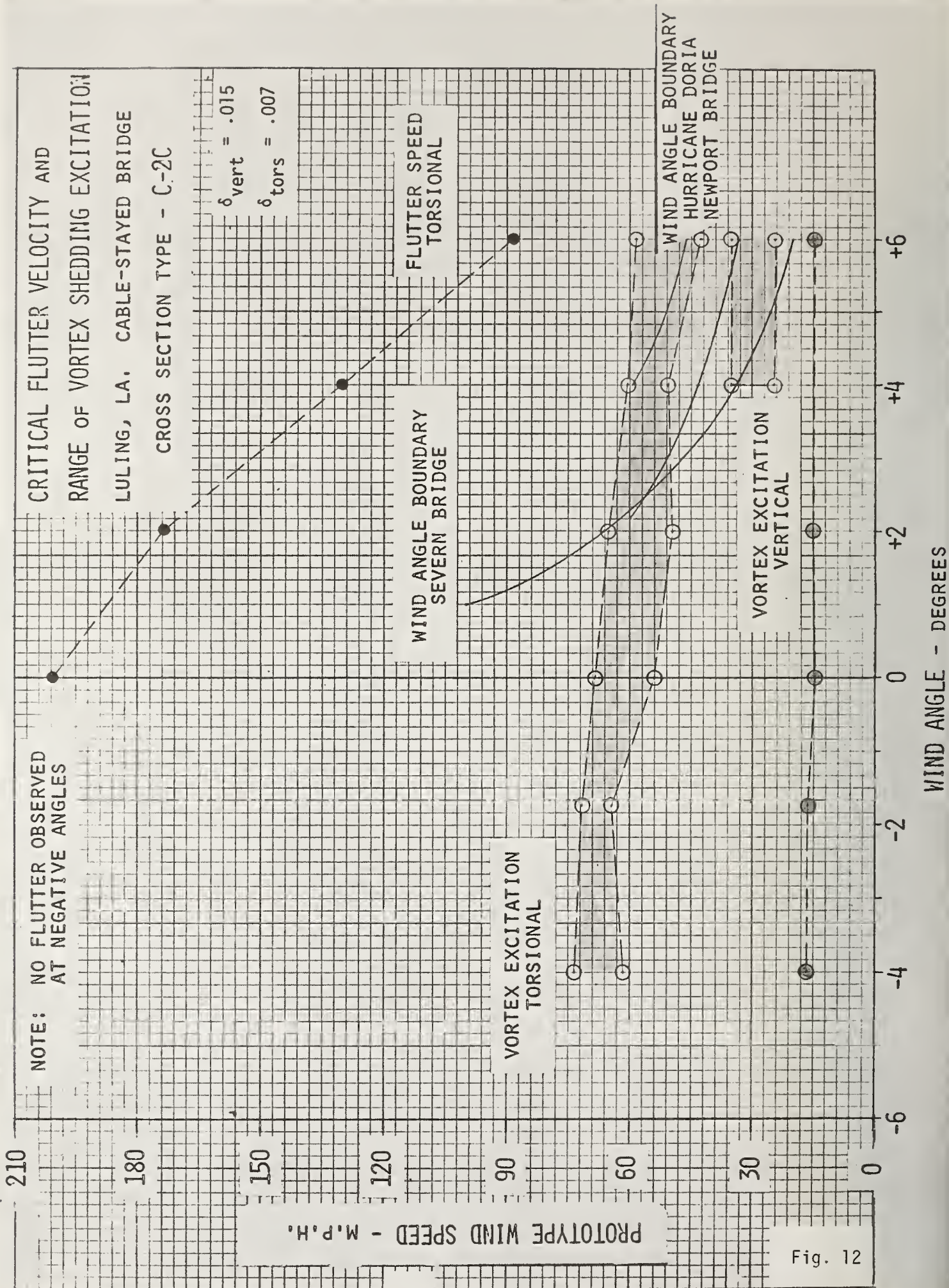


Fig. 12

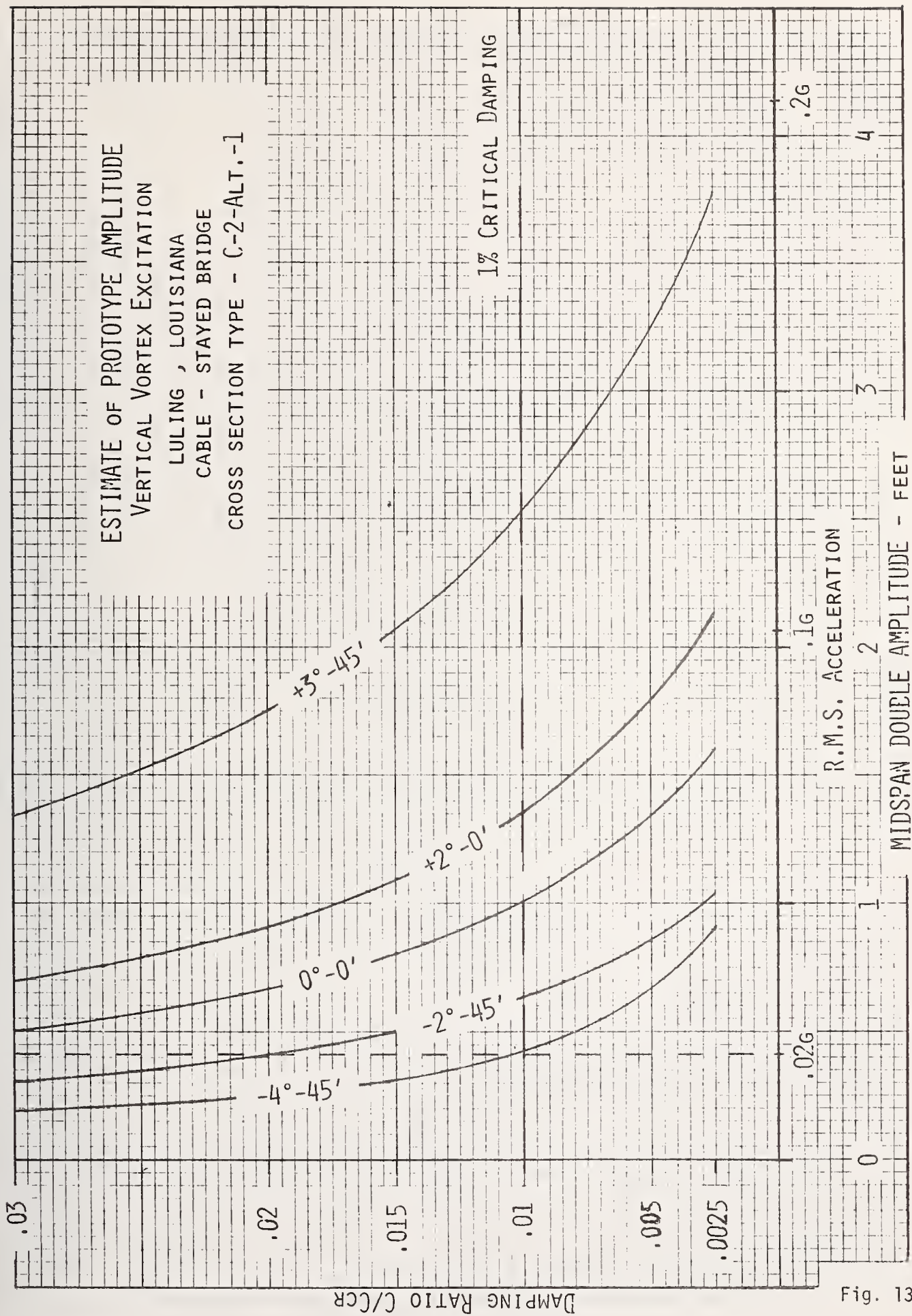


Fig. 13

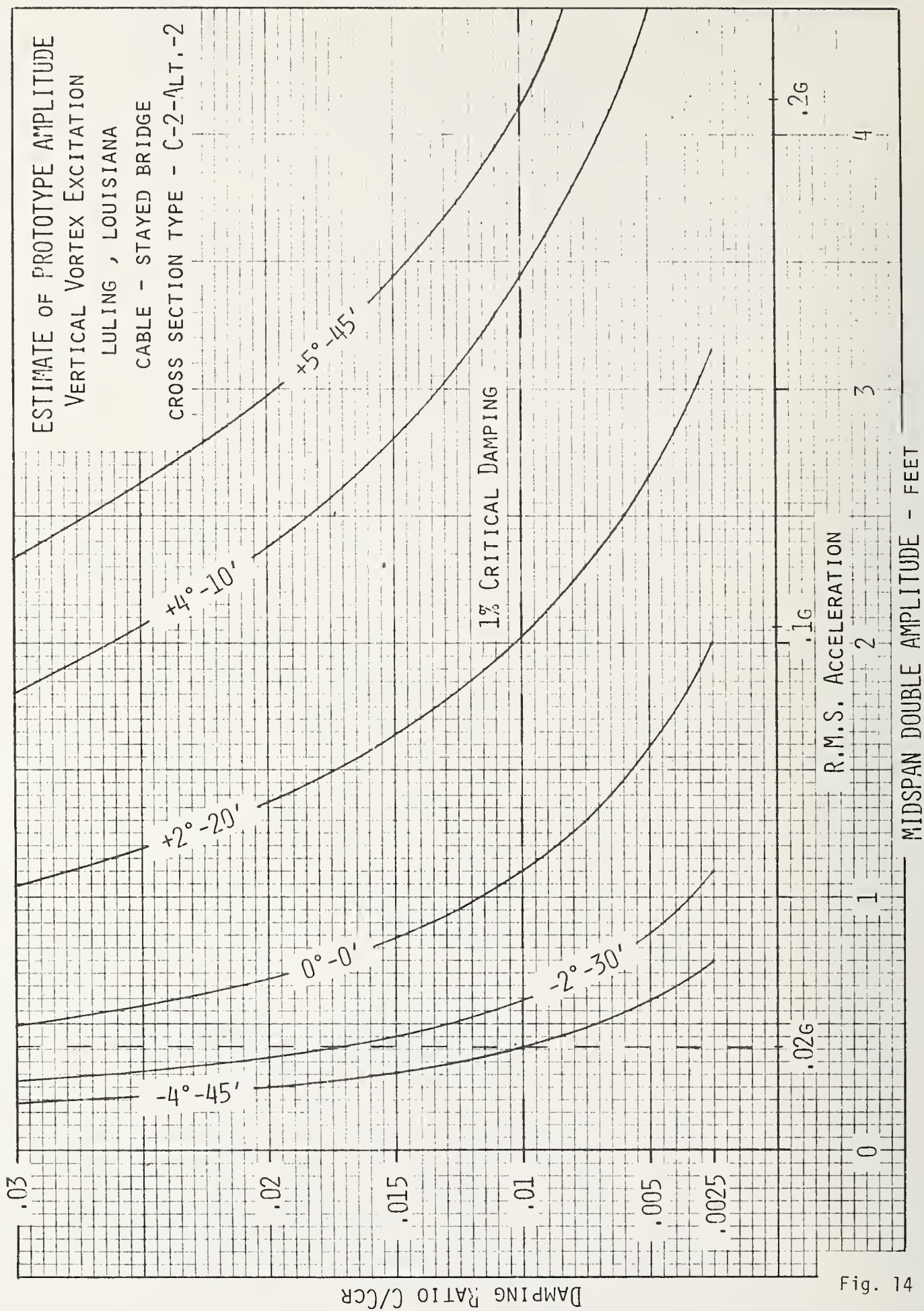


Fig. 14

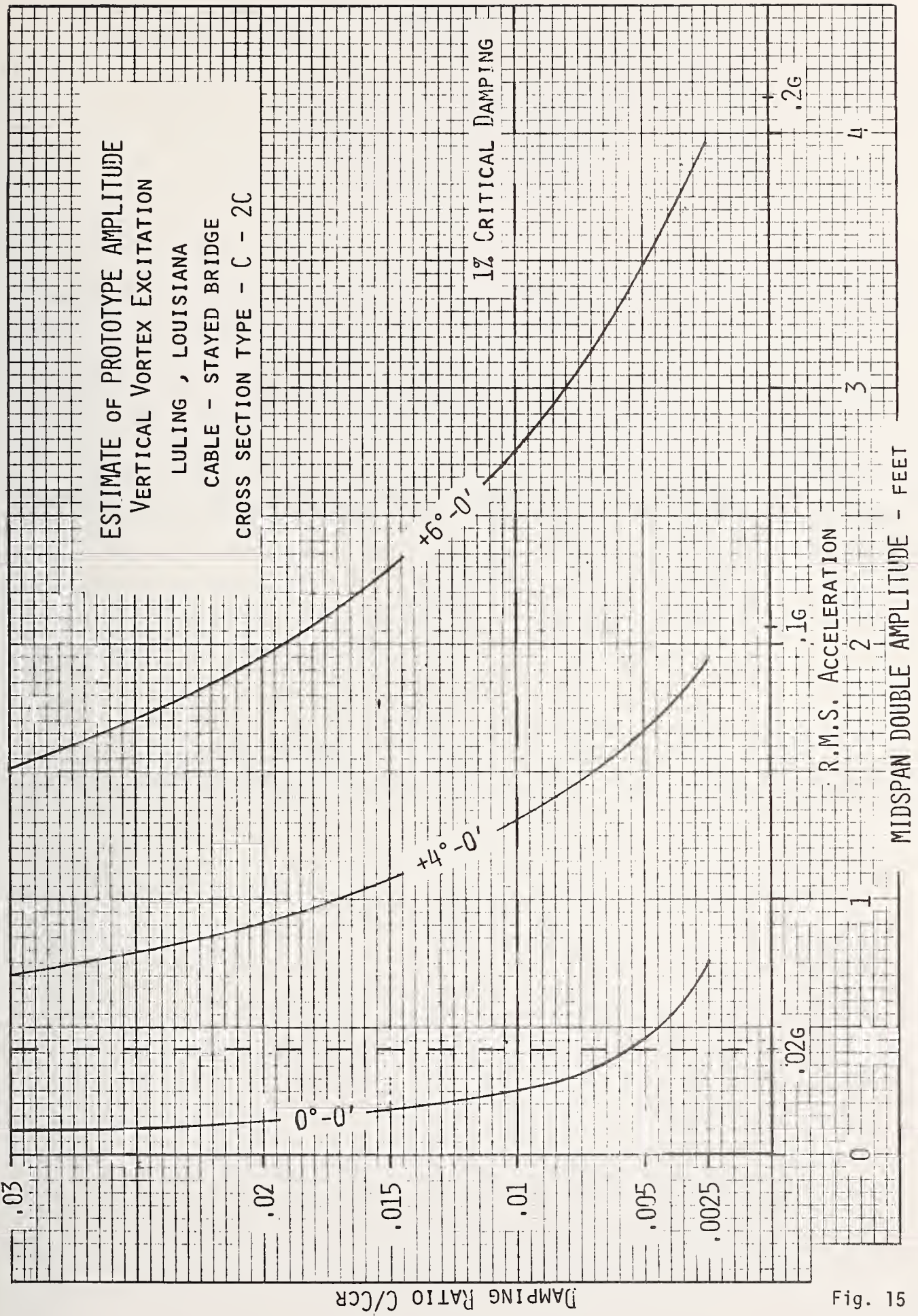


Fig. 15

THE REGIONAL DISTRIBUTION OF THE EARTHQUAKE
DANGER IN JAPAN

by

S. Hattori, Y. Kitagawa and T. Santo
International Institute of Seismology
and Earthquake Engineering
Building Research Institute
Ministry of Construction

ABSTRACT

The values of m and $\log k$ in Ishimoro-Iida's statistical Formula are derived for each component of the maximum displacement amplitude observed at many stations of the network maintained by the Japan Meteorological Agency (JMA).

A distribution map of expected maximum displacement amplitudes for the earthquake recurrence period of 100 years is made based on the derived values of m and $\log k$. The map indicates quantitatively the regional distribution of earthquake danger in and around Japan. It is seen from this map that the general level of the earthquake danger varies throughout Japan. This variation is also found to reflect the pattern of seismic activity throughout the area. The earthquake danger increases along the Pacific side of Hokkaido, Tohoku and Kanto districts and decreases in the southwestern and inland areas of Japan. Small variations are also recognized, which might suggest that the earthquake danger is affected by local geological and subsoil effects.

Key Words: Earthquakes; Earthquake Distribution; Field Data; Frequency Maps; Ground Displacement; Japan.

The data were obtained from the monthly reports of JMA (Japan Meteorological Agency) from Jan. 1967 to Jan. 1972, which give the relevant informations on a single earthquake recorded at a particular station. The data are recorded on cards for each station, with the number of cards for each year as listed in Table 1. These data are then transferred to and stored on magnetic tapes.

Seismicity in a certain area can be measured by a well-known coefficient b in a formula of $\log N = a + bM$, in which N is the frequency of the occurrence of earthquake with magnitudes of $M \pm \Delta M$, where a and b are constants.

In addition to this equation another useful formula has been derived by M. Ishimoto and K. Iida, and is;

$$n(A)dA = kA^{-m}dA \quad (1)$$

where $n(A)$ is the number of earthquakes with maximum displacement amplitude, $A \pm dA$. The two constants m and k in equation (1) have often been calculated by means of the least squares method. Recently T. Utsu [1] has reported that the coefficients in equation (1) can be calculated with high accuracy by means of the maximum likelihood method as expressed in the following formula:

$$m = \frac{S \log e}{\sum_{i=1}^I \log A_i - S \log A_j} + 1.0 \quad (2)$$

where S denotes the total number of data used and A_j is the i -th maximum displacement amplitude with the order number i from the largest value and A_j is the least value of the maximum displacement amplitudes in the data used.

The value of the coefficient k , or $\log k$, can be calculated from the following formula;

$$\log k = \log N(A \geq A_j) + \log(m - 1) + (m - 1) \log A_j \quad (3)$$

where N denotes the total number of maximum displacement amplitudes which exceed the selected level, A_j .

It must be noticed that the values of m and $\log k$ are dependent on the value of A_j . For instance, if too small value is selected for A_j , the number of data which may be used becomes smaller than the actual number owing to the limitations in the ability of observation and reading of records, which leads to situations which underestimate the value of m . Taking this into account, the data that was selected satisfied equation (1) for calculating m and $\log k$ at each station.

In the present study, the values of m and $\log k$ were calculated from the data using three components N-S, E-W and U-D, and resultants at 109 stations. In Figs. 1 and 2, the relationship of (1) cumulative frequency N versus $\log A$ and (2) N versus $\log A_j$ for the range of $\log A_j = 0.1$ to 3.0 , are shown for stations, Hikone, Okayama and Tokyo. The total number of the maximum displacement amplitudes for the N-S component given in Fig. 1(a), is 443. Because data in the range of $A_j = 0.1$ to 1.0 is small, the values of m for this range are not constant and thus were not used. The trend of the variable m relative to E-W, U-D and the resultant components, has similar trends when compared to the N-S component. Consequently in the present paper, the average value of m and the standard deviation were all calculated from the data using the N-S component, using tentative values at each station in the range of $\log A_j = 1.0$ to 2.0 at intervals of 0.1 . The average value of $\log k$ and the standard deviation were then calculated using Eq. (3). The average values of m are shown by small open circles indicated by arrows in figures 1 and 2 and as seen in Figs. 1(a) and 1(b) the trends are quite similar at Hikone and at Okayama. Examination of the Tokyo Station data shown in Fig. 2, however, is quite different. In this case, the values of m do not converge, even for a range of $\log A_j$ beyond 1.0 . Quite reasonably for this case, the values of the cumulative frequency distribution N does not show a linear relationship relative to the $\log A$. Average values of m and $\log k$, at this station have much larger standard deviations than in other cases, In Table 2, examples of the values of m and $\log k$ and their standard deviations are listed for all 109 stations. In this Table N_1 , N_2 and N_3 respectively means the total number of data, the number of data for $\log A \geq 1.0$ and for $\log A \geq 2.0$. Fig. 3 shows the differences between the values of m and $\log k$ for different components at approximately 60 stations. As can be seen from this figure, some stations have a value of m equal to 1.2 or 1.4 . These exceptional small values, however, were due to an insufficient number of data. Examination of the calculated values of m and $\log k$ using different components, showed that there was indifference from station to station, as mentioned previously.

Fig. 4(a) shows the regional distribution of the parameter m calculated from the data on N-S components, while in Fig. 4(b), the distribution of m excluding those of values of m less than 1.5 . As can be seen in Fig. 4(b), the stations at which large values of m were observed, tend to be distributed near the most active violent seismic zones in Japan. These regions are along the Pacific coast from Hokkaido and from Tohoku through the northern part of Kanto down to the southern parts of Chugoku and Kinki districts. Another large zone where m is large, is the Japan Sea along the Chubu district. The locations of the various districts and stations are shown in Fig. 5. The general tendency of the distribution of m have been found to coincide with the regional distribution of b -values which were published previously [3]. The distribution of $\log k$ parameter is shown in Fig. 6.

The frequency T (in years), when the stations experience a maximum displacement amplitude in a certain period, were calculated using the values of m and $\log k$ as follows;

Recalling that Eq. (1) shows that the variable k gives the frequency of the shock and the displacement amplitude A of 1 micron at a certain station, where this frequency is considered to be proportional to the period of the observation. Under such an assumption, the value of k for the period of T years can be extrapolated by using the following formula;

$$K = 10^{k_{61} \frac{12 \cdot T}{61}}$$

where k_{61} means the value of $\log k$ for 61 months. This means

$$\log k = k_{61} + \log(12T/61)$$

and for this paper, the value of k for $T = 100$ years will be derived. Examine now Fig. 7, which shows the regional distribution of the frequency when the maximum displacement amplitudes of 100 micron are expected in 100 years. Figs. 8(a), 8(b) and 8(c) show the regional distribution of the frequency, when the maximum displacement amplitude will exceed 100, 1,000, and 10,000 microns. For instance, as shown in Fig. 8(a), station Nemuro is expected to experience 2030 ground vibrations with a maximum displacement amplitude of more than 100 microns 100 years, which is about 20 times in one year. Similarly, the same station will in one year, experience three and 0.4 ground vibrations with a maximum displacement amplitude of 1,000 and 10,000 microns, respectively.

Conclusions

In addition to the expectancy maps given herein, other expectancy maps, as shown in Figs 9(b), (c), and (d) have been developed by H. Kawasumi [4], I. Muramatsu [5] and K. Kanai et al [6]. Comparing these figures with those presented herein, the following trends can be concluded; (1) although the data was taken from different periods, and with different accuracy, Figs. 9(a), (b) and (c) show a similar tendency in that, the earthquake danger increases along the Pacific coast of the Hokkaido, Tohoku and Kanto districts. This reflects the general pattern of seismic activity in and around Japan. However, in Fig. 9(d), the earthquake danger in Tohoku district, appears low; (2) As shown in Fig. 9(a), an additional area with high earthquake danger appears in the southern part of Kyushu, (3) high values of the earthquake danger, which seem to be abnormal, appear in Aomori ($A_{\max} = 90\text{cm}$), Akita ($A_{\max} = 60\text{cm}$) and Nagano ($A_{\max} = 50\text{cm}$) districts as shown in Fig. 9(a). In Fig. 10, the variables N vs $\log A$ and m vs $\log A_j$ are plotted for three stations, in order to check the reason for these abnormal values. With regard to m vs $\log A_j$ at Aomori and Nagano stations, the values of m increase gradually in the range of $\log A = 1.0 - 2.0$ and are approximately constant for the $\log A$ greater than 2.0. As was described previously,

m was measured at all stations in the range of $\log A = 1.0 - 2.0$. Therefore, the values of m are underestimated at these two stations. As seen in Eq. (3), an overestimated value of A is derived by an underestimation of m, which is why A_{\max} is obtained at Aomori and Nagano. In the case of Akita, however, the local ground condition should be taken into account.

References

1. Japan Meteorological Agency, 1967.1 - 1972.1, the Seismological Bull. of the Japan Meteorological Agency.
2. Utsu, T., A Method for Determining the Value of b in a Formula $\log n = a - bM$ showing the Magnitude-Frequency Relation for Earthquakes, the Geophys. Bull. of the Hokkaido Univ., 13 (1965), 99 - 104.
3. Hattori, S., Seismicity in and near Japan - Regional Distribution of b values in $\log n = a - bM$, Bull. IISSE, 12(1974), 59-82.
4. Kawasumi, H., Measures of Earthquake Danger and Expectancy of Maximum Intensity throughout Japan as inferred from the Seismic Activity in Historical Times., Bull. Earthq. Res. Inst., 21(1951), 469 - 481.
5. Muramatsu, I., Expectation of Maximum Velocity of Earthquake Motion with in 50 years through Japan, Sci. Rep. Gifu Univ., 3(1966), 470 - 481.
6. Kanai, K. and Suzuki, T., Expectancy of the Maximum Velocity Amplitude of Earthquake Motions at Bed Rock, Bull. Earthq. Res. Inst., 46(1968), 663-666.

Table 1 The Number of Data Cards

Year	Number of Cards
1967	11,448
1968	24,192
1969	14,796
1970	11,718
1971	11,232
1972	972
Total	74,358

Station	comp	N1	N2	N3	m	s. d	log k	s. d
NEMURO	(1)	709	535	115	1.886	0.131	3.733	0.328
	(2)	703	533	125	1.858	0.137	3.693	0.350
	(3)	703	452	81	1.931	0.126	3.713	0.311
	(4)	2215	1520	321	1.887	0.130	4.185	0.327
ASAHI-KAWA	(1)	672	451	65	1.864	0.055	3.521	0.132
	(2)	662	450	74	1.853	0.053	3.505	0.125
	(3)	630	397	53	1.865	0.039	3.427	0.099
	(4)	1964	1298	192	1.860	0.045	3.964	0.104
HAKODATE	(1)	1167	796	112	1.992	0.122	4.039	0.284
	(2)	1162	796	112	1.967	0.104	3.984	0.243
	(3)	1062	472	62	2.001	0.095	3.758	0.243
	(4)	3391	2064	286	1.984	0.106	4.419	0.250
HACHINHE	(1)	1167	884	144	2.020	0.164	4.158	0.400
	(2)	1189	861	126	2.038	0.164	4.161	0.350
	(3)	943	433	64	1.951	0.089	3.660	0.223
	(4)	3299	2178	334	2.013	0.141	4.516	0.342
SENDAI	(1)	1359	953	181	1.800	0.047	3.737	0.120
	(2)	1349	954	169	1.820	0.046	3.751	0.122
	(3)	1293	588	85	1.920	0.082	3.717	0.207
	(4)	4001	2475	435	1.831	0.050	4.195	0.130
NIIGATA	(1)	662	615	167	1.742	0.087	3.539	0.233
	(2)	674	622	171	1.729	0.080	3.519	0.210
	(3)	575	446	94	1.866	0.119	3.598	0.306
	(4)	1911	1683	432	1.762	0.087	4.004	0.230
WAJIMA	(1)	646	536	69	2.082	0.144	4.011	0.335
	(2)	655	550	71	2.070	0.149	4.011	0.345
	(3)	361	274	25	2.271	0.221	4.036	0.494
	(4)	1662	1360	165	2.105	0.153	4.456	0.353
TOKYO	(1)	1219	983	186	1.868	0.092	3.907	0.240
	(2)	1201	934	173	1.897	0.109	3.949	0.274
	(3)	922	646	117	1.919	0.105	3.802	0.266
	(4)	3342	2563	476	1.889	0.100	4.365	0.256

Table 2 Samples of the calculated values of m and log k and their standard deviations (s. d) at various stations.

N1, N2 and N3 respectively means the total number, the number of data of $A \geq 1.0$ and of $A \geq 2.0$. Component : (1) N-S, (2) E-W, (3) U-D, (4) resultant

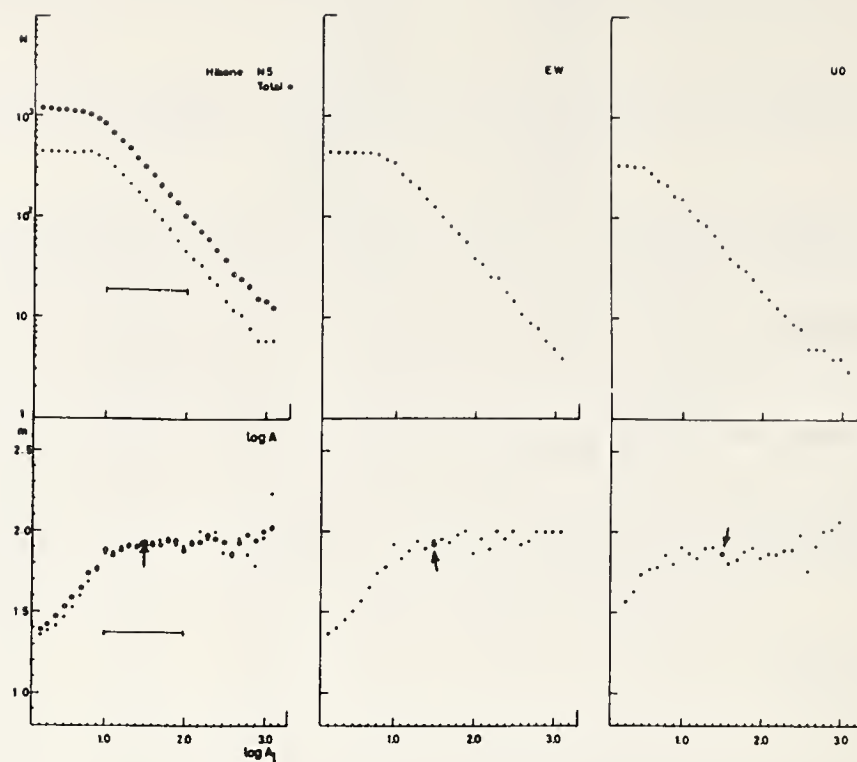


Fig. 1 (a) Relations of N versus $\log A$ and m versus $\log A_j$ at Hikone station

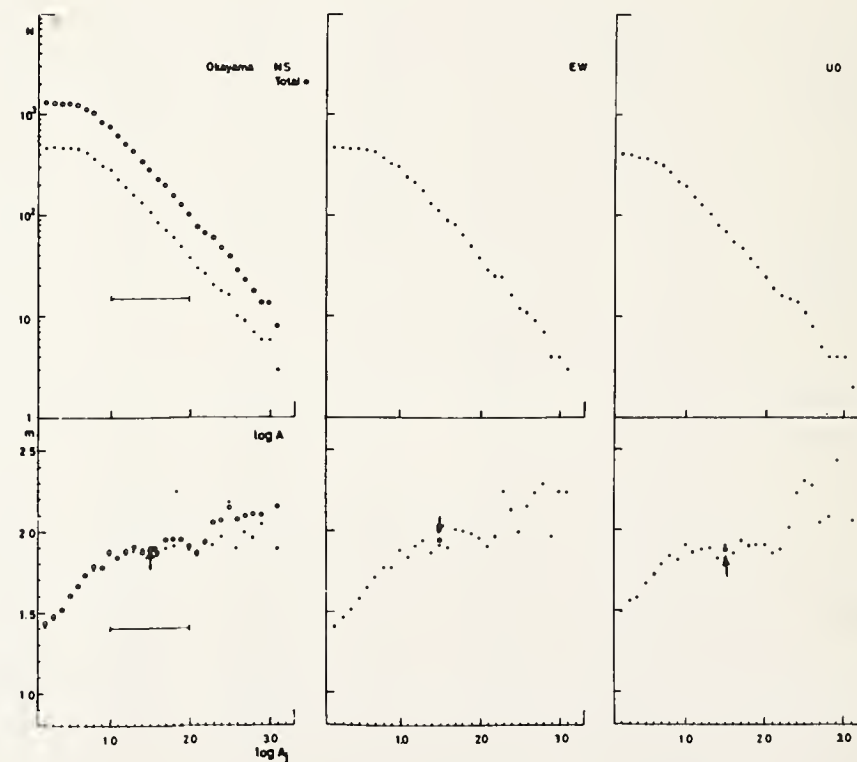


Fig. 1 (b) Relations of N versus $\log A$ and m versus $\log A_j$ at Okayama station

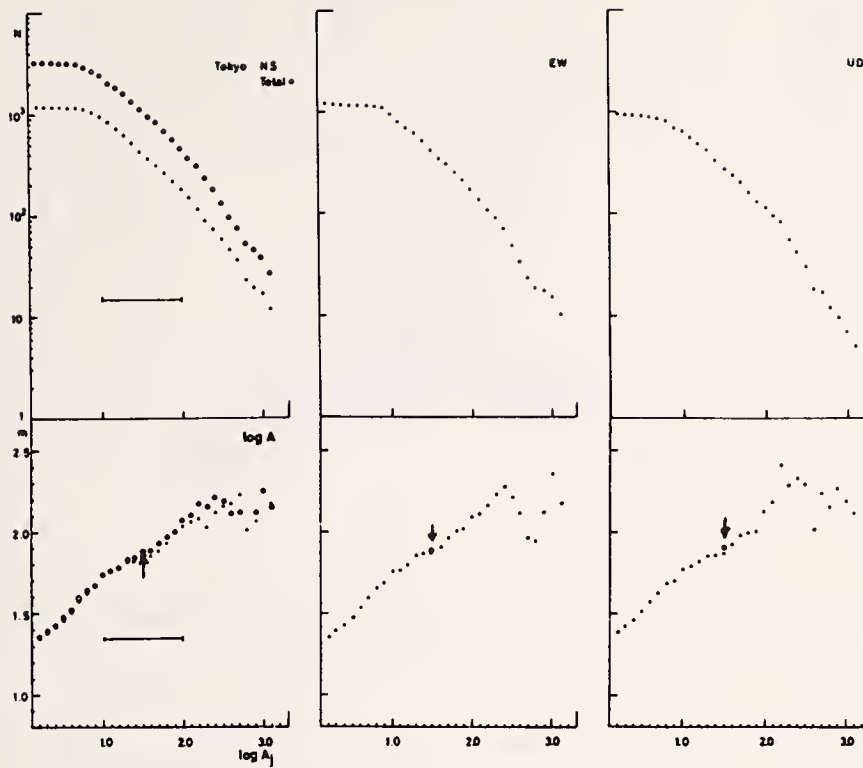


Fig. 2 Relations of N versus $\log A$ and m versus $\log A_j$ at Tokyo station

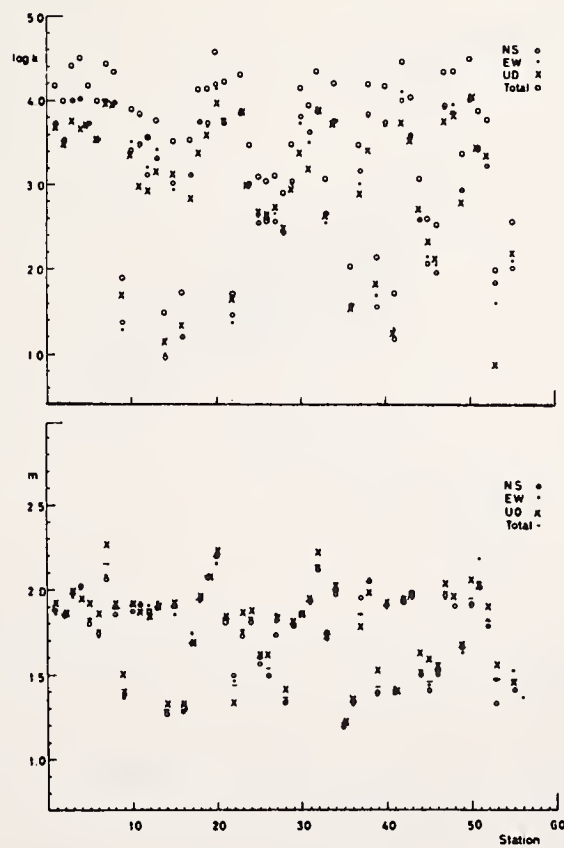


Fig. 3 Values of m or $\log k$ obtained from three components and from resultant many stations

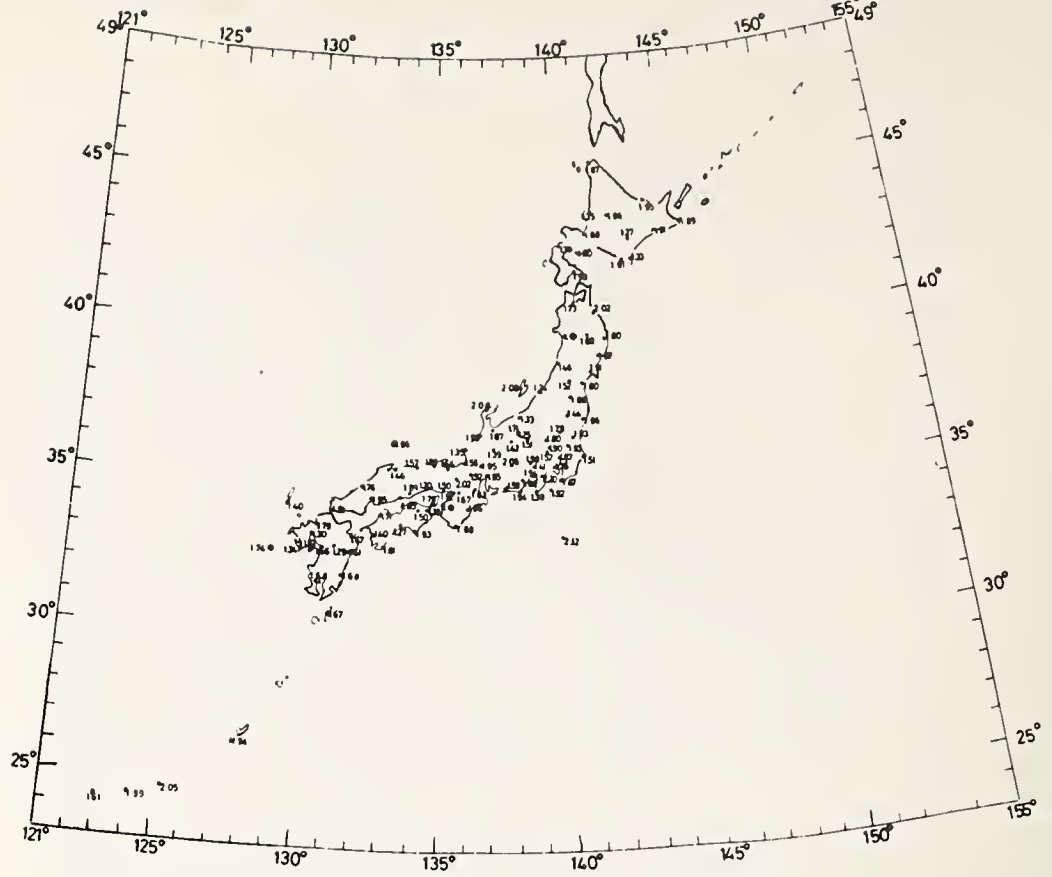


Fig. 4 (a) Regional distribution of the values of m

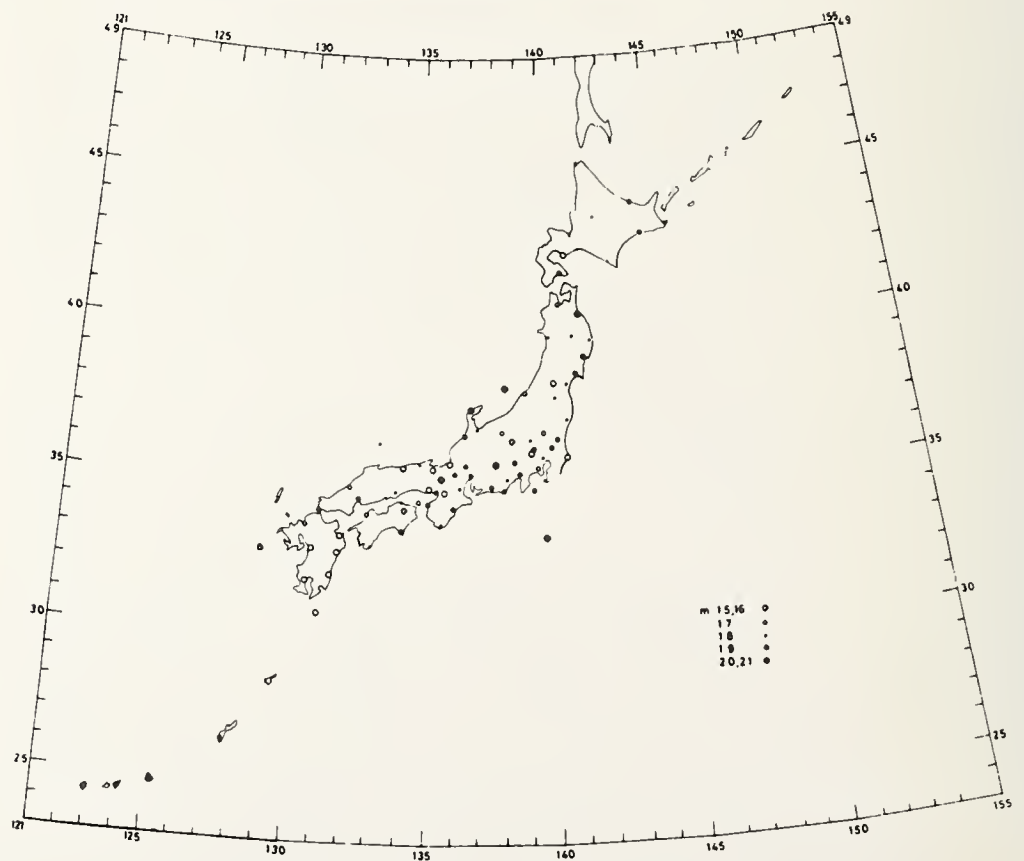


Fig. 4 (b) Regional distribution of the values of m excluding unreliable values of less than 1.5



Fig. 5 Location of stations and districts which appear in the present paper

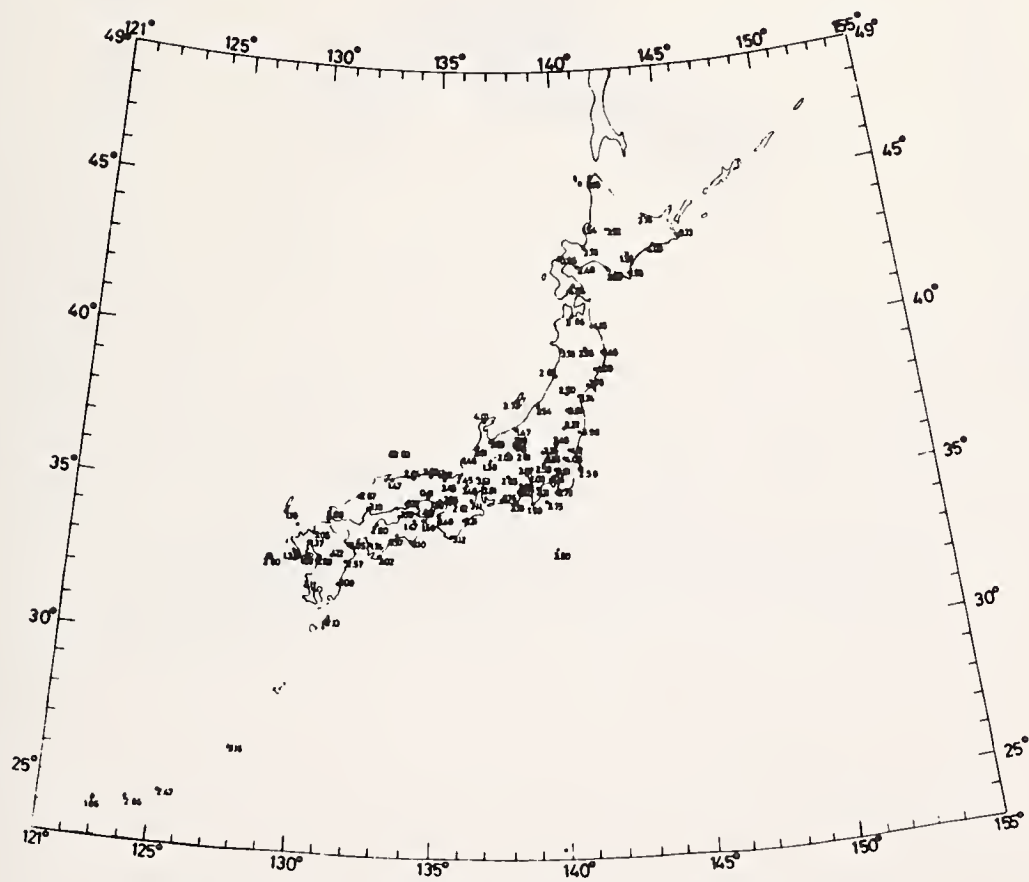


Fig. 6 Regional distribution of the values of $\log k$



Fig. 7 Regional distribution of the frequency when maximum displacement amplitudes of 100 micron will be observed in the coming 100 years

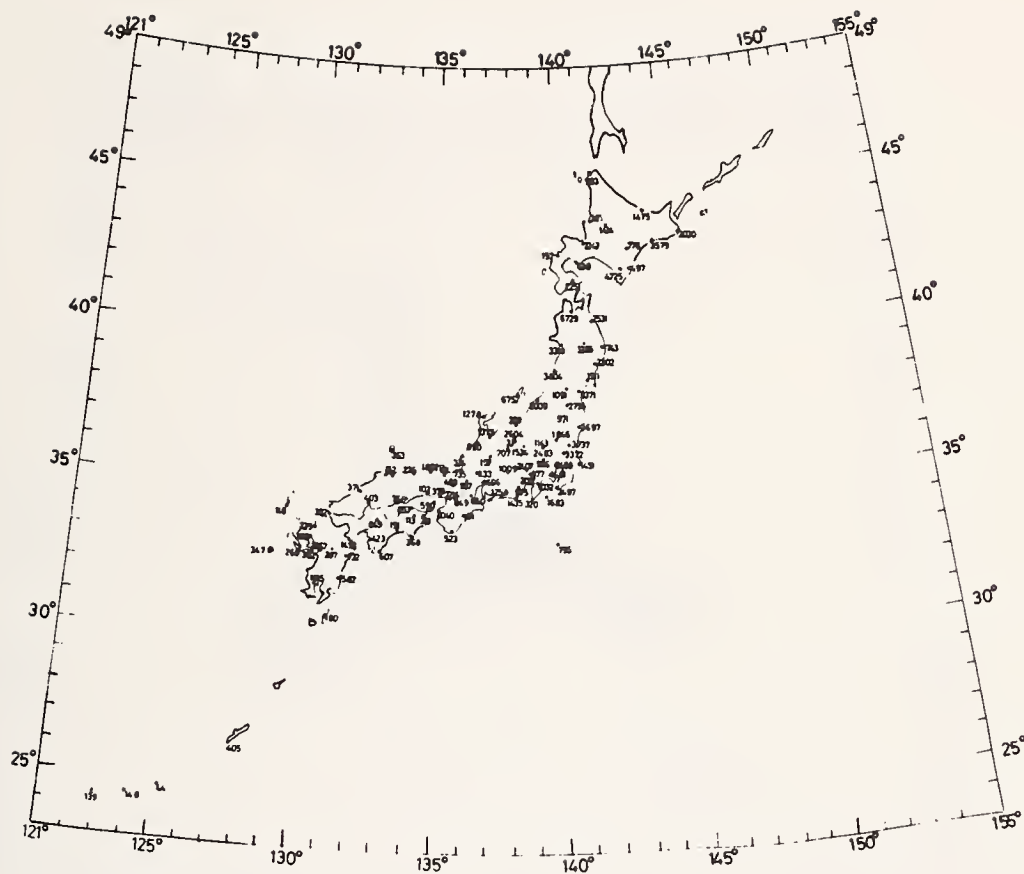


Fig. 8 (a) Regional distribution of the frequency when maximum displacement amplitudes of larger than 100 microns will be observed in the coming 100 years

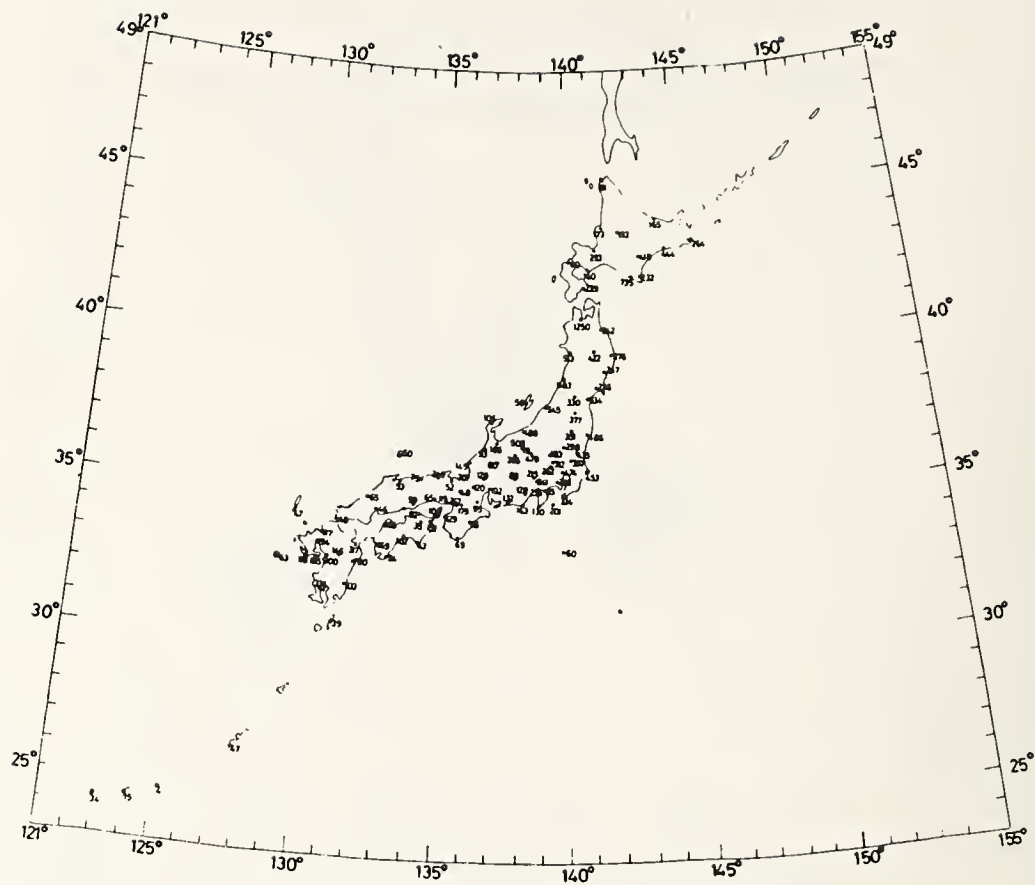


Fig. 8 (b) Regional distribution of the frequency when maximum displacement amplitudes of larger than 1,000 micron will be observed in the coming 100 years

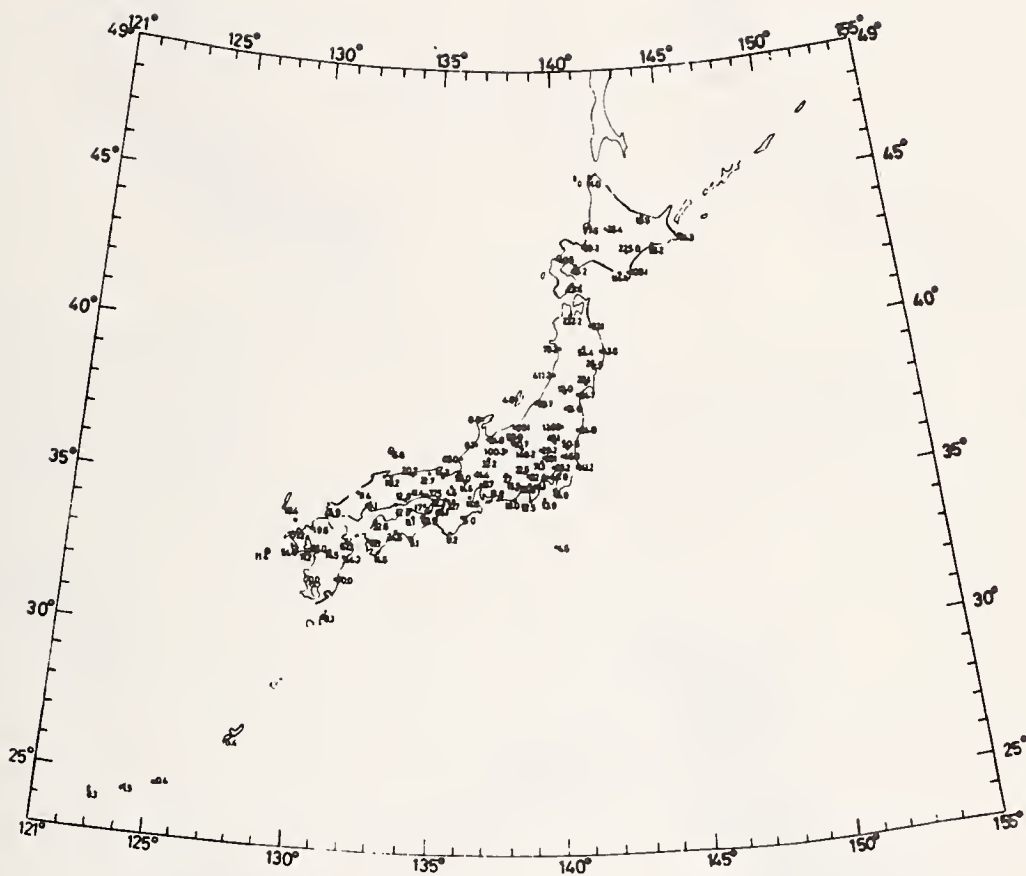
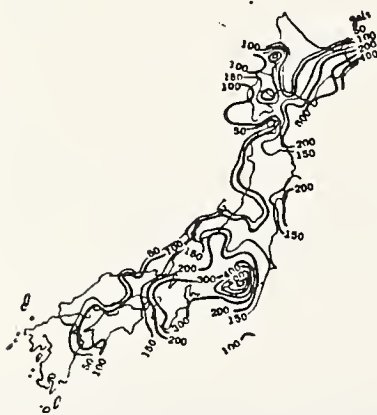


Fig. 8 (c) Regional distribution of the frequency when maximum displacement amplitudes of larger than 10,000 micron will be observed in the coming 100 years



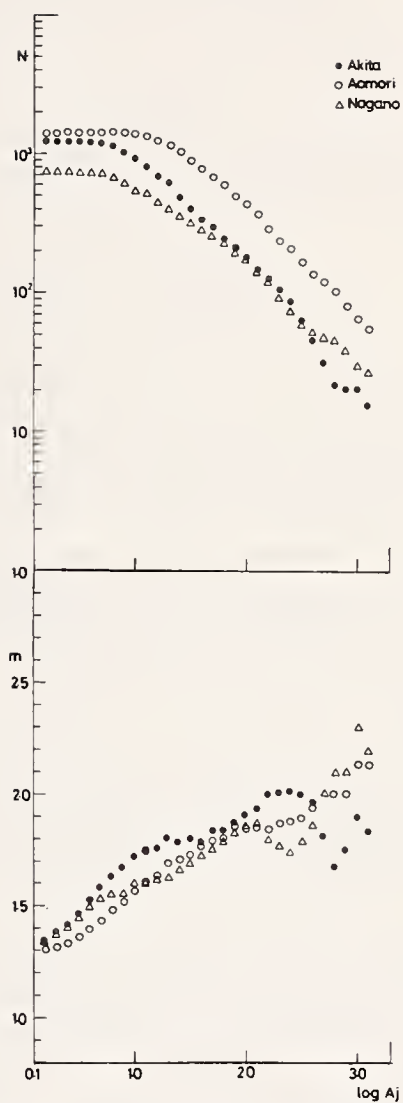


Fig. 10 Relations of N versus $\log A$ and m versus $\log A_j$ (N-S component) at Aomori, Akita and Nagano stations

QUANTIFICATION OF SEISMICITY

by

Tsutomu Terashima and Tetsuo Santo
International Institute of Seismology
and Earthquake Engineering,
Building Research Institute
Ministry of Construction

ABSTRACT

A new seismicity index is proposed in this paper. This index is defined by the following equation;

$$S_T = \left(\frac{\sum_{M \geq 6} N(M)}{T} \right) \Delta \leq 100 \text{ km } M \geq 6$$

where, $N(M)$ represents the number of shallow earthquakes with $M \geq 6$ which have occurred within a epicentral distance Δ of 100 km during the period T (year). Using this criterion, seismicity index maps in or near Japan for two different periods have been made.

Application of this index indicates that a remarkable change of S_T was found in southern part of Boso Peninsula before and after Great Kanto Earthquake of 1923. Therefore, in the field of earthquake engineering, these seismicity index maps can be used as a zoning map of earthquake risk.

Key Words: Earthquake Distributions; Epicenters; Maps; Seismicity Index.

Introduction

Since C.F. Richter (1) defined the magnitude scale (M) of earthquakes, each earthquake has been compared with each other quantitatively by this magnitude.

Relative comparisons of seismicities among various regions, however, have never been made quantitatively, therefore, an attempt to quantifying the seismicity is made in this study.

Definition of Seismicity Scale

Fig. 1 shows epicentral distributions of 3147 remarkable and moderate earthquakes which have occurred in or near Japan during a period from 1900 to 1950. In this figure, the active areas are easily seen qualitatively. If we add the epicenters of smaller earthquakes to this figure, however, the outline of the Japan Islands will disappear by the numbers of dots of the epicenters. Therefore, by this ordinary method, it is very difficult to distinguish between active and nonactive areas.

Fig. 2 shows another method of expressing seismicity by using different marks for different magnitudes. This method, however, is also insufficient to distinguish quantitatively the seismicity of various regions.

Consider the following seismicity index S_T , which is defined here as a quantitatively seismicity scale.

$$S_T = \left(\frac{\sum N(M)}{M_{26} T} \right) \quad \Delta \leq 100 \text{ km} \quad M \geq 6$$

where $N(M)$ is the number of shallow earthquakes with magnitude greater than 6 which have occurred within the epicentral distance of 100 km around a point. When T is taken as 100 years, we shall express S by removing the suffix T , and call the S as the "standard seismicity index".

As seen in Fig. 3, world-wide distributed stations can detect the occurrences of all earthquakes of $M \geq 6$. Therefore, the above definition aims to present only those earthquakes which have $M \geq 6$, which generally cause the most disaster. The limitation of $\Delta \leq 100$ km in the definition of seismicity index S_T was made because the diameter of focal region of the earthquake of $M = 8$ is almost 100 km in diameter. Tsuboi's [2] result also shows that the diameter of the earthquake province in or near Japan is almost 250 km.

Seismicity Index S_T in or near Japan

A value of S_T equal to S_{86} at 735 points in or near Japan centering in the meshes with 0.5° of longitudes and latitudes was calculated during the period of 1885 through 1970. As shown in Fig. 4, the total number of earthquakes measured were 1296, with the highest area of seismicity index equal to 2. This means that earthquakes of intensities of $M \geq 6$ have occurred twice or more in a year. The area, with an index S_{86} or $0.2 \geq S_{86} \geq 0.1$, therefore, represents those locations where earthquakes have the same magnitude which have taken place once in 5 to 10 years. Seismicity regions of $S_{86} \geq 2$ is twenty times larger than that of the region of $S_{86} \leq 0.1$.

Tsuboi [3] has conducted similar studies as presented herein, however, since magnitudes of earthquakes in or near Japan were not sufficiently defined at that time, areas of known earthquakes were used instead of magnitudes. Tsuboi [3] index was called "Passive seismicity index number" as is shown in Fig. 5. The patterns of the contour lines on land as shown in Fig. 4 and Fig. 5 are very similar to each other, however the indexes are different as shown in Fig. 4, the mean frequency of earthquakes ($M \leq 6$) per year is seen clearly but the mean frequency is not distinguished in Fig. 5.

A map of seismicity index S_{45} (1926-1970) after the Kanto Great Earthquake (1923) is shown in Fig. 6, which was made in order to see if the seismicity index changes before and after that Great Earthquake. A remarkable difference is revealed in the southern Boso Peninsula as shown in Fig. 4 and Fig. 6. In this area, the seismicity index is $2 \geq S_{86} \geq 1$ as shown in Fig. 4, while the value is $S_{45} \leq 0.1$ as shown in Fig. 6. This means that the seismicity index has changed to a value of 1/10 of that of the total interval in this area. Dambara [4] has made a cumulative earthquake energy map in or near Japan as shown in Fig. 7. An interesting fact in examining this data is that there is a close interrelation between the contour lines in Fig. 6 and the darkness in Fig. 7. It has also been pointed out by Mogi [5] and Brune [6] that low seismicity sometimes appears before the occurrence of a great earthquake.

Conclusions

A new method of estimating quantitatively the seismicity is proposed. In the field of earthquake engineering, zoning maps for earthquake risk have been determined by a statistical method based on expected acceleration or intensity in various areas. The seismicity index maps presented in the present paper have been developed without considering the expected acceleration and or intensity in various areas. They have been made only to represent the seismicity in various areas precisely and quantitatively. The new seismicity index map, however, will be available as zoning map for earthquake risk.

A seismicity index of S_{45} after 1923 reduced to about 1/10 of S_{86} after 1885 in the area of southern Boso peninsula, which is an area of high density earthquake energy. The above result show that there is an interesting relationship between the occurrence of large earthquakes and the change of S_T .

In the future, similar seismicity maps will be developed for a certain magnitude ranges and the work will be extended to microearthquakes.

References

1. Richter, C.F.: An Instrumental Earthquake Magnitude Scale, Bull. Seism. Soc. Amer., 25 (1935), 1-32.
2. Tsuboi, C.: Earthquake Province - Domain of Sympathetic Seismic Activities Jour. Phys. Earthq., 6(1958), 35-49.
3. Tsuboi, C.: Passive Seismicity Index Number in Japan and Vicinity, Bull. Geophys. Inst. Univ. of Tokyo, 12(1947), 1-6.
4. Damabara, T.: Accumulation of Earthquake Energy (in Japanese), Rep. Coord. Com. Earthq. Prediction 5(1971), 74-78.
5. Mogi, K.: Some Features of Recent Seismic Activity in and Near Japan (1). Bull. Earthq. Res. Inst., 46(1968), 1225-1236.
6. Brune, J.N. and C.R. Allen: A Microearthquake Survey of the San Andreas Fault System in Southern California, Bull. Seism. Soc. Amer., 57 (1967), 277-296.

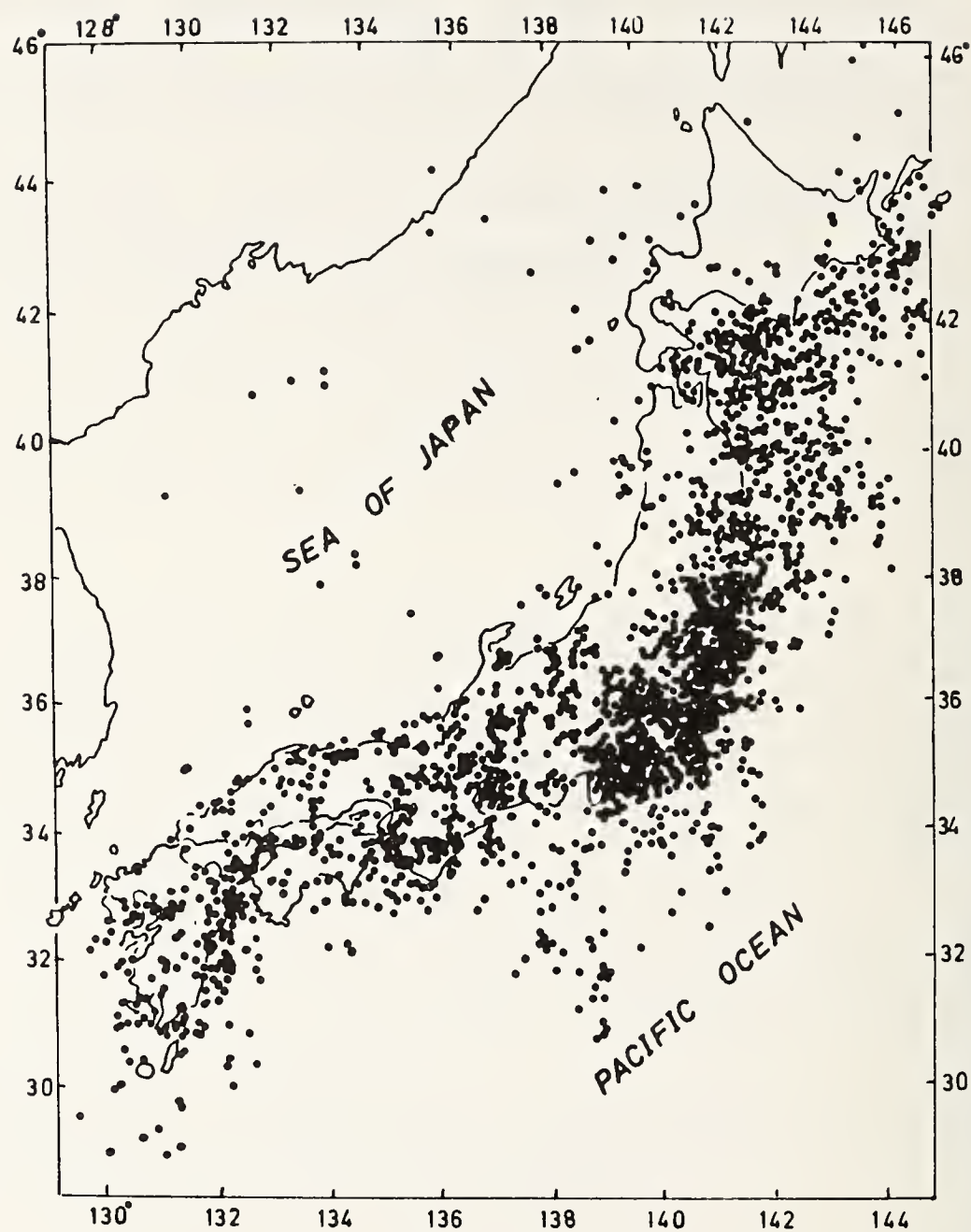


Fig. 1 Epicentres of 3147 earthquakes which occurred in or near Japan in 1900 ~ 1950 (Felt beyond 200 km)



Fig. 2 Epicentral distribution of shallow earthquakes which occurred in or near Japan in 1885 ~ 1970. ($M \geq 6.0$)

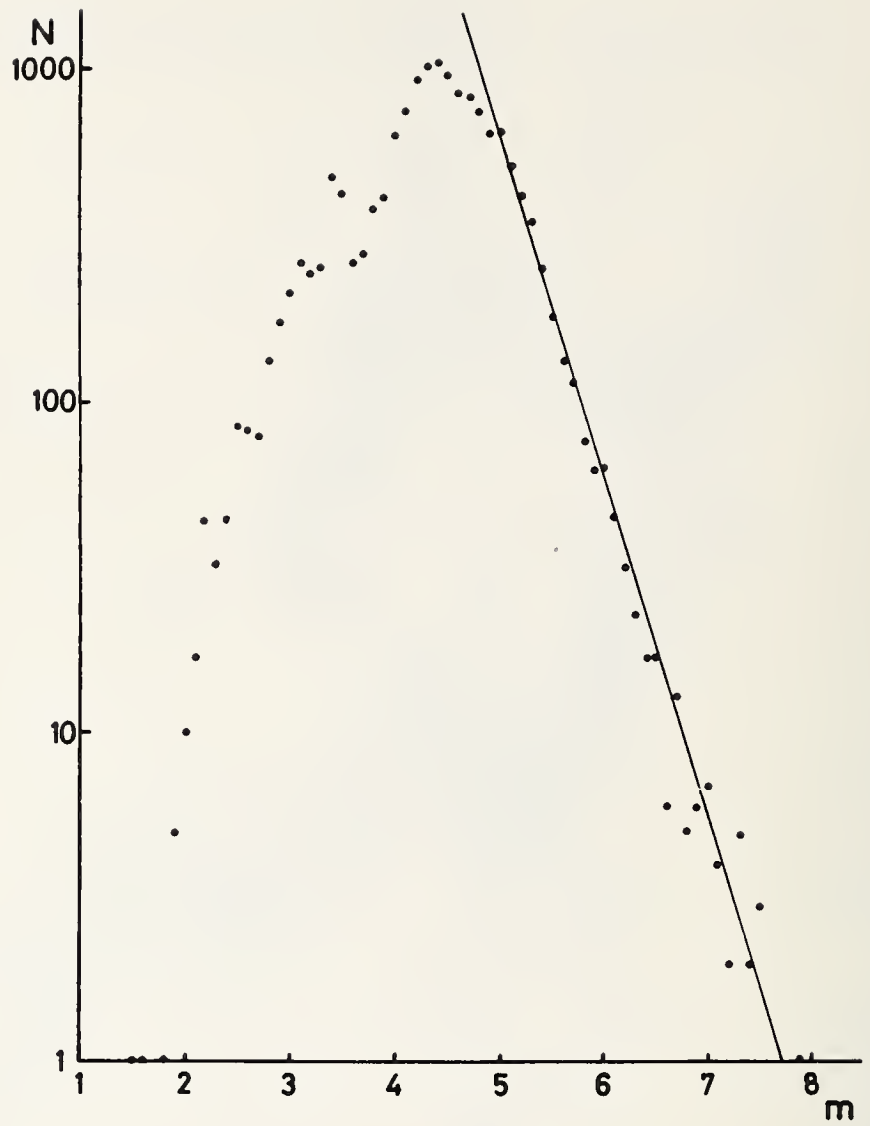


Fig. 3 Reccurrence curve of earthquakes with various magnitude of earthquakes in the world in 1968.



Fig. 4 Seismicity map of index S_{86} (1885 - 1970).



Fig. 5 The map of "Passive seismicity index number"
(After C. Tsuboi [3]).



Fig. 6 Seismicity index map of S_{45} (1926 ~ 1970).

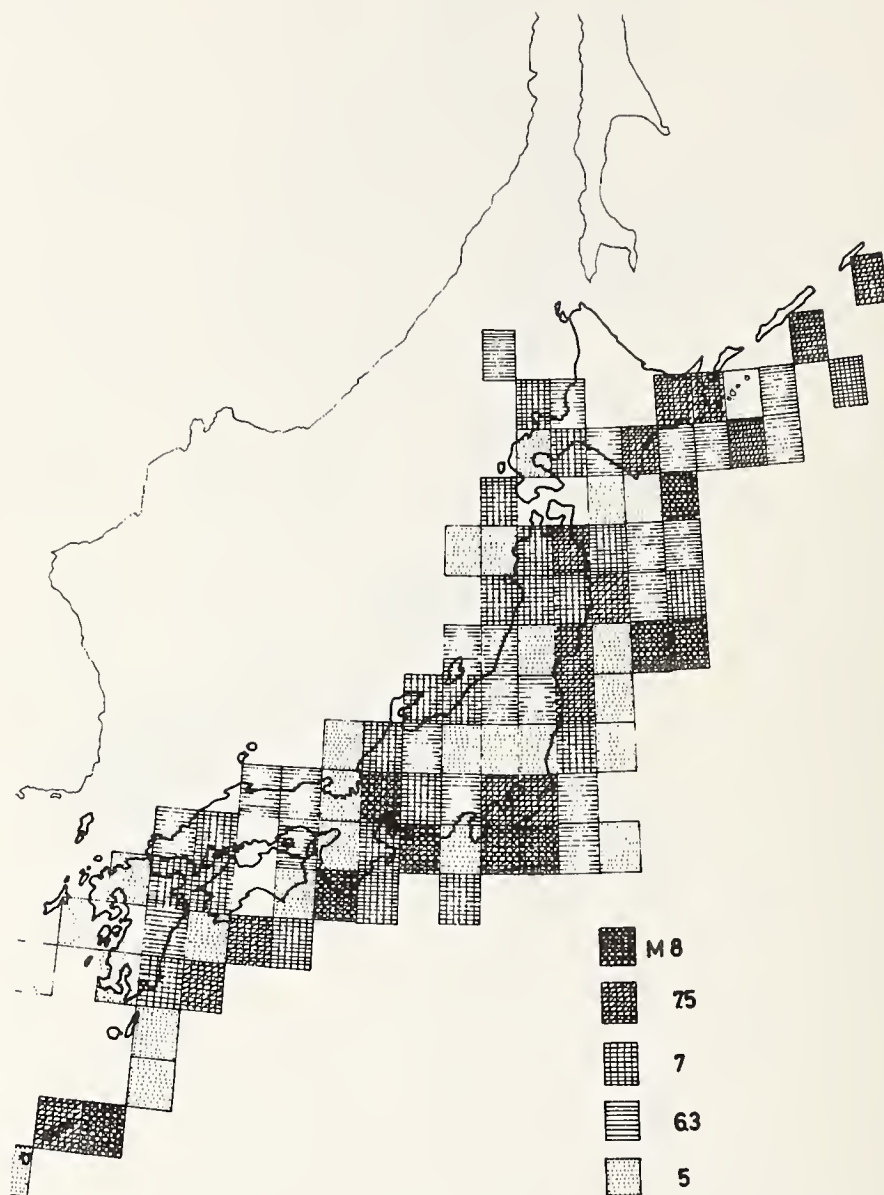


Fig. 7 Accumulation of earthquake energy in or near Japan
(After Dambara [4]).

MAINTENANCE OF THE STRONG-MOTION ACCELEROGRAPH
AND THE DATA PROCESSING OF THE RECORDS

by

Eiichi Kuribayashi
Chief, Earthquake Resistant Structures
Section, Structure and Bridge Division,
Public Works Research Institute, Ministry
of Construction

and

Hajime Tsuchida
Chief, Earthquake Resistant Structures
Laboratory, Structures Division, Port
and Harbour Research Institute, Ministry
of Transport

and

Makoto Watabe
Chief, International Institute of Seis-
mology and Earthquake Engineering, Building
Research Institute, Ministry of Construction

ABSTRACT

The observation of strong-motion earthquakes, located at harbour, public works and buildings throughout Japan by the national research institute has been made. These observations will be discussed, herein, in addition to such items as the maintenance and checks of the strong-motion accelerographs, main records, processing and analyses of records, and the availability of the data to the public.

Key Words: Accelerographs; Earthquake Data; Earthquake Records; Field Observations; Strong-motion Accelerographs.

Introduction

1. History of strong-motion earthquake observations in Japan

The SMAC type strong-motion accelerograph now being used in Japan and in Central and South America, Southeast Asia, and Middle and Near East, was developed by the Strong-Motion Earthquake Observation Committee. The development of this instrument required 2 years and was supported by science research funds of the Ministry of Education in 1950. The instrument has been improved since then and is more suitable to Japanese climate in the resistance against moisture, cold, etc.

In October, 1953 after completion of the strong-motion accelerograph, the Resources Council, Prime Minister's Office recommended the following to the prime minister; "to secure the source of necessary revenue and to improve the setup and consolidation of the necessary strong-motion earthquake observation network and to establish a system required for its operation, in approximately 3 years," and further recommended in January, 1955 that permanent station plan of strong-motion accelerographs be established.

Later, in view of the disaster caused by the Niigata Earthquake in 1964, the Science Council of Japan recommended to the prime minister in November, of that same year; execute a concentrated set of stations to measure strong-motion earthquakes". This recommendation asked for stations at every 50 km throughout the country, thus providing one yardstick for observation density. Further in October, 1971, the Science Council of Japan requested the prime minister to examine the previous recommendations, given earlier.

From 1953 to the end of March, 1974, about 850 strong-motion accelerographs were installed. When the observations were started, the communication among the observation agency and the publicity service were performed by the Strong-Motion Earthquake Observation Committee, which is controlled by the Investigation Board of Resources, Prime Minister's Office. In December, 1956, the controlling authority of the Committee was transferred to Earthquake Research Institute, University of Tokyo. In 1960, the principal strong-motion earthquake records were published by the Committee.

The number of SMAC strong-motion accelerographs, installed after the Niigata Earthquake, increased suddenly in comparison with previous installations, and thus it is difficult for the Strong-Motion Earthquake Observation Committee to examine these. In this situation, the Liaison Conference for Promotion of Strong Motion Earthquake Observation Project comprising concerned government offices, heads of concerned agencies and specialists, was established in the National Research Center for Disaster Prevention, Science and Technology Agency. The conference group decided to be responsible for communication and coordination of the nationwide promotion of the strong-motion earthquake observation project. The conference participants analyzed the present state of stationary strong-motion accelerographs, and discussed how to increase the observation network, and at the same time provided a publicity service for collection of the principal records. In February, 1972, the group arranged and published their opinions regarding the improvement of the observation network. According to the publications, they proposed to establish 2,141 strong-motion accelerograph stations throughout the country. Therefore, even if all the strong-motion accelerographs

presently installed are considered to be effectively operating, installation of about 1,300 additional strong-motion accelerographs is necessary.

2. Necessity to strengthen and enlarge the strong-motion earthquake observation network.

The strong motion earthquake observations stated herein, refers to the measurement of acceleration amplitude waveforms caused by tremors of the ground and structures at the time of a strong-motion earthquake. Such measurements relate to the reading of the measured waveforms, and to the primary analyses of the magnitude of the acceleration amplitude, periodical characteristic of the waveforms, etc.

Strong-motion earthquake observations and the subsequent analyses of the magnitude of the acceleration amplitude and the periodical characteristic of the waveforms has resulted in relationships between the magnitude of the earthquake, epicenter distance, seismic center depth, topography, geology, scales, construction, and material of the structures.

The analytical results of the strong-motion earthquake observations give quantitative information and thus will permit an establishment of countermeasures for the earthquake disaster prevention for each region of the country and for type of soil. It further rationalizes the seismic design of structures built on the ground, and moreover rationalizes the aseismatic design of the structures which grow diverse, massive, and complex, considerably contributing to safe and economical constructions of these structures. An example of such a highly dense network, for measuring strong-motion earthquakes, has been established around Los Angeles, California, USA. These observations were initiated in 1932, and have since obtained 250 strong-motion accelerographs records prior to the 1971 Los Angeles Earthquake.

In this country, strong-motion earthquake observations were initiated in March, 1953, when a strong-motion accelerograph (SMAC type) made in Japan, was installed in the Earthquake Research Institute, University of Tokyo. Since then, various universities, government agencies, and various private groups have cooperated in the enlargement and strengthening of the strong-motion earthquake observation network. Finally at the end of March, 1974, the total number of SMAC strong-motion accelerographs stationed throughout Japan was about 850, and though not reaching the required density.

The strengthening and enlargement of the strong-motion earthquake observation network is necessary in order to achieve the aim described previously, thus it is still desirable to increase the density of this still sparse observation network.

Strong-Motion Earthquake Observations in Ports and Harbours

1. Present state of the observation network

The strong-motion earthquake observations of port and harbour areas in Japan, have been executed since 1962 under the cooperation of Port and Harbour Research Institute and various agencies concerned with ports and harbours. This has been executed under an agreement initiated by a research group consisting of the Port and Harbour Bureau of Ministry of Transport, respective District Port Construction Bureaus, Port and Harbour Research Institute, and other concerned agencies. As of December, 1974, the observation network consists

of 65 strong-motion accelerographs, installed at 44 ports. Figure 2-1 shows the locations of the ports and harbours, where the strong-motion accelerographs are installed. Figure 2-2 shows the number of installed accelerographs per year. There are 2 types of strong-motion accelerographs that used in observation network: one was a SMAC-B₂ strong-motion accelerograph and the other a ERS strong-motion accelerograph. The description of the SMAC-B has been reported previously (2-1). The ERC strong-motion accelerograph is an accelerograph with a moving type coil transducer, which is available as Type A with a magnetic tape recorder, and as Tape B or C with an electromagnetic oscillicgraph. Types A and B record 2 horizontal components, and Type C records 2 horizontal components and a vertical component. The ERS strong-motion accelerograph can be used with the transducer and the recorder. This provides an advantage, for observing the earthquake response of port and harbour structures in which strong-motion accelerograph rooms are impossible to make.

2. Maintenance and check of strong-motion accelerographs

The strong-motion accelerographs, installed in port and harbour areas are maintained by the construction work offices, etc. at the respective ports. The staff in charge of the maintenance and check of the strong-motion accelerographs (normally the staff for public works) are assigned to conduct periodical checks (twice a month) and to perform special checks after the occurrence of earthquakes of II or more in the earthquake intensity scale of Meteorological Agency.

Also, once or twice a year, a detailed check is made by the manufacturer engineers of the strong-motion accelerographs. In addition, the Port and Harbour Research Institute conducts training of the staff in charge of operations, every year. The training is practical, and relates to handling of the strong-motion accelerographs by the engineers dispatched from the manufacturers of the strong-motion accelerographs. A strong-motion accelerograph is initiated when the starter senses the tremors of magnitude 50 to 10 gals. When a strong motion accelerograph does not start at the time of an earthquake, it is difficult to judge whether the tremors were too small or there was failure of the accelerograph. For this reason, a strict acquisition rate of records cannot be shown. However, what will be introduced is a case to show the record acquisition state of the observation network. At the time of the Tokachi-Oki Earthquake in 1968, 15 strong-motion accelerographs located in the ports and harbours of Hokkaido, and Tohoku district recorded the tremors. Only one accelerograph did not record, due to its own failure.

3. Principal records

From those records obtained by the strong-motion earthquake observations in port and harbour areas, those exceeding about 100 gals in the maximum acceleration are shown in Table 2-1 and are classified by each observation point. As an example of recorded wave-forms, the record of the Tokachi-Oki Earthquake in 1968 at Hachinohe Port is shown in Fig. 2-3.

4. Processing of records

a) Storage of records

All the records obtained at the respective observation points, are sent to the Port and Harbour Research Institute, to be catalogued and stored. Copies of

records are also sent to the respective observation points. The records acquired are classified for each earthquake every 2 months, and with a "Strong-Motion Earthquake Observation Table" showing the maximum acceleration of each component of the respective records, which are sent to the parties concerned.

b) Digitization of records

For those records which were obtained on the ground and exceed 50 gals in maximum acceleration, the horizontal components are digitized.

The record by an SMAC-B₂ strong-motion accelerograph is copied by contact printing on Mylar-based sensitive paper, and is digitized by a semi-automatic digitizer. The digitizer places a cursor on the position requiring digitization, coordinate values are then punched on a paper tape by pressing a switch. The time intervals used during the digitization, are 0.01 sec. The numerical values which were punched on the paper tape are then read by an electronic computer, and reproduced as waveforms by a graphic output unit in order to confirm that the readings were correct. Any errors noticed are then corrected. The corrected records provide amplitude values at unequal time intervals, and are converted into amplitude values at the equal time intervals of 0.01 sec by interpolation, and are then recorded on magnetic tape. In principle, the zero-line is not corrected, however when the zero-line is not properly inserted for those waveforms reproduced by the graphic output unit, the digitization is re-evaluated. However, if time is not available because of the many records to be processed, the waveforms are enlarged by the graphic output unit, in order to determine the corrective amount of the zero-line position, for correction in the electronic computer.

The records from the ERS-B/C strong-motion accelerograph is digitized using a different digitizer than that used for the SMAC-B₂ strong-motion accelerograph. This digitizer is interlocked with a computer and if an operator moves the cursor along the recorded waveforms, an amplitude value is stored in the computer each time the cursor moves 0.1 mm along the time base.

After end of digitization, the numerical values stored in the computer are reproduced by a digital-to-analogue converter as an analogue voltage which are recorded by a pen-writing oscillograph. After conformation that the recorded waveforms have been correctly digitized, numerical values are punched to the paper tape. They are then read by another computer, and recorded on magnetic tape together with the records of the SMAC-B strong-motion accelerographs.

No corrections are made, to the ERC-B/C strong-motion accelerograph records. The minimum time intervals for digitization, relate to the recording paper feed rates of the respective strong-motion accelerographs. These rates are 0.005 sec. for Type B and 0.0025 sec. for Type C. However, the records which are stored on the magnetic tape, have the same time intervals as those of SMAC-B strong-motion accelerograph. It was experimentally confirmed, that the digitization of the ERC-B/C strong-motion accelerograph records, could be reproduced with an accuracy which causes no viewing difficulty for practical use.

c) Spectral analysis

For all the digitized records, the response spectra and Fourier spectra are calculated. Other various spectra are calculated according to necessity.

5. Opening of data

The records obtained by the strong-motion earthquake observations in port and harbour areas, are published in the "Annual Report on Strong Motion Earthquake Records in Japanese Ports" ²⁻²⁾. The annual report covers the maximum acceleration of each component of every record, the seismic center location, magnitude, seismic intensity at the respective location for the earthquake corresponding to each record. Moreover, the ground recordings for those with accelerations of 20 gals or greater have their waveforms reproduced, and for those with maximum accelerations of 50 gals or greater have their waveforms digitized with response spectra and Fourier spectra provided.

The published annual reports extended from 1963 to 1974 ²⁻²⁾. Also the record of the Tokachi-Oki Earthquake in 1968, has been published separately ²⁻³⁾.

The data where each strong-motion accelerograph has been installed, are published as "Site Characteristics of Strong Motion Earthquake Stations in Ports and Harbours in Japan" ^{2-4, 2-5, 2-6)}. The data at these observation points, covers the geographical features where the installations are located such as the configurations of the buildings, foundations of the strong-motion accelerographs, design drawings of the strong-motion earthquake observation rooms, and soil histograms. The results of these observations are given in the annual report as in the analytical results such as average response spectra and seismic tremor characteristics of the ground ^{2-7, 2-8)}.

Strong-Motion Earthquake Observations at the Public Works Research Institute

1. History of strong-motion earthquake observations at the Public Works Research Institute

The strong-motion earthquake observations at the Public Works Research Institute, were initiated in 1957 when an SMAC type Strong-motion accelerograph and an electromagnetic strong-motion accelerograph were installed in Kinki Regional Construction Bureau. Seventeen years later, at the end of March, 1974 a total of 189 strong-motion accelerographs were installed for the public works facilities using the research funds of the Public Works Research Institute and funds from various civil engineering construction projects.

This report describes the history, system and future promotion of strong-motion earthquake observations at the Public Works Research Institute, and refers to the entire nation and Ministry of Construction projects and their inter-relationship.

2. Progress of the strong-motion earthquake observations

a) Observation stations

The strong-motion earthquake observations, at the civil engineering work facilities such as bridges, dams, embankments and tunnels are executed under the cooperation of various agencies. These agencies consist of the Public Works Institute, Regional Construction Bureaus, local governments (Civil Engineering Works Department, Board of Project), 4 public corporations concerned with

civil engineering works, and the Hokkaido Development Agency. Since the observations were started in 1957, with the use of an electromagnetic type strong-motion accelerographs at the Sarutani Dam in the Kinki Regional Construction Bureau, additional observation stations have increased gradually. Since the Niigata Earthquake in 1964, the installation of additional strong-motion accelerographs was promoted and increased by notification of the Director of the Road Bureau. At the end of March, 1974, 189 SMAC type strong-motion accelerographs were installed at 96 stations and electromagnetic type strong-motion accelerographs with 448 components, were installed at 48 stations. The locations of the observation stations of the SMAC type strong-motion accelerographs and the electromagnetic type strong motion accelerographs are shown in Figs. 3-1 and 3-2. The number of installed accelerographs per year, are shown in Table 3-1, and the numbers of installed accelerographs per structural type are shown in Table 3-2.

b) Strong-motion accelerographs

The strong-motion accelerographs used for observation are the SMAC type strong-motion accelerographs and electromagnetic type strong-motion accelerographs, with the SMAC type, especially Type B₂, used predominantly. However, recently, Type E₂ and Type Q, which allows one to measure the components in a shorter period than permitted by Type B₂, were installed. The electromagnetic type strong-motion accelerograph uses an electromagnetic method for the transducer, and an electromagnetic oscillograph or magnetic recorder for the recorder. In using a transducer for the strong-motion accelerograph, the moving coil type accelerometer is used most often, variations of the transducer in size and weight, is considered dependent on the installation location and where the SMAC type strong-motion accelerograph cannot be installed. Recently, observations of seismic tremors in the ground under the surface of the ground have been executed. At present such observations, by the electromagnetic type accelerographs, have been made at 15 stations (149 components) out of 48 stations. The number of measuring components and units used of each electromagnetic type strong-motion accelerograph differ according to each station.

c) Observed records

The records obtained from the initiation of the observations until the present consist of about 3,817 Sheets (including 869 Sheets for the Matsushiro Earthquake Swarm) as recorded by the SMAC type strong-motion accelerographs, and about 210 Sheets by the electromagnetic type strong-motion accelerographs. Most of the records listed values of less than 100 gals, and the number of records of 100 gals or more were about 77 (including about 30 records for the Matsushiro Earthquake Swarm) as shown in Table 3-3. The largest recorded waveforms obtained to date were from Uwajima City, Ehime Pref., which had a maximum acceleration of 438 gals, with the waveforms as shown in Figs. 3-3 and 3-4.

3. Observation net-work

The strong-motion accelerographs was installed according to the public works construction sites. Since the past several years, the increase in the number of installed accelerographs has shown a tendency toward an uneven distribution in specific areas, this then shows what areas need accelerographs installed. The ideal plan, for stationing strong-motion accelerographs, is to obtain a record in the adjacent area of the epicenter when an earthquake with V or more seismic intensity (JMA) occurs in any part of Japan. The present status, however, makes it impossible to approach these ideal conditions in the near future. Therefore, the following network has been drafted to promote a strong-motion earthquake observation project.

The network involves the installation during the next five years (1975-1979), and to install others according to necessity. The network plan was drafted per the following conditions:

- (1) The entire land area of Japan should be covered with 258 equilateral triangle meshes (one side is about 50 km), for the stationing at least 1 observation station in 1 mesh.
- (2) Covering all the meshes in Japan, uniformly with extreme urgency.
- (3) At least one each, at the top and bottom of a structure, with a total of two sets, should be installed at one observation station.
- (4) Consideration of those installed strong-motion accelerographs, from other ministries, should be taken into consideration.

In order to determine the total number of strong-motion accelerographs to be installed in the future, the present stationing state was investigated as shown in Fig. 3-5. The meshes, without strong-motion accelerographs can be selected as dark meshes shown in Fig. 3-6, and where, 146 stations (292 sets) require installation. The complete installation is planned for completion in the latter 3 years of the five-year project. The draft of the network is still under adjustment with the sponsoring organizations.

4. Checks and collection of records

The maintenance and control of the strong-motion accelerographs, related to the civil engineering works facilities, have been executed by the notification from the Director of the Roads Bureau and the Director of the River Bureau. These notifications were delivered in April, 1970, and have been instituted by the offices controlling the facilities in which the strong-motion accelerographs were installed. Examination of the strong-motion accelerographs involve periodic checks and special checks by the staffs of respective offices. Also technical checks by special engineers, of the manufacturers of the strong-motion accelerographs, have been made.

a) Periodic check

A check of the equipment has been conducted every 2 weeks, in order to confirm the preparedness of the equipment

b) Special check

When there is an earthquake of II or more on the seismic intensity of JMA, in the neighborhood of the observation station, a special check is

conducted to collect a record.

c) Technical check

This check is conducted, by a special engineer of the manufacturer of the strong-motion accelerograph, once or twice a year.

5. Collection, storage, analyses and publication of the records

All the seismic records obtained at the respective observation stations are mailed to the Public Works Research Institute for arrangement and storage. The arrangement and analyzing work of the seismic data and records are performed based on the flowchart as shown in Fig. 3-7. When the records are obtained, those with a maximum acceleration of 50 gals or more are digitized. The digitization is performed by use of a semi-automatic digitizer, according to the flowchart as shown in Fig. 3-8. The resolution of the digitizer is 25 microns, and the overall precision is 0.125 mm. The digitized records are subjected to a circular correction (in case of SMAC-B₂), a zero-line correction and a time base correction by an electronic computer. The data is converted into numerical values at 0.01 sec. intervals, by linear interpolation. Also developed from the waveform analyses, are autocorrelation coefficients, Fourier spectra, power spectra and various response spectra which are digitized and is further processed for graphic output unit.

The publication of the observation data and the strong-motion earthquake records, are published every year. The recorded waveforms of the previous year are copied in full-scale, and arranged in order to give of the various contrast seismic values. The tables of the numerical values are also published, when a predetermined volume of data is accumulated. The data published to date are contained in 12 books (references 3-1 to 3-6, 3-9, 3-11, 3-13, 3-16, 3-17) for strong-motion earthquake records and 5 books (3-7, 3-8, 3-14 and 3-15) for tabular numerical values.

Strong-motion Earthquake Observations at the Building Research Institute

1. History of strong-motion earthquake observations, concerned with building

In 1954, a strong-motion accelerograph Type SMAC-A, was installed at the Building Research Institute by the Director of Housing Bureau, Ministry of Construction. The observation network, close to the number of present strong-motion accelerographs, was then formed in the 1960s. The types of strong-motion accelerographs that were installed, were Type SMAC-A, Type DC developed jointly with the Research Institute, and Types SMAC-B₁ and SMAC-B₂, improved version of SMAC-A. Since the initially installed SMAC-A type became superseded, the SMAC-M type was intended for complete automation and digitization by the 2nd joint development with the Research Institute. This type has been used since 1973 as a strong-motion accelerograph. In 1974, the mobile observation network, comprising several strong motion accelerographs commonly called "Caravan" was initiated for installation. This is to be preferably installed for a period of several years in the place most likely to be subjected to strong-motion earthquakes according to the information relating to the prediction of earthquakes. Also, if the intended strong-motion record can be obtained, it is to be moved to the next place with high earthquake occurrence probability. In the building field, the Earthquake Research Institute of the University of Tokyo has been performing strong-motion earthquake observations together with this research institute.

However, in order to maintain the increased number of installed strong-motion accelerographs, the National Research Center for Disaster Prevention and the Science and Technology Agency have shared a part of the observation network. The strong-motion accelerographs related to buildings are primarily installed in the multistory structures with 45 m or more height these buildings are constructed by special permission of the Minister of Construction according to the stipulations of Article 38 of the Building Standard Law. The number of installed strong-motion accelerographs of this kind has sharply increased in accordance with the increase of construction of multistory buildings as shown in Fig. 4-1. However, the maintenance and control capacity of the Building Research Institute Earthquake Research Institute of University of Tokyo, the National Research Center for Disaster Prevention, and parts of private and public corporation, are beyond their capacity.

2. Present state of strong-motion earthquake observation network related to buildings

The Building Research Institute installs strong-motion accelerographs about every 100 km along the coasts throughout Japan. These installations are mainly in the neighborhood of the foundations of the buildings. As shown in Fig. 4-2, 31 strong-motion accelerographs are installed in 18 places. There are 8 sets of Type SMAC-A, 6 sets of Type SMAC-B 9 sets of Type SMAC-M and 8 sets of Type DC.

The numbers of strong-motion accelerographs relating to buildings and the agencies in charge of maintenance and control are shown in Table 4-1. In addition, the Building Research Institute set up the afore-said "Caravan" at 2 places. Each Caravan has strong-motion accelerographs on the foundations in the neighborhood of the vertexes of an equilateral triangle with about 1 km sides. Recorded are the absolute time and common time in order to allow accurate acquisition of the propagation direction of seismic waves, etc. One Caravan is installed in the Numuro Peninsula, which is said to have residual energy in the seismic center, with the expected seismic scale similar to that of the previous time, and the other Caravan is installed in the neighborhood of "Omaezaki" facing the Sea of Enshu since the next big earthquake is expected to occur in the Sea of Enshu trough with a magnitude of 8.

3. Maintenance and check of strong-motion accelerographs related to building

The organization system of maintenance and control in the Building Research Institute is shown in Fig. 4-3. The Building Research Institute asks local engineers concerned with the buildings at the observation points to perform maintenance and check at the observation spots with due remuneration. The local staffs performed a monthly check, and when they find any trouble and shortage of spare parts, etc. they inform the Building Research Institute. The Building Research Institute then dispatches a repairman or sends spare parts to the location. When a strong-motion earthquake has occurred in the neighborhood of any location, the local staff instantly checks the strong-motion accelerograph, and if there is any record available, he enters the data and puts the record in a metallic cylinder. The cylinder is then sent by airmail to the Building Research Institute, irrespective of the magnitude of the record. Moreover, in order to improve the technique knowledge of the maintenance and checks performed by the staff concerned with strong-motion earthquake observations, a short study course has been given every three years by

Building Research Institute. The maintenance and check of the strong-motion accelerographs related to buildings are vary in their systems and organizations, etc. In agencies other than the Building Research Institute consist of the following:

An agency in charge of observations has one responsible technician concerned with, strong-motion earthquake observations and he maintains, checks, ment.

The actual maintenance, checks and repairs are performed by an external engineering contractor at an interval once or twice a year. The strong-motion earthquake records are collected by the responsible technician of the agency or the external engineering contractor. A common trouble with all the agencies is obtaining the budget for maintenance, checks, and repairs. This is because the fund must be raised from the budget under another item, and does not appear as an independent budget.

4. Processing method of strong-motion earthquake records

Since the record processing method is about the same among all agencies related to buildings, the processing method employed by the Building Research Institute will therefore be introduced herein. The Building Research Institute uses roughly 3 types of strong-motion accelerographs: (1) those obtained by smoked paper recording, (2) those obtained by stylus paper recording, and (3) those obtained by magnetic tape recording. In the former two types, the original record is copied by contact with the negative plate, and is digitized according to the flowchart shown in Fig. 4-2, the data is then analyzed by the computer, for generation of a list of digitized data. In case of the magnetic tape, the record is directly digitized by a high speed analogue-to-digital converter, and then analyzed as described in Fig. 4-2. The utilization of strong-motion earthquake records do not require immediate evaluation. However, the publishing of the analyzed results, before general engineers and administrators lose their interest in the earthquake, is necessary in order to provide them with the significance of the strong-motion earthquake observations. Therefore, the Building Research Institute has prepared a completely new process for all records, thus permitting the data to be distributed within 4 days after collection.

5. Publication of records

The strong-motion earthquake observation records related to building, which have acceleration values exceeding 40 gals, are sent to the Liaison Committee for Promotion of the Strong-Motion Observation Project. These records are then published semi-annually as original records (analogue values) including the additional information relative to the seismic center, seismic scale, time magnitude, and seismic scale distribution at various places. The Building Research Institute published the digitized tables and analyzed results of the main strong-motion earthquake records in Annual Research Work of the Building Research Institute, the B.R.I. Research Paper, the News of Japan Society for Earthquake Engineering Promotion, etc. In addition, about once a decade, the "Digitized Strong-Motion Earthquake Accelerogram in Japan" is also published. This data contains earthquakes location of each observation point, incessant tremor Fourier spectra of the point, the external view photo and sectional view of the building in which each strong-motion accelerograph is

installed, strong-motion records and their digitized tables, response spectra of dislocation, speed and accelerations.

6. Examples of the principal strong-motion earthquake records

Table 4-2 shows the records which have a maximum acceleration exceeding 100 gals, and from those records obtained on the 1st floor of foundation of the building. Also from these records illustrated are the data of the strong-motion earthquake record obtained at Kawagishi-cho Apartment of the occasion of the Niigata Earthquake (June 16, 1964). This earthquake was the most significant in the history of strong-motion earthquake observations in Japan, and the record of the strong-motion accelerograph of Hiroo Town Office on the occasion of the Hitaka Sandei Earthquake (July 21, 1970) which recorded the largest acceleration as of this date.

References

- (2-1) Present Status of the Observations of Strong-Motion Earthquakes in Japan, T. Ariga, The 1st Joint Meeting of Wind and Seismic Effects, U.J.N.R., 1969.4
- (2-2) Annual Report on Strong-Motion Earthquake Records in Japanese Ports (1974), E. Kurata, I. Ishizuka and H. Tsuchida Technical Notes of the Port and Harbour Research Institute, No. 202, 1975.3
- (2-3) Strong-Motion Earthquake Records on The 1968 Tokachi-Oki Earthquake and its After Shock, H. Tsuchida, E. Kurata and K. Sudo, Technical Notes of the Port and Harbour Research Institute. No. 80, 1969.6
- (2-4) Site Characteristics of Strong-Motion Earthquake Stations in Ports and Harbours in Japan (Part I), H. Tsuchida, T. Yamada and E. Durata Technical Notes of the Port and Harbour Research Institute. No. 34, 1967.11.
- (2-5) Site Characteristics of Strong-Motion Earthquake Stations in Ports and Harbours in Japan (Part II), E. Kurata, H. Tsuchida and K. Sudo Technical Notes of the Port and Harbour Research Institute. No. 107, 1970.12
- (2-6) Site Characteristics of Strong-Motion Earthquake Stations in Ports and Harbours in Japan (Part III), E. Kurata and I. Ishizuka, Technical Notes of the Port and Harbour Research Institute. No. 156, 1973.3
- (2-7) Average Response Spectra for Various Subsoil Conditions, S. Hayashi, H. Tsuchida, and E. Kurata, The 3rd Joint Meeting of Wind and Seismic Effects, U.J.N.R. 1971.5
- (2-8) Characteristics of Baserock Motions Calculated from Strong-Motion Accelerograms, S. Hayashi, H. Tsuchida and T. Uwabe, The 5th Joint Meeting of Wind and Seismic Effects, U.J.N.R. 1973.5
- (3-1) PWRI, "Strong-Motion Earthquake Records from Public Works in Japan (The Matsushiro Quake Swarn, December 9, 1965 - February 28, 1966, The Ochiai Bridge)", Technical Memorandum of P.W.R.I., No. 163, April 1966.
- (3-2) PWRI, "Strong-Motion Earthquake, Records from Public Works in Japan (The Matsushiro Quake Swarn, March 1 - June 22, 1966, The Ochiai Bridge)", Technical Memorandum of P.W.R.I., No. 194, July 1966.
- (3-3) PWRI, "Strong-Motion Earthquake Records from Public Works in Japan (1961-1966)", Technical Memorandum of P.W.R.I., No. 217, December 1966.
- (3-4) PWRI, "Strong-Motion Earthquake Records from Public Works in Japan (The Matsushiro Quake Swarn, June 25-December 1, 1966, The Ochiai Bridge)", Technical Memorandum of P.W.R.I., No. 254, March 1967.
- (3-5) PWRI, "Strong-Motion Earthquake Records from Public Works in Japan (The Matsushiro Quake Swarn, Mary 27-October 23, 1966, The Susobana Dam)", Technical Memorandum of P.W.R.I., No. 263, March 1967.
- (3-6) PWRI, "Strong-Motion Earthquake Records from Public Works in Japan (1967)", Technical Memorandum of P.W.R.I., No. 341, February 1968.
- (3-7) PWRI, "Digitized Data of Strong Motion Earthquake Records (No. 1)", Technical Memorandum of P.W.R.I., No. 317, March 1968.
- (3-8) PWRI, "Digitized Data of Strong-Motion Earthquake Records (No.2)", Technical Memorandum of P.W.R.I., No. 318, March 1968.
- (3-9) PWRI, "Strong-Motion Earthquake Records from Public Works in Japan (1968)", Technical Memorandum of P.W.R.I., No. 430, April 1969.

- (3-10) PWRI, "Digitized Data of Strong-Motion Earthquake Records (No. 3)", Technical Memorandum of P.W.R.I. No. 461, May 1969.
- (3-11) PWRI, "Strong-Motion Earthquake Records from Public Works in Japan (1969)", Technical Memorandum of P.W.R.I. No. 641, March 1971.
- (3-12) PWRI, "Strong-Motion Earthquake Records from Public Works in Japan (1970)", Technical Memorandum of P.W.R.I. No. 718, March 1972.
- (3-13) PWRI, "Strong-Motion Earthquake Records from Public Works in Japan (1971)", Technical Memorandum of P.W.R.I., No. 805 March 1973.
- (3-14) PWRI, "Digitized Data of Strong-Motion Earthquake Records No. 4", Technical Memorandum of P.W.R.I. No. 877, December 1973.
- (3-15) PWRI, "Digitized Data of Strong-Motion Earthquake Records, Revision (No.1-No.3)", Technical Memorandum of P.W.R.I. No. 876, December 1973.
- (3-16) PWRI, "Strong-Motion Earthquake Records from Public Works in Japan (1972)", Technical Memorandum of PWRI No. 713, March 1974.
- (3-17) PWRI, "Strong-Motion Earthquake Records from Public Works in Japan (1973)", Technical Memorandum of P.W.R.I. No. 967, November 1974.

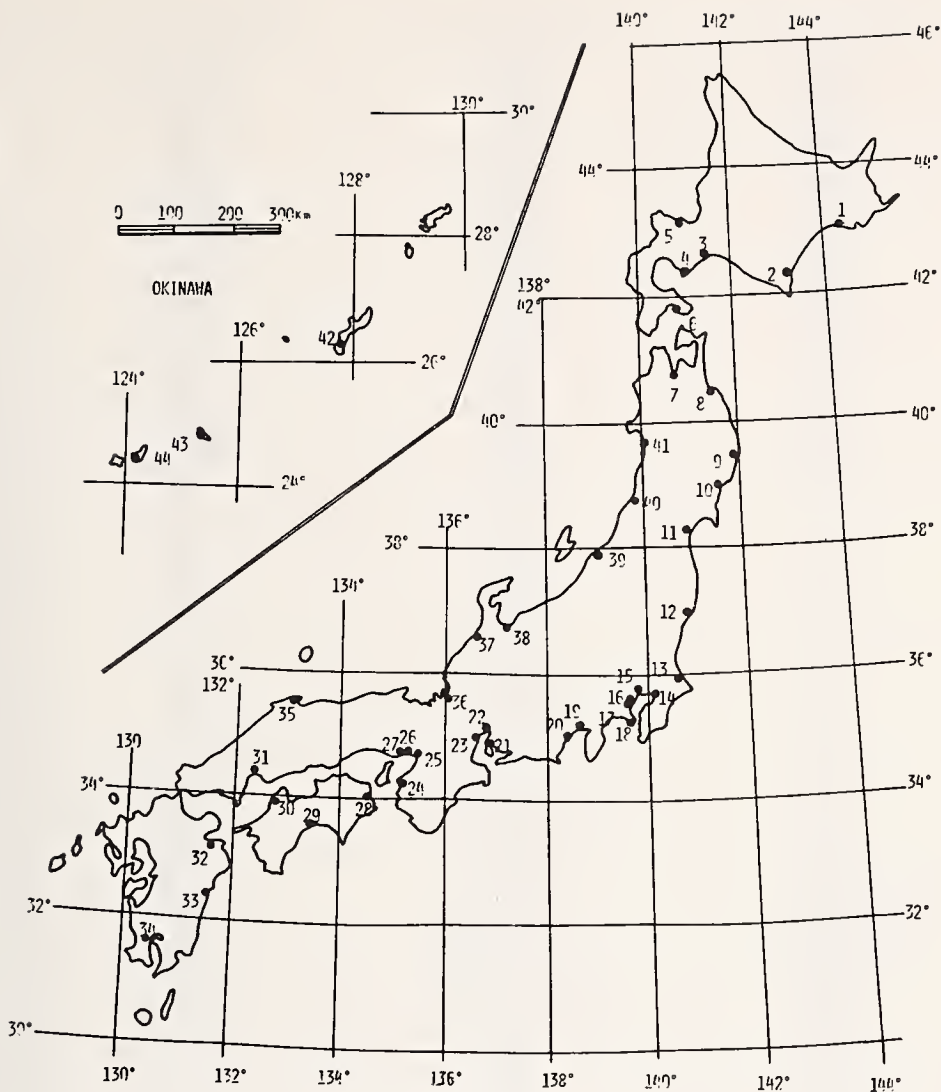


Fig. 2 - 1

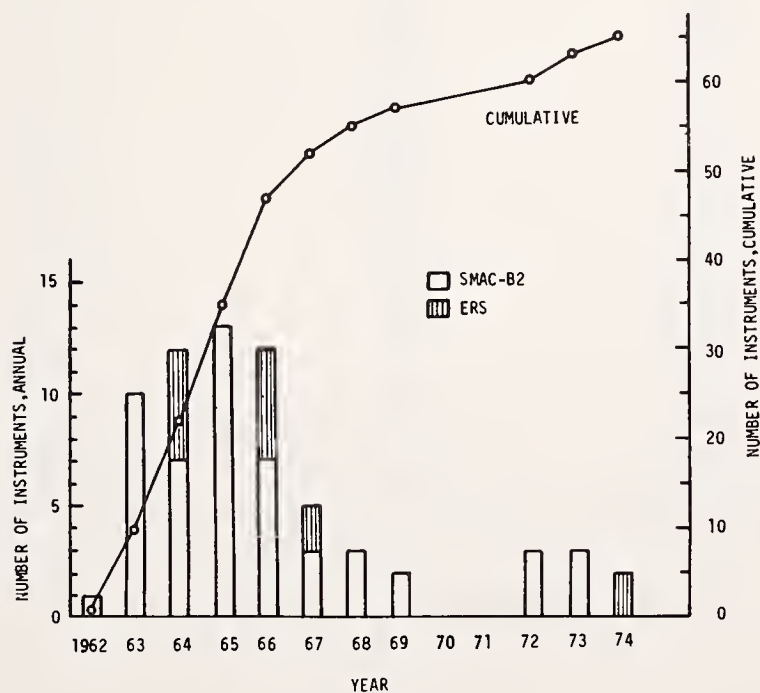


Fig. 2 - 2

S-252 HACHINOHE-S

1968-05-16-09-45

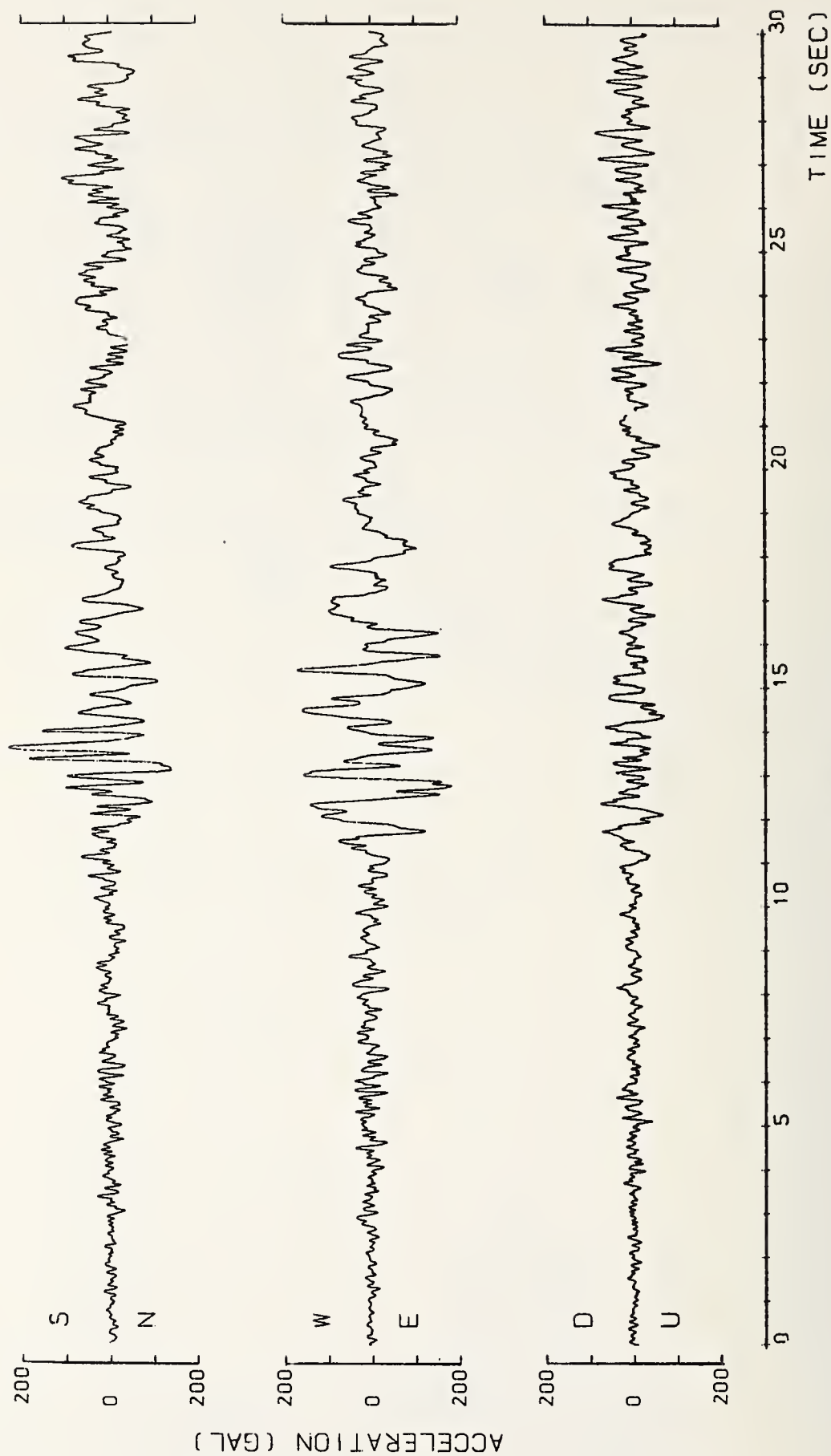


Fig. 2 - 3 (I)

S-252 HACHINOHE-S

1968-05-16-09-45

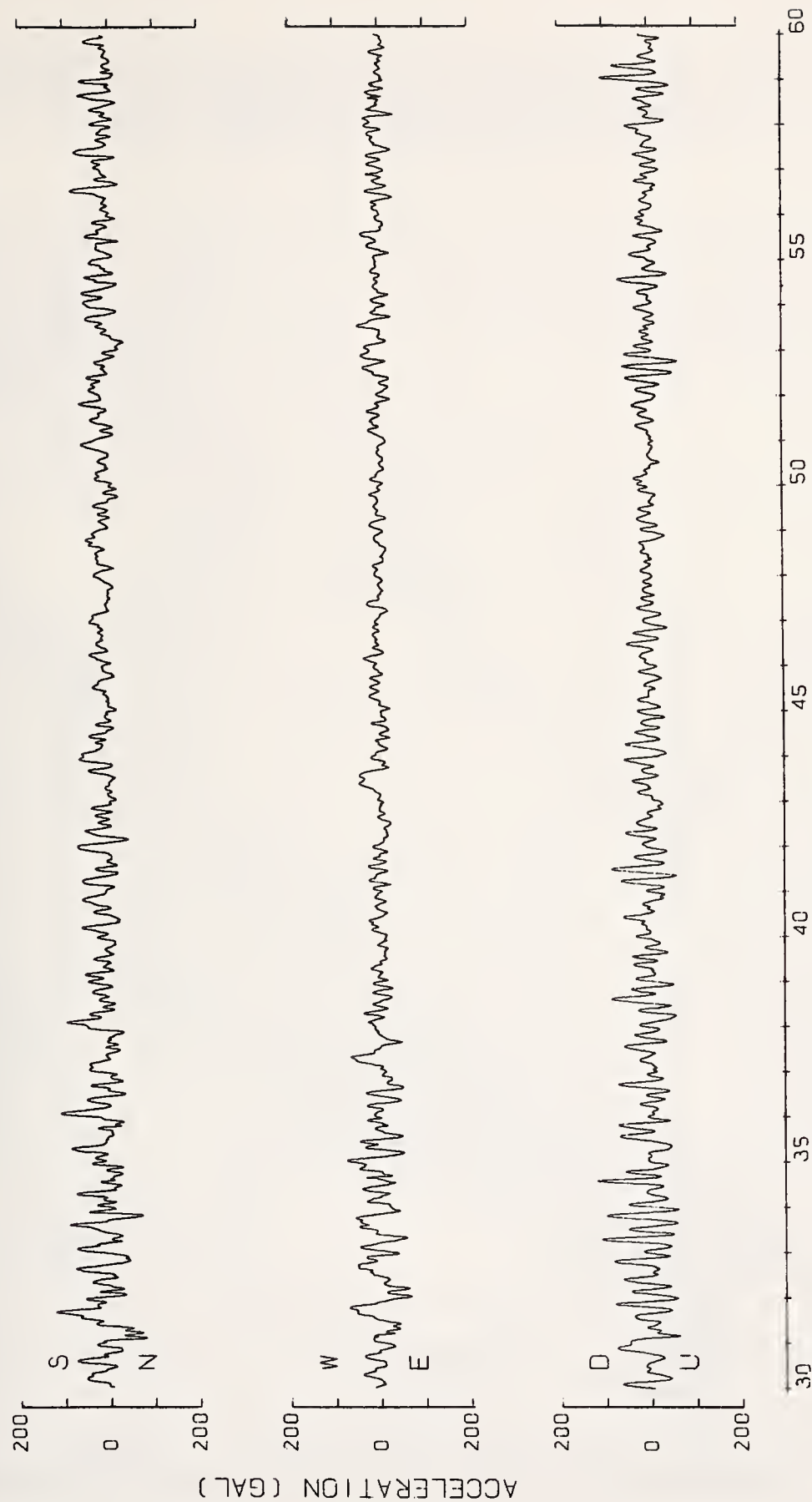


Fig. 2 - 3 (II)

Fig. 3-1 Sites of Strong-Motion Seismograph Stations for SMAC-Type Accelerographs. - Observation Network of Ground Motions and Earthquake Responses of Highway Bridges, Tunnels, Dams and Embankments - as of March, 1974

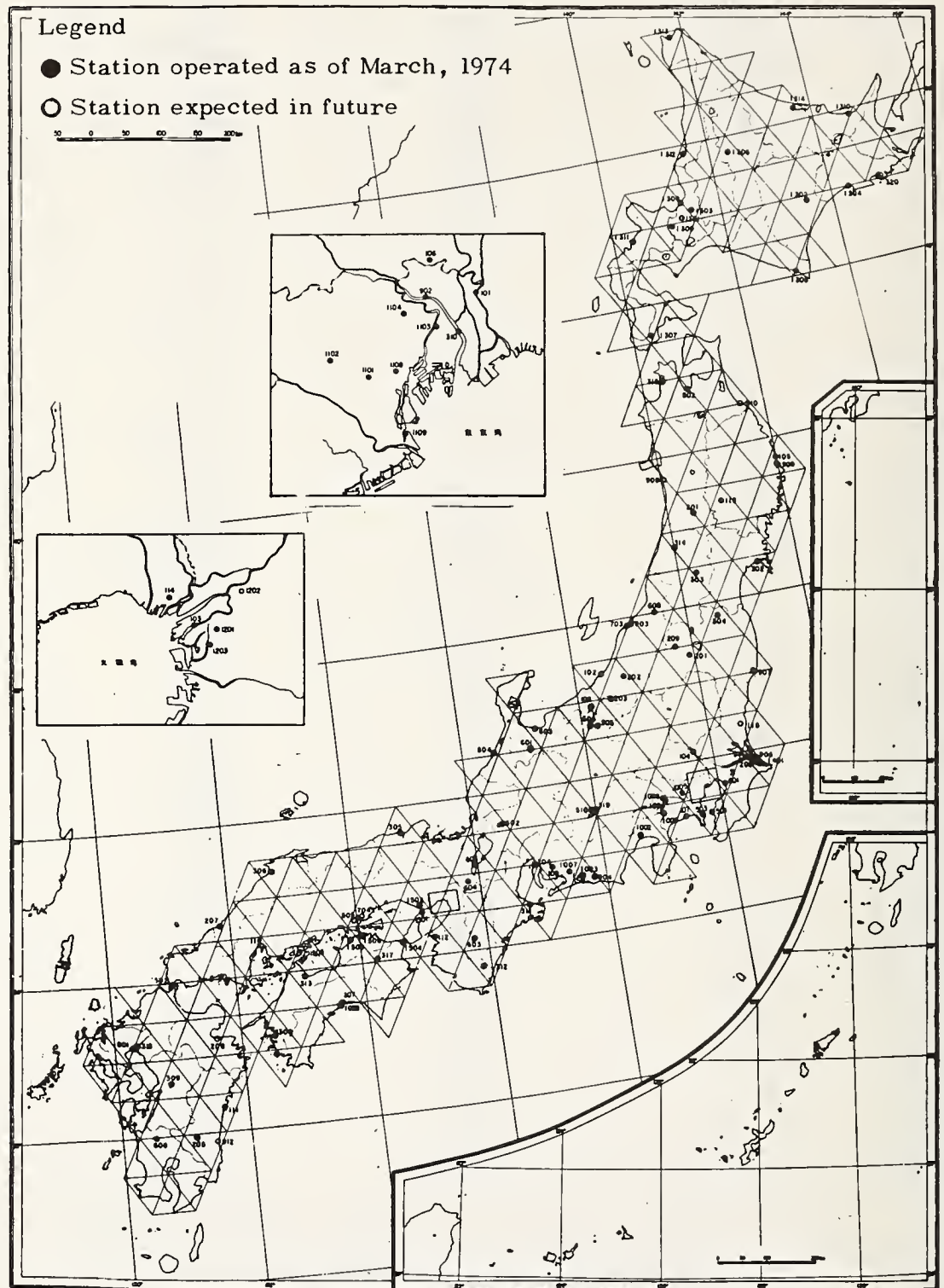


Fig. 3-2 Sites of Strong-Motion Seismograph Stations for Electro-Magnetic Type Seismographs. - Observation network of Ground motions and Earthquake responses of Highway bridges, Dams and Embankments - as of March, 1974



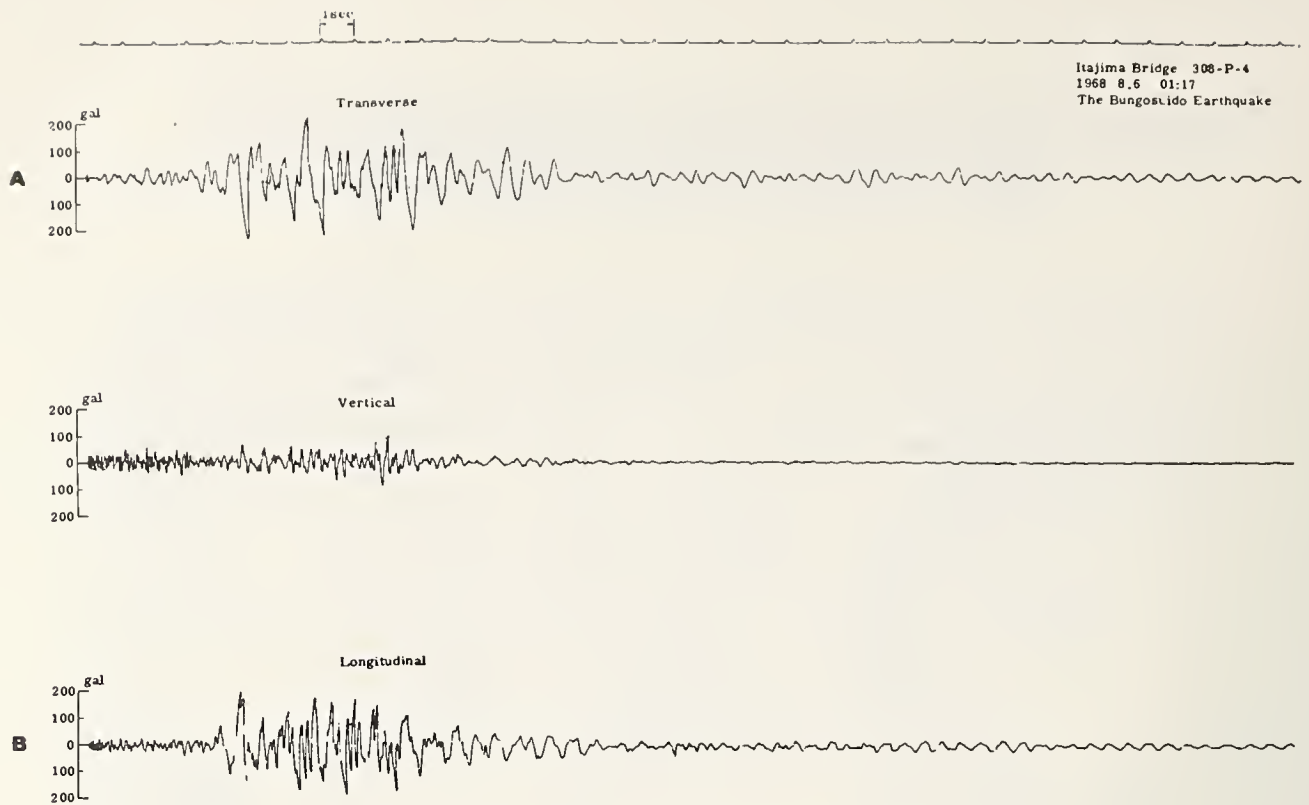


Fig. 3-3 Acceleration records at the Itajima Bridge during the Bungosuido Earthquake of August 6, 1968

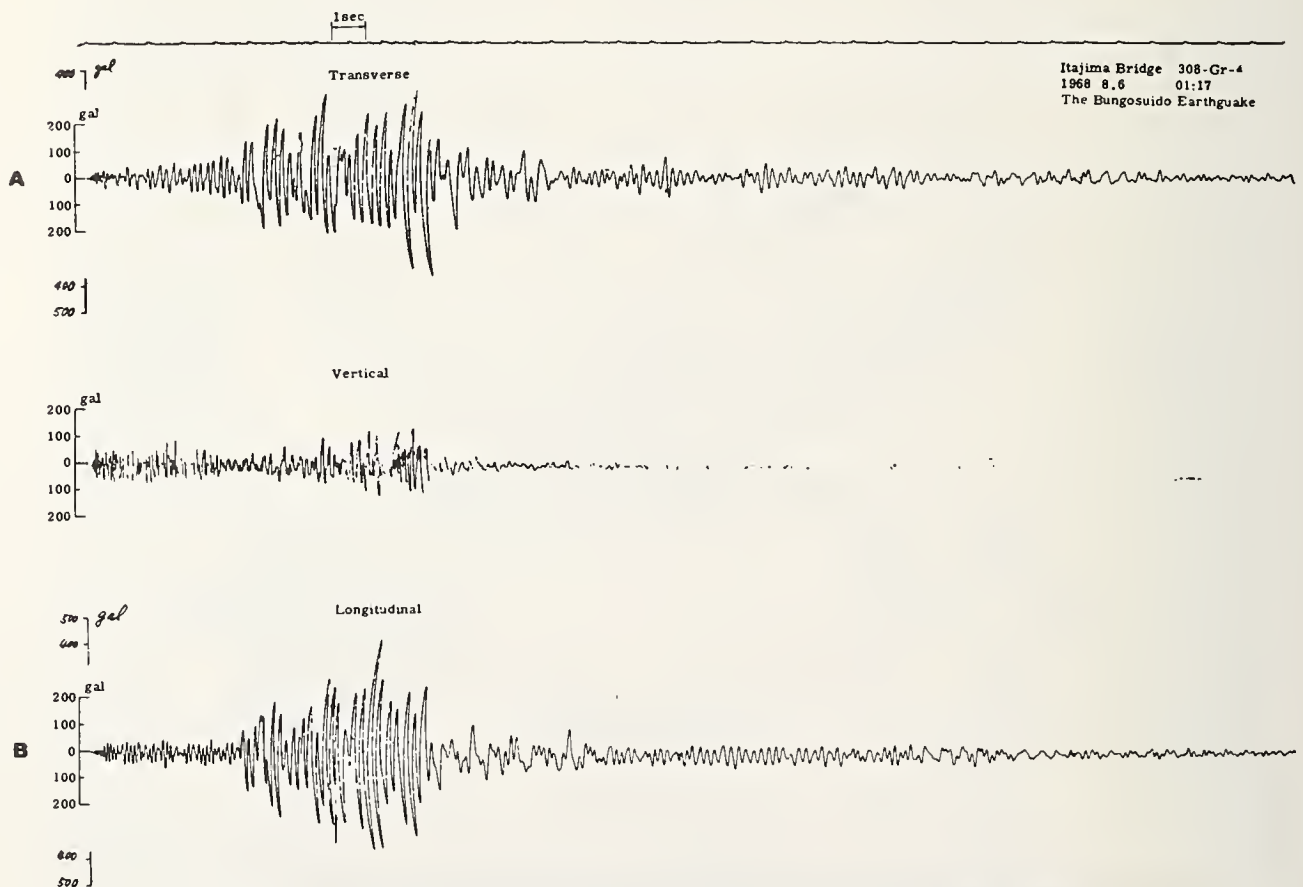


Fig. 3-4 Acceleration records on the ground surface nearby the Itajima bridge during the Bungosuido Earthquake of August 6, 1968

Fig. 3-5 Distribution of Strong-Motion Observation Stations of Japan,
as of March, 1974

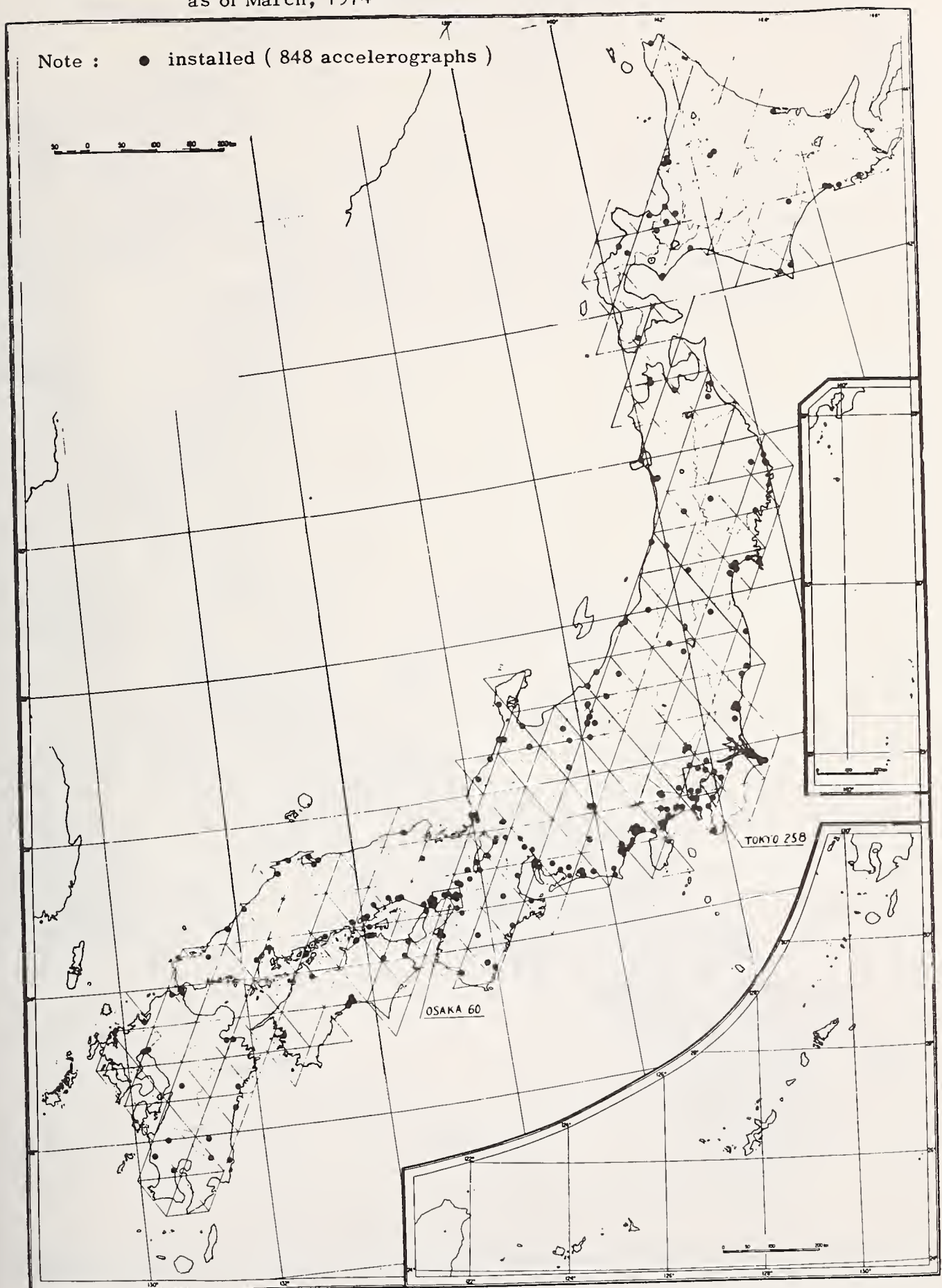
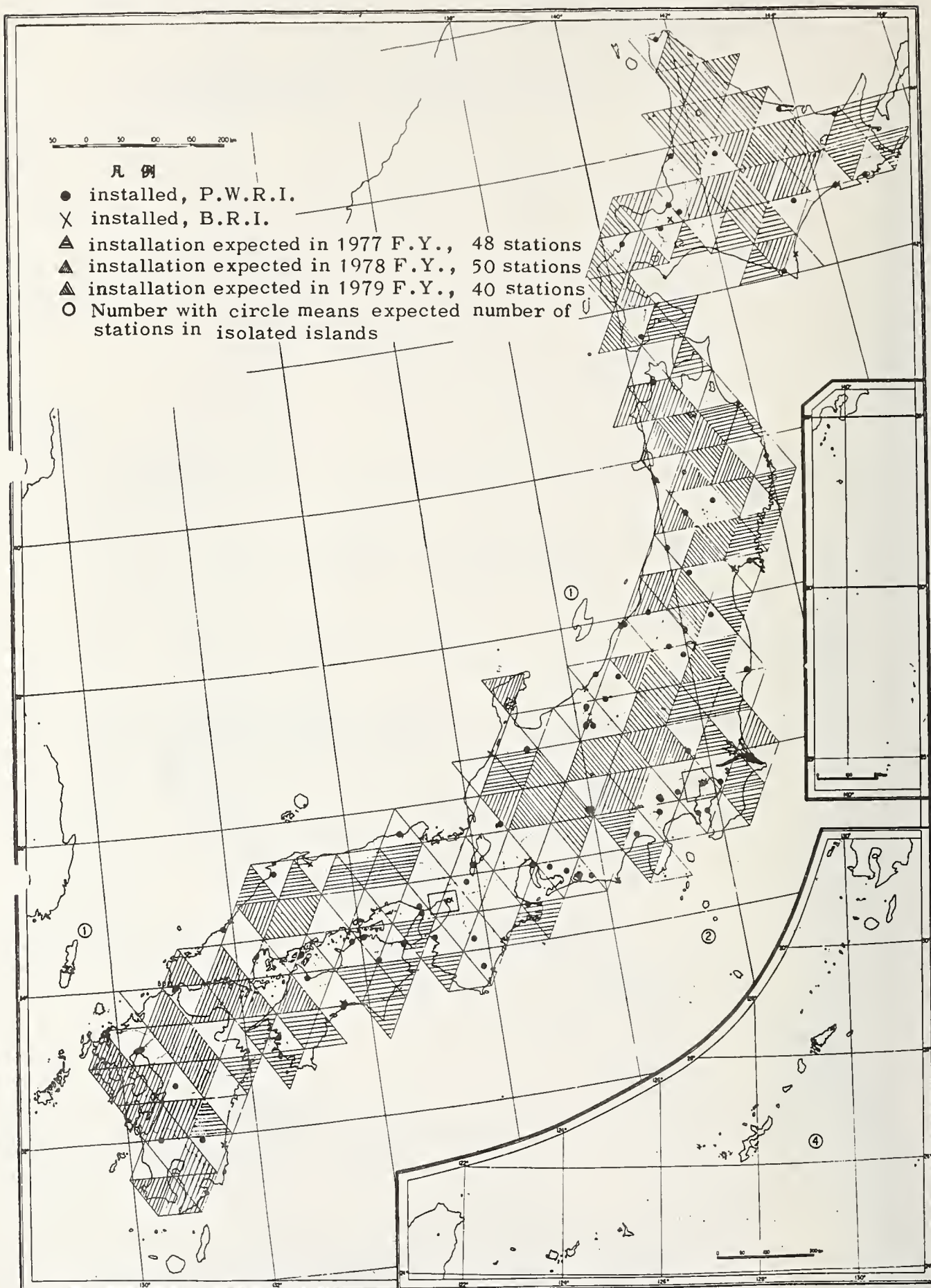


Fig. 3-6 Proposed networks of Strong-Motion Observation Stations of Ministry of Construction, as of March, 1974



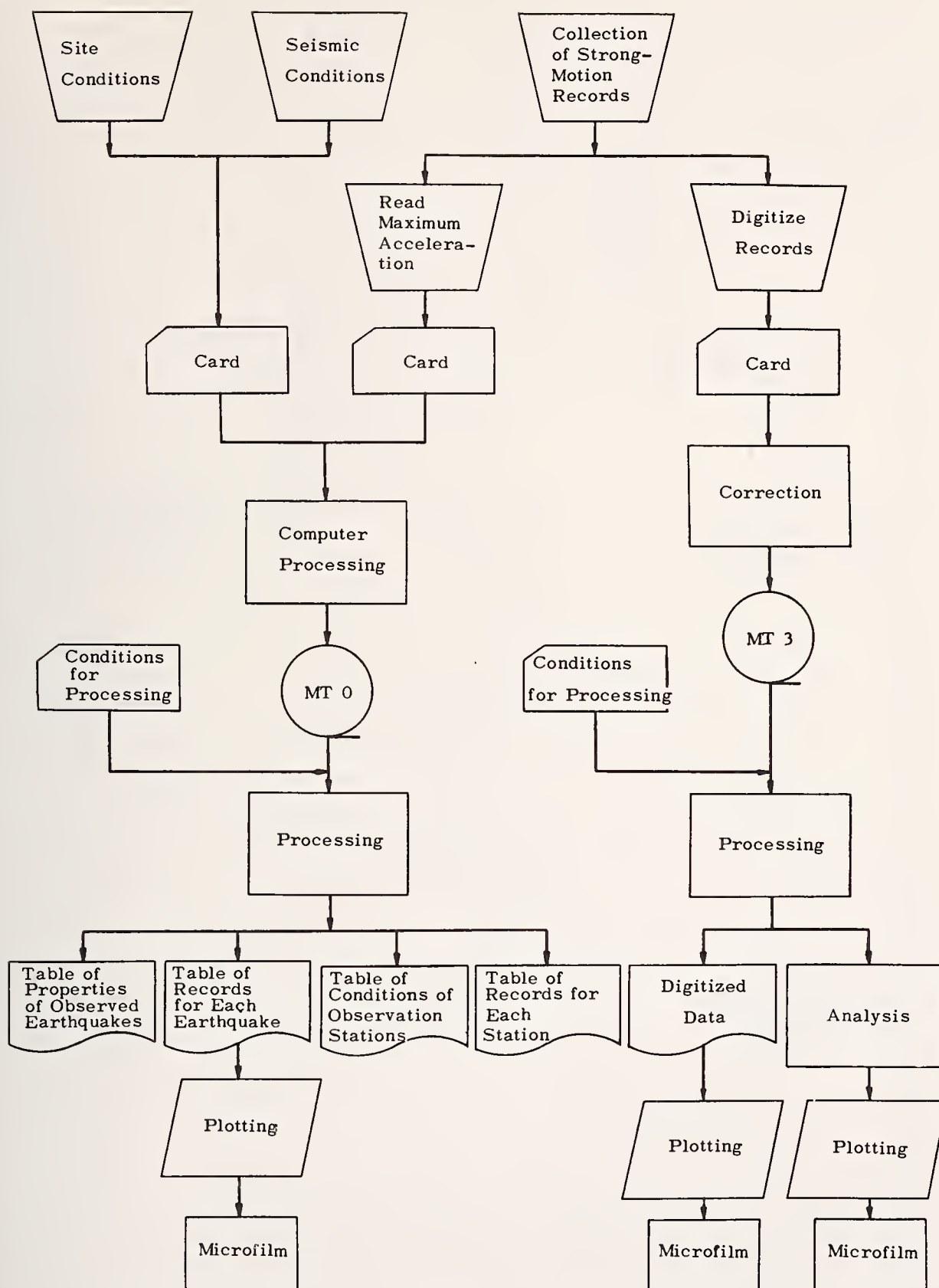


Fig. 3-7 Flowchart for Processing Strong-Motion Observation Data
(Strong-Motion Records and Seismic Conditions)

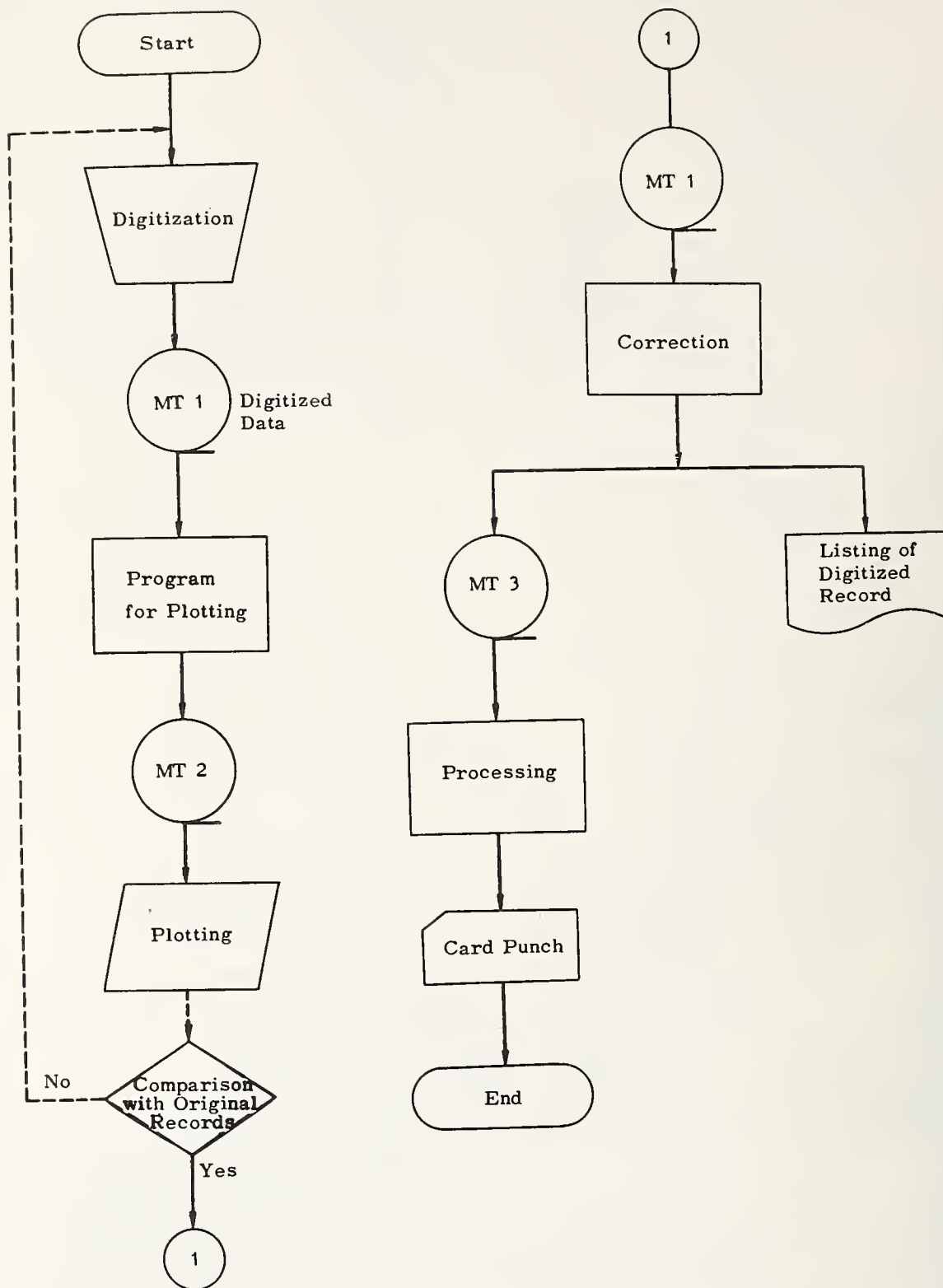
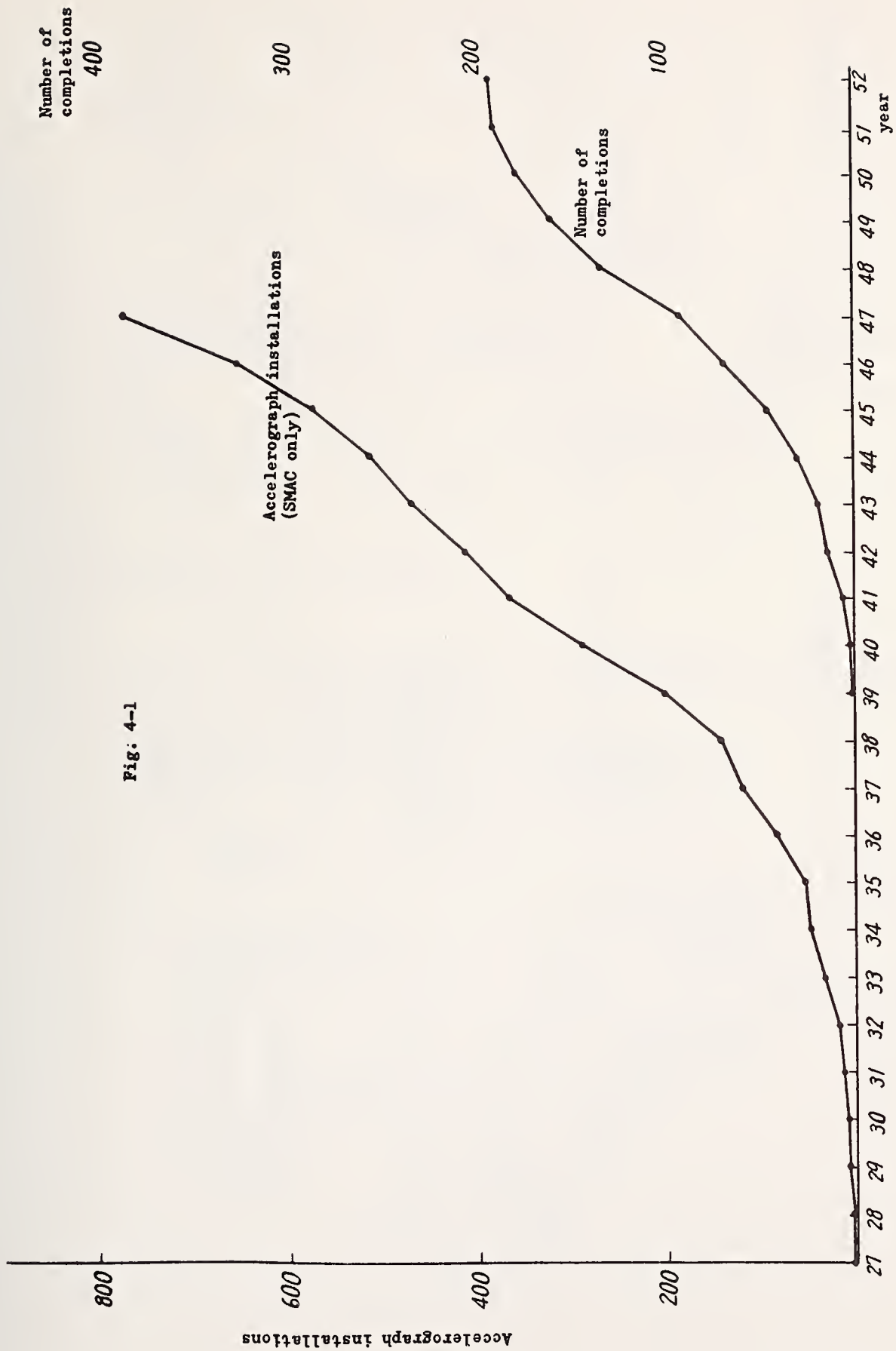


Fig. 3-8 Digitization of Strong-Motion Records



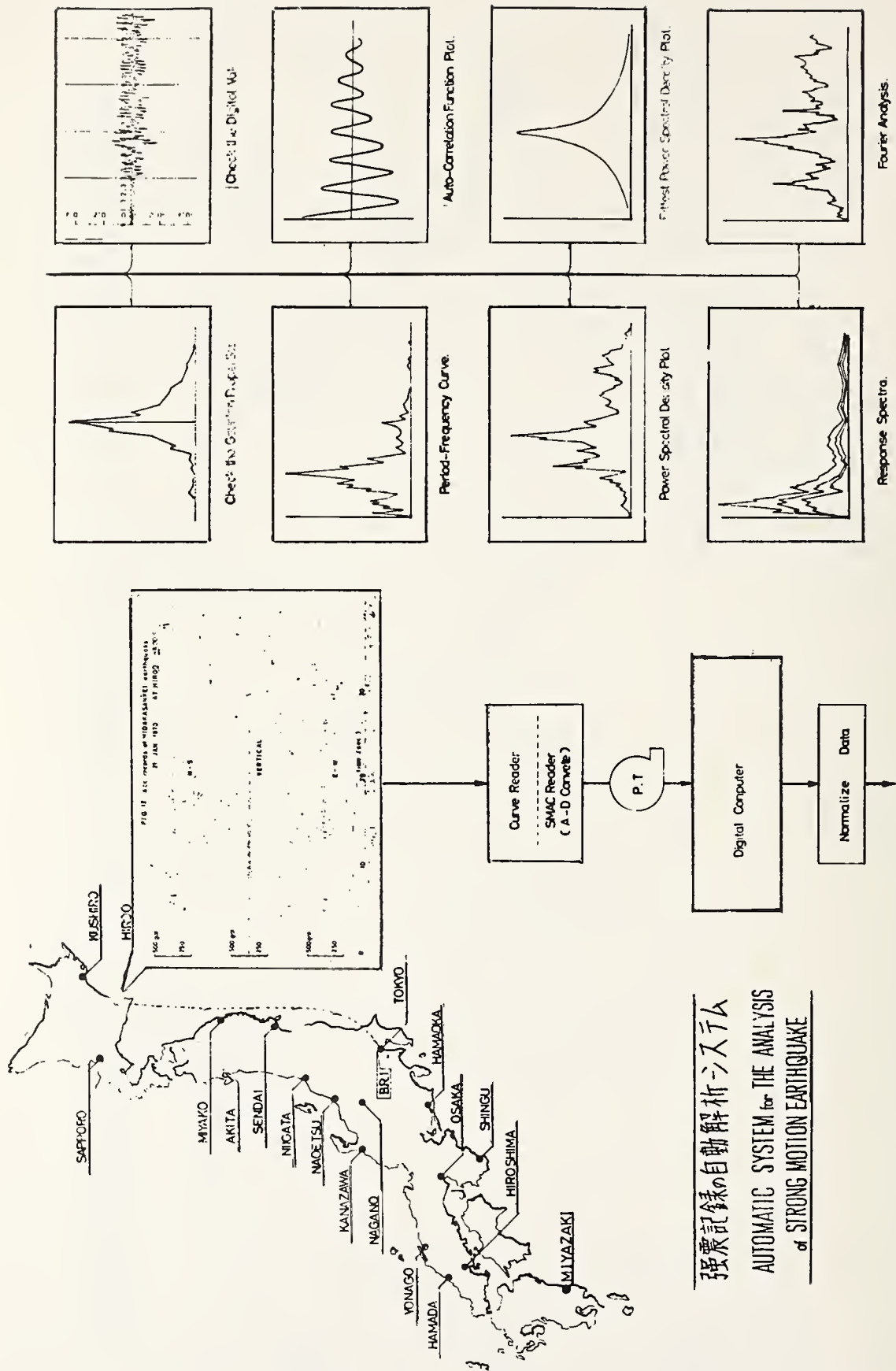
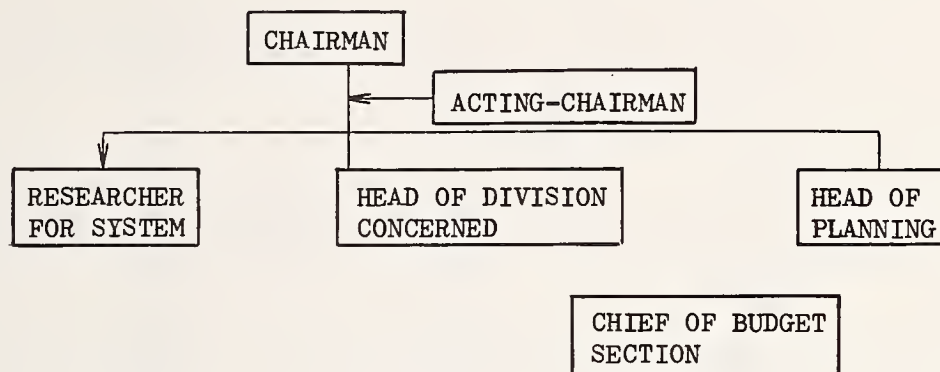


Fig. 4 - 2

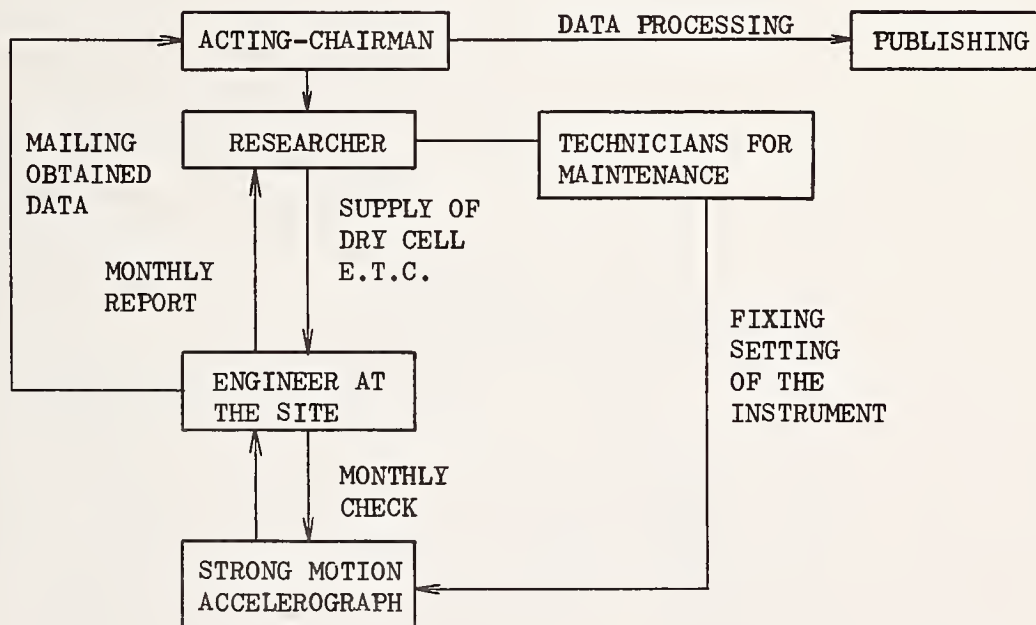
Fig. 4-3

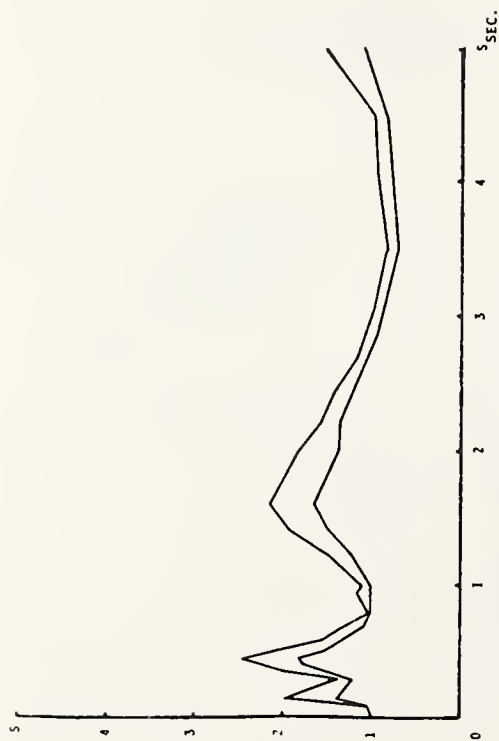
SYSTEMS FOR STRONG MOTION OBSERVATION IN B.R.I.

a) DECISION MAKING

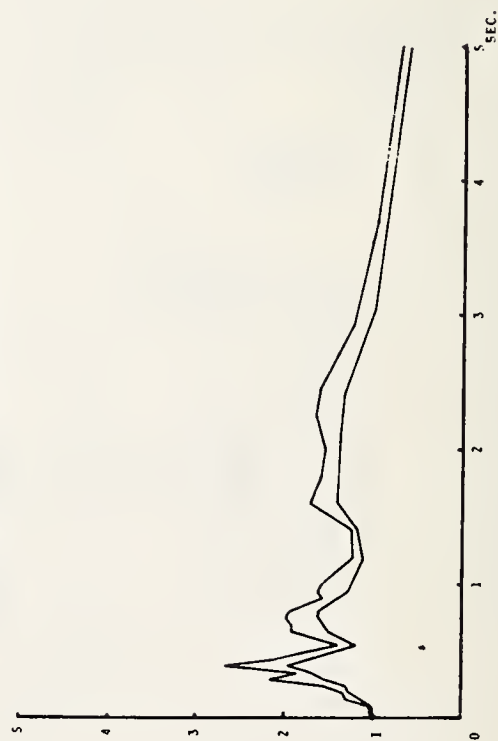


b) MAINTENANCE AND DATA PROCESSING



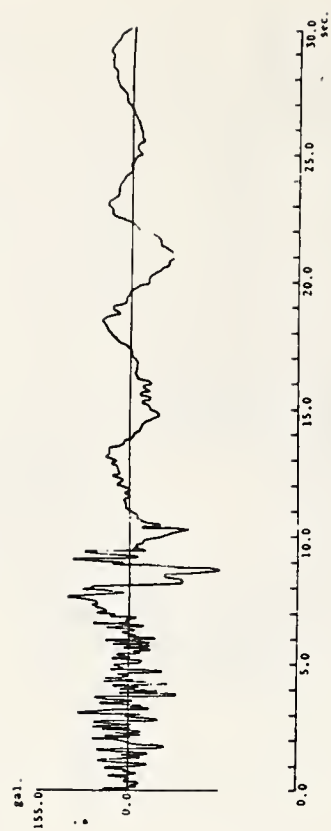


KANAGISHI CHO APARTMENT NO.2 (N11GATA 701) 1964.6.16 NS
MAX.ACC.155.00

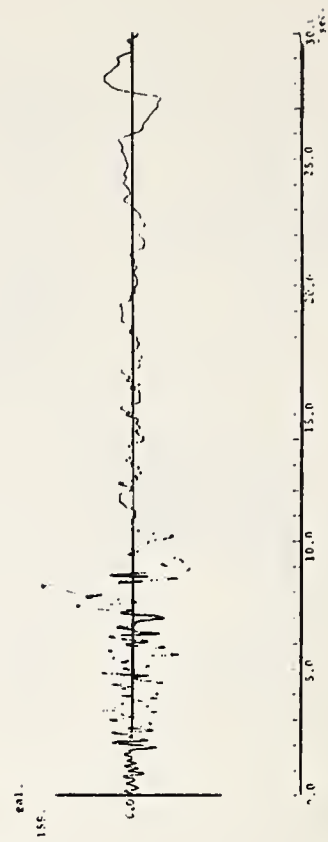


KANAGISHI CHO APARTMENT NO.2 (N11GATA 701) 1964.6.16 EW
MAX.ACC.155.00

Fig. 4 - 4



KANAGISHI CHO APARTMENT NO.2 (N11GATA 701) 1964.6.16 NS
MAX.ACC.155.00



KANAGISHI CHO APARTMENT NO.2 (N11GATA 701) 1964.6.16 EW
MAX.ACC.159.00

KANAGISHI CHO APARTMENT NO.2 (N11GATA 701) 1964.6.16 EW
MAX.ACC.159.00

Fig. 4 - 5

Accelerogram of Hidaka Sankai Earthquake

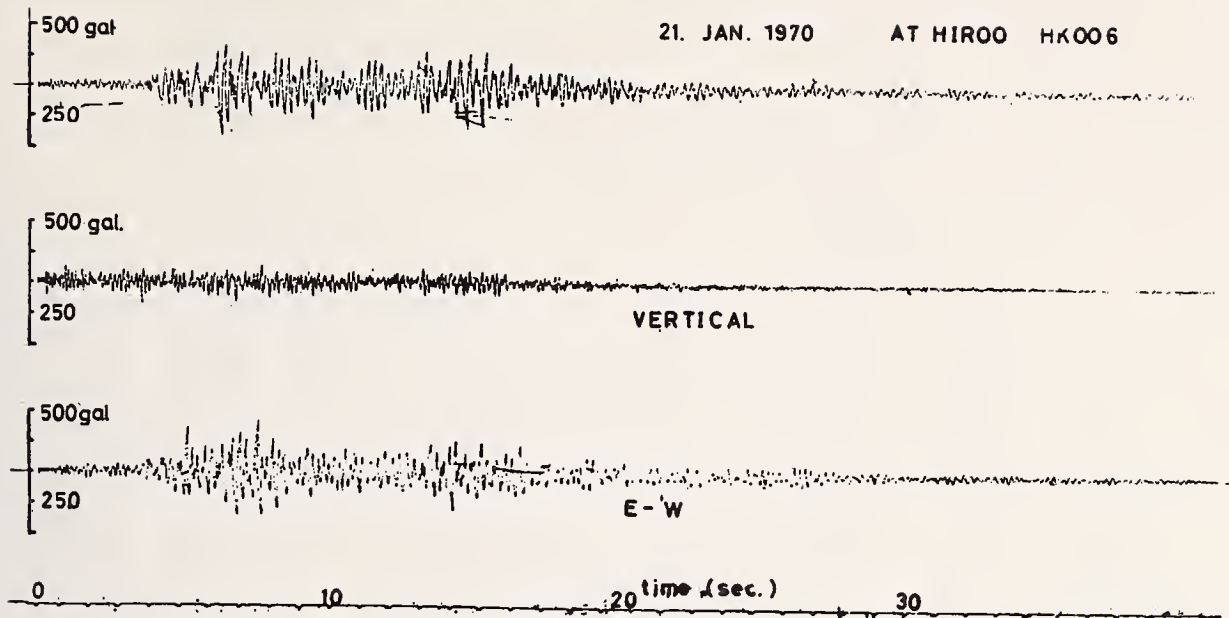
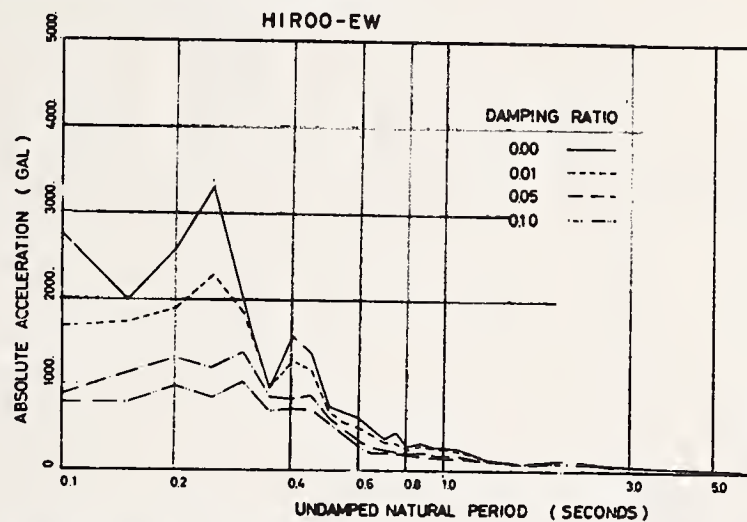


Fig. 4 - 6

Response Spectrum Absolute Acc.



Response Spectrum Absolute Acc.

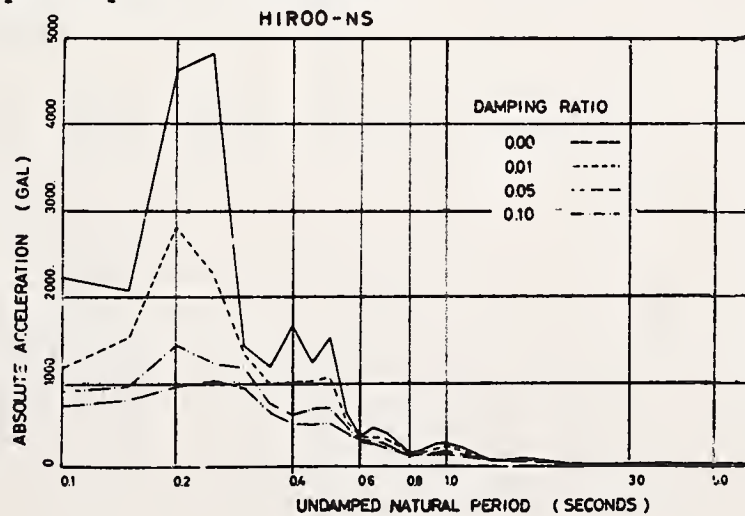


Fig. 4 - 7

Table 2-1 The records obtained by the Strong-Motion Earthquake observations in port and harbour areas

Record of Acceleration				Data of Earthquake				
Station	Record No.	Max. Acceleration (gal)	(km)	Date	Lat.	Long.	Depth (km)	Mag.
Kushiro - S	S-733	166	127	1973-06-17-12-55	42°58'	145°57'	40	7.4
Muroran - S	S-234	205	280	1968-05-16-09-49	40°44'	143°35'	-	7.9
Aomori - S	S-235	208	233	1968-05-16-09-49	40°44'	143°35'	-	7.9
Hachinohe - S	S-252	233	178	1968-05-16-09-49	40°44'	143°35'	-	7.9
Miyako - S	S-236	112	184	1968-05-16-09-49	40°44'	143°35'	-	7.9
"	S-312	110	103	1968-06-12-22-42	39°25'	143°08'	-	7.2
"	S-537	115	15	1970-04-01-23-23	39°45'	142°03'	80	5.8
Kashima - S	S-647	127	12	1971-10-11-19-16	35°54'	140°33'	40	5.2
Shinagawa - S	S-340	113	51	1968-07-01-19-45	35°59'	139°26'	50	6.1
Shimizu - S	S- 74	107	21	1965-04-20-08-42	34°53'	138°18'	20	6.1
Wakayama - S	S-265	253	6	1968-03-30-04-04	34°10'	135°10'	0	5.0
Hosojima - S	S-544	122	54	1970-07-26-07-41	32°04'	132°02'	10	6.7

Table 3-1 Annual Progress of the Number of SMAC Type Accelerographs

Year	1957	1958	1959	1960	1961	1962	1963	1964	1965	1966	1967	1968	1969	1970	1971	1972	1973	Total
Number of Instruments	1	0	0	3	5	10	0	18	29	36	15	18	12	4	16	18	3	189

Table 3-2 Number of Strong-Motion Seismograph Station and that of Instruments in Relation to the Variety of Structures

Operated as of March 1973

Variety of Structures	Number of Stations	
	SMAC Type	Electro-Magnetic Type
Bridge	72 (153)*	13
Tunnel	1 (3)	0
Dam	8 (12)	17
Embankment	3 (6)	5
Future Structure Site	9 (9)	8
Others	3 (6)	1
Total	96 (189)	45

* Number of Instruments

Table 3-3 The Strong-Motion Earthquake Records Exceeding about 100 Gals in: the Maximum Acceleration

Station	Record No.	Max. Acceleration (gal)		Date	Position of focus			Station	Record No.	Max. Acceleration (gal)		Date	Position of focus		
		Hori. A	Verti. cal		Long.	Lat.	D. km			Hori. A	Verti. cal		Long.	Lat.	D. km
Yoneyama Br.	102-Gr-16	106.3	36.3	115.6	138°21'	37°08'	0.0	Ochiai Br.	905-B-63	290.0	40.0	82.5	138°13'	36°34'	0.0
Masaki Br.	105-P-3	52.0	16.5	163.5	142°0'	40°51'	80.0	"	905-A-169	107.5	30.0	22.5	138°13'	36°34'	0.0
Kinokawa Br.	112-P-2	55.0	30.0	115.0	135°10'	34°10'	0.0	"	905-B-74	102.5	27.5	37.5	"	"	0.0
Uonuma Br.	202-P-10	57.5	20.6	121.9	138°21'	37°08'	0.0	"	905-A-196	105.0	22.5	32.5	138°17'	36°34'	0.0
Shinyavata Br.	204-P-9	100.0	12.5	50.0	136°56'	32°02'	40.0	"	905-B-83	110.0	30.0	42.5	"	"	0.0
Omitava Br.	206-Gr-2	90.0	22.5	135.0	140°53'	35°34'	60.0	"	905-B-91	70.0	20.0	100.0	138°17'	36°34'	0.0
"	206-P-2	150.0	15.0	135.0	"	"	"	"	905-B-95	130.0	65.0	-	138°21'	36°33'	0.0
Tabatsu Br.	207-P-1	118.0	20.0	75.0	132°32'	32°17'	30.0	"	905-B-107	130.0	55.0	100.0	138°12'	36°32'	0.0
Yuhei Br.	301-Gr-7	157.5	47.5	147.0	140°45'	39°12'	0.0	"	905-B-155	145.0	15.0	50.0	138°11'	36°33'	0.0
"	301-P-9	121.4	60.5	155.4	"	"	"	"	905-B-162	115.0	60.0	50.0	138°07'	36°26'	0.0
Itoijima Br.	308-Gr-1	186.3	43.0	169.9	132°32'	32°17'	30.0	"	905-B-175	113.0	15.0	25.0	138°09'	36°31'	0.0
"	308-P-2	375.0	55.0	213.0	"	"	"	"	905-B-181	290.0	45.0	110.0	138°10'	36°36'	0.0
"	308-Gr-4	360.9	140.0	437.5	132°23'	33°18'	40.0	"	905-C-93	110.0	23.0	105.0	"	"	0.0
"	308-P-4	233.0	100.0	200.0	"	"	"	"	905-B-182	160.0	20.0	28.0	138°10'	36°30'	0.0
"	308-P-6	65.0	20.0	100.0	132°24'	33°22'	40.0	"	905-B-183	120.0	5.0	25.0	138°10'	36°30'	0.0
"	308-Gr-7	85.0	25.0	130.0	132°24'	33°20'	40.0	"	905-A-387	120.0	10.0	20.0	138°09'	36°26'	10.0
"	308-Gr-8	170.0	60.0	228.0	132°27'	33°21'	40.0	"	905-P-400	113.0	25.0	33.0	138°11'	36°34'	0.0
"	308-Gr-11	100.0	26.3	113.8	132°02'	32°04'	10.0	"	905-Gr-257	100.0	15.0	35.0	138°11'	36°29'	10.0
Hirai Br.	310-P1-12	108.0	30.0	63.0	139°26'	35°59'	50.0	"	905-Gr-263	30.0	55.0	127.0	138°15'	36°34'	10.0
"	310-P2-12	128.0	30.0	60.0	"	"	"	"	905-Gr-264	160.0	27.5	37.5	138°15'	36°31'	0.0
Toyohama Br.	311-Gr-6	130.0	36.9	123.8	137°10'	34°26'	40.0	"	905-Gr-264	113.8	25.0	37.5	138°14'	36°33'	10.0
"	311-P-7	246.3	46.3	261.3	"	"	"	P.W.R.I. Kashima EL.	906-Gr-12	55.6	12.5	137.5	140°33'	35°54'	40.0
"	311-P-9	100.0	12.5	25.0	136°56'	32°02'	40.0	"	906-Gr-17	100.0	12.5	75.0	140°40'	35°39'	50.0
Kiyokawa Br.	314-P-1	106.3	12.5	75.0	139°57'	38°36'	20.0	"	906-Gr-22	143.8	43.8	137.5	141°15'	35°45'	40.0
Abbehi Br.	320-Gr-1	93.7	0.0	118.7	145°57'	42°58'	40.0	"	1004-P-1	85.0	15.0	125.0	139°26'	35°59'	50.0
"	320-P-1	94.7	87.5	125.0	"	"	"	Chuo-Highway Sakaigawa*B	1005-P-1	178.0	15.0	48.0	"	"	"
Biwako Br.	401-P1-1	145.0	10.0	75.0	137°06'	35°45'	10.0	"	1006-P-1	61.3	42.5	196.9	138°58'	35°33'	10.0
Kannonzaki	503-Gr-18	118.8	25.0	56.3	139°56'	35°31'	60.0	"	1108-P-2	173.0	25.0	140.0	139°26'	35°59'	50.0
Amagase Dam	604-Pa-2	17.0	73.0	40.0	135°39'	34°55'	10.0	"	1108-P-3	125.0	28.0	120.0	140°09'	35°31'	70.0
Susobana Dam	605-Gr-26	125.0	56.0	143.0	138°12'	36°34'	0.0	"	1302-P1-5	112.5	25.0	131.3	143°35'	40°44'	0.0
Ariake-Sea Emb.	801-Gr-1	118.0	13.0	83.0	130°12'	33°06'	10.0	"	1302-P1-8	125.0	82.5	87.5	143°08'	42°23'	50.0
Ochiai Br.	905-A-46	117.5	35.0	22.5	138°17'	36°33'	0.0	"	1302-P2-8	100.0	37.5	52.5	"	"	"
"	905-B-11	217.5	32.5	42.5	"	"	"	"	1303-Gr-1	174.9	40.0	181.3	143°35'	40°44'	0.0
"	905-A-56	190.0	42.5	147.5	138°19'	36°35'	0.0	"	1303-Gr-2	170.9	20.0	96.9	142°51'	41°25'	40.0
"	905-B-18	212.5	45.0	187.5	"	"	"	"	1305-Gr-11	105.0	45.0	147.5	143°08'	42°23'	50.0
"	905-C-7	142.5	32.6	225.0	"	"	"	Shinshikari Br.	1305-P-5	182.5	85.0	147.5	"	"	"
"	905-A-81	145.0	37.5	45.0	138°19'	36°33'	0.0	"	1401-Ea-4	180.0	15.0	210.0	140°53'	35°34'	60.0
"	905-B-33	302.5	42.5	45.0	"	"	"	"							
"	905-C-13	62.5	27.5	125.0	"	"	"	"							
"	905-B-39	141.3	25.0	35.0	138°19'	36°33'	0.0	"							

Table 4-1 Accelerograph installations relative to buildings
and power supply facilities

Installations for buildings (including the ground)

District	Number of cases	SMAC	DC	Total
Hokkaido	3	9	1	10
Tohoku	3	7	2	9
Tokyo	76	197	5	202
Kanto	23	39	10	49
Aichi pref.	11	22	0	22
Chubu	5	17	5	22
Osaka	15	36	1	37
Kinki	2	4	0	4
Chugoku	6	9	1	10
Shikoku	1	3	1	4
Kyushu	1	13	0	13
Total	152	356	28	384

Installations for power supply facilities

Organization	Number of cases	SMAC	DC	Total
Hokkaido Electric Power	1	1		1
Tohoku Electric Power	4	5		5
Tokyo Electric Power	7	11		11
Hokuriku Electric Power	2	3		3
Chubu Electric Power	4	10	1	11
Kansai Electric Power	6	13		13
Chugoku Electric Power	1	1		1
Shikoku Electric Power	3	5		5
Kyushu Electric Power	3	4		4
Electric Power Development	2	5		5
Japan Nuclear Power Generation	3	6		6
Japan Atomic Energy Research Institute	2	2		2
	4	8		8
Total	42	73	1	74

Tab. 4-2

MAIN LIST OF ACCELEROGRAMS

(MAX. ACC. EXCEEDS MORE THAN 100 GAL)

DATE AND NAME OF EARTHQUAKE	EPICENTER	DEPTH km	STATION		MAX. ACCELERATION	
					gal	
IBARAGI-OKI E.Q. Feb. 5, 1964	140.9° E 36.3° N	60.0	KANTO 601	Genken kisho- shitsu	NS	175.0
					EW	105.0
NIGATA E.Q. May 16, 1964	139.2° E 38.4° N	40.0	NIGATA 701	Kawagishi cho apartment	NS	155.0
					EW	159.0
TOKACHI-OKI E.Q. May 16, 1968	143.6° E 40.7° N	0	HK 006	Hiroo	NS	182.0
					EW	165.0
HIGASHIMATSUYAMA E.Q. January 1, 1968	139.4° E 36.0° N	50.0	TOKYO 101-2 (TK-024)	E.R.I.	NS	106.15
					EW	103.68
"	"	"	TOKYO 116-2 (TK002)	I.I.S.E.E.	NS	79.45
					EW	111.65
HIDAKA-SANKEI E.Q. Jan. 21, 1970	143.3° E 42.3° N	60	HK 006	Hiroo	NS	412.0
					EW	437.0

THE UNITED STATES STRONG-MOTION NETWORK:
FIELD OPERATIONS

Richard P. Maley
U. S. Geological Survey
San Francisco, California

ABSTRACT

The national strong-motion instrumentation network operated by the Seismic Engineering Branch of the U. S. Geological Survey is the system established to record the strong motions of damaging earthquakes in the United States. From the original 50 C&GS Standard instruments installed in the 1930's, the network has expanded to more than 1300 accelerographs, with 9 different models, located in 35 states and 9 Central and South American countries.

The network operations section of SEB conducts three interrelated field programs: instrument installation, routine maintenance, and earthquake record recovery. At the present time the large majority of instruments being installed are self-contained three-component accelerographs that record on 70-mm film. Some remote-sensor accelerographs are also being located on structures. Routine maintenance intervals have been lengthened from 2 months a few years ago to 4 months, with the exception of a trial area in Los Angeles where a 6 month interval is now in effect. The higher reliability of modern instrumentation has made this extended maintenance schedule possible. As the network expands, it may be necessary to develop a Remote Interrogation System to provide a method of determining the criterion of the instruments' vital functions by telemetry. After significant earthquakes, SEB personnel promptly collect and develop earthquake records and attach permanent labels providing sufficient data for most analyses. The records are then transmitted to the data management section for further processing.

Key Words: Accelerographs; Earthquake Data; Earthquake Records; Field Stations;
Strong-motion Network.

Introduction

In 1932 the United States Coast & Geodetic Survey (C&GS) inaugurated a program of strong-motion seismological work designed to furnish the engineer and interested others with data considered essential to the design of earthquake resistant structures (Cloud, 1964). The responsibility for organizing an instrumentation network to achieve this objective was assigned to the Seismological Field Survey (SFS) in San Francisco, California, the predecessor to the current operating unit, the Seismic Engineering Branch (SEB) of the Office of Earthquake Studies, U. S. Geological Survey (USGS). The program was initiated with the installation of nine low-sensitivity short-period seismographs (accelerographs) in structures selected for special studies by local engineers. Less than 8 months later instruments installed at Los Angeles, Vernon and Long Beach recorded the disastrous 1933 Long Beach earthquake. These first useful records of damaging earthquake motions showed amplitudes as large as 0.25g, thus justifying the program and furnishing the impetus for additional efforts. Consequently, the network was rapidly expanded to 50 instruments located principally in the San Francisco and Los Angeles areas but extending to other seismic regions of the western United States as well. The principal instrument used in this network was the strong-motion accelerograph designed by the C&GS in cooperation with the U. S. Bureau of Standards.

During the period 1936 to 1963 the program was marked by a gradual improvement of instrumentation and methodology and a slow increase in the total number of strong-motion seismographs. Over this period SFS developed numerous innovations that were subsequently incorporated into the existing instrumentation. These included among others, the design of a unifilar accelerometer, a strong-motion displacement meter, and light-tight recording assembly. Because the original accelerograph was relatively large and required extensive maintenance at frequent intervals, the network was increased by only 28 units between 1936 and 1963.

In 1963 the first commercially designed accelerograph featuring numerous engineering and electronic improvements was marketed in California. This instrument overcame many of the inadequacies of the earlier accelerograph and consequently ushered in an era of substantial expansion in the strong-motion network. With the development of several newer and less expensive instruments in recent years, the network has continued to enlarge at an accelerating pace. Between 1963 and the present time the number of accelerographs increased from 70 to approximately 1300. Instrumentation is now located in 35 states, including Hawaii and Alaska, and in 9 Central and South American countries (Figures 1 and 2). Because of the expanded network, field offices have been established at Los Angeles, California, at Las Vegas, Nevada, and at Columbia, South Carolina.

From its inception, the program has received the cooperation of numerous outside organizations and individuals. In the early years, housing and facilities were provided by private and public organizations, and in recent years, a large number of accelerographs purchased by other organizations have been incorporated into the network. In fact, more than 900 of the accelerographs installed since 1963 have been included through the cooperation of two federal agencies (the Corps of Engineers and the Veterans Administration), two State of

California agencies (the Division of Mines and Geology and the Department of Water Resources), and the numerous building departments whose codes require instrumentation at various levels of high-rise buildings. The building code requirements were initiated in 1965 when the cities of Los Angeles and Beverly Hills passed ordinances requiring three accelerographs in newly constructed buildings over six stories high with an aggregate floor area of 60,000 square feet or more, and every building over ten stories high, regardless of floor area. This requirement became more wide-spread when it was adopted by numerous other communities in California as a result of being included in the appendix of 1970 Uniform Building Code (Maley and Dielman, unpublished data). At this time, approximately one-half of the total number of accelerographs in the network are those in high-rise buildings.

Operation of the Network

Instrumentation. The majority of accelerographs in the USGS National Network are the photo mechanical type. Each instrument contains accelerometers, trigger, timer and recorders all housed in one instrument case. The typical accelerometer is a pendulum with a mirror designed to reflect a beam of light on to translating photographic film or paper. Although there are six different models of this type in the network, only two are still in general production, the Kinometrics SMA-1 and the Teledyne-Geotech RFT-350 (Table 1).

1) The Standard C&GS accelerograph records on 152-mm (6 inch) or 304-mm (12 inch) photographic paper. It is triggered by an oil damped one-second horizontal pendulum that makes an electrical contact when displaced. The instrument has a fixed operating cycle of approximately 1 minute and is capable of recording five or six separate events. Several disadvantages, other than its large size (33 x 50 x 115cm), include a relatively high standby current, lack of an internal calibration system, and the need for a darkened room to change the photographic paper. The instrument has not been manufactured for several years and is slowly being phased out of the network.

2) The AR-240, the first comparatively modern accelerograph, was designed and marketed in the United States in 1963. It records on 304-mm photographic paper and is capable of numerous operations because the supply magazine can accomodate rolls of paper 23m (75 feet) to 46m (150 feet) long. The instrument is triggered by a magnetically damped one-second electrical contact pendulum similar to that in the Standard C&FS accelerograph. The operating cycle is electronically designed to allow continuous operation during an earthquake and then for an additional 7 seconds after the last pendulum contact. There is an internal calibration system that may be activated by switches on the outside of the case thus allowing the easy recording of period and damping at each inspection. Light-proof supply and take-up magazines provide for the retrieval of records in a lighted room.

3) The MO-2 accelerograph has a fixed 47 second operating cycle and is capable of registering a maximum of nine distinct events. It records on 35-mm film and is triggered by an electronic vertical starter that is nominally set to initiate operation at .01g. The instrument has no internal calibration system. Records are collected in a light-proof container, although with some difficulty because the film must be mechanically rewound after recording an event.

4) The RFT-250 operates similar to the previously described AR-240 but is somewhat smaller and records on 70-mm film. Improvements include the elimination of standby current drain and the incorporation of sealed rechargeable batteries into the instruments base plate.

5) The RFT-350 is a re-engineered version of the RFT-250. It possesses basically the same characteristics except for the addition of an electronic "omnittrigger" that features a combination of three triggering transducers, two horizontal and one vertical. The starting threshold level is adjustable but is normally set for .01g.

6) The SMA-1, a relatively small accelerograph (20 x 20 x 31cm), records on 70-mm film. It has the usual features of modern strong-motion instrumentation including light-proof film supply containers capable of holding 23 m of film, an operate cycle that continues 6 to 20 seconds after the last triggering pulse, internal sealed batteries and a simple calibration system. The instrument is triggered by a vertical transducer calibrated to start at .01g between 1 and 10 Hz. An electrical contact 1-second pendulum starter is an optional feature. Approximately 30 SMA-1's now in the field are equipped with WWVB radio receivers that impress real time signals (GMT) on the record. Because the identification code appears on WWVB once each minute, it is necessary to have a minimum 70-second operating cycle on these instruments to assure recording of the complete code.

Recently several accelerographs utilizing remotely located unbounded-strain-gage or force-balanced accelerometers have been installed in the network (Table II). The transducers are encased in small metal boxes ideally suited for mounting in relatively un-accessible locations, such as in the embankment of earthfill dams or on a particular frame member of a building. The incoming data are transmitted by wire to a centrally located recorder for amplification and signal filtering. The signals are then sent to a bank of galvanometers where the deflections of a light beam are registered in the usual manner on translating photographic film. Sensitivity of the components, although adjustable, is normally set to approximately 1.9 cm/g, similar to the 70-mm film recording accelerographs. The adjustable triggering threshold is set for .01g and is accomplished by either using a signal from the accelerometers or by separate starters.

As an optional feature, a digital delay memory (DDM) may be incorporated into the system, thus allowing the recording of data from the transducers prior to actuation of the recording unit. The DDM continuously monitors the transducer output but records the data only if the signal proves strong enough to trigger the instrument. Since the data are continuously stored for a short preset interval and discarded if not significant, it is possible to record the entire earthquake from a time shortly before the P-wave arrival. The present photo mechanical accelerograph will miss the initial P-wave motion and frequently will not trigger until the S-wave arrives. The DDM functioned well during testing, and a six-channel unit has recently been incorporated in one of SEB's recorders for field evaluation.

Instrument Installation.

Prior to preparation of a site for installation of one or more accelerographs, the SEB consults with the instrument owner to see that proper facilities are available. Recommended site criteria include the following: (1) housing that provides ample room for routine maintenance plus protection from weather, flooding and human interference, (2) a concrete pad or floor (well anchored to underlying soil or rock if at ground level), (3) an electrical outlet for a trickle charger, and (4) the correct shielded interconnecting cable if more than one accelerograph is to be installed.

After station preparations have been completed, the instrument is set in place by driving a self drilling anchor into the concrete and bolting the unit securely to the floor. Both the SMA-1 and RFT-350, the only self-contained accelerographs currently available, are mounted by a single anchor that passes through the center of the base plate. Instruments installed in a structure are normally aligned with the horizontal accelerometers parallel and transverse to the structure's axes. Those located along major fault zones as free-field instruments are situated with the horizontal components parallel and transverse to the trace of the fault.

A trickle charger is connected to the batteries to assure maintenance of proper charge level. When no electricity is available or it is not economically feasible to bring in electrical lines, a solar panel is installed to supply the trickle charging function. Although modern instruments have an event indicator that reveals whether triggering has occurred, an external counter is also attached to show the number of operations between inspections.

When all adjustments have been completed, a test is conducted to record the alignment of traces and the period and damping of individual accelerometers. This record is returned to the office for developing, calculation of instrumental constants, and permanent storage in the station file. After the instrument cover has been replaced, a similar test record is put on the film so that calibration data will always precede any earthquake record.

The final procedure at installation is to fill out an inspection form providing both information relevant to the instrument's functioning condition (battery voltage, lamp voltage, etc) and sufficient details to determine the station location, accelerograph orientation, local contacts and access to the site (Figure 3). This information is used by the technicians to fill out access sheets that are later put in field notebooks so that any SEB member may independently enter the station to service the instrument or recover earthquake records (Figure 4).

Photographs are normally taken before leaving the site to show the instrument in place, its housing, and the major structure associated with it.

Routine Instrument Maintenance

At set intervals one of the SEB technicians visits each accelerograph station and inspects the instrument to see that all components are operating properly and to make any adjustments and changes required to keep the equipment functioning at its maximum efficiency. The following procedures are carried out during an inspection:

- 1) Check the event counter for possible operations. If it reads anything other than zero, the potential record is recovered as though it were from an earthquake.
- 2) If the film supply indicator shows that less than half of the film remains, it is replaced with a new roll. In any event, the film is replaced at intervals of every two years or less depending upon the heat and humidity in the instrument room.
- 3) Manually displace the trigger pendulum to see that it starts the accelerograph.
- 4) Observe the light traces to see that they are on the collimating lens at the correct level and that they are spaced at designated locations across the film.
- 5) Visually check the data traces for damping deflections and free period oscillations.
- 6) Note whether the time marker solenoids are deflecting properly. Since the advent of crystal regulated timers, it is seldom necessary to make regular tests of the time rate accuracy.
- 7) Measure the charge current with the instrument on standby and the battery load voltage while the accelerograph is running.
- 8) Measure lamp current for the nominal operating value.
- 9) Where several instruments are interconnected, verify that timing and starting signals are being transmitted between the various units.
- 10) Check instruments with a WWVB radio receiver for radio reception and an impressed signal on the time mark solenoids.

After these procedures have been completed, an inspection form (Figure 3) is prepared. The inspection forms consist of four copy NCR paper so that one duplicate may be left with the instrument, the second in the station files, the third with the instrument owner, and the fourth in a master file at SEB's main office in San Francisco.

There are a large number of problems that may be observed during an inspection, but most of these are minor and inconsequential to the efficient acquisition of strong-motion data. Some of the more serious malfunctions that cause total instrumental failure or jeopardize the recording system are summarized in the following paragraphs.

- 1) Loose instrument mounting. Frequently the anchors imbedded in concrete loosen after installation resulting in a loose instrument within the next several months. Re-tightening the anchor nut eliminates this problem.
- 2) Electronic breakdown. A number of solid-state failures may occur including those within circuit boards regulating the trigger and operate cycle. In the first instance, the instrument will not start and in the second instance, the instrument will not turn off after having been triggered. Other failures have occurred in circuit boards governing the motor drive, time pulse generator, and calibration systems. The inspecting technician carries a supply of these components in the field and can readily replace the malfunctioning units when they are discovered.
- 3) Power loss. Power loss has been a major long-standing problem with strong-motion accelerographs but of a diminishing nature since small trickle chargers were installed on the batteries after SEB's experiences in the 1971 San Fernando earthquake (Maley, 1971). Some of the problems that remain are the occasional breakdown of chargers, normal battery

failure, loss of electrical power and subsequent charge current, and the corrosion of battery terminal connectors.

4) Mechanical maladjustments. The 1-second horizontal pendulum starters may become offset and if this is sufficient to make the electrical contact, the instrument will trigger and not turn off until the batteries have gone dead. The electronic vertical starters sometimes sag until they come to rest on their lower stops.

Other problems in this category include trace drift that may result in total loss of one or more channels of data, the loss of time mark solenoid deflections resulting in the omission of time signals on the record, and complete or partial failure of the film drive mechanism.

5) Environmental problems. Excessive heat and humidity may cause impairment of the normal instrumental operation. Occasional flooding has occurred, resulting in total disablement as well as an expensive repair bill. Human interference is also a problem, sometimes merely from the curious but at other times from vandals bent on destruction. In one instance, a locked accelerograph building was broken into and the instrument pried off its mounting and then thrown into an irrigation canal.

Most of these problems can be handled immediately during the inspection, but when field repairs are not expedient, the instrument is removed and taken to a SEB shop for renovation.

Until the mid 1960's the national network consisted chiefly of Coast and Geodetic Survey Standard accelerographs and a lesser number of AR-240's. At that time it was particularly important to see that each instrument was kept in good operating condition because there were relatively few stations to record any one earthquake. Since the existing accelerographs were slightly less reliable than those developed in recent years, a maximum inspection interval of 2 months was considered necessary to obtain a high data return. As the network was rapidly enlarged by the influx of newer and more reliable instruments, the inspection period was lengthened to 3 months. Even with this quarterly scheduling, it was impossible for the limited SEB staff to keep up with the accelerating number of new installations and inspections required.

After a 1974 study of maintenance procedures in the network, that was by now heavily weighted with highly reliable instrumentation, it was determined that the service interval could be further lengthened to 4 months with no significant decrease in operating efficiency. The entire network is now being maintained at 4-month intervals except where chargers have not yet been installed and for more than 100 buildings in the Los Angeles area a test is being conducted using 6-month inspections. This excludes some more critical or trouble-prone stations that are serviced more frequently. Should this test prove successful, SEB intends ultimately to convert the entire network to a 6-month maintenance schedule. Because a large part of technician time is expended in simply traveling to the stations, the less frequent inspection interval provides for more time to be used in servicing the instrument, thus resulting in better performance. This trend was indicated by the 1974 study of maintenance procedures.

SEB is striving to achieve a 95% success rate in keeping the instrumentation operational. This seems to be a desirable goal when one considers the unpredictable recurrence interval for strong earthquake motion at any particular location. An instrument may remain virtually idle and not record important data for 20 years, but when an earthquake does occur, if the instrument is not operational, a unique opportunity for recording damaging motion at that site may be lost. The extremes in significant recording intervals are shown by Long Beach, where an important record was obtained 8 months after the instrument was installed (only several records of minor importance have been obtained subsequently), and San Diego, where no significant record has been obtained in the 41 year history of the station. The necessity of keeping instruments in good condition in the eastern United States is of even greater importance because the probability of a damaging earthquake occurring in any period of time is considerably less than in California.

A longer inspection interval will help keep pace with the maintenance of a rapidly expanding network for some time, but if in the next several years the number of accelerographs doubles or triples, some alternative methods must be considered. One that perhaps offers the most promise for the future is the development of a Remote Interrogation System (RIS) to determine instrument operating capability by a telemetry link to a central control unit.

The development of a RIS could allow maintenance personnel to remotely interrogate any accelerograph for the condition of vital instrument functions such as proper triggering, battery voltage under load, amount of film remaining, and the number of events recorded. The interrogation could be preprogrammed to cover any set of stations or manually operated to select an arbitrary group of stations. SEB technicians may effectively inspect the network at frequent intervals and yet make actual on-site field maintenance visits only when serious malfunctions are observed. It is anticipated that other than such required maintenance trips, each instrument would be thoroughly serviced annually.

A second function of the RIS would be to query the event counter of any selected group of instruments after a local earthquake. Although most felt earthquakes are not of engineering significance, records at a particular site may be of special value to some engineers, geologists, or seismologists. The event-counter interrogation would simplify the recovery of such records and would, to some extent, define the time of occurrence of minor earthquake records that are collected during routine servicing.

Besides its obvious advantages, the RIS would pay for itself over a period of years by reducing the mean annual maintenance costs, primarily that of travel and manpower. As the system become operational, it would allow an increase in the network size while permitting more effective use of personnel.

Earthquake Record Recovery

Post earthquake procedures in the handling of records cover three broad phases: 1) the actual retrieval of records from individual instrument sites, 2) the photographic development of records, and 3) the labeling of the records with sufficient data for most routine analyses. Because of the large number of small earthquakes that occur in California, this is nearly a continual process although at a substantially lower level than after

a significant event.

A casual review of the number of records obtained during some recent earthquakes shows the magnitude of the recovery and documentation that will be required during future large shocks. In 1968, 114 records were obtained from a magnitude 6.5 earthquake that occurred 210 km from Los Angeles. During the 1971 San Fernando earthquake, 241 accelerograms and at least 100 aftershock records were recorded. The magnitude 5.9 Point Mugu earthquake in 1973 produced 318 accelerograph records. Even the recovery of lesser interest records, such as from the Point Mugu earthquake, presents a formidable task.

The interrogation system proposed above will be of considerable assistance in record recovery as it may be used to monitor instrument operations after locally felt earthquakes that otherwise are not damaging and of relatively little significance. For instance, frequent smaller earthquakes are felt in the Los Angeles area, but it is impossible to determine which instruments have been triggered without actually visiting each site.

Considering the present size of the network in southern California, an earthquake in the magnitude 6.5 range near Los Angeles would result in 700 original records and at least 200 aftershock records. It is estimated that some 3,500 feet of data would be simultaneously obtained on a variety of recording media, i.e., 152-mm and 304-mm photographic paper and 35-mm and 70-mm film. To collect, develop, and label such a large set of records from a single event is a project of staggering proportions, particularly when a large amount of time must be allotted to dealing with the inquiries from engineers, scientists, and public officials. For example, it took nearly 4 weeks effort by the entire SFS staff just to collect and develop all the records obtained during the Sanfernando earthquake.

After an earthquake, SEB field personnel proceed to the spicentral area as rapidly as possible to retrieve records and return the instruments to their pre-earthquake condition. They carry sufficient provisions needed for extensive recovery, especially loaded film and paper magazines to replace those that have substantially reduced supplies because of the earthquake operations. Upon entering the station the technician will check the signal counter, put calibration data on the record, and advance sufficient film into the take-up magazine to assure protection from light when the instrument is opened. The record is then removed and labeled (etched on film or written on paper) with the station name, accelerograph serial number, date of record recovery, and date of earthquake, if known. Finally, the accelerograph is restored to its normal operating condition and the counter reset to zero.

The records are returned to the local SEB office for photographic processing. In the past, this has been accomplished by sight developing because of the instruments' variable lamp intensity and the possibility of accidental fogging during record recovery. Considering the potentially large number of records from future earthquakes, some effort is being expended to provide automatic developing procedures. A paper accelerogram processor is being tested that will develop, fix, and dry the records in one operation. A 70-mm film dryer is now in operation, and the use of complete film processing systems are being investigated.

After development, the records are temporarily labeled by affixing a gummed sticker with the station name, instrument number, and date of the earthquake. Permanent labels are later produced by typing the following information on matte-finish mylar plastic: station name, permanent station number, instrument type and serial number, data of earthquake in both GMT and local time, and the physical constants of the individual components including orientation, sensitivity, period and damping (Figure 5). These labels are spliced directly to the original record, normally just in front of the pre-earthquake calibration data. The records are then transferred to SEB's data management section for the production of distribution copies and subsequent processing and analysis.

ACKNOWLEDGEMENTS

The strong-motion program conducted by the Seismic Engineering Branch, U. S. Geological Survey is supported by National Science Foundation grant (NSF-CALL4). The author is indebted to the staff of the Seismic Engineering Branch who provided numerous valuable suggestions during the preparation of this paper.

References

1. Cloud, W. K., 1964, The cooperative program of earthquake investigations, in Carder, D.S., ed., Earthquake investigations in the western United States, 1931-1964: Dept. of Commerce, Coast and Geodetic Survey Pub. 41-2, p. 3-4.
2. Halverson, H. T., 1969, Some recent developments in strong-motion seismographs: Teledyne-Geotech Pub., Monrovia, California, 32 p.
3. Kinematics Inc., 1974a, SMA-1 strong-motion accelerograph: specification sheet, Kinematics, San Gabriel, California 2p.
4. Kinematics Inc., 1974b, Preliminary data sheet, CR-1 central recorder, Kinematics, San Gabriel, California, 3p.
5. Maley, R. P., 1971, A statistical summary of accelerograph performance during the earthquake of February 9, 1971, in Hudson, D. E., ed., Strong-motion instrumental data on the San Fernando earthquake of February 9, 1971: California Institute of Technology and Seismological Field Survey, NOAA, Dept. of Commerce, p. 54-76.
6. Nimbus Instruments, 1974, TMA-100 dynamic recording system, West Sacramento, California, Nimbus Instruments, 4p.
7. Teledyne-Geotech, 1973, System description RRA-100, Garland, Texas, Teledyne-Geotech, 7p.

TABLE I

Characteristics of Self Contained Photo-Mechanical Accelerographs*
in the United States Network

<u>Instruments</u>	C&GS Standard	AR-240	MO-2	RFT-250	RFT-250	SMA-1
<u>Components</u>	3	3	3	3	3	3
<u>Accelerometer Period (Sec)</u>	.04--.09	.05	.03	.045	.045	.04
<u>Sensitivity (cm/g)</u>	6-20	7.6	1.5 horiz. 2.2 vert.	1.9	1.9	1.9
<u>Photo Recording Medium</u>	152 or 304 mm paper	304-mm paper	35-mm film	70-mm film	70-mm film	70-mm film
<u>Recording Speed (cm/sec)</u>	2	2	1.5	1	1	1
<u>Trigger</u>	horizontal	horiz.	vertical	horizontal	2 horiz. 1 vert.	vert. horiz.
<u>Manufacturer</u>	out of pro- duction	out of production	Victoria New Zealand	out of pro- duction	Teledyne- Geotech, U.S.A.	Kine- metrics, U.S.A.

* Data from Halverson (1969) and Kinematics (1974a).

TABLE II

Characteristics of Accelerographs in the United States Network
With Remotely Located Sensors*

<u>Instruments</u>	TMA-100	RRA-100	CR-1
<u>Components</u>	up to 6	3	up to 12**
<u>Accelerometer Period (sec)</u>	.01	.01	.02
<u>Nominal Sensitivity (cm/g)</u>	1.9	1.9	1.9
<u>Recording Film</u>	89-mm film	70-mm film	178-mm film
<u>Recording Speed (cm/sec)</u>	1-20	1	1
<u>Trigger</u>	2 horizontal 1 vertical	2 horizontal 1 vertical	vertical horizontal (optional)
<u>Manufacturer</u>	Nimbus	Teledyne-Geotech	Kinemetrics

* Data from Kinemetrics (1974b) Nimbus (1974) and Teledyne-Geotech (1973).

** Manufacturer offers up to 25 channels but USGS uses a maximum of 12 channels.

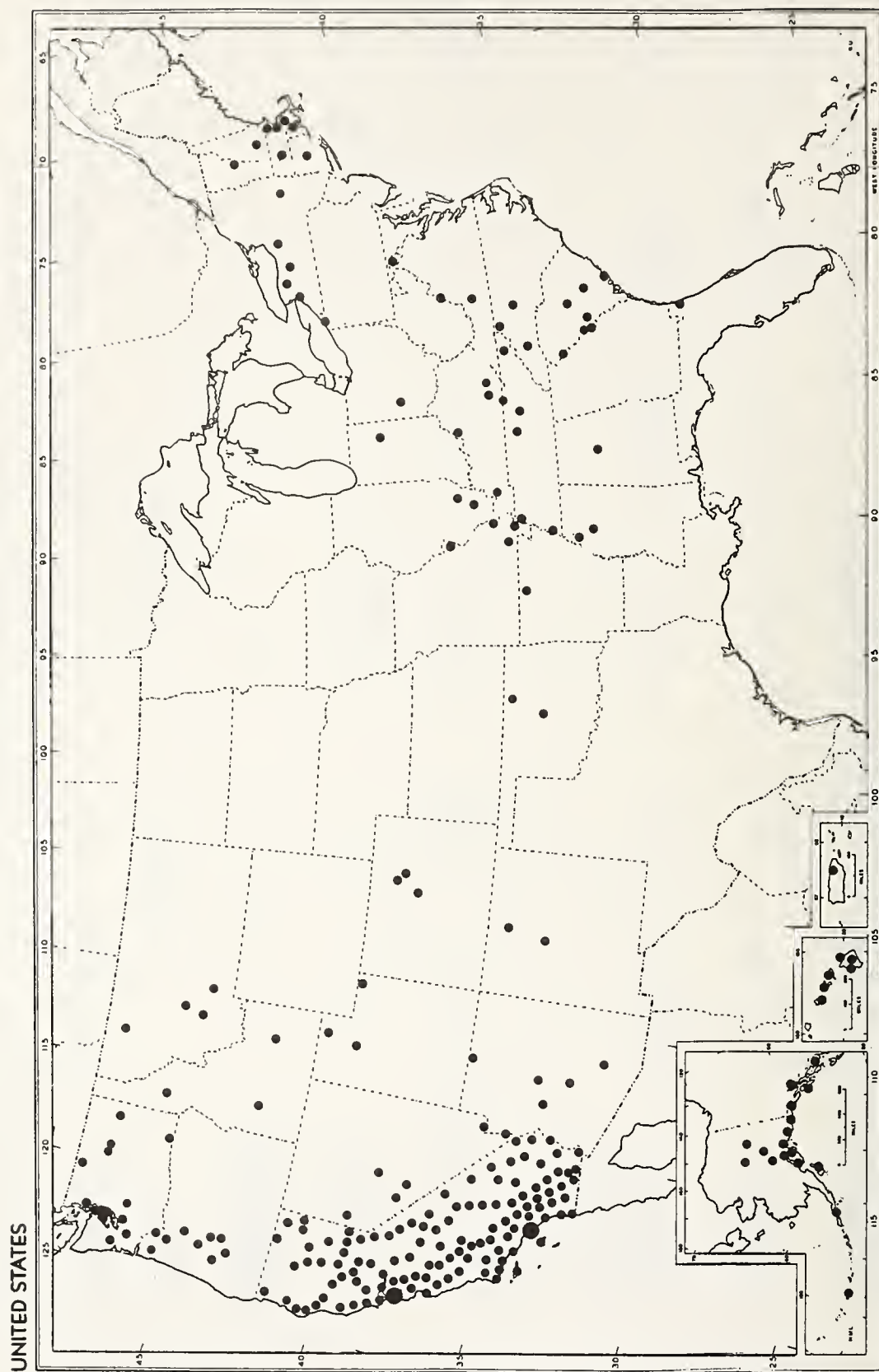


Figure 1. Accelerograph stations in the United States, 1 April 1975.

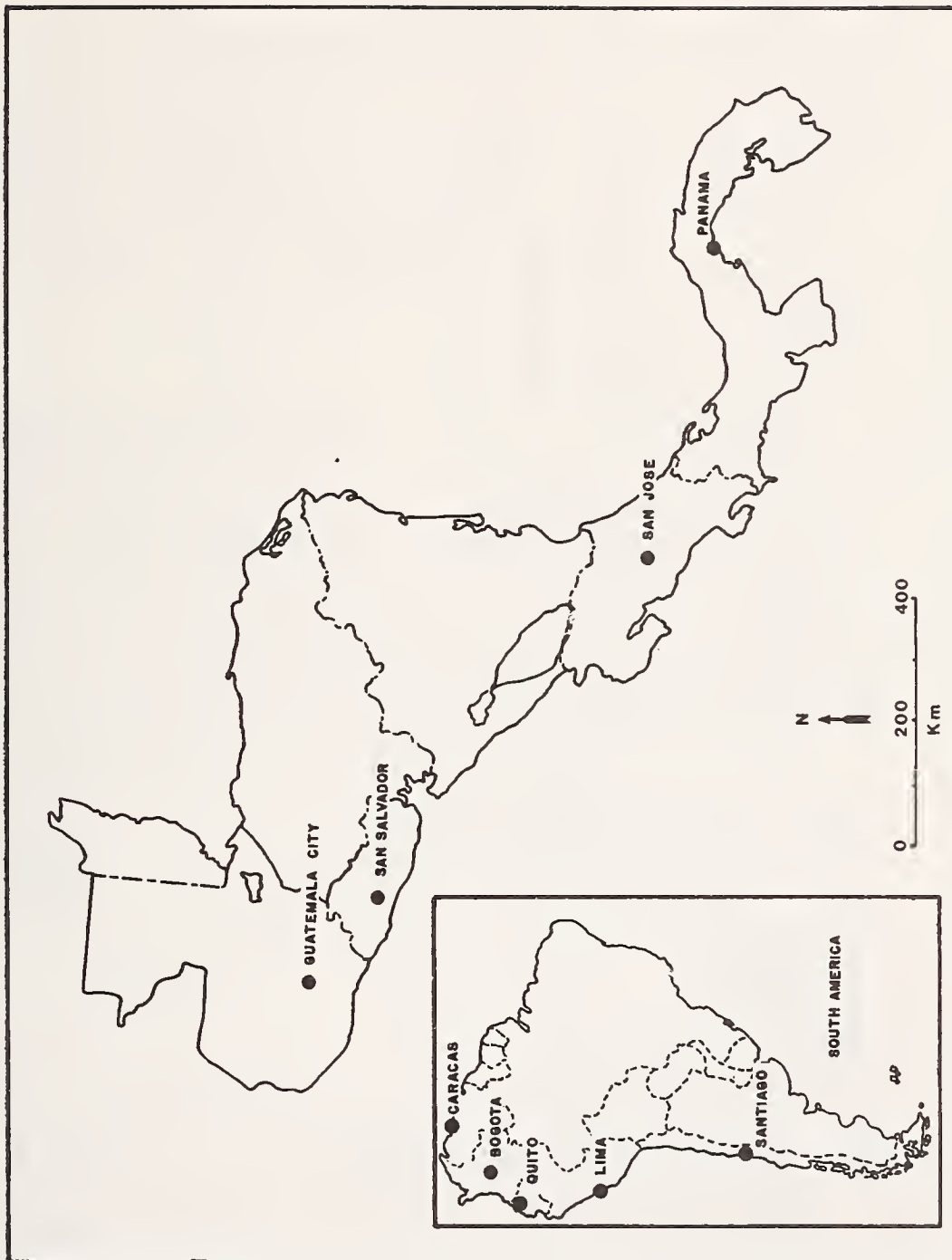


Figure 2. Accelerograph stations in Central and South America.

ACCELEROGRAPH INSPECTION		Observer	S.N.	Date
Seismic Engineering USGS		W. J. N.	SMA 1742	3 March '75
		Station	Level	
		Bonds Corners, California	Ground	
COMMENTS		Instrument is located in fire dept. storage room, 700 Diaz Road. Bill Setchell, chief, telephone (714) 361-8209. Access between 0600 and 2000.		
Earthquake Date	Installation			
Counter	0			
Battery Load V	13.1			
Lamp ma/V	3.2 v			
Charge Rate	23 ma			
Battery in-Date	3/75			
Film in-Date	3/75			
Starter Check	OK			
Clock Rate	OK			
NEEDS				

L = South
 V = Down
 T = East

Figure 3. Accelerograph Inspection form prepared for a new installation. The same form is used for routine maintenance visits.

U. S. GEOLOGICAL SURVEY
SEISMIC ENGINEERING

DATE 6-5-74

STATION 11611 San Vicente Blvd. STATION # 875

ADDRESS Brentwood CITY Los Angeles

CONTACT Fad Wiley PHONE 826-0889

POSITION Building Engineer KEYS 1

INSTRUMENTS SMA-1 s/n 1414 Grnd L- S 05 W
s/n 1415 6th V- Down
s/n 1416 Roof(11) T- S 85 E

TOPO SHEET Beverly Hills CO-ORD 34.05 N 118.25 W

THOMAS MAP P.# LA-41 CROSS STREETS S. Vicente - Bringham

OWNER CODE LA ORIENTATION VERIFIED Yes

DESCRIPTION Enter pkng. from rear. Ground - enter acc. room from
driveway to ground level pkng. (San Vicente side). 6th - en central
core east of el. Roof - el. to 10, NW stairs to roof, 3rd door
in penthouse.

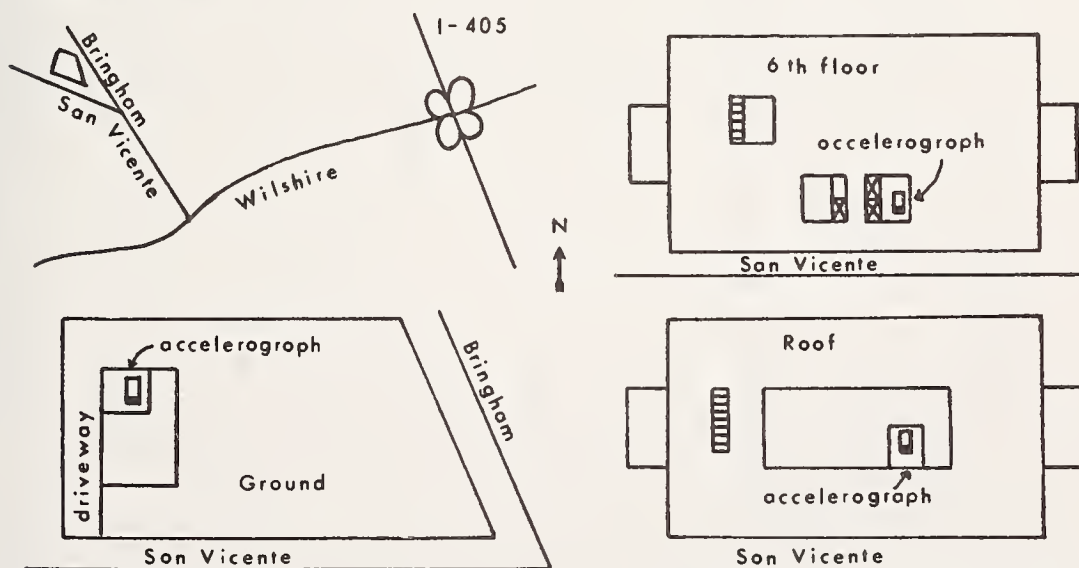


Figure 4. Typical accelerograph station access sheet.

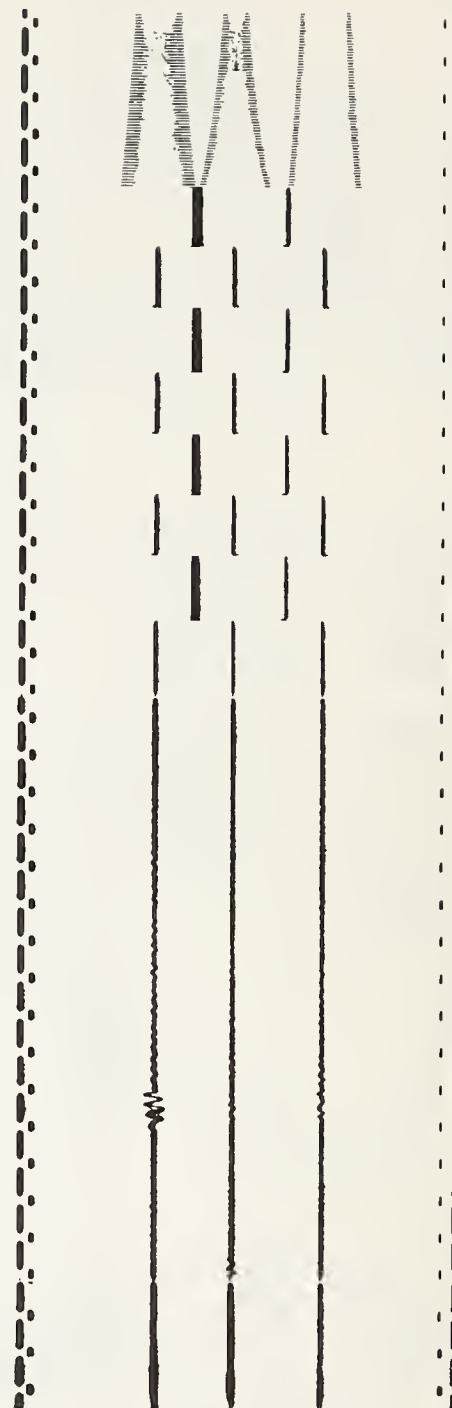
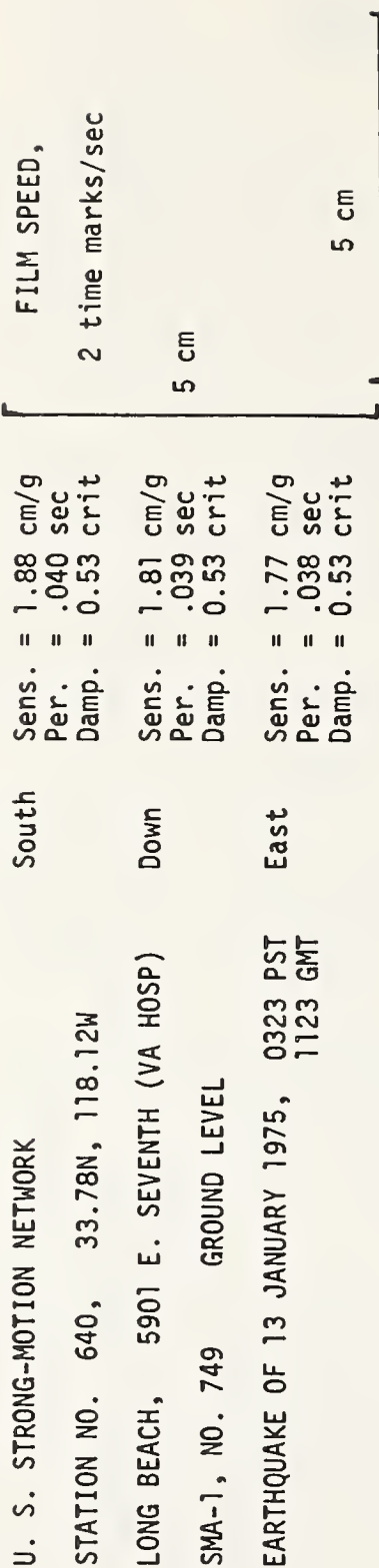


Figure 5. Details of an accelerograph record with a standard label. The pre-earthquake calibration pulses were omitted for reproduction.

Strong-Motion Data Management

by

Christopher Rojahn
U. S. Geological Survey
San Francisco, California

ABSTRACT

The Seismic Engineering Branch (SEB), of the Office of Earthquake Studies, U. S. Geological Survey, is funded by the National Science Foundation and is responsible for the development and maintenance of a national network of strong-motion instruments and for the processing, management, and dissemination of data obtained from those instruments. Data management is central to the entire strong-motion program; it serves as a focal point for the functions of archiving the records, processing the data, and disseminating both the data and information about the program to the user community. In the archival phase, all records are stored by station and cataloged both by event and by station. In data processing, all significant ground and basement level records are digitized after which the raw digitized data is used to generate the following: uncorrected acceleration time-histories; velocity and displacement time-histories; and various forms of frequency domain spectra. Both SEB and the Environmental Data Service of the National Oceanic and Atmospheric Administration are involved in the data and information dissemination operation. Each organization distributes data, whereas SEB is solely responsible for the dissemination of information about the strong-motion program. Various U. S. Geological Survey professional papers and circulars are the primary media through which the latter function is accomplished.

Key Words: Accelerographs; Data Processing; Earthquake Records; Strong-motion Data

Introduction

The Seismic Engineering Branch (SEB) of the Office of Earthquake Studies, U. S. Geological Survey (Department of Interior), is responsible for the development and maintenance of a national network of strong-motion instruments and for the processing, storage, and dissemination of data obtained from those instruments. In order to carry out these responsibilities, SEB concentrates its efforts on the following activities: program management, network design, network operations, data management, and research and applications. Data management, the subject of this paper, is central to SEB's entire strong-motion program. It serves as a focal point for the functions of (1) archiving the records, (2) processing the data, and (3) disseminating both the data and information about the program to the engineering seismology research community, the structural design community, and regulatory agencies at the Federal, State, and local levels. All three functions are discussed in detail in subsequent portions of this paper.

Background Information

SEB's data management functions were first outlined in a proposal submitted to the National Science Foundation (NSF) in July 1974. During the year prior to that time, SEB operated under general NSF funding in a transitional stage during which its responsibilities and functions were formulated and defined in detail. Before that, (i.e., up until May 27, 1973, when SEB was formed as part of the U. S. Geological Survey), the office existed as the Seismological Field Survey (SFS) in the National Oceanic and Atmospheric Administration (NOAA) of the U. S. Department of Commerce. In general, the SFS had fewer responsibilities, a smaller staff, and substantially less funds. In particular, the data management function was the responsibility of NOAA's Environmental Data Service (EDS).

As a result of the July 1974 proposal, NSF awarded SEB a grant of \$700,000 annually to develop and assume primary responsibility for the U. S. strong-motion program. The funding was approved in principle for five years and will be increased annually in accordance with a nominal inflation factor. Of the total annual amount, \$240,000 has been allocated for data management (FY 1975). This level of funding has enabled SEB to acquire three additional staff members in data management. Consequently, in addition to the project chief, there are now six persons working on data management--one geophysicist, one mathematician, one computer specialist, two physical science technicians, and one clerk typist. In contrast, there are 16 persons assigned to other SEB projects (22 staff members in total).

In its present form the national network of strong-motion instruments contains approximately 1300 accelerographs located primarily in California but also throughout the remainder of the seismically active areas of the U. S. The instruments are owned by Federal, State, and local agencies, universities, private firms and individuals, and other independent groups. SEB acts as the primary coordinator for the development and maintenance of the entire network and assumes overall responsibility for record collection, record archiving, data analysis and data dissemination.

At present, the vast majority of instruments in the network are triaxial optical-

mechanical accelerographs that record three strong-motion traces per record. Among the new installations, however, are remote recording systems that record up to 12 strong-motion traces per record. In addition, direct digital recording systems are also expected to be installed in the near future. These differences in the types of recording systems and the number of traces per record have made it necessary to design a data management system that can handle a variety of data forms.

Archival System

As of December 31, 1974 approximately 3200 strong-motion records had been obtained from the national network of strong-motion instruments. Although the first record was generated in 1932, the vast majority have been obtained since the mid-1960's, when the number of instruments in the network began to increase rapidly. Many of the records are on 6-inch and 12-inch (152-mm and 305-mm) paper, a few are on 35-mm film, but most are on 70-mm film. It is expected that most of the records obtained in the near future will be on 70-mm film, a substantial number of others will be on various sizes of paper and film (12-inch, 35-mm, and others), and a few will undoubtedly be on magnetic tape.

The records are archived by station, which is defined as the geographic location at which an instrument(s) is (are) located (e.g. a building housing three instruments constitutes one station). There are one or more storage containers (depending on the number of existing records) reserved for each station. The 35-mm and 70-mm film records are stored in 2 7/8-inch (73-mm)-high, 3 3/4-inch (95-mm) inner diameter light-weight metal canisters; the larger film and paper records are stored in 15-inch (381-mm)-long, 2 7/8-inch (73-mm) inner diameter medium-wall cardboard tubes. Each container is labeled with the station name (address or structure title), assigned station number, and date of event(s) of records stored therein. Measures have been taken to ensure that the archival room is as fire-proof as possible.

Prior to permanent storage, the records are labeled, and high-quality digitizable mylar copies are made of all those considered significant (in general, ground or basement level ~~records~~ having a maximum acceleration greater than, or, equal to 0.10g). Beginning in middle or late 1975, one mylar copy will be sent to each of the following: the SEB branch office in Los Angeles; the California Institute of Technology in Pasadena; the Environmental Data Service, NOAA, in Boulder, Colorado; and the instrument owner. All other records are archived without being copied unless there is a specific request to do so.

One other important part of the archival process is the preparation of an "event and station information card" (figure 1) for each strong-motion record. The card is prepared as soon as a record is received and contains all pertinent station and event information, instruments constants, maximum accelerations and epi-central distance. One copy is filed in a station file, and a duplicate is placed in an event file. Eventually, the information from both files will be published in catalog form and will be made available on a computerized data file that can be queried by remote terminal.

Data Processing System

SEB's data processing system is evolving from in-house developments, but much of it is patterned after the methodology developed by the California Institute of Technology (CIT) during the digitization and analysis of the February 9, 1971 San Fernando earthquake strong-motion records (1). Prior to the award of the 1974 NSF grant, SEB's data processing system was smaller in scope though similar in form. Presently, it is being expanded to handle a large volume of records in a relatively short time.

As a matter of course, SEB plans routinely to process all significant ground and basement level records. The processing of each record can be subdivided into several phases: record digitization; conversion of raw digitized data to uncorrected data; conversion of uncorrected data to corrected data and the generation of velocity and displacement time-histories; and the generation of various forms of frequency domain spectra. Phases two through four are accomplished through the use of three computers, a CDC 6400, CDC 6600, and a CDC 7600, all of which are located in Berkeley, California. All computer programs are submitted in batch or time-share mode either at Berkeley or via one of the remote terminal systems at the U. S. Geological Survey (USGS) computer center in Menlo Park, California.

The first phase of data processing (i.e. record digitization) is not carried out in-house. Instead, digitization services are being procured from the following external organizations: Dynamic Graphics of Berkeley, California; I/O Metrics of Sunnyvale, California; and EDS/NOAA of Boulder, Colorado. Dynamic Graphics uses a manual film-plane digitizer and is presently able to digitize both enlarged film and normal-sized paper records on a routine basis. The system is particularly appropriate for those records that cannot be digitized automatically, that is, those records that are not well defined, are non-continuous, and have overlapping traces. Normally, the firm is requested to digitize all peaks, valleys, and inflection points at a minimum rate of 50 points per second. I/O Metrics has developed an automatic, laser-beam, trace-following, film-plane digitizer and has satisfactorily demonstrated its capabilities in a limited trial. Film records may be digitized directly, whereas paper records must be reproduced on 70-mm film before digitization. The system is especially appropriate for well defined, continuous, non-overlapping traces, and is notable for its high processing speed potential (the firm estimates that it can accurately digitize an average-sized strong-motion record in half an hour). Normally, records are digitized in increments ranging in width from 25 to 50 microns. EDS uses an automatic faster-scanning, equal-increment digitizing system (VISICON) which is capable of scanning a 12 x 25-inch (305 x 635-mm) record at a maximum rate of 200 samples per inch (approximately 79 samples per centimeter). Records digitized on the system are currently being evaluated by SEB. It is anticipated, however, the system will be satisfactory for processing both paper and enlarged film records. In total, the three external organizations collectively provide SEB with the capability for digitizing a large volume of records in a relatively short time.

SEB requires that each external organization submit its digitized data on magnetic tape or punched cards in a preselected format, and that it be accompanied by a full-scale plot of the data (a plot at 3x's scale is also frequently required for film records). Each

plot then undergoes a quality control check whereby it is visually compared to the original record (or 3x's scale copy) with the aid of a low-power magnifying lens. If the plot of the digitized data appears to be truly representative of its analog counterpart the digitized data are accepted for subsequent phases of processing. If not, the original record is redigitized.

In the second phase of data processing, the raw digitized data are converted to what is referred to as "uncorrected data" (2). At this time, all paper or film distortions are removed, and acceleration and time are cross-correlated in order to express acceleration as a function of time. The final product is permanently retained on either magnetic tape or punched cards (in the near future, such data will also be stored on microfilm), on a digital listing, and as a time-history plot.

During the third phase, uncorrected data are converted to "corrected data" (3), and velocity and displacement curves are generated. Instrumental and baseline corrections are first applied to obtain true ground acceleration (corrected data). Single and double integration processes are then used to generate velocity and displacement time-histories. The data are permanently retained on either magnetic tape or punched cards (in the near future, such data will also be stored on microfilm), on digital listings, and in plot form.

During the fourth and final phase of data processing, various forms of frequency domain spectra are generated. Along these are the spectra routinely calculated and plotted by CIT (4, 5) during the processing of the San Fernando earthquake strong-motion records: maximum relative velocity response spectra (figure 2); relative displacement, pseudo velocity response, and pseudo acceleration spectra plotted on tripartite paper (figure 3); and Fourier amplitude spectra (figure 4). In addition, SEB has developed two other forms of plots (6) that give substantially more insight into the nature of strong-motion: relative velocity response envelope spectra (figure 5), and time-duration spectra of the response envelope (figure 6). All five forms of spectra are permanently retained on digital listings and in plot form.

Data And Information Dissemination System

Information about the SEB strong-motion program is disseminated solely by SEB, whereas the actual strong-motion data are disseminated both by SEB and EDS. EDS is the distributing agency for the uncorrected and corrected data generated by SEB. Such data are made available in punched card form and on magnetic tape (7 or 9-track). EDS also provides analog copies of strong-motion records on 70-mm film clips (approximately 8x's reduction) and on 35-mm film reels (12's reduction) and is being requested to develop the capability to produce blue-line full-scale analog copies. Beginning in middle or late 1975, SEB will publish routine data reduction and analysis results in a series of U. S. Geological Survey professional papers. It is expected that each professional paper will cover one calendar year and will contain the following data for all significant ground and basement level records generated in that year: uncorrected and corrected acceleration time-histories; velocity and displacement time-histories; and the five forms of spectra des-

cribed in the section on data processing. In addition, SEB also distributes, upon request, blue-line analog copies of all records not made available through EDS.

Information about the strong-motion program is disseminated primarily through the following publications: the "Seismic Engineering Program Report," a USGS circular published quarterly; "Strong-Motion Accelerograph Station Locations Listing," a USGS circular published annually; "Strong-Motion Accelerograph Station Descriptions" (tentative title), a series of USGS professional papers; and "Catalog of Strong-Motion Records," tentatively planned as a joint USGS/NOAA publication (to be issued as a USGS professional paper). All circulars are issued free of charge on request (the current mailing list contains names and addresses of approximately 2300 recipients). The professional papers receive a limited free distribution but can be purchased for a nominal fee.

The first issue of the "Seismic Engineering Program Report" (7) was published in December 1974 as U. S. Geological Survey Circular 713. It contains a listing of 1972 and 1973 accelerograph records and a description of the then-current status of the SEB strong-motion program. The second issue, scheduled for publication in the spring of 1974, contains a listing of 1974 accelerograph records, two articles by SEB staff members (one on the Latin American and Caribbean strong-motion programs and one on recent developments in strong-motion instrumentation), and notes on record corrections and the availability of strong-motion data. Future issues will contain similar information with all listed data as current as practicable.

The first issue of the "Strong-Motion Accelerograph Station Locations Listing" is scheduled for publication in mid-1975. It will contain the following data for all stations installed in the national network prior to January 1, 1975: station number, location, country, structure type/size, instrument location(s), coordinates, and source(s) for data. The list will be routinely updated in the "Seismic Engineering Program Report." The second issue of the listing will contain the same information for all stations installed prior to January 1, 1976 and will be published in early 1977. Similar listings will be published annually thereafter.

The content and format for "Strong-Motion Accelerograph Station Descriptions" have not yet been firmly established. It is probable, however, that the descriptions will contain the following: location data including the geographic coordinates, road and topographic maps, and an exterior photograph; geologic data including a brief seismic history of the area, the proximity of faults, if any, a verbal description of the regional and local geology, cross-section(s), formation descriptions, and depth to water table; and soils data, when available, including boring logs and measurements of density, standard penetration values, and P- and S-wave velocities. If there is a structure at the site, each station description will (tentatively) include: typical plan view(s) indicating lateral force resisting elements, orientation, dimensions, and the center of mass and center of rigidity of each floor or mass element; typical section(s) of the full structure showing dimensions; general design information (e.g., mode shapes and frequencies); and the source where additional information may be obtained (e.g., the design engineer).

It is planned that the "Catalog of Strong-Motion Records" contain a listing of all

accelerograph records obtained from the national network of strong-motion instruments since its inception in 1932. Records will be listed both by event and by station showing epicentral distance, maximum acceleration whenever available, and various data sources. The frequency of publication has not yet been established, but is expected to be annually, biannually, or even less frequently.

Summary

The Seismic Engineering Branch (Office of Earthquake Studies, U. S. Geological Survey) is funded by the National Science Foundation and is responsible for the development and maintenance of a national network of strong-motion instruments and for the processing, management, and dissemination of data obtained from those instruments. Data management is central to the entire strong-motion program; it serves as a focal point for the functions of archiving the records, processing the data, and disseminating both the data and information about the program to the user community. In the archival phase, all records are stored by station and cataloged both by event and by station. In data processing, all significant ground and basement level records are digitized after which the raw digitized data is used to generate the following: uncorrected and corrected acceleration time-histories; velocity and displacement time-histories; and various forms of frequency domain spectra. Both SEB and EDS are involved in the data and information dissemination operation. Each organization distributes data, whereas SEB is solely responsible for the dissemination of information about the strong-motion program. Various U. S. Geological Survey professional papers and circulars are the primary media through which the latter function is accomplished.

Acknowledgments

The author gratefully acknowledges Chuck Knudson, Dick Maley, and Fritz Matthieson for their help in reviewing and editing this manuscript.

References

1. Trifunac, M.D., and Lee, V., 1973, Routine computer processing of strong-motion accelerograms: California Institute of Technology report N. EERL 73-03, 360 p.
2. Earthquake Engineering Research Laboratory (EERL), 1969, Strong-motion earthquake records, Volume I-uncorrected accelerograms: California Institute of Technology report No. EERL 70-20, part A, 203 p.
3. Earthquake Engineering Research Laboratory (EERL), 1971, Strong-motion earthquake records, Volume II-corrected accelerograms and integrated ground velocity and displacement curves: California Institute of Technology, report N. EERL 71-90, part A, 321 p.
4. Earthquake Engineering Research Laboratory (EERL), 1972, Analyses of strong-motion earthquake accelerograms, Volume III-response spectra: California Institute of Technology report No. EERL 72-80, part A, 272 p.
5. Earthquake Engineering Research Laboratory (EERL), 1972, Analyses of strong-motion earthquake accelerograms, Volume IV-Fourier amplitude spectra: California Institute of Technology report No. EERL 72-100, part A, 164 p.
6. Perez, Virgilia, 1974, Time dependent spectral analysis of thirty-one strong-motion earthquake records: U. S. Geological Survey open-file report, 141 p.
7. U. S. Geological Survey (USGS), 1974, Seismic engineering program report, October-December, 1974: U. S. Geological Survey circular 713, 19 p.

STATION INFORMATION:

No. 117
 Location El Centro, California
(Imp. Val. Irrig. Dist.)
302 Commercial
 County Imperial
 Coordinates 32.79N, 115.55W
 Structure 2-story building

EVENT INFORMATION:

Date 5/18/40 Local Time 2037 PST
 Location 10 km NE of Calexico, Calif.
 Coordinates 32.72N, 115.50W
 Magnitude 6.7 Max. Intensity X
Cal. Tech./
 Information Source/Date U. S. Earthquakes-1940
 Epicentral Distance 9 km (6 miles)

Instr Loc/Type/Ser No	Component	Sensitivity	Period	Damping	EVENT MAX ACCEL
Basement	N - S	27.4 cm/g	.099 sec	.55 crit	.314g
S-M	E - W	26.9 cm/g	.100 sec	.53 crit	.169g
FS-4	Vertical	24.8 cm/g	.095 sec	.57 crit	.259g

Figure 1.

Station and event information card used by SEB to catalog information on strong-motion accelerometer records.

RELATIVE VELOCITY RESPONSE SPECTRUM

111A001 40.001.0 EL CENTRO SITE IMPERIAL VALLEY, ARIGATION DISTRICT MAY 18, 1940 - 2037 PST
 DAMPING VALUES ARE 0, 2, 5, 10 AND 20 PERCENT OF CRITICAL

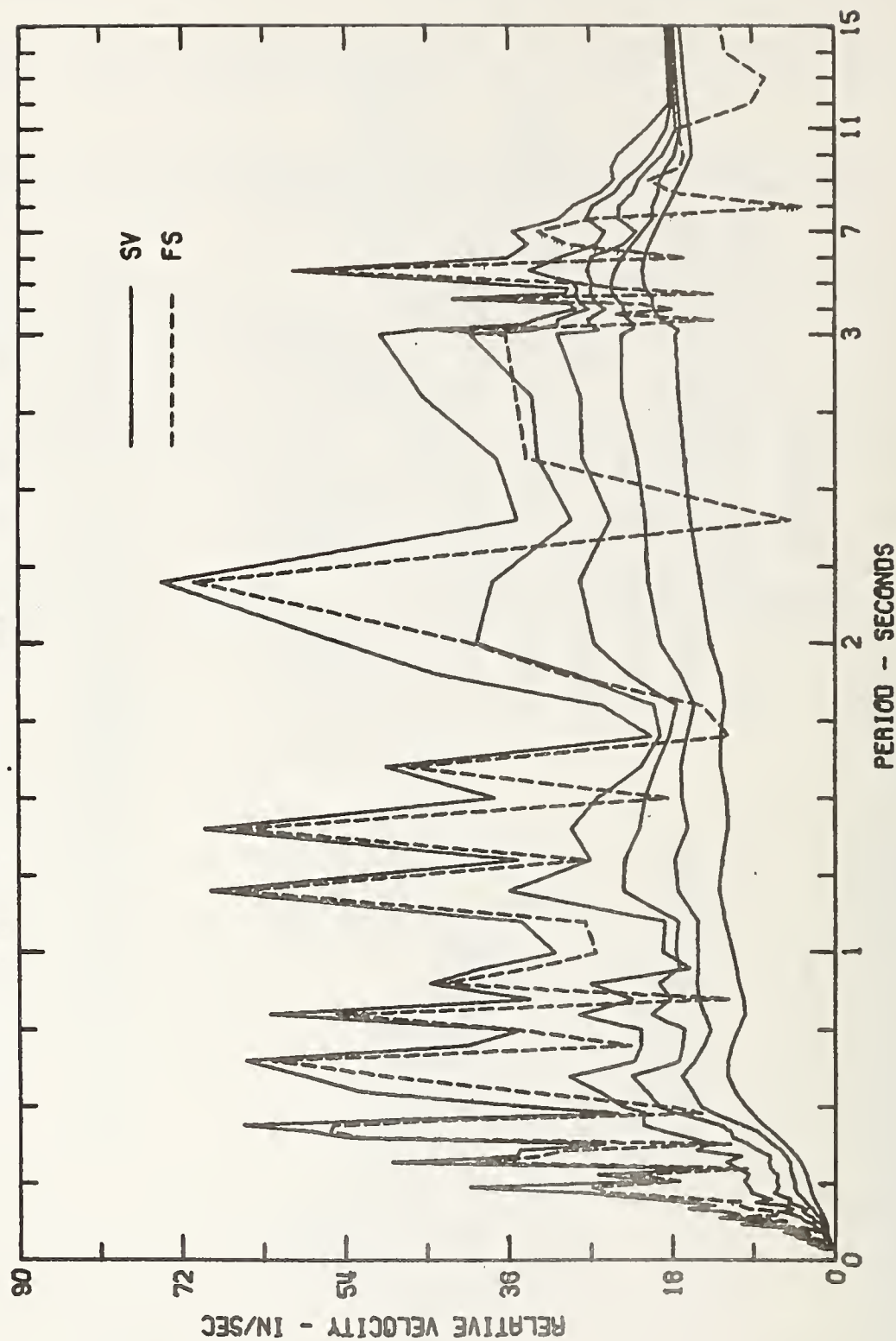


Figure 2.
 Maximum relative velocity response spectrum.

RESPONSE SPECTRUM

IMPERIAL VALLEY EARTHQUAKE MAY 18, 1940 - 2037 PST

111A001 40.001.0 EL CENTRO SITE IMPERIAL VALLEY IRRIGATION DISTRICT COMP S90H

DAMPING VALUES ARE 0, 2, 5, 10 AND 20 PERCENT OF CRITICAL

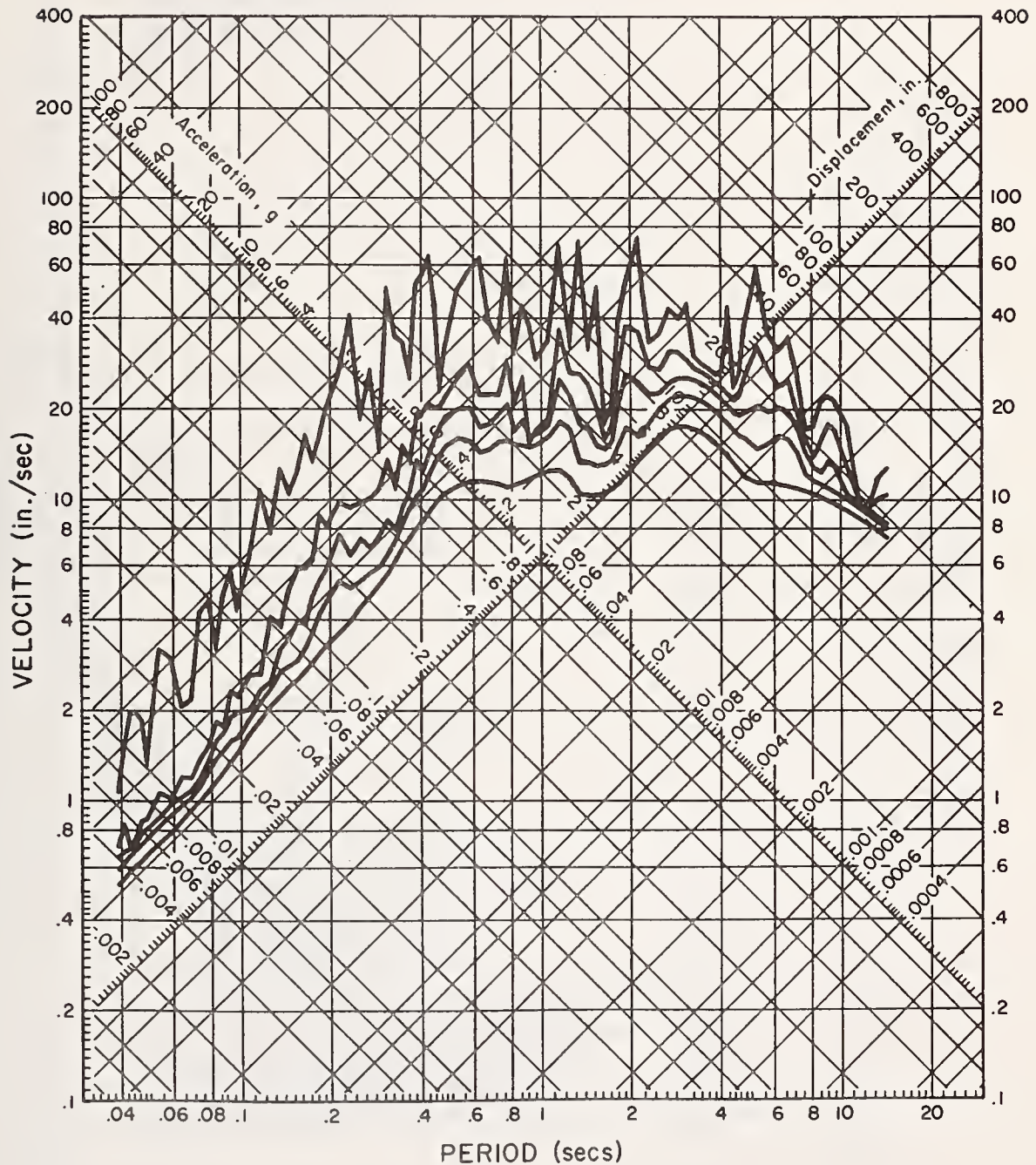


Figure 3.

FOURIER AMPLITUDE SPECTRUM OF ACCELERATION
 IMPERIAL VALLEY EARTHQUAKE MAY 18, 1940 - 2037 PST
 IVR001 40.001.0 EL CENTRO SITE IMPERIAL VALLEY IRRIGATION DISTRICT COMP S90W

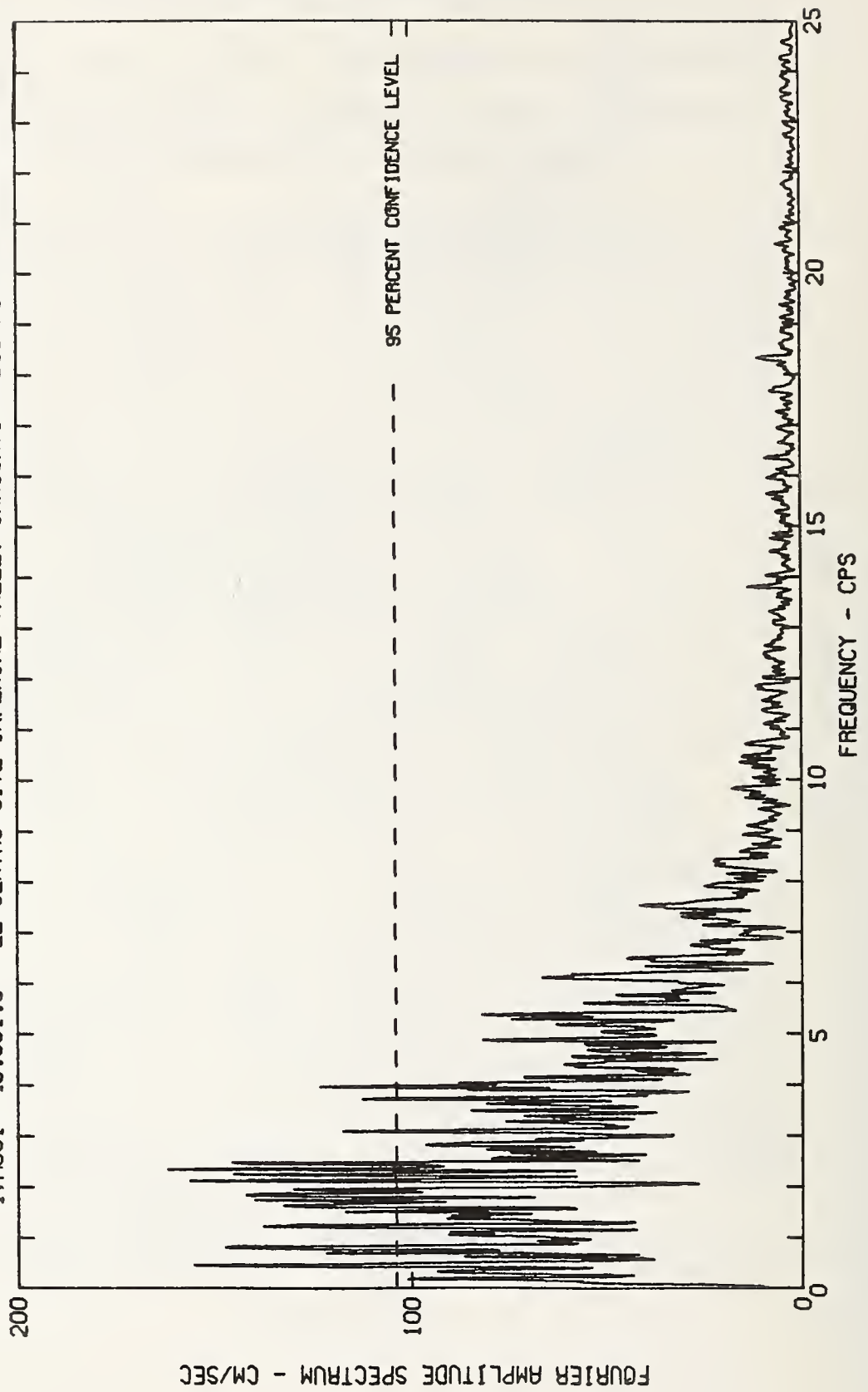
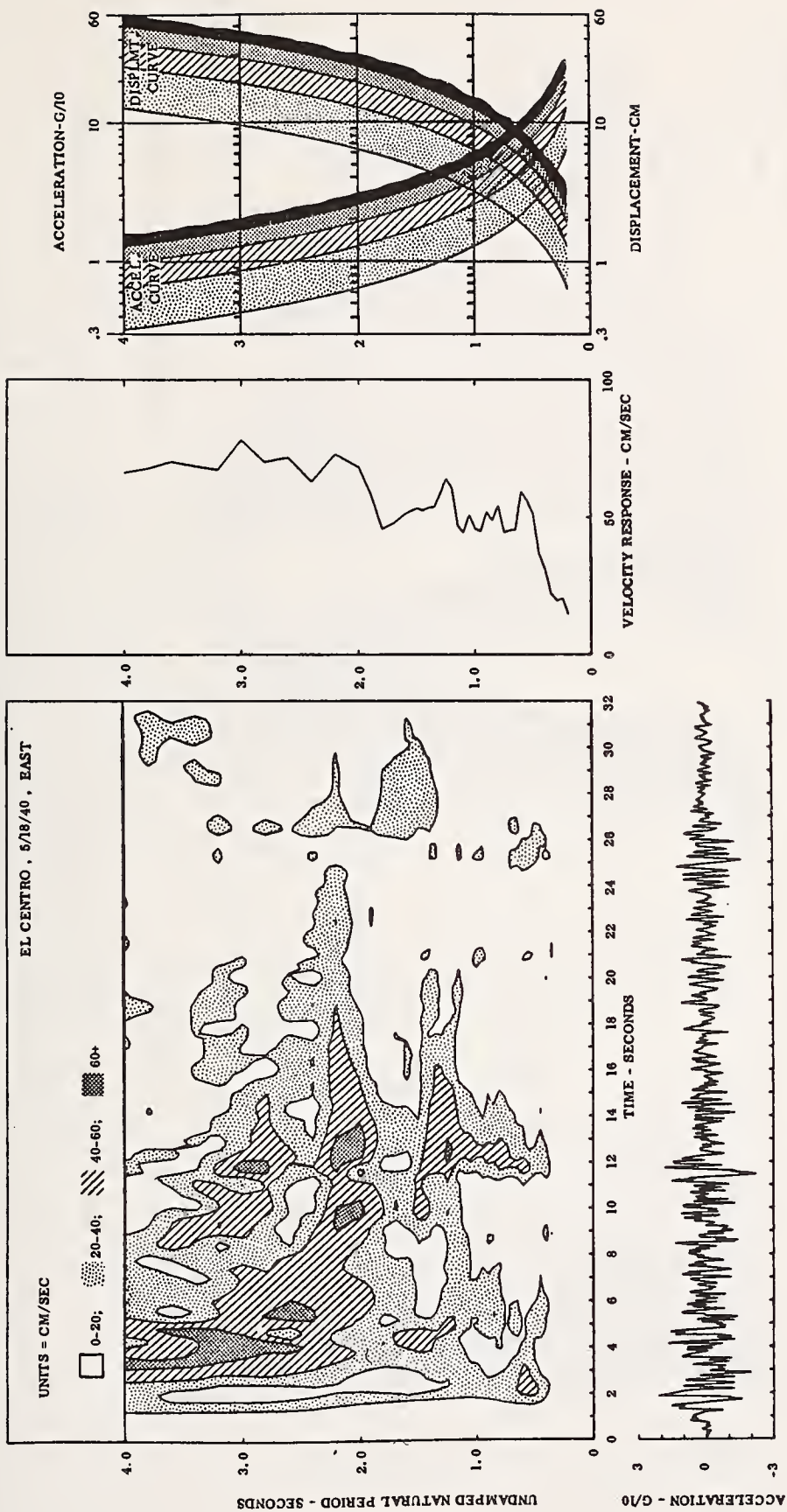


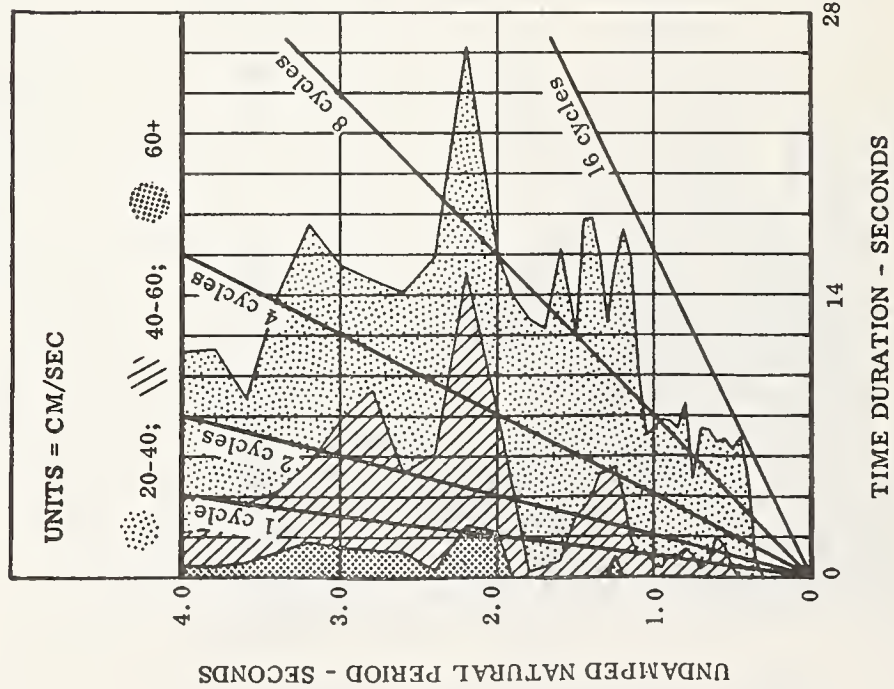
Figure 4.
 Fourier amplitude spectrum.



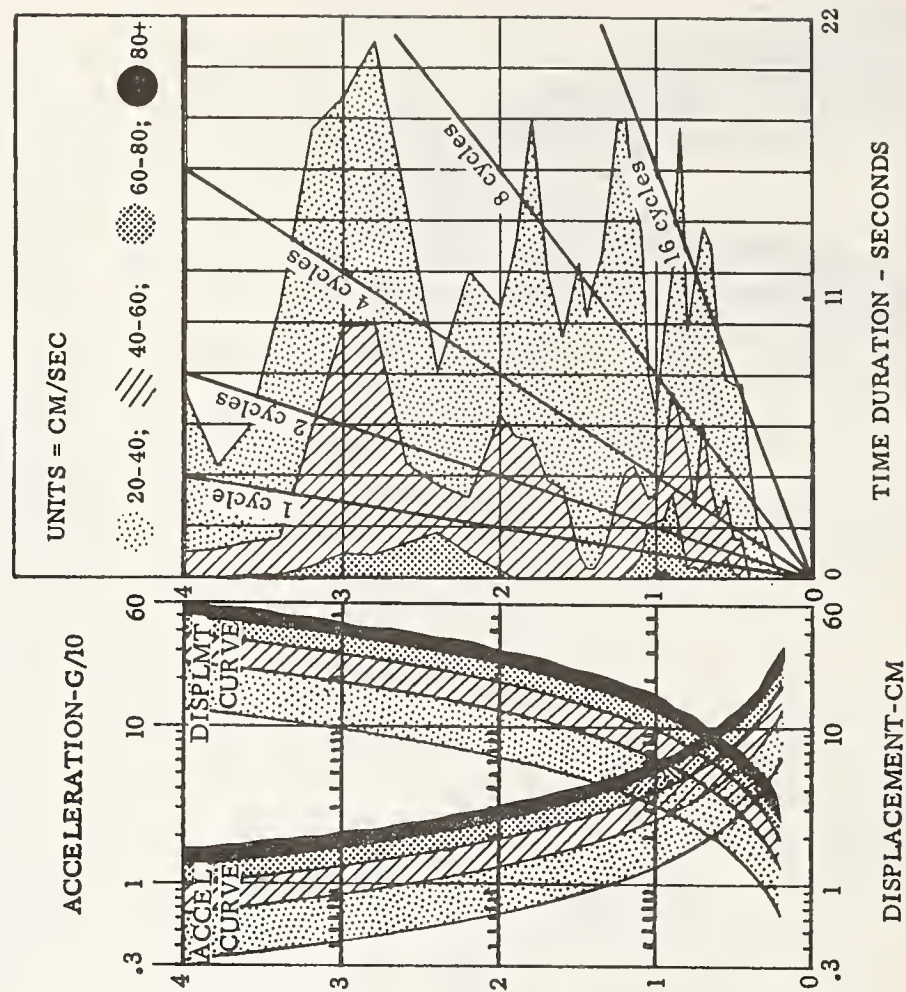
Relative velocity response envelope spectrum (VRES) at 5 % critical damping, El Centro, California, 5/18/40, East component.

Figure 5.
Relative velocity response envelope spectrum.

EL CENTRO , 5/18/40 , EAST



EL CENTRO , 5/18/40 , NORTH



Time duration spectra of the response envelope at 5% critical damping - El Centro, California, 5/18/40.

Figure 6.
Time-duration spectrum of the response envelope.

BRIEF REVIEW ON LIQUEFACTION
DURING EARTHQUAKES IN JAPAN

by

Eiichi Kuribayashi
Chief of Earthquake Engineering Research Section
Public Works Research Institute

and

Fumio Tatsuoka
Research Engineer
Earthquake Engineering Research Section
Public Works Research Institute

ABSTRACT

To correlate the actual liquefaction phenomena and site conditions, a literature survey about the liquefaction phenomena caused by earthquakes during the last century in Japan was performed. A liquefaction distribution map of Japan and the regional maps of Kanto, Nobi and Hokuriku are presented and the factors related to liquefaction are discussed. During the last century liquefaction in sub-soils have been observed at some hundred sites during 44 earthquakes where the sites were limited to alluvial deposits and reclaimed lands. Furthermore, it was found that liquefaction occurred repeatedly in different earthquake zones. The estimated JMA intensity scale factor, at the liquefied sites was more than five which means a maximum acceleration of 80 to 250 gals. The extent of the liquefied zones are limited, depending on the magnitude of the earthquake.

Key Words: Alluvial Deposits; Earthquakes; Epicentral Distance; Liquefaction; settlement; Soils.

Introduction

Most structural damage, caused by settlement or inclination due to liquefaction of saturated sandy subsoil, has inevitably occurred during major earthquakes. In accordance with the prediction of liquefaction potential of subsoils, a number of research efforts have been expended by means of laboratory tests and in-situ tests. Meanwhile, correlations between the actual liquefaction phenomena and the site conditions has rarely been investigated. Recently, case reviews on the correlation of liquefaction have been performed at several sites in Japan (Miyabe, 1933, Kishida, 1969, Ishihara, 1974 and Iida, 1974). Because many interesting facts have been obtained from these reviews, more reviews on this subject are expected. This report contains the results of a literature survey about liquefaction phenomena caused by earthquakes during the last century in Japan.

Liquefaction distribution maps since 1972 are presented first and the factors related to liquefaction are then discussed. In the literature on earthquakes, which caused damage, there contains much description of the liquefaction of the sub-soil. However, most of the descriptions before 1868, the identification of liquefaction and its characteristics, have been scientifically qualified. In the description, evidences of liquefaction in the sub-soil are given from i) water spouting with sand or mud from wells or cracks in the ground, ii) sand boils or sand volcanoes, iii) excessive settlements of heavy structures placed on sand layers, and iv) uplifting of wooden piles from rice paddy, or of caissons under construction from river beds. About 150 papers or reports have provided information on liquefaction during 44 earthquakes, as listed in Table-1.

Liquefaction Distribution Maps

Forty-four earthquakes have caused liquefaction of the sub-soil in Japan during the past century. The epicenters of the earthquakes and locations where liquefaction has occurred is shown in Fig. 1. The characteristics of the earthquakes, which include date, magnitude, focal depth, epicenter location and the number of the deaths are also listed in Table 1. Large earthquake magnitudes cause liquefactions in wide areas except for several cases, as shown in Fig. 1. Among the large scale earthquakes were No. 4 (Nobi), No. 12 (Gono), No. 15 (Kanto), No. 22 (Nishi-Saitama), No. 34 (Fukui) and NO. 42 (Niigata) as shown in Table 1 which caused wide distribution and violent liquefaction of the sub-soil. Moderate scale earthquakes, No. 6 (Shonai), No. 8 (Rikuu), No. 16 (Tajima), No. 31 (Tonankai), and No. 44 (Tokachi-oki) caused local violent spouting of water or a number of large sand volcanoes.

Microscopic features of the regions of liquefaction are closely distributed as shown in Figs. 2, 3 and 4 which depict Kanto, Nobi and Hokuriku regions, respectively.

Kanto Region

In the Kanto region during the earthquake No. 5 (Tokyo), spouting of water with dark blue or black fine sand from cracks of subground were observed in many places. In Fig. 2 the sites of liquefaction are denoted by solid circles with numeral characters of 1 to 18, which are distributed only in alluvial areas and close to the epicenter. About 30 years after this earthquake, the Kanto region was subjected to earthquake No. 15 (Kanto), which

was one of the most disasterous earthquakes in Japanese history. Sites of liquefaction, during this earthquake, as denoted by hollow triangles in Fig. 2 are very widely scattered in the alluvial plains in the Kanto region. It is interesting to note that many liquefied sites are concentrated on the original winding river course of the existing Tone river located in the north east of Tokyo. About three hundred and fifty years ago, the estuary of the Tone River was linked by man to the Pacific Ocean. The original Tone River had flowed into Tokyo Bay, depositing a very deep and soft sand layers. Because the river course was modified, a higher potential of liquefaction was retained in the original site in comparison with the ordinary site in Kanto plain. In addition to the earthquakes described above, earthquakes No. 7 and No. 22 (Nishi Saitama) during this century has caused liquefaction of sub-soil in this area. In addition to the Kanto area, sand boils, sand volcanoes, uplifting of wooden piles and caissons during the earthquake No. 15 (Kanto) were reported as shown in Fig. 2, where representative liquefied sites are denoted by characters a, b, ... k. For example, the site a is the reclaimed land in Kawasaki City, where water with dark blue and grey fine sand ejected from many cracks. At site b near the epicenter, seven wooden piles uplifted about 60 cm from the rice paddy during the quake. These piles were used as bridge piles about 800 years ago over the original Sagami River. At site c many caissons for a bridge foundations under construction uplifted from the river bed of the Sagami River. More details of liquefaction situations are reported in another paper (Kuribayashi, Tatsuoka and Yoshida, 1974).

Earthquake No. 22 (Nishi Saitama) in 1931 also induced liquefaction at many locations along the original and existing courses of the Tone River. The liquefaction sites during this earthquake, are denoted by hollow circles as shown in Fig. 2. Severe water spouting conditions were observed at sites around Fukiage City, located about 20 km east from the epicenter. Large amounts of water, with dark blue and grey fine sand, were ejected about 30 cm high from several hundred of these sand volcanoes. Furthermore, the ground surface of these liquefied sites settled about 15 cm and the spouted water covered the ground to a depth of about 15 cm.

Nobi (Mino-owari) Region

The Nobi Region has been inflicted by four violent earthquakes during the past century, which induced liquefaction at many sites as shown in Fig. 3. The most violent was No. 4 (at Nobi) in 1891 which caused wide spread and violent liquefaction of the Nobi Plain and Fukui Plain. These locations are shown by solid triangles in Fig. 1 and by hollow triangles in Fig. 3, respectively. The liquefied sites were limited to the alluvial soft deposits along the Kiso, Nagara and Ibi Rivers in Nobi Plain and to the sites along the river in the Fukui Plain which is to the north of the epicenter. It should also be mentioned that the earthquake No. 34 in 1948 (Fukui) also induced liquefaction in the entire Fukui Plain as shown in Fig. 1. One of the most violent water spouting conditions occurred during earthquake No. 4 and is denoted by a character "a" in Fig. 3. During this earthquake near the Shonai River, water with sand ejected over 2 m high from wells and deposited sand on the roofs of nearby houses. Also at the site "b", on the right bank of the Shonai River to the south of the site "a", twelve hundred sand boils were observed. The extent

of liquefaction can be evaluated in that 40 km² of rice paddies and fields in the Prefectures of Aichi and Gifu, were impossible to cultivate due to sand boils, necessitating repairs and reconstruction.

Eighteen years after this earthquake, earthquake No. 12 (Gono) caused liquefaction at many locations in the northwestern part of the Nobi Plain where liquefaction was previously caused by earthquake No. 4. Many areas liquefied during this earthquake, and are denoted by hollow circles as shown in Fig. 3. These areas are tightly distributed and are surrounded by the Ibi, Nagara and Kiso Rivers.

Earthquake No. 31 (Tonankai), during the end of World War II caused liquefaction in the coastal region which has soft alluvial deposits. These locations are between the Cape Omaezaki and the Lake Hamana and in the south coastal part of Nagoya City, which had been reclaimed during the past hundred and fifty years before this earthquake. The liquefied sites described above are expressed by hollow triangles as shown in Fig. 1 and solid triangles as shown in Fig. 3. In the south coastal region of Nagoya City damage to wooden houses such as settlement and inclination was caused by a very large quantity of ejected sand and water. Also, many sand boils and water spoutings were observed at the sites of severely damaged aeroplane factories at Nishi-inaei town, denoted as character "c" in Fig. 3. During earthquake No. 32 (Mikawa), violent boiling of sand and water was again observed at the sites of these same factories.

In general, the characteristics of earthquakes of large magnitude, but with offshore epicenters such as the earthquakes No. 31 (Tonankai), No. 33 (Nankai) and No. 44 (Tokachi-oki), will cause liquefaction at soft deposits in the coastal regions as shown in Figure 1.

Hokuriku Region

Fig. 4 shows the liquefaction history of Prefectures of Yamagata and Niigata during the past century. Earthquake No. 6 (Shonai), caused liquefaction at many sites, which are denoted by hollow triangles as shown in Fig. 4(b). In Sakata City, located at the river mouth of Mogami River, numerous sand boils were observed with the largest sand volcano reported having a height of 60 cm and about 3 m in diameter. The area where the sand boiled most violently was covered by sand deposits, similar to seashore areas. Similar violent sand boils were observed at site 2, shown in Fig. 4(b), where the largest one was about 9 m in diameter. The liquefaction site is at the same location as caused by earthquake No. 42 (Niigata), as shown in Fig. 4 (b).

Earthquake NO. 42 (Niigata) is very famous for its wide spread liquefaction, and the subsequent damage to modern buildings and civil engineering structures. Because the details of this earthquake have been reported in detail by many others, only a summary will be given in this paper. Liquefied zones during this earthquake are denoted by hatched zones, with numbers of 1 to 13, as shown in Fig. 4. It is important to note that these zones are limited to the original riverbeds of the rivers of Shinanao, Agano etc. For example, the zone expressed by the character "a" in Fig. 4 (a), is the original riverbed of the Anago River which was connected to the Shinano River at the river mouth about three

hundred years ago. This zone was then reclaimed about fifty years ago by depositing sand. The national highway No. 7 passes through this zone, and its low bank composed of 1 m of sand settled down about 1 m and moved laterally 4 m during the earthquake. This was caused by liquefaction of the sandy bank and sandy ground, because boiled sand covered the road surface and one truck on the bank sank into the ground.

Discussions and Remarks

The study of the liquefaction phenomena caused by different earthquakes indicated the following;

(i) Re-liquefaction has observed in 7 zones, shown by symbols "a" to "g" in Fig. 1 and as listed in Table 2. This suggests that re-liquefaction will occur if the proper soil conditions are present.

(ii) One of the causes of liquefaction in sub-soils is the intensity of the quake. Earthquake intensity, at the liquefied site, were estimated by comparing the liquefaction distribution map and the intensity scale distribution map. From this procedure, it was found that the estimated earthquake intensity in JMA (Japan Meteorological Agency) scale at the liquefied sites was greater than five, which means that accelerations of 80 gals to 250 gals occur

(iii) As is well known, liquefaction zones increase during the larger earthquakes. Fig. 5 shows the maximum epicentral distance of the liquefied sites R (km) and the magnitude of the earthquake M. Using the procedure presented by Fukuoka (1971), the following is obtained;

$$\log_{10} R = M - 5.7 \quad (1)$$

where Eq. (1) is based on the data obtained from earthquakes NO. 33 (Nankai) and No. 42 (Niigata). It should also be noted that examination of Fig. 5 indicates the following

$$\log_{10} R = 0.87 M - 4.5 \quad (2)$$

where the lower bound for $M > 6.0$ is expressed by

$$\log_{10} R = 0.77 M - 3.6 \quad (3)$$

From the data obtained on 44 earthquakes, a lower bound of the liquefaction R-M relationship can be anticipated by Eq. (3) or Fig. 5. On the basis of this relation liquefaction may not occur at any site when the distant site exceeds that value expressed by Eq. (3). For $M = 7.0$, for example, liquefaction may not occur at distance greater than 60 km from the epicenter.

Conclusions

A survey of many reports on earthquakes during the last century, shows that liquefaction in sub-soils are induced at many sites. In Japan during 44 earthquakes, liquefied sites were limited to alluvial deposits and reclaimed lands. Liquefaction generally occurred at original river beds which was reclaimed during the past several hundred years and in reclaimed lands along seas or lakes. Such liquefaction increases as the earthquakes with magnitude increase have an offshore epicenter. Furthermore, it could be noted that liquefaction has occurred repeatedly during different earthquakes in several zones. An estimated JMA intensity scale factor at the liquefied sites, was greater than five. A lower bound of liquefaction potential can be defined as a relationship between epicentral distance and magnitude of earthquake on the basis of this discussion.

Acknowledgments

The writers would like to express appreciation to Professor T. Mogami, Professor M. Fukuoka, Dr. T. Okubo, Assistant Professor K. Ishihara and Mr. T. Iwasaki for their helpful suggestions. This research was performed with an assistance of Mr. S. Yoshida, Earthquake Engineering Research Section, P.W.R.I. The writers wish to acknowledge his helpful cooperations.

References

1. Fukuoka, M., (1971), "Memories of Earthquakes and Foundations", Bridges and Foundations, Vol. 5, No. 10. (in Japanese).
2. Iida, K., (1974), "Past Earthquakes and Damages in Nagoya City", Report of Committee for Disaster Prevention of Nagoya City (in Japanese).
3. Ishihara, K., (1974), "Liquefaction of Subsurface Soils During Earthquakes", Technocrat, Vol. 7, No. 5.
4. Kishida, H., (1969), "Characteristics of Liquefied Sands During Mino-Owari, Tohnankai and Fukui Earthquakes", Soils and Foundations, Vol. IX, No. 1.
5. Kuribayashi, E., Tatsuoka, F. and Yoshida, S., (1974), "Liquefaction History in Japan During the Last Century", Bull. of Public Works Research Institute, No. 30. (in Japanese)
6. Miyabe, No., (1933), "On the Abnormality of Ground Water During Earthquakes", Earthquakes, Vol. 5. (in Japanese).

Table 1. List of Earthquakes which induced liquefactions (1872 - 1968)

Earthquake	Year, Month, Date	Magnitude	Focal depth (km)	Epicenter	Number of the death	Earthquake	Year, Month, Date	Magnitude	Focal depth (km)	Epicenter	Number of the death
1. Hamada	1872. 3. 14	7. 1		34. 8°N, 132. 0°E	552	23. Noto	1933. 9. 21	6. 0	15	37. 1°N, 137. 0°E	3
2. Koshigun	1887. 7. 22	6. 1		37. 7°N, 139. 0°E	0	24. Shizuoka	1935. 7. 11	6. 3	10	35. 0°N, 138. 4°E	9
3. Kumamoto	1889. 7. 28	6. 3		32. 8°N, 130. 7°E	20	25. Kawachi-yamato	1936. 2. 21	6. 4	20	34. 5°N, 135. 7°E	9
4. Nobi (Mino-Owari)	1891. 10. 28	8. 4(7. 9)		35. 6°N, 136. 6°E	7, 273	26. Kinkazan-oki	1936. 11. 3	7. 7	0	38. 2°N, 142. 2°E	0
5. Tokyo	1894. 6. 20	7. 5		35. 7°N, 139. 9°E	31	27. Oga	1939. 5. 1	7. 0	0	39. 95°N, 139. 8°E	27
6. Shonai	1894. 10. 22	7. 3		39. 2°N, 139. 5°E	726*	28. Nagano	1941. 7. 15	6. 2	5-20	36. 7°N, 138. 3°E	5
7. Tone-karyu	1895. 1. 18	7. 3		35. 9°N, 140. 4°E	9	29. Tottori-ken-oki	1943. 3. 4, 3. 5	6. 1, 6. 1	20, 20	35. 6°N, 134. 2°E	0
8. Rikuu	1896. 8. 31	7. 5		39. 5°N, 140. 7°E	209	30. Tottori	1943. 9. 10	7. 4	10	35. 5°N, 134. 2°E	1, 083
9. Kamitakai	1897. 1. 17, 4. 30	6. 3, 6. 3		36. 6°N, 138. 2°E	0	31. Tonankai	1944. 12. 7	8. 0	0	33. 7°N, 136. 2°E	998
10. Minami Unomagun	1898. 5. 26	6. 7		36. 9°N, 138. 9°E	0	32. Mikawa	1945. 1. 13	7. 1	0	34. 7°N, 137. 0°E	1, 961
11. Fukuoka	1898. 8. 10, 8. 12	6. 5, 6. 5		33. 5°N, 130. 2°E	0	33. Nankai	1946. 12. 21	8. 1	30	33. 0°N, 135. 6°E	1, 330
12. Gono (Ane-gawa)	1909. 8. 14	6. 9		35. 4°N, 136. 3°E	41	34. Fukui	1948. 6. 28	7. 3	20	36. 1°N, 136. 2°E	3, 895
13. Ugoen	1914. 3. 15	6. 4		39. 5°N, 140. 4°E	94	35. Tokachi-oki	1952. 3. 4	8. 1	4. 5	42. 15°N, 143. 85°E	28
14. Shimabara	1922. 12. 8	6. 5, 5. 9		32. 7°N, 130. 1°E	30	36. Daishoji-oki	1952. 3. 7	6. 8	20	36. 45°N, 135. 20°E	7
15. Kanto	1923. 9. 1	7. 9		35. 2°N, 139. 3°E	99, 331	37. Tokushima-nambu	1955. 7. 27			33. 80°N, 134. 30°E	1
16. Tajima	1925. 5. 23	7. 0		35. 7°N, 134. 8°E	428	38. Futatsui	1955. 10. 19	5. 7	0-10	40. 3°N, 140. 2°E	0
17. Kitatango	1927. 3. 7	7. 5	10	35. 6°N, 135. 1°E	2, 925	39. Nagaoka	1961. 2. 2	5. 2	20	37°27'N, 138°50'E	5
18. Ishinomaki	1927. 8. 6					40. Hyuganada	1961. 2. 27	7. 0	40	31°36'N, 131°51'E	2
19. Sekihara	1927. 10. 27	5. 3	0-10	37. 5°N, 138. 8°E	0	41. Miyagiken- hokubu	1962. 4. 30	6. 5	0	38°44'N, 141°08'E	3
20. Kaga-nanseibu	1930. 10. 17					42. Niigata	1964. 6. 16	7. 5	40	38°21'N, 139°11'E	26
21. Kiraizū	1930. 11. 26	7. 0	0-5	35. 1°N, 139. 0°E	272	43. Ebino	1968. 2. 21 2. 22/ 3. 25	5. 7, 6. 1 5. 6/5. 7, 5. 4	0 0/0, 10	38°01'N, 130°43'E	3
22. Nishisaitama	1931. 9. 21	7. 0	10-20	36. 1°N, 139. 2°E	16	44. Tokachi-oki	1968. 5. 16	7. 9	0	40°44'N, 143°35'E	49

* in Yamagata Prefecture only

Table 2. Zones where re-liquefactions were observed

a, b, , g correspond to those in Fig. 1.

Zones	Earthquakes
a: the narrow zone along the Omono River in the northwest of Oomagari city in Akita Prefecture	No. 8 (Rikuu) and No. 13 (Ugosen)
b: on the left side at the river mouth of Mogami river	No. 6 (Shonai) and No. 42 (Niigata)
c: in the original river course of Tone river in the notheast of Tokyo	No. 5 (Tokyo), No. 7 (Tonekaryu), No. 15 (Kanto) and No. 22 (Nishi-Saitama)
d: on the both sides of Chikuma river near Nagano city	No. 9 (Kamitakai) and No. 28 (Nagano)
e: in the southern part of Fukui plain	No. 4 (Nobi) and No. 24 (Fukui)
f: in the nothwestern part of Nobi plain	No. 4 (Nobi) and No. 12 (Gono)
g: in the southern part of Nobi plain	No. 31 (Tonankai) and No. 32 (Mikawa)

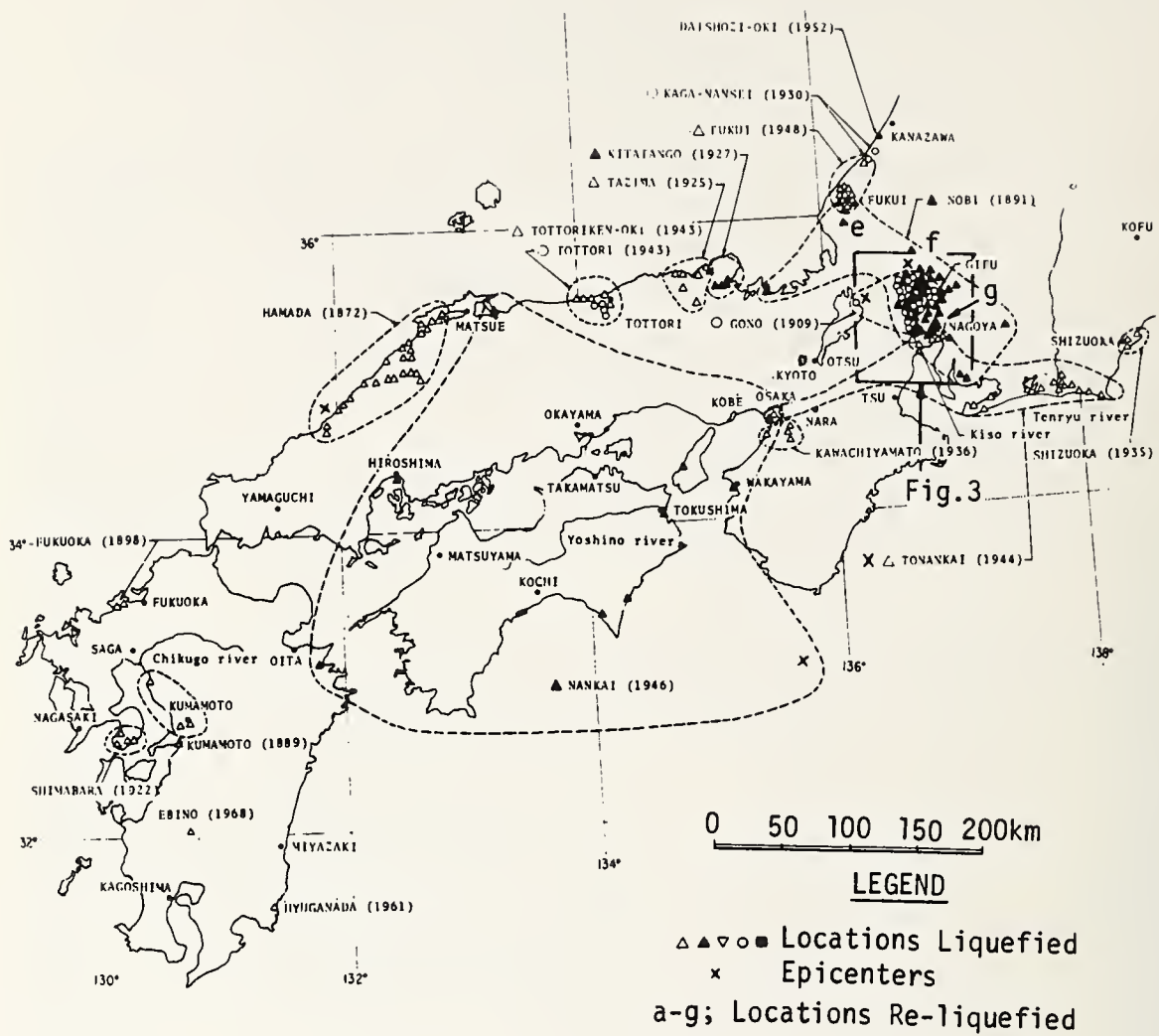


Fig. 1 Liquefaction distribution map (Japan)



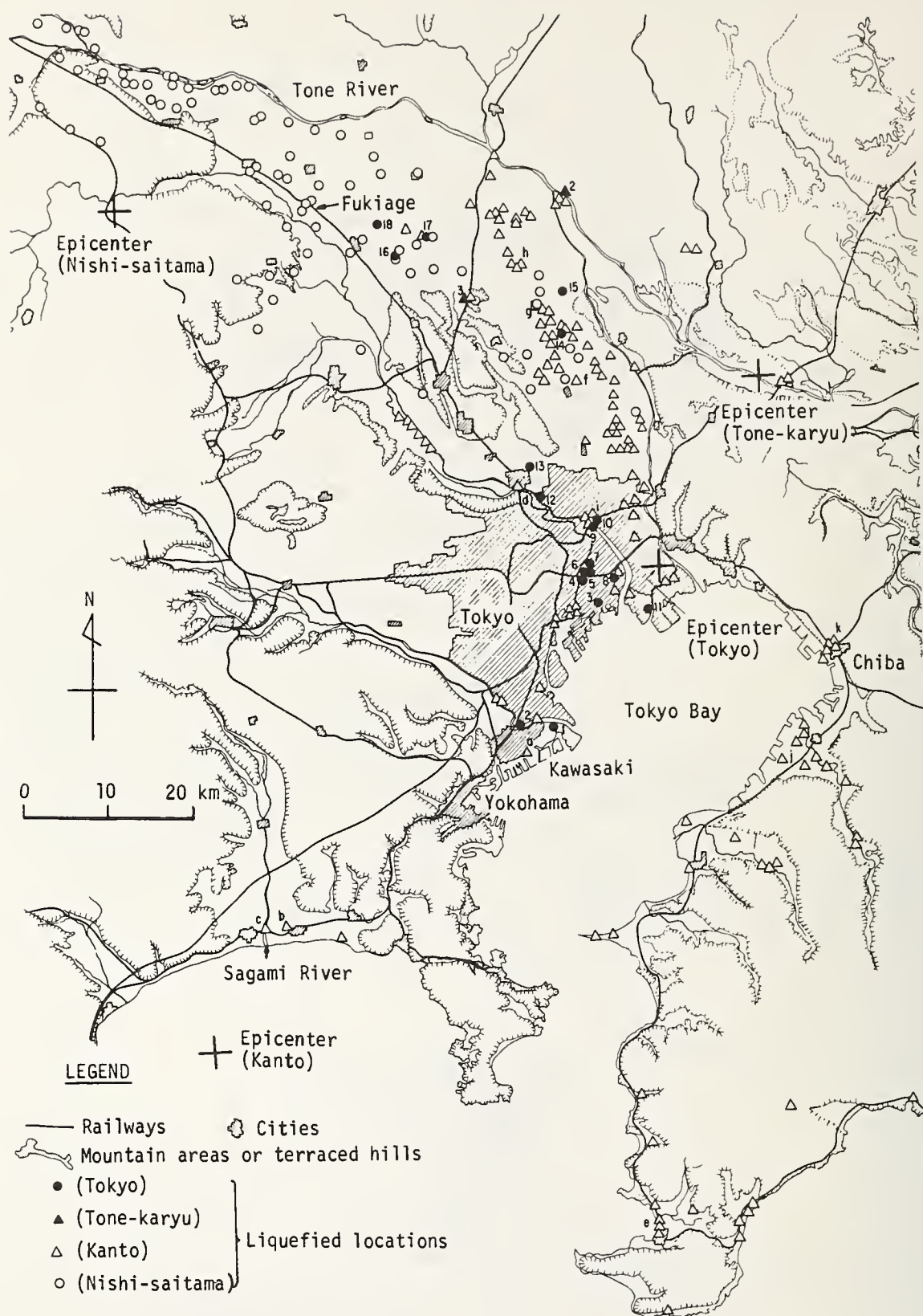


Fig. 2 Liquefaction distribution map (Kanto region)

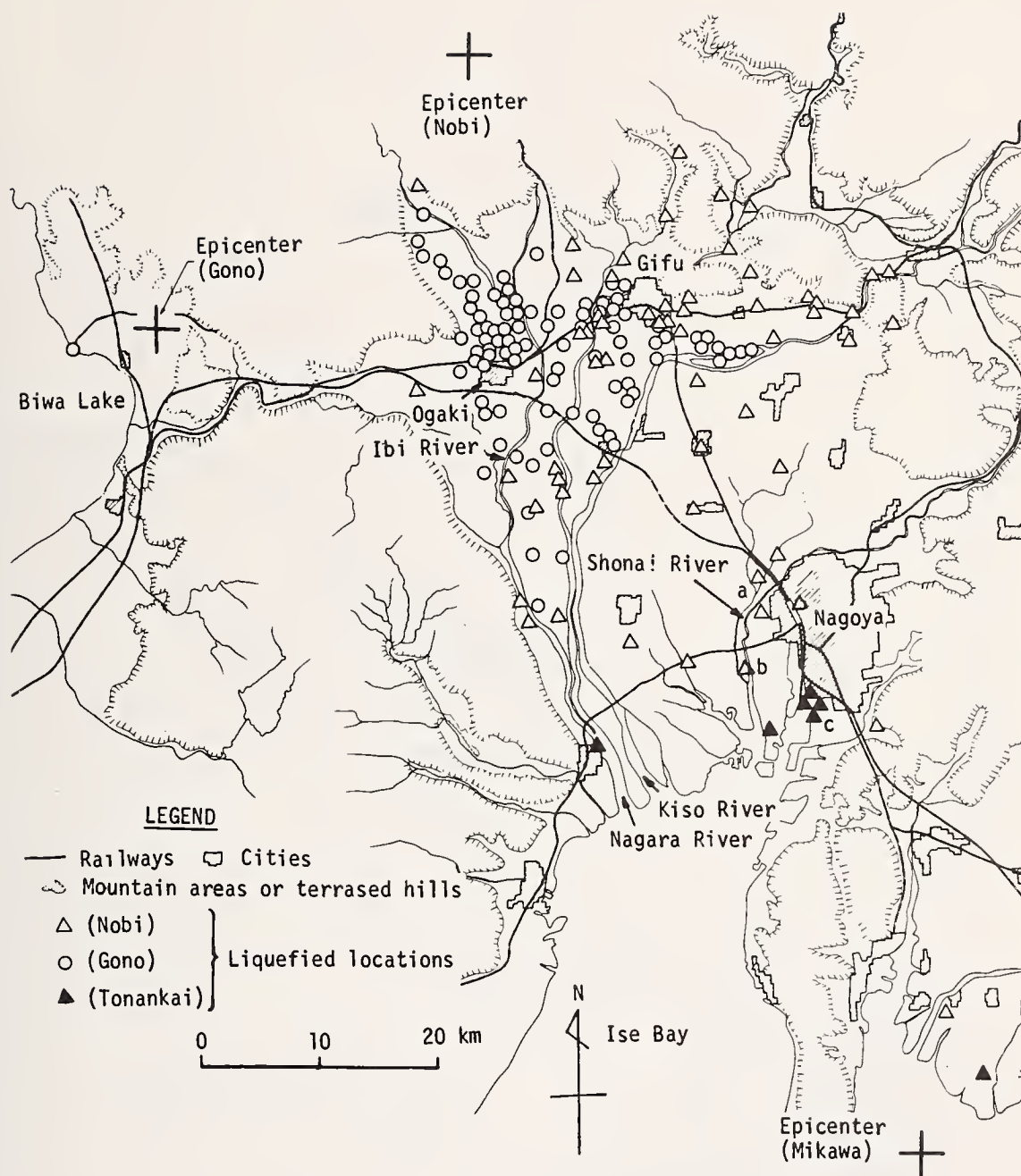


Fig. 3 Liquefaction distribution map (Nobi region)

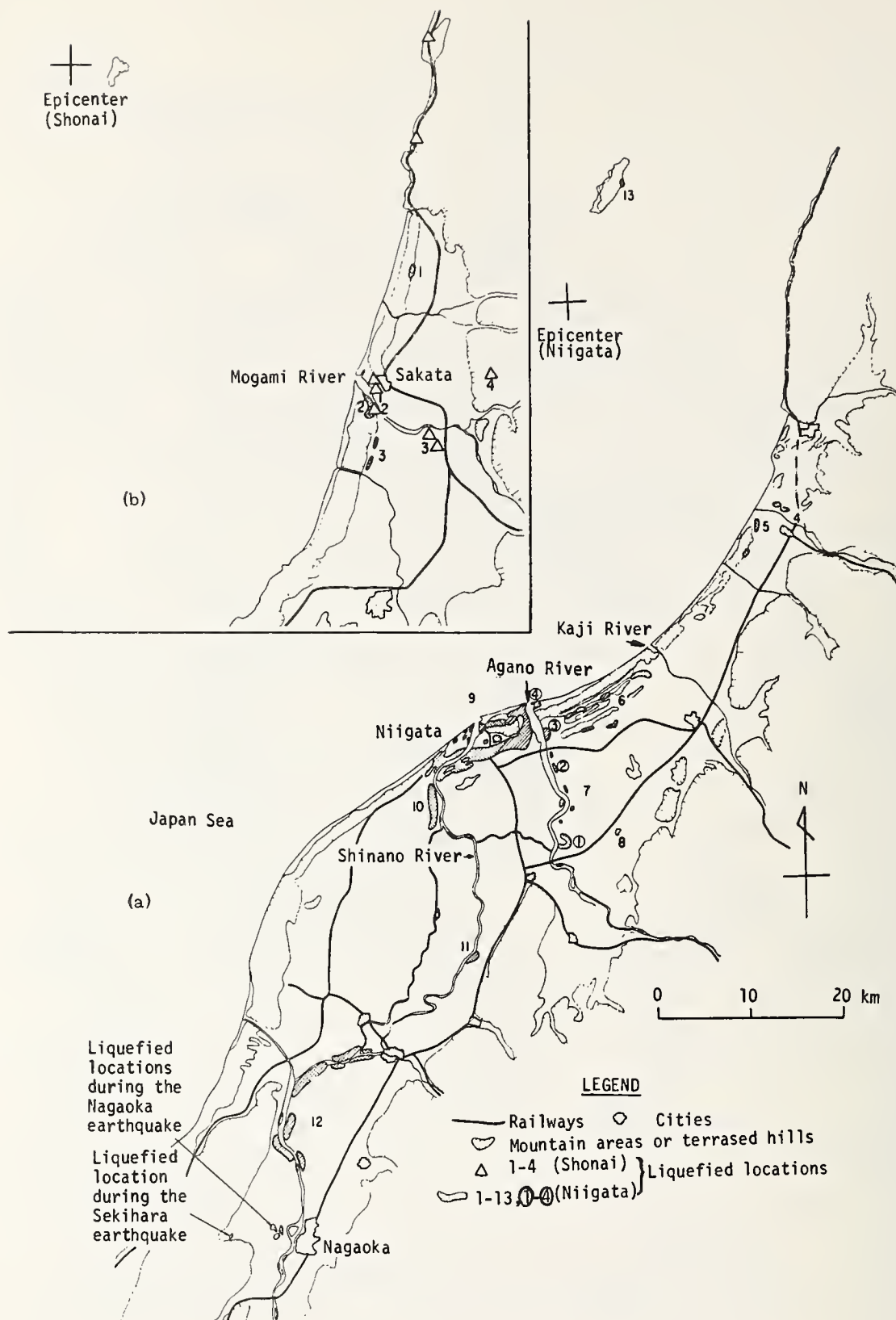


Fig. 4 Liquefaction distribution map (Hokuriku region)

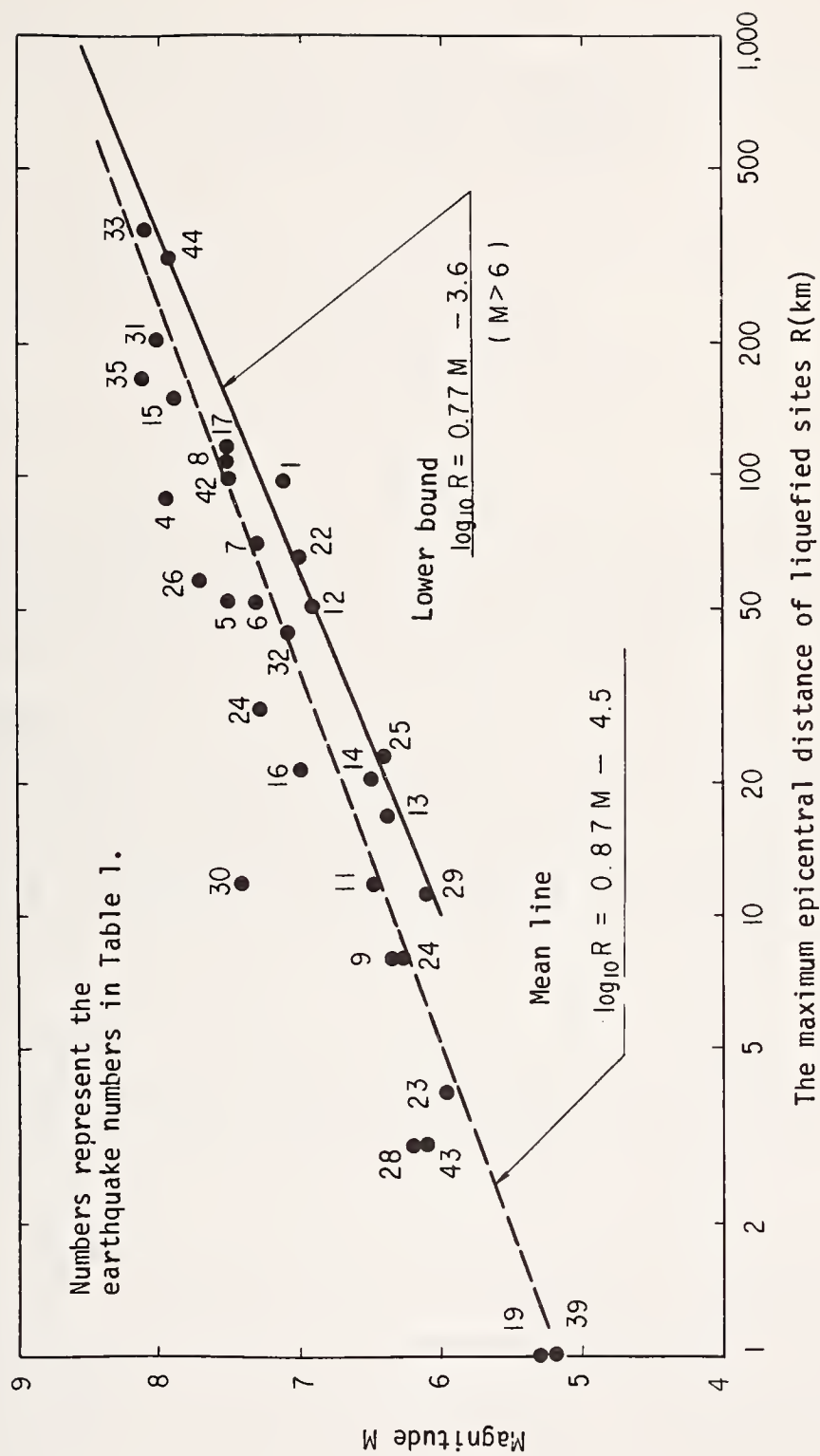


Fig. 5 Relationship between the maximum epicentral distance of liquefied sites R and magnitude M

VIBRATION TEST ON SETTLEMENT
OF SUBMERGED SAND LAYER

by

K. Sawada
Chief, Soil Dynamics Section
Public Works Research Institute
Ministry of Construction

and

Y. Koga
Research Engineer
Soil Dynamics Section
Public Works Research Institute
Ministry of Construction

ABSTRACT

A series of vibration tests on submerged sand layer model, using a large shaker table, was performed in order to establish a method which can predict the liquefaction and settlement phenomenon of sandy ground during earthquakes. As a result of these tests, information concerning the vibration behaviour during the liquefaction phenomenon and subsequent settlement behaviour was obtained. Examining these test results and assuming that the vibration and settlement behaviour of a sand layer in the sand container is one-dimensional, it has been found that the test and analysis results agree quite favorably. Therefore, if the shear stress in the ground can be reasonably estimated, the amount of settlement of the sand due to earthquakes can be estimated by this analysis method proposed herein.

Key Words: Earthquakes; Liquefaction; Sand Layer; Shake Table; Vibration Tests; Void Ratios.

Preface

The building of a structure on a sandy ground, where liquefaction is likely to occur at the time of an earthquake, requires the following sequence of steps in order to perform a aseismic design.

- (1) Determine whether or not a liquefaction phenomenon will occur in the ground which is to support the building and then establish the degree of reduction of the bearing capacity and the amount of settlement which may be generated. Then estimate whether or not certain measures are required to minimize the effects.
- (2) If design revisions are required, then improvements to the foundation or the type of structure, or improvements to the ground are necessary so that a liquefaction phenomenon be either prevented or reduced.

The methods of determining or estimating liquefaction phenomena are based on a method from sand element tests (1-3).

At a previous meeting, a method employing blasting vibrations to predict liquefaction, was presented. The results to be presented herein, however, will involve the analysis of experiments with a model sand layer using a large shake table. This experiment was performed jointly by the Public Works Research Institute, Ministry of Construction, the Kanto Engineering and Mechanical Laboratory, Ministry of Construction and the National Research Center for Disaster Prevention, Science and Technology Agency.

Method of Experiment

The container used for the experiment is a steel box having inner dimensions of 8 m (length) x 5 m (height) x 2 m (depth) as shown in Photo 1. In the experiment, the box was installed with its longitudinal direction aligned with the horizontal vibrating direction of the slab table and the sand layer of thickness of 4 m, was submerged in water up to the surface. The sand used in the experiment is mountain sand taken from Sengen-Yama in Chiba Prefecture, Japan, which has physical properties as shown in Table 1. A belt conveyor and bucket were used to place the sand into the box for forming the sand layer. The sand was compacted by stepping or a vibro-rammer for every sand layer thickness of 30 or 50 cm. A quality control test, including measurement of density, was performed for each of sand layer. Upon formation of each sand layer, the layer was then submerged in water. After inducing series of vibrations and subsequent measurements, the water and sand were discharged from the sand box and a new sand layer was formed for the next experiment. This type of experiment was conducted three times with respect to a homogenous sand layer. Three additional tests were conducted with respect to a case where a model object was buried in the sand layer.

The following types of vibrating methods were used in each experiment;

(1) Resonance Test

This test had a table acceleration equal to 20 gal, and a step sine frequency of 1 to 20 c/s. The vibrations were applied for a fixed period of 20 to 30 sec. This test was intended to examine the dynamic properties, including modulus of elasticity and damping factor.

(2) Liquefaction Test

The test level of acceleration of the table was changed by means of sine waves near the 1st resonant frequency and were applied for a fixed period of 60 to 100 sec. This experiment was intended to examine the effects of excess pore water pressure and the resulting settlement in the sand layer. In this experiment, where the excess pore water pressure was developed, the sand layer was allowed to stand for about 1 hour after completion of the vibration test sequence. The application of next vibration stage was initiated after the excess pore water pressure was dissipated.

Table 2 describes the conditions for each model experiment, including the number of times the sand layer has formed the vibrating conditions.

Illustrated in Fig. 1 is an example of the arrangement of the instruments buried in the sand layer.

Results of Experiment

(1) Characteristics of the Sand Layer

The density of sand layer varied considerably with each model, as affected by the method of compaction. For example, in the case of the 1st experiment, the dry density (γ_d) was $1.41 \sim 1.52 \text{ g/cm}^3$, the average value was 1.48 g/cm^3 , void ratio (e) was $0.77 \sim 0.91$ and the average value was about 0.82.

(2) Resonance Test

Examples of the resonance curve obtained from resonance tests are illustrated in Fig. 2(a) through (c). Illustrated in Fig. 2(a) and (b) are the response characteristics of the sand layer for experiment 1-1, relative to distance from the end face. For this experiment, the frequencies at the 1st and 2nd resonances are 10 and 17 c/s respectively. This shows that there is little difference relative to distance from the end face, but it can be seen that the magnification of acceleration varies with the distance from the end face. For example, with respect to 10 c/s which can be thought of a 1st resonance frequency Fig. 3 shows the distribution of the magnification of the acceleration which indicates that the farther from the end face, the larger the magnification of the acceleration. Experiment 3-1, as illustrated in Fig. 2(e), is different from the experiment 1-1 as illustrated in Fig. 2(a) and (b) with respect to density and table acceleration level.

(3) Liquefaction Test

The characteristics of the behaviour of the sand layer during liquefaction can be represented by the pore water pressure, settlement amount and acceleration of the sand layer.

Examples of the time-course changes of these factors are illustrated in Fig. 4 through Fig. 6. Illustrated in Fig. 4 is an example in which both the excess pore water pressure and the settlement are small due to the small table acceleration. In this case, the acceleration of the sand layer except the upper part of the sand layer shows almost a steady state where the table acceleration is constant. The acceleration of the upper part of the sand layer shows a trend in which it continues to increase even after the table acceleration has become steady and then suddenly decreases after it has reached a peak value. This phenomena is caused by first an increase of the excess pore water pressure in the upper

part of the sand layer. This increase in the excess pore water pressure over a certain value causes the rigidity of the sand layer to lower (or causes the deformation characteristics to increase) due to a reduction of the effective confining pressure. This resulting phenomenon causes an increase in acceleration of the sand layer, and if the excess pore water pressure further increases, the shear strength of that layer and the lower layer will reduce. This will result in a condition in that the vibration from the lower part cannot be transmitted to the upper part and the acceleration of the sand layer will suddenly decrease.

In the case of experiment No. 1-4 (Fig. 5), the table acceleration is larger than that of experiment No. 1-3 (Fig. 4), and both the excess pore water pressure and the settlement amount are comparatively larger than those in the experiment No. 1-3.

In experiment No. 1-4, the excess pore water pressure increases starting from the upper part of the sand layer, with a maximum value nearly equal to the effective overburden pressure in each layer. This condition shows that all layers have reached complete liquefaction. The range in which the phenomenon of a sudden decrease in acceleration of the sand layer occurs is deeper than that sand layer in the experiment No. 1-3, and researched a depth of 3 meters.

Experiment No. 3-4 (Fig. 6), is the case where the void ratio of sand layer is less than that of experiment No. 1-4. However, despite the fact that the table acceleration and vibrating period was larger than those generated experiment No. 1-4, the excess pore water pressure and the amount of settlement generated was smaller.

Fig. 7 shows the vertical distribution of the acceleration and excess pore water pressure previously given by Fig. 5. The process in which a sudden decrease of acceleration on the upper part of the sand layer progresses to a deeper part with the passing of time can readily be seen. One thing of interest in comparing the vertical distribution of excess pore water pressure, as illustrated in (b) and the corresponding experiment period versus the amount of settlement (Fig. 5(c)), is that for the period between 0 to 40 sec, the water pressure gradient at a position 1 m from the bottom is downward and the pore water tends to flow into the lower layer, so that at the position 1 m from the bottom, uplift must occur rather than settlement, as illustrated in Fig. 5(c), during the period, a considerably amount of settlement is observed. This condition is caused by air bubbles in the pores which have been compressed due to the generation of excess pore water pressure, since the sand layer had not been completely saturated. This mechanism can also be concerned by noticing first that the water level, on the sand layer surface, after vibration is lower by several cm compared to the level before vibration is applied. In addition, since the degree of saturation of the pore water of the sand layer can not be measured directly, an unsaturated sand layer was formed separately in a small container, similar to that of the experimental sand layer. Then the unsaturated sand layer was gradually submerged in water from the bottom. The initial degree of saturation of the sand layers formed by the method, was then estimated at 75 to 85% by the weight measurement method and by means of an air meter used to measure the air volume in concrete.

Discussion

As described earlier, the primary aim of the resonance test is to calculate the vibration behaviour of the sand layer subjected to large input vibrations, and to compare the results with analytical values. In this paper, however the analytical results will be omitted and we will discuss the method of analyzing the liquefaction and settlement processes of the experimental sand layer.

(1) One-dimensional settlement of the sand layer

The vibration behavior of the sand layer in the sand box, and the subsequent deformations are three-dimensional. However, since the excess pore water pressure, that is measured shows almost the same behavior regardless of the distance from the end face at the same depth, the amount of settlement can be presumed to be one-dimensional. Furthermore, it is generally difficult to analyze multidimensional deformations, therefore, if a one-dimensional settlements can be estimated, the results can be adequately applied to actual problems. Thus for the experimental sand layer, such assumptions were made considering the horizontal ground expanding indefinitely and then analyzing the process of liquefaction and settlement.

(a) In the normal theory of consolidation, the deformations of a sand layer are generated as a result of the outflow of pore water. In these tests, however the sand layer is assumed to be in an unsaturated state with air remaining in the pores and that the air is combined with the pore water and flows together. This assumes that the porewater is compressible.

(b) It is thought that the excess pore water pressure, generating a pore water flow, is generated internally by cyclic shear.

(c) It is assumed that the ordinary Darcy's law can be applied to the pore water flow.

From these assumptions, the excess pore water pressure and the void ratio in the sand layer can be represented as follows;

$$\Delta u = B \cdot f\left(\frac{\tau_d}{\sigma'_{vc}}, e, K_o\right) \cdot \sigma'_{vo} \cdot \frac{\Delta t}{T} + \frac{B}{C} \cdot \frac{k}{r_w} \cdot \frac{\partial^2 u}{\partial Z^2} \cdot \Delta t \quad (1)$$

$$\begin{aligned} \Delta e = & (1-B)(1+e) \cdot C \cdot f\left(\frac{\tau_d}{\sigma'_{vc}}, e, K_o\right) \cdot \sigma'_{vo} \cdot \frac{\Delta t}{T} \\ & + B(1+e) \cdot \frac{k}{r_w} \cdot \frac{\partial^2 u}{\partial Z^2} \cdot \Delta t \end{aligned} \quad (2)$$

where,

$$B : \text{Pore pressure coefficient } \frac{1}{1+eC_f/(1+e)C} \quad (3)$$

C : Compressibility of sand

C_f : Compressibility of pore water (including air)

$$\frac{1-(1-H)S_{r1}}{p1 + \Delta u} \quad (4)$$

$$p1 + \Delta u$$

H : Henry's coefficient of solubility

S_{r1} : Degree of saturation

p1 : Absolute pore pressure (added value by atmospheric pressure and static water pressure, considered to be equal to pore water pressure and pore air pressure)

f : Pore water pressure generation function due to cyclic shear (described later)

τ_d : Cyclic shear stress

σ'_{vc} : Effective overburden pressure used for pore water pressure generation function

e : Void ratio

K_o : Coefficient of horizontal earth pressure at rest

σ'_{vo} : Initial effective overburden pressure

T : A period of vibration

k : Coefficient of permeability

γ_w : Unit weight of water

Z : Depth from the surface of sand layer

The meaning of the pore water pressure generation function f by cyclic shear shall be defined as follows. In the instance of saturated and undrained conditions, if one cycle is applied, the following equation can be obtained, where C_f=0, B=1, k=0 and t=T, in Eq. (1)

$$\Delta u = f \left(\frac{\tau_d}{e_{vc}}, e, K_o \right) \cdot \sigma'_{vo} \quad \dots\dots\dots (5)$$

$$\Delta e = 0$$

Consequently, f·σ'_{vo} represents the pore water pressure generated per cycle under said conditions. This is based on results of undrained, cyclic, simple shear tests which have been reported. This pore water pressure generation function f was obtained based on the following assumptions and method.

- (a) The increase in the excess pore water pressure, sand subjected to cyclic shear, is the sum of the increments due to cyclic shear and the increments due to an increase in lateral pressure due to the lateral displacement being confined ⁴⁾.

Consequently, the excess pore water pressure Δu generated per cycle of cyclic shear the sand is given by the following equation;

$$\frac{\Delta u}{\sigma'_{vo}} = f_1 \left(\frac{3}{1 + 2 K_o} \cdot \frac{\tau_d}{\sigma'_{vo}} \right) \quad (6)$$

Hence, f_1 can be obtained by the isotropic cyclic triaxial test as follows;

$$\frac{\Delta u}{\sigma'_{30}} = f_1 \left(\frac{\sigma_d}{2 \sigma'_{30}} \right) \quad (7)$$

σ'_{30} : The initial effective lateral pressure

σ_d : Cyclic axial stress

- (b) The pore water pressure generation function f_1 is obtained from a conventional cyclic triaxial test. These tests yield the stress and the generated pore water pressure. However, there is generally a wide variance in the test results. Consequently, by plotting the relationship of $(\sigma_d/2\sigma'_{30} \text{ vs } n_\ell)$ obtained from the liquefaction test, an average relation is estimated from the following equation⁵⁾;

$$\frac{\Delta u}{\sigma'_{30}} = \left(1 - \frac{\Delta d}{2 \sigma'_{30}} \frac{1}{\sin \phi_\ell} \right) / n_\ell \quad (8)$$

Where ϕ_ℓ : Angle of internal friction mobilized when the initial liquefaction is generated.

n_ℓ : Cycles of loading for generating the initial liquefaction

For the tests reported herein, $\sigma_d/2\sigma'_{30}$ vs n_ℓ is plotted as shown in Fig. 8.

- (c) A relationship for general density can be obtained from the following equation with respect to the stress ratio at which liquefaction is generated;

$$\left(\frac{\sigma_d}{2 \sigma'_{30}} \right) D_r = \left(\frac{\sigma_d}{2 \sigma'_{30}} \right) D_r = 50\% \frac{D_r}{50} \quad (9)$$

Based on these assumptions, the function of the generation of pore water pressure in sand is estimated as illustrated in Fig. 9. This function is used as f in the previous equation (1) and (2).

The increments Δu and Δe , the excess pore water pressure and void ratio respectively from equation (1) and (2), are closely related to each other as shown in Fig. 10. This diagram can be interpreted as follows, i.e. path AB represents the entire process that

occurs, which means first reduction of the effective stress due to an excess pore water pressure generated when the sand layer is vibrated. The pore water then flows out and as a result the void ratio is changed. Then the excess pore water pressure is entirely dissipated and stability is attained. Path CF represents the changed path which occurs in a short time interval Δt . If this path is divided into $CF = CE + EF$, CE corresponds to the 1st terms of equations (1) and (2) respectively. Thus the 2nd term deformation path in this case of the undrained condition. An alternate path occurs when the sand layer is placed under a drained condition as shown in path EF. That is the deformation under the drained condition of an unsaturated sand layer in a short time interval can be obtained as the sum of the deformation under the undrained condition of an unsaturated sand and the deformation under the drained condition given thereafter.

The coefficient of compressibility C in equations (1) and (2) was obtained in the following manner. As shown for path EF, the excess pore water pressure was generated by the undrained cyclic shear and then by draining of the sand. The coefficient of compressibility in the recompression process is then obtained. An example of this experiment is illustrated in Fig. 11.

Also illustrated in the same diagram is the static virgin compression curve of this sand. Examining these results the following can be stated;

(a) Until the initial liquefaction point is exceeded, the coefficient of compressibility in the recompression process is smaller than the coefficient of compressibility under the virgin compression process.

(b) When the sand is recompressed, exceeding the initial liquefaction point, the compressibility is as nearly same as the virgin compressibility curve.

(2) Numerical analysis of liquefaction and settlement process

Considering the above, the following assumptions were made in the numerical analyses of the liquefaction and settlement processes as will be described later.

(a) When an excess pore water pressure is generated and exceeds the initial liquefaction point, thus causing compression of the sand, a virgin compression curve is used.

(b) During the process, in which the density increases higher than that of the past minimum void ratio, a virgin compression curve is used.

(c) In the deformation paths other than the above (a) and (b), an unloading or recompression curve is used.

(d) The generation of an excess pore water pressure function f does not occur until the time the excess pore water pressure reaches the initial liquefaction point, $\sigma'_{vc} = \sigma'_{vo}$, when the initial liquefaction point has been exceeded, $\sigma'_{vc} = \sigma'_v$ (σ'_v represents the effective overburden pressure at that time), and the working shear stress also decreases in the form of contacting with the failure envelope line.

Since a vibration analysis and subsequent evaluation of the shear stress of a sand layer, which has changes in its physical properties subsequent to an increase in the excess pore water pressure, is difficult to determine, the following method was employed.

(a) The vibration mode of the sand layer, for liquefaction test, was assumed as the 1st mode. The displacement amplitude was obtained from the amplitude of the measured acceleration and the distribution of the shear stress is then estimated from these results. During this time, when the table acceleration level increases, as seen in Fig. 5(a) on the upper part of the sand layer, the acceleration decreases due to generation of the excess pore water pressure thus making it difficult to estimate the shear strain. Therefore, assuming that the shear strength does not decrease, the standard shear strain distribution corresponding to the individual table acceleration level is estimated from this study.

(b) Now by multiplying the standard shear strain distribution by the shear modulus, in which the reduction effect ⁷⁾ of the strain level is introduced from Richart's experimental equation ⁶⁾ for the shear modulus in an infinitesimal strain level of sand, a shear stress distribution is calculated. When the excess pore water pressure exceeds the initial liquefaction point, this shear stress is decreased to a form which contacts the failure envelope. Examples of changes of the excess pore water pressure and the settlement amount with time have been calculated for the experiments and are illustrated in Figs. 12 and 13. Figs. 12 and 13 correspond to experiment No. 1-3, experiment No. 1-4 as illustrated in Fig. 4 and 5. According to the calculated results for the experiment No. 1-3, the excess pore water pressures in the upper layer ($Z = 0.5, 1.0$ m) increases considerably, consequently in the earlier stage of vibration the settlement amount is a little larger than that of the experiment. Also the excess pore water pressure is larger than measured in middle part of the sand layer and the final calculated settlement amount is larger than that measured. According to the calculated values for experiment No. 1-4, the excess pore pressures in the lower layer ($Z = 3.0, 4.0$ m) increases slowly, but the settlement behavior agrees approximately with the measured results. The cause for these differences, apart from the assumptions in the calculations, are the large errors in estimating the shear strain in the sand layer and compaction due to the preceding vibration. The settlement behaviour of the sand layer shows that the calculated results agree comparatively well with the measured values. From the aforementioned, the method for liquefaction and settlement analysis introduced herein is rather effective to the analysis for this vibration test of model sand layer.

Conclusion

The following conclusions can be derived from the results of the experiments and analyses as described previously;

- (1) In the liquefaction test, when the excess pore water pressure increases to a certain value, the magnification of the acceleration increases and then suddenly decreases.
- (2) The higher the table acceleration and the larger the void ratio, the larger is the excess pore water pressure and the amount of settlement that is generated.
- (3) The compression phenomenon of the air in the pores increases the settlement of the sand layer.
- (4) From examination of the experimental results in line with the analytical method proposed herein, it has been found that there is excellent correspondence between the experiment

data and the analysis.

If this method is used to estimate the amount of settlement of the sand at a construction site, it is important to properly estimate the shear stress in the sand. Also, at the construction site, the ground below the water level is saturated and the duration of an earthquake is relatively shorter than that which occurred in the experiment described in this paper. Consequently, a simplified method, has been developed. This method is based on the assumption that the amount of settlement during an earthquake is small, and therefore the ground is nearly in an undrained condition. The excess pore water pressure then generated is estimated, and the settlement amount is determined as a static deformation due to the outflow of the pore water after the earthquake.

References

1. Seed, H.B. and Idriss, I.M.: Simplified Procedure for Evaluating Soil Liquefaction Potential, Proc. of ASCE, SM 9, 1971.
2. Japan Road Association: Aseismic Design Mannual of Road Bridge (in Japanese), 1972.
3. Florin, V.A. and Ivanov, P.L.: Liquefaction of Saturated Sandy Soils, Proc. of 5th Int. Conf. on S.M.&F.E., Vol. 1, 1961.
4. Ishihara, K. and Li, S.: Liquefaction of Saturated Sand in Triaxial Torsion Shear Test, Soils and Foundation, Vol. 12, No. 2, 1972.
5. Shibata, T.: Liquefaction Phenomenon of Saturated Sand (in Japanese), Preprints of 16th Symposium of SM (JSSMFE), 1971.
6. Richart, F.E., Jr., Hall, J.R. and Wood, R.D.: Vibrations of Soils and Foundations, Prentice-Hall, Inc., 1970.
7. Hardin, B.O. and Drnvich, V.P.: Shear Modulus and Damping in Soils: Design Equations and Curves, Proc. of ASCE, SM 7, 1972.

Table 1 Index properties of the test sand

Properties		Values
Specific gravity G_s		2.71
Optimum water content	$\omega_{opt} (\%)$	13.4
Maximum dry density	$\gamma_d \text{ max } (g/cm^3)$	1.742
Maximum void ratio	$e \text{ max}$	1.02
Minimum void ratio	$e \text{ min}$	0.57

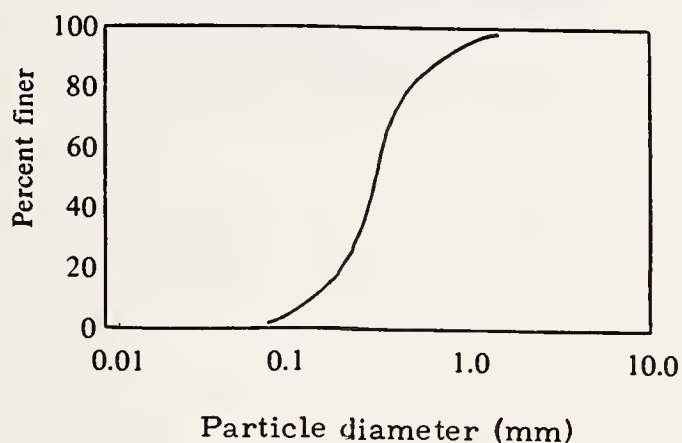


Table 2 Test Condition

Vibration Method Model	Resonance test	Liquefaction test			
	1	2	3	4	5
1	6 ~ 13 gal	37 *gal	61 gal	138 gal	274 gal
	1 ~ 20 c/s	12 c/s	11 c/s	10 c/s	9 c/s
	$\bar{e}_0 = 0.82$	74**sec	76 sec	84 sec	92 sec
2		57 gal	100 gal	132 gal	283 gal
		12 c/s	11 c/s	10 c/s	9 c/s
	$\bar{e}_0 = 0.73$	69 sec	72 sec	81 sec	78 sec
3	7 ~ 19 gal	66 gal	99 gal	219 gal	365 gal
	1 ~ 20 c/s	12 c/s	11 c/s	10 c/s	9 c/s
	$\bar{e}_0 = 0.68$	93 sec	88 sec	103 sec	85 sec

* Stationary value of table acc.

** Total duration of vibration



Photo. 1 Model sand box

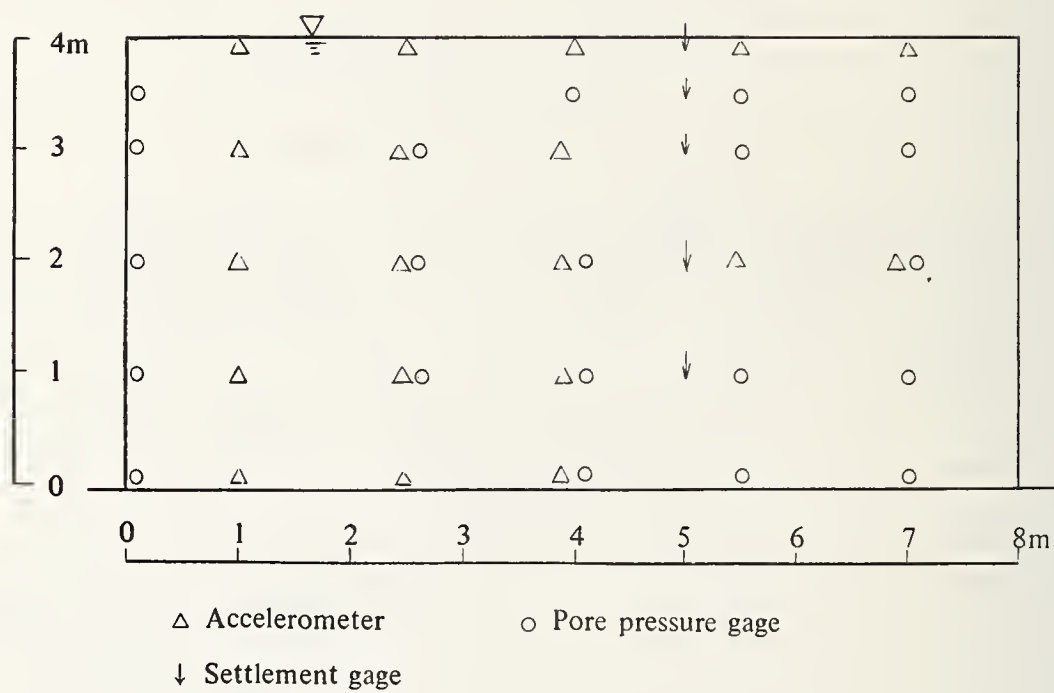


Fig. 1 Arrangement of meters

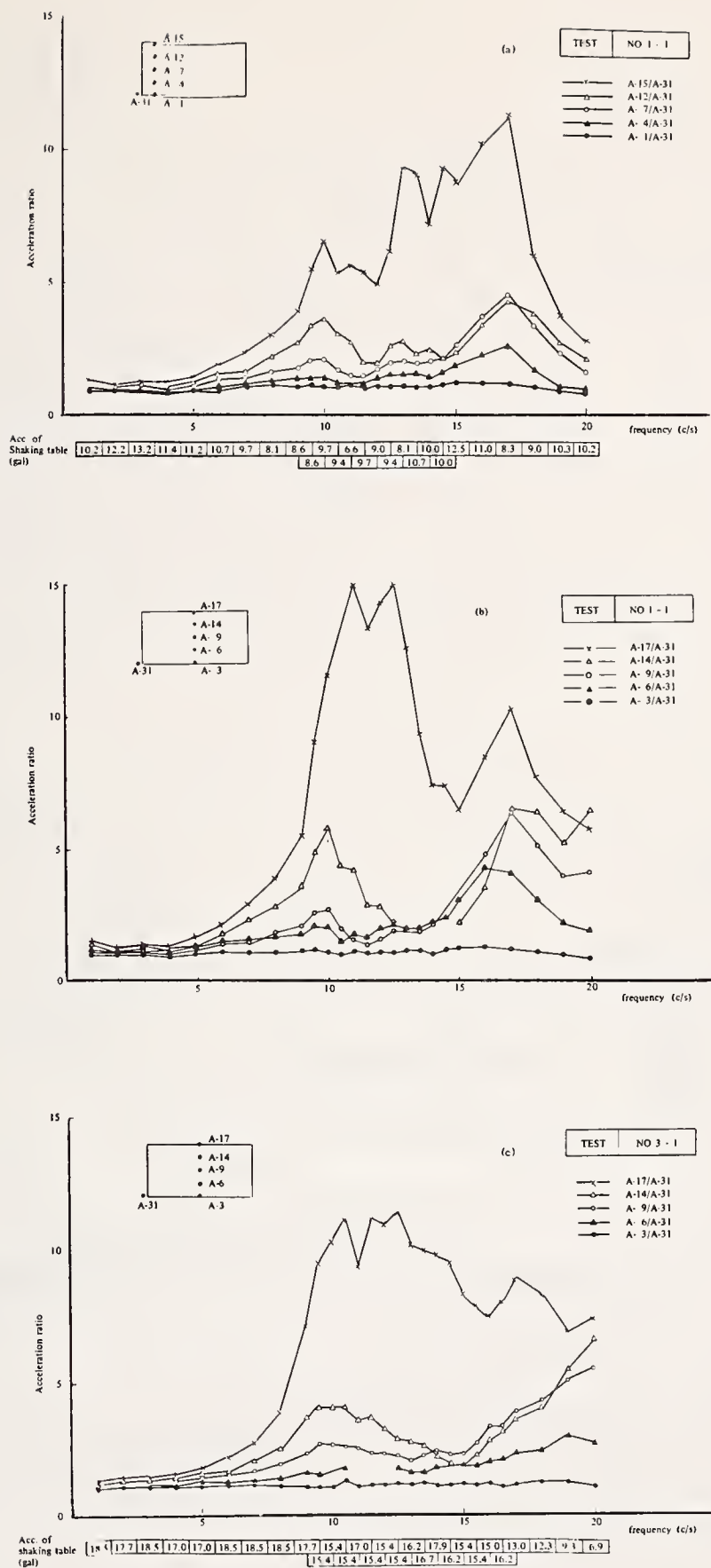


Fig. 2 Examples of resonance curves

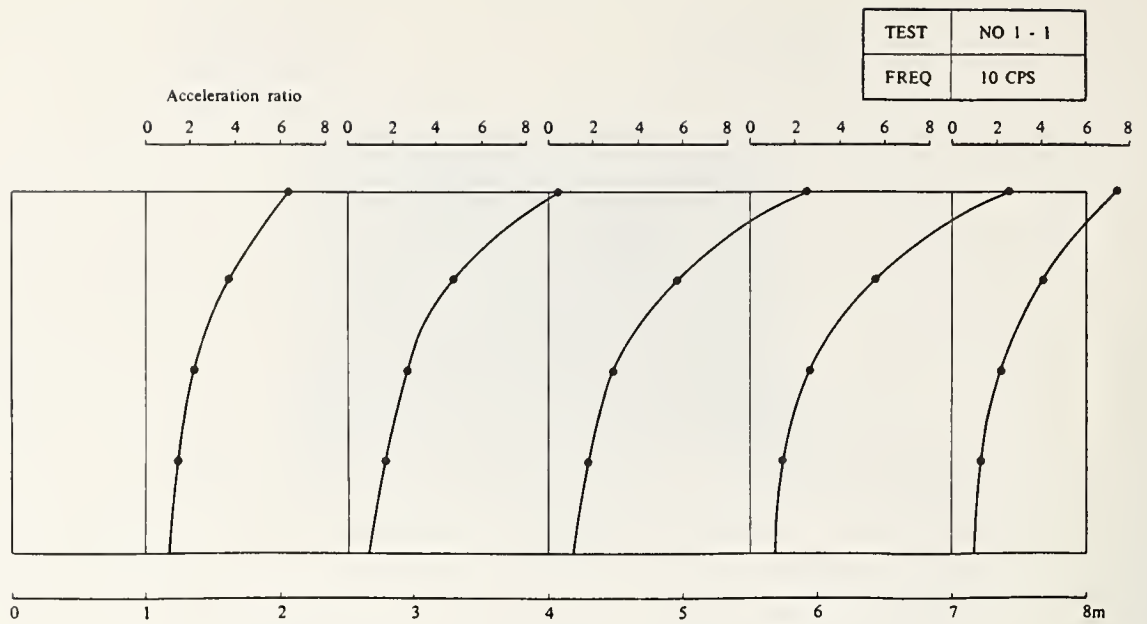


Fig. 3 Distribution of acceleration in sand layer

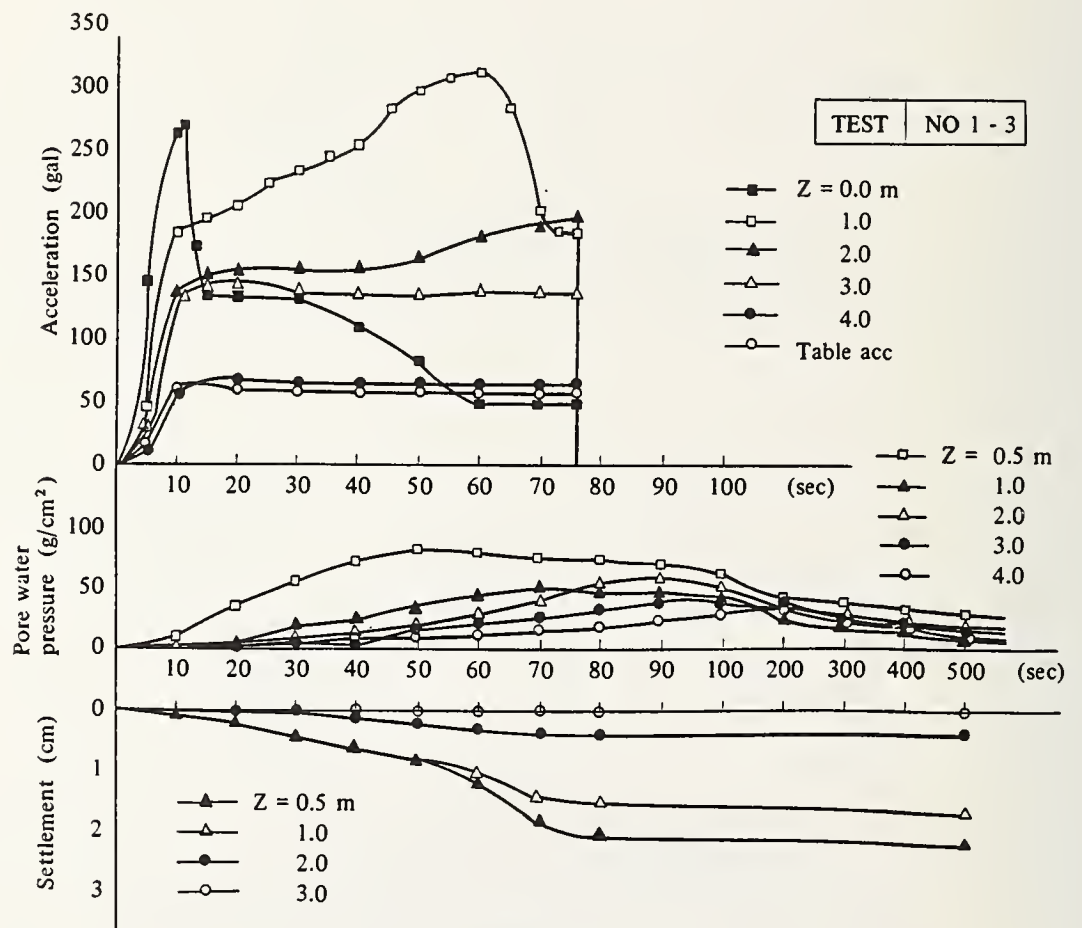


Fig. 4 Acceleration, excess pore water pressure and settlement data (Test No. 1-3)

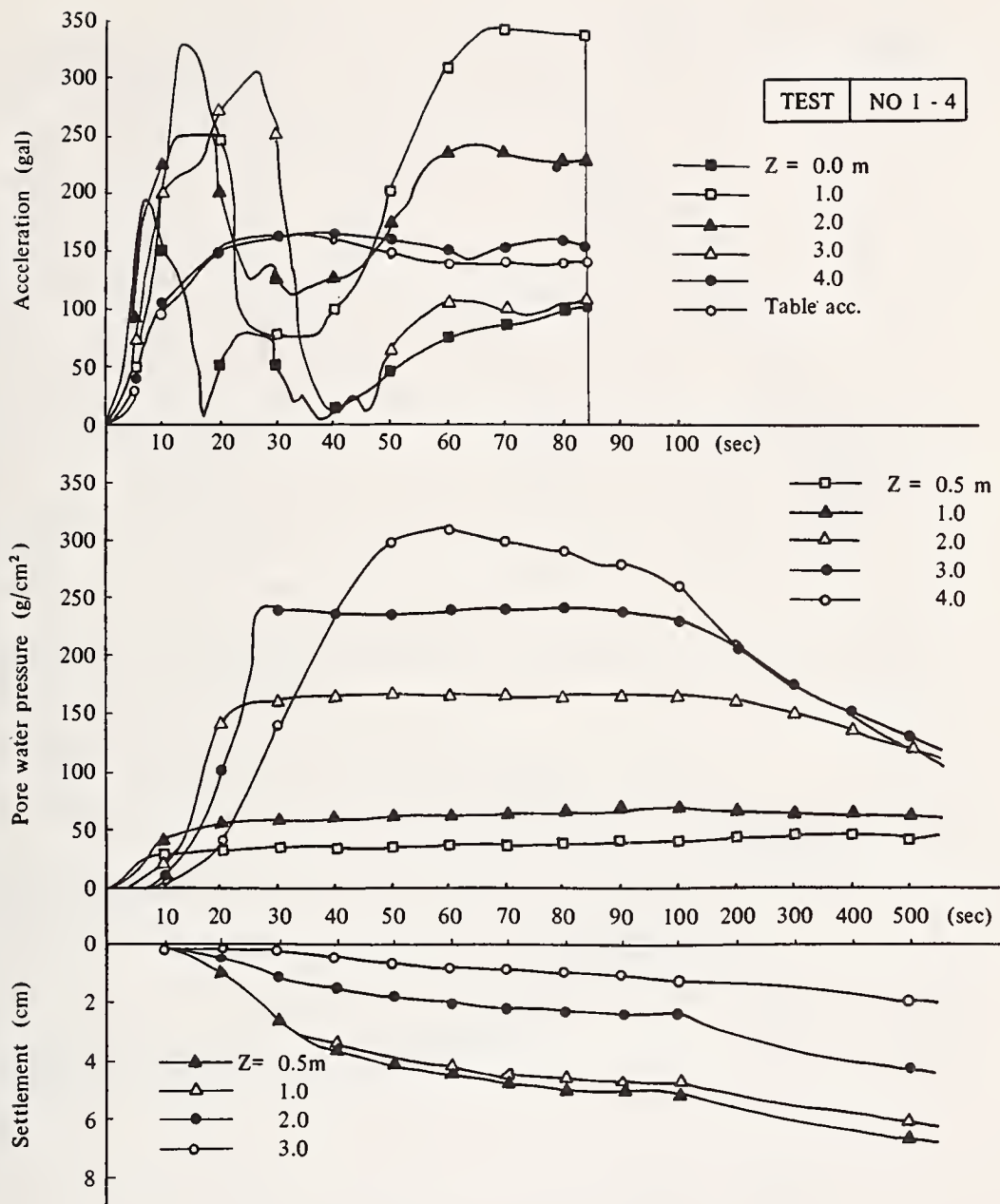


Fig. 5 Acceleration, excess pore water pressure and settlement data (Test No. 1-4)

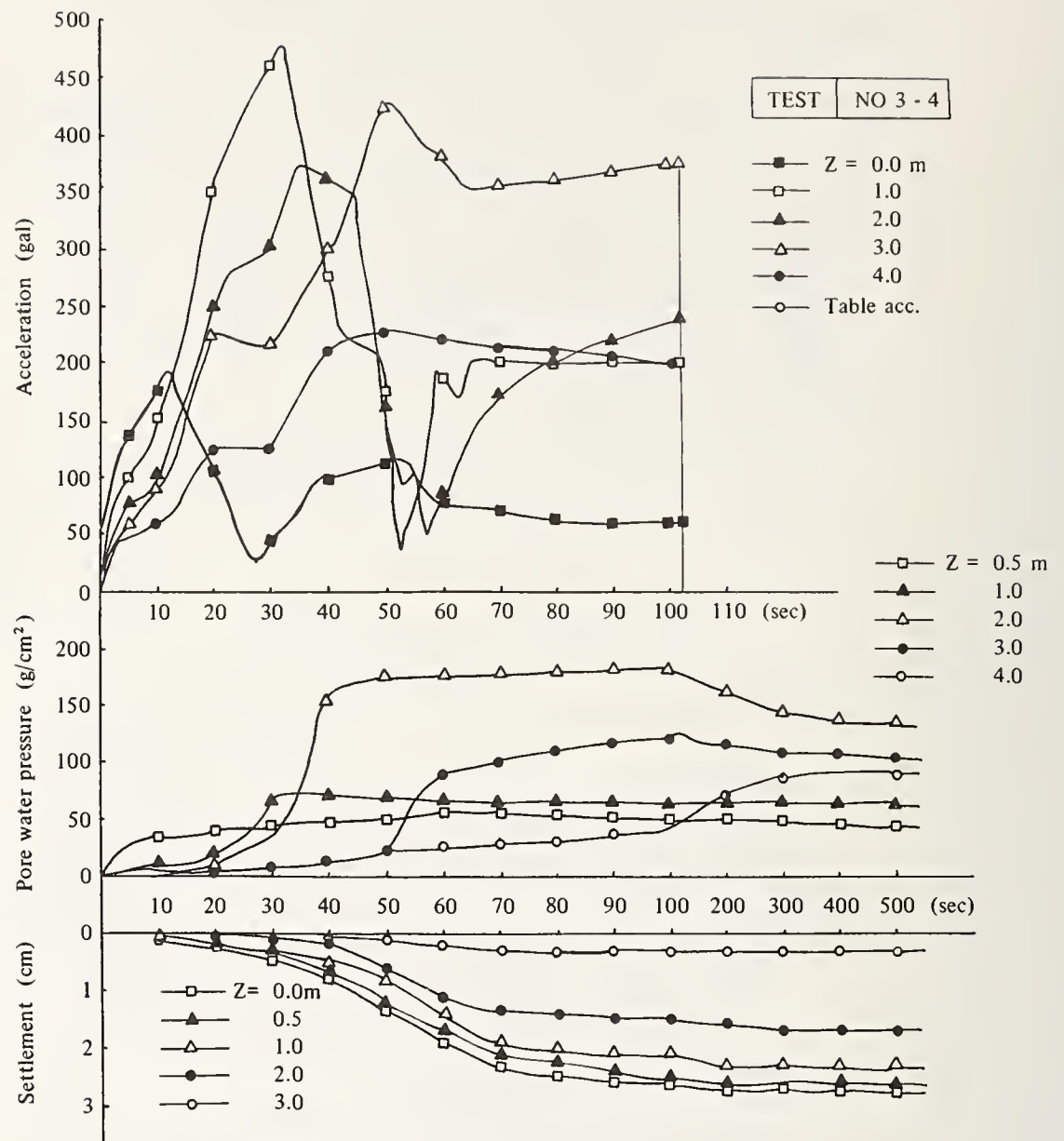


Fig. 6 Acceleration, excess pore water pressure and settlement data (Test No. 3-4)

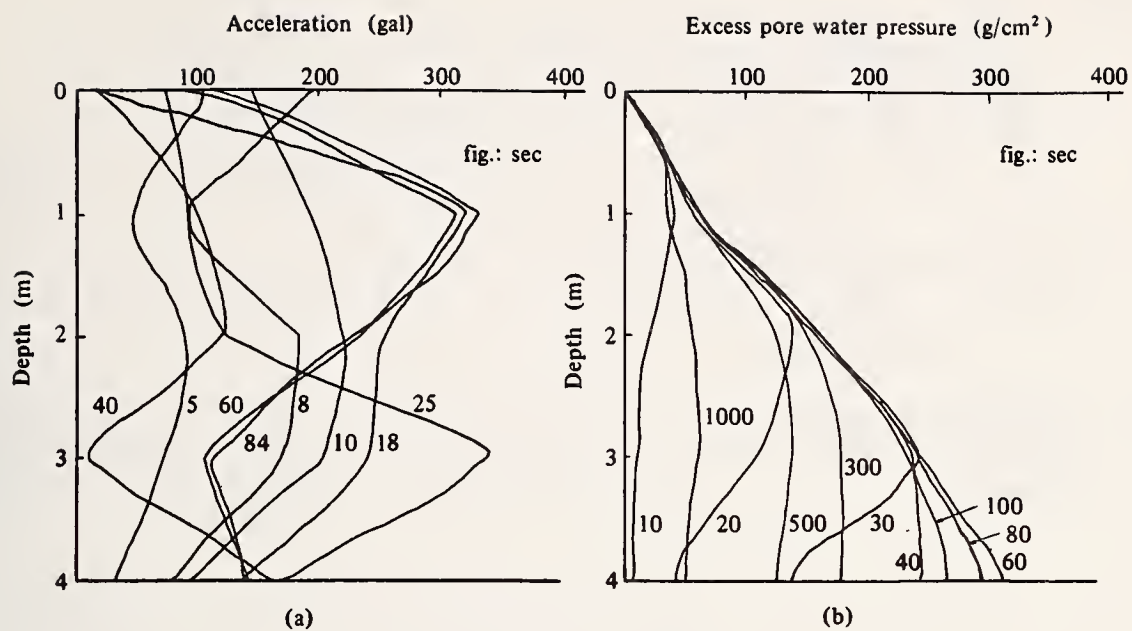


Fig. 7 Vertical distribution of acceleration and excess pore water pressure

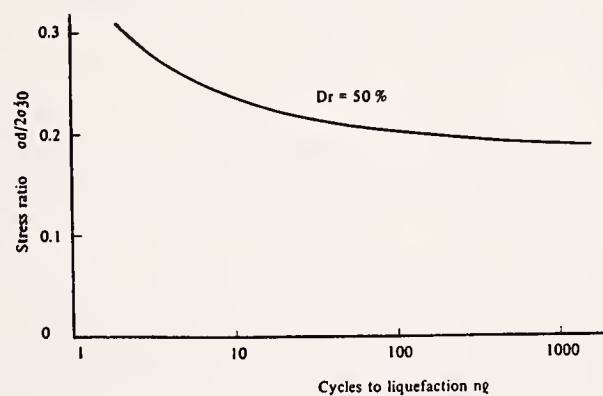


Fig. 8 Liquefaction characteristics of test sand

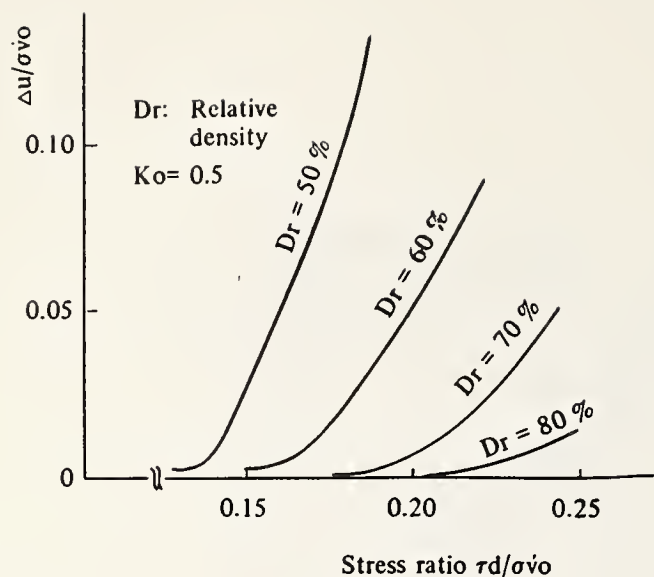


Fig. 9 Generation function of excess pore water pressure

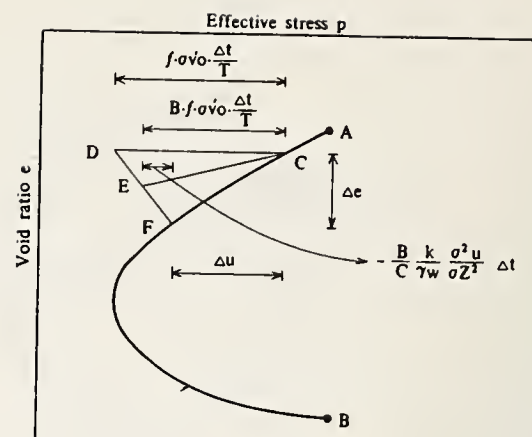


Fig. 10 Schematic relationship between void ratio and effective stress due to vibration

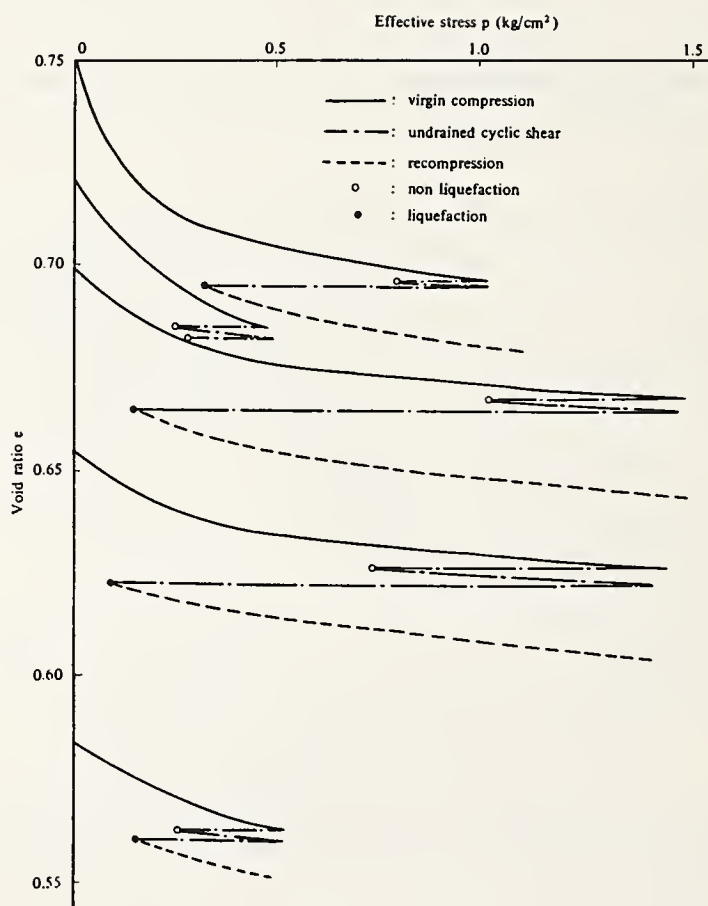


Fig. 11 Compression characteristics of test sand

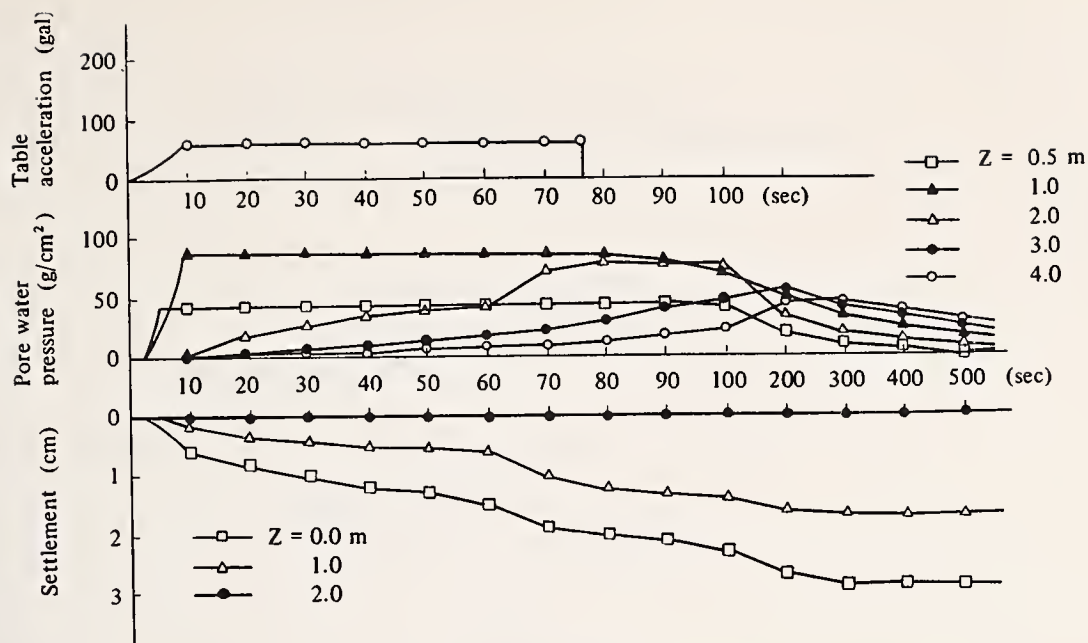


Fig. 12 Calculated results of excess pore water pressure and settlement (Test No. 1-3)

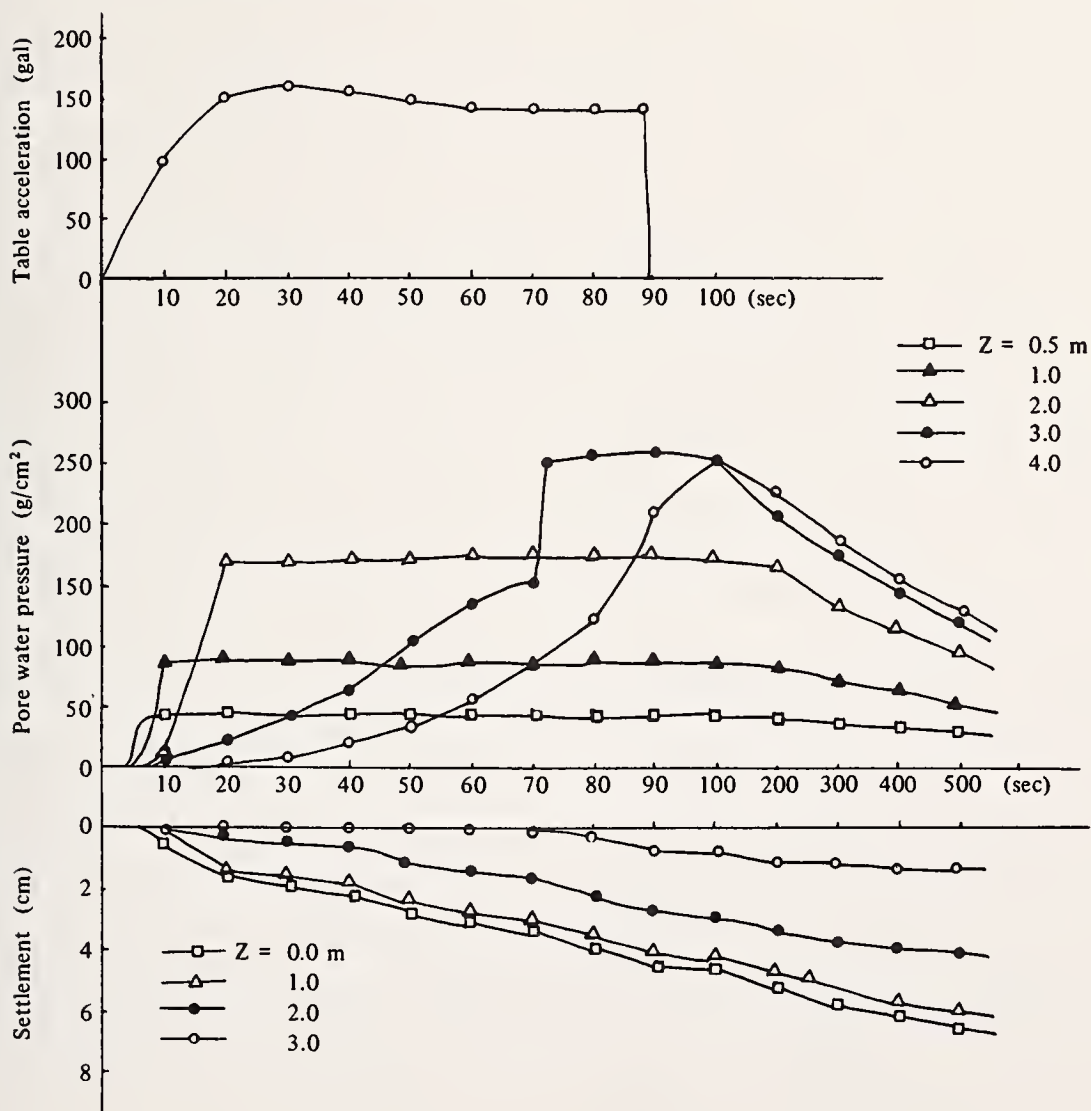


Fig. 13 Calculated results of excess pore water pressure and settlement (Test No. 1-4)

STUDY ON EARTHQUAKE RESPONSE OF
STRUCTURES BY CONSIDERING NON-DETERMINISTIC
VARIABLES

by

Yutaki Yamazaki
Structures Division

and

Yasunori Koizumi
Director
Building Research Institute
Ministry of Construction

ABSTRACT

The seismic design coefficient has been widely used because of its simplicity. This design technique provides a safeguard against earthquakes but contains many problems when replacing the dynamic forces with static forces. In addition, the earthquake resistant properties of high-rises or buildings can be investigated by a simulation analysis, using many past earthquake records as input excitation. This type of dynamic analysis of a structure has been made possible by use of electronic computers. In this analysis, an actual structure is transformed into a vibration model, then the structure is subjected to earthquake ground motions, which are simulated by an electronic computer. As an alternate scheme, from a stochastic point of view, vibrational properties of structures subjected to earthquake ground motions have been investigated by utilizing the concept of random vibrations. The theory of random vibration, for dynamic response of structures, considers that earthquake ground motions can be essentially predicted as deterministic phenomena and that the vibrational behaviour of structures during these earthquakes can be predicted stochastically. Studies on developing a more reasonable design method have been conducted using the experiences obtained from earthquake disasters and the analyses of earthquake phenomena. The non-deterministic phenomena of earthquake ground motions will be treated essentially by the application of the theory of random vibration to the earthquake engineering. However, it is also true that a structure cannot be handled as a deterministic system, because the dynamic property variables of an actual structure, such as the masses, spring constants and damping constants, cannot be evaluated deterministically when the structure is designed. Hence, a structure must be designed by considering the nondeterministic properties of the structure as well as those of earthquake ground motions. In this thesis, a theoretical treatment of the earthquake response problems of a structure with nondeterministic variables have been discussed and a reasonable design technique of a structure with appropriate safety has been suggested.

Key Words: Probability, deterministic, earthquake, structures, random vibrations, safety, dynamics.

Introduction

Vibrational properties of structures, subjected to earthquake ground motions, have been investigated by utilizing the concept of random vibrations. The theory of random vibrations for the dynamic responses of structures is based on the stochastic point of view that earthquake ground motions cannot be predicted as a deterministic phenomena and that the vibrational behaviour of structures during earthquakes must be investigated stochastically. However, it is also true that a structure cannot be examined as a deterministic system, because the dynamic property variables of an actual structure, such as masses, spring constants and damping constants, cannot be evaluated deterministically when the structure is designed. Hence, a structure must be designed by considering the non-deterministic properties of the structure as well as those of the earthquake ground motions. There has been many papers concerning the dynamic response of a structure subjected to earthquake ground motions by application of the theory of random vibrations since E. Rosenblueth⁽¹⁾ and H. Tajimi⁽²⁾. The theory for a stationary random response of a linear lumped-mass system has been studied by one of the authors⁽³⁾. Expansion of this theory is explained in this paper, in which all variables are regarded as non-deterministic. The fundamental formula obtained by Taylor's series of a function $f(r)$, of the vector of random variables r , is applied to this expansion. There are papers^{(4) (6)} in which the properties of stochastic variation of the eigen values and earthquake responses of a structure are investigated which demonstrate application of this formula. In this paper, the theoretical expansion is conducted in order to obtain a general and meaningful solution of the earthquake response of a structure. The theory of the earthquake response of a structure described herein has the following characteristics;

- (1) The structure is a one-dimensional linear multi-degree-of-freedom system with masses, springs and dashpots.
- (2) The structure is subjected to a stationary random excitation, having any distribution of power spectral density
- (3) The structural response can be stochastically predicted in consideration of the interaction effect between the structure and the ground.

Response of a Structure Subjected to a Random Disturbance

The earthquake response of one-dimensional linear multi-degree-of-freedom system with masses, springs, and dashpots as shown in Fig. 1 is analyzed as follows; The interaction effect between a structure and the ground is considered by application of sway and rocking springs. The earthquake ground motion, which affects the structure, is assumed to be a stationary random process with an amplitude distribution of Gaussian order with a zero mean value.

The equations of motion of the system subjected to an earthquake ground acceleration \ddot{x}_g is generally represented by

$$[M] \{\ddot{Z}\} + [C] \{\dot{Z}\} + [K] \{Z\} = -[M_E] \ddot{x}_g \quad (1)$$

where

$$\left. \begin{aligned} \{M\} &= \begin{bmatrix} m_1 & & & & & \\ & m_2 & & & & \\ & & \ddots & & & \\ & & & m_N & & \\ & 0 & & & m_0 & \\ & & & & & I \end{bmatrix} \\ \{M_E\} &= \{m_1 \ m_2 \ \dots \ m_N \ m_0 \ 0\}^T \\ \{Z\} &= \{Z_1 \ Z_2 \ \dots \ Z_N \ Z_0 \ \Theta\}^T \end{aligned} \right\} \quad (2)$$

$$\{K\} = \begin{bmatrix} k_1 & -k_1 & 0 & 0 & 0 & \dots & 0 & 0 & -k_1 \bar{H}_1 \\ -k_1 & k_1 + k_2 & -k_2 & & & & 0 & 0 & k_1 \bar{H}_1 - k_2 \bar{H}_2 \\ 0 & -k_2 & k_2 + k_3 & & & & \cdot & 0 & k_2 \bar{H}_2 - k_3 \bar{H}_3 \\ 0 & 0 & -k_3 & & & & \cdot & \cdot & \cdot \\ & & & \cdot & & & \cdot & \cdot & \cdot \\ & & & \cdot & & & \cdot & 0 & k_1 \bar{H}_1 - k_{i+1} \bar{H}_{i+1} \\ & & & \cdot & & & \cdot & \cdot & \cdot \\ & & & 0 & & & 0 & 0 & \cdot \\ & & & -k_{N-1} & & & 0 & k_{N-2} \bar{H}_{N-2} - k_{N-1} \bar{H}_{N-1} \\ 0 & 0 & & 0 & k_{N-1} + k_N & & -k_N & k_{N-1} \bar{H}_{N-1} - k_N \bar{H}_N \\ 0 & 0 & 0 & 0 & -k_N & k_N + k_s & k_N \bar{H}_N & k_R + \sum_{i=1}^N k_i \bar{H}_i^2 \\ -k_1 \bar{H}_1 & k_1 \bar{H}_1 - k_2 \bar{H}_2 & k_2 \bar{H}_2 - k_3 \bar{H}_3 & & k_{N-1} \bar{H}_{N-1} - k_N \bar{H}_N & k_N \bar{H}_N & k_R + \sum_{i=1}^N k_i \bar{H}_i^2 \end{bmatrix} \quad (3)$$

m , m_0 and I : masses of each story and the foundation and the moment of inertia about the center of the foundation, respectively

k , k_s and k_R : spring constants of each story, sway and rocking springs, respectively

\bar{H} : story height

The damping matrix $\{C\}$ is prescribed here by

$$\{C\} = \frac{2 h_1}{\omega_1} \{K\} \quad (4)$$

where ω_1 and h_1 is the fundamental circular frequency and damping constant of the system, respectively.

The vector of the relative floor displacement $\{Z\}$ is expressed in terms of the normal mode matrix $[\phi]$ and the vector of normal coordinate $\{\eta\}$, namely

$$\{Z\} = (\phi) \{\eta\} \quad (5)$$

Substituting Eq. 5 into Eq. 1, the equations of motion of the system are expressed into each mode as follows.

$$\ddot{\eta}_j + 2\zeta_j \omega_j \dot{\eta}_j + \omega_j^2 \eta_j = -\Gamma_j \ddot{x}_g \quad (6)$$

where

$$\zeta_j = \frac{h_j}{\omega_j} \omega_j \quad (7)$$

$$\Gamma_j = \{\phi_j\}^T \{M_E\} \quad (8)$$

In the above expression, the mode matrix $[\phi]$ is normalized. In this case, a generalized mass matrix M^* , given by Eq. 9, corresponds to a unit matrix E .

$$\{M^*\} = [\phi]^T \{M\} [\phi] \quad (9)$$

The autocorrelation function of the normal coordinate η_j is represented by

$$R_{\eta_j}(\tau) = \int_{-\infty}^{\infty} S_{\eta_j}(p) e^{ip\tau} dp \quad (10)$$

where $S_{\eta_j}(p)$ is the power spectral density function of η_j . Defining $H_j(ip)$ and $S_{\ddot{x}_g}(p)$ as the function of the frequency response of the system and the power spectral density function of a ground acceleration \ddot{x}_g , respectively, it follows that:

$$S_{\eta_j}(p) = |H_j(ip)|^2 S_{\ddot{x}_g}(p) \cdot \Gamma_j^2 \quad (11)$$

$$R_{\eta_j}(\tau) = \Gamma_j^2 \int_{-\infty}^{\infty} |H_j(ip)|^2 e^{ip\tau} S_{\ddot{x}_g}(p) dp \quad (12)$$

Utilizing the relation

$$R_{\dot{\eta}_j}(\tau) = -\frac{d^2}{d\tau^2} R_{\eta_j}(\tau) \quad ,$$

the autocorrelation function of $\dot{\eta}_j$ is represented by

$$R_{\dot{\eta}_j}(\tau) = \Gamma_j^2 \int_{-\infty}^{\infty} |H_j(ip)|^2 p^2 e^{ip\tau} S_{\ddot{x}_g}(p) dp \quad (13)$$

Representing the power spectral density function of the ground acceleration \ddot{x}_g as a sum of the power spectral density functions of the single-degree-of-freedom systems excited by white noise accelerations, the function is expressed by

$$S_{xg}''(p) = \sum_{s=1}^L S_{s xg}''(p) = \sum_{s=1}^L \frac{1 + 4\xi_s^2 \left(\frac{p}{\omega_{gs}}\right)^2}{\left\{1 - \left(\frac{p}{\omega_{gs}}\right)^2\right\}^2 + 4\xi_s^2 \left(\frac{p}{\omega_{gs}}\right)^2} S_s \quad (14)$$

where ω_g , ξ and s are the natural circular frequency and the damping constant of the single-degree-of-freedom system and the constant power spectral density of the white noise acceleration, respectively. In general, the following relationship exists between the response Z_i of i -th story and Z_s of the s -th one.

$$\overline{Z_i Z_s} = \sum_j \sum_k \phi_{ij} \phi_{sk} \overline{\eta_j \eta_k} = \sum_j \phi_{ij} \phi_{sj} \overline{\eta_j^2} = \sum_j \phi_{ij} \phi_{sj} R\eta_j(0) \quad (15)$$

From the above relationship, the mean square values of the responses Z_i and \dot{Z}_i become

$$\overline{Z_i^2} = \sum_j \phi_{ij} R\eta_j(0) \quad (16)$$

$$\overline{\dot{Z}_i^2} = \sum_j \phi_{ij}^2 R\eta_j(0) \quad (17)$$

Substituting Eqs. 12 to 14 into Eqs. 16 and 17, the following equations are finally obtained.

$$\overline{Z_i^2} = \sum_s \sum_j \phi_{ij}^2 \chi_{sj} \frac{C_{sj}}{D_{sj}} \quad (18)$$

$$\overline{\dot{Z}_i^2} = \sum_s \sum_j \phi_{ij} \chi_{sj} \frac{E_{sj}}{D_{sj}}$$

where

$$\begin{aligned} \chi_{sj} &= \pi \frac{\Gamma_j^2 S_s}{\omega_j^4} \\ C_{sj} &= {}_2A_{sj} {}_3A_{sj} - {}_1A_{sj} {}_4A_{sj} + {}_3A_{sj} {}_6A_s^2 \\ D_{sj} &= {}_1A_{sj} ({}_2A_{sj} {}_3A_{sj} - {}_1A_{sj} {}_4A_{sj}) - {}_3A_{sj}^2 \\ E_{sj} &= {}_3A_{sj} + {}_1A_{sj} {}_6A_s^2 \end{aligned} \quad (19)$$

and

$$\begin{aligned} {}_1A_{sj} &= {}_5A_j + {}_6A_s \\ {}_2A_{sj} &= \frac{1}{\omega_{gs}^2} + {}_5A_j {}_6A_s + \frac{1}{\omega_j^2} \\ {}_3A_{sj} &= \frac{{}_8A_j}{\omega_{gs}^2} + \frac{{}_6A_s}{\omega_j^2} \\ {}_4A_{sj} &= \frac{1}{\omega_{gs}^2 \omega_j^2} \end{aligned} \quad (20)$$

$$\begin{aligned} {}_s A_j &= \frac{2 \zeta_j}{\omega_j} \\ {}_s A_s &= \frac{2 \xi_s}{\omega_{gs}} \end{aligned} \quad (20)$$

The mean square values of the relative displacement and velocity at each story are given by similar expressions namely;

$$\begin{aligned} \overline{(Z_i - Z_{i+1})^2} &= \sum_j \sum_j \{ \phi_{ij} - \phi_{i+1j} \}^2 x_{sj} \frac{C_{sj}}{D_{sj}} \\ \overline{(\dot{Z}_i - \dot{Z}_{i+1})^2} &= \sum_j \sum_j \{ \phi_{ij} - \phi_{i+1j} \}^2 x_{sj} \frac{E_{sj}}{D_{sj}} \end{aligned} \quad (21)$$

The mean square values of the relative story displacement and velocity, subtracting the rocking effect, are also given by

$$\begin{aligned} \overline{(Z_i - Z_{i+1} - \bar{H}_i Z_{N+2})^2} &= \sum_j \sum_j \{ \phi_{ij} - \phi_{i+1j} - \bar{H}_i \phi_{N+2j} \}^2 x_{sj} \frac{C_{sj}}{D_{sj}} \\ \overline{(\dot{Z}_i - \dot{Z}_{i+1} - \bar{H}_i \dot{Z}_{N+2})^2} &= \sum_j \sum_j \{ \phi_{ij} - \phi_{i+1j} - \bar{H}_i \phi_{N+2j} \}^2 x_{sj} \frac{E_{sj}}{D_{sj}} \end{aligned} \quad (22)$$

The mean squares of the responses are given by Eqs. 18, 21 and 22. The maximum displacements can be estimated by application of Eq. 23, derived by S.O. Rice, to these mean squares, providing the process is a stationary random and a Gaussian distribution with zero mean value.

$$|x|_{\max} = \sqrt{2 \sigma_x^2 \log_e \left(\frac{T}{\pi} \frac{\sigma_{\dot{x}}}{\sigma_x} \right)} \quad (23)$$

where σ_x , $\sigma_{\dot{x}}$ and T represent the standard deviation of the responses x and \dot{x} and the duration time of the responses, respectively. The mean squares, obtained by Eqs. 18, 21 and 22, correspond to the standard deviation of the responses which have zero mean values. Hence, the maximum responses can be estimated by substituting Eqs. 18, 21 and 22 into Eq. 23, respectively.

Mean Value and Variance of a Function Composed of Stochastic Variables

Considering $f(r)$ being a function of the vector of random variables r , this function can be expanded in Taylor's series about the mean values of r . Truncating the series after the third term, the following equations are obtained.

$$f(r) = f(\bar{r}) + \sum_{\ell} \frac{\partial f(\bar{r})}{\partial r_{\ell}} (r_{\ell} - \bar{r}_{\ell}) + \frac{1}{2} \left[\sum_{\ell} (r_{\ell} - \bar{r}_{\ell}) \frac{\partial}{\partial r_{\ell}} \right]^2 f(\bar{r}) \quad (24)$$

Based on the assumption that the variables r are stochastically independent of each other, namely the covariance of r_k and r_ℓ is equal to zero for the case of $k \neq \ell$, the mean value of the function $\overline{f(r)}$ is directly obtained from this equation, which gives;

$$\begin{aligned}\overline{f(r)} &= E[f(r)] = E[f(\bar{r})] + \frac{1}{2} E \left[\left(\sum_{\ell} (r_{\ell} - \bar{r}_{\ell}) \frac{\partial}{\partial r_{\ell}} \right)^2 f(\bar{r}) \right] \\ &= f(\bar{r}) + \frac{1}{2} \sum_{\ell} \frac{\partial^2 f(\bar{r})}{\partial r_{\ell}^2} \text{Var}(r_{\ell})\end{aligned}\quad (25)$$

where $\text{Var}(r_{\ell})$ means the variance of the variable r_{ℓ} . The variance of the function, $\text{Var}(f(r))$, is given by

$$\text{Var}(f(r)) = E[(f(r) - \overline{f(r)})^2]$$

Substituting Eqs. 24 and 25 into the above equation, the following relation is finally obtained;

$$\text{Var}(f(r)) = \sum_{\ell} \left(\frac{\partial f(\bar{r})}{\partial r_{\ell}} \right)^2 \text{Var}(r_{\ell}) + \frac{1}{2} \sum_k \sum_{\ell} \left(\frac{\partial^2 f(\bar{r})}{\partial r_k \partial r_{\ell}} \right)^2 \text{Var}(r_k) \text{Var}(r_{\ell}) \quad (26)$$

Eqs. 25 and 26 are the fundamental formulas concerning the mean value and variance of the function $f(r)$, respectively. Neglecting the third term of the right hand side of Eq. 24, the following formulas are obtained, instead of Eqs. 25 and 26;

$$\overline{f(r)} = f(\bar{r}) \quad (27)$$

$$\text{Var}(f(r)) = \sum_{\ell} \left(\frac{\partial f(\bar{r})}{\partial r_{\ell}} \right)^2 \text{Var}(r_{\ell}) \quad (28)$$

The pair of Eqs. 25 - 26 and Eqs. 27 - 28 are called the formulas of " the Second Expansion of Probability Variance " and " the first Expansion of Probability Variance ", respectively, in this paper.

Earthquake Response of Structures by Considering Nondeterministic Variables

The theoretical approach, concerning an earthquake response of a structure subjected to a random disturbance, has been given in part 2. The fundamental stochastic variables r , considered in this application, are masses m , spring constants k , a fundamental damping constant of the parameters concerning power spectral properties of the ground motions, namely ω_g , ξ and s . All the variables are shown in Table 1. Consequently, the number of fundamental stochastic variables are $2N+3L+6$, where N and L are the number of stories of the structure and the number of peaks on the spectrum of the ground motions, respectively.

Applying the formulas of "the First Expansion" Eqs. 27 and 28 into the maximum response $|x|_{\max}$ given by Eq. 23, the following equations are obtained.

$$\overline{|x|_{\max}(r)} = |x|_{\max}(\bar{r}) \quad (29)$$

$$\text{Var}(|x|_{\max}(r)) = \sum_{\ell} \left(\frac{\partial |x|_{\max}(\bar{r})}{\partial r_{\ell}} \right)^2 \text{Var}(r_{\ell}) \quad (30)$$

The former equation can be directly evaluated. However in order to solve the latter equation, the following is required. First Differentiate Eq. 23 with respect to variable r_{ℓ} , which gives the following equations for each condition of the subscript ℓ .

for $\ell=1$ (r_{ℓ} corresponds to duration time T)

$$\frac{\partial |x|_{\max}(\bar{r})}{\partial r_{\ell}} = \frac{\sigma_x^2}{T} \frac{1}{\sqrt{2\sigma_x^2 \log_e \left(\frac{T}{\pi} \frac{\sigma_{\dot{x}}}{\sigma_x} \right)}} \quad (31)$$

for $\ell \neq 1$

$$\begin{aligned} \frac{\partial |x|_{\max}(\bar{r})}{\partial r_{\ell}} = & \frac{1}{\sqrt{2\sigma_x^2 \log_e \left(\frac{T}{\pi} \frac{\sigma_{\dot{x}}}{\sigma_x} \right)}} \left[2\sigma_x \log_e \left(\frac{T}{\pi} \frac{\sigma_{\dot{x}}}{\sigma_x} \right) \left(\frac{\partial \sigma_x}{\partial r_{\ell}} \right) \right. \\ & \left. + \frac{\sigma_x}{\sigma_{\dot{x}}} \left\{ \sigma_x \left(\frac{\partial \sigma_{\dot{x}}}{\partial r_{\ell}} \right) - \sigma_{\dot{x}} \left(\frac{\partial \sigma_x}{\partial r_{\ell}} \right) \right\} \right] \end{aligned} \quad (32)$$

The variance σ_x^2 and $\sigma_{\dot{x}}^2$ correspond to mean squares $\overline{Z^2}$ and $\overline{\dot{Z}^2}$, respectively, for relative displacements to the ground, namely

$$\begin{aligned} \sigma_{xi}^2 &= \overline{Z_i^2} \\ \sigma_{\dot{x}i}^2 &= \overline{\dot{Z}_i^2} \end{aligned} \quad (33)$$

The following equations are directly obtained by differentiating Eqs. 33 and 18 with respect to r_{ℓ} .

$$\begin{aligned} \frac{\partial \sigma_{xi}}{\partial r_{\ell}} &= \frac{1}{2\sigma_{xi}} \left(\frac{\partial \overline{Z_i^2}}{\partial r_{\ell}} \right) \\ \frac{\partial \sigma_{\dot{x}i}}{\partial r_{\ell}} &= \frac{1}{2\sigma_{\dot{x}i}} \left(\frac{\partial \overline{\dot{Z}_i^2}}{\partial r_{\ell}} \right) \end{aligned} \quad (34)$$

and

$$\begin{aligned}
 \frac{\partial \bar{Z}_i^2}{\partial r_\ell} &= \sum_s \sum_j \left[2\phi_{ij} \left(\frac{\partial \phi_{ij}}{\partial r_\ell} \right) \chi_{sj} \frac{C_{sj}}{D_{sj}} + \phi_{ij}^2 \left(\frac{\partial \chi_{sj}}{\partial r_\ell} \right) \frac{C_{sj}}{D_{sj}} \right. \\
 &\quad \left. + \phi_{ij}^2 \chi_{sj} \left\{ \frac{1}{D_{sj}} \left(\frac{\partial C_{sj}}{\partial r_\ell} \right) - \frac{C_{sj}}{D_{sj}^2} \left(\frac{\partial D_{sj}}{\partial r_\ell} \right) \right\} \right] \\
 \frac{\partial \bar{Z}_i^2}{\partial r_\ell} &= \sum_s \sum_j \left[2\phi_{ij} \left(\frac{\partial \phi_{ij}}{\partial r_\ell} \right) \chi_{sj} \frac{E_{sj}}{D_{sj}} + \phi_{ij} \left(\frac{\partial \chi_{sj}}{\partial r_\ell} \right) \frac{E_{sj}}{D_{sj}} \right. \\
 &\quad \left. + \phi_{ij}^2 \chi_{sj} \left\{ \frac{1}{D_{sj}} \left(\frac{\partial E_{sj}}{\partial r_\ell} \right) - \frac{E_{sj}}{D_{sj}^2} \left(\frac{\partial D_{sj}}{\partial r_\ell} \right) \right\} \right]
 \end{aligned} \tag{35}$$

For relative story displacements and those subtracting the rocking effect, Eqs. 21 and 22 are applied instead of Eq. 18. The unknowns in the above equations are differential of χ_{sj} , C_{sj} , D_{sj} , E_{sj} , and ϕ_{ij} . These are derived in the following

$$\frac{\partial \chi_{sj}}{\partial r_\ell} :$$

Differentiating Eq. 18-1 with respect to r_ℓ , the differential of χ_{sj} is represented by

$$\frac{\partial \chi_{sj}}{\partial r_\ell} = \frac{\Gamma_j}{\omega_j^4} \pi \left[2S_s \left(\frac{\partial \Gamma_j}{\partial r_\ell} \right) + \Gamma_j \left(\frac{\partial S_s}{\partial r_\ell} \right) - 4 \frac{\Gamma_j S_s}{\omega_j} \left(\frac{\partial \omega_j}{\partial r_\ell} \right) \right] \tag{36}$$

where $\partial \Gamma_j / \partial r_\ell$ is obtained by Eq. 8, or;

$$\begin{aligned}
 \frac{\partial \Gamma_j}{\partial r_\ell} &= \left\{ \frac{\partial \phi_j}{\partial r_\ell} \right\}^T \{ M_E \} + \{ \phi_j \}^T \left\{ \frac{\partial \omega_j}{\partial r_\ell} \right\} \\
 \frac{\partial C_{sj}}{\partial r_\ell}, \quad \frac{\partial D_{sj}}{\partial r_\ell} \quad \text{and} \quad \frac{\partial E_{sj}}{\partial r_\ell} &:
 \end{aligned} \tag{37}$$

The differential of C_{sj} , D_{sj} , and E_{sj} , referring to Eqs. 19-2 to 19-4 are represented as follows;

$$-\frac{\partial C_{sj}}{\partial r_\ell} = -{}_4A_{sj} \left(\frac{\partial {}_1A_{sj}}{\partial r_\ell} \right) + {}_3A_{sj} \left(\frac{\partial {}_2A_{sj}}{\partial r_\ell} \right) + ({}_2A_{sj} + {}_6A_s^2) \left(\frac{\partial {}_3A_{sj}}{\partial r_\ell} \right) \quad (38)$$

$$-{}_1A_{sj} \left(\frac{\partial {}_4A_{sj}}{\partial r_\ell} \right) + {}_2{}_3A_{sj} {}_6A_s \left(\frac{\partial {}_6A_s}{\partial r_\ell} \right)$$

$$\frac{\partial D_{sj}}{\partial r_\ell} = ({}_2A_{sj} {}_3A_{sj} - {}_2{}_1A_{sj} + A_{sj}) \left(\frac{\partial {}_1A_{sj}}{\partial r_\ell} \right) + {}_1A_{sj} {}_3A_{sj} \left(\frac{\partial {}_2A_{sj}}{\partial r_\ell} \right) \quad (39)$$

$$+ ({}_1A_{sj} {}_2A_{sj} - {}_2{}_3A_{sj}) \left(\frac{\partial {}_3A_{sj}}{\partial r_\ell} \right) - {}_1A_{sj}^2 \left(\frac{\partial {}_4A_{sj}}{\partial r_\ell} \right)$$

$$\frac{\partial E_{sj}}{\partial r_\ell} = {}_6A_s^2 \left(\frac{\partial {}_1A_{sj}}{\partial r_\ell} \right) + \left(\frac{\partial {}_3A_{sj}}{\partial r_\ell} \right) + {}_2{}_1A_{sj} {}_6A_s \left(\frac{\partial {}_6A_s}{\partial r_\ell} \right)$$

(40)

The unknowns, $\partial {}_iA_{sj}/\partial r_\ell$ in the above equations are derived from Eqs. 20-1 to 20-6, respectively;

$$\left. \begin{aligned} \frac{\partial {}_1A_{sj}}{\partial r_\ell} &= \left(\frac{\partial {}_3A_j}{\partial r_\ell} \right) + \left(\frac{\partial {}_6A_s}{\partial r_\ell} \right) \dots\dots\dots (1) \\ \frac{\partial {}_2A_{sj}}{\partial r_\ell} &= -\frac{2}{\omega_{gs}^3} \left(\frac{\partial \omega_{gs}}{\partial r_\ell} \right) + \left(\frac{\partial {}_6A_s}{\partial r_\ell} \right) {}_5A_j + {}_6A_s \left(\frac{\partial {}_5A_j}{\partial r_\ell} \right) - \frac{2}{\omega_j^3} \left(\frac{\partial \omega_j}{\partial r_\ell} \right) \dots\dots\dots (2) \\ \frac{\partial {}_3A_{sj}}{\partial r_\ell} &= \frac{1}{\omega_j^2} \left(\frac{\partial {}_6A_s}{\partial r_\ell} \right) - 2 \frac{{}_6A_s}{\omega_j^3} \left(\frac{\partial \omega_j}{\partial r_\ell} \right) + \frac{1}{\omega_{gs}^2} \left(\frac{\partial {}_5A_j}{\partial r_\ell} \right) - 2 \frac{{}_5A_j}{\omega_{gs}^3} \left(\frac{\partial \omega_{gs}}{\partial r_\ell} \right) \dots\dots\dots (3) \\ \frac{\partial {}_4A_{sj}}{\partial r_\ell} &= -\frac{2}{\omega_j^2 \omega_{gs}^3} \left(\frac{\partial \omega_{gs}}{\partial r_\ell} \right) - \frac{2}{\omega_j^3 \omega_{gs}^2} \left(\frac{\partial \omega_j}{\partial r_\ell} \right) \dots\dots\dots (4) \\ \frac{\partial {}_5A_j}{\partial r_\ell} &= 2 \left\{ \frac{1}{\omega_j} \left(\frac{\partial \zeta_j}{\partial r_\ell} \right) - \frac{\zeta_j}{\omega_j^2} \left(\frac{\partial \omega_j}{\partial r_\ell} \right) \right\} \dots\dots\dots (5) \\ \frac{\partial {}_6A_s}{\partial r_\ell} &= 2 \left\{ \frac{1}{\omega_{gs}} \left(\frac{\partial \xi_s}{\partial r_\ell} \right) - \frac{\xi_s}{\omega_{gs}^2} \left(\frac{\partial \omega_{gs}}{\partial r_\ell} \right) \right\} \dots\dots\dots (6) \end{aligned} \right\} \quad (41)$$

where $\partial \zeta_j / \partial r_\ell$ is obtained Eq. 7, namely

$$\frac{\partial \zeta_j}{\partial r_\ell} = \frac{\omega_j}{\omega_1} \left(\frac{\partial h_1}{\partial r_\ell} \right) + \frac{h_1}{\omega_1} \left(\frac{\partial \omega_j}{\partial r_\ell} \right) - \frac{h_1 \omega_j}{\omega_1^2} \left(\frac{\partial \omega_1}{\partial r_\ell} \right) \quad (42)$$

The other unknowns in the above equations, namely $\partial \phi_{ij} / \partial r_\ell$ and $\partial \omega_j / \partial r_\ell$ are obtained by an application of the formulas of "the First Expansion" to an eigen value problem. (4) (6)

Therefore, the right hand side in Eq. 3- can be calculated with the above equations, which are represented by the differential of the fundamental variables shown in Table 1. Therefore, the mean value and variance of the maximum response $|x|_{\max}$ of a structure can be theoretically estimated by Eqs. 29 and 30, if the mean value and variance of the fundamental variables are determined. The above-mentioned relationship, used to obtain the mean value and variance of the maximum response of a structure subjected to earthquake ground motions, are based on the formulas of "the First Expansion", namely Eqs. 27 and 28. Applying the formulas of "the Second Expansion" represented by Eqs. 25 and 26 instead of "the First Expansion" to this problem, instead of Eqs. 29 and 30, the following equations are obtained;

$$\overline{|x|_{\max}(r)} = \overline{|x|_{\max}(\bar{r})} + \frac{1}{2} \sum_{\ell} \left(\frac{\partial^2}{\partial r_{\ell}^2} |x|_{\max}(\bar{r}) \right) \text{Var}(r_{\ell}) \quad (43)$$

$$\begin{aligned} \text{Var}(|x|_{\max}(r)) &= \sum_{\ell} \left(\frac{\partial}{\partial r_{\ell}} |x|_{\max}(\bar{r}) \right)^2 \text{Var}(r_{\ell}) \\ &+ \frac{1}{2} \sum_k \sum_{\ell} \left(\frac{\partial^2}{\partial r_k \partial r_{\ell}} |x|_{\max}(\bar{r}) \right)^2 \text{Var}(r_k) \text{Var}(r_{\ell}) \end{aligned} \quad (44)$$

The remaining unknown term is $\frac{\partial^2}{\partial r_k \partial r_{\ell}} (|x|_{\max}(\bar{r}))$, in the above equations as the first terms of the right hand side in the above both equations have been derived. This term can be easily derived in the same way as described above. The derivation of the theoretical relationship concerning "the Second Expansion" is omitted in this paper.

Earthquake Response of a Three-Storied Structure

In this section, the theory concerning the earthquake response of a structure, described in the previous section, is applied to a 3-story reinforced concrete structure with sway and rocking springs under the foundation. The dynamic behaviour of the structure shown in Fig. 2 is analyzed as follows. The constants of the structure, such as masses and spring constants, are shown in Table 2, where m_0 , I , k_s and k_R are the mass of the foundation, the moment of inertia about the center of the foundation, sway and rocking spring constants, respectively. The sway and rocking spring constants, k_s and k_R , are obtained by the

relationship, in which k_H and k_V are the dynamic coefficients of subgrade reaction in horizontal and vertical directions, respectively.

$$k_S = k_H \cdot B \cdot L, \quad k_R = k_V \cdot \frac{BL^3}{12}$$

B and L: breadth and longitude of the foundation, respectively

$$k_H = \text{kg/cm}^3$$

$$k_V = 4\text{kg/cm}^3$$

spring constant k is estimated on the following considerations;

Table 2 Parameters of 3-storied Structure analyzed

Mass			Spring		
Element	Mean Value	Coefficient of Variation	Element	Mean Value	Coefficient of Variation
m_1	0.130 $\text{ton}/\frac{\text{cm}}{\text{sec}^2}$	0.17	k_1	177.8 ton/cm	0.1
m_2	0.198	0.17	k_2	418.6	0.1
m_3	0.204	0.17	k_3	363.0	0.1
m_0	0.400	0.17	k_S	1300	0.2
I	39373 $\text{ton}\cdot\text{cm}\cdot\text{sec}^2$	0.17	k_R	$2.166 \times 10^8 \text{ton}\cdot\text{cm}$	0.2

Considering a structure having a relatively rigid horizontal members, spring constants of each story of the structure, k, are represented by

$$k = \sum_{i=1}^N k_i \quad (45)$$

where k_i are the values of horizontal rigidity of each vertical member at a corresponding story and these can be obtained by the method of D-value. Applying the formulas of "the First Expansion" to Eq. 45, the mean value and variance of the spring constant k are represented by

$$\bar{k} = \sum_{i=1}^N k_i$$

$$\text{Var}(k) = \sum_{i=1}^N \text{Var}(k_i) \quad (46)$$

Therefore, the coefficient of variation $\tilde{\sigma}_k$ of the spring constant k is represented by

$$\tilde{\sigma}_k = \text{Var}(k)/\bar{k} = \sqrt{\sum_{i=1}^N \text{Var}(k_i) / \sum_{i=1}^N \bar{k}_i} \quad (47)$$

Considering that the mean value and variance of all vertical members have the same value, Eq. 47 becomes

$$\tilde{\sigma}_k = \sqrt{N \text{Var}(k) / N \bar{k}} = \tilde{\sigma}_k / \sqrt{N} \quad (48)$$

where $\tilde{\sigma}_k$ is the coefficient of variation for the horizontal rigidity of each vertical member at a story. Based on the statistical arrangement of materials, the coefficient of variation $\tilde{\sigma}_k$ for the horizontal rigidity of reinforced concrete columns is estimated as 0.3. The values of the coefficients of variation, shown in Table 2, were obtained by application of Eq. 48 in which $\tilde{\sigma}_k=0.3$. The values of the coefficients of variation for sway and rocking spring constants, k_s and k_R , are 0.2. These values were estimated from the variation of the natural period among many standard 5-story apartment houses constructed by the Japan Housing Corporation. The values of the coefficients of variation for mass were determined by the relationship which is obtained by application of the formulas of "the First Expansion" to the equation of eigen value on a single-degree-of-freedom system. In this case, the coefficient of variation for the natural period of the system is assumed to be $\tilde{\sigma}_T=0.1$. The mean value and coefficient of variation of the damping constant, for a fundamental mode used in this example, are $h_1=0.06$ and $\tilde{\sigma}_{h_1}=0.3$, respectively. These were determined by a statistical analysis of the materials concerning damping constants of many actual structures. Finally, the properties of the earthquake ground motions must be determined. In this example, it is assumed that the structure is constructed in Muroran, where many strong earthquakes have been observed. Fig. 3 shows the power spectra of a ground accelerations observed in Muroran Harbor. However, a simulated power spectra corresponding to those of the observed earthquakes can be obtained by use of Eq. 14, where parameters ω_g , ξ and s in Eq. 14 are assumed as stochastic variables. Fig. 4 shows the simulated power spectra. These two figures, Figs. 3 and 4, are quite similar to each other. Therefore, the simulated power spectra shown in Fig. 4 were utilized in the following numerical calculation. The prescribed mean value and variance of parameters ω_g , ξ and s on the simulated power spectra are shown in Table 3. The standard deviation of the ground

Table 3 Constants for Simulated Power Spectral Density Function of Earthquake Ground Motion at Muroran Harbor

	Mean Value	Coefficient of Variation
Predominant Frequency ω_g	15.57 rad/sec	0.16
Damping ξ	0.235	0.08
Power Level S	38.55 gal ² /rad/sec	0.17

motions, having this simulated power spectra, $\sigma_{\ddot{x}_g}$, is 70 gals. The maximum acceleration is about 3 times as great as the standard deviation in this case, namely 210 gals. The mean value and coefficient of variation for a time duration of the ground motions are assumed to be $\bar{T}=30$ seconds and $\tilde{\sigma}_T=0.2$.

Fig. 5 shows the stochastic distribution of the maximum responses. The solid lines in the figure show the mean values of the maximum displacements. The broken chain lines show the confidence band located on either side of the mean value at a distance of the standard deviation and the maximum displacements corresponding to 95% probability. The probability distribution of the maximum responses is assumed to be Gumbel's First Asymptotic Distribution. The coefficient of variation of the maximum displacements and the ratios of the mean maximum displacements, corresponding to 95% probability to the maximum displacements, are shown in Fig. 6. The coefficients of variation of the maximum displacements are about 0.3 to 0.4 and the maximum displacements, corresponding to 95% probability, are about 1.8 times as much as the mean maximum displacements. This fact shows that the stochastic variation of the earthquake response of a structure is extremely important in designing a structure with proper safety against earthquake ground motions.

Effect of Stochastic Variables to Variation of Earthquake Response of a Structure

The structure model used in the previous section is examined again in this section. The coefficients of variation of the stochastic variables, used in the previous section, are employed as the standard values of these coefficients of variation. Varying independently all the coefficients of variation of each one of all stochastic variables, in the range of 0.05 to 0.4, gives the results shown in Figs 7 to 9. The significant features in these figures are as follows:

- (1) The most influential factor in the variation of the maximum displacements is the variation of the predominant frequency ω_g of the earthquake ground motions.
- (2) The variation of the spring constants k of the structure is the most influential factor, as well as the predominant frequency ω_g of the earthquake ground motions, to the variation of the maximum story displacement.
- (3) The variation of mass m , fundamental damping constant h_1 of the structure and the damping constants ξ in the power spectra of the earthquake ground motions are not significant.
- (4) The variation of the spring constants of the structure is not influential in the variation of the maximum response of the foundation. Similarly, the variation of the sway and rocking constants is not influential in the variation of the maximum response of the structure, except for the foundation.
- (5) The variation of the duration of time of the earthquake ground motion is not an important factor.

In this example, the predominant period of the earthquake ground motions is 0.4 seconds, while the fundamental period of the structure is 0.38 seconds. Therefore, it is natural that the variation of the predominant frequency of the earthquake ground motion is an important influential factor with respect to the variation of the maximum response. Hence, it must be recognized that the feature described in (1) is not general. It is expected that the variation of the predominant frequency of such earthquake ground motions as white noise excitations are not effective with respect to the variation of the maximum response.

Conclusion

A study of the stochastic earthquake response of a structure, which consists of a nondeterministic stochastic variables, is explained in this paper. If the statistic properties of the nondeterministic variables relating to the problem of earthquake responses of structures can be obtained with sufficient accuracy, then the response properties of a structure subjected to earthquake ground motions can be reasonably evaluated by the stochastic theory described herein.

References

1. Emilio Rosenblueth: "Some Applications of Probability Theory in Aseismic Design", Proceedings of the 1st World Conference on Earthquake Engineering, 1956.
2. Hiroshi Tajimi: "Earthquake Responses of Structures Estimated by Statistical Method", Transactions of the Architectural Institute of Japan, No. 603, 1958.
3. M. Ozaki, M. Watabe, M. Hirose, Y. Matsushima and Y. Yamazaki: "Earthquake Response Prediction of Reinforced Concrete Buildings", Transactions of the Architectural Institute of Japan, No. 171, 1970.
4. T.K. Hasselman and G.C. Hart: "Modal Analysis of Random Structural Systems", Journal of the Engineering Mechanics Division, Proceedings of the American Society of Civil Engineers, June, 1972.
5. M. Hoshiya and H.C. Shah: "Free Vibration of Stochastic Beam-Column", Journal of the Engineering Mechanics Division, Proceedings of the American Society of Civil Engineers, August, 1971.
6. Yutaka Matsushima: "Perturbation of Earthquake Responses for Systems Composed of Stochastic Variables", Transactions of the Architectural Institute of Japan, No. 210, 1973.

Table 1 Actual Variable Factors Corresponding to Probabilistic Variable r_L

r_L	Duration Time	r_L	Earthquake Property	r_L	Damping	r_L	Mass	r_L	Spring
r_1	T	r_2	ξ_1	r_{3L+2}	h_1	r_{3L+3}	M_1	r_{3L+5+N}	k_1
		r_3	ω_{g1}			r_{3L+4}	M_2	r_{3L+6+N}	k_2
		r_4	S_1						
		r_5	ξ_2						
		r_6	ω_{g2}						
		r_7	S_2						
						r_{3L+2+N}	M_N	$r_{3L+4+2N}$	k_N
						r_{3L+3+N}	M_0	$r_{3L+5+2N}$	k_S
						r_{3L+4+N}	I	$r_{3L+6+2N}$	k_R
		r_{3L-1}	ξ_L						
		r_{3L}	ω_{gL}						
		r_{3L+1}	S_L						

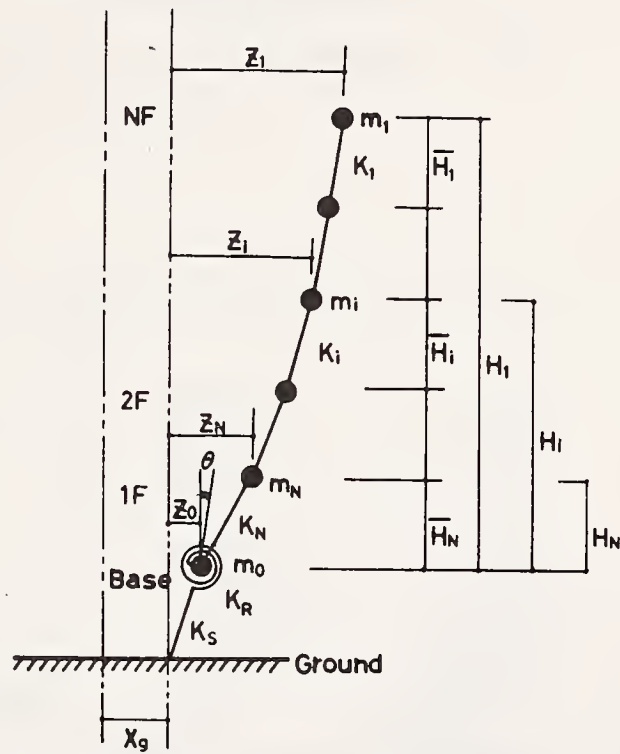


Fig1. Idealization of Structure subjected to Earthquake Ground Motion

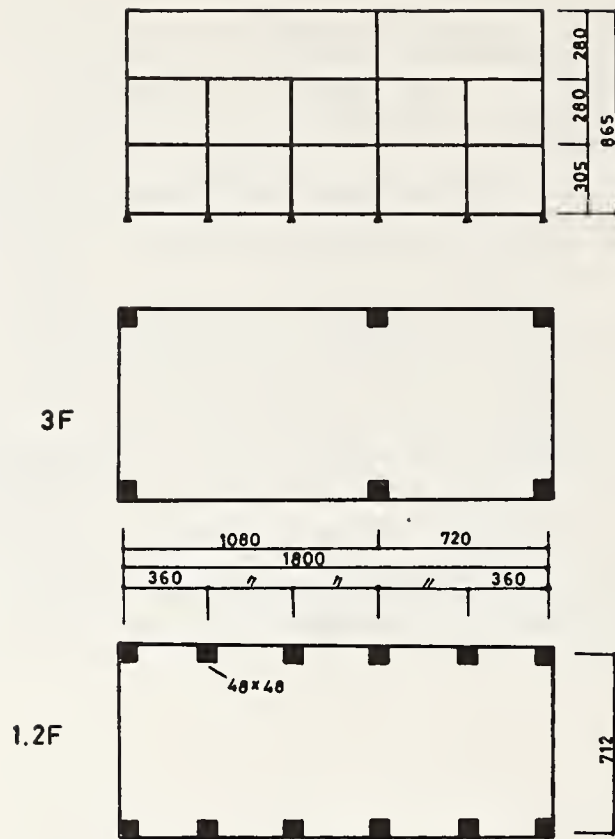


Fig.2 3-storied Structure analyzed

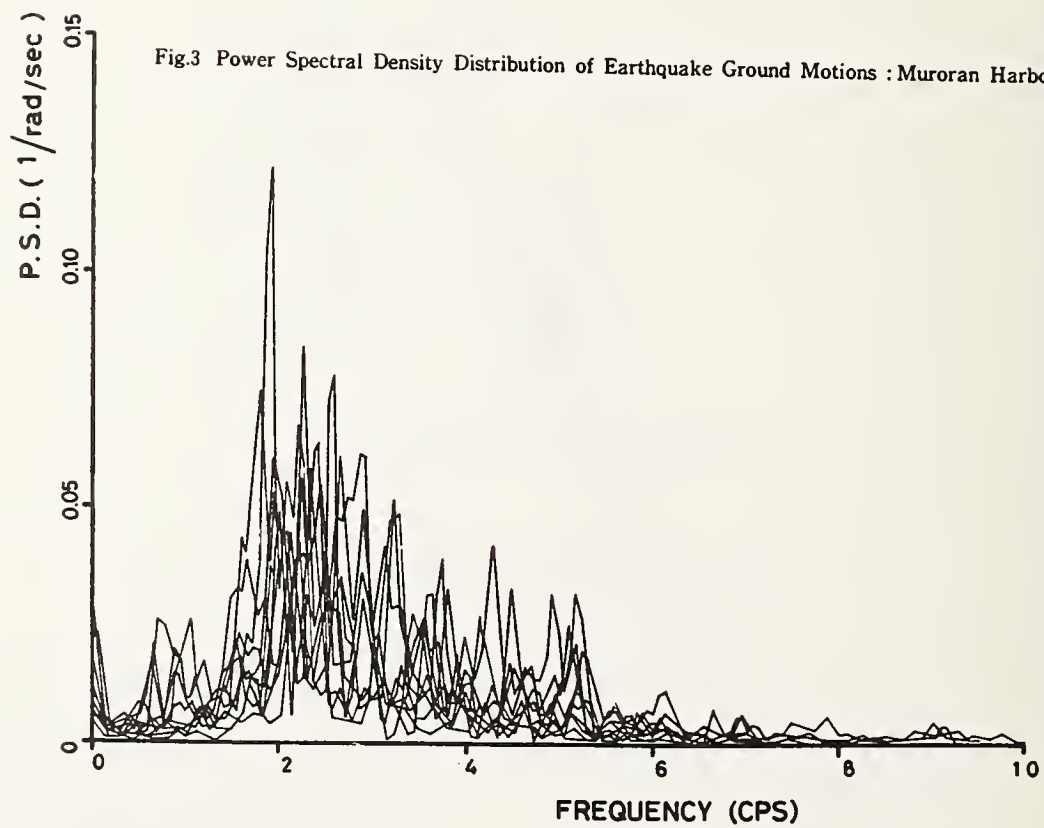


Fig.3 Power Spectral Density Distribution of Earthquake Ground Motions : Muroran Harbor

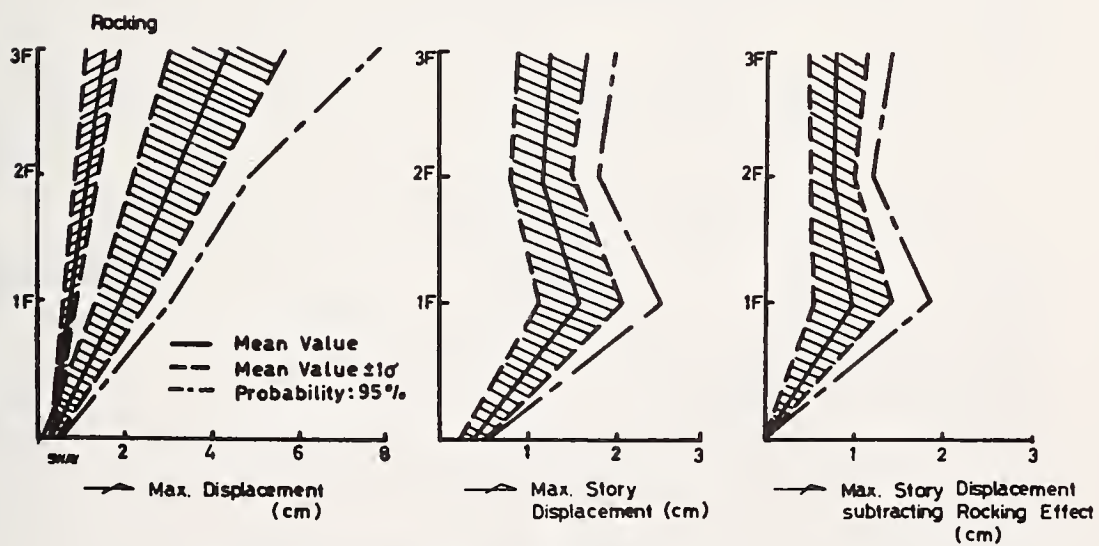
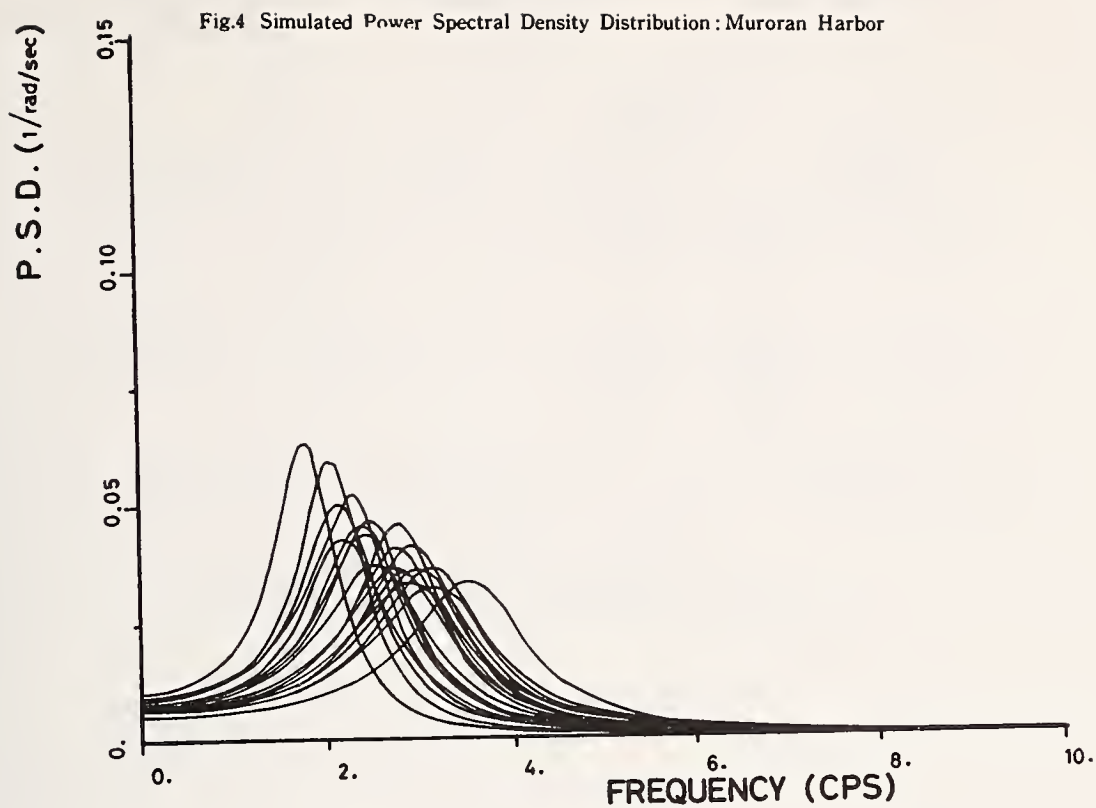


Fig.5 Probability Distribution of Maximum Response

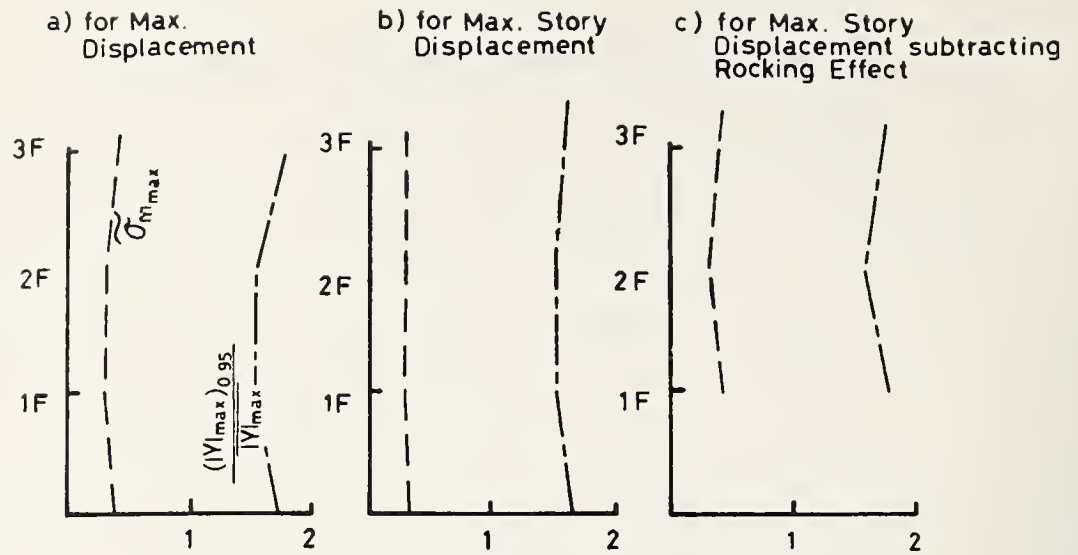


Fig.6 Coefficients of Variation $\tilde{\sigma}|Y|_{\max}$ and Ratio of Maximum Response corresponding to Probability 95% to Mean Maximum Response $(|Y|_{\max})_{0.95} / \overline{|Y|_{\max}}$

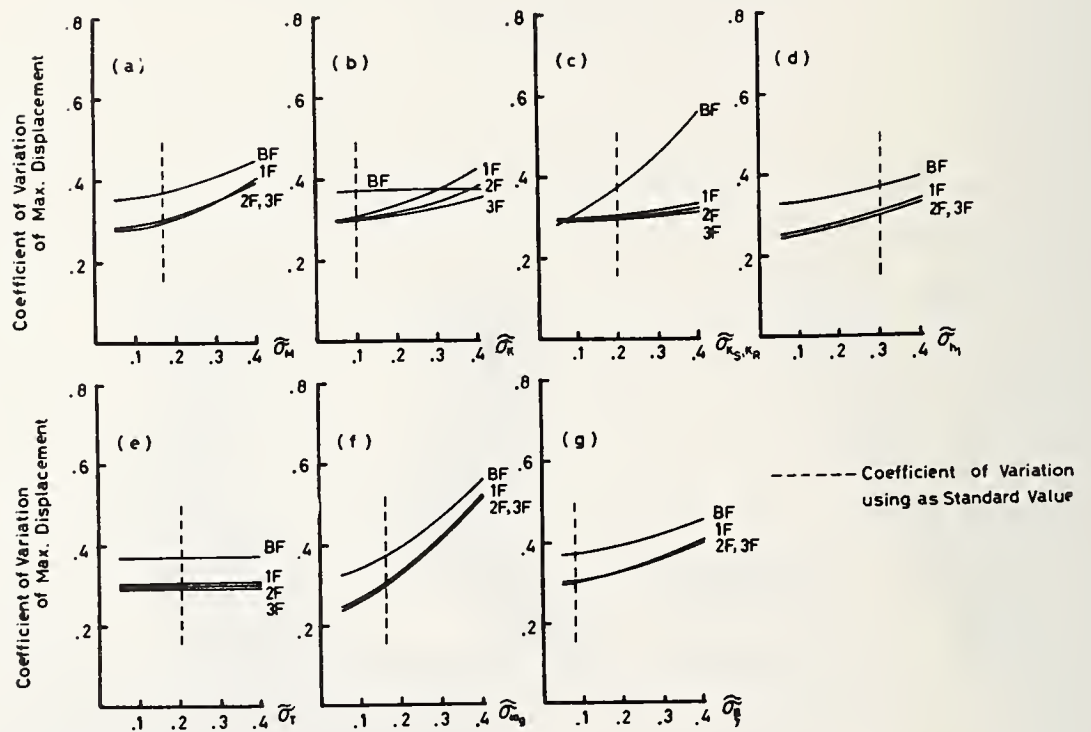


Fig.7 Relation between Coefficient of Variation of Maximum Displacement and of Variables on Input and System

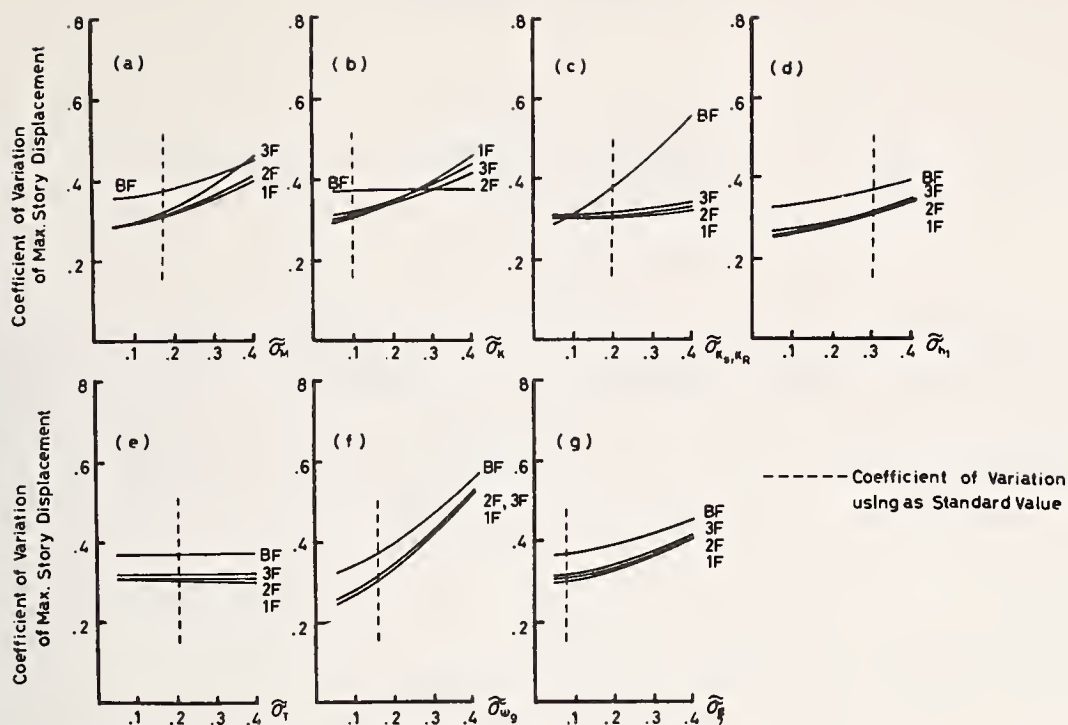


Fig.8 Relation between Coefficient of Variation of Maximum Story Displacement and of Variables on Input and System

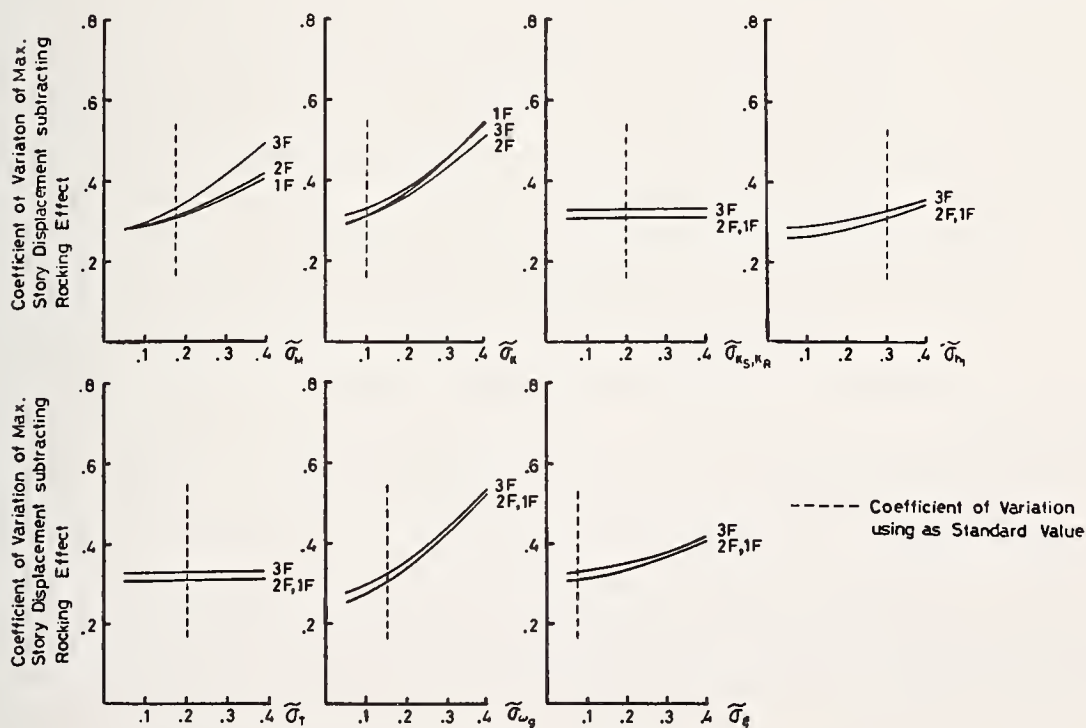


Fig.9 Relation between Coefficient of Variation of Maximum Story Displacement subtracting Rocking Effect and of Variables on Input and System

LEAST WEIGHT STRUCTURES FOR
THRESHOLD FREQUENCIES

by

R. D. McConnell
Graduate Student
Catholic University
Washington, D.C.

ABSTRACT

This paper demonstrates a method for designing least-weight, or optimized, structures when a threshold frequency (within appropriate force factors) is known. The process is highly amenable to a job-by-job application due to its simplicity. Small mathematical models of a structure can be analyzed by a hand-calculator while standard static-load finite element programs can be used for large structures.

Key Words: Least weight, optimization, structures, frequency response.

Introduction

Aerospace designers have long been designing component structures to a minimal-fundamental, or "threshold", frequency specification. In general, dynamic force levels imposed in such designs are determined by the principal inertial force excitations to which the structure under design will be subjected at frequencies known to be below the specified "threshold design frequency". Undoubtedly such concepts may have been used in various earthquake-related analyses and designs. More formalized procedures as specified by various codes, however, fall into two categories: a table of component forces (which often result in grossly conservative or grossly underdesigned structures); or sophisticated computer analyses using detailed models which undergo dynamic time-history force simulations. Such sophistication is well known to be expensive, time-consuming and somewhat arbitrary in earthquake analyses due to the approximations used as the forcing functions. Such large programs often have the hazards of inadequacies in the mathematical algorithms and error-conditioning problems with large models.

Although it may not appear as generally applicable for ground-supported structures, the design of substructures for earthquake induced forces could use such aerospace methods. By "substructures" here is meant any component structure for which the predominant frequency to which it may be subjected is known to a reasonable degree of accuracy. For example, radio towers, watertanks, electrical gear, etc. which are supported by larger structures will be subjected to the natural frequencies of the "base structure" regardless of the earthquake spectrum. (Technically, "larger" structure would imply considerably higher dynamic modal-mass) By knowing the approximate amplification factors for the principal contributing frequencies (and corresponding base-excitation levels) of the "base structure," a substructure specification for the 1) dynamic amplification factor, 2) arbitrary safety-factor and 3) threshold design frequency can be determined. (This has assumed consideration, where necessary, for an assumed mass-spring representing the substructure as part of the "base structure" model.) The arbitrary factor-of-safety would take into consideration the spread between the specified threshold design frequency and the fundamental (or major contributing) frequency of the "base structure", in addition to the assumed possible accrued errors in the particular analyses.

For these reasons, this paper demonstrates a method for designing least-weight, or optimized, structures when a threshold frequency (with appropriate force factors) is known. The process is highly amenable to a job-by-job application due to its simplicity. Small mathematical models of a structure can be analyzed by a hand-calculator while static-load finite-element programs can be used for larger structures. Design (member-selection) methods, whether by hand or by special program algorithms, becomes the same common set of procedures as would be introduced in any optimum-design methods.

Structural Optimization Methods

With the increasing availability and intricacy of finite-element matrix programs for structural analysis, there has been a growing interest in, and development of structural optimization procedures to augment those programs. They generally optimize by minimizing weight and/or cost or a similar objective function. Finite-element programs use matrix

representations, or idealizations, of real structures for the purpose of behavioral analyses under various loading conditions and constraints.

Most methods and applications involving optimization of dynamic properties and behavior of structures have, in general, incorporated the basic procedures of prior studies in optimization under static load conditions.

The goal in structural optimization is to minimize a prescribed merit function. This merit function could be weight, cost, fabrication criteria, or a combination of these (7). Active constraints on the minimization of the merit function (or "optimality criterion") would be the analysis equations for the set of design variables, such as stress solutions for the design of the members. Side-constraints would be limits on displacements, minimum member sizes, etc. These constraints must not be violated when optimizing the mathematical representation of the structure to a particular merit-function. In those cases where the geometry is to be optimized, volume or space constraints may be imposed.

Structural optimization methods can be divided into two general categories: mathematical programming involving search techniques, and optimality procedures. The principally identified methods in the first category are feasible-usable direction (16), gradient projection (17), optimum vector (8,9), linear programming (15) and allocation (13), all being defined as explicit minimization processes. Implicit minimization methods in the same general mathematical search category are steepest descents (18), adaptive gradients (19), variable metric (20) and conjugate gradients (21). These identities are indicative of the redesign search routine algorithm. "Implicit" methods use penalty functions (14) to transform a constrained minimization problem to an unconstrained one. Conceptually, these can also transform discrete values of the design variables into general unconstrained functions.

The optimality procedures include fully-stressed design (22, 23, 24, 25, 26, 27, 4), uniform strain-energy density (28, 29, 27), simultaneous buckling (30, 6), and limit design (10, 12, 3).

Most examples demonstrated in the mathematical search technique group have been small, simple models of structures, generally involving static loading conditions. These procedures are very time-consuming, may not monotonically converge and involve much programming effort (8, 9, 16).

Virtually all practical applications involving larger model representations of real structures have employed one of the optimality methods. Conceptually, the optimality methods require solution of first derivatives of the merit function, or a substitute function in which case the method is classified as a substitute optimality process. (For example, the use of fully-stressed convergence is substituted for minimum weight.) In the actual iterative procedures, derivatives are not calculated specifically, hence the redesign calculations are relatively few. In the mathematical search technique, however, second derivatives must be extracted or approximated at each iteration to determine sensitivity coefficients for redesign toward a minimum of the merit function.

The two substitute optimality methods which have been used with success are fully-stressed design and uniform strain-energy density design. These have been used for linear-elastic design structures. With the exception of such techniques as penalty functions (14) in the mathematical search procedures, in general, with the exception of specific side-constraints, must have equivalent linearized functional representation. Such linear representation of discrete values are generally approximate and cannot always be so expressed.

In the realm of optimization of structures, the penalty function, or unconstrained optimization, techniques have not been very efficient. Such penalty functions introduce near-singularities in the search process with consequent instabilities (7).

Most literature on applications and comparative reviews conclude that the more efficient and successful methods have been those of the optimality, or substitute optimality category.

It has long been known that simple structures optimized under a one-load condition will converge to a determinate structure in the absence of side-constraints which maintain minimum sizes for all members in the original structure (25). (One frequency constraint is considered the dynamic equivalent of a one load-condition.) That determinate structure will have member sizes determined only by the forces in the members. The allowable stress could be prescribed by strength, yield or buckling criteria, and may be different for each member.

The two methods used today for practical size problems under dynamic constraints or loading conditions are, as in the case of static loads, the substitute optimality approaches of fully-stressed design and uniform strain-energy density design. These two produce the same optimum structure when the structure is made of only one material.

In the case of resonant frequency optimization by fully-stressed methods, the allowable stress is uniform for all members in the structure. This is to say that if strength criteria do not preclude the adjusted stress-level, fully-stressed methods in the dynamic resonance case will reduce the stresses uniformly (thereby increasing sizes) to provide the stiffness sought. This step is often called "proportioning". Re-analysis is then necessary as the mode-shape, and consequently the effective force-distribution, changes. As noted earlier, side-constraints may be introduced to preserve strength in particular members.

The primary use of structural optimization procedures in dynamics problems has been to optimally adjust the fundamental frequency of the structure while assuring all additional strength requirements.

One reference (25), is of particular note here in that it is a representative practical application of optimizing a real structure to a fundamental frequency threshold level by the fully-stressed substitute optimality approach. The authors, Young and Christiansen, point out that they do not find an absolute, or global, optimum, but they do produce a "good, efficient structure."

Their procedure was essentially: 1) produce an original design; 2) analyze for resonant frequencies in the reduced models, mode shapes and corresponding modal forces in the detailed model; and 3) redesign (or proportioning). These three steps, basic design, analysis and redesign, are the fundamental steps common to all iterative optimization methods.

This paper describes a simple, stable method for adjustment of the entire frequency set to a minimum level. The structure adjusted by this efficient method will be simultaneously optimized to a least weight criterion without requiring the use of eigenvalue/eigenvector extraction routines, or algorithms to transpose mode shapes to forces. This procedure converges rapidly and requires only standard finite-element programs for static-load conditions.

Procedure

For those cases where the entire set of eigenvalues is shifted to provide a fundamental frequency above a prescribed minimum level, proportioning of the structure is possible. Methods for total adjustment with proportioning have been presented in the literature as described earlier. It is often possible, however, to obtain such results by a rapidly converging, stable process using finite-element programs written for static-load analyses. The economy so realized, as contrasted to the use of eigenvalue extraction routines, permits the use of larger, more detailed models in these instances. The element of instability of comparable methods in the literature is principally inherent in the algorithms used to transpose mode-shapes to relative forces in the structural elements (25, 4). Modal extraction and transposition are not explicitly required in the familiar Rayleigh energy method to obtain the fundamental frequency of a structure. Also, by using the more detailed model of a structure, rotary inertias generally become insignificant. Their exclusion in a Rayleigh approximation, consequently, does not seriously affect the results.

Static equivalent loads which can be factored by any arbitrary constant, are imposed by ratio and direction in accordance with the assumed (approximate) fundamental mode-shape. Resulting forces are then extracted by the routine stiffness matrix procedures for static loads. The force set is then linearly proportioned to achieve a fully-stressed state in that member which experiences the numerically largest force using the prevailing size of that member. All members are then simultaneously proportioned to the forces and scaled by the ratio of λ_F/λ_E where λ_F is the desired eigenvalue level and λ_E is the currently extracted approximation. The process is repeated using applied forces proportional to the latest mode-shape. The iteration is complete in the Rayleigh method when the λ_E extracted approximates λ_F desired.

This modified Rayleigh method is simultaneously converging to the true-mode shape of the fundamental mode while being proportioned accordingly.

In most cases, an approximate mode-shape is known. When this is not the case, it would be advisable to use a procedure such as the "inverse power method with shifts" to extract the fundamental frequency and its corresponding mode-shape for only the first step⁽¹¹⁾. Following adjustments, the routine Rayleigh method, as modified above, may then be used.

Convergence can be assured by checking the total structural weight upon each successive redesign step. If there is a divergence due to a poor estimated mode-shape, it is only necessary to carry the Rayleigh iteration to successive steps (without proportioning) until convergence is assured. The advantages of this method, in contrast to those in the literature, are 1. since only the fundamental frequency is of concern, the Rayleigh method is efficient and economical; and 2. the element forces are already known during each step to the process.

The following is a statement of the basic Rayleigh iterative steps.

$$\omega^2 = \frac{\sum_{r=1}^j F_{ri} \phi_r''}{A'' \sum_{r=1}^j M_r (\phi_r'')^2}$$

Where F_{ri} are the inertia forces corresponding to an assumed (or prior calculated) mode shape.

$A'' \phi_r''$ are the deflections due to F_{ri} where ϕ'' is the normalized vector; (5).

Example

A simple 3x3 matrix model is shown in Figure 1. The schematic spring model corresponding to the structural model is identical to one used in Reference (5). The first iteration cycle is identical. The subsequent steps toward weight/frequency optimization can be compared with the elementary method, in that reference, whereby only the extraction of the original fundamental frequency was required.

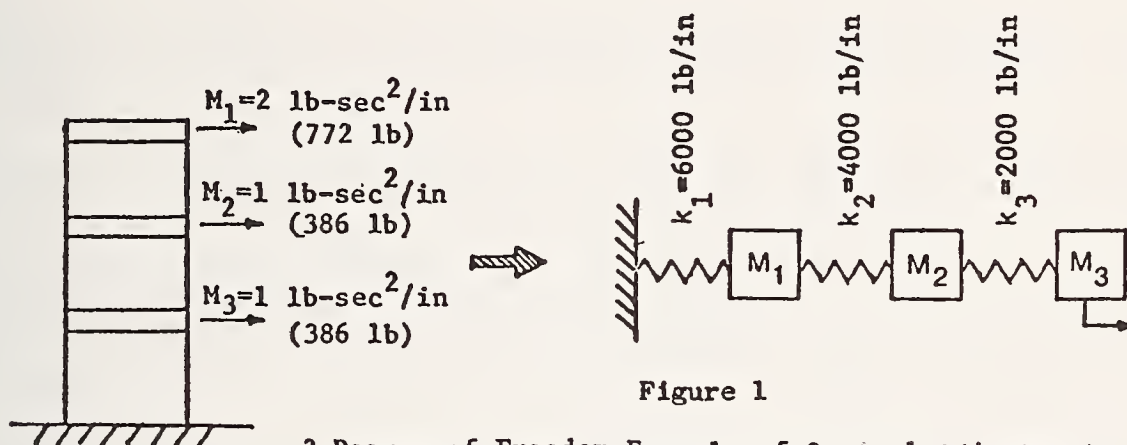


Figure 1
3 Degree-of-Freedom Example of Optimal Adjustment
of Fundamental Frequency by Rayleigh Method

Table 1 illustrates the steps in a simultaneous Rayleigh extraction of the fundamental frequency of this structure while proportioning members to optimize its weight. It concurrently shifts the fundamental frequency to a prescribed threshold level of $\omega = 30$ rad/sec.

The assumed mode shape is obtained by a lg. force on each mass. The first cycle produces a frequency of 28.2 rad/sec, and a mode shape of 1, 2.02 and 3.22. The spring stiffnesses (used in the Fig. 1 schematic to illustrate the method) are then adjusted to 6000, 4340, and 2670 lb/in to result in a uniform stress. This is obtained in this case by assuming the effective spring lengths equal and spring stiffnesses proportional to area. If a spring, therefore, has twice the area, it has twice the weight (for the same lengths) and will take twice the force at the same stress. The mode shape to which this model must converge can be recognized to be 1, 2, 3 for these conditions. That "computed mode shape" is achieved in

second cycle following proportioning of the springs. That cycle produced a frequency $\omega = 29.5$ (increased due to the basis of the spring proportioning).

The third cycle is exact, in this instance, as the assumed and computed mode-shapes are identical. The resulting frequency is 29.3. An adjustment by ω_2^2/ω_1^2 of the stiffnesses to produce 30. rad/sec results in the minimum total weight springs as shown.

Conclusion

In conclusion, the above example has demonstrated "fully-stressed" optimization concurrent with threshold-frequency adjustment by a procedure so simple as to permit the solution, in this instance, by the use of a hand calculator. The use of a model used earlier in texts (to demonstrate the Rayleigh method) was to permit comparison with this paper's augmented method. In addition, the particular model was thought to be of an "optimal" variation in member sizes (for first-mode stresses) at the beginning of the process. Further efficiency in weight was obtained.

The possible applications to earthquake design of sub-structures become most apparent upon reviewing the reasons for such requirements and applications in the design of aerospace structures.

References

1. McConnell, R. D.: Direct Optimization of Dynamic Response of Structures by Spectral Synthesis. Ph.D Thesis, Catholic University, 1974.
2. Gere, J. M.; Weaver, W.: Analysis of Framed Structures. Van Nostrand, Princeton, New Jersey, 1965.
3. Hodge, P.; Prager, W.: A Variational Principle for Plastic Materials with Strain Hardening. Jour. Math. Physics, Vol. XXVII, 1948, pp. 1-10.
4. Rubin, C. P.: Minimum Weight Design of Complex Structures Subject to A Frequency Constraint. AIAA Journal, Vol. 8, No. 5, 1970.
5. Biggs, J. M: Introduction to Structural Dynamics. McGraw-Hill Book Co., New York, 1964.
6. Shanley, F. R.: Weight-Strength Analysis of Aircraft Structures. McGraw-Hill Book Co., New York, 1952, pp. 1-260.
7. Melosh, R. J.: A Plan for Computer-Assisted Optimization of Structures. NAS 5-11779, NASA, G.S.F.C., Greenbelt, Md. 1970.
8. Gelatly, R. A.: Development of Procedures for Large-Scale Automated Minimum-Weight Structural Design. AFFDL-TR-66-180, Air Force Flight Dynamics Laboratory, Wright-Patterson AFB, Dec. 1966.
9. Gelatly, R. A.; Burno, J. A.: Development of Procedures for Large-Scale Automated Minimum-Weight Structural Design, Supplement 1, Programmer Documentation. AFFDL-TR-66-180, Supplement 1, Air Force Flight Dynamics Laboratory, Wright-Patterson AFB, Dec. 1966.
10. von Mises, R.: Mechanik der festen Korper im Plastish-deformablen Zustand. Nachr. Kgl. Ges. Wiss. Gottingen, Math-Physic Klasse, 1912, pp. 582-592.
11. McCormick, C. W., Editor: The NASTRAN User's Manual. NASA SP-221, National Aeronautics and Space Administration, Washington, D.C. Oct. 1969.
12. Nadai, A.: Plasticity, A Mechanics of Plastic State of Matter. McGraw-Hill Book Co., New York, 1931.
13. Melosh, R. J.; Luke, R.: Approximate Multiple Configurition Analysis and Allocation for Least Weight Structural Design. AFFDL-TR-67-59, Air Force Flight Dynamics Lab., Wright-Patterson AFB, 1967.
14. Fiacco, A. V.; McCormick, G. P.: Computational Algorithm for the Sequential Unconstrained Minimization Technique for Nonlinear Programming, Part II. Management Science, Vol. X, No. 4, pp. 601-617.
15. Pope, G. C.: Application on Linear Programming Techniques in the Design of Optimum Structures. AGARD Symposium on Structural Optimization, Istanbul, Oct. 1969.
16. Zoutendijk, G.: Method of Feasible Directions. Elsevier Publishing Co., Amsterdam, 1960.
17. Rosen, J. B.: The Gradient Projection Method for Nonlinear Programming. Jour. SIAM Appl. Math., Vol. IX, No. 4, Dec. 1961, pp. 514-532.
18. Cauchy, A. L.: Methode Generale pour la Resolution des Systems d'equations simultanee. Compes rendu de l'Academie des Sciences de Paris, Vol. XXV, pp. 536-538, 1947.
19. Rosenbrock. H. H.: An Automated Method for Finding the Greatest or Least Value of a Function. Computer Jour., Vol. III, 1950.

20. Fletcher, R.; Powell, M. J. S.: A Rapidly Convergent Descent Method for Minimization. Computer Jour., Vol VI, 1963, pp. 163-168.
21. Fletcher, R.; Reeves, C.M.: Function Minimization by Conjugate Gradients. Computer Jour., Vol. VII, 1964, pp. 149-154.
22. Maxwell, J. C.: Scientific Papers II. Cambridge University Press, 1890, pp. 175-177. (Reprinted by Dover Publications, New York, 1952.)
23. Michell, A. G. M.: The Limits of Economy of Material in Frame-Structures. Phil. Mag. (London), Ser. 6, Vol. VIII, No. 47, Nov. 1904, pp. 589-597.
24. Cilley, F. H.: The Exact Design of Statically Indeterminate Frameworks: An Exposition of its Possibility, but Futility. Trans. ASCE, Vol. XLIII, June 1900, pp. 353-407.
25. Young, J. W.; Christiansen, J. N.: Synthesis of a Space Truss Based on Dynamic Criteria. Jour. Struct. Div. ASCE, Vol. SCII, No. ST6, Dec. 1966, pp. 425-442.
26. Gellatly, R. A.; Gallagher, R. H.; and Luberacki, W. A.: Development of a Procedure for Automated Synthesis of Minimum Weight Structures. FDL-TR-64-141, Wright-Patterson AFB, Ohio, 1964.
27. Venkayya, V. B.; Khot, N. S.; and Reddy, V. S.: Energy Distribution in a Optimum Structural Design. AFFDL-TR-68-156, Wright-Patterson AFB, Ohio March 1969.
28. Prager, W.; Taylor, J. E.: Problems of Optimal Structural Design. Trans. Jour. Appl. Mech. ASME, Vol. XXXV, Series E, No. 3, Mar. 1968, pp. 102-106.
29. Taylor, J. E.: Maximum Strength Elastic Structural Design. Jour. Eng. Mech. Div. ASCE, EM3, June 1969, pp. 653,663.
30. Gerard, G.: Minimum Weight Analysis of Compressive Structures. New York University Press, New York, 1960.

Cycle	Mass Point	Assumed Shape ϕ'_r	$F_{r1} = \frac{M_r}{\phi'_r}$	Proportioned Stiffnesses (lbs./in.)	Computed Deflections $A'' \phi'_r$	Computed Shape ϕ''_r	$F_{r1} \phi''_r$	$M_r (\phi''_r)^2$
1	1	1.00	2.00	6000	0.001042	1.00	2.00	2.00
	2	1.75	1.75	4000	0.002104	2.02	3.54	4.08
	3	2.50	2.50	2000	0.003354	3.22	8.05	10.37
			$\omega^2 = \frac{13.59}{0.001042 \times 16.46} = 792$		$\omega = 28.2$		$\Sigma 13.59$	$\Sigma 16.46$
2	1	1.00	2.00	6000	0.001207	1.00	2.00	2.00
	2	2.02	2.02	4340	0.002414	2.00	4.04	4.00
	3	3.22	3.22	2670	0.003621	3.00	9.66	9.00
			$\omega^2 = \frac{15.70}{0.001207 \times 15.00} = 867$		$\omega = 29.45$		$\Sigma 15.70$	$\Sigma 15.00$
3	1	1.00	2.00	6000	0.001167	1.00	2.00	2.00
	2	2.00	2.00	4285	0.002334	2.00	4.00	4.00
	3	3.00	3.00	2571	0.003501	3.00	9.00	9.00
			$\omega^2 = \frac{15.00}{0.001167 \times 15.00} = 857$		$\omega = 29.27$			

$$\omega_1^2 / \omega_2^2 = 900/857 \quad \times \quad \begin{Bmatrix} 6000 \\ 4285 \\ 2571 \end{Bmatrix} = \begin{Bmatrix} 6301. \\ 4500. \\ 2700. \end{Bmatrix} = \Sigma 13501$$

Springs Optimized to $\omega = 30$.
vs. $900/791 \times 12000 = 13653$.

Table 1
Solution of Optimal Adjustment of Fundamental
Frequency by Rayleigh Method

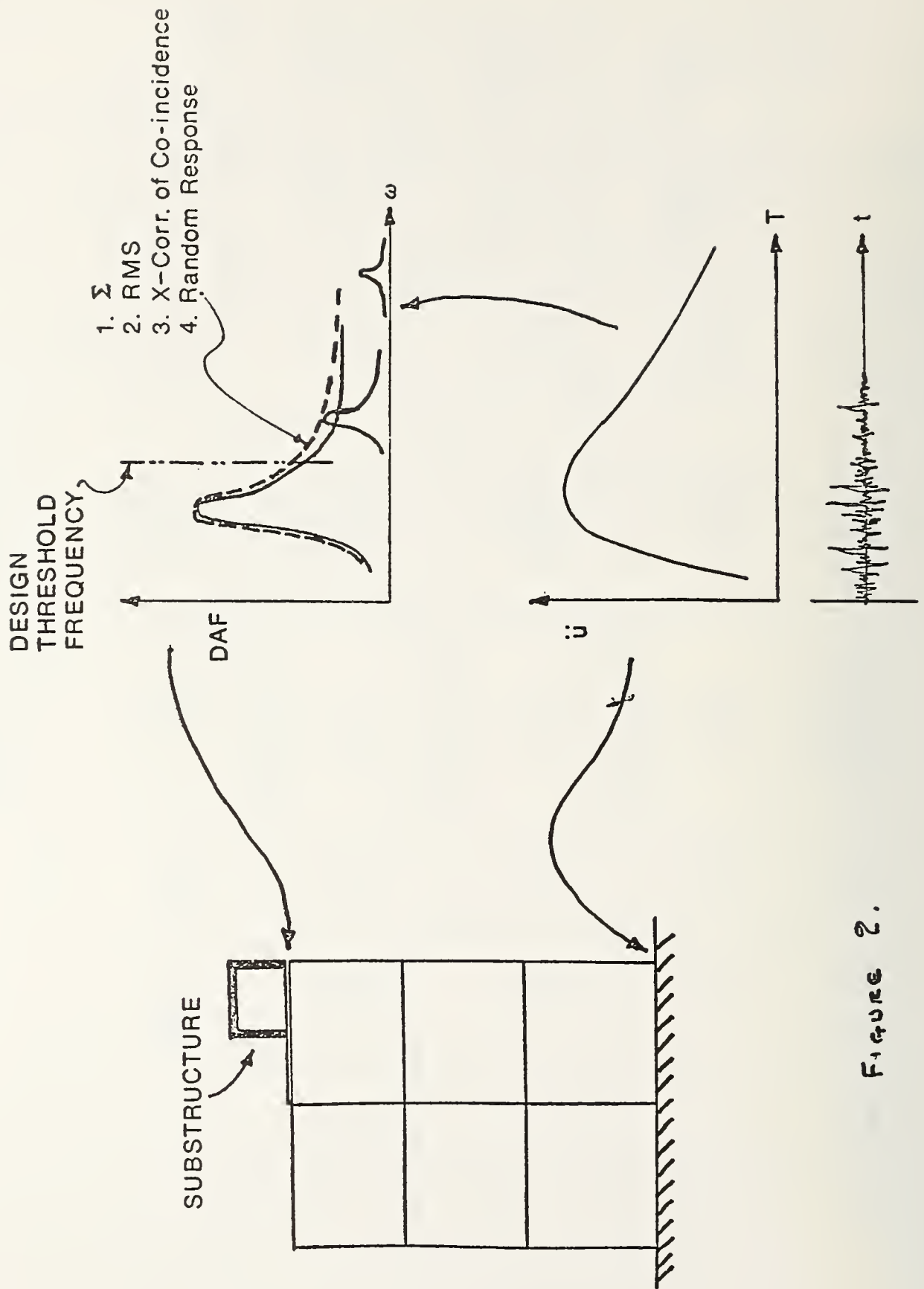


Figure 2.

DUCTILE SHEAR WALLS IN EARTHQUAKE-RESISTANT MULTISTORY BUILDINGS

by

Mark Fintel
Director, Engineering Services Department
Portland Cement Association
Skokie, Illinois 60076

ABSTRACT

Slender shear walls in multistory buildings are discussed in this paper and answers are given to such questions as "Why do we need them?" and "What do we know about their design?". Also discussed are the historical development of the use of shear walls, their performance in earthquakes of the past 10 years (both good and bad), and finally, the available design information and our future needs in the area of design of shear walls for strength, stiffness and ductility, as well as needs in the area of analysis for the dynamic response of shear wall structures.

Key Words: Buildings; Damage; Dynamic Response; Earthquakes; Safety; Shear Wall; Stiffness.

Slender shear walls can be defined as vertical cantilevers, with various cross sections such as: rectangular (a vertical plate), I, box, and other elevator walls. The shear walls support the vertical load, in addition to their function to stiffen the frames in their resistance to lateral loads due to winds, earthquake or blast. Although interior and exterior concrete walls have been used to stiffen structures as long as reinforced concrete itself has been in use, the modern concept of shear walls designed as vertical slender cantilevers were first utilized in 1948 in housing projects in New York City and in Chicago in buildings designed for wind forces, to augment the lateral resistance of the frames.

In nonearthquake areas of the United States and Canada concrete buildings with more than 15 to 20 stories are usually designed with shear walls, primarily to improve their stiffness. Economically, the inclusion of shear walls seems to be the least expensive way to increase the overall rigidity of concrete buildings, since they serve the triple function: to support gravity loads, to provide lateral resistance, and to function as a wall.

Analysis for lateral loads of buildings containing shear walls was carried out initially, in the 1950s, by assigning all the lateral loads to the shear walls, since it was felt that the very big difference in stiffness between the shear walls and the frame would cause the shear walls to accept the total lateral loads. This inaccurate assumption may have been conservative for the computation of shear wall moments; it is, however, not conservative for the frame, and particularly in the upper parts of the building.

Formal procedures for shear wall-frame interaction were first introduced in the early sixties. Fig. 1 shows the concept of the interaction, with the resulting internal forces, which substantially increase the overall stiffness of the combined system.

Most of the recent prominent ultra-high-rise reinforced concrete buildings were built without any additional cost for the lateral resistance, which was mostly accommodated within the 33 percent increase in the allowable stresses when lateral loads are considered. The high lateral rigidity was achieved as a result of the shear wall-frame interaction.

Performance in Earthquakes

To judge the merits of shear walls for earthquake resistance, an examination of their performance in earthquakes should be made, and particularly the comparative behavior of frame buildings and buildings containing shear walls during the earthquakes of the last 10 years, starting with the earthquake of Managua, and going back in chronological order to the other earthquakes.

Managua Earthquake, 1972

The earthquake of Managua of Dec. 23, 1972 seems to be the most significant of the recent earthquakes,¹ since side by side were two buildings (Fig. 2) representing the two different structural systems. The building on the left is the 15-story Banco Central which is principally a frame building, while the building on the right is the Banco De America, an 18-story shear wallframe interactive system.

The Banco Central was designed in the early 1960s; the structural system of the tower (Fig. 3) is a one-bay frame with two small reinforced concrete cores and an infilled wall at the end of the building. These stiff elements may have done the structure more harm than

good by introducing torsion due to their off-center location.

The building was subjected to violent shaking, as could be observed from the damage of the nonstructural elements, both inside and outside (Fig. 4). Except for the 4th floor steel roof over the auditorium which fell off its support, the only structural damage observed in the building was some ripping between the off-center core and the slab. The structural frame of the tower itself showed little distress. There was evidence of yielding at some junctions between the columns and the beams; however, the structure had enough ductility (whether designed for it or not) to sustain the large distortions. Inside, however, the building was in shambles over most of the stories, due to the extremely violent shaking experienced by the building.

In contrast, the building across the corner, the 18-story Banco De America, (Fig. 2) exhibited an entirely different performance, both inside and outside. The plan of the building contains four centrally located cores, arranged symmetrically within the peripheral column system as shown in Fig. 5. The cores are interconnected by two rows of stocky beams, many of which are penetrated by ducts. A general comment: the number of shear walls in this building is substantially higher than is usually provided in wind-resisting buildings of comparable height and plan size.

The interconnecting beams between the cores suffered repairable shear damage through most of the height of the building. Observing the large amount of flexural reinforcement in the beams, it should be recognized that it is almost impossible to provide enough shear capacity (whether the beams are penetrated by ducts or not) to be able to develop flexural hinging at the ends of the beams.

There was very little evidence throughout the height of the building of any violent shaking. All the furniture was in place, and there was no discernible nonstructural damage.

A comparison of the above two buildings shows that both were well designed and well constructed, within several years of each other. Both buildings were designed according to the United States west coast standards in force at the time of their design. Although both buildings were subjected to the same earthquake motion, one had very severe architectural damage; the other could be reoccupied immediately while the repairs proceeded. There was only one difference between the two buildings - a healthy system of shear walls which restricted the interstory distortions, thus providing damage control.

Figs. 6 and 7 show another pair of comparative buildings from the Managua earthquake. Both of these 5-story buildings were located in areas of high damage. The 5-story Insurance Building (Fig. 6) outwardly appeared so badly damaged that people did not trust themselves to enter it for several days. Later inspection showed that, although the exterior masonry walls and the interior partitions were badly damaged, there was little structural damage to the building's moment-resistant frame.

In contrast, the 5-story Enaluf Building (Fig. 7) which has a relatively large reinforced concrete core in addition to the frame, went through the earthquake exceptionally well. The only structural distress was slight horizontal cracking in several of the exterior first story columns, and a shear wall on the ground floor had some damage adjacent to a duct

penetration. Otherwise, neither structural nor serious nonstructural distress appeared in the building.

Performance of Other Modern Frame Buildings in Managua

There were also a number of other well-designed moment-resisting frame buildings in the 6-8 story range. They were all subjected to intense shaking and large distortions as evidenced by the severe damage to their nonstructural components and finishes. All of them exhibited sufficient ductility, since there was almost no structural distress. They all performed according to the present code philosophy - little or no structural distress, however, quite a bit of nonstructural damage.

The 8-story Supreme Justice Building had minimal structural distress, but the inside was in shambles.

The 8-story Social Security Building (Fig. 8) outwardly showed no distress except for the collapsed roof over the elevator machine room, and little structural distress on the inside. However, the nonstructural damage was considerable and the staircases were full of partition debris and could not have been used to evacuate people had the earthquake occurred during the daytime.

The 8-story Telecommunications Building had post-tensioned beams on the column lines spanning across the entire building. There was an off-center core at the far end of the building was in evidence; however, the post-tensioned beams of the tower showed (with one exception) no substantial structural damage.

Summarizing the behavior of this group of frame buildings, it is evident that the buildings had enough ductility, whether intentionally designed for it or not, to sustain the large distortions to which they were subjected during the earthquake. The high degree of economic damage these buildings suffered was apparently not so much from the ground shaking as from an inadequate design philosophy - a philosophy in which we design the structure for large distortions, but we do not detail the rest of the building (which in many cases comprises up to 80 percent of the value) to accommodate the large distortions without damage.

Of particular interest was the performance of the National Theatre, built several years ago in the style of the Lincoln Center in New York. The structure contains a U-shaped reinforced concrete shear wall around the auditorium within another U-shaped shear wall of columns and beams infilled with 18-in. thick solid masonry around the lobby and stage. Except for a few marble statues which were thrown off their pedestals, there was no evidence that the building had just gone through an earthquake. Neither structural nor nonstructural damage could be found.

San Fernando Earthquake, 1971

The Indian Hill Medical Center is an example of an acceptable earthquake performance of a shear wall-frame type building. The building was restored and put back into operation within a short period after the earthquake. The structure of the Indian Hill Medical Center consists of beam column frames supplemented by shear walls. The shear walls exhibited some diagonal cracking and other local distress; they were repaired by increasing their thickness.

On the compound of the Veteran's Administration Hospital, where some buildings of 1920 vintage collapsed, several auxiliary buildings built as reinforced concrete boxes went

through the earthquake without structural damage; even the chimney of the central boiler plant had only some sliding at a cold joint. Unfortunately, these cases of excellent behavior somehow escaped the attention of the profession, which was busy examining the collapses.

Caracas, Venezuela Earthquake, 1967

Fig. 9 shows a multistory building with a very flexible skeleton of the type prevalent in Caracas.² There were no shear walls used in the Caracas buildings. The skeletons were filled with brittle and weak hollow clay tile infill walls. During the earthquake the buildings were subjected to large distortions and the weak partitions exploded, as shown in Fig. 10. It is obvious that such damage should have been expected from buildings with flexible skeletons undergoing large distortions and filled with brittle partitions.

The 17-story Plaza One Building was the only complete shear wall building in Caracas. It was located within an area of extremely high damage. As seen in Fig. 11, one of its neighbors, a 10-story building, collapsed while the other surrounding structures suffered severe damage. The Plaza One Building went through the earthquake without any damage whatsoever. The building has shear walls in both directions.

Skopje, Yugoslavia Earthquake, 1963

Many of the residential buildings in Skopje up to 10 stories high had two shear walls, all across the width, flanking the central stairway. The shear walls were usually non-reinforced of poor quality concrete. Nevertheless, the rigidity of the shear walls did not permit interstory distortions, and consequently, there was no damage. In some instances slip of the cold joints between successive story lifts was observed.

Fig. 12 shows the 14-story Party Headquarters, which was the only building in Skopje with a structure similar to our shear wall-frame systems. Being the party headquarters, it was designed more carefully and constructed with greater attention to quality. Three non-reinforced shear walls in the center were of good quality concrete. Although it is known that the building underwent severe shaking during the earthquake (according to witnesses who were thrown from one end of the room to the other), there was neither structural nor nonstructural damage in the building, with the exception of the elevators which did not function after the earthquake.

Misbehavior of Shear Walls

The preceding description of performance in past earthquakes showed many examples of good behavior of buildings containing shear walls. On the opposite side of the spectrum there are two distinct categories of misbehavior of shear wall buildings during earthquakes: (a) interrupted shear walls, and (b) brittle linkage between coupled shear walls.

The Olive View Hospital (San Fernando) shown in Fig. 13 is an example of interrupted shear walls. The upper four stories contained shear walls; however, they were undesirable in the ground floor due to the architectural layout, and were, therefore, omitted. The building distorted during the earthquake by more than 2 feet within the ground story. In retrospect, it seems that in this building the ductility available in the upper stories was of little benefit because the presence of shear walls did not allow any distortions; while the extremely high amount of ductility available in the columns of the ground story

did not really do very much good in keeping the building intact, except possibly preventing total collapse of the ground story.

Discussion

If we look back and review what we have learned from the previous earthquakes, I believe that we were extremely eager during the last decade to verify the viability of the concept of the ductile moment-resistant frame. Consequently, after each of the past earthquakes, we have introduced some improvement to the ductile moment-resistant frame, i.e., after Caracas we increased substantially the overturning moment; after other earthquakes, other details were modified. However, I believe that we have not thoroughly examined the basic concept of our earthquake design philosophy as related to reinforced concrete. For, I believe if we were to make a thorough examination, we would probably find that the ductile moment-resisting frame without shear walls is a relatively poor structural system for residential and office buildings which contain a lot of nonstructural elements that are not designed and detailed to accommodate the large earthquake distortions of the moment-resistant frame.

A brief look at the history shows that the ductile moment-resistant frame evolved in the 1950s out of the moment-resistant frame which, at that time, was the only system for multi-story buildings for both steel and concrete. By adding ductility to the then available system, we created a convenient solution to the problem of earthquake resistance. However, in the meantime, better and more efficient structural systems for multistory structures (both in steel and concrete) were developed for wind resistance. Actually, the last moment-resistant frame utilized in the east for a very tall building was the 60-story steel framed Chase Manhattan Bank in New York, built in the early 1960s. At that time, this 60-story building utilized about 45 lb of steel per square foot of floor area (220 kg/m^2). Today, 60-story buildings are built with about 20 lb of steel per square foot (98 kg/m^2), while buildings in the 100-story range are built with slightly over 30 lb of structural steel per square foot of floor area (146 kg/m^2).

The emphasis on ductility as the key to survival of moment-resisting open frames led to the adoption of concrete structures reflecting characteristics more common to steel buildings, rather than taking advantage of the strength, stiffness, and ductility inherent in the natural forms to which concrete lends itself, such as shear walls. Recent experience has demonstrated that the twin requirements of safety and damage control can be better met by structures possessing adequate stiffness, such as shear walls can most economically provide, when coupled with sufficient ductility or energy-absorption capacity. This is especially desirable for apartment and office buildings, where considerable nonstructural damage can result from excessive interstory displacements during an earthquake. When sufficient lateral stiffness is built into a structure by the introduction of ductile shear walls, so that large lateral displacements are prevented, it is doubtful if the connected frame in a frame-shear wall building will ever undergo the distortions which would call for the ductility which we now design into them.

It seems that for uses like parking garages, stadiums, bridges, and the like, the ductile moment-resistant frame without shear walls is an excellent earthquake resistant

system. However, for apartment and office buildings in which 80 percent of the value is nonstructural, we should have more damage control than the ductile moment-resistant frame can provide.

Shear Walls As Elements

Shear walls can be classified as (a) short shear walls (h/d , less than about $1/2$), and (b) slender shear walls (h/d , more than 2). Short shear walls are mostly governed by their shear strength, while slender shear walls are cantilever beams controlled by flexure. If special details are utilized in slender walls, they can be detailed to have sufficient ductility.

Another possible classification of shear walls is according to the geometry of the section: rectangular sections, and I-sections representing both I and box sections as used in cores. An important difference between plain rectangular sections and flanged sections is the degree to which shear (i.e., diagonal tension) contributes to the total distortion.

The current state-of-the-art shear wall design consists of individual developments on a number of aspects-only bits and pieces-with a rational approach slowly emerging.

Testing of Shear Walls

Tests of infilled one- and two-story concrete frames were conducted in the fifties. After a period of nearly 20 years, testing of shear walls was initiated several years ago, and some of the new studies have already been reported in the technical journals. There have been a number of experimental investigations of short shear walls to determine their shear strength at the PCA laboratories with both monotonic and cyclic loading.^{3,4,5} Results of some of these studies have formed the background for the shear provisions for shear walls in the 1971 ACI Code.⁶ Also, a test series of long shear walls with monotonic loading has been carried out at PCA.⁷ Investigations on coupled shear walls were carried out very successfully in New Zealand.⁸ A series of dynamic tests on shear wall assemblies on the shaking table has been initiated and is underway at the University of Illinois. In addition, several universities are preparing test series on various aspects of slender shear walls.

Analytical Investigation of Shear Wall Sections

A series of analytical studies to investigate the strength, stiffness, and ductility of shear wall sections was carried out recently at the PCA.⁹ The mathematical model used for the development of the interaction diagrams of shear wall sections is based on the non-linear beam theory. The mathematical model for the "computer test series" has the obvious shortcoming of simulating only monotonic loading, since no model of possible effects on concrete due to cyclic loading has yet been developed.

Despite this shortcoming, this series of computer studies gives us a better understanding of the influence of the variables affecting strength, stiffness, and ductility of shear walls. In addition, the mathematical model has the capability to consider confinement in any part of the section.

The nonlinear beam theory assumes the strains to vary linearly across the section, while the stresses in both the concrete and the reinforcement vary non-linearly according to their actual stress-strain relationships, as shown in Fig. 14.

Two principal sections were investigated: a rectangular section with uniformly distributed reinforcement and reinforcement bunched at the ends; and an I-section with concentrations of reinforcement in the flanges. The latter section represents box or I-sections as used in elevator cores.

Since we are interested in the properties at maximum capacity, rather than at the code "ultimate" (which is at the first yielding) it is important to model the properties of the materials, particularly after yielding, as accurately as possible. For the steel reinforcement there is good stress-strain information available; for the stress-strain characteristic of concrete a complex equation was developed based on all tests reported in the literature. The complexity of the expression is not objectionable, since it is intended for computer application; accurate presentation of both the ascending and descending branches of the stress-strain curve was the most important consideration.

The load-moment interaction diagram shown in Fig. 15 is the envelope of maximum capacity, at whatever strain this may occur, rather than for the customary concrete strain of 0.003. It is found that the strain of the concrete at which maximum capacity occurs increases as the eccentricity increases, from about 0.002 for the compression controlled branch of the interaction diagram to three to four times as much for the tension controlled branch (zero axial load). The reason for this increase: as the steel stretches in yielding, the concrete strain increases progressing along the descending branch; the strain hardening of the steel causes an increase of the strength of the section. Computation of design strength based on concrete strain of 0.003 for all eccentricities is conservative. The deformation capacity of the section from the onset of yielding of reinforcement until its final rupture, or until the compression failure of the concrete, is the section ductility.

Also, the available section ductility was investigated as related to the axial load level. The plot in Fig. 16 of sectional ductility against axial loads shows that the I-section with confined flanges has a substantial ductility even at balanced load level. Obviously, all these analytical findings will have to be confirmed by laboratory tests.

Needed Studies

Further work is needed in both the analytical and experimental areas to supplement the present knowledge for a complete procedure for earthquake resistant shear wall type buildings. Extensive shear tests have been carried out for monotonic and cyclic loading on short shear walls. Experimental testing for cyclic reversed loading is needed to further investigate the effect of the many variables and to perfect the reinforcing details to assure an optimum strength, stiffness, and ductility of slender shear walls. Important variables to be considered are the arrangement of reinforcement, details for confinement, details for splices, effects of strength of concrete, influence of floor level construction joints, and others. Also, the extent of the yielding region needs to be investigated experimentally. The studies should encompass rectangular, dumbbell, I-sections, and walls with openings. Experimental studies would provide moment-rotation and shear-deflection

characteristics needed to develop a mathematical model to be used for dynamic response studies of structures containing shear walls. Also dynamic experimental studies on the shaking table are desirable to ascertain the reproducibility of the general response characteristics using mathematical models.

In the area of analytical dynamic response studies, work is needed on shear wall and shear wall-frame type structures to determine the ductility demands on shear walls. Also, the required stiffness of the structure to respond to various categories of earthquake ground motions should be investigated to determine the eventual number of shear walls needed in a building to control its earthquake response.

Conclusion

In conclusion, it should be pointed out that until now safety against collapse has been the major preoccupation of earthquake engineering. However, we now should enter a second stage of our development in which, in addition to safety, damage control should be our major goal. Judging from the behavior of multistory reinforced concrete buildings in earthquakes, it seems that to achieve damage control the ductile shear wall may be the most logical solution. Actually, from observations in earthquakes, it seems that we can no longer afford to build our multistory buildings without shear walls.

References

1. Fintel, Mark, "Quake Lesson from Managua: Revise Concrete Building Design?", Civil Engineering - ASCE, V. 43, No. 8, Aug. 1973, pp. 60-63.
2. "Preliminary Report - The Behavior of Reinforced Concrete Structures in the Caracas, Venezuela Earthquake of July 29, 1967", Portland Cement Association, Skokie, 1967, 51 pp.
3. Corley, W. Gene, and Hanson, John M., "Design of Earthquake-Resistant Structural Walls", Proceedings, Fifth World Conference on Earthquake Engineering (Rome, 1973).
4. Brada, F., "Shear Strength of Low-Rise Walls with Boundary Elements", PhD Thesis, Lehigh University, Bethlehem, Pa., 1972.
5. Barda, F., Hanson, John M., and Corley, W. Gene, "An Investigation of the Design and Repair of Low-Rise Shear Walls", Proceedings, Fifth World Conference on Earthquake Engineering (Rome, 1973)
6. Cardenas, A.ex, Hanson John M., Corley, W. Gene, and Hognestad, Eivind, "Design Provisions for Shear Walls", ACI Journal Proceedings, V. 70 No. 3, Mar. 1973 pp. 221-230.
7. Cardenas, Alex E., and Magura, Donald D., "Strength of High-Rise Shear Walls-Rectangular Cross Sections", Response of Multistory Concrete Structures to Lateral Forces, SP-36, American Concrete Institute, Detroit, 1973, pp. 119-131.
8. Pauley, T., "Some Seismic Aspects of Coupled Shear Walls", Proceedings, Fifth World Conference on Earthquake Engineering (Rome, 1973).
9. Slase, E. A. B., and Fintel, Mark, "Strength, Stiffness and Ductility Properties of Slender Shear Walls", Proceedings, Fifth World Conference on Earthquake Engineering (Rome, 1973).

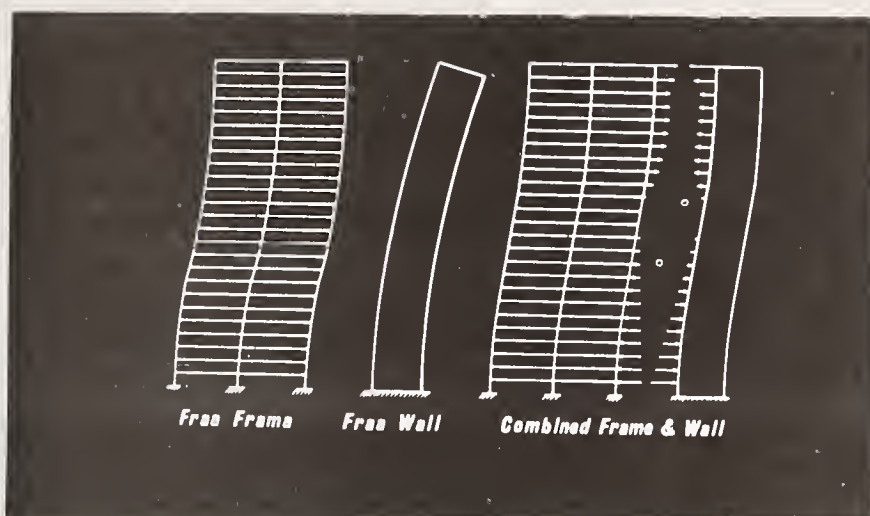


Fig. 1—Shear wall-frame interaction



Fig. 2—Two recent Bank Buildings in Managua, representing different structural systems. On the left, Banco Central and on the right, Banco de America.

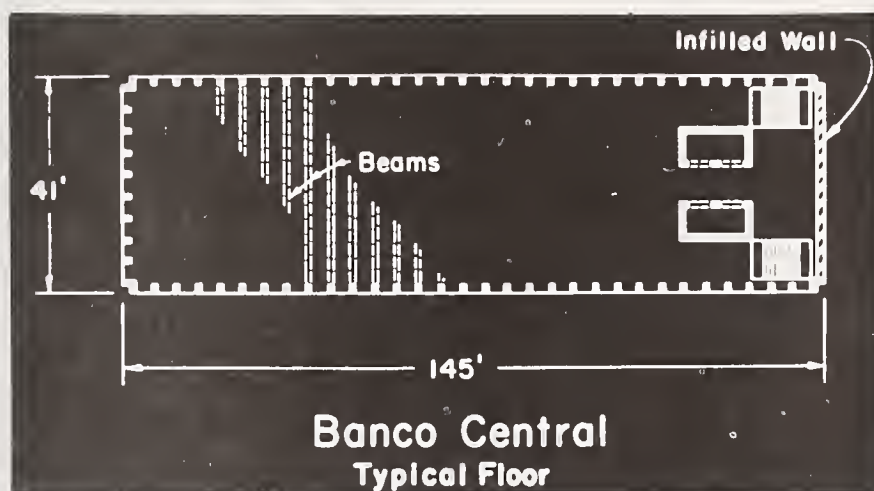


Fig. 3—Banco Central—Plan



Fig. 4—Banco Central—Inside damage

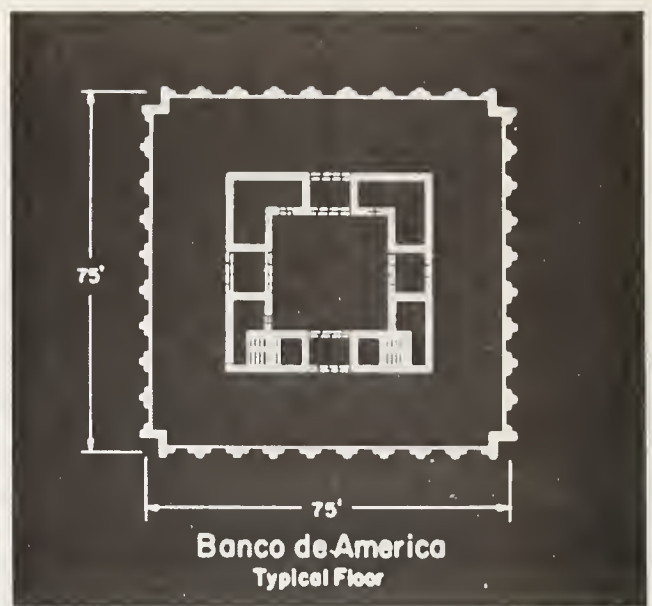


Fig. 5—Banco de America—Plan

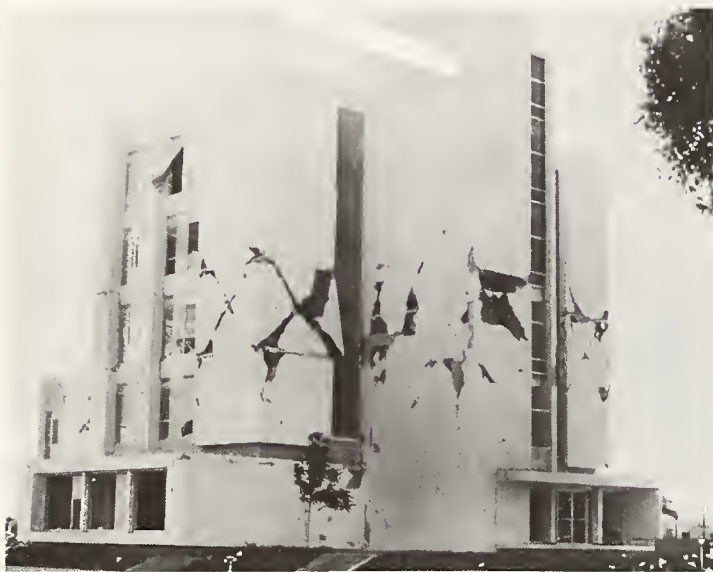


Fig. 6—Insurance Building—Managua



Fig. 7—Enaluf Building—Managua



Fig. 8—Social Security Building—Managua



Fig. 9—Typical skeleton of a multi-story building in Caracas, Venezuela



Fig. 10—Damage to brittle hollow clay tile infill in Caracas, 1967



Fig. 11—The Plaza One Building—Caracas



Fig. 12—Party Headquarters, Skopje, Yugoslavia



Fig. 13—Olive View Hospital—San Fernando

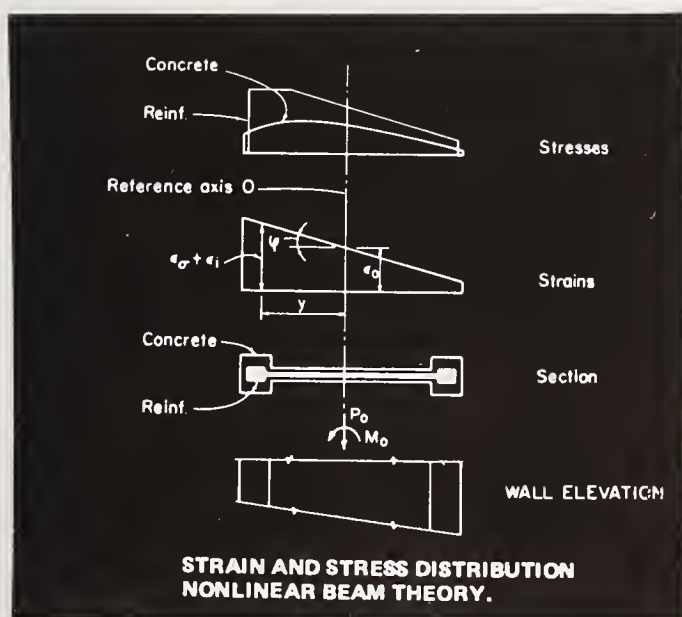


Fig. 14—Nonlinear beam theory assumptions

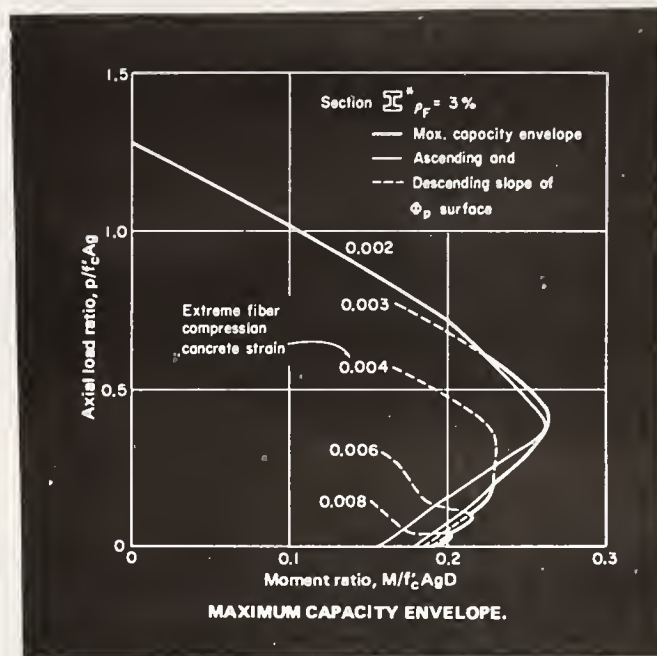


Fig. 15—Load-moment interaction envelope

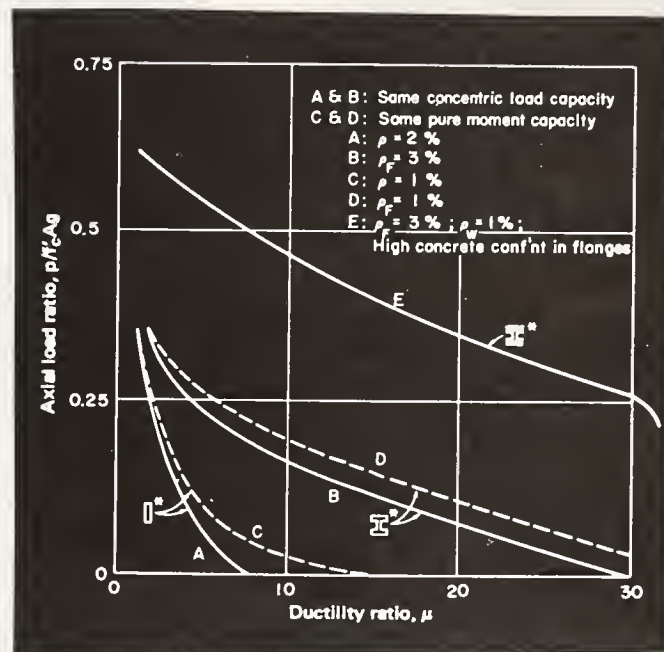


Fig. 16—Ductility versus axial load

SURVEILLANCE OF CORPS OF ENGINEERS STRUCTURES
IN EARTHQUAKE-PRONE AREAS

by

Keith O. O'Donnell
Office, Chief of Engineers
Washington, D.C.

ABSTRACT

This paper explains the program which the Corps of Engineers has adopted to assess the effects of earthquake activity concerning the structural behavior of Civil Works hydraulic structures. The program encompasses reporting earthquake effects and an instrumentation system on dams and appurtenant structures for monitoring. Post-earthquake inspections will be conducted to detect significant structural distress and provide information for the necessary remedial measures for damaged structures. The strong motion instrumentation will provide a record of ground and structure motion during earthquakes. Data provided from this program should be an aid in selecting design earthquakes and may provide preliminary guidance in design procedures for use in predicting, from small earthquakes, the behavior structures subjected to larger design earthquakes. The accumulated information from the entire program should help in improving the design criteria for future designs.

Key Words: Earthquakes, Hydraulic Structures; Inspection; Instrumentation; Strong-motion Accelerographs.

Reporting Earthquake Effects

General

In 1969 the Corps of Engineers established a program for assuring the structural integrity and operational adequacy of major Civil Works structures following the occurrence of significant earthquakes. This program is primarily concerned with damage surveys following the occurrences of earthquakes greater than Richter Magnitude 5. The evaluation of structures following an earthquake is of paramount concern to insure structural stability, safety and operational adequacy for structures whose failure or partial failure would endanger lives or cause substantial property damage. Structures included in the program are dams, navigation locks, powerhouses and appurtenant structures which are operated by the Corps of Engineers. Other facilities such as major levees, flood walls and pumping stations which are designed and constructed by the Corps of Engineers are included although their maintenance and operation are by other agencies.

Guidelines for Post-Earthquake Inspections

Earthquakes may cause hidden or obvious damage to all types of structures. It is intended that prompt post-earthquake field inspecting and reporting will aid in determining the appropriate remedial measures for structures that have been damaged. All important Civil Works structures within a prescribed area that has been subjected to an earthquake of sufficient magnitude to produce a Modified Mercalli Intensity of 5 (MM5) or greater will be inspected for damage. This prescribed area is defined as the area enclosed by the Intensity 5 Contour or "isoseismal." Information to identify the prescribed area usually can be obtained from the Coast and Geodetic Survey or U.S. Geological Survey. However, since the qualitative or quantitative ground motion data are usually not immediately available, the prescribed area for post-earthquake inspection will be determined by magnitude scale. For a Richter Magnitude less than 5.0, no inspection is required unless specific reports of possible damage are received from project offices. For a Richter Magnitude 5.0 through 7.0, inspection of projects within 200 miles of the epicenter is required and for a magnitude exceeding 7.0 inspection is required within 500 miles of the epicenter.

There are many types of structural damage induced by ground motion from earthquakes that need to be reported. Any change in appearance or functional capability of a major Civil Works structures should be evaluated. Examples would include cracked or shifted bridge pier footings or other concrete structures; turbidity or changed static level of water wells; cracks in concrete dams or earth embankments; misalignment of hydraulic control structures or gates; loss of freeboard by settlement; development of a localized quick condition within an embankment section or new seepage paths through an embankment or foundation.

Inspection and Evaluation

Generally, the structures that would be of most concern following an earthquake are also the structures which are covered under the periodic inspection program which the Corps of Engineers adopted in 1965 for major Civil Works structures. Where feasible, the instrumentation and prototype testing program included in the periodic inspection program to monitor structural performance will serve in the post-earthquake safety evaluation program. Addi-

tional special types of instrumentation are incorporated in selected structures in which it is desirable to measure forces, pressures, loads, stresses, strains, displacements, deflections or other conditions concerning damage and structural safety in case of an earthquake.

A report will be prepared of the post-earthquake inspection of each selected structure which will include summaries of instrumentation and other observation data, for permanent record and reference purposes. The U.S. Army Waterways Experiment Station at Vicksburg, Mississippi is assigned the responsibility for analyzing and interpreting the earthquake data obtained from the strong motion instrumentation.

Earthquake Aftershock Measurements

A field team has been formed at the Waterways Experiment Station which is capable of being mobilized immediately upon notification of the occurrence of an earthquake that might be expected to produce significant ground motion from aftershocks at any project operated by the Corps of Engineers. The objective of the field team is to provide a capability for rapid response to earthquake occurrences in recording response of installation, such as dams, to earthquake aftershocks. Instrumentation will be utilized to supplement existing instruments which may have been installed as a part of the Corps of Engineers strong-motion instrumentation program. The measurements obtained will provide approximate input for analysis of the response of the structures under loading by more severe earthquakes. Additionally, they will provide input for the analysis of other similar structures, and by comparison of observed and calculated response of the structures, allow evaluation of existing analytical procedures and aid in developing improved methods for seismic design.

The instruments presently available for this purpose include four Teledyne model RFT-250 accelerographs, which have response ranges from 0.25g to 1.0g, and four Kinemetric SMA-1 strong-motion accelerographs with 1.0g maximum range, incorporating WWVB time base radio receivers. These instruments record accelerations on 3-orthogonal axes, and the standard time base will permit correlation of events that are recorded on the various instruments. This equipment is maintained on standby so that it is available on a 24 hour basis. The equipment is packaged so that it may accompany the field team aboard commercial aircraft.

Seismic Instrumentation Program

General

The Corps of Engineers has adopted a policy providing seismic instrumentation for Civil Works structures in regions of significant seismic activity to measure ground motion and response of the structure. Each installation is planned to suit the particular structure, geologic and seismic conditions. The seismic instrumentation includes strong-motion recording accelerographs, peak recording accelerographs, seismoscopes, and hydrodynamic pressure gages. The types of strong-motion accelerographs used by the Corps of Engineers are shown on Figures 1 and 2. Figure 3 shows the peak recording accelerograph and Figure 4 the seismoscope. The seismic zone map of the United States for the contiguous states is shown in Figure 5.

Seismic Instrumentation for Concrete Dams and Intake Towers

The normal installation for concrete dams 150 feet or over in height in all seismic risk Zones 4 or 3 and those in Zones 2 in the western part of the United States consists of a

minimum of three strong-motion accelerographs. One accelerograph is located on top of the higher dam monoliths, one in the upstream gallery near the base of the same monolith and one in the bedrock foundation at a distance downstream of the toe of about three times the dam height. For the larger dams (300 feet and over), or where foundation conditions warrant, a fourth accelerograph should be located about mid-height of the principal instrumented monolith. For dams 150 feet or more in height in Zones 2, other than in the western part of the United States, at least one strong-motion accelerograph is located on the bedrock structure near the dam to record ground motion. Intake gate towers 150 feet or more in height located in Zones 4 or 3 and in Zone 2 in the western part of the United States are usually instrumented with one accelerograph at the base and one at the top of the tower.

Instruments which are suitable for installation at concrete dams are strong-motion triaxial instruments such as Kinemetrics SMA-1, manufactured by Kinemetrics, Inc., San Gabriel, California and Teledyne RFT 250 or RFT 350, manufactured by Earth Sciences Division of Teledyne Corp., Pasadena, California. The accelerographs should have a maximum operating range up to 0.5g or 1.0g. The 1.0g instruments would be appropriate at the crest of high dams and the 0.5g instruments at other locations near or at the ground surface. Seismoscopes to measure the relative response of different foundation or geologic formations within the immediate project vicinity are installed to supplement the conventional strong-motion accelerographs located at the foundation or abutments. Hydrodynamic pressure gages are installed on the upstream face of high dams and intake towers (over 300 feet) to measure the increased pressure of the reservoir water during earthquake occurrences.

An example of seismic monitoring instrumentation for concrete dams is that of Dworshak Dam which is shown on the drawing of Figure 6. This dam is located on the North Fork of the Clearwater River in Idaho and has a maximum structural height of 717 feet. The instruments at Dworshak consist of four time recording strong-motion accelerographs, thirteen triaxial peak accelerographs and six dynamic water pressure cells. These instruments are generally located within the highest monolith of the dam, in the powerhouse superstructure concrete walls, around the lake in the vicinity of the dam and at two bridges located approximately 18 and 40 miles upstream from the dam. Three Kinemetric, Type SMA-1 accelerographs are located in monolith 23 in small instrument rooms at elevation 980, 1260 and 1603. The fourth SMA-1 is located on the right bank 1430 feet downstream of the dam in a steel and concrete vault. This fourth instrument is to measure ground shock-wave intensity for a basis of comparison of intensities measured at different locations within the structure. Six dynamic water pressure cells are located on the upstream face of the dam at elevations 1050, 1160, 1220, 1280, 1350 and 1435 to measure and record water pressure changes against the structure in the event of an earthquake. Four of the triaxial peak recording accelerographs are located in the powerhouse, three in the thin superstructure walls and one in the substructure to monitor and compare shock-wave accelerations. Five triaxial peak recording accelerographs are installed around the lake in the vicinity of the dam to monitor possible varying intensity of ground shock-waves at different locations. The other four triaxial accelerographs are located at the two bridges upstream from the dam.

Seismic Instrumentation of Earth and Rock-Fill Dams

Earth and rock-fill dams 100 feet high and greater and located in seismic risk zones 2, 3, and 4 are instrumented for strong-motion measurements. All areas west of the Rocky Mountains are considered at least zone 2 for instrumentation purposes. Dams less than 100 feet high and/or located in zones other than stated above are considered for instrumentation dependent upon embankment and foundation materials, particularly if such materials are considered susceptible to liquefaction. Locations of instruments for an embankment dam are shown on Figure 7. All embankment dams in seismic zone 4 and in zones 3 west of the Rocky Mountains are instrumented in accordance with Category C as depicted in Figure 7 except in special cases where more complete measurements are desired and in these cases Category D is followed. Most other structures are instrumented in accordance with Category B.

The strong-motion accelerographs, such as the Teledyne RFT-250 or 350 and Kinemetric SMA-1 are also recommended for embankment dams. Because of difficulties with transmission of signals from transducers to remote recorders, central recording systems are not generally recommended. Seismoscopes are used on different geologic deposits in the immediate vicinity of the dams to provide an estimate of the influence of geologic conditions on ground motion intensity and to supplement ground motion information obtained from the accelerographs. However, seismoscopes are not installed on embankment dams because of the difficulty in interpreting the records from this type of installation.

Seismic Hazards of Reservoirs and Landslides

Experiences elsewhere in the world have indicated that the filling of large reservoirs might induce earthquake activity. An example of this is the Koyna Reservoir in India. The Corps of Engineers has designed and built a number of high dams with large reservoirs and no earthquake activity has been reported as a result of reservoir filling. The Corps' high dams are as follows: 34 dams over 200 feet high, 15 dams over 300 feet high, 6 dams over 400 feet high and 2 dams over 600 feet high. Of these dams 24 have a reservoir volume larger than one million acre feet. Special microseismic instrumentation to measure reservoir effects has been installed at several projects.

The importance of possible landslides into the reservoir cannot be overlooked. While not caused from earthquake activity, the Corps of Engineers had an experience at Libby Dam when during construction a small slide occurred in bedrock at the left abutment which damaged the concrete plant. As a result a comprehensive study was made to determine possible effects should a geologically similar landslide into the reservoir develop. A model was built at the Waterways Experiment Station to measure the effects of such a landslide. To increase stability and minimize concern at Libby Dam, a massive rockfill buttress was constructed along the upstream abutment slope. Extensive instrumentation was developed to detect and measure changes in subsurface conditions indicating potential instabilities. The instruments included the following: extensometers, porepressure measuring devices, inclinometers, and micro acoustic noise transducers.

Strong-Motion Instrumentation Installations

As of July 1974, 38 dam projects had been instrumented with 117 strong-motion accelerographs, 52 seismoscopes and 18 peak recording accelerographs. Additional instrumentation is currently planned for 56 projects which includes 171 strong-motion accelerographs, 50 seismoscopes and 17 peak recording accelerographs. The status of the instrumentation program is shown in Table 1.

Seismic Engineering Branch of the U.S. Geological Survey (USGS) is responsible for maintenance of the strong-motion instruments installed on Corps of Engineers structures. The record of ground and structure motion during earthquakes should provide valuable information to form a basis for selecting design earthquakes and for establishing the validity of dynamic design procedures. Also, the record of small earthquakes will be helpful in making preliminary estimates of the behavior of the structures during larger design earthquakes.

The instrumentation program is of great importance to the Corps of Engineers because of the many large reservoir projects for which the Corps is responsible. It is hoped that should significant earthquakes occur, the results of seismic instrumentation will give a better understanding of dynamic response of structures and perhaps lead to improved designs for seismic behavior.

References

1. Engineer Regulation ER 1110-2-1802, 10 September 1969, "Reporting Earthquake Effects", Corps of Engineers, U.S. Army.
2. Engineer Technical Letter ETL 110-2-130, 30 July 1971, "Seismic Instrumentation of Concrete Dams and Intake Towers", Corps of Engineers, U.S. Army.
3. Engineer Regulation ER 1110-2-103, 9 August 1974, "Strong Motion Instruments for Recording Earthquake Motions on Dams," Corps of Engineers, U.S. Army.
4. Engineer Technical Letter ETL 110-2-195, 9 September 1974, "Instrumentation for Measurement of Earthquake Motion and Instrument Shelters for Earth and Rock-Fill Dams," Corps of Engineer, U.S. Army.
5. Engineer Circular EC 110-2-151, 26 September 1974, "Status Report of CE Strong Motion Instrumentation Program for Measurement of Earthquake Motions," Corps of Engineers, U.S. Army.

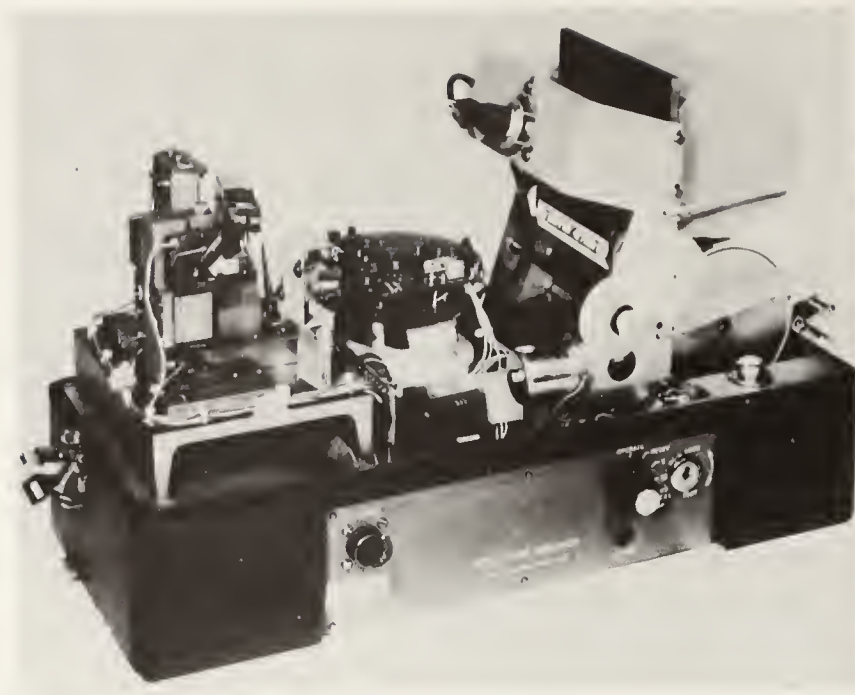


Figure 1 RFT-350 strong motion accelerograph.

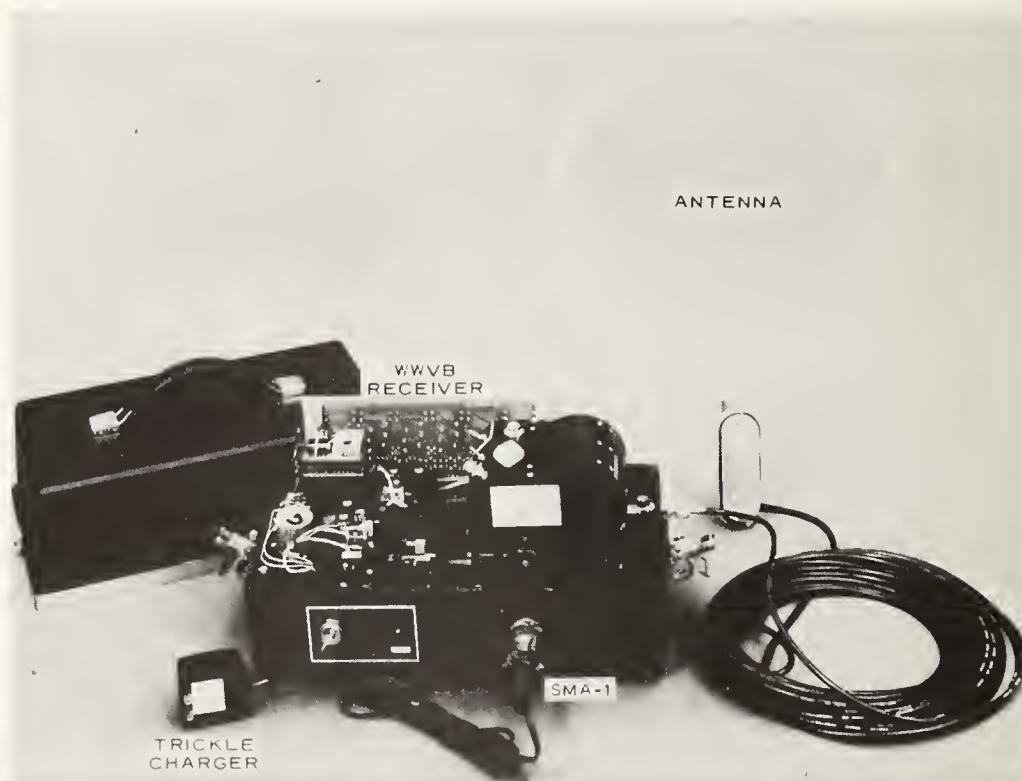


Figure 2 SMA-1 accelerograph with WWVB receiver, antenna, and trickle charger.

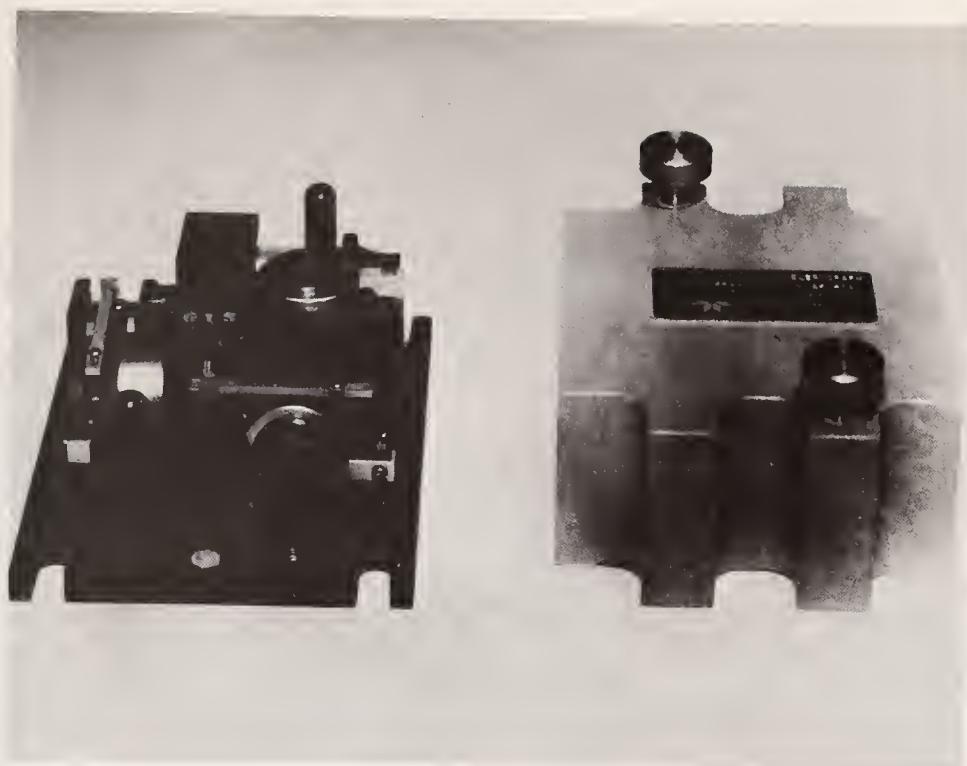


Figure 3 PRA-103 peak recording accelerometer.



Figure 4 Wilmot SR-100 seismoscope with cover.

VI-56

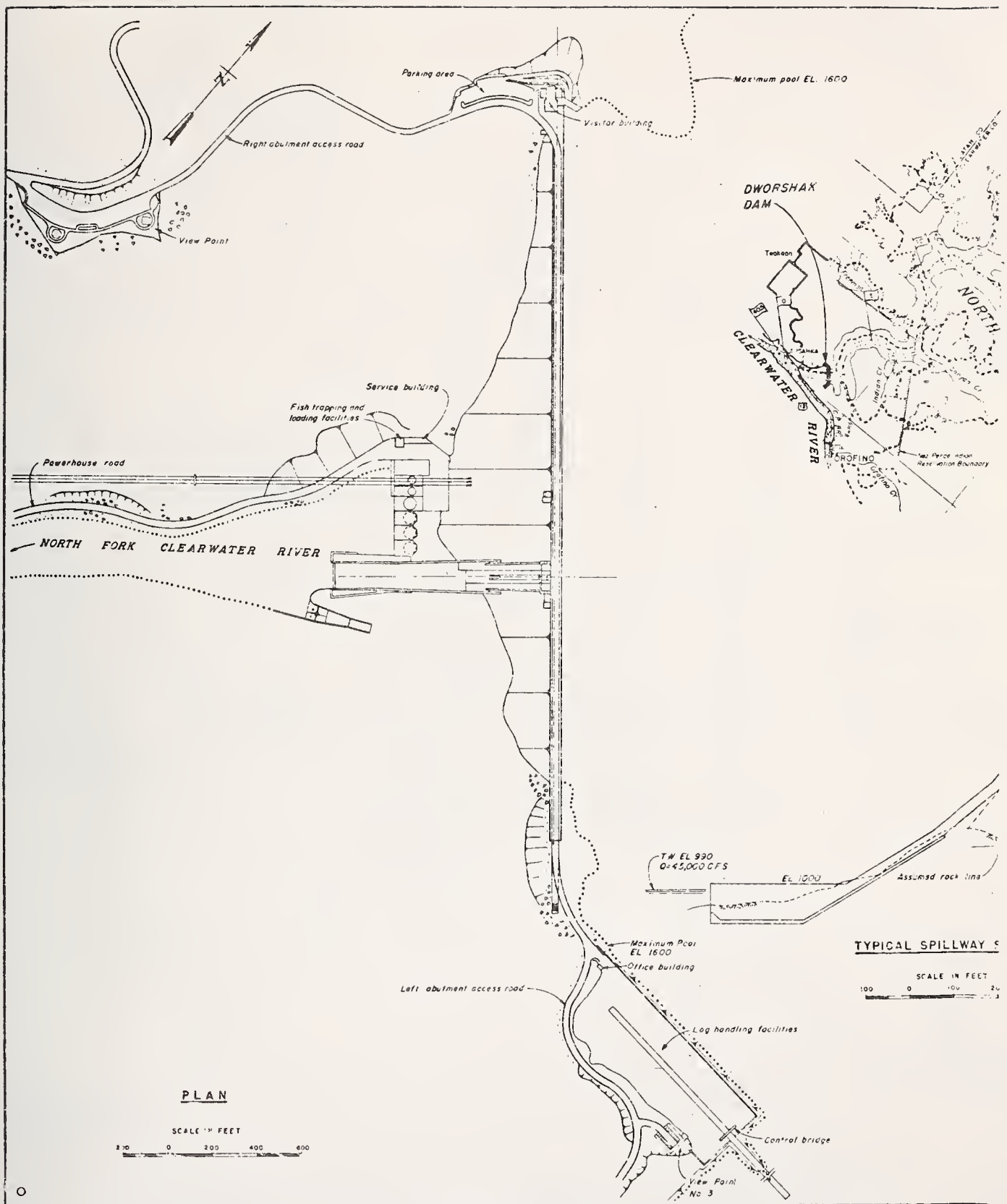


Figure 6-1

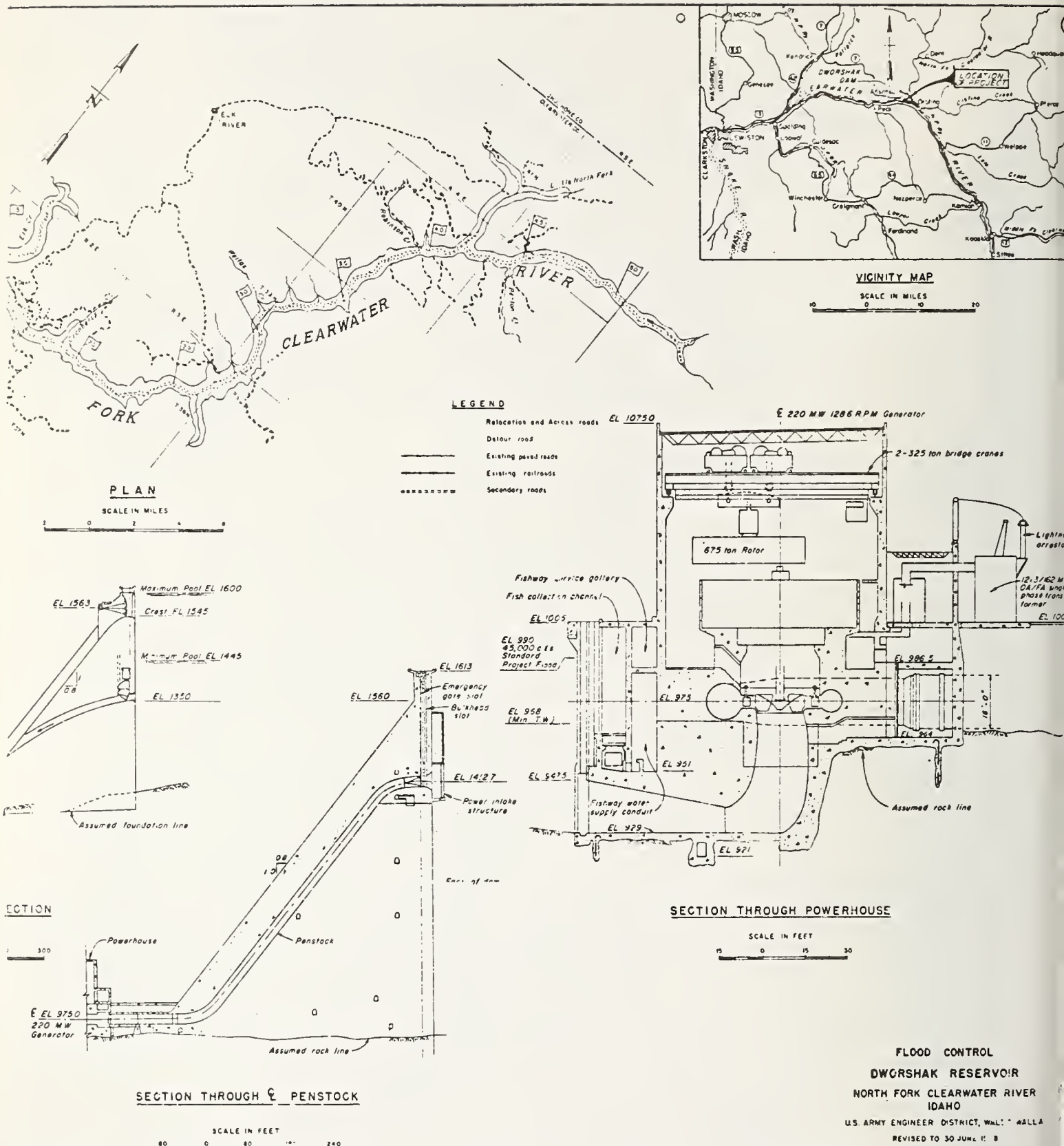
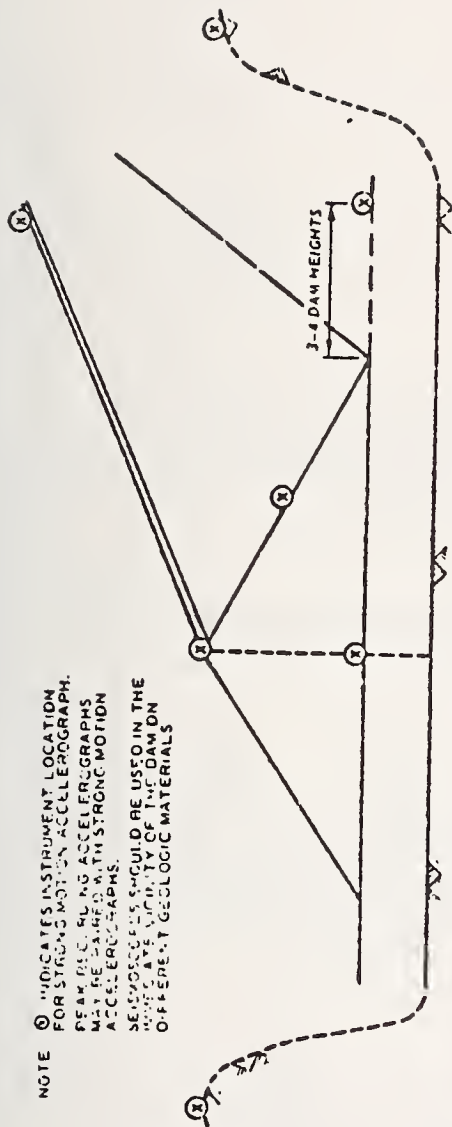


Figure 6-



REQUIREMENTS FOR DIFFERENT CATEGORIES OF INSTRUMENTATION

CATEGORY	INSTRUMENTATION
A. ABSOLUTE MINIMUM	1 INSTRUMENTS ON ABUTMENT (PROVIDED ABUTMENT MOTIONS NOT INFLUENCED BY LOCAL TOPOGRAPHY. OTHERWISE ANY LOCAL RELATIVELY FLAT ROCK OUTCROP) 1 INSTRUMENT ON CREST OF DAM
B. DESIRABLE MINIMUM:	2 INSTRUMENTS ON ABUTMENTS (USE RELATIVELY FLAT LOCAL OUTCROP IN LIEU OF ONE ABUTMENT LOCATION IF ABUTMENT MOTIONS LIKELY TO BE INFLUENCED BY TOPOGRAPHY) 2 INSTRUMENTS ON CREST AT DIFFERENT EMBANKMENT HEIGHTS, ONE AT MAXIMUM EMBANKMENT HEIGHT
C. DESIRED NORMAL:	2 INSTRUMENTS ON ABUTMENTS (AS IN B ABOVE) 2 INSTRUMENTS ON CREST (AS IN B ABOVE) 1 INSTRUMENT ON DOWNSTREAM SLOPE (0.4 TO 0.5H ABOVE BASE OF EMBANKMENT) 1 INSTRUMENT ON FOUNDATION LEVEL IN FREE FIELD DOWNSTREAM (IF SOIL)
D. DESIRED FOR MORE COMPLETE COVERAGE:	2 INSTRUMENTS ON ABUTMENTS (AS IN B ABOVE) 2 INSTRUMENTS ON CREST (AS IN B ABOVE) 1 INSTRUMENT ON DOWNSTREAM SLOPE (AS IN C ABOVE) 1 INSTRUMENT IN FREE FIELD DOWNSTREAM (AS IN C ABOVE) 1 INSTRUMENT AT FOUNDATION LEVEL ON AXIS OF EMBANKMENT (IF SOIL FOUNDATION)

Fig. 7 Strong motion instrument locations for earth and rockfill dams

Revised as of 1 July 1974

STRONG-MOTION INSTRUMENTATION AT CE PROJECTS
OPERATIONAL OR PLANNED AND TO BE SERVICED BY SEISMIC ENGINEERING

TABLE 1

Division	District	Project	State	Accelerographs		Seismoscopes		Peak Accel	
				Operational	Planned	Oper.	Plan.	Oper.	Plan.
NPD	Portland	Cougar	OR	6-SMA-1	--	--	--	--	--
		Green Peter	OR	2-AR-240	--	6	--	2	--
		Lookout Point	OR	1-SMA-1	--	--	--	--	--
		Lost Creek	OR	6-SMA-1	6	--	--	--	--
		Blue River	OR	5-SMA-1	--	--	--	--	--
		Detroit	OR	3-SMA-1	--	--	--	--	--
		Hills Creek	OR	3-SMA-1	--	--	--	--	--
	Seattle	Libby	MT	--	4	--	--	--	--
		Chief Joseph	WA	3-SMA-1	--	--	--	--	--
		Howard Hanson	WA	2*	3	--	--	--	--
		Mud Mountain	WA	2-SMA-1	1	--	--	--	--
		Wynoochee	WA	3-SMA-1	--	--	--	--	--
		Dworshak	ID	6-SMA-1	--	--	--	--	6
		Lower Granite	WA	--	2	--	--	--	9
		Lucky Peak	ID	5-SMA-1	--	--	--	--	--
	Walla Walla	Ririe	ID	--	5	--	--	--	--
		Snettishom	AK	--	2	--	--	--	--
		Alamo	AZ	2-RFT-250	1	3	--	--	--
		Brea	CA	--	3-SMA-1	--	--	--	--
		Carbon Canyon	CA	1-RFT-250	2-SMA-1	--	--	--	--
SPD	Los Angeles	Mojave	CA	4-SMA-1	--	--	--	--	--
		Prado	CA	--	3	--	--	--	--
	Alaska	Salinas	CA	1-AR-240	--	--	--	--	--
		San Antonio	CA	1-RFT-250	2-SMA-1	--	--	--	--
		Sepulveda	CA	--	2-SMA-1	--	--	--	--
		Whittier Narrows	CA	1-RFT-250	2-SMA-1	--	--	--	--

(Continued)

* Tape recorded units, not serviced by Seismic Engineering

STRONG-MOTION INSTRUMENTATION AT CE PROJECTS
OPERATIONAL OR PLANNED AND TO BE SERVICED BY SEISMIC ENGINEERING

TABLE 1

Division	District	Project	State	Accelerographs		Seismoscopes		Peak Accel.	
				Operational	Planned	Oper.	Plan.	Oper.	Plan.
MRD	Sacramento	Black Butte	CA	2-RFT-250 2-RFT-350	--	2	--	--	--
		Isabella	CA	5-RFT-250 1-RFT-350	--	5	--	--	--
		Martis Creek New Hogan	CA	5-SMA-1 2-RFT-250	--	--	--	--	--
		Pine Flat	CA	1-RFT-350 3-RFT-250	--	2	--	--	--
		Terminus	CA	1-RFT-350 3-RFT-250	--	3	--	--	--
		Coyote Warm Springs	CA	3-RFT-250 3-SMA-1	--	--	--	--	--
	San Francisco		CA						
			CA						
	Kansas City	Tuttle Creek	KS	--	?	--	--	--	--
		Milford Dam	KS	--	?	--	--	--	--
SWD	Omaha	Chatfield Dam	CO	--	5	--	--	--	--
	Albuquerque	Cochiti	NM	4-SMA-1	3-SMA-1	4	4	--	--
	Little Rock	Norfolk	AR	2-SMA-1	--	--	--	--	--
	Tulsa	Kaw	OK	--	2-SMA-1	--	2	--	--
NCD	Buffalo	Mt. Morris	NY	--	4	--	1 or 2	--	--
LMVD	Memphis	Wappapello	MO	3-SMA-1	--	6	--	--	--
		Rend Lake	IL	3-SMA-1	--	6	--	--	--
	St. Louis	Arkabutla	MS	3-SMA-1	--	7	--	--	--
		Sardis	MS	3-SMA-1	--	6	--	--	--

(Continued)

STRONG-MOTION INSTRUMENTATION AT CE PROJECTS

OPERATIONAL OR PLANNED AND TO BE SERVICED BY SEISMIC ENGINEERING

TABLE 1

Division	District	Project	State	Accelerographs		Seismoscopes		Peak Accel.	
				Operational	Planned	Oper.	Plan.	Oper.	Plan.
ORD	Louisville	Brookville Dam	IN	--	3	--	--	--	--
		Cagles Mill Dam	IN	--	3	--	--	--	--
		Monroe Dam	IN	--	3	--	--	--	--
		Nolin R. Dam	KY	--	3	--	--	--	--
	Nashville	Rough R. Dam	KY	--	3	--	--	--	--
		Wolf Creek	KY	2-SMA-1	3	--	1	--	1
		Center Hill	TN	2-SMA-1	3	--	2	--	1
		Barkley	KY	--	6	--	2	--	1
		J. Percy Priest	TN	2-SMA-1	3	--	2	--	1
		Dale Hollow	TN	--	4	--	2	--	1
	Huntington	Laurel River	KY	--	3	--	1	--	1
		R. D. Bailey Dam	WV	--	1	--	--	--	--
		Bluestone	WV	--	1	--	--	--	--
		J. W. Flannagan	VA	--	1	--	--	--	--
NET		Ball Mt. Lake	VT	3-SMA-1	--	--	--	1	--
		Colebrook R. Lake	CT	--	3-RFT-250	--	--	--	--
		Littleville Lake	MA	--	3-RFT-250	--	--	--	--
		Franklin Falls	NH	--	3-RFT-250	--	--	--	--
		Union Village	VT	--	3-RFT-250	--	--	--	--
		Everett	NH	--	3-RFT-250	--	--	--	--
		Hodges Village	MA	--	3-RFT-250	--	--	--	--
		Knightville	MA	--	3-RFT-250	--	--	--	--
		Surry Mt.	NH	--	3-RFT-250	--	--	--	--
		N. Hartland	VT	--	3-RFT-250	--	--	--	--
		N. Springfield	VT	--	3-RFT-250	--	--	--	--
		Townshend Lake	VT	--	3-RFT-250	--	--	--	--

(Continued)

STRONG-MOTION INSTRUMENTATION AT CE PROJECTS
OPERATIONAL OR PLANNED AND TO BE SERVICED BY SEISMIC ENGINEERING
(Concluded)

TABLE 1

Division	District	Project	State	Accelerographs		Seismoscopes		Peak Accel.	
				Operational	Planned	Oper.	Plan.	Oper.	Plan.
NAD	Norfolk New York	Gathright	VA	--	4	--	--	--	--
		Waterbury	VT	--	3(est)	--	--	--	--
	Baltimore	Wrightsville	VI	--	3(est)	--	--	--	--
		Arkport	NY	--	3(est)	--	--	--	--
SAD	Wilmington	John H. Kerr	VA	--	5	--	3	--	--
		Philpott	VA	--	2	--	--	--	--
	Charleston	W. Kerr Scott	NC	--	3	--	3	--	--
		Clark Hill	GA	--	6	--	3	--	--
	Savannah	Hartwell	GA	--	5	--	3	--	--
		Buckman Lock	FL	1-SMA-1	--	--	--	--	--
	Jacksonville Mobile	Allatoona	GA	--	5	--	3	--	--
		Buford	GA	--	3	--	3	--	--
	Walter F. George	Coffeeville	CA	--	1	--	2	--	--
		Carters	AL	--	1	--	6	--	--
			GA	--	3	--	6	--	--

SCHOOL AND HOSPITAL CONSTRUCTION IN CALIFORNIA

by

John. F. Meehan
Research Director, Supervising Structural Engineer
Structural Safety Section
Office of Architecture and Construction
Department of General Services
State of California

ABSTRACT

The California State Legislature has adopted statutes concerning the regulation of the design and construction of public school buildings and hospitals. These statutes were brought about because of the rather poor performance of these types of buildings in California earthquakes. Events leading up to these statutes and the methods of their enforcement will be discussed.

Key Words: Building Codes; Building Regulations; Design Criteria; Earthquakes; Hospitals; Schools.

Public Schools

The 1933 Long Beach, California earthquake produced great damage to public school buildings throughout the devastated area. It occurred at 5:54 p.m. on Friday, March 10, 1933 and, as usual during this time on a Friday evening, there were essentially no students or teachers in the buildings. Had the earthquake occurred during school hours the number of deaths to the school children would have been horrifying. The California State Legislature requires school attendance of the youngsters and recognizing that earthquakes may occur at a time of full occupancy of the children, took measures to prepare and adopt the Field Act within a month after the earthquake. The rapidity of the passage of this legislation clearly indicates the gravity and concern of the legislature and the public. Each earthquake that has occurred in California since 1933 has proven the wisdom of this Act. Reports of earthquake damage in California usually point out the good performance of post-Field Act school building construction. (1, 2, 3, 4, 5, 6, 7, & 8)

Field Act and Enforcement

The Field Act will be briefly explained and the method of its enforcement by the Structural Safety Section (SSS) of the Office of Architecture and Construction (OAC) in the Department of General Services (DGS) will be described. The Field Act is given in Section 3 of Title 21, California Administrative Code (CAC).

The Act applies to all new public school buildings and to all additions or alterations of schools costing more than \$10,000. The plans and specifications must be prepared by registered structural engineers and/or architects in the private sector. The complete construction documents including the structural design calculations, geologic reports, application and fee are submitted to SSS. The prints of the plans and specifications are reviewed (checked) and comments are marked on them by registered structural engineers in the SSS for conformance with seismic design regulations. To accomplish this, the structural plans and the structural or anchorage aspects in the architectural, mechanical and electrical plans are rather closely checked. The plans and specifications are returned to the structural engineer or architect for correction. The tracings and marked documents are then returned to SSS and compared (back checked) by the SSS representative working together with the responsible structural engineer and/or architect. Upon mutual agreement of the revisions, the tracings are stamped approved. A corrected set of approved stamped documents are filed with SSS. Competitive bids are taken and the contract may then be let by the school district to the lowest responsible bidder. All change orders and addenda must also be signed by the architect or structural engineer and approved by SSS. Continuous on-site inspection of all phases of the construction is required by the Field Act and is provided by a construction inspector approved by the structural engineer and/or architect in responsible charge of construction, the school board and the SSS. Materials of construction to be tested and special inspections to be performed are established at the time of back check. Reports are filed by private sector testing laboratories to assure material conformance with the requirements of the approved documents. The structural engineer and/or architect in charge of construction are required to supervise or observe the work of construction. Certificates verifying that the construction fully complies

with all of the requirements of the approved documents are filed by the structural engineer, architect, construction inspectors, testing laboratories and contractor. Making a false statement is a felony. Field personnel from SSS also visit the projects periodically to review the construction for possible design and construction errors. A fee of one-half of one percent of the construction cost is paid by the school district to the SSS to fund this operation.

It has been frequently expressed by structural engineers in the private sector that the reasons for the good performance of public school buildings in earthquakes are because the designs are prepared by capable personnel; the independent review of the plan details by structural engineers equally capable as those who originally designed the structure to assure code compliance and design concept; the inspection provided by the responsible designers; the continuous detail inspection provided by the approved construction inspectors; and the review of the construction by the SSS structural engineers for conformance of design principles. In general it is required to pay close attention to proper detailing of the structure and provide complete and logical means of resisting lateral loads giving full consideration to deflections and displacements.

The Field Act also established that regulations may be adopted pursuant to the legislation. These regulations, adopted by SSS, are those of the 1973 Uniform Building Code together with certain nominal additions and deletions found necessary to accomplish the requirements of the Field Act. These amendments are printed in Title 21, CAC. The lateral force provisions are basically those recommended by the Seismology Committee of the Structural Engineers Association of California. A copy of Title 21, CAC, can be obtained from State of California, Documents Section, P.O. Box 20191, Sacramento, Calif. 95820.

Title 21, California Administrative Code (CAC) and Uniform Building Code (UBC)

Exceptions

The regulations adopted to administer the Field Act are given in Groups 1 and 2 of Title 21, CAC. The detail technical regulations are given in Group 3, Article 23 through Article 47. All of the items given in Title 21, CAC in article 23 through 47 are exceptions or additions to the 1973 UBC. Just a few of these will be mentioned here.

Loading

The minimum acceptable base shear KC factor for any one and two story building is 0.10 as mentioned in Section T21-2316(d) (1) and all frames must meet the ductile requirements. This base shear factor seldom is applied, as most designs proposed are based upon a base shear of 0.133, and further, the framing is usually of shear wall design concept.

Any single mass structure on a single column or of a type where a single column must provide the total lateral resistance, the lateral force base shear KC factor must be 0.30, and the column must meet the ductile requirements.

Also if building frames are designed for a base shear KC factor of 0.30 or more, the frame need not be ductile but the columns must be ductile. Most frames are designed under this basis.

In the near future Title 21, CAC will probably be revised to require a KC base shear factor of 1.5 times the code force when the building is located near established active faults.

Drift is controlled in Section T21-2307(c). This section requires the maximum drift of 1/16" per foot of height. The drift is also limited to 1/32" per foot of height of opening where glass is installed in the walls which may deflect in the plan of the wall and the glass is not separated from the frame such that any in-plan deflection will transfer load into the glass. In tests, reported by this author at the Second World Conference on Earthquake Engineering in Tokyo, it was shown that glass fails at about 1/16" per foot of height when bedded in stiff mastic and the glass frame cannot rotate. Wall deflection limitations applied perpendicular to the wall is also given in Section T21-2307(c).

There are diaphragm span/depth ratios given in Table T21-23L. These ratios are primarily to control deflection and stress in the horizontal diaphragms which, in effect, also control the flexibility of the horizontal diaphragms. Controls are also provided for vertical diaphragms in this table.

Masonry

All masonry construction requires inspection by a specially approved masonry inspector. His duties are described in Section 2401 of Title 21, CAC. This section also requires cores of the completed walls to be taken and tested in shear and compression. Cores not only provide an indication of the strength of the materials but also provide an excellent means of determining the quality of workmanship within the wall.

The allowable stresses in masonry are given in Article 24, but under most designs the stresses in masonry seldom control the design. All masonry must be reinforced. Maximum spacing of reinforcing is limited to 24 inches each way in walls and extra ties are required at the ends of all columns and around bolts. Such reinforcing greatly increases the toughness of the wall. High and low lift grouting is allowed but it is imperative that it be reconsolidated at the proper time and again after the next lift of grout is placed, also it is strongly recommended that an expansive type admixture is used in the grout. Both of these conditions, the reconsolidation and the expansive admixture, greatly reduces the amount of internal shrinking cracks in the grout. Unreinforced masonry or cavity wall construction is not allowed.

Methods of rehabilitating existing masonry construction is given in Section T2102422.

Wood

Article 25 of Title 21, CAC covers the requirements for wood. The exceptions are rather nominal. The maximum adjustment for stress for duration of loading is limited to 15% increase. The allowable nail stresses are higher than those given in the current UBC because of the success of designs provided under Title 21, CAC. As an example, the allowable shear load on an 8d common nail in Title 21, CAC is 100 pounds whereas the allowable is 78 pound in the 1973 UBC. These nail stresses have been used successfully since the Field Act became effective in 1933.

Glue lam construction, Section T21-2511, basically conforms to current industry standards except the maximum moisture content at time of gluing relates to the expected moisture content in the area when the building is situated. That is, the maximum allowable moisture content along the sea coast is 16% whereas in the desert areas it is limited to 10%. Continuous inspection by a specially approved inspector is required for glue lab

beam construction.

Unblocked plywood diaphragm allowable loads are a bit lower than that permitted by UBC as given in Section T21-2514.

Rather complete details are usually given on the plans showing wood framing, openings in floors and walls, notching, etc. Also careful attention has always been paid to properly anchor wood roofs and floors to masonry or concrete walls.

Concrete

Much of the material in Title 21, CAC in the concrete section refers to proportions, mixing and placement. There are several additional design and construction requirements such as those given in Section T21-2406 which call attention to the requirements for clean construction joint; additional column ties are required by Section T21-2607 on the ends of all columns; the column ties shall terminate in a 135° bend with 6" extension; Section T21-2614 requires height/thickness ratio of bearing walls to be not more than 30 and not more than 36 for non-bearing walls, precast walls require special trim wall reinforcing, anchorage and other requirements; Section T21-2618 requires grouting of all post-tension tendons anchored with friction type anchors; and Section T21-2621 contains controls on pneumatically placed concrete.

Steel and Iron

Article 27 covers steel and iron. There is little difference between the basic UBC requirements and Title 21, CAC. There are, however, controls on steel deck used as diaphragms and load test requirements of steel joists if analyses cannot be readily performed. Welding inspection is required by capable inspectors who must use all means necessary to assure himself of the proper quality of the weld.

Foundations

Under foundations, the additional special requirements are for inspection of engineered fill, piles and other miscellaneous items.

Veneer

All veneer over 3/8" in thickness must be anchored by mechanical means. Details of anchorage and reinforcing of the masonry is given in Article 30. Walls to which veneer is applied must have stiffness of L/600. The connection is usually by means of sheet metal dove-tail anchors. The anchor slot is cast into the concrete walls or nailed with 10d common nails at 12" oc. A nail placed vertically between the end of the anchor and the back of the slot to take up any slack in the connection. A number 9 wire is placed horizontally in the mortar joint in each horizontal joint containing an anchor. The maximum spacing of anchors is about 16" oc horizontally and 12" vertically.

Although currently not required by code, it is this authors preference to omit any veneer, or glass over exit doors.

Roofing

Article 32 provides for anchoring the roofing to the structure including tile. The anchorage of each tile by means of non-corrodible wires or nails is required to prevent the tile from sliding off the roof and falling to the ground during earthquake motion.

Ceilings

Plaster ceilings must be wire-tied to the ceiling framing to prevent the ceiling from falling. It was learned that ceiling fastened to wood framing only by means of nails in withdrawal will allow the ceiling to fall in one single large piece somewhat like a blanket. Complete details for all types of ceilings and light fixture anchorages must be shown on the drawing.

Anchorage

Items such as boilers, water tanks, fixtures, cabinets, shelves, window sash, ceilings, heaters, etc. must be properly anchored to the structure and are shown on the approved detail drawings.

Field Act Advisory Board

The SSS has an Advisory Board composed of four structural engineers, four architects, a mechanical engineer and an electrical engineer from the private sector who serve without pay. Representatives of various state agencies are ex-officio members. This board provides advice on technical and administrative matters relating to the regulations and enforcement of the Field Act.

Other Legislation

When the Field Act was first adopted in 1933 it related only to new construction and it remains so today. Existing buildings were not mentioned. Legislation was later adopted in the Garrison Act which provided that, if a building was examined and found unsafe and the building was allowed to continue in operation without correction and without attempting to obtain funds for the correction if no funds were available, the school board members were individually liable. Many old school buildings were, therefore, never examined to determine whether they were unsafe. In 1967 legislation was adopted to require a structural examination of all school buildings constructed prior to 1933. In 1968 the statutes were changed and provided that if found unsafe and not corrected, such buildings could not be used for school purposes after June 30, 1975. In 1975 legislation was added to provide that if definite steps were taken by June 30, 1970 to correct the deficiency, the building could be used until June 30, 1977.

When the Field Act was first adopted there was no control established concerning the location of the school site. As a result, many school buildings were located very close to active faults. In 1967 legislation was enacted to require a geologic hazards report and to prohibit siting new schools on active faults or on other geologic hazards. It was later amended to also require a geologic hazards report for building additions on existing sites.

Currently a geologic hazards report is required when deemed necessary by SSS.

Hospitals

Hospital buildings have frequently been damaged from the larger earthquakes in California and therefore were evacuated just at a time when they were most critically needed to serve the victims from other damaged man-made structures.

Following the 1971 San Fernando earthquake, where 50 deaths or 85% of the total deaths of patients or employees resulted from hospital building collapse or inoperative equipment, where four hospitals were evacuated, and where 17 hospitals were damaged, legislation was

passed by the state legislature in 1972 requiring construction approval procedures similar to those in the Field Act to apply to hospitals. There are some differences.

The Department of Health (DH) administers the act, but is required to contract with the DGS to perform a similar service on hospitals as they do on public school buildings. It requires that all plans and specifications shall be prepared under the responsible charge of a California registered architect or structural engineer or both; it requires that a structural engineer shall sign plans and specifications related thereto; it requires a geologic hazards report on all but the small buildings; it requires the geologic data to be reviewed by an engineering geologist and the structural design to be reviewed by a structural engineer; it requires a fee based upon the estimated cost and a further fee based upon the final cost; it requires continuous on-site inspection by competent personnel and administration of the work of construction to be under the responsible charge of such structural engineer or architect; it requires signed certificates indicating conformance with the approved documents from all those involved in the construction; it authorizes the DH to adopt regulations with the advice of the DGS to carry out the desires of the bill; and it establishes a Building Safety Board to advise and act as an appeals board with regard to seismic safety; and it established that any person who violates the provisions are guilty of a misdemeanor. This bill is Chapter 1130 of the 1972 Statutes and is given in Division 12.5 of the Health and Safety Code.

The SSS enforcement of this act is quite similar to the procedures followed under the Field Act and will not be repeated here.

Building Regulations

The legislation mandates that "...hospitals...be completely functional to perform all necessary services...to resist, insofar as practicable, the forces generated by earthquakes, gravity and winds..." places a new direction in building codes. Recognizing this and the need for immediate input from the private sector, DH contracted with a structural engineer, a mechanical/electrical engineer and an architect as consultants to SSS to prepare the regulations. They were adopted as emergency measures, then public hearings were held when input was provided by the Seismology Committee of the Structural Engineers Association of California and other interested groups.

The building regulations for California hospitals are given in Title 17, CAC and contains the special provisions for the seismic load levels and performance. The remainder of the regulations are essentially those required for public school buildings. As mentioned previously, these latter regulations consist of the 1973 Uniform Building Code as the basic code, together with nominal additions and deletions found necessary to accomplish the desired results. A copy of Article 23, General Design Requirements can be obtained from the State of California. The remaining regulations are essentially those given in Title 21, CAC.

A few of the highlights for earthquake forces of Article 23, General Design Requirements in Title 17, CAC will be presented. There are two basic methods of design. One may be by dynamic analysis, Method A, and the other by static analysis, Method B. Section T17-2314 of Title 17, CAC requires that buildings over 160 feet in height or those with highly irregular

shapes, or other unusual structural features must have a Method A or a dynamic analysis. This requires that the structural and deflection capacities shall be sufficient to resist the effects of earthquakes upon the structure as determined by dynamic analyses. These analyses shall be based upon the ground motion prescribed for the site in a geotechnic report. The report shall consider the seismic event that may be postulated with a reasonable confidence level within a 100 year period.

The analyses may be based on appropriate time-histories or response spectra with percentages of critical damping consistent with the strain levels in the structural materials. All natural modes of vibration with periods greater than 0.05 seconds shall be considered in the analyses. If the stresses calculated by elastic analyses exceed the nominal yields stress of the structural materials, the structural elements to be used shall be justified by approved methods which reconcile the equivalent inelastic deformations with the ductility of the structural elements.

The base shear resulting from the dynamic analyses shall be not less than 80% of the base shear calculated from the provisions of Method B. If the base shear as determined by dynamic analyses must be increased to meet this requirement, the design spectra shall be normalized to a proportionately higher value.

Under Method B, the static analysis, the lateral load level has been raised above that provided for other occupancies given in the Uniform Building Code. The base shear equation is

$$V = KCW$$

where K shall be 3.00 for all buildings, the value of C is the same as that given in the 1973 Uniform Building Code, except that the combined value of KC shall be 0.25 for all and two story buildings and need not exceed 0.25 for any building. The method for calculating the period, T, and the load distribution is the same as that of the 1973 Uniform Building Code. Since all of California is located in Zone 3 of the Uniform Building Code, zone factors are not mentioned in these regulations and the importance factor currently being considered for inclusion in the Uniform Building Code is included in the KC value. All lateral force resisting frames must be ductile; however, in one and two story buildings when the KC value used in the design is 0.50 or more, the frames need not be ductile but the columns must be ductile. The C_p table is more extensive than that given in the Uniform Building Code and the load level is higher in all cases. Anchorage requirements for such items, equipment, elevators, piping, cabinets, lights, ceilings, partitions, etc. are presented.

Building Safety Board

The states establish the formation of a Building Safety Board to advise the DH with regard to seismic structural safety and to act as a board of appeals in the enforcement of the Act. This board is composed of members qualified by close connection with hospital design and construction and are highly knowledgeable in their respective fields with particular reference to seismic safety. The board consists of eleven members of which there are two structural engineers, two architects, one engineering geologist, one soils engineer and one hospital administrator appointed by the Director of Public Health from nominations of

technical and professional associations. There are also six ex-officio members from state offices.

This board has provided a great deal of input to the Department of Health concerning the operation of this Act. It reviews the regulations to be adopted, has studied and recommended methods of approving work in existing buildings and advises the Department as requested.

The board has established standing sub-committees on structural, architectural, mechanical and electrical, geotechnic and hospital operations. These committees act as liaison between the board and the respective technical associations and provide advice on assigned subjects. There are also ad hoc committees on appeals procedure, plan checking fees, board rules and procedures, and legislative intent. A board member is the chairman of each sub-committee and ad hoc committee.

References

1. Steinbrugge, K. V. and Moran, D. F., An Engineering Study of the Southern California Earthquake of July 21, 1952 and of Its Aftershocks. Bulletin of the Seismological Society of America, April, 1954, p. 344 and p. 255.
2. Steinbrugge, K. V., Cloud, W. K., and Scott, N. H., The Santa Rosa California Earthquakes of October 1, 1969, Coast and Geodetic Survey, 1970, p. 38 and p. 10.
3. Steinbrugge, K.V., Schader, E. E., Bigglestone, H. C., and Weers, C. A., San Francisco Earthquake of February 9, 1971, Pacific Fire Rating Bureau, p. 2.
4. Meehan, J. F., Degenkolb, H. J., Moran, D. F., Steinbrugge, K. V., Cluff, L. S., Carver, G. A., Matthiesen, R. B., and Knudson, C. F., Managua Nicaragua Earthquake of December 23, 1972, Reconnaissance Report, Earthquake Engineering Research Institute, 1973, p. 167.
5. National Academy of Sciences, National Academy of Engineering, The San Fernando Earthquake of February 9, 1971, p. 13.
6. Jennings, P. C., Engineering Features of the San Fernando Earthquake, California Institute of Technology EERC 71-02, p. 276.
7. National Bureau of Standards, Engineering Aspects of the 1971 San Fernando Earthquake Building Science Series 40, 1971, p. 311.
8. Steinbrugge, K. V., Schader, E. E., Earthquake Damage and Related Statistics, San Fernando Earthquake February 9, 1971, U. S. Department of Commerce, 1973, Vol. I, Part B, p. 713.

IMPROVED EARTHQUAKE RESISTIVE DESIGN AND
CONSTRUCTION OF SINGLE-FAMILY RESIDENTIAL DWELLINGS

by

G. Robert Fuller, P.E.
Office of Underwriting Standards
Housing Production and Mortgage Credit
Federal Housing Administration
U.S. Department of Housing and Urban Development

ABSTRACT

This paper presents results of the research program being carried out by the Applied Technology Council (ATC) of the Structural Engineers Association of California (SEAOC) under the sponsorship of the U.S. Department of Housing and Urban Development. The objective of this project was to review and evaluate available manuals, literature and standards concerning design and construction of residential dwellings and response of such structures to earthquake motions; and to then develop a manual of recommended practice for earthquake resistive design and construction. This manual would be primarily directed toward builders, building officials, field inspectors, and house designers and would contain recommended construction details, architectural layouts, design recommendations and types of construction recommended or to be avoided. The manual is now in draft form and copies are available for review. A synopsis of research results developed to date will be presented in this paper. Code comparisons, problem areas, tentative recommendations will be discussed.

The research contract with ATC is not due for completion until June 30, 1975, therefore this paper is an interim report. The final report with the completed manual will be distributed to members of the U.S. - Japan Panel on Wind and Seismic Effects, when available.

Key Words: Buildings; Building Codes; Construction; Dwellings; Earthquakes; Seismic Design Criteria.

Introduction

The U.S. Department of Housing and Urban Development (HUD) awarded a one year contract to the Applied Technology Council (ATC) of the Structural Engineers Association of California, on June 30, 1974. The primary objective of this research is to develop a "Manual of Recommended Construction Practice for Earthquake Resistive Residential Dwellings" to be used by builders, building officials, field inspectors and house designers.

The manual is to explain the structural behavior of single-family and townhouse residential construction subjected to forces produced by earthquake shocks. HUD Minimum Property Standards and other building code requirements will be illustrated. Sound practical construction methods and details for the reduction of structural damage due to earthquakes, will be covered. The manual will also illustrate recommended construction details, architectural layouts, types of construction recommended, or to be avoided, and methods of installing mechanical equipment to resist seismic forces.

Scope of Manual

Tasks

Several tasks make up the total project:

Task 1: Review of Literature: Review literature and reports on damage to residential structures as a result of recent earthquakes. An analysis and bibliography of literature reviewed outlining the engineering causes for identified damage to buildings and outlining possible solutions and corrective actions was required.

Task 2: Review HUD Minimum Property Standards (MPS) and Building Code Requirements: Review the HUD-MPS, Manual of Acceptable Practice and appropriate building codes to determine their adequacy for preventing earthquake damage to single-family residences. Recommend improvements in terms of structural performance based on reviewed reports of past earthquakes.

Task 3: Develop Construction Details: Develop typical engineering drawings, illustrations and details which are required to resist earthquake forces with appropriate descriptions and explanations to be easily understood by non-technical representatives of the housing industry. Details are to be categorized, as appropriate, by Seismic Zones 1, 2, and 3 as delineated in the Uniform Building Code, "Seismic Risk Map of the United States." Illustrations shall include the types of construction most commonly used for residential dwellings in earthquake prone areas of the country, i.e.: wood frame with siding, wood frame and brick veneer, wood frame and stucco, brick or concrete block masonry, steel or aluminum frame with siding or masonry veneer and other prevalent conventional combinations of framing, materials, and building components.

Construction details will include those for basement and slab foundations, dwelling structures, utility and mechanical equipment installation, chimneys and fire places, attached garages, and other architectural and structural components which may affect the strength, rigidity or stability of dwellings.

Task 4: Prepare Manual and Supplementary Engineering Analysis Report:

Task 4: Prepare Manual and Supplementary Engineering Analysis Report: To include the following general subjects:

1. Introduction
2. Commentary on principles of seismic force design.
3. Illustrative typical construction details. Description and discussions of details, as developed in Task 3.
4. Recommendations:
 - a. Concerning plan checking
 - b. Concerning construction inspection at site
5. Summary, general conclusions and recommendations
6. Supplementary engineering analysis report including discussion of theory and design calculations to justify typical details developed to resist seismic forces.

Task 5: Presentation Material: Presentations to include 35mm slides, text material and voice tape which will be used to explain contents of the manual to user groups - builders, building officials and designers.

Task 6: Presentations to User Groups: Four presentations to home builder organizations with invitations to designers and building officials to acquaint them with contents of manual. Presentations will be conducted in Los Angeles, San Francisco, Portland and Seattle at different times.

Major progress has been achieved on all of the tasks preliminary to the final presentations. Following is a general synopsis of accomplishments to date including philosophical discussions by the subcontractor to ATC: Ralph W. Goers and Associates of Los Angeles, California.

General Philosophy

Economic considerations must be reviewed not only in terms of life/safety but also damage control. Single-family dwellings always perform well in terms of life/safety. However, since HUD is an insuring agency, damage control should also be a factor. There is no doubt that if more shear resistance were provided in residences, damage figures would be considerably lessened. The approach to be used in the Manual should be that houses, like other structures, should conform to design requirements of the Uniform Building Code (UBC). Arbitrary requirements and exceptions in the UBC for single-family framed structures should not be permitted unless justified by a thorough structural analysis covered under this research project. It is the intent to minimize the degree of damage rather than prevent all damage.

This approach will either limit design or more probably add some additional cost to home construction. There is little doubt that the additional cost is the least expensive earthquake insurance available. However, the final decision will be up to HUD after reviewing all of the applicable data concerning earthquake probability, intensity and frequency and if justified by reference literature, field observations or calculations.

Finally, governmental agencies have normally led the way in developing both social and structural changes in our system. It seems only logical that requirements should exceed building code minimums where such can be justified by reference literature, field observations or calculations.

Seismic coefficients for single-family construction are not specified in some jurisdictions and also vary from code to code. It is felt that the UBC value of 0.133g for Zone 3 is sufficient. This would coincide with field observations of damage and with current HUD-MPS requirements. This conclusion is felt to be justified by the following:

1. One-story homes performed reasonably well in San Fernando earthquake and they probably would have performed even better if built according to the proposed manual.
2. Factors of safety for plywood diaphragms are consistently at or above 3.0. Therefore, houses properly designed and constructed using plywood shear panels to resist 0.133g would actually be capable of resisting 0.40g ultimate load.

Virtually all homes built recently have wood framed second floors and roofs. Current engineering analysis generally assumes the wood diaphragm to be flexible, therefore lateral loads are distributed to shear walls on a tributary area basis. Field observations indicate that this assumption is not necessarily correct. Preliminary calculations show that the second floor diaphragm is approximately ten times as rigid as the longest transverse shear wall. Relative rigidities of shear resisting elements used in single-family framed construction are difficult to determine. General conclusions, however, can be reached on how shear resisting elements act in relation to small wood diaphragms.

Analysis reveals that shears are generated in the first story walls of a small two-story house in excess of allowable values for any of the shear-resisting materials required by Section 2518(f)5 of the UBC. Proposed requirements will either result in plywood shear panels or much longer panels of material of lesser shear resistance for two-story and split-level homes.

A split-level house plan was analyzed by use of tributary area method. This typical type of house received severe damage in one case and collapsed in two other cases during the San Fernando earthquake. Analysis revealed that the wall between the garage and family room would receive around three-quarters of the total lateral load. If the diaphragm were analyzed as a cantilever beam in houses of this type, the interior wall would receive close to 100% of the lateral load. It was found that one of the greatest deficiencies of wood frame construction is its lack of resistance to torsional racking. In the one case examined the floor diaphragm rotated in plan, lifting the rear wall from its foundation and leaving only the center wall to resist further earthquake motions. It is obvious from these previous examinations that analysis techniques must be evaluated and perhaps be revised.

Collection of Data

Several interviews have been completed or arranged with architects, engineers, HUD officials, building department officials and building contractors in several areas of the U.S. A questionnaire has also been developed for mailing to all HUD Field Offices to determine types of single-family construction most prevalent in the U.S. (see Attachment No. 1). Construction methods will also be determined.

Preliminary information indicates that in earthquake prone areas of the U.S., over 90% of all houses presently being constructed are wood frame with either stucco, wood siding or masonry veneer as an exterior finish and either plaster or gypsum drywall on the interior.

Data is being collected on shear wall diaphragm properties for the multitude used: plywood, stucco, lath and plaster, gypsum wall board (drywall), fiberboard and others.

Organization of Manual

The following is a general outline of the proposed manual:

Introduction

Acknowledgements

Chapter I - Purpose and Use of Manual

1. Audience
2. Economics vs. Safety
3. Definitions
4. Geographical Scope (Seismic Zone Map)
5. Observations of Earthquake Damage
6. Use of Manual

Chapter II - Principles of Seismic Design

1. Inertial Movement
2. Walls as Vertical Beams
3. Floor and Roof Diaphragms
4. Shear Wall Diaphragms
5. Shear Resistance of Materials (Graphs & Tables)
 - a. Roofs
 - b. Floors
 - c. Walls
6. Chords and Struts
 - a. Splices and Connections
7. Load to Shear Wall Calculations
8. Effects of Deformation
 - a. Glazing
 - b. Other brittle materials
9. Fireplace and Chimney Design and Anchorage
10. Mechanical Equipment
11. Other Non-Structural Items
12. Basement Construction
13. Layout Configurations
14. Glossary of Terms

Chapter III - Construction Details

1. Shear Wall Design and Details
 - a. Hold-Down Anchors
 - b. Sill-Bolt Size and Spacing
2. Shear Transfer Details
3. Struts and Chords
4. Connection of Studs to Sill Plates

5. Exterior Corner Framing and Anchors
6. Fireplaces
7. Mechanical Equipment
8. Other Non-Structural Items
9. Masonry Construction
10. Steel Frame Houses

Wind design will be covered to the extent that comparisons can be made between wind and earthquake forces for the entire structure not for individual elements. Seismic Zones 1 and 2 in the U.S. will be covered together since wind forces generally govern. Seismic Zone 3 will be covered in a separate section. Even though wind could govern in some areas, the dynamic effort of earthquakes precludes a comparison with wind forces.

Review of Building Codes and HUD Minimum Property Standards

Uniform Building Code (1973 Edition)

1. Sec. 2308 Wind Pressure: Buildings shall be designed for wind pressures indicated in tables and maps. Uplift wind pressures for enclosed buildings are $3/4$ of the uniform wind pressures specified and for unenclosed buildings are $1\ 1/4$ times those specified. Overturning moments calculated shall not exceed $2/3$ of dead load resisting moment.

Based on experience in Phoenix and Los Angeles, failures due to wind are generally caused by uplift on the roof or to walls by inadequate anchorage of walls to roof or other supporting diaphragms. The conclusion drawn from observing wind damaged homes is that either the factor for uplift on unenclosed structures or the wind zone map is incorrect. Horizontal wind pressures as applied to the whole structure appear to be too high.

Despite the fact that uplift forces seem to be critical, overturning requirements for shear walls are questionable since shear forces appear to result in answers which are too high.

2. Sec. 2313 Anchorage: Masonry and concrete walls shall be anchored to all floors and roofs to resist a minimum force of 200 plf of wall or the calculated horizontal force, whichever is greater; continuous crossties shall be provided in roof and floor systems between diaphragm chords.

The force requirement of 200 plf appears to be too low. In many areas of the country this anchorage requirement and the diaphragm crossties are virtually ignored. This has proved disastrous not only for earthquake loads but also for wind forces as well. The manual will provide for minimum sill bolts and horizontal connections to roof framing, roof sheathing or blocking between roof framing members.

3. Sec. 2314 Earthquake Regulations: This section defines various systems utilized to resist earthquakes, formulas to determine equivalent static forces for design, distribution of horizontal loads, overturning, setback requirements, etc.

As applied to residential construction, this section specified that virtually all residences are "box systems" without vertical load carrying space frames.

Lateral forces are resisted by shear walls or braced frames and the force to be resisted in 0.133 times gravity loads.

4. Sec. 2514 Wood Diaphragms: Connections and anchorages capable of resisting design forces shall be provided between diaphragms and resisting elements. In buildings of wood frame construction where rotation is provided for, depth of diaphragm normal to open side shall not exceed 25 feet nor $2/3$ diaphragm width, whichever is smaller. Straight sheathing shall not be permitted to resist shears in diaphragms acting in rotation.

One-story, wood-framed structures with depth normal to open side not greater than 25 feet may have depth equal to width. Where calculations show that diaphragm deflections can be tolerated, depth normal to open end may be increased to a depth to width ratio not greater than $1\ 1/2:1$ for diagonal sheathing or $2:1$ for special diagonally sheathed or plywood diaphragms.

In masonry or concrete buildings, lumber and plywood diaphragms shall not be considered to transmit lateral forces by rotation.

The provisions for rotation as presently written are considered to be one of the most controversial items in the UBC in light of the 1971 San Fernando Valley earthquake. Many residential structures which had to depend on the principle of rotation in order to remain standing, fared reasonably well. Generally though, this type of structure has more than average damage and in some cases collapsed. Improperly braced cripple stud walls, improperly tied levels of split-level homes and the principle of rotation are the three principle causes of residential damage due to earthquakes. The manual will recommend that rotational principles of design be used for one-story detached garages.

5. Sec. 2517 Structural Roof Sheathing: Plywood roof sheathing is used in most home construction in the U.S., but various other systems are used in the Los Angeles area. Most of these other systems would not qualify as diaphragms. Despite this, there was little damage to roofs from the San Fernando earthquake. This was probably due to the fact that interior walls stopped at the ceilings and the roofs only carried their own weight. The manual will, therefore, not specify as does the UBC that structural roof sheathing shall be designed to support all loads specified in the Code.
6. Sec. 2518(f)5 Bracing: All exterior walls and main cross-stud partitions shall be effectively and thoroughly braced at each end and at least every 25 feet of length by one of several methods which include let-in $1" \times 4"$ diagonal braces, diagonal wood boards, plywood sheathing, fiberboard sheathing and gypsum board sheathing panels.

Braced panels shall be 48" in width. Solid sheathing shall be applied continuously on the first story exterior walls of all wood framed buildings three stories in height. Solid sheathing shall be applied on either face of the first story exterior walls of all wood framed buildings two stories in height in Seismic Zone 3. These braced wall sections shall be located at each end and at least 25% of linear

length of wall shall be braced. All vertical joints shall occur over studs and horizontal joints shall occur over blocking unless panels are 4'x8' applied vertically.

Poor performance of let-in braces was observed after the San Fernando earthquake. Particle-board is allowed by the Code although no shear values are specified. Some of the materials specified for sheathing have no minimum attachment specified. The sheathing specified is to be used in Seismic Zone 3 even though higher shear forces may occur for two-story residential structures in areas having wind loads of 20 psf or higher. Calculations show that if no interior shear walls are provided, all of the sheathing materials specified for exterior walls will be overstressed if a two-story building experiences a 20 psf wind load. If an interior shear wall does exist at the center line of the structure; fiber-board, gypsum board and particle board would still be overstressed.

Calculations also show that the Code requirements for overturning are conservative. Even if no interior shear wall exists and if the exterior walls are of minimal length, overturning will not be a problem.

7. Sec. 2518(f)6 Cripple Walls: Foundation cripple walls are framed walls less than full story height that extend from foundation wall to the floor or roof level. Such walls shall be braced as required for first-story exterior walls. Solid blocking may be used to brace cripple walls having a stud height of 14" or less.

Some split-level homes in the San Fernando earthquake were constructed with cripple walls. Most of these houses suffered severe damage caused by collapse of the cripple-stud walls. Let-in braces are not adequate and will not be allowed in the manual.

8. Sec. 2518(g)6 Blocking: Rafters more than 8" in depth shall be supported laterally at ends and at each support by solid blocking unless nailed to header, band or rim joist or to an adjoining stud.

Prefabricated roof truss-rafters are used predominately in today's housing construction. When roof rafters are used, they generally are less than 8' deep. In any case, blocking is seldom specified and shear transfer is not achieved. The manual will probably require solid blocking for truss-rafters and all other rafters.

9. Chapter 37 - Masonry or Concrete Chimneys, Fireplaces and Barbecues: Many differences exist between the Code, HUD-MPS, and other building codes and standards. The manual will specify requirements as verified by calculations or observations.

10. General Requirements

- a. Roof Diaphragms: Roof diaphragms, as opposed to ceiling diaphragms, play a small part in transferring lateral loads in residential construction. Since the roof diaphragm is generally more limber than the ceiling, loads in the direction of framing are taken by the ceiling to interior crosswalls. Specific requirements for roof diaphragms, in the opinion of the contractor, accomplish little and only add to cost.

b. Roof Framing Blocking: The Code stipulates that blocking for 2x4 through 2x8 roof framing members may be omitted. Normal procedure in California, however, is to provide such blocking. Blocking for roof trusses is generally not provided in the Phoenix, Arizona area. Because of relatively low shear forces, blocking may not be needed continuously. Some shear transfer is required and this is difficult to provide without some blocking. It is suggested that a minimal length (as little as six feet) of blocking should be provided near ends of each individual roof. Blocking requirements will be specified for prefabricated roof trusses.

c. Conventional Construction Provisions: These Code provisions imply that all residential construction can be considered as "conventional." However, many types of construction are very unconventional and may require further design considerations:

- 1) Cathedral ceilings with high shear walls. Shear walls may still be four foot wide and overturning forces may be considerable.
- 2) Large rooms and long unbraced walls may be critical. Fewer interior walls to resist earthquakes may be provided.
- 3) Two-story homes may have insufficient shear walls.
- 4) Broken roof diaphragms may occur in split-level homes and in other unusual configurations.
- 5) Partial second floors very often do not have adequate shear walls near interior extremities.

Economy of construction must play a very important role when considering modifications to requirements for home construction. Some design requirements in the Code should therefore be revised in the manual. Other normal engineering procedures not specifically mentioned in the Code will be ignored. Bracing requirements provided in the manual will obtain the most in structural integrity for the least cost.

11. Shear Resisting Materials and Shear Walls: In order to obtain the most efficiency from shear resisting materials and to obtain the most liberal interpretation for the design of shear walls, the following provisions will be contained in the manual.

a. The designer will be instructed to use full dead load for resistance to overturning moments. Many engineers use a lesser, more conservative value. The Code specifies full dead load but the Los Angeles City Building Code allows 75% of dead load. Hold-down anchors have not been required for home construction except in those isolated cases where engineering design is provided. These anchors frequently cause problems in the field because of misplacement, incorrect installation and the problem of covering bolt heads or nuts, etc. For those reasons, it is felt desirable to eliminate the need for anchors where at all possible. The manual will have provisions to allow designers greater latitude in selecting shear wall lengths, spacing and location to preclude hold-down anchors.

b. Shear values for differing materials applied to each side of the same wall are proposed.

c. The height to width ratio for fiberborad, stucco, gypsum lath and plaster and gypsum board will be increased from 1 1/2:1 to 2:1 as implied in Section 2518(f)5 of the Code.

12. Sill Bolts: The Code stipulates that sill bolts shall be 1/2-inch diameter embedded at least 7" into concrete and spaced not more than six feet apart, with a minimum of two bolts per piece and one bolt within 12" of each end. The manual will require that sill bolts be placed in accordance with shear in the wall which will increase the number in some cases.

Los Angeles City Building Code (1972 Edition)

1. Sec. 91.2305-Horizontal Forces (a) General: Requirements of this section do not apply to any conventional framed one-story, Type V building accessory to dwelling, provided building is not an unusual shape or size and not subjected to unusual loading conditions. This would exempt most garages. The manual will clarify this requirement.
2. Sec. 91.2305(h) Overturning: 75% of dead load may be used to reduce tensile stresses caused by seismic overturning moments. The manual will specify full dead load as stated in the review of the UBC.
3. Sec. 91.2306-Design for Horizontal Force (b) Anchorage:
 - a. Walls anchored to continuous footings do not need to be anchored to floors that are within four feet of the footings.
 - b. When roofs, including their supporting joists, beams or purlins, are constructed of metal and are not designed as diaphragms to resist horizontal forces anchors may be spaced at greater than four feet on center. These provisions will be contained in the Manual.
4. Division 24 - Masonry, Table 24-H, Note No. 5: Shear walls which resist seismic forces shall be designed to resist 1.5 times forces as determined by Sec. 91.2305 (d)2. The allowable shears in Table 24-H are lower than the UBC values. The manual will use shear values from the UBC but will require the 1.5 factor for overturning.
5. Division 25 - Wood, Table 25-H,-Allowable Shear for Diaphragms and Shear Walls: This table sets forth allowable shear values for 1" and 2" straight sheathing, 1" and 2" diagonal sheathing, fiberboard wall, sheathing, expanded metal lath with cement plaster, gypsum lath and plaster, and gypsum wallboard. Several clarifying notes are appended. Table 25-C contains relative strength values of bolts, nails, screws and connectors in different species of wood. The shear values in Table 25-H are at variance with the UBC. However, the format is excellent and will be incorporated in the manual. No similar table to 25-C is contained in the UBC - it therefore will be printed in the manual.

6. Sec. 91.2512(b) Design Considerations: Wood diaphragms and wood shear walls shall be considered flexible and shall not be used to transmit rotational forces unless otherwise approved. Wood diaphragms in houses are not necessarily flexible, therefore, the manual will present some design criteria.

HUD Minimum Property Standards (MPS) (1973 Edition)

A preliminary review of the MPS has been completed and several sections may be affected by the manual. In addition some general comments were offered by the contractor which will not affect the manual directly, but may affect implementation of its requirements. Specific commentary will not be known until the manual is fully developed. It is intended to then reference the manual in the MPS manual of Acceptable Practice with applicable commentary.

Conclusion

It has been the intent of the author to present a status report on the research project undertaken by the Applied Technology Council for HUD. Major pertinent areas of concern and conflicts between various building codes under which most U.S. housing is constructed, are discussed with an attempt made to present their treatment in the proposed "Manual of Recommended Construction Practice for Earthquake Resistant Residential Dwellings."

The paper was prepared from a review of draft documents submitted by the subcontractor: Ralph W. Goers and Associates, Sherman Oaks, California to Mr. Roland L. Sharpe, Executive Director of the Applied Technology Council, Palo Alto, California. This review and analysis of recommendations are solely the interpretation of the author and do not necessarily reflect the official position of the U.S. Department of Housing and Urban Development, the Applied Technology Council, or the subcontractor.

ATC-4-SCA1
"MANUAL OF RECOMMENDED CONSTRUCTION PRACTICE FOR
EARTHQUAKE RESISTIVE RESIDENTIAL DWELLINGS"

GENERAL

1. What building code (or codes) are used in your area? _____

2. If the code utilized is local, is it based on:
A. BOCA _____
B. Southern Building Code _____
C. Uniform Building Code _____
D. Other (specify) _____
3. A. Snow load or roof live load is _____ psf.
B. Wind load (not zone) for lowest building is _____ psf.
C. Residential floor live load is _____ psf.
4. Is residence roof and floor framing "designed" (by span tables or actual engineering)? Yes _____ No _____
5. What seismic zone are you in (if known)? 0 _____ 1 _____ 2 _____ 3 _____
6. Are small commercial buildings in your area required to be engineered by a licensed engineer? Yes _____ No _____
If yes, are wind or seismic designs required? Yes _____ No _____
7. Are residences and tracts plan checked? Yes _____ No _____
By whom? Licensed engineer _____
Licensed architect _____
Unlicensed personnel _____
8. What is your estimate of the percentage of tract type housing designed by -
Architects _____ %
Building Designers _____ %
Drafting services _____ %
Contractor employee _____ %
Other (specify) _____

9. What percentage of homes in your area are "split-level"? (Split-level: two or more floor elevations approximately one-half story apart in height) _____ %

ROOF AND FLOOR FRAMING

1. Are any systems other than wood frame used for floor and roof framing? (Specify) Material
Roof: _____ % used
Floor: _____ % used
2. Are roof truss designs normally engineered by the fabricator?
Yes _____ No _____
3. What is the weight range of roofing materials used?
Material Weight
Heaviest _____ psf
Lightest _____ psf

4. Is blocking between wood framing members required at

Roof Yes _____ No _____

Floor Yes _____ No _____

5. Listed in descending order of use (most common first) what sheathing materials are used?

Roof

Floor

_____	_____
_____	_____
_____	_____

6. What species and grade of lumber are most commonly used for roof and floor framing?

Species	<u>Roof</u>	Grade	Species	<u>Floor</u>	Grade
_____	_____	_____	_____	_____	_____
_____	_____	_____	_____	_____	_____
_____	_____	_____	_____	_____	_____

7. Are you familiar with the terms roof and floor diaphragms? Yes ___ No ___
At what size building do you almost always require they be designed? _____

8. What percentage of roof framing utilizes prefabricated roof trusses?
_____ %

WALL FRAMING

1. Please list the types of wall framing and exterior finishes used in your area with your estimate of the percentage of tract type homes built using that system. (Examples: Brick Masonry, Block Masonry with or without interior furring, wood studs with all walls veneered, wood studs and fiberboard, etc.)

	<u>Materials</u>	<u>Percentage</u>
A.	_____	_____
B.	_____	_____
C.	_____	_____
D.	_____	_____
E.	_____	_____
F.	_____	_____
G.	_____	_____

2. What types of interior finishes are commonly used in your area?

	<u>Materials</u>	<u>Percentage</u>
A.	_____	_____
B.	_____	_____
C.	_____	_____
D.	_____	_____
E.	_____	_____

3. Are masonry exterior walls in residential construction

- A. Fully reinforced _____
- B. Partially reinforced _____
- C. Unreinforced _____

4. Are all masonry walled houses (exterior and interior) built with any frequency in your area? Yes _____ No _____
5. Do you require dowels to the footing to match vertical reinforcing in
 A. Residence Yes _____ No _____
 B. Commercial Buildings Yes _____ No _____
6. Species and grade for wood studs are

7. Are methods of attachment of wood stud wall finish material specified in your code? Yes _____ No _____
 If yes, do these requirements pertain to residences? Yes _____ No _____
 By your best estimate, are these requirements met in the field (for residences)? Yes _____ No _____
8. What type, size and spacing of sill plate attachment (to foundation or slab) do you require?

9. Although this question is difficult to estimate, we ask your indulgence. For the average one-story house and the average two-story house, if a horizontal line were drawn across the front and rear elevations (first floor for two-story) such that as much of the line as possible crossed windows, doors and other openings, what percentage of the line would be across such openings?

	<u>One-story</u>	<u>Two-story</u>
Rear Elevation	_____	_____
Front Elevation	_____	_____

FOUNDATIONS

1. Are slabs on grade used in your area? Yes _____ No _____
 If so, what is required thickness? _____
 Are they required to be reinforced? _____
 Type of reinforcing? _____
2. What percentage of homes in your area have basements? _____ %
 Are basement walls - Concrete _____
 Masonry (type) _____
 Other (specify) _____
 Is reinforcing steel required? Yes _____ No _____
 What reinforcing? _____
3. What is minimum size footing required?

	<u>One-story</u>	<u>Two-story</u>
Depth below grade:	_____	_____
Width:	_____	_____

4. What is frost line depth? _____
5. Are exterior footings normally
- A. Full width pour _____
 - B. Footing and footing wall _____
 - C. Other (Specify) _____
6. Is reinforcing normally required in footings? Yes ____ No ____
If so, what and where _____
7. Are houses frequently built in your area with the lowest story one half story below grade? Yes ____ No ____
- Are one or more sides frequently at grade when this construction is used? _____

Will you include, please, any "hand-out" sheets or other information pertaining to residential construction, fireplace construction, foundation requirements, etc. which your department utilizes?

SPECIAL CONDITIONS IN YOUR AREA -- OR OTHER COMMENTS --

by

Seiichi Inaba
National Research Center for Disaster Prevention
Science and Technology Agency

ABSTRACT

In Japan, it is necessary to build an increasing number of nuclear power plants in order to overcome the energy problem. Also, an increasing number of large oil tanks have been built in order to increase the amount of standard crude oil. It has, therefore, become important in engineering to design aseismic structures for nuclear power plants, oil plants, gas tanks, and other industrial plants for the purpose of preventing disasters due to the earthquake. Under these circumstances, several dynamic tests of plant structures have been conducted by using a large-scale shake table of the National Research Center for Disaster Prevention (VRCDP) in Tsukuba New Town. This report will present in general the results of dynamic tests on a graphite shielding structure, oil tanks, fuel assemblies of nuclear reactor, and a container vessel of thin shell.

Key Words: Aseismic Design; Dynamic Tests; Nuclear Reactors; Oil Tanks; Power Plants; Shake Table.

Introduction

A large-scale shake table, of the NRCDP, was built in 1970. Since then, a number of vibration tests on structures have been conducted under a joint research program with engineers of other research organizations. Most of the dynamic test projects have been related to problems concerned with soils, soil-structures, and soil-structure interaction. Some of the test results have been reported at a previous Joint Panel on Wind and Seismic Effects.

Dynamic Test of a Graphite Shielding Structure

The dynamic test of a graphite shielding structure, used for fast reactors, was conducted by the Power Reactor and Nuclear Fuel Development Corporation and the Building Research Institute in June, 1971, using the large-scale shake table of NRCDP.

The graphite shielding structure is a masonry-type structure, composed of a great number of graphite blocks to fill the space between the reactor vessel and a safety vessel. It is necessary to leave gaps between the blocks in order to account for dimensional changes due to thermal expansion and radiation effects. The graphite blocks are connected by graphite shear keys, and the outside rows of the blocks are linked by steel pins to the safety vessel.

Aseismic stability of this structure was to be obtained directly from the vibration test, because it is difficult to theoretically analyze structures with many gaps. The half scale model of the graphite shielding structure was built using the same materials as those of the prototype. Eleven layers of the graphite blocks were piled up and jointed to a cylindrical cell of 3200 mm in outer diameter, 2270 mm in inner diameter, and 1067 mm in height.

The model structure was tilted 30 degrees and then 45 degrees on the shake table in order to apply the lateral force for a static test. Dynamic tests were conducted by inducing sinusoidal waves of various frequency range including the design earthquake waves. Measurements of stresses in the representative blocks and keys, stresses of the pins, relative displacements of the blocks, and accelerations of the graphite blocks were made throughout during the tilting test and the vibration test. After completion of these tests, an ultimate strength test was conducted by applying static loads, to determine the ultimate strength of several graphite blocks of 1 or 3 layers and 3 rows connected by the shear keys and pins.

The results of the ultimate strength test showed that the ultimate limit acceleration of the blocks corresponds to the collapse mode around the pin hole, (the limit acceleration for the pin) this limit acceleration was 52.4 g and the ultimate limit acceleration of the blocks, corresponding to the collapse mode around the key way, (the limit acceleration for the key) was 57.3 g.

The results of the static tilting test indicate that the limit acceleration for the pin key were 31.8 g and 56.9 g respectively, as obtained from the measured stress values due to the lateral force of 45° inclination. Therefore, the stress concentration on the model structure for the actual number of rows was greater than that of three rows. The dynamic amplification was determined from vibration tests data, and the values for the pin and for

key were 6.8 and 3.5 respectively. Thus, the limit acceleration for the pin was 4.7 g and that for the key was 16.3 g. The vibration test of the 1/2 scale simulation model shows that the limit acceleration was 4.7 g, which is equivalent to 2.3 g on the prototype structure according to the similarity law.

The results of the response analysis of the reactor building and the safety vessel supporting the graphite shielding structure indicate that the maximum response acceleration of a design earthquake (0.15 g at the base of the building foundation) was 0.43 g at the elevation of the graphite shielding structure.

From these results, it is considered, therefore, that the graphite shielding structure was aseismic. The safety vessel had high stiffness and the earthquake response of the vessel was uniform in the vertical direction. The effect of insufficient number of layers for the model can be ignored. The design of the graphite shielding structure can be applied to other areas of greater earthquake design for this reactor, if the pin is reinforced.

Dynamic Test of Fuel Assembly for Nuclear Reactor

The fuel assembly of a nuclear reactor is one of the most important parts of the reactor, as it contains the boiling water, and, thus, it is necessary to evaluate its dynamic characteristics. The dynamic test of such a fuel assembly, was conducted by Hitachi and the NRCDP in June, 1974.

A unit of 4 fuel elements was used for the test, and had a dimension of 4,500 mm in length, containing 49 fuel rods inside the channel box with dimension of 138 mm and 2.03 mm in thickness. The model fuel rods were made from lead, which had a density approximately equivalent to that of uranium dioxide. The four fuel element unit was fixed to the supporting system inside a steel tank, which had a dimension of 800 mm in diameter and 5200 mm in height.

The lateral vibration forces were applied at two horizontal directions 0 degree and 45 degrees. These angles were between the side of the fuel element and the direction of the dynamic force. The influence of the inserted control rod insert and the gap between the fuel elements was studied. The effects of the boiling water inside the reactor core were also examined by filling the tank with water and thus simulating submerged conditions.

The upper joints of the fuel element are composed of channel fasteners with the upper lattice panel and channel fasteners (designated as a spring joint) was fixed by a spring in the original design. The tests were conducted using a wedge type fastener in order to study the influence of the fixed supporting system (designated as a pin joint).

The dynamic response of the structure was measured by accelerograms attached to the fuel assembly, tank, and the shake table. Sinusoidal waves, with a frequency range between 3.0 and 8.0 Hz at a sweeping speed of 0.025 Hz/sec, were induced for the vibration tests. The input accelerations were between 0.1 g and 0.3 g and were chosen in order to test the influence of the various vibrational forces on the response structure. The design earthquake response waves, obtained from the analysis, were also applied to the model structure under several maximum acceleration steps.

There was not much difference in the frequency characteristics, for the test results, when considering high to low frequencies. This means that the non-linearity of the upper spring joint was not as assumed. The acceleration perpendicular to the direction of the dynamic force of the vibrating elements was $1/3$ of that of the direction of table vibration. The measured accelerations during the 45 degree vibration test was smaller than those during the vibration of the 0 degree test, with the difference becoming smaller between the test values, as the vibration force was increased. The dynamic amplification ratio was greater for the 0 degree test than for the 45 degree vibration test. For the tests with the spring joint system, the resonant frequency became higher and the amplification ratio increased with an associated increase of the applied force. In the case of the pin jointed system, the amplification ratio of the elements was constant even when the applied input force was increased. The resonant frequency of the fuel assembly, with inserted control rods, was not different from that of the structure without control rods. When the fuel assembly was immersed into the water, the amplification factor of the fuel element with control rods was reduced to a range between $1/2$ to $1/4$ of that of the element without control rods. The data indicate that the control rods can cause damping, and thus will reduce the dynamic response due to earthquake. The amplification ratio obtained from the earthquake vibration tests were between 1.1 and 1.3, and thus the dynamic amplification ratio of 2.0 used for the actual design of fuel element is conservative.

The results of the dynamic tests show that it is necessary to design the structural fuel assembly, without control rods and with the force direction at 0 degrees. The non-linear characteristics of the fixed joint system causes no problem on the response analysis under the comparatively greater design accelerations and also when the fuel assembly is submerged into the water.

Dynamic Test of Thin Shell Container Vessel

The container vessels for the nuclear reactor are shell type vessels with additional structure elements inside the wall. It is generally assumed that such vessels will show a complicated dynamic response due to earthquakes. The dynamic test of a model thin shell container vessel was therefore conducted by the Hitachi and the NRCDP in July, 1974 after completion of the fuel assembly act.

The model structure was domed shaped and had a dimension of 2400 mm in diameter, 3600 mm in height and 2 mm thick, and was made of vinyl chloride resin. The model had a circular flange bonded to the bottom of the vessel which was then bolted to the large-scale shake table. The model container vessel had supplementary weight inside the shell wall and a stiffener belt outside the vessel. The model was subjected to sinusoidal vibration waves forcing out various frequencies and acceleration.

The accelerations of thin shell in the normal direction and the stresses of the shell in radial and vertical directions were measured using accelerograms and strain gages.

The results of the dynamic tests indicate that the vibrational behavior of the this shell type vessel simulates beam type vertical vibrations. The resonant frequency was approximately 19 Hz, which was not influenced by the supplementary weight or by the

stiffener. In the range of the low frequencies shell type characteristic vibrations were noted but the amplifications were smaller than those observed for the beam effect. The shell response increases the resonant frequencies but reduced the dynamic amplification in the lower frequency range.

Dynamic Test of Oil Tank

In order to increase the crude oil reserve in Japan, it is necessary to build super-scale crude oil storage tanks. The dynamic test of a model oil tank, was therefore conducted in order to confirm the aseismic stability of floating roof tanks. Such tanks are considered to be suitable for super-scale oil tanks. The dynamic test of a model tank was conducted by Nippon Kokan (NKK) and the NRCDP in February, 1974.

The purpose of the test was to establish the sloshing movement of fluid in the tanks, examine the stresses in the shell wall, and to design the aseismic floating roof tanks. The wave heights of the fluid, the dynamic pressure, the velocity, and the strains in the tank shell were measured to obtain the dynamic characteristics of the tank and the contained fluid. Sinusoidal, triangular and rectangular waves were applied for the dynamic test, as were earthquake simulated waves of six representative earthquakes.

Three model tanks were built on the shake table. A cylinder type model used for a sloshing test had a diameter of 2860 mm, a height of 1219 mm and a steel plate thickness of 4.5 mm. The rectangular type model also used for sloshing test had a length of 2000 mm, a width of 1000 mm, a height of 1000 mm, and a steel plate thickness of 4.5 mm. The third model was a cylinder type which had a diameter of 2190 mm, a height of 914 mm, a steel sheet thickness of 0.4 mm and was constructed for the dynamic tests. The cylinder type model tank used for the sloshing test was also used to determine the damping effects of a floating roof with damping fins. The results of the dynamic tests showed that the stresses in the cylinder wall due to the vibrational force were greater than those assumed from the analyses. The wall stresses due to sloshing fluid however were less than the stresses assumed from the analysis. The natural frequency of the sloshing fluid was in good agreement with those obtained from the theoretical analysis. When sinusoidal waves representing the natural frequency of 0.5 Hz for the first mode, 1 Hz of the second mode, and 1.2 Hz of the third mode were applied to the model tank, the sloshing phenomena in resonance were caused by the vibration of the sinusoidal waves. No sloshing phenomenon was observed in the range of frequency which were different from the natural frequencies.

In order to reduce the sloshing movement of the fluid surface, dynamic tests were conducted for the following cases; (1) using a floating roof, with fins for damping, (3) using a floating with water on the top of the roof. The result of the tests with a floating roof, showed that the damping coefficient was not different from that of the free surface fluid. In the case of the test for a tank with a floating roof with damping fins, the damping coefficient of the sloshing was three times as much as that of free surface sloshing. In the case of the test for tanks with a floating roof with water on the top as weight, the damping coefficient was two times as much as that of the free surface sloshing. This means

that the damping fins are quite effective in reducing the sloshing movement.

Conclusion

This paper has briefly described the dynamic tests using the large-scale shake table of the NRCDP, and the obtained results on structures for nuclear power plants and oil tanks, these tests are quite important in order to prevent disasters due to the earthquakes.

The oil tank fires, due to the Niigata Earthquake in 1964, and the crude oil leakage and pollution caused by the collapse of tanks in the Inland Sea in Okayama in 1974, and the possible Kawasaki Earthquake predicted from data on ground upheaval, have aroused concern in the field of earthquake engineering and in the aseismic stability of structures in industrial plants. However the industry and private organizations are primarily responsible for the design of such structures and the government institutions can only regulate the design of such structures. It is therefore necessary to develop the theoretical analysis of the dynamic behavior of plant structures and also to test large-scale structure on a shake table. In addition, it is necessary to improve the shake table, development of techniques for dynamic tests, and studies regarding simulation and modeling.

The Resources and Energy Agency of the Ministry of International Trade and Industry has appropriated part of the funds to build a new large-scale shake table in their budget for the fiscal year of 1975-1976. The shake table, of dimension of 30 m square can support a test structure of 1000 tons and was built for the dynamic testing of structures for future nuclear power plants. However, there are still many problems concerned with the construction of such super-scale shake tables.

It is hoped that by exchanging technical information through the Joint Panel on Wind and Seismic Effects, many of these problems can be solved.

Bibliography

Kawaguchi, O., Watabe, M., et al., "Special Aseismic Design Engineering and Development for Fast Reactor", Proceedings Vol. I, Engineering of Fast Reactors for Safe and Reliable Operation, Karlsruhe, 1973.

SHEET PILE FOUNDATION AND ITS STRUCTURAL
CHARACTERISTICS AGAINST HORIZONTAL LOADS

by

Kenji Kawakami
Tadyoshi Okubo
Keiichi Komada
and

Michio Okahara
Structures & Bridges Division
Public Works Research Institute
Ministry of Construction

ABSTRACT

The general response of sheet pile foundations, relative to analytical and experimental studies, are discussed. Test results are given, in addition to the development of general design equations.

Key Words: Foundation; Lateral Loads; Sheet Piles; Structural Analysis; Tests.

1. Introduction

Sheet pile foundations consist of steel piles with joints, driven into the ground to form a closed unit. This is a unique foundation structure and was developed by the Japanese steel manufacturers. Since this foundation uses steel piles, it has advantages in that the work can be mechanized and completed within a shorter period of time and that the dimensions and penetration length of the foundation can be freely chosen. The enclosure of the sheet piles also can be used for a cofferdam by making their joints watertight.

The sheet pile foundation was first used in 1965, for the foundation of blast furnaces, and was used for bridge construction in 1969. Owing to its outstanding advantages, the sheet piling method has been used in the construction of some 148 foundations for 40 bridges, and it will probably be used more frequently in the future. This method has primarily been used for such cases that cannot use caissons or piled foundations, because the ground and water depth conditions are poor and the dimensions are large.

The sheet pile foundation is considered to be a structure having mechanical characteristics intermediate between the caisson foundation and piled foundation. It is therefore, necessary to establish more efficient design of the sheet pile foundation, by making further investigations on its mechanical characteristics.

In this paper, we would like to discuss the structure of the sheet pile foundation, the presently used design method¹⁾, past performances, and the results of in-site experiments. Also to be presented will be the results of an analysis we have made in an attempt to clarify the structural characteristics of the sheet pile foundation. The sheet pile foundation has such complicated structural characteristics, that we have advanced only one step in its investigation.

We will not discuss the use of the sheet pile foundation for cofferdam, in this paper.

2. Sheet Pile Foundation Structure⁽¹⁾

2-1 General Definition

The sheet pile foundation is defined as a structure that forms a circular, elliptical or rectangular enclosure with steel-pipe or H-shaped steel piles driven into the ground. Their heads are rigidly connected, and the joints are so treated that the required horizontal resistance and vertical bearing capacity is developable. As will be seen from the examples given later, it can be said that steel-pipe piles can be used in many instances. As for the treatment of the joints, they are grouted with mortar to prevent the passage of water, because the sheet pile foundation is also used to serve as a cofferdam. The grouting of the joints with mortar, although it is a technically difficult work, is employed because the weak points of the sheet pile foundation lies in the joints and its strength can be increased by the treatment of such joints. Much is expected in the development of efficient joints for the future.

2-2 Material

The material that is used for the sheet pile foundation is steel, which has sufficient strength, quality and sectional characteristics to satisfy its structural configuration. As a rule, the steel shall be over 8 mm in thickness. The sheet pile

foundation utilizes steel piles or H-shaped steel sheets, whose shapes and dimensions are described at the end of this paper. The shapes of steel piles and joints are shown in Fig. 2-1 and their dimensions and weights are given in Table 2-1. Typical values are given in the figure 2-1. The steel used in the making of the sheet piles are defined by JIS A5528 and is as follows.

Steel-pipe piles: SY24

H-shaped steel sheet piles: SY30, SY40

The allowable stress intensities for the steel piling, as given in the chapter devoted to surveying and designing in the Specifications for Substructure Design of Highway Bridges, are given herein in Table 2-3.

2-3 Structural Types

The sheet pile foundations can be classified by shape into two types, that is, the well type which is formed with the piles of equal length driven to the bearing stratum and the pronged type in which some of the piles are driven to the bearing stratum. These two basic forms of sheet pile foundations, can be further divided into several types according to the cross sectional contour, number of foundations, and joint grouting method as shown in Table 2-4.

As was mentioned previously for the well type, all the piles are driven to the bearing stratum and the head of piles are rigidly connected by a footing. However, when the bearing stratum is located at a relatively great depth, it has greater vertical load bearing capacity than horizontal capacity. In such cases it is more economical to employ the pronged type, in which some piles are driven to the bearing stratum while others are stopped midway between the ground surface and the bearing stratum, thereby reducing the quantity of steel piling.

The sheet pile foundations can have such cross sectional contours as circular, oval and rectangular, as illustrated in Fig. 2-2. In the case of caisson foundations, the cross sectional contour greatly influences the speed at which the construction work can be conducted. In this method, however, the work differs little from the conventional piling work, therefore the cross sectional contour arrangement has little influence on the speed of construction.

The sheet pile foundations can be divided into five types, as illustrated in Fig. 2-3, according to the differences in the head and coffering. Class (1) is called the "rising" type, in which the footing is above the water surface. Class (2) is called the "closing" type in which a closing wall is built independent of the foundation body and footing. Class (3) is called the "coffering" type, in which the sheet piles rise above the water surface to form a cofferdam and the coffering parts of the sheet piles are above the water, after the foundation body and footings are completed. Class (4) is called the "semi-rigid" type, in which the inside of the wall is partially excavated and filled with concrete. Class (5) is called the "rigid" type, in which the inside of the well is excavated down to the bearing stratum and filled with concrete.

The sheet pile foundation was used as a foundation for the first time in conjunction with the blast furnaces at the Mizushima Iron Works of Kawasaki Steel Corporation. In addition, after repeated tests on models and actual sheet pile foundations, this method was used in the construction of bridges for the first time on the Ishikari Kako Bridge (Hokkaido), 1969) and then for the Omigawa Bridge (Chiba Prefecture, 1970) and the Senbonmatsu Bridge (Osaka City, 1970).

As noted the first application of this method was in the construction of a blast furnace foundation, with the development and research of the sheet pile foundation conducted by several major steel manufactures. Apart from the blast furnace foundations, this method was also used in various civil engineering works, such as dolphins and scale pits at the iron works. At that stage, development and research projects were conducted, thereby developing the fundamental techniques for its application in the construction of bridge foundations.

The sheet pile foundation, is considered to have a rigidity close to that of the caisson foundation, and can be built almost in the same manner as the piled foundation and is well suited for labor-saving and rapid construction work. This method has so many advantages, that the Ministry of Construction granted research subsidies to the steel manufactures in 1969, in order to encourage their research relative to the workability and structural characteristics of sheet pile foundations. In this relation, the steel manufacturers took the initiative to form a sheet pile foundation research committee which included university professors and government officials, in order to conduct the four research projects⁽³⁾. These projects were; (1) investigations on pile driving accuracy, (2) the water seepage prevention, (3) the integrity of piling and concrete grouting, and (4) vibration characteristics. As a result of these studies, the "Specification for Designing and Construction of Sheet Pile Foundations" was published in January, 1972. Although this is a Specification, which was developed from nongovernment basis unlike the technical standards set up by the Ministry of Construction i.e. the Specification for Highway Bridge Design and the Specification for Substructure Design of Highway Bridges, it has been widely used in the actual design and building of bridge foundations.

One of the most outstanding features of the sheet pile foundation is that the coffering method can be used. As a matter of fact, this particular type has been used in most of the sheet pile foundations constructed. Fig. 2-4, shows the steps involved in construction of this type of the sheet pile foundation. The building of a pile foundation in water requires a cofferdam, a great deal of money, and takes a long time to complete the work when the water is deep. The mechanical stability of a cofferdam is not fully understood. In this foundation type, the cofferdam is built with the same structural material as the foundation body, therefore, it has a very high degree of safety. It is possible to further increase the safety by filling the gaps between the cross beams of H-shaped steel sheet piles and steel-pipe piles, thereby integrating the timbering and cofferdam. If the sheet pile foundation is to be effective as a

cofferdam, it is necessary to have watertightness of the joints, and have a proper technique in cutting of the steel pipe piles in water in order to have an efficient and economical product.

3. Designing of Sheet Pile Foundations

3-1 Fundamentals of Design

The basic principles to be considered in the design of sheet pile foundations are listed below;

- (1) The maximum ground reaction on the well bottom and at the distant ends of the prongs of sheet pile foundations must not exceed the allowable bearing capacity of the ground at the given position.
- (2) The shear resistance on the well bottom of a sheet pile foundation must not exceed the allowable shear resistance between the well bottom and the ground.
- (3) The displacement of a sheet pile foundation must be considered, by considering the allowable amount of displacement that is determined in relation to the superstructure.
- (4) The intensity of stress, in the various parts of a sheet pile foundation, must not exceed the allowable stress intensity.
- (5) Since the horizontal resistance of a sheet pile foundation is treated as a beam on an elastic foundation, as in the case of a piled foundation, there is no need to consider the ground reaction on the front surface of the foundation.
- (6) In the case of a sheet pile foundation, whose displacement is large and natural frequency is long, it is preferable, if the responsible engineer deems it necessary, to make a dynamic analysis, such as analysis will take the superstructure into consideration, and to make a comprehensive study of displacements and stresses in the structural members.

3-2 Determination of Load

The loads to be used in the design of sheet pile foundations shall comply, as a rule, with Chapter 2 "Loads" in the part devoted to investigations and design in general in the "Specification for Substructure Design of Highway Bridges" and Chapter 3 "Loads" and Design Conditions to be Considered in Earthquake Resistant Design in the "Specification for Earthquake Resistant Design of Highway Bridges".

The loads to be considered include live loads, dead loads, earth pressures, water pressures, buoyancy, effects of temperature changes, effects of earthquakes, snow load etc.

3-3 Allowable Vertical Bearing Capacity

The allowable vertical bearing capacity shall be determined, taking into consideration the degree of importance of the structure, as follows;

- (1) Vertical load test
- (2) The formula for statical bearing capacity
- (3) Estimated values when the values are proven correct
- (4) Formula for the statical bearing capacity

When calculating the allowable vertical bearing capacity, several formulas, not merely one formula, should be used so that a comprehensive study may be made from the results of all such calculations. The allowable bearing capacity is a value to be obtained by dividing the ultimate bearing capacity, obtained from the statical formulas, by a safety factors given in Table 3-1.

The conception of the bearing area, when calculating the bearing capacity of the ground and the bearing capacity calculation formulas, are shown in Table 3-2. The symbols used in Table 3-2 are as follows;

Ra: Allowable bearing capacity of a sheet pile (kg)

S: Safety factor

ℓ_1 : Length of penetration of well (cm)

ℓ_2 : Length of prong (cm)

U: External circumference (cm)

U_o : Circumferential length of prong (cm)

n_1 : Number of sheet piles forming the well

n_2 : Number of prongs

qd: Ultimate bearing capacity of the ground at the distant end of sheet pile (kg/cm²)

f: Frictional force on the circumferential surface of well (kg/cm²)

f_o : Frictional force on the circumferential surface of prong (kg/cm²)

3-4 Horizontal Resistance

(i) Flexural rigidity

The flexural rigidity is considered to vary according to the treatment of the joints between the sheet piles, the treatment of the heads of sheet piles, the type of soil, and the shapes and dimensions of the sheet pile foundations.

As a matter of convenience, the flexural rigidity can be obtained by using the following formula as obtained from the experiments;

$$E_I = E \left(\sum_{i=1}^{n_1} I_i + \mu \sum_{i=1}^{n_1} A_i y_i^2 \right) \quad (3-1)$$

where

E: Elastic modulus of sheet pile (2.1 x 10⁶ kg/cm²)

I: Moment of inertia of sheet pile foundation (cm⁴)

I_i : Moment of inertia of i-th sheet pile (cm⁴)

n_1 : Number of sheet piles

A_i : Sectional area of i-th sheet pile (cm²)

y_i : Distance of i-th sheet pile from the center axis of sheet pile foundation (cm)

v: Composite efficiency of sheet pile foundation (0 to 1.0).

The reference values are shown in Table 3-3.

(ii) Coefficient of ground reaction

The coefficient of the ground reaction, is defined as the split line gradient of the load-displacement curve. That is,

$$K = \frac{P}{y} \quad (3-2)$$

where

K: Coefficient of ground reaction (kg/cm^3)

The ground reaction coefficients include horizontal ground reaction coefficient (K_H), vertical ground reaction coefficient (K_V), and horizontal shear spring coefficient (K_s).

P: Load intensity (kg/cm^2)

y: Amount of displacement (cm)

(1) Method of estimating the ground reaction coefficient, in the well type of sheet pile foundation

o Method of estimating the horizontal ground reaction coefficient

$$K_{H1} = K_{H0} \left(\frac{B}{30} \right)^{-\frac{3}{4}} = 12.8 K_{H0} B^{-\frac{3}{4}} \quad (3-3)$$

where

K_{H1} : Horizontal ground reaction coefficient (kg/cm^3)

K_{H0} : This is the horizontal ground reaction coefficient (kg/cm^3) which is equivalent to the value obtained by the plate loading test using 30 cm diameter rigid disk and can be expressed by the following formula including the 20% share by the side.

$$K_{H0} = \frac{1.2}{30} \alpha E_o = 0.040 \alpha E_o$$

B: Load width (cm)

E_o : Modulus of deformation of ground (kg/cm^3) measured or estimated by the methods shown in Table 3-4.

α : Coefficient which are used normally or at the time of earthquakes. Shown in Table 3-4.

o Vertical ground reaction coefficient

$$K_{V1}, K_{V2} = K_{V0} \left(\frac{B_v}{30} \right)^{-\frac{4}{3}} = 12.8 K_{V0} B_v^{-\frac{4}{3}} \quad (3-4)$$

where

K_{V1} : Coefficient of vertical ground reaction at the well bottom (kg/cm^3)

K_{V2} : Coefficient of vertical ground reaction at the prong end (kg/cm^3)

K_{vo} : The vertical ground reaction coefficient (kg/cm^3) equivalent to the value obtained by the plate loading test using a 30 cm diameter disk and can be obtained by the following formula.

$$K_{vo} = \frac{1}{30} \alpha E_o \quad 0.033 \alpha E_o$$

B_v : Equivalent load width of foundation (cm), which can be obtained by the following formula.

$$B_v = A_v$$

E_o : Modulus of deformation of ground measured or estimated by the methods shown in Table 3-4 (kg/cm^3)

α : Coefficients to be used normally or at the time of earthquakes. Shown in Table 3-4.

A_v : Base area surrounded by the outer and inner circumferences of the foundation (cm^2)

When the ground beneath the base of the sheet pile foundation changes in the direction of the depth, or when there exists a particularly weak stratum, the following should be considered;

o Horizontal shear spring coefficient

$$K_s = \lambda K_v l$$

K_s : Shear spring coefficient of the well bottom (kg/cm^3)

(iii) Calculation of horizontal resistance

Assuming the sheet pile foundation to be a beam on an elastic foundation, its horizontal resistance shall be obtained by the following formula.

$$EI \frac{d^4 y}{dx^4} = -ky \quad (3-5)$$

where

k : Horizontal ground reaction coefficient (kg/cm^3)

y : Amount of displacement (cm)

x : Depth from the ground surface (cm)

Both the well type and the pronged type of the sheet pile foundation shall be such a structure that there exist a horizontal spring, vertical spring and shear spring on its front, side and bottom. Furthermore, in the case of the well type, the bottom shall receive a vertical ground reaction proportional to the vertical displacement and a shear resistance proportional to the horizontal displacement.

When the penetration length is short for its rigidity, and the shear deformation is so large in amount that it cannot be ignored, the foundation must be designed by taking the shear deformation into consideration.

(1) Design of the well type sheet pile foundation

A mechanical model of this type foundation, is illustrated in Fig. 3-1.

o Basic Formulas

The following, are the basic equations relative to the model shown in Fig. 3-1.

$$\begin{aligned} EI \frac{d^4 y_0}{dx^4} &= 0 \\ EI \frac{d^4 y_1}{dx^4} &= -P \end{aligned} \quad (3-6)$$

where

$$P = E_s y_1 = K_H D y_1 \quad (\text{cm})$$

D: Load width of sheet pile foundation (cm)

y_0, y_1 : Displacement (cm)

The following are the general solutions to equations (3-6).

For the part above the ground

$$y_0 = A_0 x^3 + B_0 x^2 + C_0 x + D_0$$

For the part under the ground

$$\begin{aligned} y_1 &= e^{-\beta x} (A_1 \sin \beta x + B_1 \cos \beta x) \\ &+ e^{\beta x} (C_1 \sin \beta x + D_1 \cos \beta x) \end{aligned} \quad (3-7)$$

The unknown constants can be determined by substituting the following boundary conditions into the general equations;

$$\left. \begin{aligned}
x = -h & : -EI_{y0}'' = -M_0 \\
& -EI_{y0}''' = -H_0 \\
x = 0 & : y_0 = y_1, y_0' = y_1' \\
& y_0'' = y_1'', y_0''' = y_1''' \\
x = \ell & : -EI_{y1}'' = K_{v1} I_1 y_1' \\
& -EI_{y1}''' = -K_s A'_v y_1
\end{aligned} \right\} \quad (3-8)$$

However, when a tensile force is acting on the well bottom, the solution must consider I_1 (moment of inertia well bottom), and A'_v (effective loading area of well bottom), which ignore the part where the tensile force is acting.

3-5 Section Forces

The stress intensity in the vertical direction of the well type sheet pile foundation can be calculated, using the section forces of the well. Using the vertical force the horizontal force and bending moment working on the top of the well is then obtained, and then the stresses. When the composite efficiency exceeds 0.5, the equation (3-9) shall be used and when it does not exceed 0.5, equation (3-10) shall be used.

$$\sigma = \frac{V_0}{n_1 A_0} \pm \frac{M_0}{I} y \quad (3-9)$$

$$\sigma = \frac{V_0}{n_1 A_0} \pm M_0 \left(\frac{1-\eta}{\sum_{i=1}^n Z_i} + \frac{\eta}{Z} \right) \quad (3-10)$$

where

- σ : Stress intensity in the vertical direction (kg/cm^2)
- V_0 : Vertical force working on the top of the well (kg)
- A_0 : Sectional area of a sheet pile (cm^2)
- M_0 : Moment working on the top of the well (kg/cm)
- I : Moment of inertia (cm^4) with considering the composite efficiency (μ)
- y : Distance (cm) from the central axis of the well to the point where stress is calculated
- n_1 : Number of sheet piles in the well
- Z_i : Section modulus of each sheet pile (cm^3)
- Z_1 : Section modulus of the foundation when $\mu = 1.0$

n: Bending moment distribution constant which is determined by the composite efficiency, as shown in Table 3-5, for example.

μ	η
0.5	0.93

4. Past Pile Foundation Construction Projects (4)

Table 3-5

Important examples of sheet pile foundations, constructed prior to January 1975, are shown in Tables 4-1, 4-2, and 4-3. These tables show the project name, purchaser, location of work, starting date scale of work (basic sectional dimensions, sheet pile dimensions, number of foundations), the type of sheet pile (type, type of joints, length of joints), and the basic type. Table 4-1 shows those cases in which steel-pipe piles were used in the construction of bridge foundations. There are 37 bridges and 126 sheet pile foundations. Table 4-2 shows the cases in which steel-pipe piles were used in the construction of blast furnace foundations and other foundations. There are 14 cases and 59 foundations. Table 4-3 shows the cases in which H-shaped steel sheet piles were used. There are 6 cases and 32 foundations. A total of 148 sheet pile foundations were constructed for 40 bridges. As seen from these cases of sheet pile foundation projects, steel-pipe piles were used for most cases. There were very few cases in which H-shaped steel piles were used, and almost none in recent years. It is also noticeable that there is an increasing number of the cofferdam type, which is an important characteristic feature and merit of the sheet pile foundation.

Figs. 4-1 through 4-4 show the histograms, obtained from the data given in these tables. Fig. 4-1 shows a histogram representing rectangular or oval sheet pile foundations, using their largest width. Of the bridge foundations built with steel-pipe piles, there are 16 such foundations ranging from 10 to 15 m in width. Fig. 4-2 shows the circular-shaped sheet pile foundations, arranged by their diameters. In this instance, these are the only cases in which steel pipe piles are used. The foundations of this type, range from 5 to 10 m in diameter, and are used most often for bridges. There are as many as 30 such cases. Fig. 4-3 shows a histogram arranged by the sheet pile length. The sheet piles used most often for bridge foundations are 25 to 35 m in length. Fig. 4-4 shows a histogram arranged by the steel pipe diameter. The largest in number are the steel-pipe piles ranging from 800 to near 1000 mm in diameter. As many as 57 foundations fall into this category.

5. In-site Tests of Sheet Pile Foundations

Tables 4-1 through 4-3 show the sheet pile foundations which were constructed in the past and in-site tests (loading tests, vibration tests, in-site measurements of stresses), where the test results are rearranged in Table 5-1⁽⁴⁾, including 11 cases.

We will now discuss the results of tests conducted on the Omigawa Bridge, in which extensive data were collected. Fig. 5-1 shows a cross section of the foundation. The pile length varies from 42.6 m to 24.5 m and the foundation is of the pronged type. Fig. 5-2 shows the column section of the ground. Fig. 5-3 shows the load-displacement curve. The load was imposed in a horizontal direction around the middle of a bridge pier. The displacement measured was located in the horizontal direction at the top end of the bridge pier. When the load was 200 tons, the displacement was about 13 mm. It is noted that the curve is essentially straight, and it can be said that the test was conducted within the

elastic limits. Fig. 5-4 shows the load-angle of slope curve. The angle of the slope was measured at three points, that is, the top of the bridge pier, the top end of the top plate, and the bottom of the top plate. Fig. 5-5 shows the distribution of strains in the bridge pier. Fig. 5-6 shows the distribution of stresses in the sheet pile well. Fig. 5-7 shows the horizontal response curve for the top of the bridge pier. The natural frequency during this time was about 6Hz. Fig. 5-7 shows the vertical response curve for the bridge pier. The natural frequency at that time was about 4.5Hz.

6. Joint Characteristics of Sheet Pile Foundations⁽⁶⁾

6-1 Purpose of Joint Strength Tests

The sheet pile foundations consist mainly of steel-pipe piles driven into the ground to form a circular, oval or rectangular enclosures, with the piles being connected with one another by means of joints. Because of this connection, their structural characteristics are greatly influenced by the joints. This may be understood from the fact that the use of even the joints which have very low rigidity, gives the foundation a rigidity far greater than when no joints are used. However, the rigidity of the foundation as a whole is naturally smaller than when the joints are the same as in the case of the main pipe piles. The analysis of such a system taking into account the joint characteristics, is obviously an important item to be considered in designing sheet pile foundations. As was discussed in Chapter 3, the moment of inertia of the entire foundation is evaluated by the use of the "composite efficiency", and then assuming the foundation to be a beam on an elastic foundation. This method is very advantageous, due to its simplicity when the length is sufficiently large in comparison to the diameter. However, as the ratio of diameter to length approaches 1, it is difficult to apply this method of solution. This is because the shear deformation of the joint is ignored.

In order to consider the joint characteristics in the design of a sheet pile foundation, it is necessary to know the shear strength characteristics of the joint. There are various tests that can be performed to evaluate the shear strength of the joint. Two such tests have been conducted, as will now be described. In one test, three piles were connected in parallel and a punching load was applied to the middle pile in order to make a direct measurement of the shear strength of the joint. In another test, two piles were combined, one on top of the other to form a beam and a load is then concentrated in the middle thereof to determine the shear characteristics of the joint.

6-2 Direct Shear Test

As shown in Fig. 6-1, three piles were connected in parallel, with their joints grouted with mortar and a punching load applied to the middle pile. This test was conducted in order to obtain the relationship between the load and the amount of displacement of the piles in relation to each other. The shear stress in the joint was calculated, assuming a fracture between the steel material of the joint and mortar. There are many different shapes of joints. Used in these tests were pipe type and the CT type joints, which are shown in Fig. 6-2. The fractures considered are as illus-

trated, assuming the fracture of the joints to be the minimum area of contact, between the joint material and mortar. (The bond strength of mortar is sufficiently small compared with the compressive strength).

The results of the tests conducted on the pipe type joint will now be discussed.

Relative to the fracture of the pipe type joint, the shear strength per unit length Q and the shear stress per unit area can be easily calculated by the following formulas.

$$Q \text{ (kg/cm)} = \frac{P}{2L} \quad (6-1)$$

$$\tau \text{ (kg/cm}^2\text{)} = \frac{P}{2\pi DL}$$

where:

D: Joint pipe diameter (cm)

L: Joint pipe length (cm)

The results of the direct shear test will be graphically shown as the relationship between the superimposed load P , shear strength per unit length Q , shear stress per unit area τ and the amount of displacement between the joints. The amount of displacement and deformation between the joint and mortar, where they are in contact with each other, increased almost linearly until the load reached about 25 tons. Thereafter, it increased sharply and ruptured when the load was increased to about 50 tons. This occurred when maximum shear strength Q and maximum shear stress τ were about 250 kg/cm and 5 kg/cm², respectively. The compressive strength of the mortar which was used to grout the joints was $\sigma_{20} = 180 \text{ kg/cm}^2$.

Assuming that the mortar's Young's modulus is $E = 2.1 \times 10^5 \text{ kg/cm}^2$, the modulus of rigidity of the standard mortar G therefore is as follows;

$$G = \frac{E}{2(1+\nu)} = \frac{2.1 \times 10^5}{2(1+\frac{1}{6})} = 0.9 \times 10^5 \text{ kg/cm}^2 \quad (6-2)$$

However, from the test results, the modulus of rigidity G' can be calculated using the shear stress per unit area τ and the amount of displacement of the joints

$$G' = \tau/\gamma = \frac{1.0}{1 \times 10^{-3}/24.7} = 2.47 \times 10^4 \text{ kg/cm}^2 = \frac{G}{3.64} \quad (6-3)$$

From this result, it can be stated that the modulus of rigidity of the joints is considerably lower than the modulus of rigidity of the mortar.

6.3 Bending Shear Test

As illustrated in Fig. 6-4, two piles were combined, one on top of the other, with the joint grouted with mortar to form a beam. A concentrated load was then applied in the middle of the beam, which was freely supported in the bending shear test. Ten such tests were conducted. Various shapes of joints were used in the test, but consisted primarily of the pipe type joint and the CT type joint, which were also used in the direct shear test. The results of only one of the tests will be given herein due to space limitation. The relationship between the shear stress in the joint and the rate of decrease in the shear stress for the condition of a rigid connection is obtained from the test results. Therefore, a method which gives such a relationship obtained from the load-strain curve and a method of obtaining the information from the load-strain distribution in relation to the shear strength transmission coefficient α will be presented.

(1) A Method of Obtaining the relationship from the Load-strain Curve

The shear strength transmission coefficient α is defined as follows:

$$\tau(\text{kg/cm}^2) = \alpha \tau' \quad (0 \leq \alpha \leq 1) \quad (6-4)$$

in which τ is the joint shear stress in which the rigid connections are imperfect, and τ' is the joint shear stress between the two piles with rigidly connected. The moment of inertia I_0 would be as follows;

$$I_0 = 2I' + 2A' \left(\frac{d}{2} \right)^2 = \frac{3}{4} A' d^2 \quad (6-5)$$

where:

A' : Sectional area of a sheet pile (cm^2)

I' : Moment of inertia of a sheet pile (cm^4)

When a concentrated load P is imposed in the middle of the beam, the deflection of the centerpoint δ can be obtained as follows;

i) $\alpha = 0$ (No joint connection)

$$\delta = \frac{P \ell^3}{96 EI'} \quad (6-6)$$

ii) $\alpha = 1$ (Perfect rigid joint connection)

$$\delta = \frac{P^3}{48 EI_0} \quad (6-7)$$

iii) $0 < \alpha < 1$ (Imperfect rigid joint connection)

$$\tau = \alpha \frac{P}{2} \cdot \underbrace{\frac{A' \frac{d}{2}}{I_0}}$$

From the equilibrium of moment

$$\frac{dM}{dx} = Q - \tau \ell \frac{d}{2} = \frac{P}{2} \left\{ (1-2) \frac{1}{2} + a \frac{I'}{I_0} \right\} = \frac{P}{2} \beta \quad (6-8)$$

where:

$$\beta \doteq \frac{1}{2} - \frac{a}{3}$$

At this time, the deflection of the center point is

$$\delta = \frac{P \ell^3}{48 EI'} \cdot \beta \quad (6-9)$$

The joint shear strength Q is

$$Q = \frac{P}{3d} \cdot a \quad (6-10)$$

Thus, we can obtain the relations of P , δ and α .

(2) A Method of obtaining the Relationship from the Load-strain Distribution

Assuming two cross sectional strain distributions of the composite beam, that is, when the joint is imperfectly connected and when the joint is perfectly connected, the joint shear strength Q and the shear transmission coefficient α can be obtained as follows;

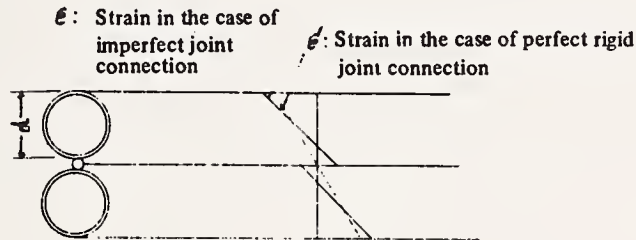


Fig. 6-5 Strain Distribution

$$Q = \int_0^d E \epsilon dx \quad (6-11)$$

α is determined from the strain distribution is defined as follows

$$\alpha = \frac{\int_0^d \epsilon' dx}{\int_0^d \epsilon dx} \quad (6-12)$$

As shown above, the shear strength transmission coefficient α can be obtained by two different methods from test results.

The bending test is illustrated in Fig. 6-6. In this test, the joint was a pipe type, and the relative size of the joint for the main pile is larger in comparison to an actual sheet pile foundation. The test results are given in Figs. 6-7 through 6-11. Fig. 6-7 shows the load-central deflection curve. It is seen that the experimental curve is approximately midway between the calculated values, in the case of rigid joint connection, and of no joint connection. When the steel material begins to yield, (the stress is about 2400 kg/cm²), the deflection increases substantially compared to an increase in load. Fig. 6-8 shows the load-deflection in the axial direction of the pipe. The values are measured to the left and right of the supports. Fig. 6-9 shows the load-strain distribution at a point 1 m away from the center point. When the load is small, the strain distribution is such that plane bearing occurs but as the load increases, the upper and lower piles gradually begin to show an independent strain distribution.

The relationship between the load and the shear strength transmission coefficient is shown in Fig. 6-10. The solid line, in this figure represent what was obtained from the load-strain curve given in Fig. 6-7. The broken line represents what was obtained from the load-strain curve given in Fig. 6-9. These two lines should agree with each other, but actually are wide apart from each other.

Apart from the above-mentioned test, ten other types of tests were conducted, and will now be described.

When the joint was not grouted with mortar, the strain distribution showed that the upper and lower piles behaved as an almost perfect single body. Examination of the load-strain curve shows that the experimental values are roughly in agreement with the calculated values for the case when there is no rigid joint connection.

None of the tests showed the results in which the two load-shear strength transmission coefficient curves were nearly in agreement with each other, but the two curves were considerably wide apart from each other. There seems to be a tendency that the shear strength transmission coefficient, which was obtained from the load-strain curve, is smaller than the actual value. The average of the load-shear strength transmission coefficient curves, obtained by the tests, is represented by the curve shown in Fig. 6-11. To obtain this curve, the shear strength of the joint (the shear strength when the joint is rigidly connected) was obtained assuming a joint fracture and it was replaced by the load.

7. New Approaches to Structural Analysis for Horizontal Resistance of the Sheet Pile Foundation (5)

7-1 Linear Interpolation Method (6) (7)

(1) Method of Analysis

The method of analysis to be used is based on the curve given in Fig. 6-11 which was obtained in the preceding chapter. The analysis of the sheet pile foundation with rigidly connected joints is obtained by U.L. Chang's formula. This formula is obtained by the group of piles method when the joints are not connected. They are linearly distributed by the shear strength transmission coefficient and thus the obtained values are taken as the analytical solution of the sheet pile foundation.

This value of α is determined from Fig. 6-11 by obtaining the joint shear stress when the joint is assumed to be rigidly connected.

The section forces of the sheet pile foundation when horizontally loaded can be obtained as follows.

(i) Section forces when the joints are rigidly connected

$$\left. \begin{aligned} I &= n I_i + \sum_i A_i y_i^2 \\ \beta &= \sqrt[4]{E_{s1} / 4EI} \\ E_{s1} &= K_B (D + d) \end{aligned} \right\} \quad (7-1)$$

where:

- I: Moment of inertia of the entire sheet pile (cm^4)
- I_i : Moment of inertia of an individual pile (cm^4)
- A_i : Sectional area of an individual pile (cm^2)
- y_i : Distance from the centroid of the whole piles to the centroid of the i-th pile (cm)

The section forces of the whole piles at an arbitrary point is

$$\left. \begin{aligned} M_1(z) &= -\exp(-\beta_1 z) \left\{ M_0 (\cos \beta_1 z + \sin \beta_1 z) + \frac{H_0}{\beta_1} \sin \beta_1 z \right\} \\ S_1(z) &= \exp(-\beta_1 z) \{ H_0 (\cos \beta_1 z - \sin \beta_1 z) - 2\beta_1 M_0 \sin \beta_1 z \} \end{aligned} \right\} \quad (7-2)$$

The bending moment, axial force and shear strength of an individual pile at an arbitrary point are

$$\left. \begin{aligned} M_{1i} &= \frac{I_i}{I} M_1(z) \\ N_{1i} &= \frac{1}{I} y_i A_i M_1(z) \\ S_{1i} &= \frac{I_i + \kappa_i}{I} S_1(z) \end{aligned} \right\} \quad (7-3)$$

where :

$$\kappa_i = A_i \left\{ \left(\frac{D}{2} \right)^2 - y_i^2 \right\}$$

(ii) Section Forces When the Joints Are Not Connected

Analysis shall be made by the use of the group pile displacement method. The analysis can be made by determining the footing displacement.

If

$$\left. \begin{aligned} K_1 &= 4EI_i \beta_2^3 \\ K_2 &= 2EI_i \beta_2^2 = K_3 \\ K_4 &= 2EI_i \beta_2 \\ K_5 &= \frac{\pi}{4} d^2 K_v \\ \beta_2 &= \sqrt[4]{E_{s1}/n (4EI_i)} \end{aligned} \right\} \quad (7-4)$$

we obtain

$$\begin{bmatrix} nK_1 & 0 & -nK_2 \\ 0 & nK_5 & 0 \\ -nK_3 & 0 & K_5 [y_i^2] + nK_4 \end{bmatrix} \begin{Bmatrix} \delta_x \\ \delta_y \\ \delta_\theta \end{Bmatrix} = \begin{Bmatrix} H_0 \\ V_0 \\ M_0 \end{Bmatrix} \quad (7-5)$$

Hence we can determine the section forces of an individual pile at an arbitrary point from the value of

$$\{ \delta_x \ \delta_y \ \delta_\theta \}^T$$

$$\left. \begin{aligned} M_{2i} &= -\exp(-\beta_2 z) \left\{ PM_{i0} (\cos \beta_2 z + \sin \beta_2 z) + \frac{PH_{i0}}{\beta_2} \sin \beta_2 z \right\} \\ N_{2i} &= PN_{i0} \\ S_{2i} &= -\exp(-\beta_2 z) \left\{ PH_{i0} (\cos \beta_2 z - \sin \beta_2 z) - 2\beta_2 PM_{i0} \sin \beta_2 z \right\} \end{aligned} \right\} \quad (7-6)$$

where:

$$\left. \begin{aligned} PH_{i,0} &= H_0 / n \\ PM_{i,0} &= -K_3 \delta_x + K_4 \delta_\theta \\ PN_{i,0} &= K_5 (\delta_y + y_i \delta_\theta) \end{aligned} \right\} \quad (7-7)$$

(iii) Section Forces When the Joints are Imperfectly Connected

The section forces can be obtained by the use of α , and thus linearly distribute the section forces of an individual pile at an arbitrary point which have been determined by (i) and (ii).

$$\left. \begin{aligned} M_i &= \alpha M_{1i} + (1 - \alpha) M_{2i} \\ N_i &= \alpha N_{1i} + (1 - \alpha) N_{2i} \\ S_i &= \alpha S_{1i} + (1 - \alpha) S_{2i} \end{aligned} \right\} \quad (7-8)$$

In this case, where the linear interpolation method is used, the shear stress of the joint is needed for determining α and it is necessary to take a representative value at the section. In determining the representative value, a value of 2/3 of the maximum shear stress is assumed, and the sectional shear flow is distributed in a parabolic form.

(2) Comparison of the Measured Values and the Analytical values of Stress Intensities in the Body of a Sheet Pile Foundation

A comparative study of the measured and analytical stress intensities in the sheet pile foundation was made. The analytical values were obtained by use of the method given by the present specification ⁽¹⁾ (two methods using the composite efficiencies of 0.5 and 1.0), the group pile method, and above-mentioned linear interpolation method giving a total of four methods. The comparison of these are shown in Figs. 7-1 and 7-2. In Fig. 7-1 the horizontal force is 160 tons and in Fig. 7-2 it is 25- tons. Apart from these values, the analytical values are compared with the measured values for the four cases. From such results, it can be said that the linear interpolation method produces values considerably close to the measured values.

7-2 Analysis, With Consideration of the Relative Displacement of Piles

(i) Derivation of the Basic Formula

A model is assumed as shown in Fig. 7-3 to represent the deformation under a load. When the structure is deformed, the plane A-A becomes stepped as illustrated due to the relative displacement of the piles. Here the following assumptions are made;

- (1) The intersections of the plane A'-A' and the center lines of the piles are on a plane B-B. This makes it possible to treat the entire behavior of the model in the same manner as a beam subjected to a shear deformation.
- (2) The shear deformation of the piles is ignored.

The basic formula is derived on such assumptions. If the displacement of pile at an arbitrary point is represented by u and w , or;

$$\left. \begin{aligned} u &= u_0 \\ w &= w_0 - \theta x - (u'_0 - u) \xi \end{aligned} \right\} \quad (7-9)$$

where:

u_0, w_0 : Components of displacement in x and Z directions

u'_0 : Differentiation for Z

The coordinate system is shown in Fig. 7-4.

The direct strain ϵ_z and the shear strain γ_{xz} are

$$\left. \begin{aligned} \epsilon_z &= w'_0 - \theta' (x - \xi) - u''_0 \xi \\ \gamma_{xz} &= u'_0 - \theta \end{aligned} \right\} \quad (7-10)$$

The formula of equilibrium is derived from the principle of virtual work as follows.

$$\begin{aligned} & \int_{z_1}^{z_2} \int_A (\sigma_z \delta \epsilon_z + \tau_{xz} \delta \gamma_{xz}) dA dz + \int_{z_1}^{z_2} q \delta u dz - \int_{z_1}^{z_2} P_x \delta u dz \\ & - \left[\nu_z \int_A (\bar{\sigma}_z \delta w + \bar{\tau}_{xz} \delta u) dA \right]_{z_1}^{z_2} = 0 \end{aligned} \quad (7-11)$$

where:

q : Ground reaction

P_x : Distributed external force working in direction

σ_z, τ_{xz} : Surface force working in Z and x direction at the sections of both ends

ν_z : x -direction component of the outward unit normal line vector of the sections of both ends

Transforming the equation (7-11), the differential equations of equilibrium expressing displacement can be obtained as follows:

$$\left. \begin{aligned} - (EA w'_0) &= 0 \\ - (EI_p u''_0)'' + \{GA (u'_0 - \theta)\}' - k u_0 + p_x &= 0 \\ - (EI^* \theta')' - GA (u'_0 - \theta) &= 0 \end{aligned} \right\} \quad (7-12)$$

where:

I^* : Moment of inertia at the gravity center due to the axial force of pile

I_p : Total of moments of inertia of all piles

If the displacement θ is eliminated from the equation (7-12), the following differential equation of equilibrium with respect to the displacement is obtained;

$$\frac{EI^*}{GA} \cdot EI_p u_0^{(6)} - E(I^* + I_p) u_0^{(4)} + \frac{EI^*}{GA} k u_0'' - k u_0 = -p_x \quad (7-13)$$

(ii) Selection of Modulus of Elasticity

The modulus of elasticity E is assumed. 2.1×10^7 (t/cm²) for steel. The shear modulus of rigidity is assumed using a model as shown in Fig. 7-5. The shear modulus of rigidity is obtained using the average elastic shear deformation of the joints for the entire piles. If the shear deformations of the joint and the main body of pile are represented by γ_c and γ_s , respectively, then;

$$\left. \begin{aligned} \tau_c &= \frac{q \cdot d}{G_c A_c} \\ \tau_s &= \frac{q \cdot D}{G_s A_s} \end{aligned} \right\} \quad (7-14)$$

where:

G_c : Shear modulus of rigidity of material of the joint

G_s : Modulus of rigidity of whole pile

The equivalent shear modulus of rigidity G can be determined by the use of the equation (7-14) as follows;

$$GA = \frac{(D+d)^2}{\frac{d^2}{G_c A_c} + \frac{D^2}{G_s A_s}}, \quad A = A_c + A_s \quad (7-15)$$

(iii) Application of a Simple Case

An application is made relative to an experimental specimen as illustrated in Fig. 7-6. The joint is grouted with cement paste, because the model is small in size. There are two models, one of them uses three piles and the other six piles. The model is assumed to be placed in the air, and the pile heads are hinged and the bottoms are rigidly connected and a horizontal load is applied to the head.

In obtaining the general solution to the equation (7-13), if the spring constant of the ground k is 0 and the x-direction distributed external force P_x

is 0, the equation (7-13) can be rewritten as follows;

$$u_0^{(6)} - \beta^2 u_0^{(4)} = 0$$

$$\beta = \sqrt{\frac{GA \cdot L (I^* + I_p)}{EI^* EI_p}} \quad (7-16)$$

The general solution to the equation (7-14) is

$$u_0 = C_1 + C_2 Z + C_3 Z^2 + C_4 Z^3 + C_5 \cosh \beta z + C_6 \sinh \beta z \quad (7-17)$$

The boundary condition for the hinged head is obtained by assuming it to be in the vertical and horizontal directions and rotation. The angle of rotation at the end of pile and for the pile as a whole are not the same, because the piles are displaced in relationship to each other. From such boundary conditions, the unknown constants $C_1 \sim C_6$ can be obtained by solving the six simultaneous equations given in Table 7-1.

(iv) Calculation Results

The displacement of the pile head and the stress in the pile body were calculated by varying the shear modulus of rigidity of the joint. The following moduli of rigidity were used.

- (G) $G_c = G_s$: The equivalent shear modulus of rigidity, when the section of the joint is assumed to be made entirely with steel
- (G) $G = \infty$: Infinite shear modulus of rigidity, that is, the shear modulus of rigidity when there is no displacement of the piles in relationship to each other

(equivalent G): The shear modulus of rigidity obtained by method (iii)

In Fig. 7-7 the ratio of (equivalent G) to (G) $G_c = G_s$ is plotted on the horizontal axis and ratio of (μ_o) to $(\mu_o) G = \infty$ on the vertical axis. If the damping rate for G_c (shear modulus of rigidity of the cement paste) is taken at 1.0, the abscissa would be 0.45. Also $\mu_o / (\mu_o) G = \infty$ would be 1.02, 1.075, 1.080 and 1.375 when N (number of piles) = 3 ($\ell = 1.615m$), $N=3$ ($\ell = 0.7m$) and $N=6$ ($\ell = 0.7m$). The bond rigidity of the cement paste and steel material is taken as 0.3 of the shear rigidity of the cement paste. Then (equivalent G)/(equivalent G) $G_s = G_c$ would be 0.19. Thus, from Fig. 7-7, $\mu_o / (\mu_o) G = \infty$ would be 1.025, 1.110, 1.125 and 1.575, respectively.

7-3 Analysis with Consideration of the Bending and Shear Deformations

(i) Derivation of Basic Formula

A model is constructed as shown in Fig. 7-8, which represents a sheet pile foundation structure. Assuming the entire piles to be an integral beam, the

basic formula is derived by taking into consideration the bending and shear deformations.

The displacement of pile at an arbitrary point

$$\left. \begin{aligned} u &= u_0 \\ w &= w_0 - \theta x \end{aligned} \right\} \quad (7-18)$$

The direct strain ϵ_z and the shear strain γ_{xz} can be obtained by use of the equation (7-16) as follows

$$\left. \begin{aligned} \epsilon_z &= w_0' - \theta' x \\ \gamma_{xz} &= u_0' - \theta \end{aligned} \right\} \quad (7-19)$$

From the principle of virtual work, the equation of equilibrium can be obtained as follows

$$\begin{aligned} & \int_{z_1}^{z_2} \int_A (\sigma_z \delta \epsilon_z + \tau_{xz} \delta \gamma_{xz}) dA dz + \int_{z_1}^{z_2} q \delta u dz - \int_{z_1}^{z_2} p_x \delta u dz \\ & - \left[\nu_z \int_A (\bar{\sigma}_z \delta w + \bar{\tau}_{xz} \delta u) dA \right]_{z_1}^{z_2} = 0 \end{aligned} \quad (7-20)$$

From the equation above, the differential equations of equilibrium expressing displacement can be obtained as follows;

$$\left. \begin{aligned} (EA w_0')' &= 0 \\ \{ GA (u_0' - \theta) \}' - ku_0 + p_x &= 0 \\ (-EI \theta')' - GA (u_0' - \theta) &= 0 \end{aligned} \right\} \quad (7-21)$$

If the displacement θ is eliminated from the equation (7-19), the following differential equation of equilibrium in relation to the displacement is obtained;

$$-EI u_0^{(4)} + \frac{EI}{GA} ku_0'' - ku_0 = p_x \quad (7-22)$$

(ii) Application of a Simple Case

Application of these equations is made relative to an experimental specimen, as illustrated in Fig. 7-6. The shear rigidity of the joint is determined by use of equation (7-15). If, in equation (7-22), the spring constant of the ground k is 0 and the x-direction distributed external force P_x is 0.

$$\mu_o^{(4)} = 0 \quad (7-23)$$

The general solution will be

$$\mu_o = C_1 + C_2 Z + C_3 Z^2 + C_4 Z^3 \quad (7-24)$$

However, the unknown constants $C_1 \sim C_4$ can be obtained from the boundary conditions as follows;

$$\left. \begin{aligned} C_1 &= \frac{P\ell^3}{3EI} + \frac{P\ell}{GA} \\ C_2 &= -\frac{P\ell^2}{2EI} - \frac{P}{GA} \\ C_3 &= 0 \\ C_4 &= \frac{P}{6EI} \end{aligned} \right\} \quad (7-25)$$

(iii) Calculated Results;

In Figs. 7-9 and 7-10, $\eta \cdot Gc$ (η is damping rate) is plotted on the horizontal axis and the horizontal displacement of pile head on the vertical axis. A comparison is then made of these results by taking into consideration the displacement of piles in relationship to each other. Fig. 7-9 shows a case in which there are six piles and the pile length is 1.615 m. Fig. 7-10 shows a case in which there are the same number of piles (6), but the pile length is 0.7 m. From these results, it may be said that the two methods of analysis produce little differences, relative to the horizontal displacement of pile heads.

Fig. 7-11 shows a comparison of the stress distribution, as obtained by the two methods of analysis. It can be said that the two methods produce great differences with regard to the distribution of stresses. Examination of the distribution of stresses measured in the in-site tests, it may be said that the analysis when taking into consideration the displacement of piles in relation to each other shows a better approximation.

8. The Problem to be Solved in the Future

The method of design of sheet pile foundations has been established. However, this type of foundation can have a wide range of dimensions, thus the design of the structures using the existing method may not be adequate to cover such a wide range of designs of the sheet pile foundations. Studies of the structural characteristics of sheet pile foundations have just been initiated with an ultimate view of establishing better design standards.

The following subjects of study are being considered;

(1) Structural Characteristics of a Sheet Pile Foundation as a Unit

- (i) Construction of mechanical models and studies of the theoretical formulas
- (ii) Comparison of the theoretical formulas and the results of loading tests
(displacements, stresses, spring constants, damping)
- (iii) Experimental investigation of the ultimate yield strength and rupturing condition (including torsion)

(2) Characteristics of Some Specific Parts of Sheet Pile Foundations

- (i) Evaluation of the rigidity of the joints
- (ii) Investigations of the joint connections of the top plates

(3) Cofferdam Type

- (i) Investigations of the stresses in the cofferdam
- (ii) Investigations of the weldability and strength in the presence of residual stresses

References

1. Sheet Pile Foundation Research Committee: Specification for Design and Construction of Sheet Pile Foundations, January 1972.
2. Keiichi Komada: The History of Development and Present State of Sheet Pile Foundations, Foundation Work, March 1975.
3. Susumu Kurata and Fumio Shima: Study on Workability and Structural Characteristics of Sheet Pile Foundation, Bridges and Foundations, Vol. 4, No. 9, September 1970.
4. Earthquake Resistant Technological Development and Research Committee: Report on Research and Development on Earthquake Resistant Technology, National Land Development Technological Research Center, March 1974.
5. Earthquake Resistant Technological Research Committee: Report on Research and Development on Earthquake Resistant Technology, National Land Development Technical Research Center, March 1975.
6. Keiichi Komada, Asao Yamakawa and Michio Okahara: Structural Characteristics of Sheet Pile Foundations (Report NO.1), Civil Engineering Technical Material, Vol. 17, No. 3 February 1975, Civil Engineering Research Association.
7. Compiled by Iwao Yoshida: Designing of Piled Foundations, Kensetsu Toshu, April 1974.

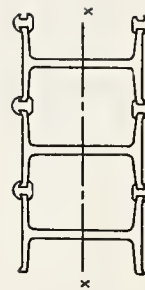
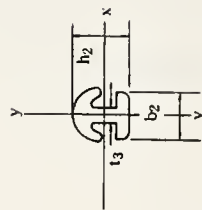
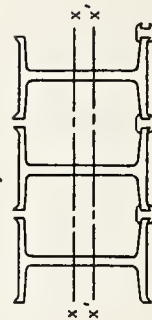
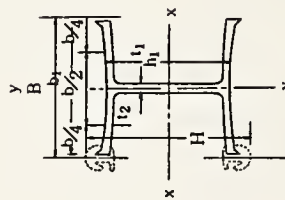
Table 2-1 Dimensions & weight of steel pipe pile

Outer diameter mm	Thickness mm	Section area cm ²	Unit weight kg/m	Moment of inertia I cm ²	Section modulus Z cm ³	Radius of gyration of area i cm	Outer surface area m ² /m
600	9	167.1	131	730×10 ²	243×10	20.9	1.88
	12	221.7	174	958×10 ²	320×10	20.8	1.88
	14	257.7	202	111×10 ³	369×10	20.7	1.88
	16	293.6	230	125×10 ³	418×10	20.7	1.88
700	9	195.4	153	117×10 ³	333×10	21.1	2.20
	12	259.4	204	154×10 ³	439×10	21.3	2.20
	14	301.7	237	178×10 ³	507×10	21.3	2.20
	16	343.8	270	201×10 ³	575×10	21.2	2.20
812.8	9	227.3	178	184×10 ³	452×10	23.4	2.55
	12	301.9	237	242×10 ³	596×10	28.3	2.55
	14	351.3	276	280×10 ³	690×10	28.2	2.55
	16	400.5	314	318×10 ³	782×10	28.2	2.55
914.4	9	340.2	267	346×10 ³	758×10	31.9	2.87
	12	396.0	311	401×10 ³	878×10	31.8	2.87
	14	451.6	354	446×10 ³	997×10	31.8	2.87
	16	534.5	420	1170×10 ³	117×10 ²	31.7	2.87
1016	9	378.5	297	477×10 ³	939×10	35.5	2.19
	12	440.7	346	553×10 ³	109×10 ²	35.4	2.19
	14	502.7	395	628×10 ³	124×10 ²	35.4	2.19
	16	595.1	467	740×10 ³	146×10 ²	35.2	2.19

Typical shapes of H-shaped steel sheet are shown in Table 2-2.

Table 2-2

Kinds	Dimensions mm						Section area cm ²	Weight kg/m	Kinds	Dimensions mm			Section area cm ²	Weight kg/cm	Section modulus cm ³			
	H	B	b ₁	h ₁	t ₁	t ₂	One sheet	One sheet	Joint	b ₂	h ₂	t ₃	One piece	One piece	I _x	I _y	Z _x	Z _y
YSPB -74	486	420	403	410	10	13.5	165.0	130		67	64	14	22.99	18.0	54,800	17,000	2,670	850



Section area cm ² /m	Weight kg/m	Moment of inertia cm ⁴ /m	Section modulus cm ³ /m
447.6	351	152,000	6,600

Section area cm ² /m	Weight kg/m	Moment of inertia cm ⁴ /m	Section modulus cm ³ /m
502.4	394	180,000	7,420

Table 2-3

kinds	steel members	allowable stress intensity (kg/cm ²)		
		SS 41	SS 50	SM 50 A
1. axial tensile stress intensity (per all section area)		1,400	1,700	1,900
2. axial compression stress intensity (per all section area) compressive members ℓ = length of members r = sectional radius of all cross section compressive added member		$0 < \ell/r \leq 110$ $1,300 - 0.06(\ell/r)^2$ $\ell/r > 110$ $7,200,000/(\ell/r)^2$ 1,300	$0 < \ell/r \leq 100$ $1,600 - 0.09(\ell/r)^2$ $\ell/r > 100$ $7,200,000/(\ell/r)^2$ 1,600	$0 < \ell/r \leq 90$ $1,800 - 0.11(\ell/r)^2$ $\ell/r > 90$ $7,200,000/(\ell/r)^2$ 1,800
3. bending stress intensity tensile fibre of beam (per all section area) compressive fibre of beam (per all section area) ℓ = distance between fixed points of flange (cm) b = width of flange in this case beam with being fixed compressive flange directly by reinforced concrete deck and so forth		1,400 $1,300 - 0.6(\ell/b)^2$ where $\ell/b \leq 30$ 1,300	1,600 $1,600 - 0.9(\ell/b)^2$ where $\ell/b \leq 30$ 1,600	1,900 $1,800 - 1.1(\ell/b)^2$ where $\ell/b \leq 30$ 1,800
4. members for axial compressive load and bending moment whose members must be calculated by formulas to be given below. for buckling about horizontal axis for buckling about vertical axis		$\frac{P}{A_g} + \frac{M}{I} y_c \frac{\sigma_{ca1}}{1,300}$ $\leq \sigma_{ca1}$ $\frac{P}{A_g} + \frac{M}{I} y_c \leq \sigma_{ca3}$ ただし $\frac{P}{A_g} \leq \sigma_{ca2}$	$\frac{P}{A_g} + \frac{M}{I} y_c \frac{\sigma_{ca1}}{1,600}$ $\leq \sigma_{ca1}$ to left	$\frac{P}{A_g} + \frac{M}{I} y_c \frac{\sigma_{ca1}}{1,800}$ $\leq \sigma_{ca1}$ to left

Table 2-4

basic type	section shape	number of foundations	treatment of joint
well type pronged type	circular oval oval rectangular other	single complex	grouting mortar welding no treatment

Table 3-1

kinds of piles & grounds kinds of times in loading	bearing pile	friction pile	
		good sandy stratum	other
normal	3	3	4
erarthquake	2	2	3

Table 3-2

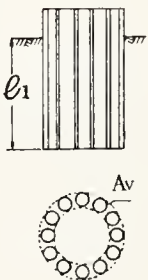
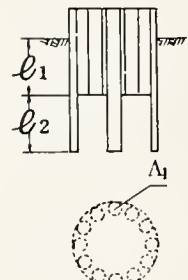
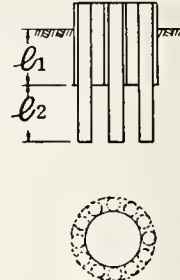
1) well	2) pronged	
	i) distance between each prong over 2.5D	ii) distance between each prong under 2.5D
		values smaller between (1) and (2)
	(1) same to 2) i)	(2)
		
$R_a = \frac{1}{n_1 \cdot S}$ $(q_d \cdot A_v + f \cdot U \cdot l_1)$	$R_a = \frac{1}{S} (q_d \cdot A_1 + f_o \cdot U_o \cdot l_2 + \frac{f \cdot U \cdot l_1}{n_1})$	$R_a = \frac{1}{n_2 \cdot S}$ $\{ q_d \cdot A_v + f \cdot U \cdot (l_1 + l_2) \}$

Table 3-3 Composite efficiencies




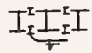

Kinds of sheet piles	Treatment of joint	Composite efficiency	Remarks
H-shaped	Filling with concrete in part of flange with dowel connectors	1.00	
	Filling with concrete in all section	1.00	
	Filling with concrete in part of flange	1.00	
	Welding 50 cm part of joint	0.40	
	Fixing the head	0.40	
Steel pipe	Grouting mortar and fixing the head	0.50	
	Fixing the head	0.30	

Table 3-4

modulus of deformation of ground by the following tests E_0 (kg/cm ²)	α	
	Normal	earthquake
a half of the E_0 obtained by the plate loading test using a 30 cm diameter disk	1	2
the E_0 measured inside a boring hole	4	8
the E_0 obtained by the unconfined compression test or the triaxial compression test	4	8
the E_0 estimated by $E_0=28N$; the N -value obtained by the standard penetration test	1	2

Table 4-1 Examples of sheet pile foundation construction works

(bridge, steel pipe pile)

(1)

name of work (bridge)	orderer	location of work (prefecture)	date of start	scale of work			type			basic type
				basic sectional dimensions	dimensions of steel pipe pile	number of foundation	type	type of joint	length of joint	
Ishikari kako	Bureau of Hokkaido	Hokkaido	44. 6 (1969)	8, 877x20, 483	812. 8x16 42, 000 x 13, 000	2	closing	pipe	40, 500	pronged
Omigawa	Chibaken	Chiba	45. 11	φ 9, 095	1, 016x14 42, 500 x 24, 500	1	"	"	41, 200	"
Nitta	"	"	45.	2, 313x3, 374	812. 8x12x35, 200	1	rising	"		well
Senbonmatsu	Osakashi	Osaka	45. 11	φ 12, 759	812. 8x13 52, 000 x 31, 000	2	"	"	50, 700	pronged
Nanko	"	"	45. 12	9, 011x9, 011	914. 4x14x64, 000	2	closing	"	28, 000	well
Shionagi	Nagoyashi	Aichi	46. 6	4, 328x7, 903	711. 2x11x20, 000	2	rising	"	18, 700	"
Osaka Port	Hanshin Highway Public Corporation	Osaka	46. 11	φ 15, 210	1, 219x13x33, 000	7	coffering	"	31, 700	"
"	"	"	46. 11	13, 350x35, 290	1, 219x13x33, 500		"	"	32, 200	"

(2)

name of work (bridge)	orderer	location of work (prefecture)	date of start	scale of work			type			basic type
				basic sectional dimensions	dimensions of steel pipe pile	number of foundations	type	type of joint	length of joint	
Yoshii	Okayama Highway Public Corporation		46. 12 (1971)	φ 13, 000		6				
Mizushima	"	Okayama	46. 12	φ 12, 936	762x9x27, 000	19	coffering	pipe	14, 000	well
Saidaiji	"	"	46. 12	φ 12, 726	914. 4x12. 7 x24, 000	6	"	"	12, 500	"
Ariake Quay	Tokyo	Tokyo	46. 12	13, 946x5, 811	914. 4x12x35, 000	2	"	"	33, 700	pronged
Hazenoura	Bureau of Kyushu	Saga	47. 7	φ 9, 081	914. 4x12x28, 870	4	"	"	22, 700	well
Shin - iinogawa	Bureau of Tohoku	Miyagi	47. 9	12, 560x9, 620 10, 600x7, 660	800x12x ^{41, 000} 75, 500	2	no closing	pipe-T	26, 000 16, 000	pronged
Shin - kitakami	Miyagiken		47. 10	12, 110x4, 010		1				
Gokeidai	Okayamaken	Okayama	47. 11	7, 581x14, 527	914. 4x12. 7 x13, 900	1	coffering	pipe	6, 500	well
Shibatani Hirano Line	Osakashi	Osaka	47. 12	15, 727x20, 376	914. 4x14x34, 500	6	"	"	33, 000	"
Shin - kitakami	Miyagiken	Miyagi	48. 1	11, 658x3, 710	800x12x32, 000	1	rising	pipe-T	30, 000	"

(3)

name of work (bridge)	orderer	location of work (prefecture)	date of start	scale of work			type			basic type
				basic sectional dimensions	dimensions of steel pipe pile	number of foundations	type	type of joint	length of joint	
Minami Quay Connection	Osakashi	Osaka	48. 2 (1973)	22, 225x15, 008	1, 200x14x28, 000	2	coffering	pipe	26, 700	"
Suehiro	Tokushima-ken	Tokushima	48. 3	φ 24, 508	914. 4x14x39, 600	2	"	"	26, 700	"
Ishikari	Bureau of Hokkaido	Hokkaido	48. 5	φ 15, 488	800x14x20, 000	2	"	"	18, 700	"
Kurogane	Nippon Steel Corporation	Hyogo	48. 5	φ 3, 910	508x12. 7x11, 000	1	in water	pipe-T	10, 500	"
Shin-ebetsu	Bureau of Hokkaido Development	Hokkaido	48. 6	φ 15, 506	800x16x27, 000	3	coffering	pipe	25, 700	pronged
Teshiokako	"	"	48. 7	φ 10, 832	800x12x20, 000	1	"	"	18, 500	"
Rokko Island Connection	Kobeshi	Hyogo	48. 9	10, 568x25, 193	1, 219. 2x16 x31, 000	5	"	"	29, 700	well
Kinuura	Aichi	Aichi	48. 11	φ 9, 081	914. 4x16x21, 000	5	"	"	20, 200	"
Shinsuigo	Bureau of Kanto	Chiba	48. 11	26, 445x16, 186	1, 219. 2x19 x57, 500	4	"	"	56, 200	"
Kofunadu	Bureau of Kyushu	Nagasaki	48. 11	φ 6, 872	914. 4x12x28, 000	4	"	"	26, 700	"
Ichikawa Waterway 3	Bureau of Kanto	Chiba	48. 12	14, 062x10, 504 other	1, 016x ¹⁴ ₁₂ x30, 000	8	no closing	pipe-T	28, 700	"

(4)

name of work (bridge)	orderer	location of work (prefecture)	date of start	scale of work			type			basic type
				basic sectional dimensions	dimensions of steel pipe pile	number of foundations	type	type of joint	length of joint	
Shin- kagasuno	Bureau of Shikoku	Tokushima	49.3 (1974)	φ 18, 684	914. 4x14x44, 000	4	coffering	pipe	41, 000	well
Edogawa Bridge Left Site	Bureau of Kanto	Chiba	49.3	15, 200x11, 700	1, 016x ¹⁴ ₁₂ x14, 000	3	no closing	pipe-T	12, 700 34, 700	"
Edogawa Bridge Right Site	"	Chiba	49.3	13, 100x9, 700	1, 016x ¹⁴ ₁₂ x28, 000	1	"	"	26, 500	"
Senboku	Osakafu	Osaka	49.5	26, 058x14, 322	1, 219. 2x16 x42, 500	2	coffering	pipe	41, 000	"
Yaegawa Side Road	Bureau of Kinki	Hyogo	49.11	2, 000x3, 954	508x9x6, 000	4	no closing	second port type	6, 000	"
Ogishima	N. K. Steel Corporation	Kanagawa	49.12	φ 8, 110	812. 8x ¹⁶ _{12. 7} x30, 000	1	"	"	30, 000	"
Jonan	Ishikawaken	Ishikawa	50.1	φ 8, 344	914. 4x16x38, 000	2	coffering	pipe	35, 800	"
Osakashi Highway	Hanshin Highway Public Corporation			32, 897x12, 422						
Osaka Gulf Circum- ference	"			35, 288. 5x13, 351						

(5)

name of work (bridge)	order	location of work (prefecture)	date of start	scale of work		type		
				basic sectional dimensions	dimensions of steel pipe pile	number of foundations	type	length of joint
"				35, 430, 7x10, 568.2		7		
				15, 210, 6x15, 210.6				
				13, 351x13, 351				
				12, 422x12, 422				
				15, 210, 6x15, 210.6				

Table 5-1

Table 7-1

c_1	c_1	c_1	c_1	c_1	c_1	c_1	
0	0	2	0	0	ρ'	0	0
0	0	0	0	0	ρ'	0	0
1	1	ρ'	ρ^2	$\cos \rho l$	$\sin \rho l$	$\rho \cos \rho l$	0
0	1	2l	$3\rho^2$	$\rho \sin \rho l$	$\rho \cos \rho l$	$\rho^2 \cos \rho l$	0
0	0	$-2(EI_p^2 + EI_p)$	$-6(EI_p^2 + EI_p)$	$\frac{EI_p^2 EI_p}{GA} \rho^4 - (EI_p^2 + EI_p) \rho^3 \cos \rho l$	$\frac{EI_p^2 EI_p}{GA} \rho^4 - (EI_p^2 + EI_p) \rho^3 \sin \rho l$	$\frac{EI_p^2 EI_p}{GA} \rho^4 - (EI_p^2 + EI_p) \rho^3 \cos \rho l$	$-EI_p$
0	0	0	6	$\rho^4 \sin \rho l$	$\rho^3 \cos \rho l$	$\rho^3 \cos \rho l$	$\frac{p}{EI_p}$

name of bridge	loading test	vibration test	measurement of stress
Kaneshiro	○	○	
Nanko	○	○	
Shiniinogawa	○		
Shinkitakamigawa		○	
Mizushima	○	○	
Nanko Connection			○
Hazenoura			○
Omigawa	○	○	○
Suehiro			○
Ishikarikako		○	
Shinsuigo			○

Table 4-2 Examples of sheet pile foundation construction works
(except bridge, steel pipe pile)

(1)

name of work	orderer	location of work (prefecture)	date of start	scale of work			type			basic type
				basic sectional dimensions	dimensions of steel pipe pile	number of foundations	type	type of joint	length of joint	
In Steel Factory	Kawasaki Steel Corporation			φ 6, 458		1				
1st ~ 4th Blast furnace	"	Okayama	41. 1 (1966)	φ 35, 402	1, 219. 2x12 x22, 000	4	Founda- tion	pipe	17, 400	well
Scale Pit	"	"	41. 6	12, 640x29, 072 other	1, 219. 2x7. 9 x23, 000 other	17		"		"
Pit	"		44. 5	12, 640x29, 072		2				
Rain-quay	"	Okayama	44. 9	φ 5, 784	762x7. 9x24, 000	7	Founda- tion	pipe		well
In Steel Factory	"		45. 1	12, 700x31, 700		2				
"	"	Okayama	45. 1	φ 13, 824	762x x16, 000	1				well
Pit	"		45. 3	7, 000x20, 100		2		pipe		
Quay	"	Okayama	45. 9	φ 15, 600	1, 117x6x21, 000	18	Founda- tion	pipe	15, 300	well

Table 4-2

(1)

name of work	orderer	location of work (prefecture)	date of start	scale of work			type			basic type
				basic sectional dimensions	dimensions of steel pipe pile	number of foundations	type	type of joint	length of joint	
Quay Detached Pier	Kawasaki Steel Corporation	Okayama	46.5	φ 5,784	762x11x29,000	1		pipe	27,700	
Dolphin	"	"		φ 5,140	762x7.9x23,000	1		"		
Quay	Car Ferry Company	Tokyo	47.11	15,248x6,946 19,992x15,248	1,016x12.7 x55,000		Founda- tion	pipe-T	46,700	pronged
Steel Tower	Chugoku Electric Power	Hiroshima	48.9 (1966)	9,127x9,127	812.8x19x22,000	1	"	Second port shaped	22,000	well
In Fukuyama Steel Factory	N.K. Steel Corporation	"	49.11	φ 8,752	812.8x19x38,000	2	"	"	22,000 38,000	pronged

Table 4-3

(2)

name of work	orderer	location of work (prefecture)	date of start	scale of work			type			basic type
				basic sectional dimensions	dimensions of H-shaped sheet	number of foundations	type	type of joint	length of joint	
Kaneshiro	Nagoya Port Association	Aichi	41.9 (1966)	1, 670x2, 090	pile YSPB-74 =48, 500	16	rising		32, 500	pronged
Dolphin	Kansai Oil	Osaka	42.3	5, 770x8, 660 1 4, 930x4, 930 2 4, 530x4, 530 4	" =39, 500	7	"		29, 500	"
"	Nippon Steel Corporation	"	42.8	2, 530x2, 530	" =30, 000	1	"		30, 000	well
"	Keihin Quay Public Corporation	Kanagawa	44.8	2, 490x2, 066	" =25, 000	2	"		25, 000	"
Takanashi-gawa Intersection	Mitsubishi Oil	Okayama	45.3	2, 510x2, 510	" =30, 000	4	rising		= 30, 000	well
Fukusoku	Gifuken	Gifu	45.10	4, 200x3, 360	" =42, 800	2	"		19, 300	pronged

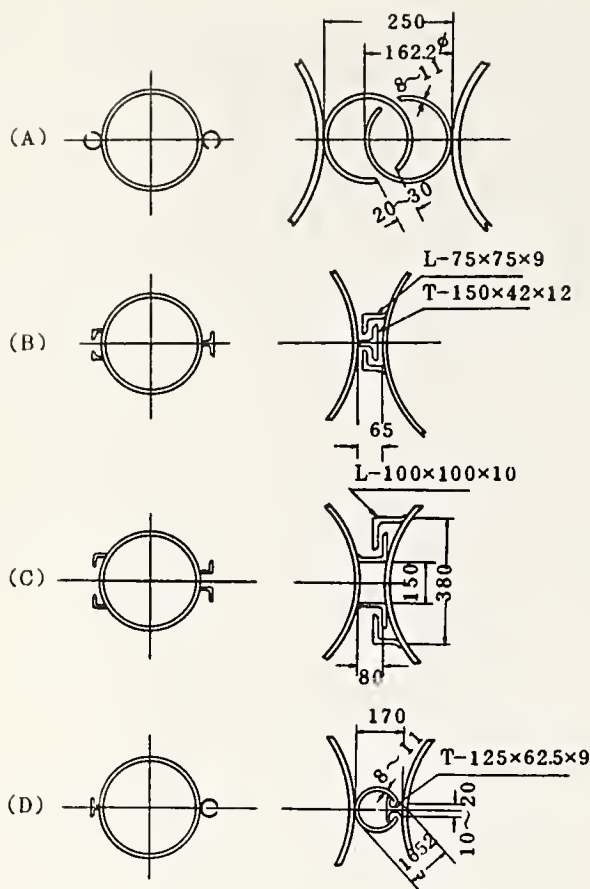


Fig. 2-1 Joint shapes of steel pipe pile

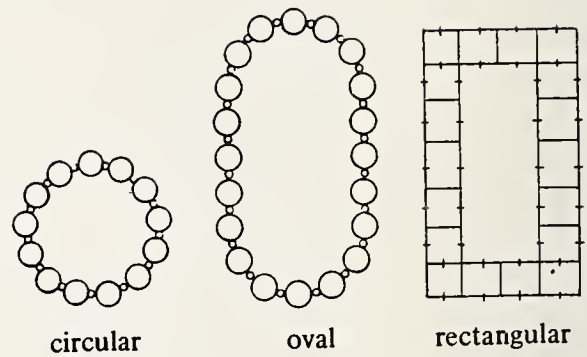
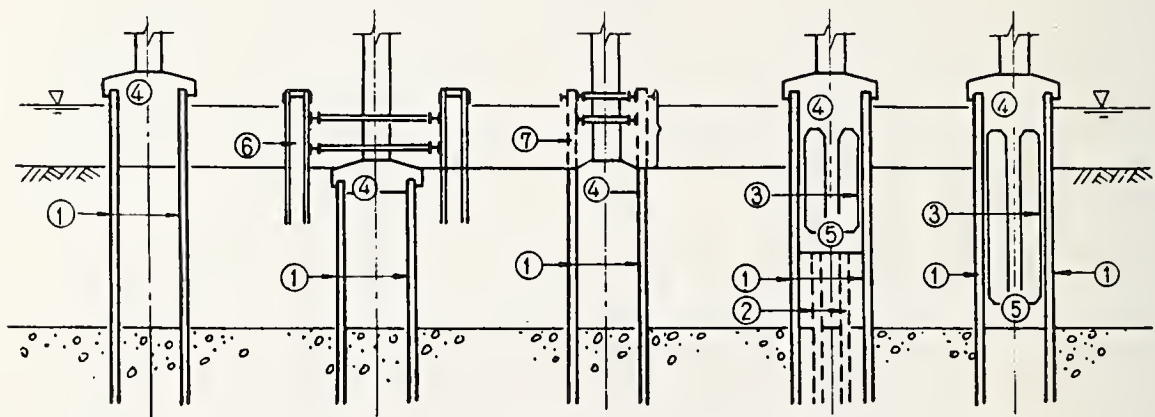


Fig. 2-2



(1) rising type (2) closing type (3) coffering type (4) semi-rigid type (5) rigid type
 ① steel pipe pile ② steel pile (if necessary) ③ the inside filled reinforced concrete ④ footing
 ⑤ bottom plate ⑥ double closing ⑦ cofferdam.

Fig. 2-3

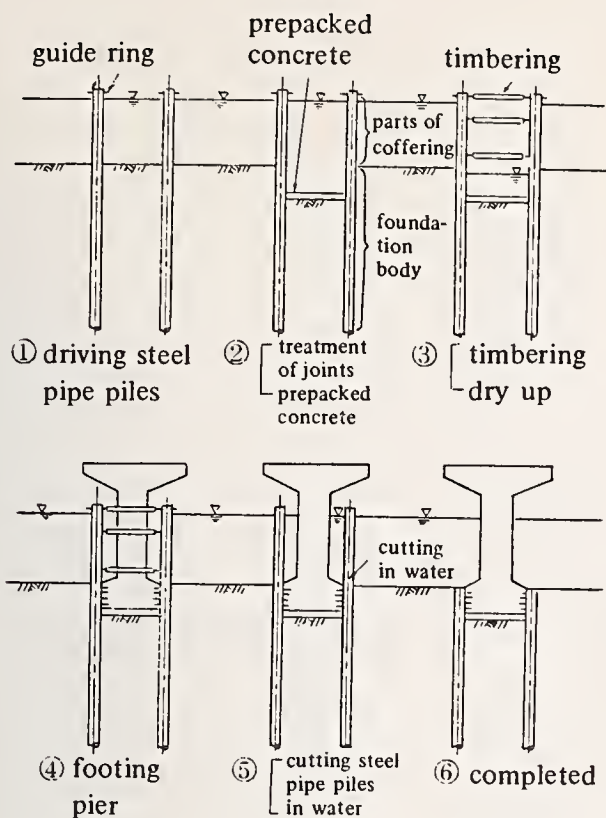


Fig. 2-4 several steps in construction of the "cofferdam" type of the sheet pile foundations

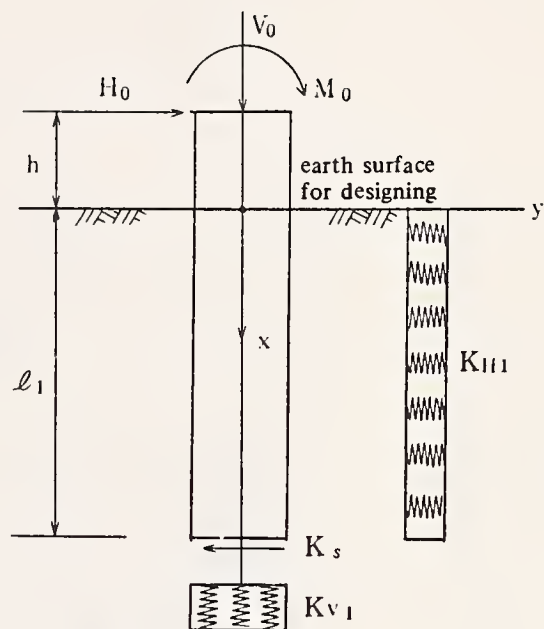


Fig. 3-1

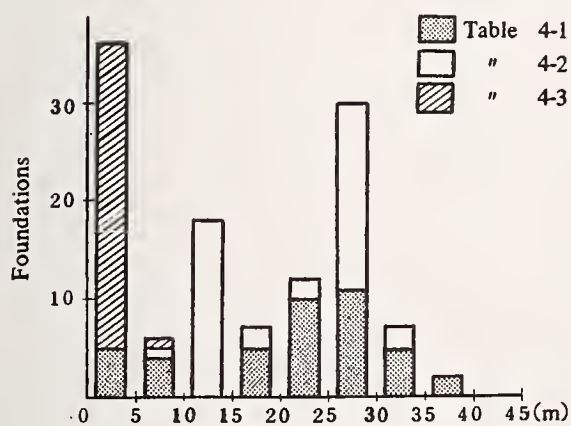


Fig. 4-1 Largest width of sheet pile foundation reclangular or oval

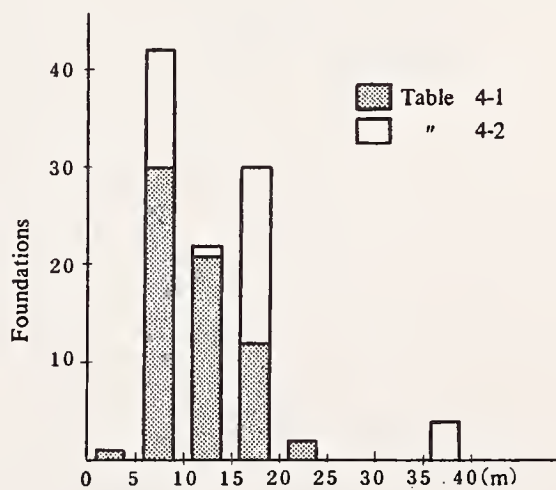


Fig. 4-2 Diameter of circular sheet pile foundation

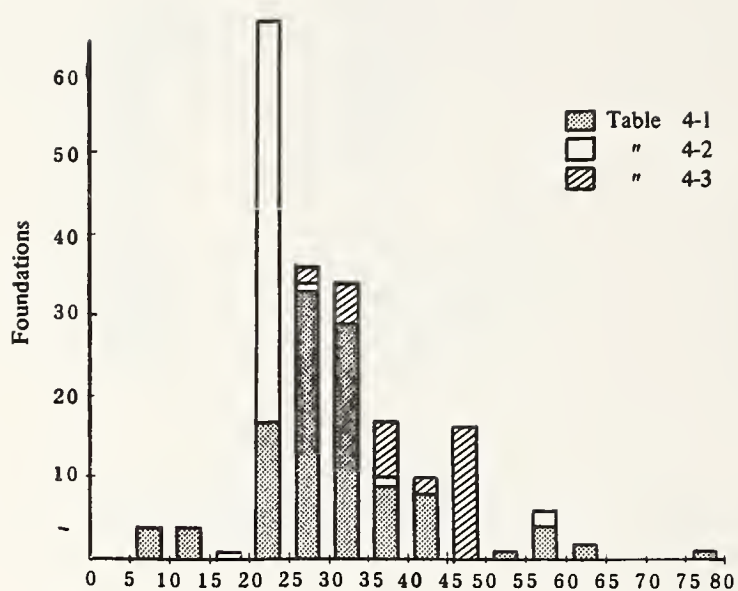


Fig. 4-3 Sheet pile length
(including length of
coffering)

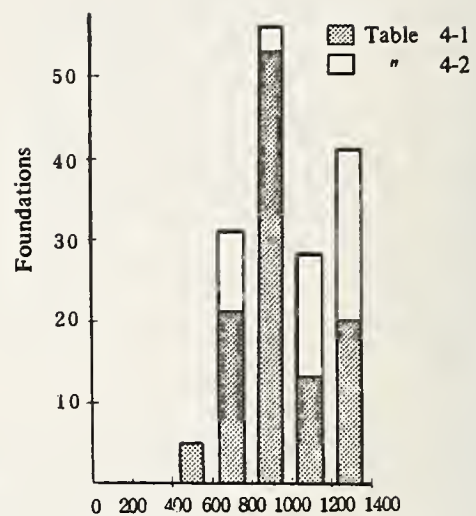


Fig. 4-4 Diameter of
steel-pipe piles

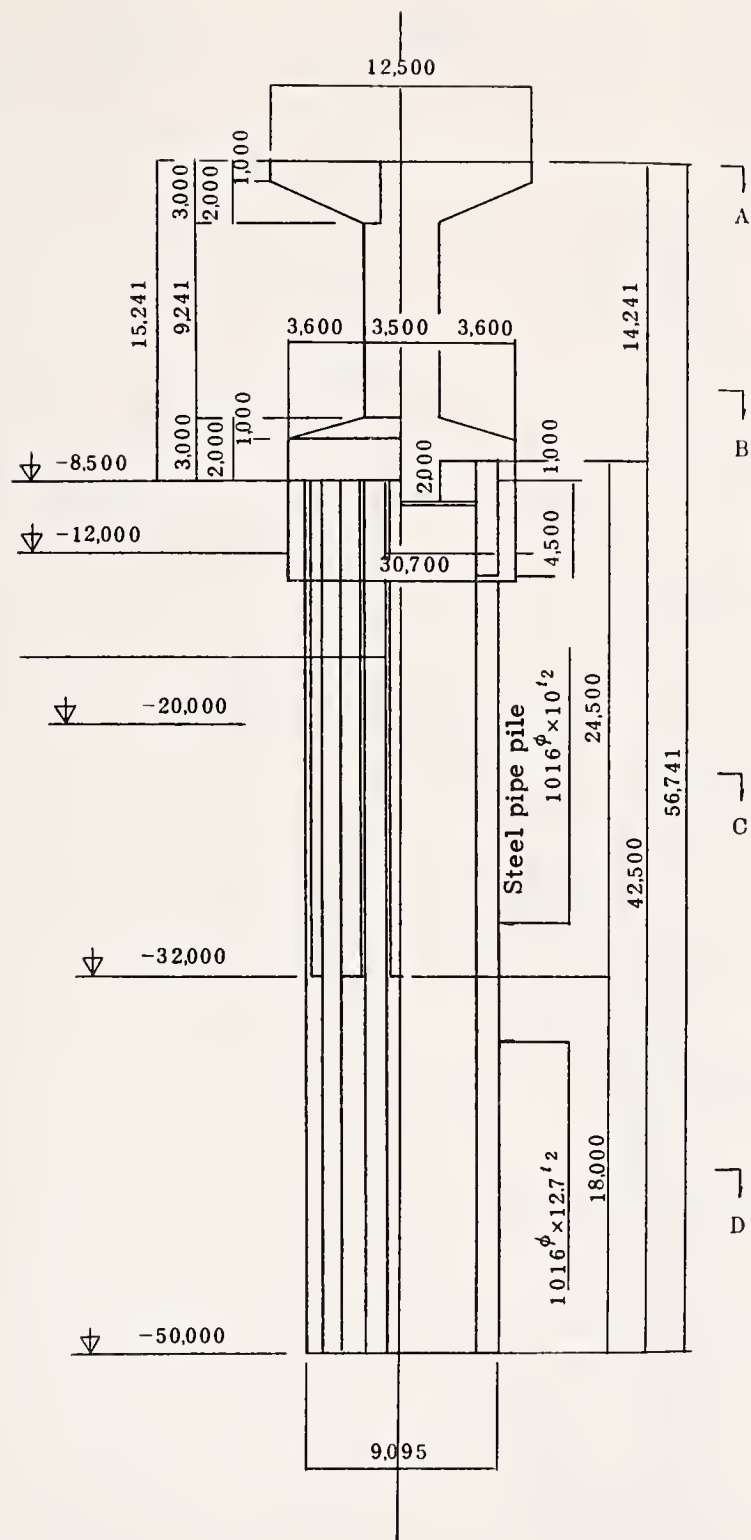


Fig. 5-1 Cross section Omigawa Bridge

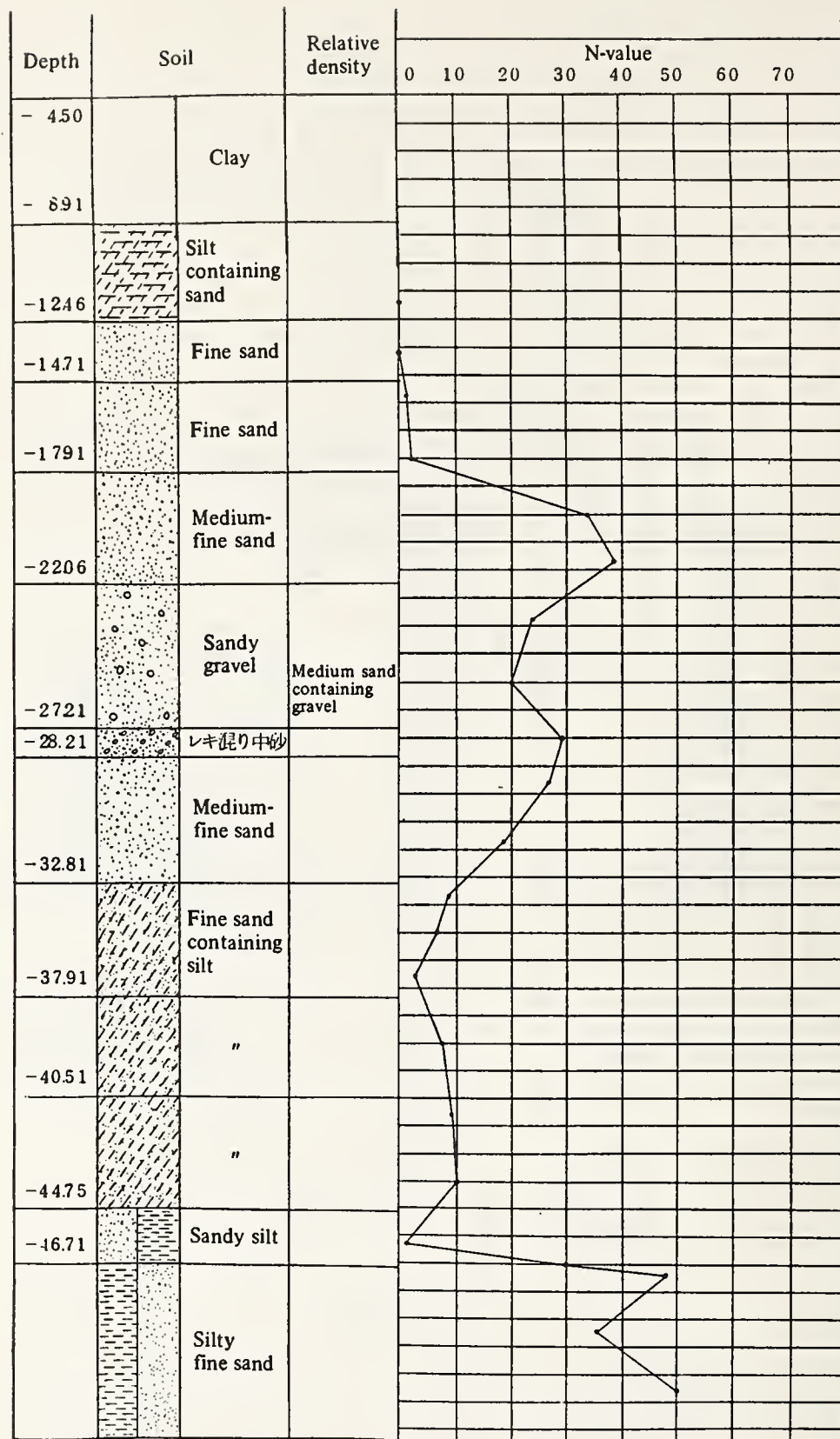


Fig. 5-2 Soil conditions; Omigawa Bridge

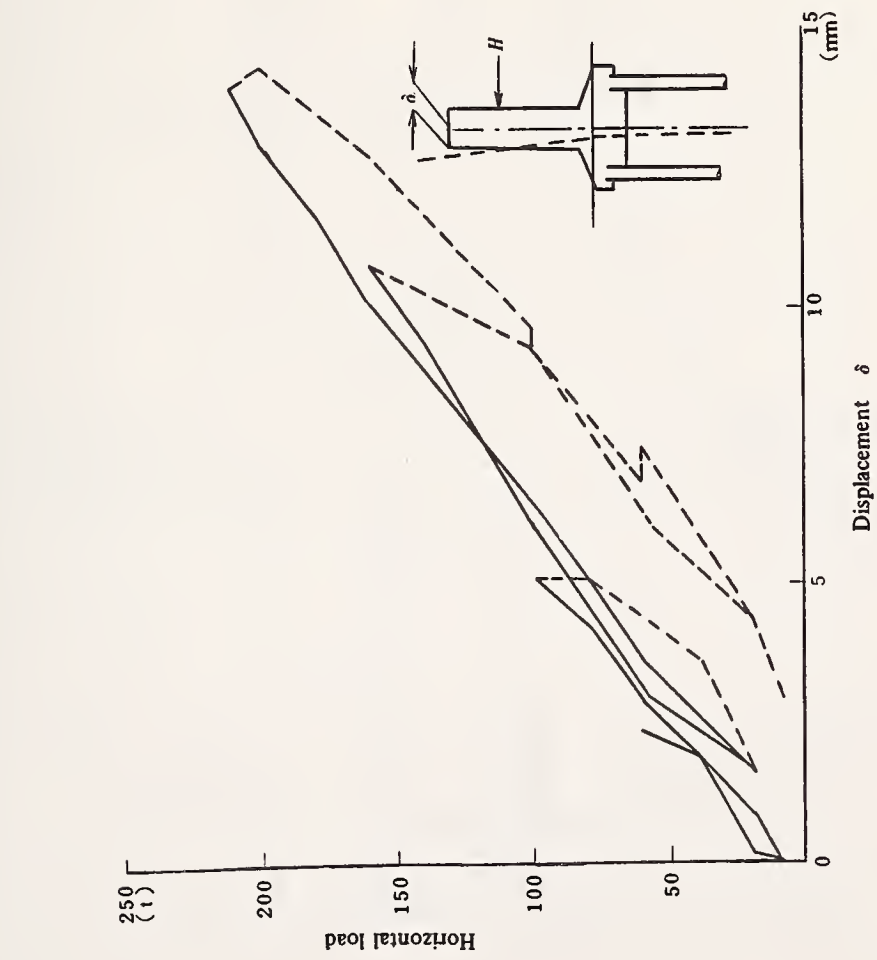


Fig. 5-3 Load-displacement curve

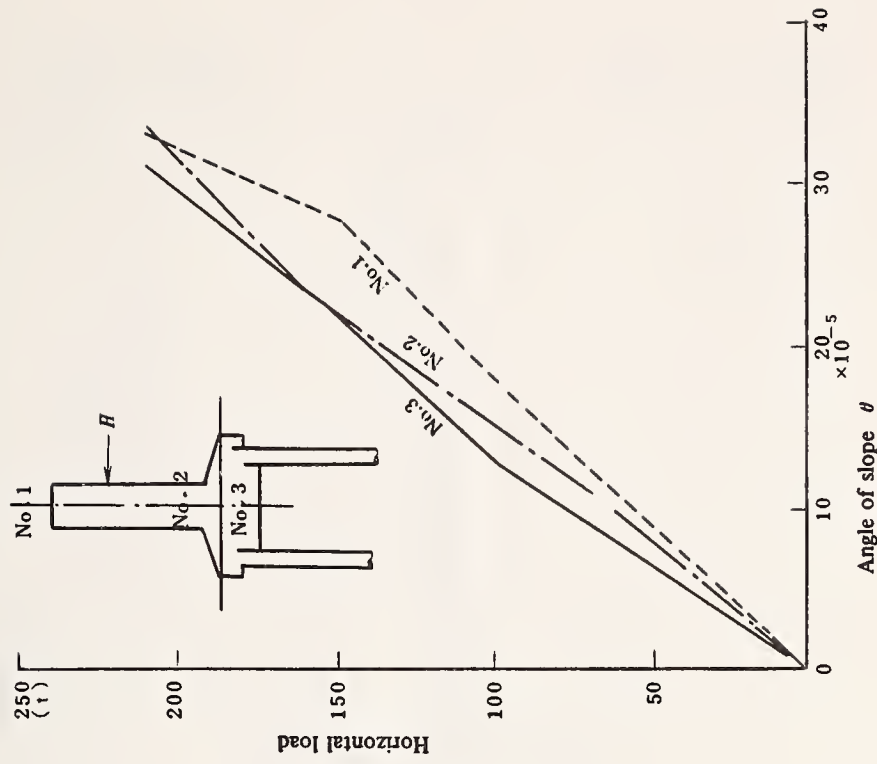


Fig. 5-4 Load-slope of angle curve

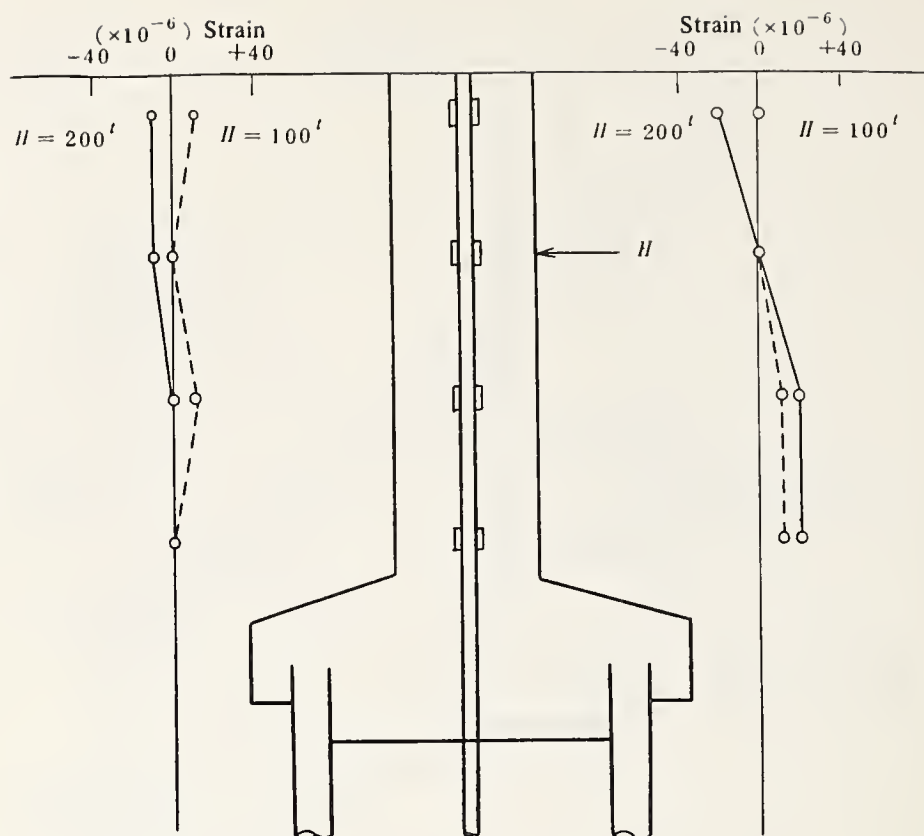


Fig. 5-5 Strain distribution in part of pier

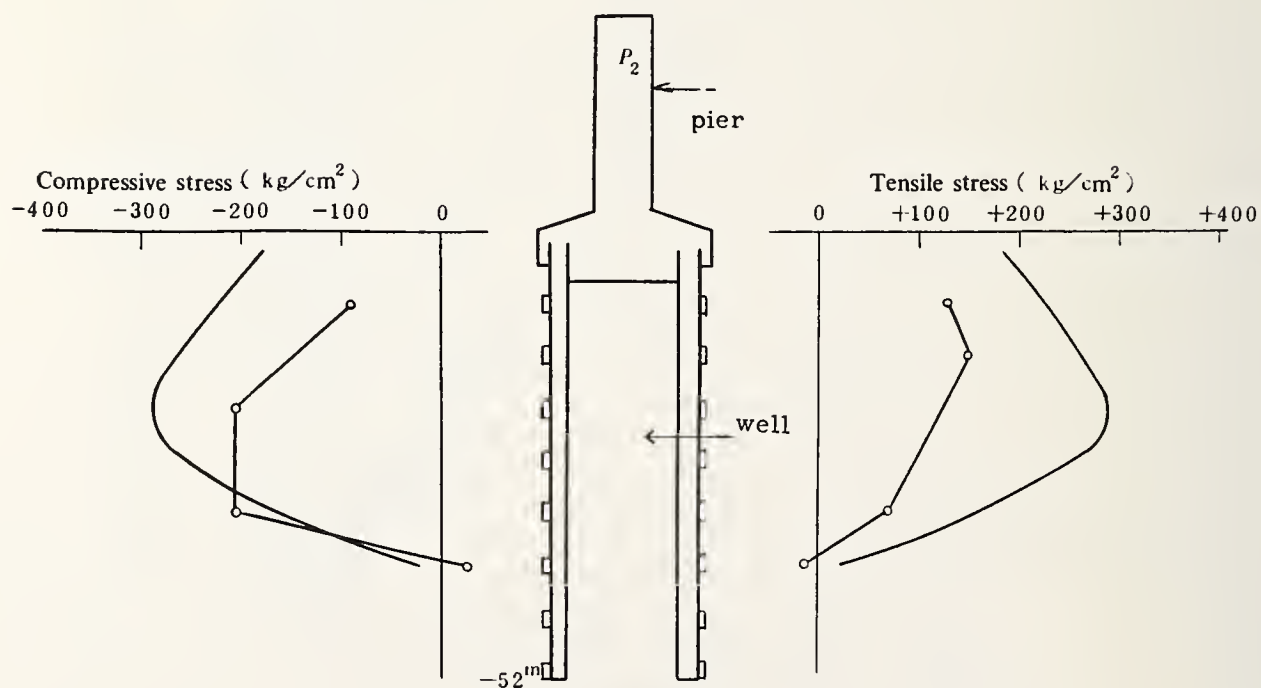


Fig. 5-6 Stress distribution

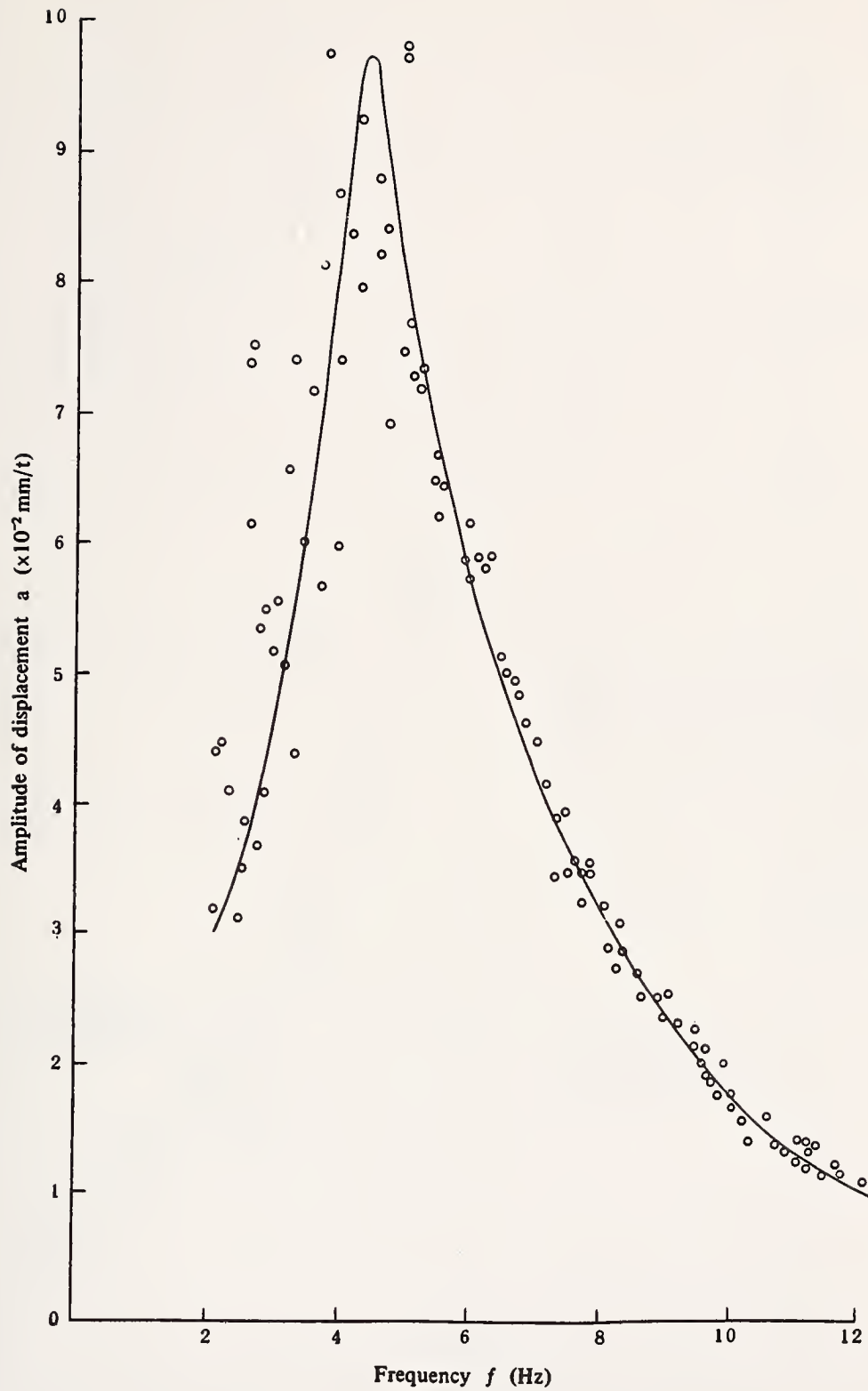


Fig. 5-7 Horizontal response on the top end

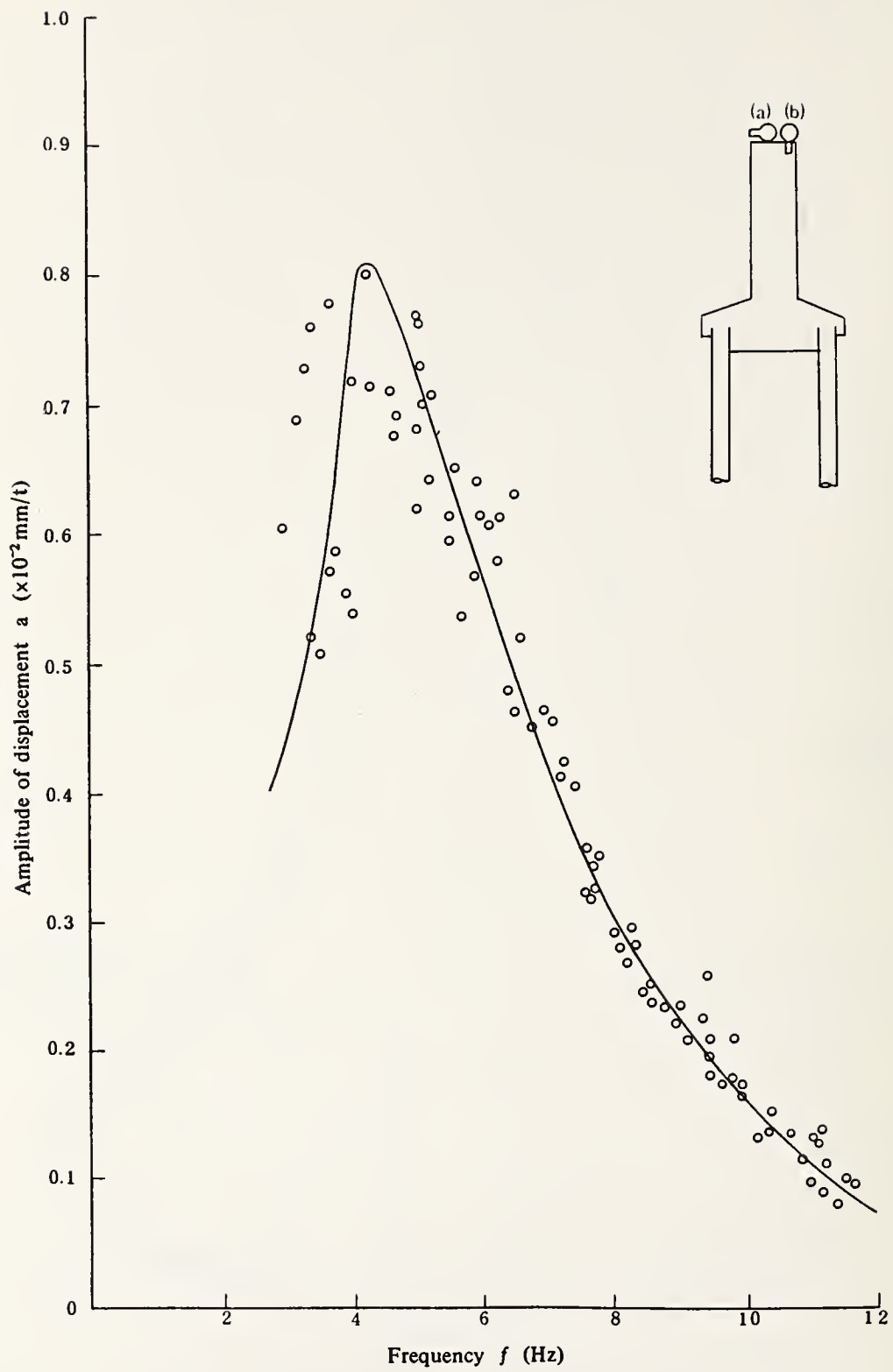


Fig. 5-8 Vertical response on the top end

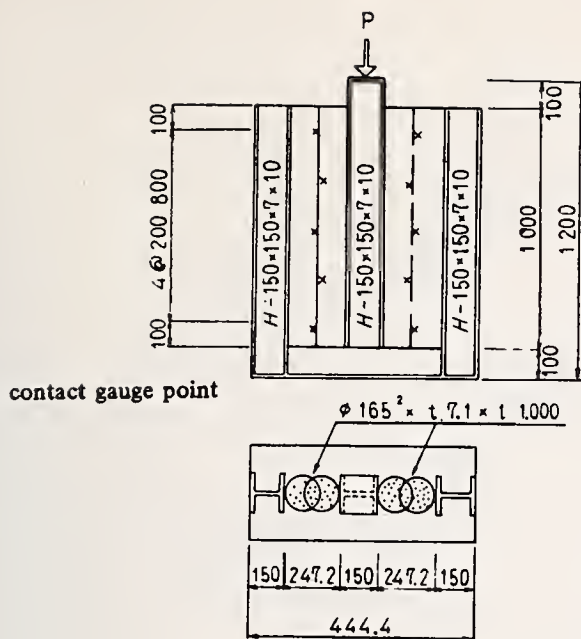


Fig. 6-1 Direct shear test

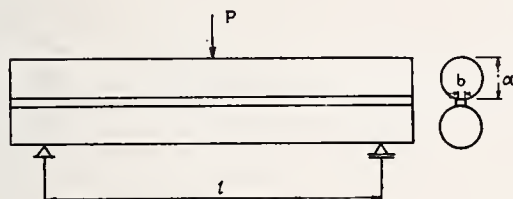


Fig. 6-4 Combined beam

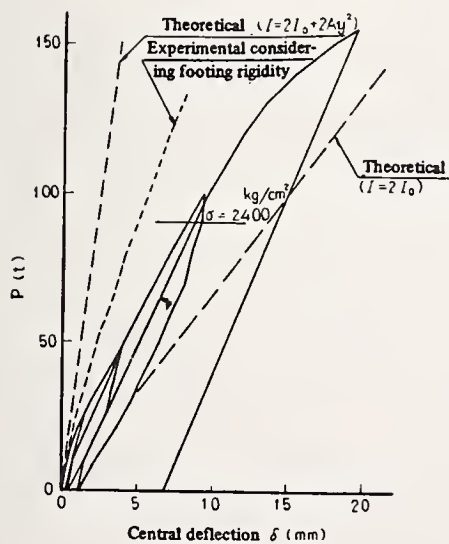


Fig. 6-7 P- δ curve

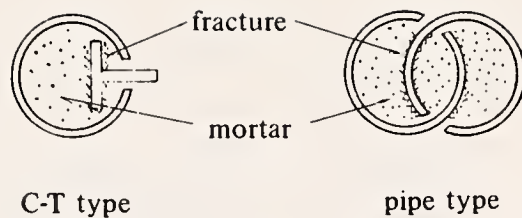


Fig. 6-2 Fracture of joint

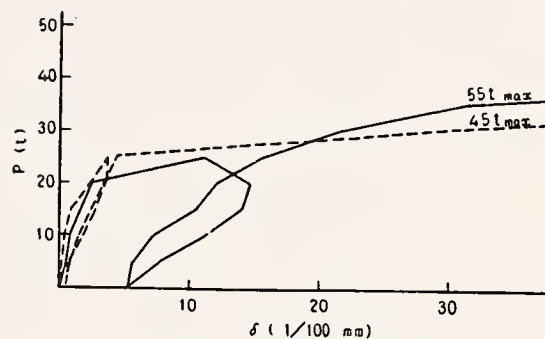


Fig. 6-3 P- τ curve

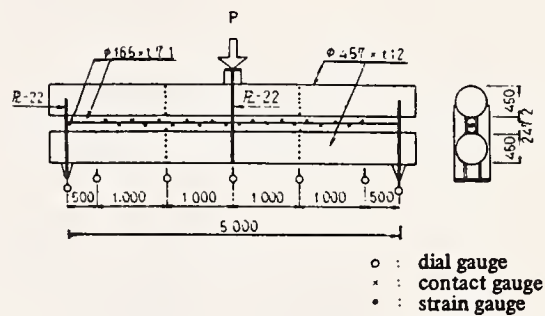


Fig. 6-6 Bending test

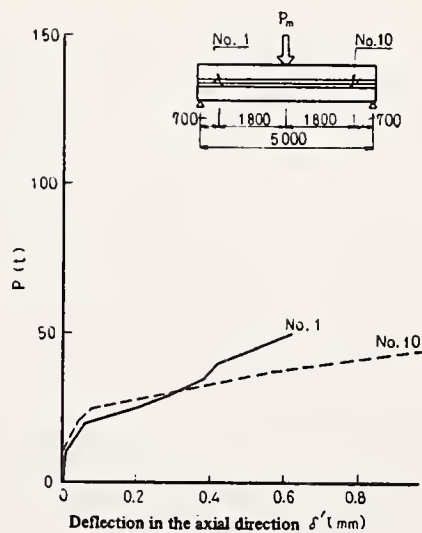


Fig. 6-8 P- δ' curve

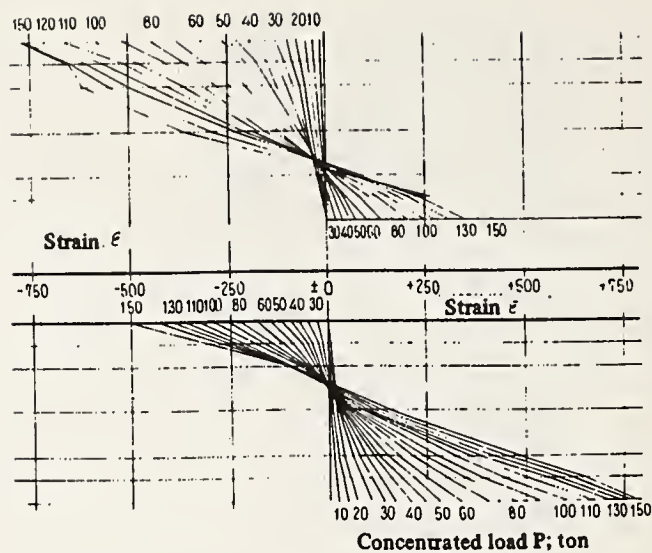
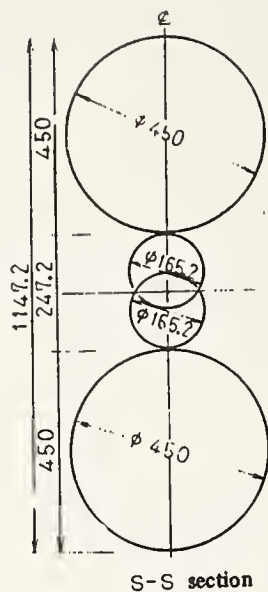


Fig. 6-9 Load-strain distribution

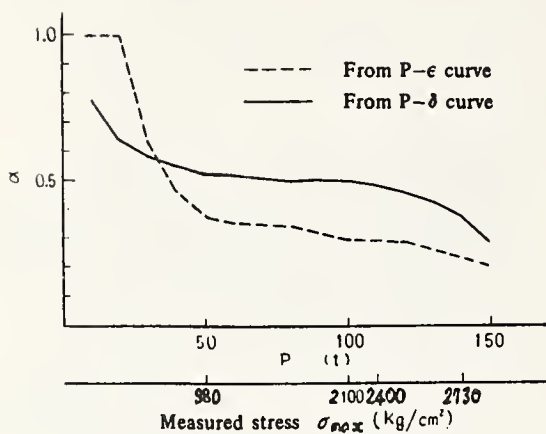


Fig. 6-10 α -P curve

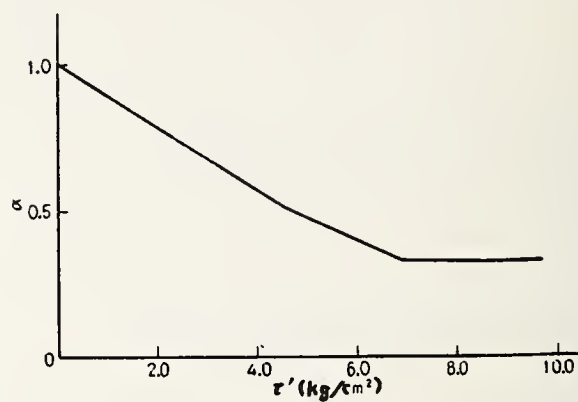


Fig. 6-11 $\alpha \sim \tau'$ curve

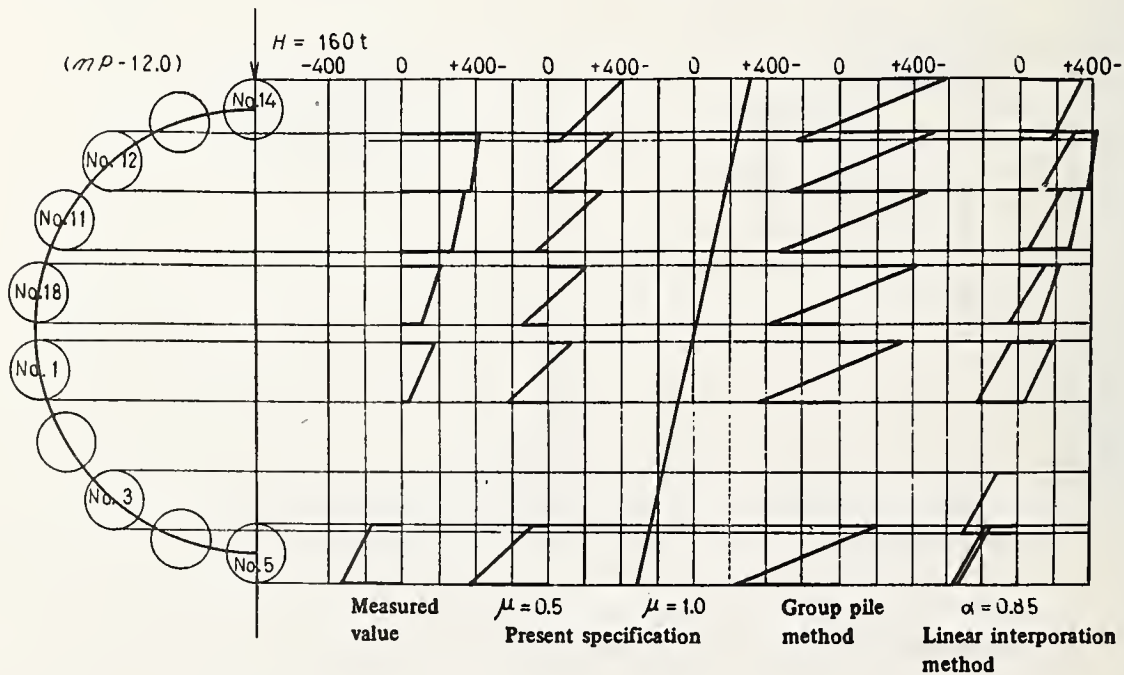


Fig. 7-1

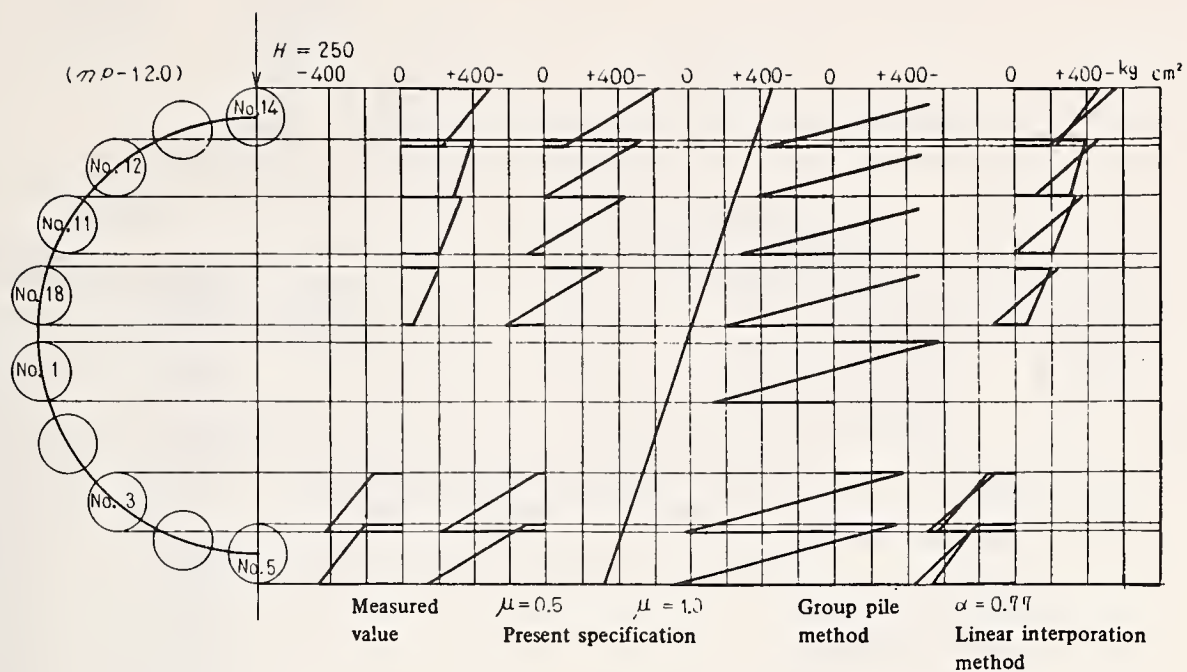


Fig. 7-2

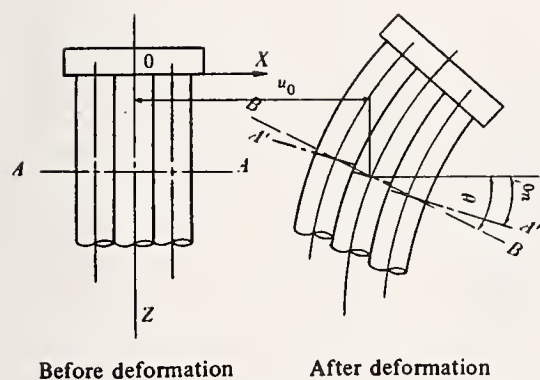


Fig. 7-3 Structural model

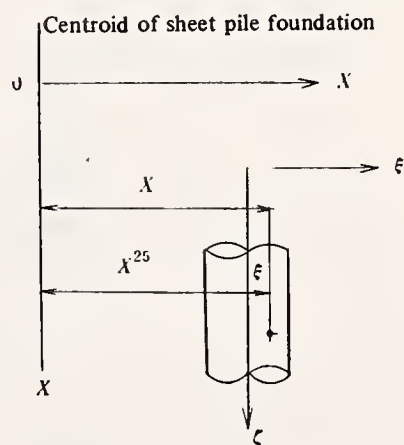


Fig. 7-4 Coordinate system

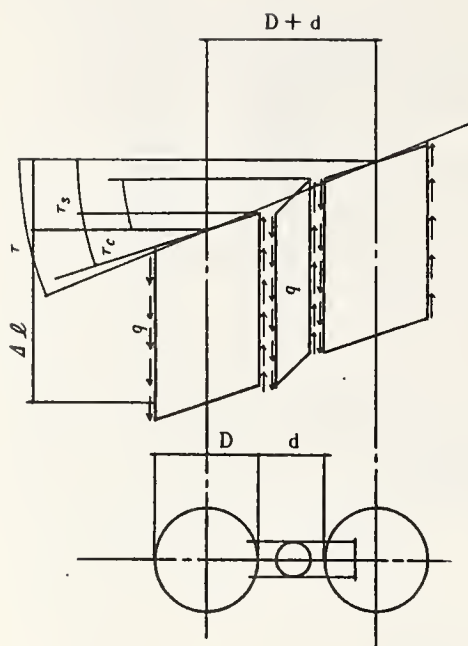


Fig. 7-5 Model of shear deformation

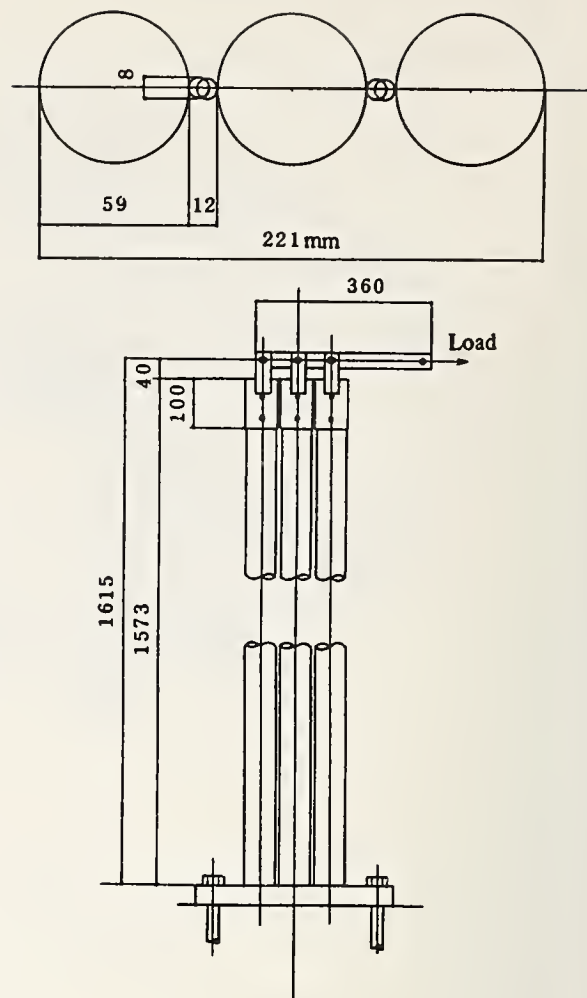


Fig. 7-6 Model for calculation

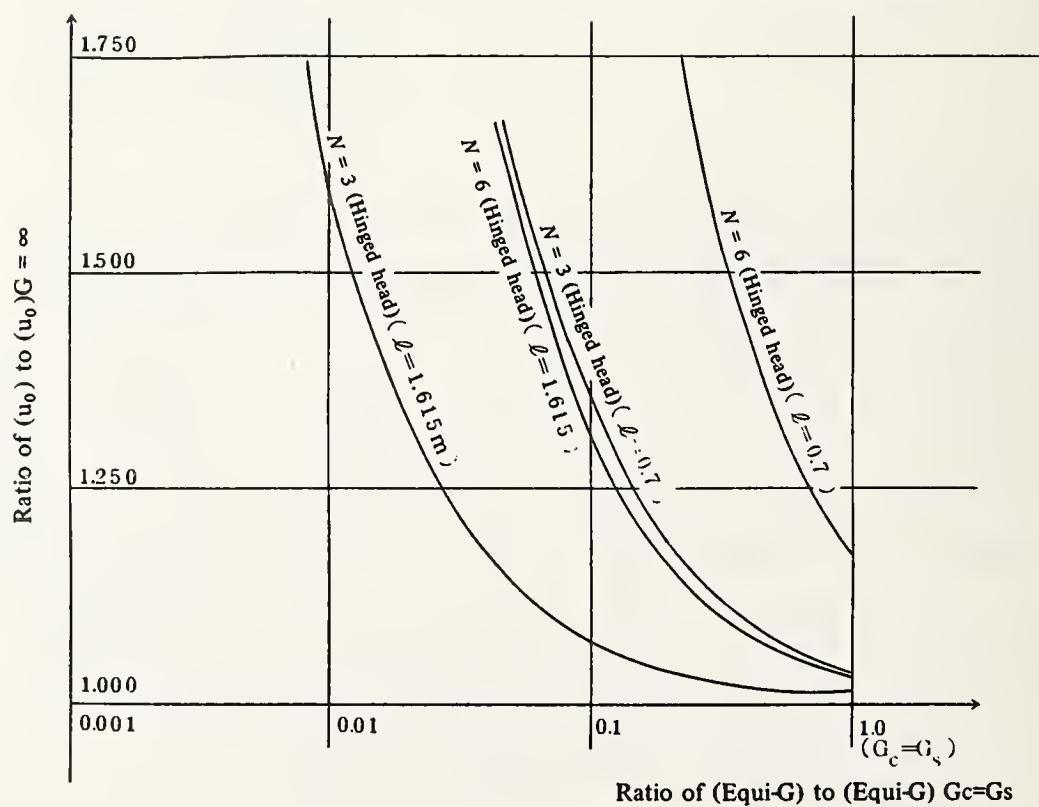


Fig. 7-7

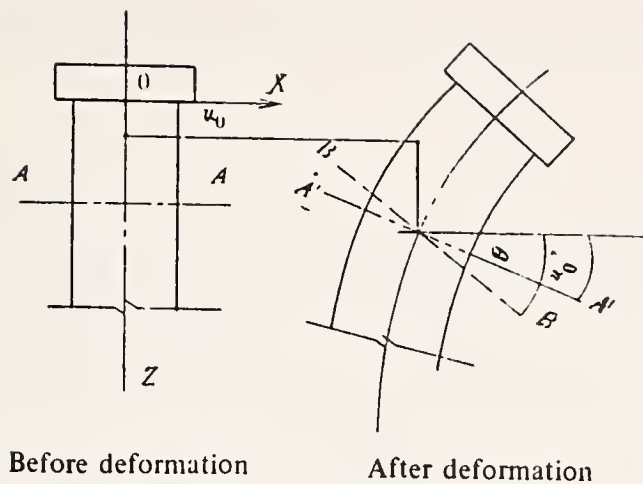


Fig. 7-8. Structural model

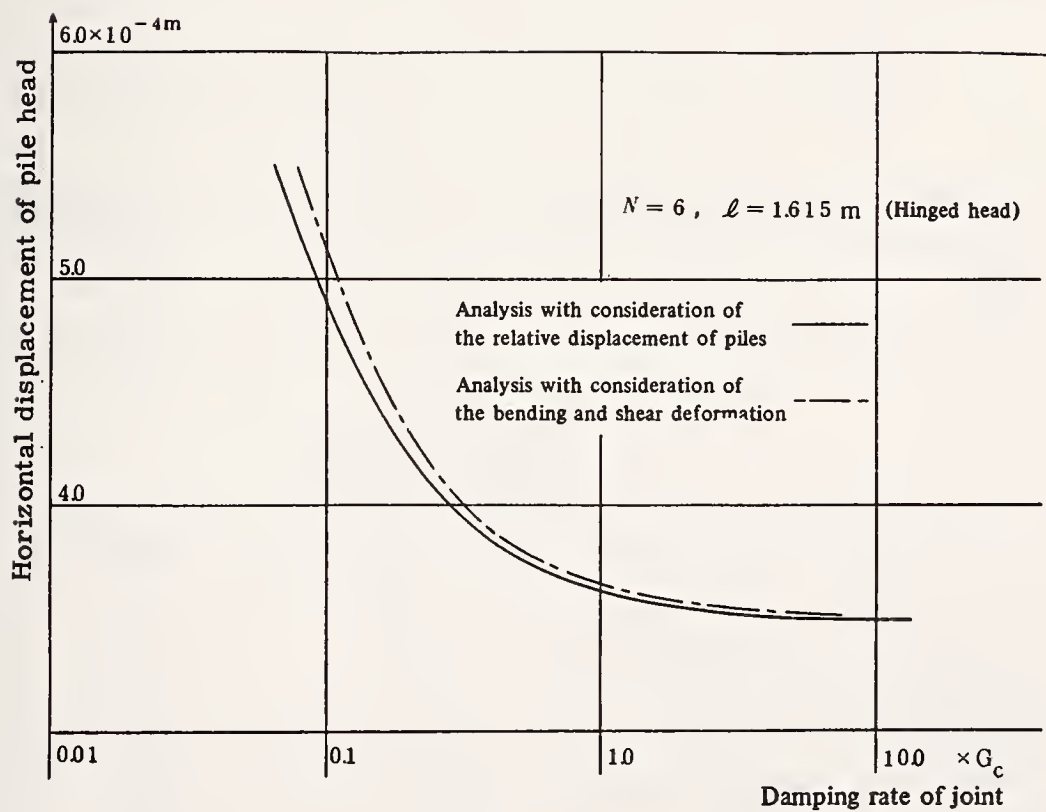
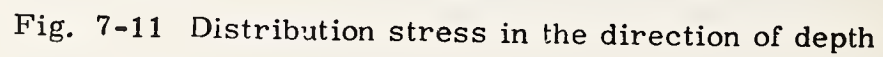
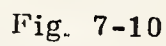


Fig. 7-9



ON SPECIFICATIONS FOR EARTHQUAKE-RESISTANT DESIGN
OF HIGHWAY BRIDGES (JANUARY, 1971)

by

Kenji Kawakami
Director, Public Works Research Institute

Eiichi Kuribayashi
Chief, Earthquake Engineering Research Section
Public Works Research Institute

Toshio Iwasaki
Chief, Civil Engineering Section, IISEE
Building Research Institute

and

Yutaka Iida
Research Engineer, Earthquake Engineering Research Section
Public Works Research Institute

ABSTRACT

This paper presents the details of new specification for Design of Highway Bridges to Resist Earthquakes, completed in January 1971 by the Highway Bridge Committee of the Japan Road Association.

Key Words: Earthquakes; Highway Bridges; Seismic Provisions; Specifications; Structural Engineering.

Introduction

In the event of a major seismic disaster, highway networks should perform their duties to facilitate evacuation, rescue and recovery operations with a minimum loss of life and property. In such a case, bridges, viaducts, etc. which constitute important parts of highways, would decide the fate of each route of a highway network. Therefore, the structural safety of these structures, against earthquakes, are extremely important.

In 1966 the Ministry of Construction commissioned the Japan Road Association to draw up a new comprehensive specification for the earthquake-resistant design of highway bridges, and accordingly provide maximum protection against earthquakes at minimum cost. In response to the commission, the Japan Road Association established a special committee to develop these new specifications, which were completed in January 1971. The Japan Road Association immediately reported to the Ministry of Construction, who then notified the highway administrative organization of these specifications. These specifications were then issued as directives of the Road and City Bureau on standards for bridges and viaducts in March 1971.

The directives issued are supplements to Article 5 of the Ministry of Construction Ordinance for the enforcement of the Road Structure Ordinance, which is a governmental ordinance. The legal conditions of this ordinance is as follows; The Road Structure Ordinance is in force and conforms with the Road Law. Article 30 of the Road Law provides that technical standards for bridges and other principal structures, which are designated by a governmental ordinance, may be subjected to a governmental ordinance. Paragraph 1 of Article 35 of the Road Structure Ordinance provides that bridges, viaducts, etc., shall be constructed of steel or concrete, of similar nature. Paragraph 2 of Article 35 provides the total design live loads shall be 20 or 14 tons, for bridges, etc. Paragraph 3 states that other matters concerned with the structural standards of bridges, etc. shall be provided by a Ministry of Construction ordinance. Article 5 of the Ministry of Construction Ordinance for the enforcement of the Road Structure Ordinance provides that bridges, viaducts, etc. shall be sufficiently safe against dead loads, live loads, wind loads, seismic effects and other loads which are expected to act on bridges and any combination of loads, considering structural types, traffic situations, topographical, geological, meteorological and other conditions.

Outline of Specifications for Earthquake-Resistant Design of Highway Bridges (January 1971)

Since 1956, the earthquake-resistant design of highway bridges had been conducted in accordance with the provisions of Section 13 (Section 2.9 in the English version) of "Specifications for Design of Steel Highway Bridges" which were issued in 1958 by the Japan Road Association. These specifications were revised in 1964 (the English version was issued in 1968) and subsequently displaced by "Specifications for Highway Bridges" in 1972, the details of which are as follows;

- (1) The horizontal design seismic coefficient shall be determined by Table 1.
- (2) The vertical design seismic coefficient shall be assumed equal to 0.10.
- (3) Increases in the allowable stresses for only seismic forces or for dead loads plus seismic loads shall be taken as

70% for steel structures

50% for concrete structures and reinforced concrete structures

Since the provisions in the Section 13 were not comprehensive, it was necessary to draw up new detailed specifications exclusively for aseismic design of highway bridges. Current "Specifications for Earthquake-Resistant Design of Highway Bridges" were issued in January 1971, by the Japan Road Association, which apply to the design of highway bridges with spans not longer than 200 meters, to be constructed on expressways, national highways, prefectural highways and principal municipal highways.

The specifications basically require that seismic coefficient methods be applied and that methods be used in determining the seismic coefficients. One method is the conventional seismic coefficient technique that applies to the design of relatively rigid structures. The other method is the modified seismic coefficient technique considering the structural response that applies to the design of relatively flexible structures. The following lists the principal points of the specifications;

- (1) The horizontal design seismic coefficient for a rigid structure is determined systematically, depending on the geographical location of the bridge site, the ground conditions at each sub-structure site, and the importance of the bridge. The horizontal design coefficient, for a flexible structure is determined as a function of the fundamental natural period of each structural system.
- (a) In the seismic coefficient method that is employed for relatively rigid structures, the horizontal design seismic coefficient (k_h) shall be determined by

$$k_h = v_1 v_2 v_3 k_0 \quad (1)$$

where :

- k_h : horizontal design seismic coefficient,
- k_0 : standard horizontal design seismic coefficient (=0.2),
- v_1 : seismic zone factor,
- v_2 : ground condition factor,
- v_3 : importance factor.

The values of v_1 , v_2 and v_3 are shown in Tables 2, 3 and 4 respectively. The definitions of classification are specified in the provisions. The minimum value of k_h shall be considered as 0.10.

- (b) In the modified seismic coefficient method considering structural response that is employed for relatively flexible structures such as a bridge with highrise piers higher than 25 m or a bridge with a fundamental period longer than 0.5 seconds, the horizontal design seismic coefficient (k_{hm}) shall be determined by

$$k_{hm} = \beta_{kh} \quad (2)$$

where :

k_{hm} : horizontal design seismic coefficient in the modified seismic coefficient method considering structural response

k_h : coefficient given by eq. (1)

β : a factor dependent on the fundamental period of the bridge, and obtained by Fig. 2. For structures whose fundamental periods are shorter than 0.5 seconds, β may be considered as 1.0.

The minimum value of k_{hm} shall be 0.05.

- (2) The vertical design seismic coefficient may generally be considered as zero, except for special portions such as bearing supports.
- (3) The horizontal design seismic coefficient for structural parts, soils and water below the ground surface may be considered as zero.
- (4) Hydrodynamic pressure during earthquakes are specified in the specifications. Earth pressures during earthquakes, however, are specified in the related specifications.
- (5) Specific attention should be paid to very soft soil layers and soil layers vulnerable to liquefaction during earthquakes. The bearing capacities of these layers are to be neglected in the design, in order to assure high earthquake-resistance for structures that are built in these layers.
- (6) Special attention should also be paid to the design of structural details, in consideration of the damage previously experienced to bridge structures. To this aim provisions are specified for bearing supports and devices for preventing bridge girders from falling.
- (7) Increases in the allowable stresses of materials may be considered in the earthquake-resistant design, magnitudes of increases for various materials are specified in several related specifications, and the increasing rates are as follows;

concrete in reinforced concrete structures;	50%
reinforcements in reinforced concrete structures:	50%
structural steel for superstructures:	70%
structural steel for substructures:	50%
concrete in prestressed concrete structures against compressive forces:	65%
foundation soils:	50%

Acknowledgments

Specifications for Earthquake-Resistant Design of Highway Bridges (January 1971) are the fruit of efforts of the Earthquake-Resistant Design Branch-Committee of the Specifications Subcommittee under the Highway Bridge Committee, the Japan Road Association. Special thanks are extended to the Branch-Committee headed by Mr. Yasuo Tada for his energetic efforts.

Table 1. Horizontal Design Seismic Coefficient (Out of Date)

Ground Conditions* Regions*	Weak	Ordinary	Firm
Where severe earthquakes have been frequently experienced	0.35~0.30	0.30~0.20	0.20~0.15
Where severe earthquakes have been occurred	0.30~0.20	0.20~0.15	0.15~0.10
Other regions	0.20	0.15	0.10

*no further description on regions and ground conditions.

Table 2. Seismic Zone Factor ν_1 for General Highway Bridges

Zone	Value of ν_1
A	1.00
B	0.85
C	0.70

Note: Refer to Fig. 1.

Table 3. Ground Condition Factor ν_2 for General Highway Bridges

Group	Definitions ¹⁾	Value of ν_2
1	(1) Ground of the Tertiary era or older (defined as bedrock hereafter) (2) Diluvial layer ²⁾ with depth less than 10 meters above bedrock	0.9
2	(1) Diluvial layer ²⁾ with depth greater than 10 meters above bedrock (2) Alluvial layer ³⁾ with depth less than 10 meters above bedrock	1.0
3	Alluvial layer ³⁾ with depth less than 25 meters, which has soft layer ⁴⁾ with depth less than 5 meters	1.1
4	Other than the above	1.2

- (Notes) 1) Since these definitions are not very comprehensive, the classification of ground conditions shall be made with adequate consideration of the bridge site.
Depth of layer indicated here shall be measured from the actual ground surface.
- 2) Diluvial layer implies a dense alluvial layer such as a dense sandy layer, gravel layer, or cobble layer.
- 3) Alluvial layer implies a new sedimentary layer made by a landslide.
- 4) Soft layer is defined in Section 3.7 "Soil Layer Whose Bearing Capacities are Neglected in Earthquake Resistant Design".

Table 4. Importance Factor ν_3 for General Highway Bridges

Group	Definitions	Value of ν_3
1	Bridges on expressways (limited-access highways), general national highways and principal prefectural highways. Important Bridges on general prefectural highways and municipal highways.	1.0
2	Other than the above	0.8

Note: The value of ν_3 may be increased up to 1.25 for special cases

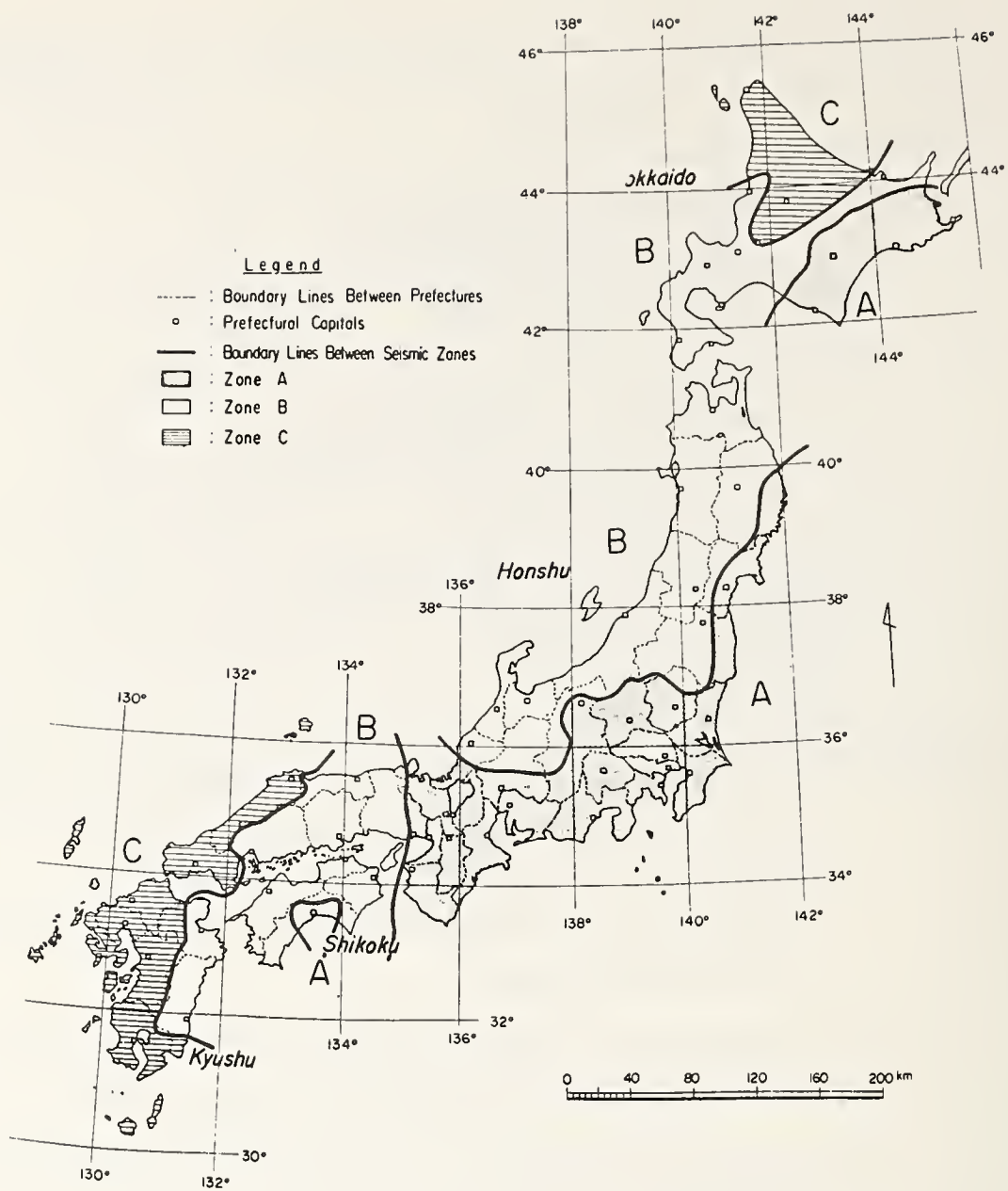


Fig. 1. Seismic Zoning Map

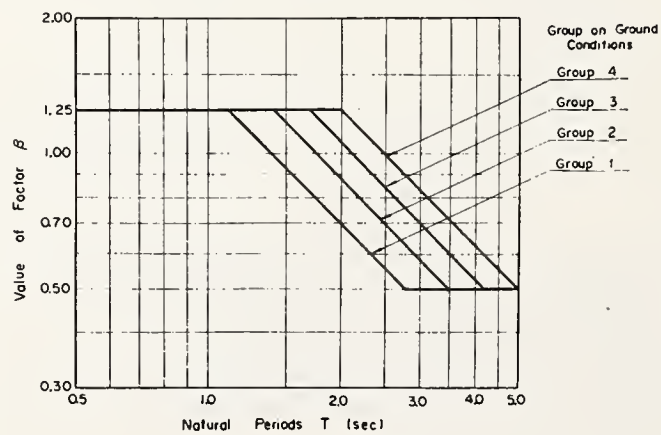


Fig. 2. Factor

APPENDIX
SPECIFICATIONS FOR EARTHQUAKE-RESISTANT DESIGN
OF HIGHWAY BRIDGES (JANUARY 1971)

Tentative English Version

JAPAN ROAD ASSOCIATION

FOREWORD

The earthquake-resistant design of highway bridges is currently being conducted in accordance with the provisions of Section 13 (Section 2.9 in the English version) of the Specifications for Design of Steel Highway Bridges. Since the provisions concerning earthquake-resistant design are not very comprehensive as stated in the preface of the Specifications, the design is in many respects dependent on the designer's interpretation. Accordingly the results of the various designs were not always consistent. To alleviate this problem it was necessary to revise the Section 13 of the Specifications and to draw up new detailed specifications exclusively for earthquake resistant design of highway bridges.

In response to the need for revisions, the Japan Road Association established the Earthquake Resistant Design Subcommittee under the Highway Bridge Committee in 1966. Between 1966 and 1968 a preliminary draft was prepared. The task was taken over by the Earthquake-Resistant Design Branch-Committee of the Specifications Subcommittee in 1968, when the Highway Bridge Committee was reorganized.

The Subcommittee and the Branch-Committee have seriously attempted to draw up the revision through surveys of the available research work, discussions with specialists from universities and other organizations, and trial calculations and bridge designs at several stages in accordance with the interim drafts, and finally completed the revision of the Specifications in 1971.

The new Specifications are completed basically in accordance with the provisions of Section 13 of the Specifications for Design of Steel Highway Bridges, and also by extensively referring to the results of recent investigations on earthquake engineering. Therefore the design methodology of Section 13 of the current Specifications was generally traced in establishing the new Specifications.

In determining the design seismic coefficient the importance factor is newly considered in addition to the traditional factors such as zone factor and ground condition factor. Moreover, for bridges which have longer natural periods the factor on the natural periods of the structures are considered.

Although the design horizontal seismic coefficient used to be 0.1 to 0.35 in the Section 13 of the current Specifications, the value is reduced to 0.1 to 0.3 and over 0.3 only for rare occasions in the new Specifications. This is based on the results of recent investigations that it seems more essential to pay attention to soil conditions rather than to the magnitude of seismic coefficients in design of bridges against seismic forces.

Since design seismic forces in the new Specifications were determined by referring to the seismic risk map expected for 75 years presented by Dr. Kawasumi and by reflecting the results of a recent study on the meteorological data since the Kanto Earthquake in 1923, seismic forces considered in the new Specifications would cover the severest earthquakes experienced in individual regions in Japan.

The seismic forces would also correspond to those due to the greatest earthquakes in the seismological point of view.

In the new Specifications the following aspects differ from the previous method.

- (1) The design seismic coefficients of a bridge are determined systematically dependent on geographical location of the bridge site, the ground conditions at each substructure site, and the importance of the bridge.
- (2) The vertical design seismic coefficients are generally neglected.
- (3) The design seismic coefficients for structural parts, soils and water below the ground surface are neglected.
- (4) Special attention is paid to very soft soil layers and soil layers vulnerable to liquefaction during earthquakes. The bearing capacities of these layers are neglected in the design in order to assure high earthquake-resistance for those structures which are constructed in these layers.
- (5) The design seismic coefficients for bridges with highrise piers are determined in accordance with the modified seismic coefficient method considering structural response, instead of the conventional way in which the design seismic coefficients increase with the height of the piers.

(6) Special attention is also paid to the design of structural details in view of earthquake damage previously experienced to bridge structures. To this end provisions are specified for bearing supports and devices for preventing superstructures from falling.

Although the Specifications were developed through extensive studies and discussions of research reports on earthquake engineering from throughout the world as well as Japan, some unexpected problems may arise when they are applied to actual structures. Because of this and the fact that technological improvements take place very rapidly, another revision will be required in the future. Everyone is urged to indicate any insufficient points or to make any suggestions for the present Specifications, so that they may be improved in subsequent revisions.

The present publication is limited to the provisions which are considered to be sufficient for the design of bridges. Comments which describe the basis and the application methods of the provisions will be issued immediately after their completion. They will be indispensable when it is necessary to revise the present Specifications again or when any parts of the provisions are found to be uncertain in their application.

Dr. Hiroshi Kawasumi, Dr. Tsutomu Terashima, and Mr. Tsutomu Tomita participated in the discussions on special matters as special members of the Committee. Their cooperation is greatly appreciated.

January, 1971

Earthquake Resistant Design Branch-Committee
Specifications Subcommittee
Highway Bridge Committee
Japan Road Association
3-3-3 Kasumigaseki
Chiyoda-ku, Tokyo

LIST OF MEMBERS

HIGHWAY BRIDGE COMMITTEE

Chairman:	Aoki, Kusuo		
Members:	Arie, Yoshiharu	Fukuda, Takeo	Fukuoka, Masami
	Hirai, Atsushi	Hiura, Taizo	Inomata, Shunji
	Kokubu, Masatane	Konishi, Ichiro	Kono, Michiyuki
	Matsuzaki, Akimaro	Murakami, Eiichi	Murakami, Tadashi
	Nakajima, Takeshi	Nakano, Takayuki	Naniwa, Hayato
	Naruse, Katsutake	Okamoto, Shunzo	Okubo, Tadayoshi
	Okumura, Toshie	Ozaki, Hisashi	Suzuki, Toshio
	Tahara, Yasuji	Tanaka, Goro	Tomonaga, Kazuo
	Uemae, Yukitaka	Yokomichi, Hideo	
Secretaries:	Komada, Keiichi	Kutsukake, Tetsuo	Miyazaki, Shoji
	Okada, Tetsuo	Sawai, Hiroyuki	

LIST OF MEMBERS

SPECIFICATIONS SUBCOMMITTEE

Chairman: Murakami, Eiichi

Members:

Adachi, Ko
 Horii, Kenichiro
 Ito, Manabu
 Kunihiro, Tetsuo
 Miyazaki, Shoji
 Nishiyama, Hironobu
 Okinaka, Koichiro
 Samukawa, Shigeomi
 Tada, Yasuo
 Tanabe, Suenobu

Fuse, Yoichi
 Inoue, Hirotsato
 Komada, Keiichi
 Maeda, Kunio
 Narita, Nobuyuki
 Okada, Tetsuo
 Saiki, Saburo
 Sawai, Hiroyuki
 Tamano, Mitsuharu

Secretaries:

Kato, Hiroshi
 Sato, Nobuhiko

Mori, Hiroaki
 Yamaki, Takashi

LIST OF MEMBERS

EARTHQUAKE RESISTANT DESIGN BRANCH-COMMITTEE

Chairman:

Tada, Yasuo

Members:

Adachi, Ko
 Asama, Tatsuo
 Ishihara, Kenji
 Keto, Hideyuki
 Kuribayashi, Eiichi*
 Nakamura, Hiroaki
 Okada, Tetsuo
 Oyamada, Yoshihiro*
 Tamura, Koichi
 Yahagi, Kaname

Arakawa, Tadashi*
 Iida, Yutaka*
 Iwasaki, Toshio*
 Kunihiro, Tetsuo
 Nakagawa, Kyoji
 Nishiyama, Hironobu
 Okubo, Teiji
 Shimokawa, Hiroshi
 Tsuji, Katsunari*
 Yoshinaka, Ryunoshin

Members with * are also secretaries.

CONTENTS

	Page
FOREWORD	(2)
LIST OF MEMEBERS	(3)
CHAPTER 1 GENERAL	(6)
1.1 Scope	(6)
1.2 Definitions of Terms	(6)
CHAPTER 2 BASIC PRINCIPLES FOR EARTHQUAKE RESISTANT DESIGN	(7)
CHAPTER 3 LOADS AND CONDITIONS IN EARTHQUAKE RESISTANT DESIGN	(7)
3.1 General	(7)
3.2 Seismic Effects	(8)
3.3 Inertia Forces	(8)
3.4 Earth Pressures during Earthquakes	(9)
3.5 Hydrodynamic Pressures during Earthquakes	(10)
3.6 Ground Surface Assumed in Earthquake Resistant Design	(11)
3.7 Soil Layers Whose Bearing Capacities are Neglected in Earthquake Resistant Design	(11)
3.8 Buoyancy or Uplifts	(11)
CHAPTER 4 DESIGN SEISMIC COEFFICIENT	(12)
4.1 General	(12)
4.2 Design Seismic Coefficient in the Seismic Coefficient Method	(12)
4.3 Factors for Modifying the Standard Horizontal Design Seismic Coefficient	(12)
4.4 Design Seismic Coefficient in the Modified Seismic Coefficient Method Considering Structural Response	(15)
CHAPTER 5 GENERAL PROVISIONS FOR DESIGN OF STRUCTURAL DETAILS	(19)
5.1 General	(19)
5.2 Devices for Preventing Superstructures from Falling	(19)
5.3 Vertical Seismic Forces for Design of Connections between Superstructures and Substructures	(20)
5.4 Methods for Transmitting Seismic Forces at Connections between Superstructures and Substructures	(20)
5.5 Devices Expected for Decreasing Seismic Forces	(21)
CHAPTER 6 MISCELLANEOUS PROVISIONS	(21)
REFERENCES*	(21)

CHAPTER 1 GENERAL

1.1 Scope

The provisions in the Specifications apply to earthquake resistant design of highway bridges with spans not longer than 200 meters, to be built on expressways, national highways, prefectural highways and principal municipal highways.

In regard to matters which are not specified herein, the following Specifications shall be conformed to, in accordance with the type of the structure considered.

Specifications for Design of Steel Highway Bridges,	Japan Road Association
Specifications for Design of Welded Highway Bridges,	Japan Road Association
Specifications for Design and Construction of Composite Beams for Steel Highway Bridges,	Japan Road Association
Specifications for Design of Reinforced Concrete Highway Bridges,	Japan Road Association
Specifications for Design and Construction of Friction Type Joints in Steel Highway Bridges Using High Strength Bolts,	Japan Road Association
Specifications for Design of Substructures of Highway Bridges,	Japan Road Association
Specifications for Prestressed Concrete Highway Bridges,	Japan Road Association

1.2 Definitions of Terms

The following definitions apply only to the provisions of these Specifications.

- (1) Earthquake: A phenomenon with propagation of vibration due to a sudden naturally occurring movement at a certain portion inside the earth.
- (2) Earthquake Ground Motion: Vibration of ground during earthquakes.
- (3) Design Seismic Coefficient: A coefficient indicating the magnitude of acceleration to be considered for earthquake-resistant design of structures, and expressed as a fraction of the acceleration of gravity.
- (4) Seismic Coefficient Method: A method for earthquake-resistant design in which seismic forces are assumed to act on structures as static forces.
- (5) Modified Seismic Coefficient Method Considering Structural Response: A method for earthquake resistant design which is developed through modification of the seismic coefficient method by considering characteristics of earthquake ground motions, dynamic properties of structures, etc. for those structures with long fundamental periods of vibration.
- (6) Modified Design Seismic Coefficient Considering Structural Response: A design seismic coefficient used in the modified seismic coefficient method considering structural response in which the design seismic coefficient is dependent on the fundamental period of the structure.
- (7) Standard Horizontal Design Seismic Coefficient: The Horizontal design seismic coefficient which applies to a bridge which is located in a zone where severe earthquakes have frequently occurred or where severe earthquakes have a high potential of occurrence, and which is constructed in soil layers with ground conditions corresponding to group 2 in Table 4.5.
- (8) Seismic Zone Factor: A factor to decrease the horizontal design seismic coefficient in accordance with the geographical location of the structural site. The factor has the value of 1.0 for those zones where severe earthquakes have frequently occurred or where severe earthquakes have a high potential of occurrence.
- (9) Ground Condition Factor: A factor to modify the horizontal design seismic coefficient depending upon the ground conditions of the structural site. The factor is intended to unify the margin of

safety against earthquake disturbances among structures constructed in various ground conditions, in consideration of damage previously experienced.

- (10) Importance Factor: A factor to modify the horizontal design seismic coefficient depending on the importance of the structure.
- (11) Inertia Force: Product of the weight of the structural body and the design seismic coefficient.
- (12) Seismic Force: Any forces such as inertia forces, earth pressures, etc. to which structures are subjected during earthquakes.
- (13) Coefficient of Subgrade Reaction: A coefficient given by the following formula, which is also shown in Section 3.1 of the Volume of Spread Foundations, the Specifications for Design of Substructures of Highway Bridges.

$$K = \frac{p}{\delta}$$

where

- K: coefficient of subgrade reaction in kg/cm³
- p: loading pressures in kg/cm²
- δ: displacement in cm

- (14) Earthquake Response Analysis: An analysis of the dynamic behavior of structures during earthquakes.

CHAPTER 2 BASIC PRINCIPLES FOR EARTHQUAKE-RESISTANT DESIGN

- (1) The earthquake-resistant design for a highway bridge shall provide sufficient stability against seismic disturbances for the structure as a unit and also for all parts thereof, including superstructures, substructures, and surrounding soils, considering topographical and geological conditions at the site.
- (2) The seismic coefficient method basically shall apply to the earthquake-resistant design of relatively rigid structures.
- (3) The modified seismic coefficient method considering structural response shall apply to the earthquake resistant design of relatively flexible structures which are of long fundamental periods of vibration, such as bridges with highrise piers.

The earthquake response analysis shall also be adopted for those structures, for which detailed investigations are required.

- (4) Particular attention shall be paid to preventing the fall of superstructures from substructures due to the movements during earthquakes.

When the design allowing for partial failures of the whole system or local failures of certain structural members is required on the basis of economical considerations, special attention to preventing the fall of superstructures shall be paid.

CHAPTER 3 LOADS AND CONDITIONS IN EARTHQUAKE-RESISTANT DESIGN

3.1 General

- (1) The following loads shall be taken into account in earthquake-resistant design. The appropriate loads shall be selected from this list on the basis of the location and the type of the structure.

- 1. Dead Loads
- 2. Earth Pressures
- 3. Hydraulic Pressures
- 4. Buoyancy or Uplifts
- 5. Effects of Temperature Change

6. Effects of Shrinkage due to Humidity in Concrete Structures (Including Creep Effects)
7. Seismic Effects
8. Effects of Friction at Bearing Supports
9. Effects of Consolidation and Settlement of Ground
10. Effects of Movements of Supports
11. Other Loads

(2) Combination of Loads

Design conditions shall be determined considering the following four cases. The combination of various loads listed above shall be decided in accordance with the provisions in individual Specifications according to the type of the bridge considered.

- Case 1 Maximum stresses will be expected in the members
Case 2 Maximum reactions will be expected in the foundation soils
Case 3 Maximum displacements will be expected at the supports
Case 4 The structure will become critical conditions due to overturning, sliding, etc.

3.2 Seismic Effects

The following seismic forces shall be taken into account to determine seismic effects in design of a bridge structure.

1. Inertia forces due to the dead weight of the structure: The magnitude of the inertia forces shall be the product of the weight of the structure and the design seismic coefficient. The design seismic coefficient shall be obtained in accordance with the provisions in Chapter 4 "Design Seismic Coefficient."
2. Inertia forces due to the superimposed weight: The magnitude of the inertia forces shall be the product of the superimposed weight and the design seismic coefficient. The design seismic coefficient also shall be obtained in accordance with the provisions in Chapter 4 "Design Seismic Coefficient."
3. Earth pressures during earthquakes.
4. Hydrodynamic pressures during earthquakes.

3.3 Inertia Forces

- (1) Both for the seismic coefficient method and the modified seismic coefficient method, bridge substructures shall be subjected to the inertia forces of superstructures during earthquakes as follows (refer to Fig. 3.1):

- (a) Horizontal seismic force acting on A_L (left abutment) shall be

$$H_{AL} = R_{AL} \cdot f_{AL} \text{-----} (3.1)$$

$$\text{where } H_{AL} \leq \frac{1}{2} k_h W_A \text{-----} (3.2)$$

In other words,

$$H_{AL} = \text{smallest of } \begin{cases} R_{AL} \cdot f_{AL} \\ \text{or} \\ \frac{1}{2} k_h W_A \end{cases}$$

- (b) Horizontal seismic force acting on P_1 (Pier 1) shall be

$$H_{AR} + H_{BL} = \text{largest of } \begin{cases} k_h W_A \text{ (} H_{BL} = 0 \text{ in this case)} \text{-----} (3.3) \\ \text{or} \\ \frac{1}{2} k_h W_A + R_{BL} \cdot f_{BL} \text{-----} (3.4) \end{cases}$$

In equation (3.4), $R_{BL} \cdot f_{BL}$ shall satisfy

$$R_{BL} \cdot f_{BL} \leq \frac{1}{2} k_h W_B \text{-----} (3.5)$$

(c) Horizontal seismic force acting on A_R (right abutment) shall be

$$H_{BR} = k_h W_B \text{-----} (3.6)$$

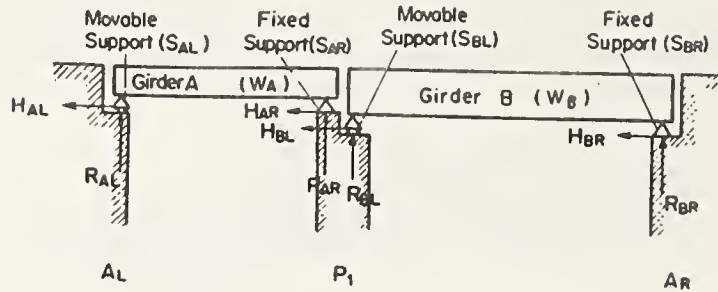


Fig. 3.1 Inertia Forces of Superstructures

where

- f_{AL} : Static friction coefficient at movable support A_L ,
- f_{BL} : Static friction coefficient at movable support B_L ,
- H_{AL} : Horizontal seismic force (inertia force or friction force) acting on A_L due to Girder A,
- H_{AR} : Horizontal seismic force (inertia force) acting on P_1 due to Girder A,
- H_{BL} : Horizontal seismic force (inertia force or friction force) acting on P_1 due to Girder B,
- H_{BR} : Horizontal seismic force (inertia force) acting on A_R due to Girder B,
- k_h : Horizontal design seismic coefficient (in accordance with the provisions in Chapter 4 "Design Seismic Coefficient": k_h in equation (4.1) for the seismic coefficient method, or k_{hm} in equation (4.2) for the modified seismic coefficient method, shall be employed),
- R_{AL} : Reaction at A_L due to W_A ,
- R_{AR} : Reaction at P_1 due to W_A ,
- R_{BL} : Reaction at P_1 due to W_B ,
- R_{BR} : Reaction at A_R due to W_B ,
- W_A : Dead weight of Girder A, and
- W_B : Dead weight of Girder B.

- (2) Inertia forces shall be assumed to act at the center of gravity of the structure. In designing the substructure, inertia forces exerted from superstructures may be assumed to act at the level of the base of the supports in the longitudinal direction to the bridge axis, and at the level of the center of gravity of the superstructures in the transverse direction.

In the transverse direction the level of the center of gravity of the superstructures may generally be taken as the lower level of the floor slab.

- (3) Inertia forces shall be assumed to come from two horizontal directions: longitudinal and transverse to the bridge axis, or parallel and perpendicular to the principal axis of any structural elements of the bridge.

3.4 Earth Pressures during Earthquakes

Earth pressures during earthquakes shall be determined in accordance with provisions in the Specifications for Design of Substructures of Highway Bridges (See Reference 1 at the end of the English

Version). The horizontal seismic coefficient in the calculation of earth pressures shall be in accordance with the provisions in Section 4.2 "Design Seismic Coefficient in the Seismic Coefficient Method."

3.5 Hydrodynamic Pressures during Earthquakes

Hydrodynamic pressures during earthquakes shall be determined by the following formulas. The pressures shall be assumed to act in the same direction as that of the inertia forces given by the provisions in Section 3.3 "Inertia Forces."

(1) Hydrodynamic Pressures on Walls

Hydrodynamic pressures acting on one side of a wall-type structure shall be determined as follows (refer to Fig. 3.2):

$$P = \frac{7}{12} k_h W_o b h^2 \text{-----} (3.7)$$

$$h_g = \frac{1}{2} h \text{-----} (3.8)$$

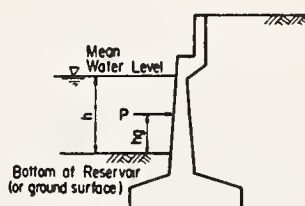


Fig. 3.2 Hydrodynamic Pressures on Wall Structures

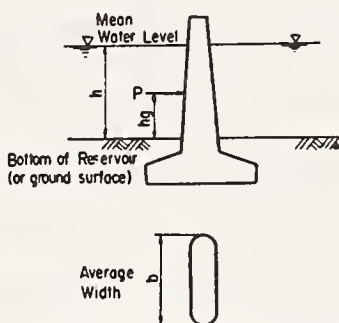


Fig. 3.3 Hydrodynamic Pressures on Column Structures

where

- b : Width of the wall in meters in the perpendicular direction to that of the pressure,
- h : Depth of water in meters,
- h_g : Height of the total hydrodynamic pressure in meters above the bottom of the water,

k_h : Horizontal design seismic coefficient given by the provisions in Section 4.2 "Design Seismic Coefficient in the Seismic Coefficient Method,"

P : Total hydrodynamic pressure in t, and

W_o : Unit weight of water in t/m³.

(2) Hydrodynamic Pressures on Columns

Hydrodynamic pressures acting on a column-type structure surrounding by water shall be determined as follows (refer to Fig. 3.3):

$$P = \frac{3}{4} k_h W_o b^2 h \left(1 - \frac{b}{4h}\right) \quad \text{for } \frac{b}{h} \leq 2 \text{ ----- (3.9)}$$

$$P = \frac{3}{8} k_h W_o b^2 h \quad \text{for } \frac{b}{h} > 2 \text{ ----- (3.10)}$$

$$h_g = \frac{1}{2} h \text{ ----- (3.11)}$$

3.6 Ground Surface Assumed in Earthquake Resistant Design

In earthquake resistant design the bearing capacities of soil layers which are specified in Section 3.7 "Soil Layers Whose Bearing Capacities are Neglected in Earthquake Resistant Design" shall be neglected. Ground surface in design shall be assumed to be the level of the lower boundary of the neglected layer, if the layer extends continuously below the actual ground surface.

For this case the neglected layer shall be assumed to have properties of zero cohesion and zero angle of internal friction.

3.7 Soil Layers Whose Bearing Capacities are Neglected in Earthquake Resistant Design

(1) Sandy Soil Layers Vulnerable to Liquefaction

Saturated sandy soil layers which are within 10 meters below the actual ground surface, have a standard penetration test N-value less than 10, have a coefficient of uniformity less than 6, and also have a D_{20} -value on the grain size accumulation curve between 0.04 mm and 0.5 mm, shall have a high potential for liquefaction during earthquakes. Bearing capacities of these layers shall be neglected in design.

Saturated sandy soil layers which have a D_{20} -value between 0.004 and 0.04 mm or between 0.5 mm and 1.2 mm may liquefy during earthquakes, and shall be given particular attention. Estimation whether or not these layers will liquefy shall be made in accordance with the available information on liquefaction problems.

When a special investigation is performed, the provisions in this item (1) in Section 3.7 may not be required to apply.

(2) Cohesive Soil Layers and Silty Soil Layers

Bearing capacities of cohesive soil layers and silty soil layers, which are within 3 meters of the actual ground surface, and are very soft such as those with the compression strength, determined by unconfined compression tests or field tests, less than 0.2 kg/cm², shall be neglected in design.

(3) Weight of Soil Layers Whose Bearing Capacities are Neglected

The weight of soil layers whose bearing capacities are neglected shall have surcharge effects on the lower ground.

3.8 Buoyancy or Uplifts

Buoyancy or uplifts shall be determined in accordance with the provisions in the Specifications for Design of Substructures of Highway Bridges (See Reference 2 at the end of the English Version).

CHAPTER 4 DESIGN SEISMIC COEFFICIENT

4.1 General

The design seismic coefficient shall generally be determined in accordance with the provisions in Section 4.2 "Design Seismic Coefficient in the Seismic Coefficient Method." For those bridges, however, which have flexible piers and long fundamental periods, such as those with piers higher than 25 meters above the ground surface, the design seismic coefficient shall be determined in accordance with the provisions in Section 4.4 "Design Seismic Coefficient in the Modified Seismic Coefficient Method Considering Structural Response."

4.2 Design Seismic Coefficient in the Seismic Coefficient Method

- (1) The horizontal design seismic coefficient shall be determined by the following formula:

$$k_h = \nu_1 \cdot \nu_2 \cdot \nu_3 \cdot k_o \text{-----(4.1)}$$

where

- k_h : Horizontal design seismic coefficient,
- k_o : The standard horizontal design seismic coefficient (= 0.2),
- ν_1 : Seismic zone factor,
- ν_2 : Ground condition factor, and
- ν_3 : Importance factor.

The value of k_h shall be rounded to two decimals. The minimum value of k_h shall be considered as 0.10. The values of factors ν_1 , ν_2 and ν_3 shall be obtained by the provisions in Section 4.3 "Factors for Modifying the Standard Horizontal Design Coefficient."

- (2) The vertical design seismic coefficient, k_v , may generally be considered as 0. Vertical seismic forces for design of bearing supports, however, shall be determined in accordance with the provisions in Section 5.3 "Vertical Seismic Forces for Design of Connections between Superstructures and Substructures."
- (3) The horizontal design seismic coefficient may be considered as 0 for structural parts, soils and water below the assumed ground surface in design. The assumed ground surface in design shall be determined in accordance with the provisions in Section 3.6 "Ground Surface Assumed in Earthquake Resistant Design."

Item (3), however, shall not apply to underground structures such as culverts.

4.3 Factors for Modifying the Standard Horizontal Design Seismic Coefficient

(1) Seismic Zone Factor

Seismic zone factor shall be determined in accordance with Table 4.1, in which the zone classification shall be determined from Fig. 4.1 or Table 4.2.

Table 4.1 Seismic Zone Factor ν_1

Zone	Value of ν_1
A	1.00
B	0.85
C	0.70

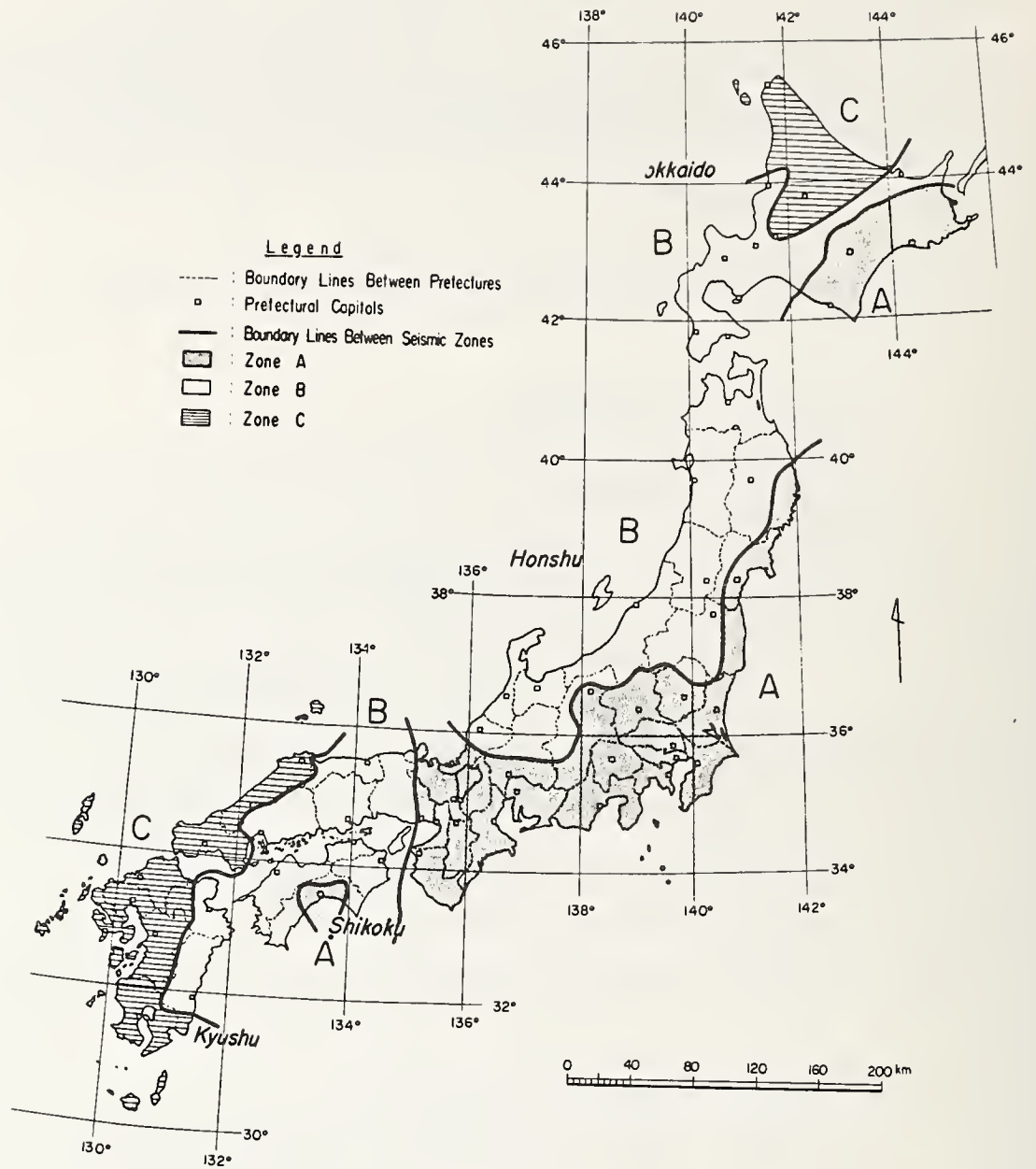


Fig. 4.1 Seismic Zoning Map

(Note)

Table 4.2, which indicates in detail the seismic zone through the use of place names, is omitted in the English version.

(2) Ground Condition Factor

Ground condition factor shall be determined in accordance with Table 4.3.

Table 4.3 Ground Condition Factor ν_2

Group	Definitions ¹⁾	Value of ν_2
1	(1) Ground of the Tertiary era or older (defined as bedrock hereafter) (2) Diluvial layer ²⁾ with depth less than 10 meters above bedrock	0.9
2	(1) Diluvial layer ²⁾ with depth greater than 10 meters above bedrock (2) Alluvial layer ³⁾ with depth less than 10 meters above bedrock	1.0
3	Alluvial layer ³⁾ with depth less than 25 meters, which has soft layer ⁴⁾ with depth less than 5 meters	1.1
4	Other than the above	1.2

(Notes)

- 1) Since these definitions are not very comprehensive, the classification of ground conditions shall be made with adequate consideration of the bridge site.
Depth of layer indicated here shall be measured from the actual ground surface.
- 2) Diluvial layer implies a dense alluvial layer such as a dense sandy layer, gravel layer, or cobble layer.
- 3) Alluvial layer implies a new sedimentary layer made by a landslide.
- 4) Soft layer is defined in Section 3.7 "Soil Layer Whose Bearing Capacities are Neglected in Earthquake Resistant Design."

(3) Importance Factor

Importance factor shall be determined in accordance with Table 4.4.

Table 4.4 Importance Factor ν_3

Group	Definitions	Value of ν_3
1	Bridges on expressways (limited-access highways), general national highways and principal prefectural highways. Important Bridges on general prefectural highways and municipal highways.	1.0
2	Other than the above	0.8

Note: The value of ν_3 may be increased up to 1.25 for special cases in Group 1.

4.4 Design Seismic Coefficient in the Modified Seismic Coefficient Method Considering Structural Response

The design seismic coefficient specified in this Section shall apply to the design of superstructures and substructures of those bridges which have flexible piers and relatively long fundamental periods, such as ones in which the height of the substructures is 25 meters or more above the ground surface in design.

The above-mentioned ground surface in design shall be specified in Section 3.6 "Ground Surface Assumed in Earthquake Resistant Design."

The Design Seismic coefficients in this Section shall be determined by modifying the horizontal design seismic coefficient in Section 4.2 "Design Seismic Coefficient in the Seismic Coefficient Method," on the basis of characteristics of strong earthquake ground motions recorded, and dynamic properties of bridge structures, such as natural periods, mode shapes and damping capacities of bridge substructures.

After obtaining the design seismic coefficient, the method for applying seismic loads for the design shall be the same as specified by the provisions in Chapter 3 "Loads and Conditions in Earthquake Resistant Design."

The provisions in this Section shall not apply to the design of superstructures of those bridges in which superstructures are flexible and have longer periods, such as suspension bridges.

4.4.1 Design Seismic Coefficient

(1) The horizontal design seismic coefficient shall be determined by the following formula:

$$k_{hm} = \beta k_h \text{-----} (4.2)$$

where

k_{hm} : Horizontal design seismic coefficient in the modified seismic coefficient method considering structural response,

k_h : Horizontal design seismic coefficient given by eq. (4.1), and

β : A factor dependent on the fundamental period of the bridge, and obtained by Table 4.5 or Fig. 4.2.

For structures whose fundamental periods are shorter than 0.5 sec., β may be considered as 1.0

The value of k_{hm} shall be rounded to two decimals. The minimum value of k_{hm} shall be considered as 0.05.

- (2) The vertical design seismic coefficient shall be provided in accordance with the provisions in Item (2) of Section 4.2.
- (3) The horizontal design seismic coefficient for the portions below the assumed ground surface in design, shall be provided in accordance with the provisions in Item (3) of Section 4.2.

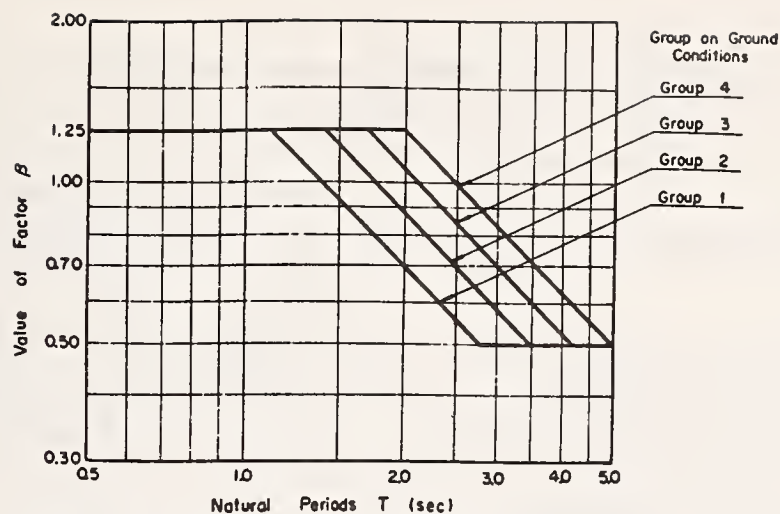


Fig. 4.2 Factor β (For reference of Table 4.5)

Table 4.5 Value of β

Group on Ground Conditions	Value of β for Fundamental Period T (sec.)		
1	$\beta = 1.25$ for $0.5 \leq T \leq 1.1$	$\beta = 1.40/T$ for $1.1 \leq T \leq 2.8$	$\beta = 0.50$ for $T \geq 2.8$
2	$\beta = 1.25$ for $0.5 \leq T \leq 1.4$	$\beta = 1.75/T$ for $1.4 \leq T \leq 3.5$	$\beta = 0.50$ for $T \geq 3.5$
3	$\beta = 1.25$ for $0.5 \leq T \leq 1.7$	$\beta = 2.10/T$ for $1.7 \leq T \leq 4.2$	$\beta = 0.50$ for $T \geq 4.2$
4	$\beta = 1.25$ for $0.5 \leq T \leq 2.0$	$\beta = 2.50/T$ for $2.0 \leq T \leq 5.0$	$\beta = 0.50$ for $T \geq 5.0$

(Notes)

- 1) Refer to Fig. 4.2.
- 2) Refer to Table 4.3 regarding groups on ground conditions.

4.4.2 Method for Obtaining Fundamental Periods

Fundamental natural periods of a bridge shall be determined for the individual system consisting of each substructure and the part of superstructures supported by it rather than for the structural system as a whole.

(1) Bridges Supported by Spread Foundations or Pile Foundations

For those bridges which are supported by spread foundations or pile foundations, the fundamental periods may be obtained from Table 4.6.

Any formulas in Table 4.6 shall apply to bridges in which the level of the base of the footing is lower than that of the assumed ground surface in design and the deformation of the substructure is mainly caused by the elastic flexural deformation of the pier which is the upper part of the substructures above the top of the footing. Therefore, they shall not apply to bridges in which the level of the base of the footing is higher than that of the assumed ground surface in design.

Table 4.6 Fundamental Periods of Bridges Supported by Spread Foundations or Pile Foundations

Type of Structural System	Direction	Formulas for Fundamental Periods	
		Material of Pier	
		Reinforced Concrete	Steel
1 A bridge where most superstructures are continuous, have fixed supports (or movable supports specified in Article 5.2.1) on most substructures, and also have rigid abutments, to one of which the extreme end of the superstructures is connected with a fixed support (See Fig. 4.3)	Transverse	$T = 2\pi \sqrt{\frac{0.3W_p + W_u}{3EI_g} h^3}$ (4.3)	$T = 2\pi \sqrt{\frac{0.3W_p + W_u}{4.5EI_g} h^3}$ (4.4)
	Longitudinal	$T = \frac{\pi}{8} \sqrt{\frac{W_p}{EI_g} h^3}$ (4.5)	
2 Other than the above: For example, a bridge with simple supports	Longitudinal or Transverse	$T = 2\pi \sqrt{\frac{0.3W_p + W_u}{3EI_g} h^3}$ (4.6)	

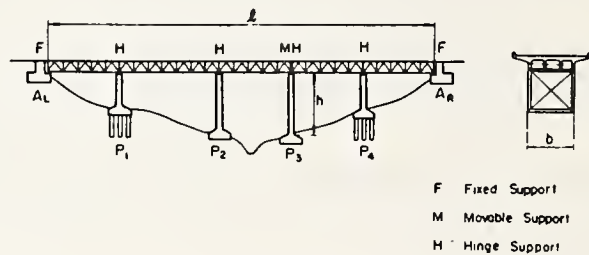


Fig. 4.3 An Example of Type 1 of Structural System in Table 4.6

where

- T : Fundamental period in second of the system consisting of a substructure and the section of the superstructures which it supports,
 W_p : The weight of the pier in t ,
 W_u : The weight of the section of superstructures in t supported by the substructure being considered,
 E : Young's modulus of the pier in t/m^2 ,
 I : Moment of inertia of the pier in m^4 in the direction considered.
 For piers with varying section with the height, I may be an average value,
 h : The height of the pier in m , and
 g : Acceleration of gravity ($= 9.8 \text{ m/sec}^2$).

(Note)

Eq. (4.4) shall apply to those bridges which have a ratio of the length between supports on both abutments to the width between outside girders, less than approximately 50 (refer to ℓ/b in Fig. 4.3).

(2) Bridges Supported by Caisson Foundations

For those bridges which are supported by caisson foundations, the fundamental periods may be obtained from Table 4.7.

Table 4.7 Fundamental Periods of Bridges Supported by Caisson Foundations

Type of Structural System		Direction	Formulas for Fundamental Periods
1	Type 1 in Table 4.6	Transverse	one of eqs. (4.3) (or (4.4), and (4.7), which gives the largest value of β
		Longitudinal	eq. (4.5)
2	Type 2 in Table 4.6	Transverse	one of eqs. (4.6) and (4.7), which gives the largest value of β
		Longitudinal	

(Note)

$$T = 2\pi \sqrt{\frac{(h + \frac{2}{3}l)^2 W_u + (\frac{1}{3}h^2 + \frac{2}{3}hl + \frac{4}{9}l^2) W_p + \frac{l^2}{9} W_c}{g \left\{ K_H \frac{bl^3}{36} + K_S \frac{Al^2}{9} + K_v l B \right\}}} \quad \text{----- (4.7)}$$

where

- T : Fundamental period in second of the system consisting of a substructure and the section of the superstructures which it supports,
 W_p : The weight of the pier in t,
 W_u : The weight of the part of superstructures in t supported by the substructure being considered,
 W_c : The weight of the caisson foundation in t,
 h : The height of pier in m,
 A : Cross-sectional area in m^2 at the base of the caisson foundation,
 I_B : Moment of inertia in m^4 at the base of the caisson foundation in the direction considered,
 K_H : Horizontal coefficient of subgrade reaction in t/m^3 at the level of the base of the caisson foundation,
 K_v : Vertical coefficient of subgrade reaction in t/m^3 at the base of the caisson foundation,
 K_S : Horizontal coefficient of subgrade reaction in t/m^3 for shear deformation at the base of the caisson foundation, and
 g : Acceleration of gravity ($= 9.8 \text{ m/sec}^2$).

CHAPTER 5 GENERAL PROVISIONS FOR DESIGN OF STRUCTURAL DETAILS

5.1 General

Every bridge structure or every portion thereof shall be designed and constructed to resist seismic forces as provided in Chapter 1 through Chapter 4 and to meet the provisions for design of structural details specified in this Chapter.

Moreover, attention shall be paid to the following respects.

- (1) For those abutments which are constructed in soft ground layers, the failure of the ground layer during earthquakes shall be checked.
- (2) For those bridges in which any adjacent substructures have different ground conditions, different type of structural systems, or different structural dimensions, special attention shall be paid to the design of structural details, considering that those two substructures may respond differently during earthquakes.
- (3) For those portions such as joints between superstructures and substructures, connections between piers and foundations, or connections between footings and piles in pile foundations, where the seismic forces may not be transmitted smoothly and seismic failure have been observed often in the past, particular attention shall be paid to the design of structural details, considering accuracy of evaluation of ground conditions, existence of construction joints, accuracy of construction, etc.

5.2 Devices for Preventing Superstructure from Falling

Movable supports shall have stoppers (special devices for resisting large movements of superstructures during earthquakes) to prevent the superstructures from falling from the substructures, caused by the dislocation of the upper shoes of the supports from the lower shoes during strong earthquakes (refer to 5.2.1).

For the girder ends one of the following methods shall be employed as well as the above-mentioned consideration.

- (1) A method extending the length between the end of the support and the edge of the substructure (or widening the width of the crest of the substructure in the longitudinal direction to the bridge axis) in order to prevent the superstructures from falling from the substructure (refer to 5.2.2 or 5.2.3).
- (2) A method connecting adjacent girders on the substructure to prevent the superstructures from falling from the substructure even if they become dislodged from the substructure (refer to 5.2.4).

5.2.1 Stoppers at Movable Supports

The allowable movable length in the design of stoppers at movable supports shall be assumed as the sum of the movement due to temperature change, the movement due to the deflection of the girder when subjected to live loads, a margin for covering construction errors, and 20 mm.

The above-mentioned provision need not apply to those stoppers which are not installed near the supports.

The horizontal design seismic coefficients for designing stoppers shall be determined by increasing the horizontal design seismic coefficient given by eq. (4.1) or (4.2) by 50% or more.

5.2.2 Method of Extending the Length between the End of the Support and the Edge of the Substructure

For those substructures which support the ends of girder, the length S (in cm) between the end of the support and the edge of the substructure, shall be equal to or more than the value given by the following formulas:

$$S = 20 + 0.5 \, l \quad \text{for } l \leq 100 \, \text{m}$$

$$S = 30 + 0.4 \, l \quad \text{for } l > 100 \, \text{m}$$

where

S : Length between the end of the support and the edge of the substructure in cm, and

l : Span length in meters.

For particularly important bridges constructed in soft ground layers (Group 4 in Table 4.3), the value of S shall be equal to 35 cm or more.

5.2.3 Suspended Joints

For suspended joints the length between the ends of girders shall be equal to 60 cm or more, as shown in Fig. 5.1. The length for those bridges constructed in soft ground layer (Group 4 in Table 4.3) shall be equal to 70 cm or more.

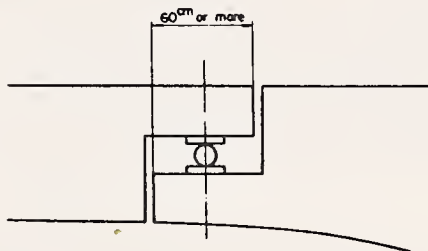


Fig. 5.1 Length between the Ends of both Girders

5.2.4 Method of Connecting Adjacent Girders

Devices for connecting adjacent girders on substructures shall have the movable length specified in Section 5.2.1, for cases in which at least one of two supports is a movable one.

The devices shall be designed to rotate freely to allow the rotation of the girder subjected to live loads, for cases in which both two supports are fixed on one pier.

5.3 Vertical Seismic Forces for Design of Connections between Superstructures and Substructures

The vertical design seismic coefficient for the design of connections between superstructures and substructures shall be assumed as 0.10. When the vertical design seismic coefficient applies upward, only seismic forces shall be considered, neglecting the effects of the dead loads.

The same value of the vertical design seismic coefficient shall be employed for the design of any connections similar to the above.

5.4 Methods for Transmitting Seismic Forces at Connections between Superstructures and Substructures

The method for transmitting seismic forces at connection between superstructures and substructures shall be as follows:

- (1) For cast-in-place reinforced concrete bridges, the means of transmission of seismic forces shall be due to the bearing pressure between the swelling at the base of the lower shoe and the concrete at the crest of the substructure. The concrete portion near the base of the lower shoe shall resist seismic forces as one body together with the pier of the substructure. In the above-mentioned cases, the means of transmission of seismic forces between the upper shoe and the girder shall be due to the anchors fixed on the upper shoe.

For a margin of safety, anchor bolts between the lower shoe and the substructure shall be designed to resist seismic forces alone, in consideration of cases where no resistance between the swelling at the base of the lower shoe and the concrete at the crest of the substructure can be expected.

The above method is recommended not only for cast-in-place concrete bridges, but, if possible, also for prefabricated concrete bridges or steel bridges.

- (2) In cases where no bearing resistance of concrete can be expected, anchor bolts shall be employed to transmit the seismic forces. In these cases one of the following two methods shall be considered.
- (a) A method in which a steel plate with anchor bolts is fixed firmly on the crest of a substructure while concrete is being placed, and then the lower shoe of the support is welded to the steel plate after the erection of the girders.
 - (b) A method in which a hole is prepared when concrete is placed, a support is set up near the hole, and then anchor bolts are fixed by placing cement mortar into the hole, or a method in which anchor bolts are set up while concrete is being placed, and then the lower shoe is fixed on the anchor bolts.
- (3) Anchor bolts used shall be 25 mm or more in diameter, and the depth of the anchor bolts fixed in the concrete shall be 10 times the diameter or more.

5.5 Devices Expected for Decreasing Seismic Forces

When any devices which are expected to decrease seismic force are employed for bridge structures, sufficient investigations shall be conducted on their effectiveness, and special attention shall be paid to preventing the superstructures from falling.

CHAPTER 6 MISCELLANEOUS PROVISIONS

When sufficient reasons exist, these Specifications need not apply to the design of bridges.

REFERENCE

References are provided exclusively in the English version.

[Reference 1]

Specifications for Design of Substructures of Highway Bridges

Volume for General Survey and Design

Part 3 Design, Chapter 2 Loads.

Section 2.5 Earth Pressures

Earth pressures acting on a wall shall be the distributed loads given by the following formulas:

(1) Normal Earth Pressures

(a) Earth pressures acting on a movable wall during normal time shall be determined by the Coulomb's theory as follows:

i) For Sandy Soils

$$P_A = \gamma \cdot K_A x + K_A q$$

$$P_P = \gamma \cdot K_P x + K_P q$$

ii) For Cohesive Soils

$$P_A = \gamma \cdot K_A x - 2C\sqrt{K_A} + K_A q$$

$$P_P = \gamma \cdot K_P x + 2C\sqrt{K_P} + K_P q$$

(b) Earth pressures on a fixed wall during normal time shall be determined by

$$P_A = \gamma \cdot K_s \cdot x + K_s q$$

(2) Earth pressures during earthquakes shall be determined by the Mononobe-Okabe method.

$$P_A = (1 - k_v) \gamma \cdot x \cdot K_{EA}$$

$$P_P = (1 - k_v) \gamma \cdot x \cdot K_{EP}$$

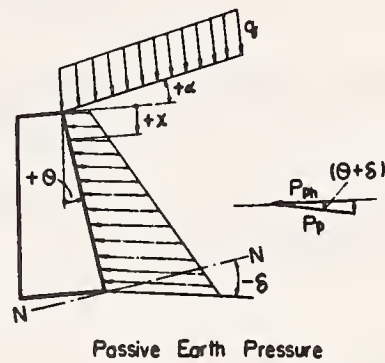
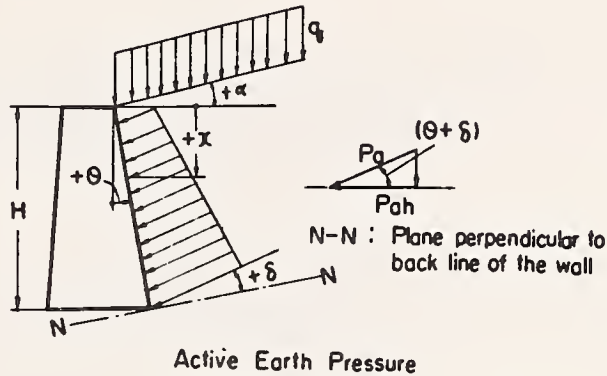


Fig. 1 Earth Pressure

where

- C : Cohesion of the soil in t/m^2 ,
- K_A : Active earth pressure coefficient for Coulomb's theory,
- K_P : Passive earth pressure coefficient for Coulomb's theory,
- K_{EA} : Active earth pressure coefficient during earthquakes,
- K_{EP} : Passive earth pressure coefficient during earthquakes,
- K_s : Earth pressure coefficient at rest,
- k_v : Vertical seismic coefficient,
- P_A : Active earth pressure in t/m^2 at depth of x meters,
- P_P : Passive earth pressure in t/m^2 at depth of x meters,
- q : Surcharge in t/m^2 on ground surface,
- x : Arbitrary depth in meters,
- α : Angle between the ground surface line and the horizontal line,
- γ : Unit weight of the soil in t/m^3 ,
- δ : Angle of friction between the wall and the soil,
- ϕ : Angle of internal friction of the soil, and
- θ : Angle between the back line of the wall and the vertical line.

(Comments)

K_A, K_P, K_{EA} and K_{EP} are expressed as follows:

$$K_A = \frac{\cos^2 (\phi - \theta)}{\cos^2 \theta \cdot \cos (\theta + \delta) \left[1 + \sqrt{\frac{\sin (\phi + \delta) \cdot \sin (\phi - \alpha)}{\cos (\theta + \delta) \cdot \cos (\theta - \alpha)}} \right]^2}$$

$$K_P = \frac{\cos^2 (\phi + \theta)}{\cos^2 \theta \cdot \cos (\theta + \delta) \left[1 - \sqrt{\frac{\sin (\phi - \delta) \cdot \sin (\phi + \alpha)}{\cos (\theta + \delta) \cdot \cos (\theta - \alpha)}} \right]^2}$$

$$K_{EA} = \frac{\cos^2 (\phi - \theta_0 - \theta)}{\cos \theta_0 \cdot \cos^2 \theta \cdot \cos (\theta + \theta_0) \left[1 + \sqrt{\frac{\sin \phi \cdot \sin (\phi - \alpha - \theta_0)}{\cos (\theta - \theta_0) \cdot \cos (\theta - \alpha)}} \right]^2}$$

$$K_{EP} = \frac{\cos^2 (\phi - \theta_0 + \theta)}{\cos \theta_0 \cdot \cos^2 \theta \cdot \cos (\theta - \theta_0) \left[1 - \sqrt{\frac{\sin \phi \cdot \sin (\phi + \alpha - \theta_0)}{\cos (\theta - \theta_0) \cdot \cos (\theta - \alpha)}} \right]^2}$$

where $\sin (\phi \pm \alpha - \theta_0) = 0$ when $\phi \pm \alpha - \theta_0 < 0$
and δ is assumed to be zero during earthquakes.

where

$$\theta_0 = \tan^{-1} \frac{k_h}{1 - k_v}$$

k_h : Horizontal seismic coefficient

k_v : Vertical seismic coefficient

[Reference 2]

Specifications for Design of Substructures of Highway Bridges

Volume for General Survey and Design

Part 3 Design, Chapter 2 Loads

Section 2.7 Buoyancy or Uplifts

When it is apparent that buoyancy forces or uplifts act on structures, they shall be taken into account in the design.

(Comments)

When it is unknown whether they act or not, both cases shall be taken into account in the design.

ON SPECIFICATIONS FOR EARTHQUAKE-RESISTANT DESIGN
OF THE HONSHU-SHIKOKU BRIDGES (JSCE 1974)

by

Ishio Kawasaki
Director, Honshu-Shikoku Bridge Authority

and

Eiichi Kurbayashi
Chief, Earthquake Engineering Research Section
Public Works Research Institute
Ministry of Construction

ABSTRACT

The following describes the general specifications for earthquake resistant design of the Honshu-Shikoku Bridges, as developed by JSCE in 1974, after significant study.

Key Words: Bridges; Earthquake Design; Earthquake Forces; Specifications; Seismic Provisions.

Introduction

The Japan Society of Civil Engineers issued "Specifications for Earthquake-Resistant Design of the Honshu-Shikoku Bridges"⁽¹⁾ in May, 1967. The Specifications were developed by JSCE's Sub-Committee (Chairman: Professor Shunzo Okamoto), which existed for a five year period. The committee started in 1962 with a commission jointly from the Ministry of Construction and the Japanese National Railways (the Japan Railways Construction Public Corporation took over the work of JNR after March, 1964). In May, 1970 three years after the completion of the above Specifications (1967), the Earthquake Engineering Committee (Standing Committee) of the JSCE established a Joint Meeting for Studying Earthquake-Resistant Design of the Honshu-Shikoku Bridges (Chairman: Professor Shunzo Okamoto), and to consider future research needs. The Joint Meeting was organized in cooperation with the regular members of the Earthquake Engineering Committee, the staff members of the Japan Highway Public Corporation, the Japan Railways Construction Public Corporation and the Honshu Shikoku Bridge Authority (the Authority was established in July, 1970), and experts from various organizations. The committee attempted to improve the Specifications (1967) in view of recent progress in the area, and presented in June, 1971 a report⁽²⁾ summarizing the results of its research activity.

Furthermore, with a commission from the Honshu-Shikoku Bridge Authority, the JSCE established a Research Sub-Committee on Earthquake-Resistant Design of the Honshu-Shikoku Bridges (Chairman: Professor Keizaburo Kubo) in June, 1971. The Research Sub-Committee's charge was to amend the Specifications for Earthquake-Resistant Design of the Honshu-Shikoku Bridges (1967) and also to clarify the design procedure details. The Research Sub-Committee studies showed that the following three subjects should be investigated extensively;

- 1) Evaluation of seismic forces--Effects of near earthquakes on structures, effects of long-period ground motions and their measuring systems, factors to be considered in determining the magnitude of seismic forces, etc.
- 2) Evaluation of dynamic characteristics of soils and foundations--Dynamic characteristics of multi-column foundations and caisson foundations with an emphasis in obtaining a design procedure based on dynamic analysis of foundations, investigations on earthquake-resistant design practices for foundations, etc.
- 3) Earthquake-resistant design practices for bridges with span length of 200 m or more (such as suspension bridges, truss bridges, etc).

The Research Sub-Committee concluded investigations on those subjects by March, 1974, and recently published the final report⁽³⁾. The report proposes revised Specifications for Earthquake-Resistant Design of the Honshu-Shikoku Bridges (1974). Although the new Specifications (1974) include the commentary which gives additional explanations necessitated for design practices, the main body of the Specifications will be introduced herein.

1. General

1.1 Scope

The provisions in the Specifications apply to earthquake-resistant design of the Honshu-Shikoku bridges.

1.2 Notations

The following notations are used in the Specifications:

Notation	Definition	Unit
A	Lateral cross-sectional area of a structure	m ²
a	Length of cross-section of a structure in the parallel direction to that of seismic motion considered	m
b	Width of cross-section of a structure in the perpendicular direction to that of seismic motion considered	m
d	Depth of water	m
h	Damping ratio	m
K _D	Design seismic coefficient	
K _R	Response seismic coefficient	
S _a	Response acceleration spectrum	cm/sec ²
S _v	Response velocity spectrum	cm/sec
T	Natural period of a structure	sec
x	Any depth below the surface of water or ground	m
α	Coefficient dependent on vibrational modes of a structure	
β	Coefficient dependent on shape of a foundation	
γ _w	Unit weight of sea water	t/m ³
μ	Modification factors necessitated in obtaining design seismic coefficient from response seismic coefficient	

2. Earthquake to be Considered in Design

2.1 Earthquake to be Considered in Design

An earthquake with the following characteristics shall be considered in design:

- 1) Magnitude: Large-scale (Namely around 8 on the Richter scale)
- 2) Location: Comparatively far from the bridge sites (Namely off Kii Peninsula, or off Tosa)
- 3) Frequency: Once or twice per one hundred years

2.2 Design Ground Acceleration

The maximum value of the design ground acceleration shall be 180 gals at the level of the surface of ground layers which support foundations at the bridge sites.

3. Basic Principle for Earthquake-Resistant Design

3.1 Method of Design Calculation

- 1) For structures whose principal dimensions are determined by some requirements other than those by earthquake resistant design, the modified seismic coefficient method considering structural response shall be adopted. The results shall generally be examined through a dynamic analysis.
- 2) For structures whose principal dimensions can be determined by requirements from earthquake-resistant design, the structural dimensions shall be determined by the response spectrum method of dynamic analysis. In such cases the results should be examined through a numerical integration method of a dynamic analysis.

4. Design by the Modified Seismic Coefficient Method Considering Structural Response

4.1 Design Procedure

In a design, based on the modified seismic coefficient method when considering structural response, the seismic forces specified in 4.2 and additional effects specified in 4.4 shall be taken into account simultaneously.

4.2 Seismic Forces

Seismic forces shall be determined by the product of structural dead weight and the design seismic coefficient. The design seismic coefficient is provided in "4.3 Design Seismic Coefficient Considering Structural Response."

4.3 Design Seismic Coefficient Considering Structural Response

4.3.1 Horizontal Response Seismic Coefficient

The horizontal response seismic coefficient (K_R) shall be determined from Fig. 1. This figure was obtained by assuming the following conditions:

- 1) Foundations are constructed directly on the Tertiary layer (or older) at the site where the surface Quaternary layer is shallow or none.
- 2) The maximum ground acceleration for design is expected to be 180 gals.

4.3.2 Vertical Response Seismic Coefficient

The Vertical response seismic coefficient shall be generally the half of the horizontal response seismic coefficient.

4.3.3 Design Seismic Coefficient Considering Structural Response

The design seismic coefficient, considering structural response, shall be determined by the following formula:

$$K_D = \mu_1 \cdot \mu_2 \cdot \mu_3 \cdot \mu_4 \cdot \mu_5 \cdot K_R$$

where K_D : Design seismic coefficient considering structural response

K_R : Response seismic coefficient (see Fig. 1) dependent on structural type and the predominant natural period.

μ_1 : Modification factor dependent on the maximum ground acceleration for design ($\mu_1 = 1.0$ for the case of 180 gals)

μ_2 : Modification factor to cover the influences of the higher modes

μ_3 : Modification factor to apply equivalent uniform seismic loads

μ_4 : Modification factor to cover the case where the direction of structural response is perpendicular to that of seismic motion applied.

μ_5 : Modification factor to be adjusted by engineering judgment.

The predominant natural period herein is the natural period corresponding to a vibration mode whose response (stress or displacement) is the most predominant in respective structural members. This predominant natural period does not necessarily coincide with the fundamental period.

4.4 Additional Effects to be Considered in Design

4.4.1 Effects of Ground Reactions on the Structural Response and Stresses

In evaluating the effects of the surrounding soil on the structural response and stresses, ground reactions shall be taken into account as the product of the structural displacement relative to the ground and the spring constant of the ground.

4.4.2 Effects of Surrounding Soil and Water on Structural Response

- 1) The surrounding soil will effect the structural response. Therefore the spring and damping factors shall be taken into account. The mass effect of the soil, however, may generally be neglected.
- 2) The effects of water shall be taken into account by applying the virtual or added mass, as described in "5.5 Effects of Surrounding Water on Structural Response".

5. Dynamic Analysis

5.1 Methods of Analysis

The following methods shall be employed in the dynamic analysis to obtain the structural response.

- 1) Response spectrum method: Calculate the maximum values of the structural earthquake response based on the response acceleration spectra specified in 5.3.
- 2) Numerical integration method: Calculate the time history of the structural earthquake response based on specific seismic motions specified in 5.4.

5.2 Application of Dynamic Analysis

In performing the earthquake-resistant design of structures, the dynamic analysis shall be employed in the following ways:

- 1) The design results obtained by using the modified seismic coefficient method considering structural response or the seismic coefficient method are examined by the dynamic analysis.

- 2) The response spectrum method of dynamic analysis is employed for structures whose dimension can be assumed by normal loads. The structural dimensions determined by this procedure are then examined by the numerical integration method of dynamic analysis.

5.3 Response Acceleration Spectrum for Dynamic Analysis

The response acceleration spectral curves shown in Fig. 2 shall apply to the response spectrum method of dynamic analysis specified in 5.1⁽¹⁾

5.4 Seismic Ground Motion for Dynamic Analysis

Seismic ground motions used for the numerical integration method of dynamic analysis specified in 5.1⁽²⁾ shall be either of the following. The maximum acceleration shall be adjusted to 180 gals by proportioning the various original acceleration records.

- 1) Typical seismic records obtained near the bridge sites
- 2) Strong motion records obtained at El Centro in 1940.

5.5 Effects of the Mass of the Surrounding Soil on the Structural Response

In the dynamic analysis of substructures, the effects of the mass of the soil on the response may generally neglected.

5.6 Effects of Surrounding Water on the Structural Response

For the portion of the structure which is in water, the virtual mass of the water converted from the hydrodynamic pressure shall be considered by the following formula:

$$M_{wx} = \alpha \beta \frac{\gamma_w}{g} A \sqrt{\frac{x}{d}}$$

where:

M_{wx} : Virtual mass (or added mass) per unit width at the depth of x below the water surface ($t \text{ sec}^2/m^2$)

α : Coefficient dependent on vibrational mode of the structure

β : Coefficient dependent on shape of the foundation

$$1) \beta = \frac{b}{a} (1 - \frac{b}{4d}) \text{ for the case of } \frac{b}{d} \leq 2$$

$$2) \beta = \frac{b}{a} (0.7 - \frac{b}{10d}) \text{ for the case of } 2 < \frac{b}{d} \leq 4$$

γ_w : Unit weight of the sea water (t/m^3)

A : Lateral cross-sectional area of the foundation

g : Gravity of acceleration ($=9.8 \text{ m/sec}^2$)

a : Length of cross-section of the foundation in the parallel direction to that of the seismic motion considered (m)

b : Width of cross-section of the foundation in the perpendicular direction to that of the seismic motion considered (m)

d : Depth of water at the site (m)

5.7 Dynamic Characteristics of Structures

1) The Directions of Seismic Motion to be Considered are;

Directions of seismic motion to be considered in dynamic analysis shall be longitudinal, transverse, and vertical.

2) Natural Frequencies and Mode Shapes:

The structural earthquake response shall be analyzed by taking into account the order of the natural frequencies and the corresponding mode shapes. These conditions are necessary in order to obtain the precise maximum response in the special consideration for erection and completed construction.

3) Damping ratios:

The damping ratios, used for dynamic analysis, shall be determined in view of the results of the appropriate investigations.

6. Safety Considerations in Earthquake-Resistant Design

6.1 Factors of Safety in the Modified Seismic Coefficient Method Considering Structural Response

6.6.1 Combination of Loads

For superstructure: Dead Load + live Load during earthquake + effects of temperature change + seismic effects + effects of movements of supports + effects of erection errors.

For substructure: Loads from superstructure + dead load + soil pressure + water pressure + buoyancy or uplift + seismic effects

6.1.2 Increase in Allowable Stresses for Steel Superstructure

The Increase in the allowable stresses for steel superstructures in earthquake resistant design shall be as follows:

For suspension bridges and long-span bridge: 1.5

For bridges other than the above: 1.7

6.1.3 Stability of Substructures

- (1) Allowable bearing capacities of soil: The ultimate bearing capacity of soil shall be evaluated in accordance with the Specifications for Design of Substructures of Highway Bridges-Volume for Design of Spread Foundations (issued by the Japan Road Association). The minimum values of the allowable bearing capacities shall be obtained by dividing the ultimate bearing capacities by the factors of safety specified in Table 1.

(2) Stability for Overturning

In normal design, the position of the resultant force acting on the foundation base shall be located within the middle third of the base. In earthquake-resistant design the force shall be located within the middle two thirds of the base. When the position of the resultant force, for the earthquake-resistant design, is outside of the middle two thirds, stability and deformation of ground and structures shall be examined.

(3) Stability for Sliding

The sliding resistance at the foundation base shall be evaluated in accordance with the Specifications for Design of substructures of Highway Bridges-Volume for Spread Foundation (issued by the Japan Road Association). The fractures safety for sliding shall be provided in Table 2.

(4) Displacement Standards for Substructures

Displacements of substructures shall be generally less than the displacement standards provided i Table 3.

6.2 Factors of Safety in the Design Based on Dynamic Analysis

Factors of Safety, of the design using the dynamic analysis, shall be in accordance with the provisions in 6.1.

References

1. Japan Society of Civil Engineers, "Technical Report of Investigations on the Honshu-Shikoku Bridges," July 1967. (in Japanese).
2. Japan Society of Civil Engineers, "Report of Research for Improving the Earthquake-Resistant Design Criteria for the Honshu-Shikoku Bridges," June, 1971. (in Japanese).
3. Japan Society of Civil Engineers, "Technical Report of Investigations on Earthquake-Resistance of the Honshu-Shikoku Bridges," September, 1974. (in Japanese).

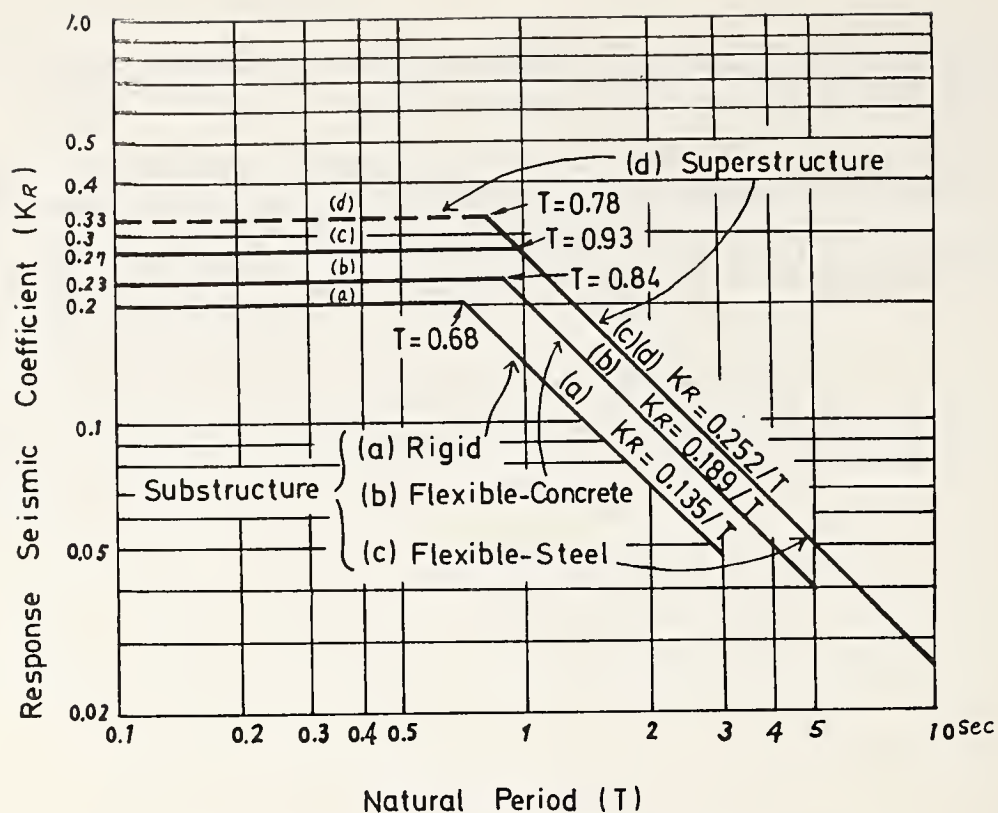


Fig. 1. Response Seismic Coefficient Used in Design

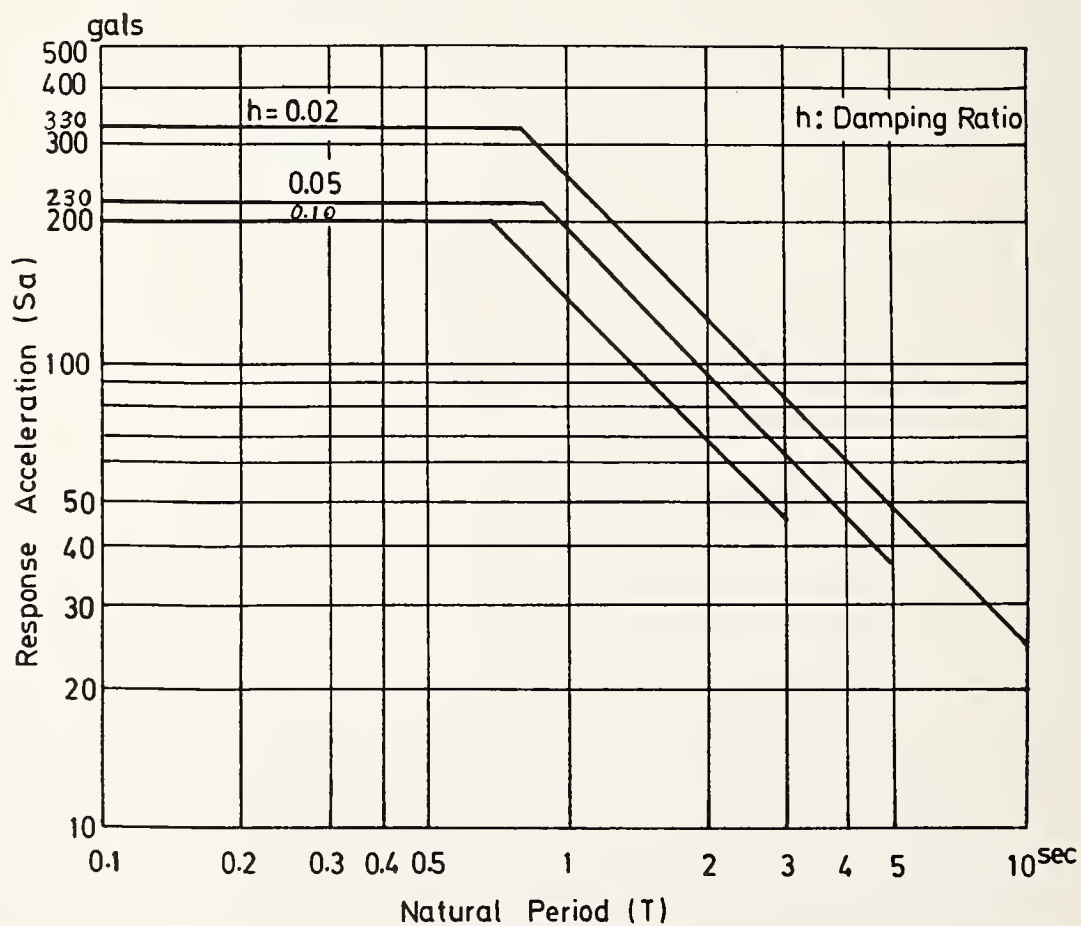


Fig. 2. Response Acceleration Spectral Curves (for maximum acceleration of 180 gals)

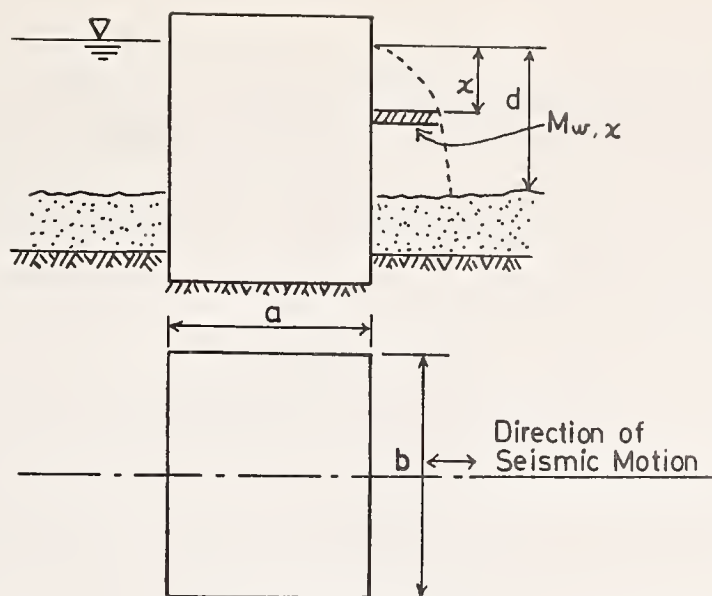


Fig. 3. Virtual mass of water

Table 1. Factors of Safety for Bearing Capacities

	Construction Manner of Foundation Base	
	Dry	Under Water
Normal Design	3.0	4.5
Earthquake-Resistant Design	2.0	3.0

Table 2. Factors of Safety for Sliding

	Construction Manner of Foundation Base	
	Dry	Under Water
Normal Design	2.0	2.5
Earthquake-Resistant Design	1.2	1.5

Table 3. Displacement Standards for Substructures

Suspension Bridges		Other Bridges
Abutments	Tower Foundations	Horizontal displacement at the level of ground surface (cm)
Horizontal displacement at the Saddle Position (cm)	Rotation at the tower base	
$\delta = 0.017l$	$\theta = 0.0055l + 2$	$\delta = 1$

l : central span length (m)

RECENT REVISION OF DESIGN STANDARDS ON
SEISMIC EFFECTS FOR PORT AND HARBOUR STRUCTURES

by

Satoshi Hayashi
Head of Structures Division
Port and Harbour Research Institute

Hajime Tsuchida
Chief of Earthquake Resistant Structures Laboratory
Structures Division
Port and Harbour Research Institute

Setsuo Noda
Chief of Subaqueous Tunnels and Pipe Lines Laboratory
Structures Division
Port and Harbour Research Institute

ABSTRACT

The design standards for port structures have been compiled four times in Japan. In these design standards, provisions on earthquake resistant design of wharves are included.

In 1950 the first design standard was published, and in 1959 and 1967 new design standards as an expansion of preceding one were compiled. Those design standards were recognized as the most advanced design procedure in the times and used very widely for design of port structures. However, the standards were not related to any law.

In 1973 Port and Harbour Law was revised and to secure the safety in ports it was assigned to establish engineering requirement of facilities in ports. The requirement has been effective since 1974 and the earthquake resistant design of the facilities are specified in it.

Key Words: Structures, Ports, Harbors, design, specifications, earthquakes.

1. Introduction

A port is an interconnection between sea transportation and land transportation and is an essential part in the activity of our modern society. Loss or even partial damage of a port, due to an earthquake, causes serious effect on the activities of a community. This is especially true after a destructive earthquake, as the port is required to function for transportation of emergency goods and materials for reconstruction of damaged facilities.

During past earthquakes, however, serious damage to port facilities has been experienced. For instance, in the Niigata earthquake of June 16, 1969, which had a magnitude 7.5, the damage to the port facilities in the Niigata port cost 22 billion yen. Wharves are major facilities in a port, and many wharves are earth retaining structures such as a gravity type quay wall and a sheetpile bulkhead. These structures support large soil areas which move in a very complex manner during earthquakes. This is one of the reasons why the port facilities were greatly affected by past earthquakes.

Because of these circumstances, intensive efforts have been made by port engineers to increase the aseismicity of port facilities, with a minimum increase of construction cost, which was acceptable to the community.

In this paper, the basic requirements and procedures for earthquake resistant design of port facilities will be presented. It is well known that a large variety of structures surrounding a port exists; however, in this paper, the authors will limit the discussion to sea walls, piers, etc., and those types of structures which exist only in a port. Therefore, the term "port structures" will mean such structures. In this report, the design standard means a compilation of typical procedures and considerations. Such standards would be allowable stresses and factors of safety for designing port structures. These design standards have been published previously four times in Japan, and their degrees of restriction to actual designs differ according to each publication.

2. History of Design Standard

The first design standard for the port structure was published by the Japan Port and Harbour Association in 1950, and was called "Manual of Harbour Construction Work (Title in Japanese: Kowan Koji Sekkei Shiho Yoran)"⁽¹⁾. The manual consisted of three parts; namely the recommendations for design of quay walls and piers, the recommendations for planning and execution of dredging and fill-up, and the recommendations for design of breakwaters.

In the recommendations for design of quay walls and piers, relative to earthquake resistant design, inertia force, earthpressure and dynamic water pressure were considered. For the estimation of the earthpressure during earthquakes, a formula proposed by Matsuo based on his experimental study⁽²⁾ was adopted. However, Mononobe-Okabe's formula⁽³⁾ for earthpressure during earthquakes was also explained as an applicable formula.

The second design standard for the port structure was published by the Japan Port and Harbour Association in 1959, called "Design Manual for Harbour Construction Work

(Title in Japanese: Kowan Koji SekKei Yoran)⁽⁴⁾. This document has been called the "Green Book" by port engineers because of the color of the cover.

In the "Green Book" the area of Japan was divided into three regions and a seismic coefficient was specified for each region. The formula to estimate earthpressure, during earthquakes, consisted of Mononobe-Okabe's formula.

The third design standard was published also by the Japan Port and Harbour Association in 1967, and was called "Design Manual of Harbour Structures in Japan (Title in Japanese: Kowan Kozobutsu Sekkei Kijun)⁽⁵⁾". This design standard had various unique characteristics, in comparison to the previous two design standards. The first quality was that the third design standard presented procedures for the design of the structures, such that even a less experienced engineer could design the structures without any other textbook, and it also presented to the engineers the background information on the procedures. As a result, the third design standard has become a publication of many pages and has the characteristics of a specialized textbook.

The second quality was that the third design standard was to be revised regularly, in order to introduce results of the most recent research and technological developments. In order to make such a condition possible and easier, the design standard was compiled such that any page could be replaced by a newly printed page.

The provisions in the third design standard, regarding earthquake resistant design, were presented at the First Joint Meeting, U.S.-Japan Panel on Wind and Seismic Effects, UJNR⁽⁶⁾, and at the Second Joint Meeting relative to the comments on the revision of the of the third design standard⁽⁷⁾.

The third design standard described previously was recognized as the best procedure at that time by the port engineers. Most of the port structures were designed according to these design standards.

3. Engineering Requirement by Port and Harbour Law

In 1973 the Port and Harbour Law was revised. Because of social demands on the safety of facilities in ports and harbours, the ministry established engineering requirements on facilities which were to be constructed in ports and harbours. In 1974, these engineering requirements were established as Ordinance No. 30 by the Ministry of Transport, which prescribes that the facilities in ports and harbours must be safe against earthquakes as well as dead load, water pressure, wave force, surcharge, impact and drag due to ships, etc. However, details on earthquake resistant design, such as design procedures, factors of safety, and allowable stresses, have not been given in the ordinance, but were specified in an order by the Director General of Bureau of Port and Harbours. Such a legal system was chosen because considerable progress in earthquake resistant design is expected in the near future, and flexibility to revise the requirements is necessary.

Even in the order of the Director of Bureau of Ports and Harbours only important points are specified. Therefore, it is recommended that the third design standard should be used as a supplement to this order.

The basic consideration of earthquake resistant design of structures, constructed mainly in ports, is the seismic coefficient method; however, earthquake resistant design depending on dynamic analysis is also acceptable.

4. Earthquake Resistant Design in the Requirement

In this section the earthquake resistant design, specified in the engineering requirements, will be described. However, the following are not a translation of the provisions, but an explanation of the earthquake resistant design. The provisions are available in the separate publication⁽⁸⁾.

4.1 Design Earthquake Load

1) Earthquake load

The earthquake loads acting on port structures should be calculated by the following formulas, where the most severe conditions should be chosen.

- i) Earthquake load = Dead load x Seismic coefficient
- ii) Earthquake load = (Dead load + Surcharge) x Seismic coefficient

The seismic coefficient is defined in the next paragraph.

2) Seismic coefficient

The seismic coefficient should be calculated by the following formula, taking regional seismicity, foundation soil and importance of the structure into consideration.

$$\text{Seismic coefficient} = \text{Regional seismic coefficient} \times \text{Factor for subsoil condition} \times \text{Importance factor}$$

In general the earthquake load is applied horizontally at the center of gravity of the structure. The earthquake load in the vertical direction is not considered, with the exception of those special structures which are influenced by a vertical load. The seismic coefficient should be calculated to two decimal places, where the last digit is set equal to 0.1, if equal to or greater than 0.08; if the digit is between 0.07 and 0.03 set the value equal to 0.05.

3) Regional seismic coefficient

Standard values of the regional seismic coefficient are tabulated in Table 1. The seismic coefficient in a region which is not described in Table 1 is determined considering seismicity of the region and the regional seismic coefficients in the neighboring regions as given in Table 1.

Fig. 1 shows the regional seismic coefficient and Fig. 2 the expected maximum acceleration of earthquakes in the next 75 years estimated by Kawasumi.

4) Factor for subsoil condition

The standard value of the factor for subsoil condition should be determined as shown in Table 2.

The classification of the subsoil condition should be assigned as shown in Table 3, considering the thickness of the quaternary deposit and the kind of subsoil.

5) Factor depending on importance of structure

The standard value of the factor relative to the importance of the structure should be determined by Table 4.

4.2 Earthpressure in an Earthquake

Lateral earthpressure of sandy soil in earthquakes is computed by using Mononobe-Okabe's formula which is derived from Coulomb's formula by statically applying the earthquake load to the soil mass in question. For horizontal ground surface, the formula is as shown in (Fig. 3).

where, p : intensity of lateral earthpressure in earthquakes (t/m^2)

w : intensity of uniform load on the ground surface (t/m^2)

k : seismic coefficient

ϕ : angle of internal friction of sandy soil ($^\circ$)

for general case $\dots 30^\circ$

for particularly good backfill $\dots 40^\circ$

γ : unit weight of soil (t/m^3); buoyed unit weight should be used below water level and the following are the standards:

above water table in backfill $\dots 1.8t/m^3$

below water table in backfill $\dots 1.0t/m^3$

h : depth from the ground surface (m)

K : coefficient of lateral earthpressure

γ : angle between wall surface and the vertical ($^\circ$)

δ : angle of friction between soil and wall ($^\circ$); usually $|\delta| \leq 15^\circ$

θ : angle given by the following equations; $\theta = \tan^{-1} k$ or $\theta = \tan^{-1} k'$

ζ : angle between failure surface and horizon ($^\circ$)

In Eqs. (2) and (3), upper signs are for active and passive earthpressure for typical values of ϕ and δ are shown in Figs. 4 and 5 respectively.

For backfill, in layers $(w + \gamma h)$ in Eq. (1), these terms should be replaced by the vertical effective stress. Below the water table the apparent seismic coefficient should be used. In calculation of the vertical effective stress the buoyed unit weight of soil is used, this causes a smaller estimation of the earthquake load acting on the soil mass, since the weight of soil mass in the air should be multiplied by the seismic coefficient. The apparent seismic coefficient compensates the difference. The apparent seismic coefficient is given by the following equation.

$$k' = \frac{\gamma'}{\gamma' - 1} k \quad \dots\dots\dots (4)$$

where; k' : apparent seismic coefficient

γ' : unit weight of saturated soil (t/m^3)

4.3. Dynamic Water Pressure

Rigid wall- and column-like structures facing the water are designed by taking the dynamic water pressure into consideration. However, the structure is retaining soil and the earthpressure is calculated by Mononobe-Okabe's formula with the apparent seismic coefficient, where the dynamic water pressure is not considered in the design calculation. The reasons for this assumption are: first, when the apparent seismic coefficient is applied for the earthpressure calculation the inertia force due to pore-water has already been considered. Also experience from structural performance during past earthquakes do not indicate the necessity to consider the dynamic water pressure acting on the face of the earth supporting structures.

4.4. Allowable Stresses

Allowable stresses of the materials are determined as shown in Tables 5 through 9. Allowable stress of tie rods must be equal to or below 40 percent of the certified yielding stress.

Allowable stresses of steel and concrete, for short period load such as earthquake load, may be equal to or smaller than 1.5 times of the allowable stresses in normal condition.

4.5. Earthquake Resistant Design Based upon Special Study

When the seismic coefficient is determined from consideration of a survey on seismicity of the region, and from the characteristics of earthquake motion and response characteristics of the ground against earthquakes, the requirement described in 4.1 need not be applied to design.

When the earthquake resistant design is confirmed by consideration of the dynamic characteristics of the structure and the investigation on the response analysis for the structure against earthquakes, the requirement described in 4.1 need not be applied.

It is advised that in case of necessity the earthquake resistant design is confirmed by the consideration of the dynamic characteristics of the structure and the investigation on the response analysis against earthquake.

4.6 Structures Other Than Port Structures

Structures other than port structures are normally designed by the design standards established for each type of structure.

1) Design Specifications for Steel Highway Bridges, established by the Japan Road Association, may be applied to the earthquake resistant design of the highway bridges.

2) Design Specifications for Steel Railway Bridges by the Japan Society of Civil Engineers or Design Specifications for Civil Engineering Facilities established by the Japan Railway Facility Association may be applied to the earthquake resistant design of the railway bridges.

3) On the earthquake resistant design of the pipe line for transporting such fluid and gaseous materials as petroleum, Fire Service Law, Oil Pipelines Enterprise Law or High Pressure Gas Control Law and regulations established to supplement these laws, may be applied.

4) On the earthquake resistant design of the buildings, Building Standard Law and regulations established to supplement the law may be applied.

5. Future Follow-up

In this report the earthquake resistant design designated by the Port and Harbour Law, has been presented. Many new types of structures are going to be constructed on or off-shore and the social demands for environmental consideration of such structures have been increasing. Because of such circumstances, revision of the Design Manual of Harbour Structures in Japan has been undertaken. The rationalization of earthquake resistant design will be achieved by this revision.

References

- 1) Manual of Harbour Construction Work, The Japan Port and Harbour Association, May 1950, 115p.
- 2) Haruo Matsuo: Experimental Study on Distributions of Earth Pressure Acting on Retaining Walls during Earthquakes, Journal of the Civil Engineering Society, Vol. 27, No. 2, February 1941, pp. 1-24
- 3) Saburo Okabe: General Theory on Earthpressure and Seismic Stability of Retaining Wall and Dam, Journal of the Civil Engineering Society, Vol. 10, No. 6, December 1924, pp. 1277-1323.
- 4) Design Manual of Harbour Construction Work, The Japan Port and Harbour Association, June 1959, 453p.
- 5) Design Manual of Harbour Structures in Japan, The Japan Port and Harbour Association, April 1967.
- 6) Satoshi Hayashi: Current Procedure for Earthquake Resistant Design of Harbour Structures in Japan, Proceedings of the First Joint Meeting, U.S.-Japan Panel on Wind and Seismic Effects, UJNR, May 1969.
- 7) Satoshi Hayashi: Comments on Revision of Earthquake Resistant Design Criteria for Harbour Structures in Japan, Proceedings of the Second Joint Meeting, U.S.-Japan Panel on Wind and Seismic Effects, UJNR, May 1970.
- 8) Ministerial Ordinance on Engineering Requirements on Port and Harbour Facilities and Its Application, The Japan Port and Harbour Association, February 1975, 94p.

Classification	Region	Regional seismic coefficient
First region	Hokkaido (Nemuro, Kushiro, Hidaka) Kanto (Chiba, Tokyo, Kanagawa) Chubu (Shizuoka, Aichi) Kinki	0.15
Second region	Hokkaido (Ishikari, Iburi, Shiribeshi, Hiyama, Oshima, Rumoi) Tohoku Kanto (Ibaragi) Chubu (Niigata, Toyama, Ishikawa, Fukui) Shikoku Chugoku (Tottori, Okayama, Hiroshima) Kyushu (Oita, Miyazaki)	0.10
Third region	Hokkaido (Soya, Abashiri) Chugoku (Shimane, Yamaguchi) Kyushu, Okinawa (Fukuoka, Saga, Nagasaki, Kumamoto, Kagoshima, Okinawa)	0.05

Table 1 Regional seismic coefficient

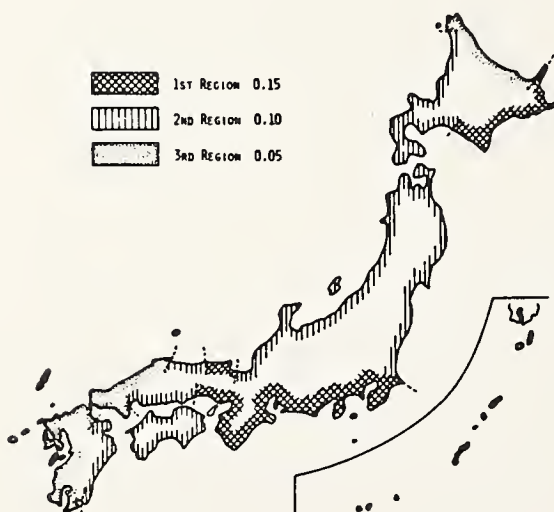


Fig. 1. Regional seismic coefficient for port structures



Fig. 2. Expectancy of maximum acceleration of earthquakes in 75 years in gals (After Kawasumi)

Classification	1st kind	2nd kind	3rd kind
Factor	0.8	1.0	1.2

Table 2 Factor for subsoil condition

Thickness of quaternary deposit	Gravel	Sand or clay	Soft ground
less than 5 m	1st kind	1st kind	2nd kind
5 - 25 m	1st kind	2nd kind	3rd kind
more than 25 m	2nd kind	3rd kind	3rd kind

Table 3 Classification of subsoil condition

Classification of structure	Characteristics of structure	Importance factor
Special class	The structure has significant characteristics described by items of (1) - (3) in A class	1.5
A class	(1) If the structure is damaged by an earthquake, a large number of human life and property will possibly be lost. (2) The structure will perform an important role on the reconstruction work of the region after an earthquake (3) The structure handles a hazardous or a dangerous object, and it is feared that the damage on the structure will cause a great loss of human life or property. (4) If the structure is damaged, economical and social activity of the region will be severely suffered. (5) If the structure is damaged, it is supposed that the repair work of it is considerably difficult.	1.2

Classification of structure	Characteristics of structure	Importance factor
B class	The structure is other than Special, A and C classes.	1.0
C class	The structure is small and easy for repairment, excepting that in Special and A class.	0.5

Table 4 Factors depending on importance of structure

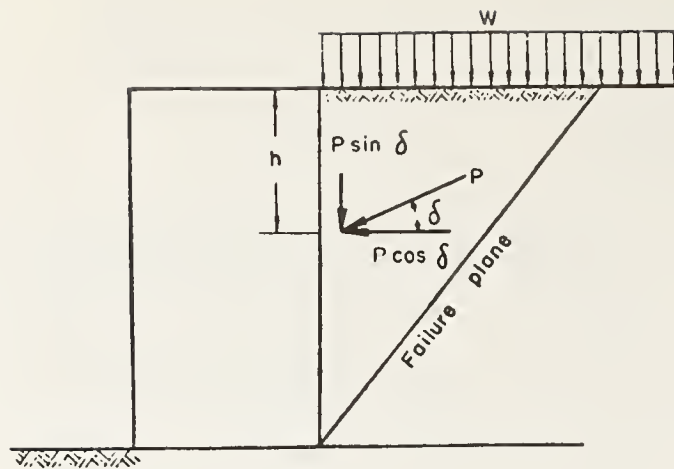


Fig. 3. Earthpressure acting on a vertical wall

$$p = (w + r \cdot h) K \quad \dots\dots\dots (1)$$

$$K = \frac{\cos^2(\phi \pm \varphi - \theta)}{\cos \theta \cdot \cos^2 \varphi \cdot \cos(\delta + \varphi \pm \theta) \left(1 \pm \sqrt{\frac{\sin(\phi \pm \delta) \sin(\phi - \theta)}{\cos(\delta + \varphi \pm \theta) \cos \varphi}} \right)^2} \quad \dots\dots (2)$$

$$\cot \zeta = \mp \tan(\phi \pm \delta \pm \varphi) + \sec(\phi \pm \delta \pm \varphi) \sqrt{\frac{\cos(\varphi + \delta \pm \theta) \sin(\phi \pm \delta)}{\cos \varphi \sin(\phi - \theta)}} \quad \dots\dots (3)$$

where; p : intensity of lateral earthpressure in earthquakes (t/m^2)

w : intensity of uniform load on the ground surface (t/m^2)

k : seismic coefficient

ϕ : angle of internal friction of sandy soil ($^\circ$)

for general case $\dots 30^\circ$

for particularly good backfill $\dots 40^\circ$

r : unit weight of soil (t/m^3 ; buoy unit weight should be

used below water level and the following are the standards:

above water table in backfill $\dots 1.8 t/m^3$

below water table in backfill $\dots 1.0 t/m^3$

h : depth from the ground surface (m)

K : coefficient of lateral earthpressure

φ : angle between wall surface and the vertical ($^\circ$)

δ : angle of friction between soil and wall ($^\circ$); usually $|\delta| 15^\circ$

θ : angle given by the following equations; $\theta = \tan^{-1} k$ or $\theta = \tan^{-1} k'$

ζ : angle between failure surface and horizon ($^\circ$)

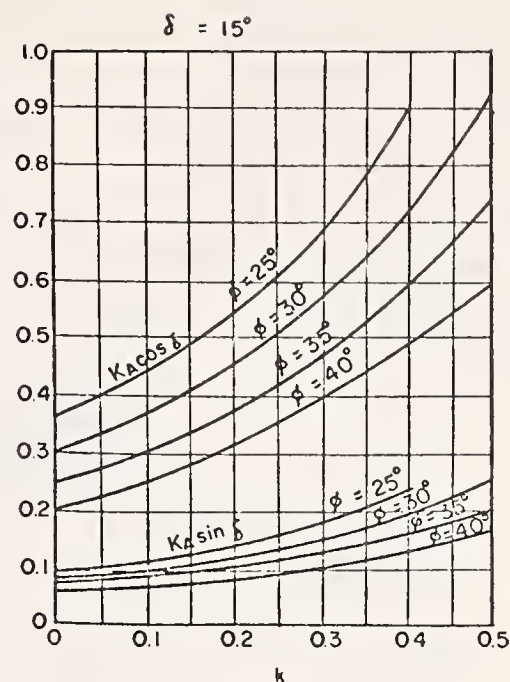
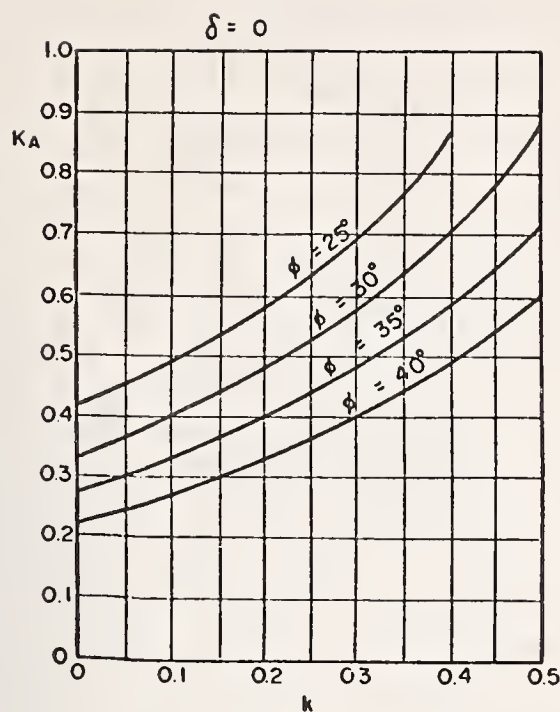


Fig. 4. Coefficient of active earthpressure by Mononobe-Okabe's formula

Kind of stress	SS 41, SM 41 SMA 41	SS 50	SM 50
Axial tensile stress (for net section)	1,400	1,700	1,900
Axial compressive stress (for gross section)	(a) $\frac{\ell}{r} \leq 20$, 1,400 (b) $20 < \frac{\ell}{r} < 93$	(a) $\frac{\ell}{r} \leq 17$ 1,700 (b) $17 < \frac{\ell}{r} < 86$	(a) $\frac{\ell}{r} \leq 15$ 1,900 (b) $15 < \frac{\ell}{r} < 80$
ℓ : effective buckling length (cm)	$1,400 - 8.4(\frac{\ell}{r} - 20)$	$1,700 - 11.3(\frac{\ell}{r} - 17)$	$1,900 - 13(\frac{\ell}{r} - 15)$
r : radius of gyration for gross section (cm)	(c) $93 \leq \frac{\ell}{r}$ $\frac{12,000,000}{6,700 + (\ell/r)^2}$	(c) $86 \leq \frac{\ell}{r}$ $\frac{12,000,000}{5,700 + (\ell/r)^2}$	(c) $80 \leq \frac{\ell}{r}$ $\frac{12,000,000}{5,000 + (\ell/r)^2}$
Bending stress (1) tensile stress for net section (2) compressive stress for gross section	1,400	1,700	1,900
Shearing stress (for gross section)	800	1,000	1,100

(unit : kg/cm²)

Table 5 Allowable stresses of structural steel

Kind of stress	SS 41, SM 41 SMA 41, STK 41	SM 50, STK 50
Axial tensile stress (for net section)	1,400	1,900
Axial compressive stress (for gross section)	Same as shown in Table-5	
Combination of axial compressive force and bending moment	$\frac{\sigma_c}{\sigma_{ca}} + \frac{\sigma_{bc}}{\sigma_{ba}} \leq 1.0$	
Shearing stress (1) with stiffener (2) without stiffener (R/t ≤ 30)	R/t ≤ 125 800 - 0.019(R/t) ² 200 > R/t > 125 75,000/(R/t) - 90 500	R/t ≤ 95 1,100 - 0.044(R/t) ² 200 > R/t > 95 75,000/(R/t) - 90 600

(unit : kg/cm²)

Notation σ_c : compressive stress of axial compressive force

σ_{bc} : compressive stress of bending moment

σ_{ca} : allowable axial compressive stress

σ_{ba} : allowable bending compressive stress shown in Table-5

R : outer radius of steel pile (cm)

t : thickness of steel pile (cm)

Table 6 Allowable stresses of steel pile materials

Kind of steel material	Allowable stress
SY 24	1,400
SY 30	1,800
SY 40	2,400

(unit : kg/cm²)

Table 7 Allowable stresses of steel sheetpile materials

Kind of reinforcing bars	SR 24	SR 30	SD 24	SD 30	SD 35	SD 40
Tensile stress	1,400	1,600	1,400	1,800	2,000	2,100
Tensile stress for fatigue loading	1,400	1,600	1,400	1,600	1,800	1,800

(unit : kg/cm²)

Nation 1) Diameter of bars is less than 32 mm

2) When design standard strength σ_{ck} is less than 180 kg/cm²

deformed bars $\sigma_{sa} \leq 1,600$ kg/cm²

round bars $\sigma_{sa} \leq 1,200$ kg/cm²

Table 8 Allowable tensile stress of reinforcing bars σ_{sa}

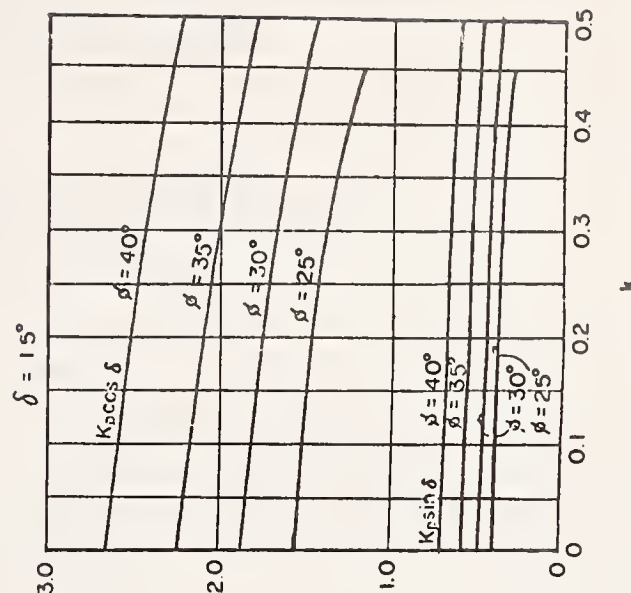
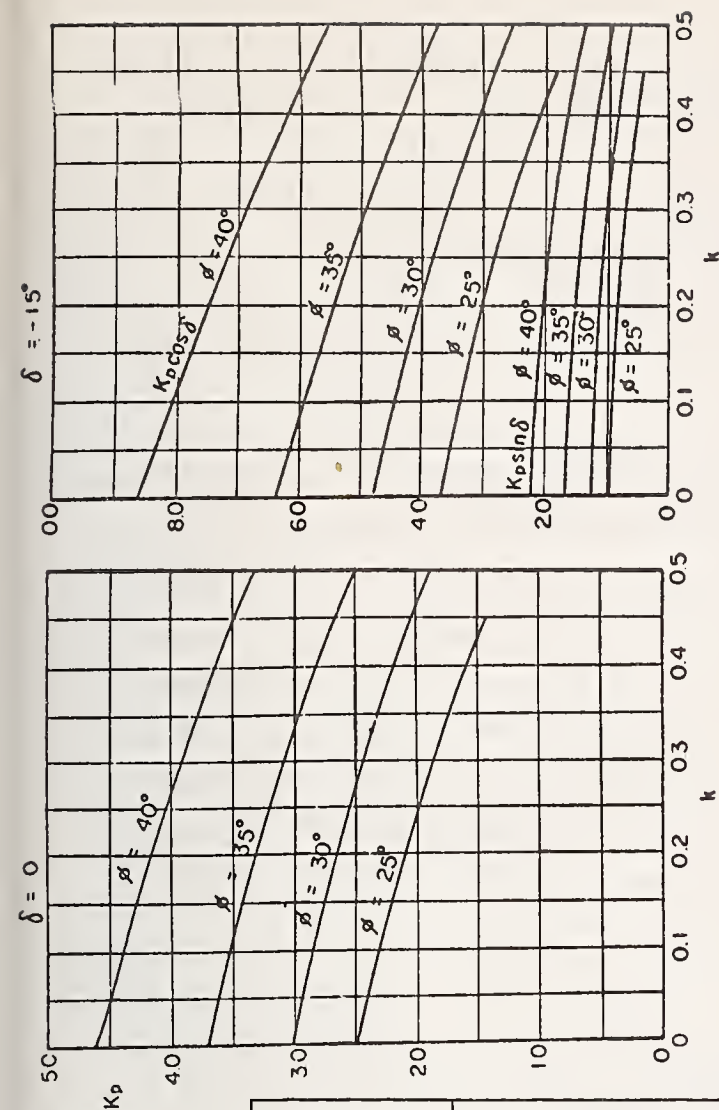


Fig. 5. Coefficient of passive earthpressure by Mononobe-Okabe's formula

Kind of stress	Items	reinforced concrete			Plain concrete
		σ_{ck}			
		180	240	300	
Flexural compressive stress	_____	$\sigma_{ca} \leq \frac{\sigma_{ck}}{3}$			$\sigma_{ca} \leq \frac{\sigma_{ck}}{4} \leq 55$
Shearing stress	$\tau_{a1} \begin{cases} \text{beam} \\ \text{slab} \end{cases}$	6 8	7 9	8 10	_____
	τ_{a2} only shear force	17	20	22	
Bond stress	round bars	7	8	9	_____
	deformed bars	14	16	18	
Flexural tensile stress	_____	0			$\sigma_{ca} = \frac{\sigma'_{ck}}{7} \leq 3$

σ_{ck} : design standard compressive strength

σ'_{ck} : design standard tensile strength

σ_{ca} : allowable stress

τ_{a1} : allowable shearing stress without calculation of diagonal tension bars

τ_{a2} : allowable shearing stress with calculation of diagonal tension bars

Table 9 Allowable stresses of concrete

JSCE SPECIFICATIONS FOR EARTHQUAKE RESISTANT DESIGN
OF SUBMERGED TUNNELS (1975)

by

Eiichi Kuribayashi
Chief, Earthquake Engineering Research Section
Public Works Research Institute
Ministry of Construction

and

Hajime Tsuchida
Chief, Earthquake Resistant Structure Laboratory
Port and Harbor Research Institute
Ministry of Transport

ABSTRACT

In response to the request from Ministry of Construction and Ministry of Transport, the Japan Society of Civil Engineers has concluded in March 1975 the final draft of the Specifications for Earthquake Resistant Design of Submerged Tunnels. The writers of this paper have worked on the drafting of these Specifications in cooperation with colleagues of the Public Works Research Institute and Port and Harbor Research Institute during the last four years.

The draft of the Specifications was adopted as Specifications for Earthquake Resistant Design of the Proposed Tunnel across Tolyo Bay. This paper presents the principal provisions and articles of the draft of the Specifications, and contains the following five chapters; General, Investigation, Earthquake Resistant Design, Dynamic Analyses, and Preservation and Countermeasure in Earthquakes.

Key Words: Aseismic Design Criteria; Design Provisions; Earthquakes; Specifications; Structural Engineering; Tunnels.

Foreword

The Committee of Earthquake Resistant Design criteria for Submerged Tunnels, chaired by Professor Shunzo Okamoto, was established by the Japan Society of Civil Engineers under a contract with the Public Works Research Institute, Ministry of Construction in July, 1971. The contract had been supported by the Institute in addition to The Second Construction Bureau for Port and Harbor, Ministry of Transport since 1972.

Since the initiation of this work, the committee has met nine times with the Sub Committee, who drafted the specifications and have met forty-four times. Through 1971 to 1972, the dynamic behavior of submerged tunnels was examined, and then the provisions of the Specifications were drafted on the bases of these results.

Prior to developing the specifications, the application of earthquake engineering and design practices to submerged tunnels both in Japan and abroad, and the general observation of submerged tunnels during earthquakes were comprehensively studied. The Committee, however, adopted the final resolution as a draft to the Specifications with due consideration that lack of sufficient examples of design applications existed. This draft will attempt to establish a meaningful specification for the future and thus provide needed experience on their application of earthquake resistant design.

The safety and stability of the submerged tunnels are important and therefore, the skeleton of the specification draft should be applied toward the design and construction of tunnels with care. The draft will, however, be an important guide in the construction and the design of tunnels.

Finally, the members of the Committee which participated in the draft of the Specifications included the Ministry of Construction, the Ministry of Transport, and the clerk of the Committee of Japan Society of Civil Engineers. Their cooperation is deeply appreciated.

1.1 Scope

The provisions in the Specification apply to earthquake resistant design of submerged tunnels.

1.2 Conformation to Specifications

In regard to matters which are not specified herein, the following Specifications shall apply in accordance with the types of structures and facilities considered.

Standard Specifications of Concrete,

Japan Society of Civil Engineers

Specifications for Design and Construction of Prestressed Concrete,

Japan Society of Civil Engineers

Specifications for Earthquake Resistant Design of Civil Engineering Structures,

Japan Society of Civil Engineers

Specifications for Earthquake Resistant Design of Highway Bridges (January, 1971),

Japan Road Association

Design Standards on Seismic Effort for Port and Harbor Structures,

Port and Harbor Association of Japan

Uniform Building Code,

1.3 Definitions of Terms

The following definitions shall apply only to the provisions of these Specifications.

Submerged Tunnel; A total structural system which are composed of submerged structures, approaches and ventilation towers.

Submerged structure; A portion of the tunnel which is under water on a water table. Those portions are constructed in the following sequence.

1st: The elements are fabricated in yards or docks

2nd: The elements are floated and towed to the construction site.

3rd: The elements are placed on a trench prepared along the site.

4th: The elements are connected together under the water tables.

5th: Over-all elements are covered with rock and soil.

Approach; Under-ground structures or exposed structures which lead from the submerged structure to airial portions.

Ventilation tower; A structure which is located at the intermediate portion of the tunnel for the purpose of construction and ventilation of the tunnel.

Seismic Deformation Method; A method for earthquake resistant design of the tunnel, in which the ground displacements at the level of an axis of the tunnel are assumed to apply seismic effects to the submerged structure.

(Fourteen additional terms, other than above, are herein omitted).

2.1 General

For earthquake resistant design of a submerged tunnel, detail investigations shall be made on earthquakes and earthquake ground motions; geology and soils; materials, and types and details of structure; preservation and counter-measures in earthquakes; and a post-earthquake inspection program.

2.2 Investigation of Earthquakes and Earthquake Ground Motions

2.2.1 Earthquakes

Investigation on earthquakes are presently being conducted in order to collect data on seismic activity in an area of a proposed submerged tunnel site. The data will be utilized for earthquake resistant design and for preservation and counter-measures in earthquakes.

2.2.2 Earthquake Ground Motions

Field observations on earthquake ground motions are being conducted in order to obtain data necessary to estimate earthquake response of soil strata and structures. Such estimations shall be taken into consideration for earthquake resistant designs and on preservation and counter-measures in earthquakes.

2.3 Investigation of Geology and Soils

2.3.1 General

Investigation on geology and soils in relationship to earthquake resistant design is divided into two categories; (1) preliminary investigation and (2) site investigation. The preliminary investigation is required in order to collect information on geology and soils in the tunnel locality, preceding the site investigation for making the site investigation efficient and effective. The site investigation is conducted in order to obtain all the necessary data for design and construction of a submerged tunnel.

2.3.2 Preliminary Investigation

In the preliminary investigation the following information shall be collected:

- 1) Topographic map; also submarine topographic map when it is necessary
- 2) Geological map
- 3) Soil profile
- 4) Soil map
- 5) Boring log

2.3.3 Site Investigation

In conducting the site investigation, the following items should be determined; possible structural types of a submerged tunnel, soil condition, and other related factors. In considering these items the following viewpoints shall be made of the site investigation.

- 1) Data necessary for determination of design earthquakes
- 2) Data necessary for structural design
- 3) Data necessary for examination of stability of soils during earthquakes

Items that are included in site investigations depend on the proposed tunnel; however, the following items shall be included in the site investigation.

- 1) Boring, sounding (normally standard penetration tests), and sampling
- 2) Laboratory tests of samples
- 3) Measurement of seismic wave velocities with boreholes.
- 4) Measurement of density of soils
- 5) Microtremor observation

2.3.4 Test Procedures

Field and laboratory tests shall be conducted in accordance with procedures specified in the Japan Industrial Standards or the Standard Specifications of the Japanese Society of Soil Mechanics and Foundation Engineering.

2.3.5 Configuration and Depth of Base-rock

In the site investigation configuration and depth of base-rock surface shall be surveyed. The base-rock surface means an interface between base-rock and surface layer.

2.4 Investigation of the Engineering Property of the Soil and Surface Layer

2.4.1 Engineering Property of the Soil and of the Surface Layer

The following are the important properties to be considered for earthquake resistant design.

- 1) Density
- 2) Elastic moduli; Young's modulus and shear modulus
- 3) Poisson's ratio
- 4) Strength parameters; angle of internal friction and cohesion
- 5) Coefficient of subgrade reaction
- 6) Strength of soils under dynamic loading
- 7) Velocities of seismic waves; velocity of longitudinal waves and velocity of transverse waves
- 8) Dynamic characteristics of subground

These properties shall be determined directly by observation or tests. Only when it is very difficult to be obtained directly, the properties can be determined indirectly using the results from standard penetration tests or other observation tests.

2.4.2 Strength of Soils under Dynamic Loading

Dynamic strength-test of soils, to examine the soil behavior under dynamic loading, is desirable.

2.4.3 Measurement of Velocities of Seismic Waves

Velocities of seismic waves shall be measured at the proposed tunnel site.

2.4.4 Measurement of Microtremor

For estimation of the dynamic characteristics of the surface layer, at the tunnel site, microtremors shall be measured and analysed.

2.4.5 Damping Factor of the Surface Layer

Damping factors of surface layer, which are applied in the earthquake response calculations and dynamic model tests shall be carefully determined based on results of field and laboratory tests.

2.4.6 Properties and Strain of the Soil

Properties of the soil and surface layer, such as elastic moduli, velocities of seismic waves, and damping factor, depend of the strain in the soil. The difference between the strain in the soil under test or observation and the strain in the soil expected during earthquakes shall be considered when the properties are used in earthquake resistant design.

2.5 Ground Failure

A submerged tunnel is supported by the surrounding soil which is usually soft, and thus the stability of a submerged tunnel depends largely on the behavior of the ground during earthquakes. Engineers concerned with the design and construction of a submerged tunnel shall have appropriate knowledge of the ground failure due to earthquakes.

2.6 Seismic Stability of the Soils

2.6.1 Stability of Sandy Soil

Liquefaction of soils around a submerged tunnel shall be avoided. When the soil is estimated to liquefy during earthquakes the soil shall be improved. Liquefaction potential shall be examined based on liquefaction case records from past earthquakes and results of research on liquefaction.

2.6.2 Stability of a Cohesive Soil

When soil at a tunnel site is cohesive, it shall be checked such that a change in the soil strength and deformation due to earthquake will never affect the stability of a submerged tunnel.

2.7 Investigation of the Materials and Structural Types

Relative to materials, types and details of a submerged tunnel, tests and investigations shall be conducted on the following;

- 1) Structural concrete
- 2) Structural steel
- 3) Watertightness of elements
- 4) Types and materials of the joints
- 5) Types of foundations
- 6) Preparation of trench bottom and backfilling

2.8 Investigation of the Preservation and Proper Countermeasures in Earthquakes

For the preservation and countermeasures of tunnels in earthquakes, traffic control systems of the tunnel shall be examined, and the interaction of the function among these systems shall be sufficiently considered.

Chapter 3 Earthquake Resistant Design

3.1 General Principle

Every partial structural system shall be designed by the seismic deformation method and the seismic coefficient in accordance with the provisions in Chapter 3 "Earthquake Resistant Design". Also the total structural system shall be designed by using the results of the dynamic response analysis with regard to the influence of the surrounding topography and geology in accordance with the provisions in Chapter 4 "Dynamic Analysis".

Equipment shall be provided for earthquake control and examination, and shall be used in accordance with the provisions in the Chapter 5 "Preservation and Countermeasures for Earthquakes".

3.2 Design Requirements

- 1) Not only the submerged structure but also the total structural system, including the effects of the surrounding topography and geology, shall be designed to provide sufficient stability against seismic disturbances.
- 2) Every structural system of the submerged tunnel shall be designed in accordance with the displacements of the surrounding ground during earthquakes and design seismic coefficients. The structural system shall be designed and the results examined by the dynamic response analyses.
- 3) The structural system in which the rigidity changes, i.e. joints, hinges and other parts, shall be designed with regard to the effects the change in rigidity has on the system and seismic resistance of the submerged tunnel.
- 4) For the preservation and countermeasures of the tunnel during earthquakes, the reliability of the operation of the systems of the submerged structure, the approach, the ventilation tower and other equipment shall be considered.

3.3 Loadings and other Conditions in the Earthquake Resistant Design

3.3.1 General

- 1) The following Loadings and Conditions shall be taken into account in earthquake resistant design. The Appropriate Loadings shall be selected from this list on the basis of the location and the type of the structure.
 - a) Dead Loads
 - b) Earth Pressures
 - c) Hydrostatic Pressures
 - d) Buoyancy or Uplift
 - e) Live Loads
 - f) Effects of Consolidation and Settlement of the Sub-ground
 - g) Effects of Temperature Change

- h) Effects of Shrinkage due to Humidity in Concrete Structures
- i) Other Loadings (Tidal Waves, etc.)
- 2) The following seismic effects shall be taken into account in earthquake resistant design.
 - a) Displacement of the sub-ground or structures in earthquakes
 - b) Inertia forces due to the dead weight of the structure
 - c) Earth pressures in earthquakes
 - d) Hydrodynamic pressures in earthquakes

3) Combination of Loads

Design conditions shall be determined considering the loading conditions a) through h), given in the preceding article (1) and in addition the loading effects h) and i) in accordance with the site conditions.

3.3.2 Ground Displacement in Earthquakes

- 1) The displacements of the subsurface ground in which the submerged tunnel is embedded shall be determined in accordance with the provisions given in Section 3.4.2.1 "Ground Displacement in Earthquake Resistant Design". The ground Displacement for the design of submerged structures shall be taken as the ground displacement at the level of the longitudinal axis of the structure.
- 2) The plane where the ground displacements are applied, shall be taken as the horizontal and the vertical plane on the axis respectively.

3.3.3 Inertia Forces (omitted)

3.3.4 Earth Pressures due to Earthquakes (omitted)

3.3.5 Hydrodynamic Pressures due to Earthquakes (omitted)

3.3.6 Soil Layers Where the Bearing Capacities are Neglected in Earthquake Resistant Design (omitted)

3.4 Design Earthquake Ground Motion

3.4.1 General

- 1) The ground Displacement and the design seismic coefficient shall be taken into account in the design of the submerged tunnel
- 2) The submerged structure shall be designed by the seismic deformation method and the seismic coefficient method.
- 3) Ventilation towers and other structures can be designed by the seismic coefficient method.

3.4.2 Design Earthquake Ground Motion

3.4.2.1 Ground Displacement in the Earthquake Resistant Design

The ground displacement, in the earthquake resistant design, shall be evaluated on the basis of the ground displacement considering the nature of the earthquake ground motions and the soil conditions.

3.4.2.2 Base Rock Accelerations in Earthquake Resistant Design

- 1) The horizontal base rock acceleration, in earthquake resistant design, shall be evaluated in accordance with the intensity of the earthquakes at the construction site and the importance of the submerged tunnels.
- 2) The vertical base rock acceleration, in earthquake resistant design, shall be taken as one half of the horizontal base rock accelerations.

3.4.2.3 Design Seismic Coefficient in the Seismic Coefficient Method (omitted)

3.5 Earthquake Resistant Design of Submerged Structures

3.5.1 General

The submerged structure shall be principally designed by the seismic deformation method. However, the seismic coefficient method can be applied to the design of the transverse tunnel sections and the examination of possibility of the sliding of the submerged tunnel.

3.5.2 Seismic Deformation Method

The submerged structure shall be designed in accordance with the Seismic Deformation Method.

3.5.3 Seismic Coefficient Method (omitted)

3.6 Earthquake Resistant Design of Ventilation Tower

3.6.1 General

The earthquake resistant design of the ventilation tower shall provide appropriate stability against seismic disturbances for the total structural system of the submerged tunnel, considering the conditions for the connection with the submerged structure.

3.6.2 Earthquake Resistant Design of the Ventilation Tower

The ventilation tower can be designed by the seismic coefficient method. The design seismic coefficient, in the seismic coefficient method, shall be determined in accordance with the provisions in Section.

3.4.2.3 "Design Seismic Coefficient in the Seismic Coefficient Method"

The directions of the inertia forces and the design method shall be determined in accordance with the provisions in individual related Specifications, according to the type of the ventilation tower considered and the conditions of the construction site.

3.7 Earthquake Resistant Design of Approaches

3.7.1 General (omitted)

3.7.2 Earthquake Resistant Design of Approach (omitted)

3.8 Stability of Subgrounds

3.8.1 General

The stability of the ground around the submerged structure shall be evaluated.

3.8.2 Stability Analysis of Ground

The Stability of the ground can be analyzed by the seismic coefficient method assuming a slip plane. Also the submerged structure shall be analyzed to avoid the critical damages due to the ground displacement evaluated by the dynamic analyses.

3.8.3 Stability of the Soil-use for Submerged Structure Fill

1) Liquefaction

A soil which is prone to liquefaction during earthquakes shall not be used for soil fill for submerged structures. The estimate of liquefaction shall be evaluated in accordance with the provisions given in Section 2.6.1 "Stability of Sandy Soils".

2) Examination of Sliding

The stability of the sliding of submerged structures in the transverse direction shall be analyzed in accordance with the provisions in Section 3.5 "Earthquake Resistant Design of Submerged Structure".

3.9 Allowable Stresses

3.9.1 General

The allowable stresses of the materials, and the increase of the allowable stresses for earthquake resistant design shall be determined in accordance with the structural types and the importance of the structures.

The stresses shall be required to be based on the various Specifications and the consideration of the assumptions in the design and the procedure and operation in the construction.

3.9.2 Allowable Stresses of Concrete

- 1) The allowable stresses of concrete, for use in submerged tunnels, shall conform to the provisions specified in the following:

Standard Specifications of Concrete,
Japan Society of Civil Engineers

- 2) The allowable stress of concrete placed in water shall be determined on the basis of experiments of simulated field conditions, because of the lack of reliability of the uniform quality of the concrete.

3.9.3 Allowable Stress of Steel

- 1) The allowable stress of steel used for submerged tunnels shall conform to the provisions specified in the following Specifications.

For reinforcing Bars;

Standard Specifications of Concrete,
Japan Society of Civil Engineers

For Structural Steel, Except for Reinforcing Bars;

Standard Specifications for Highway Bridges, Part of Steel Bridges,
Japan Road Association

- 2) In the case of minor cracking of the concrete, the allowable tensile stresses shall be designated in accordance with the effect of cracking of concrete.

3.9.4 Increase in the Allowable Stresses in the Earthquake Resistant Design

- 1) Use of the allowable stresses specified in the provisions of the Section 3.9.2 "Allowable Stresses of Concrete" and the Section 3.9.3 "Allowable Stresses of Steel", the increase of the allowable stresses shall be allowed in accordance with the following combination of loadings;

Table 3.3

Combination of Loading	Limitation of Increase of Allowable Stress
Ordinary Load + Earthquake Loading	50%
Ordinary Load + Effect of Temp. Change + Shrinkage + Earthquake Loading	65%

Note) In this table, the fundamental allowable tensile stress shall conform to the provisions of Section 3.9.2 "Allowable Stresses of Steel".

- 2) If the provisions of the Section 3.9.1 "Allowable Stresses of Concrete" and the Section 3.9.3 "Allowable Stresses of Steel" are not used in the evaluation of the gross allowable strength of the section of the structural member, the allowable stresses for ordinary conditions and seismic conditions or the safety factor shall be determined on the basis of the experiments or equivalent measures.

3.10 Earthquake Resistant Design in Detail

3.10.1 General	(omitted)
3.10.2 Attached structure	(omitted)
3.10.3 Pile Foundation	(omitted)
3.10.4 Ventilation tower	(omitted)

Chapter 4 Dynamic Analysis

4.1 General

The dynamic analysis for the design of a submerged tunnel is divided into the dynamic analysis for the partial structural system and the dynamic analysis for the total structural system.

4.2 Earthquake Response Analysis

4.2.1 General

The earthquake response analysis for the submerged tunnel shall be conducted for the individual items of the structural system, such as the surrounding ground, the

submerged structure and the ventilation tower, in addition to the total structural system. The analysis shall consider the dynamics of the soil-structure interaction and the characteristics of earthquake ground motions by using the method which can simulate the dynamic response of the submerged tunnel as close as possible.

4.2.2 Method of Earthquake Response Analysis

The earthquake response analysis can be conducted by using one of the following two methods.

- (A) method using the averaged response spectrum,
- (B) method using the original record of earthquake motions.

4.2.3 Mechanical Model

The mechanical model, for the earthquake response analysis, shall be individually designated to represent such structural systems as the ground, the submerged structure, the ventilation tower and the submerged tunnel of the total system and taking into account if necessary the effects of the existence of the water. The dynamic properties of the ground, such as natural period, vibration mode, damping characteristics and the dynamic characteristics of the submerged structure and the attached structures, and the dynamic interaction among the ground and the structures shall be taken into account in representing mechanical mode.

4.2.4 Input Earthquake Motion

The input earthquake ground motion shall be designated by the maximum acceleration and the characteristics specified in the provisions of Chapter 2 "Investigation".

The input earthquake ground motion shall be applied to the base rock.

4.3 Dynamic Model Test

(omitted)

4.4 Designation of Safety

(omitted)

Chapter 5 Preservation and Countermeasures in Earthquakes

5.1 General

For the purpose of preservation and countermeasures in earthquakes, earthquake equipment shall be installed in the submerged tunnel. The security and the stability of the tunnel are guaranteed completely by using the equipment and also conducting inspections.

5.2 Preserving Equipment

For the purpose of the preservation and countermeasures in earthquakes, the following equipment shall be installed. This equipment shall be guaranteed to have normal operation during earthquakes and have periodical inspections.

- 1) Sensor, recorder and system of notification for earthquake ground motion
- 2) Sensor, recorder and system of notification for the level of tidal wave and tsunami
- 3) Traffic control system during and after earthquake
- 4) Sensor, recorder and system of notification for settlement and spill water
- 5) System for evacuation and induction
- 6) Emergency power plant

- 7) System for inspection of traffic
- 8) Drainage and system of protection for inundation
- 9) Other (strain-meter, stress-meter, etc)

5.3 Preserving Operation

By employing the preserving equipments, the countermeasure for the security of traffic and the safety of the structure shall be applied in accordance with the intensity of earthquakes at the location of the tunnel.

5.4 Inspection for preservation

The tunnel structure shall be maintained by inspection, for proper preservation. The inspection shall be periodically conducted, and also the temporary inspection shall be conducted during earthquakes of the strong intensity.

5.5 Investigation after earthquakes

The administrator of the submerged tunnel shall immediately conduct an investigation of every portion of the tunnel after earthquakes of high intensity. The results of the investigation and the proper countermeasures shall be employed and recorded.

JOINT RESEARCH PROGRAM UTILIZING THE
LARGE SCALE TESTING FACILITIES (FREE DISCUSSION)

by

Makota Watabe
Senior Staff Scientist
Structures Division
Building Research Institute

and

Masaya Hirosawa
Senior Staff Scientist
Structures Division
Building Research Institute

and

Shinsuke Nakata
Researcher
Structures Division
Building Research Institute

ABSTRACT

Recently the United States and Japan have made progress in aseismic design of R.C. Structures based on the testing of R.C. members, in which these tests have shown the importance of ductility in columns. However there are a few seismic studies based on the loading tests of full size structures. Fortunately, in Japan there is the greatest loading test facilities in the world, with new larger facilities now under construction. By using these facilities full size aseismic tests can be conducted. This proposal provides a plan for the testing of reinforced concrete structures with shear walls, which should be the first step toward developing an international aseismic code.

Key Words: Dynamic Testing; Lateral Load Simulation; Models; Shake Tables; Testing.

Recent Research Progress

R.C. structures are generally recognized to have sufficient earthquake resistance. However in 1968, the Tokachi-Oki earthquake induced extensive damage to school buildings in Japan. In 1971, the San Fernando earthquake induced severe damage to hospital buildings in the USA. Examination of the earthquake damage indicated that many R.C. columns sustained severe damage, particularly shear failures. Thus, the problem of the need for ductility of R.C. column was reconfirmed. Therefore, since 1973, a research project was organized by the Ministry of Construction which included tests of about 200 R.C. column specimens. The following lists some of the results obtained from these tests;

- (1) All types of failure modes of the columns were defined precisely from the tests. They consist of shear diagonal tension failure, shear compression failure, shear tension failure, bond splitting failure, and buckling of the main bars. Empirical equations relative to strength associated with each mode were then established.
- (2) Load-deflection curves of all type of columns were standardized and the limitation of web reinforcement (quantity, shape and arrangement) for ductile members was determined.

Further Problem

At present many experimental studies have been conducted on columns, beams and shear walls. However, there are many fields still unexplored. For example, the seismic tests (static and dynamic) of full size structures with slabs, shear walls and foundations need investigations. These test results would provide insight on the difference between the behavior of a structure and unit member, especially the anchorage of the main bars or ground effects on the walls, etc. Previous studies on the structural damage due to earthquake were based only on member tests in the laboratory, and the behavior of entire structures had to be based on many engineering assumptions, which may lead to some errors. Full size structural testing should be made in order to avoid such errors.

Planning of Test

a) Testing Facilities

In Japan, there are large dynamic and static testing facilities and many others now under construction. Two such facilities are described below;

(Large Scale Earthquake Simulator)

This simulator system is housed in the National Research Center for Disaster Prevention and located in Tsukuba Research and Education City (that is now under construction). The performance of this simulator is shown in Table 1. The test platform is 15 by 15 meters in plan, which allows free motion in two directions. The effective weight on the platform is 500 ton (horizontal motion), and 200 ton (vertical motion). The test platform is actuated by a 360 ton capacity hydraulic actuator at a maximum acceleration of 500 gals and a maximum velocity of 37 cm/sec and a maximum displacement of ± 30 mm under dynamic conditions. Fig. 1 shows the relationship between acceleration, frequency and weight.

(Large Size Loading Facility)

This facility is for both static and dynamic full size structural tests using hydraulic serve actuators, which are not under construction. The plan and section of this facility are shown in Fig. 2. The facility consists of two blocks A and B, and a wall for horizontal reaction which is located along the periphery of the blocks. B block has two reaction walls in two directions. All the testing systems, loading, vibration and measurement are directly controlled by a computer system in this facility. Fig. 3 shows an example of the testing capacity of this system.

b) Description of Test Structure

As a first stage of the testing project, it is proposed that a four story building with shear walls be tested, as shown in Fig. 4. The type of shear walls will include normal types, precast walls and slip walls. Conducting of this test will permit solution of such problems as the actual behavior of shear walls, effects of the foundation, soil conditions and the mechanism at structural yielding. The test structure as shown in Fig. 4, is one example, other types of buildings however, should be included in the project, i.e. structures without shear walls and with short columns or long columns, long span structures and many types of ground conditions.

Conditions

Important buildings and materials must be protected during strong earthquakes. From this viewpoint, therefore, our first study should be the development of full size aseismic tests using Japanese large scale facilities. Systematic full size tests in cooperation between the U.S.A. and Japan will permit a better understanding of factors in order to establish an international standard aseismic design code.

Table 1 Capacity of Vibration Table

Table	15m x 15m , weight 160 tons
Vibration system	Electric oil compression
Max. power	360 tons (90 tons x 4)
Max. weight	500 tons (horizontal) 200 tons (vertical)
Max. amplitude	30 mm
Max. velocity	37 cm/sec
Max. acceleration	0.55 g (horizontal) 1.0 g (vertical)
Frequency	0.1-50 HZ
Structure	24m x 42.5m H=12.2m
Crane	30 tons and 5 tons

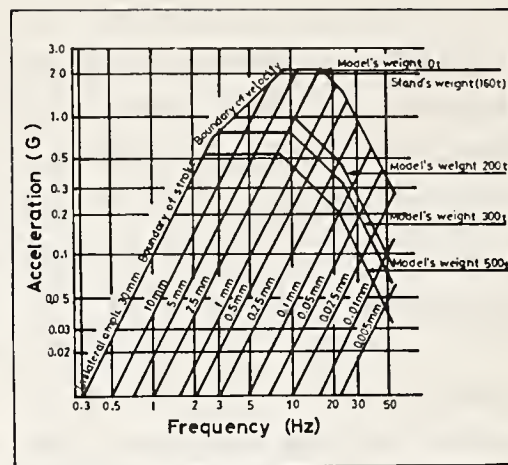


FIG 1 VIBRATIONAL CAPACITY

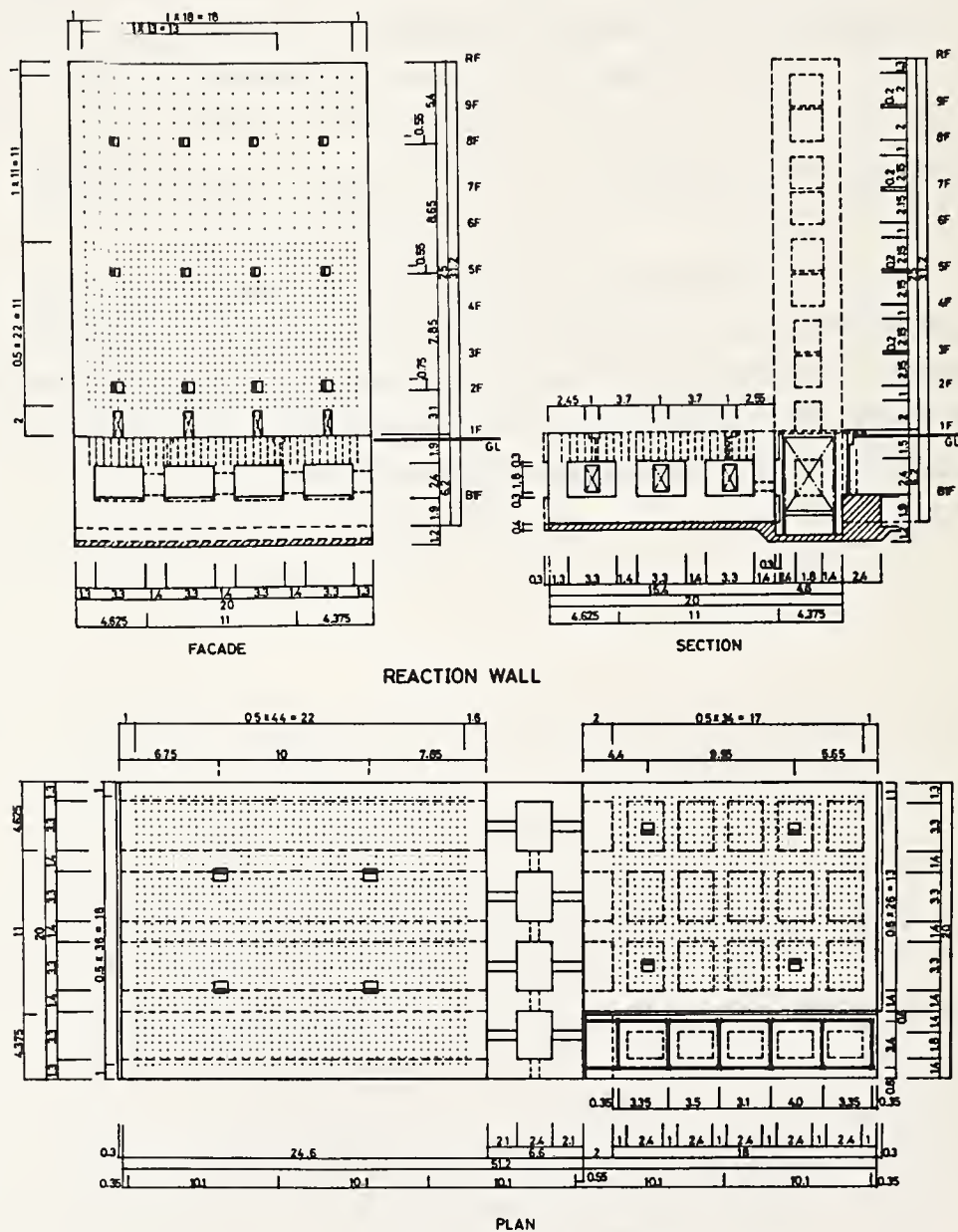


FIG 2 LARGE SCALE ASEISMIC FACILITY

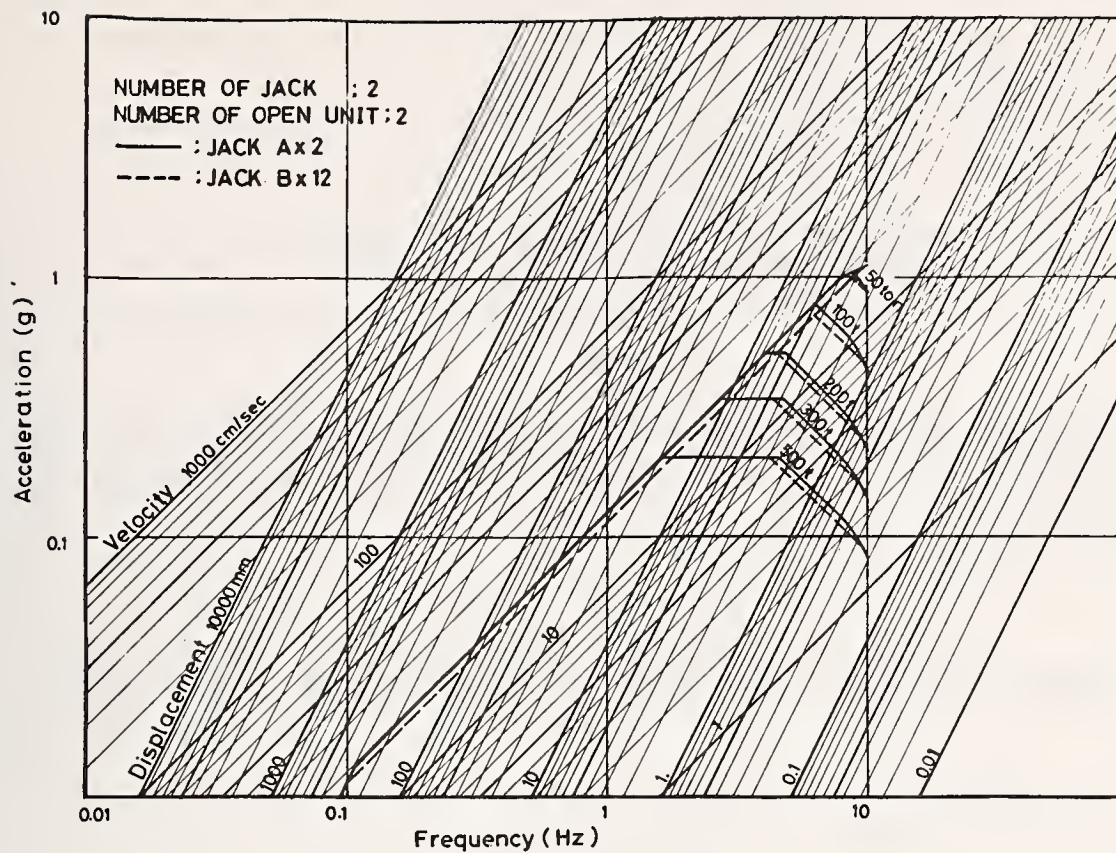


FIG 3 DYNAMIC CAPACITY

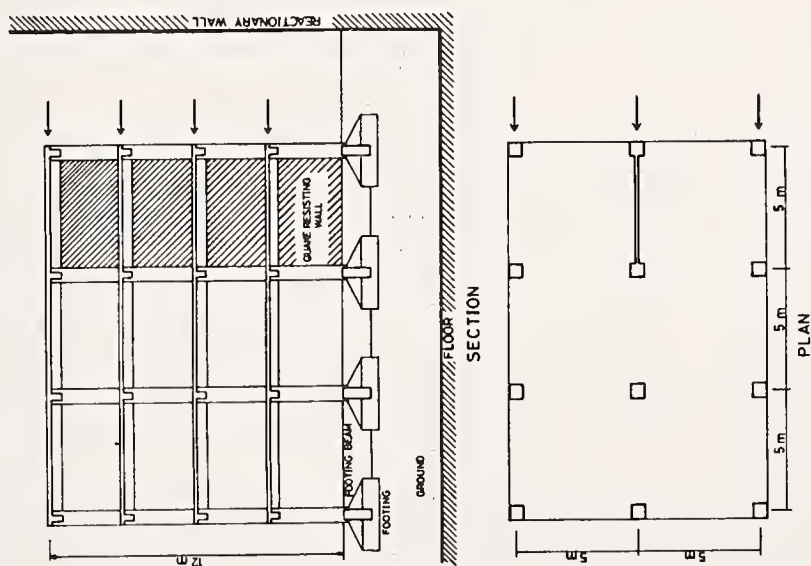


FIG 4 TEST BUILDING

EARTHQUAKE DISASTER MITIGATION:
A Joint Research Approach

by

Charles C. Thiel

and

John B. Scalzi

Program Managers, Earthquake Engineering
Research Applications Directorate (RANN)
National Science Foundation

ABSTRACT

This paper discusses the current earthquake research being undertaken in the USA under sponsorship of the NSF. In addition, possible cooperative research studies between the USA and Japan are described.

Key Words: Buildings; Earthquakes; Research; Structures; Structural Engineering.

Introduction

Numerous recent publications attest to the seriousness of the hazard presented by earthquakes to the peoples and economies of the United States and Japan. The damaging quakes of this decade are grim reminders of the severe impacts of the 1923 Tokyo and 1906 San Francisco events. In the intervening years these cities have grown, concentrating substantially greater populations likely to experience earthquakes of comparable intensity. Urbanization combined with industrialization are increasing our vulnerability not only to calamitous life losses but to major economic disruption and dislocation through lost industrial capacity.

These are not problems without potential resolution. It is a tenet of engineering that we can devise strategies at some cost that will reduce the potential for disruption. It is this belief that drives the research process to discover and develop better economic design and construction practices. Our joint national interests in this area are consistent and compatible: to control the consequences of earthquake occurrences through limiting life loss and injury, property damage and social disruption.

The United States program of research in earthquake mitigation is directed at the development of

- (A) economically feasible design and construction methods for building earthquake resistant structures of all types, and for the identification and repair of existing hazardous structures;
- (B) an operational program for predicting damaging earthquakes and their physical effects in the seismically active regions of the United States;
- (C) procedures for integrating data and information about seismic risk with on-going land use planning and regulation activities;
- (D) procedures for identifying, evaluating and accurately characterizing seismic hazards in earthquake-prone regions;
- (E) improved understanding of the social and economic consequences of individual and community decisions on earthquake-related issues, emphasizing risk control, pre-event planning, issuance of warnings, provision of emergency services, rescue, recovery and redevelopment; and
- (F) methods and procedures for the control or alteration of seismic phenomena and their effects on existing structures.

The achievement of these objectives will require the concerted effort of many professionals working in concord.

The problem posed by earthquakes to the U.S. are comparable in most ways to those posed to Japan. Both our countries have embarked on extensive programs of research in engineering, seismology, geology and the social sciences to develop earthquake mitigation procedures consistent with the above objectives. It is certainly true, in the U.S., and almost surely true in Japan that the magnitude of the research problems we face are significantly greater than the man power and financial resources we can bring to bear to resolve them. Under the auspices of the U.S. - Japan Panel on Wind and Seismic Effects we are now

meeting for the seventh time to discuss our mutual problems and accomplishments. This is a vital element in keeping ourselves jointly informed of the work being pursued in our respective countries. We believe that it is now time to escalate our activities to the next logical plateau: the conduct of joint and complementary research projects.

First an observation. This Panel has by the very nature of its membership been strongly oriented toward engineering problems. But the problems we face in earthquake disaster mitigation are not simple engineering, or for that matter seismological, economic or political. There appear to be eight approaches to limiting earthquake impact, four each of a physical and social type:

- Control the event by prevention or modification of the event;
- Anticipate the event so that remedial actions may be taken;
- Identify the seismic potential of areas;
- Construct facilities so as to perform acceptably during and after the event;
- Plan for the warning, response, and recovery to the event;
- Distribute the economic risk;
- Generate and select alternative physical development plans; and
- Adopt and enforce zoning, construction and management standards.

Clearly if our panel is going to focus on the problem of reducing earthquake impacts, we must extend its membership (or foster companion panels) to take advantage of the experience and capabilities of the other disciplines. The area of earthquake prediction is a vital area, advancing quickly in our respective countries. This panel could act as a focus for the exchange of mutually beneficial data and accomplishments. We propose, at the least, to extend the Panel's activities to include prediction as a sub-panel, possibly meeting separately. In the main, we propose to extend the Panel to address the full range of earthquake disaster mitigation methods.

As noted above we also feel that it is time for us to begin the pooling of our joint national research resources to resolve problems of public safety. As noted in the appended list, the NSF program has made substantial investments in research in a variety of areas. In keeping with our goal to extend the scope of the Panel's activities, we propose that six specific areas be targeted for potential joint research:

1. Public policy implications of earthquake prediction;
2. Large scale destructive testing;
3. Design of industrial facilities;
4. Instrumentation at foreign sites;
5. Land use planning;
6. Structural upgrading, repair and retrofitting;

These areas will be discussed individually below:

1. Public Policy Implications of Earthquake Prediction

The issuance of predictions of damaging earthquakes in selected geographic areas may well be upon us. Forecasts could be one mechanism for reducing potential loss and disruption from earthquakes. With extended lead times, actions could be taken to inspect and strengthen buildings, upgrade the seismic resistance component of building code requirements

so all new structures would be less susceptible to damage, improve land use zoning regulations to limit or prohibit construction in especially hazardous areas and, of course, as the forecasted event day approaches, plans for partial or complete evacuation could be carried out.

On the other hand, the negative consequences could be enormous if an extended period of uncertainty follows a forecast for a damaging earthquake. Public and Private investment agents may drastically reduce their construction and development in the area as well as curtail production and commercial activity that could trigger an extended showdown in the local economy which would be reflected in increased unemployment, reduced private income, shrinking tax base, and increased demands for public services.

Today there is no base of scientific knowledge to provide information on the benefits or disbenefits of such actions. Limited studies have been initiated in the United States. They are, however, confined by the time frame in which the research must be accomplished and by the need to validate policy recommendations by observing the public's response to actual predictions. A joint program of cooperative research could materially reduce the time frame in which this research is completed and lead to a better utilization of earthquake prediction for the public benefit. We propose a four item cooperative program to achieve the following objectives:

1. To develop and interpret a comprehensive set of empirically based findings regarding the probable response of organizations and individual citizens to early credible earthquake forecasts;
2. To develop and apply an effective means of informing organizations and the public of the findings and their implications;
3. To test in a rigorous fashion the impact of these findings on organizations; and
4. To prepare recommendations for legislative and administrative actions.

To facilitate such a program we propose that a bilateral meeting between appropriate officials and researchers be concerned in the near future to plan such a program.

2. Large Scale Destructive Testing of Structures

In the area of structural analysis and design we have relied heavily on our technical capabilities with theory and computers to develop concepts for design of structures to resist earthquake forces. Many of these concepts have evolved from post-inspections of earthquake damage and shake table results. As beneficial as these concepts are there are many factors which cannot be evaluated by inspection or small scale tests.

Among the parameters for which better data is required are: the three dimensional behavior of full size structures and individual components subjected to controlled seismic type forces, the determination of the structural damping characteristics caused by the various elements in a building, the connections of various structural components and equipment, the forces acting on various equipment caused by the interaction of the structure and the equipment, the attachment of non-structural items and other items which are either too large or too cumbersome to be handled on a shake table or confidently by analysis.

A plan to obtain the required data could be formulated by a Joint U.S.-Japan program consisting of: (a) large scale testing of existing structures of various types of materials

and construction, (b) pseudodynamic tests on full size specimens or structures constructed to obtain specific data, (c) shake table verifications where required for the pseudo-dynamic tests or for specimens which may be considered full size.

At the present time a few projects are underway to investigate the behavior of masonry construction by pseudo-dynamic test methods. Large joint specimens of reinforced concrete frame and shear walls are being analyzed and tested by pseudo-dynamic test procedures.

The results of these tests could be verified by full size structural tests to evaluate the time behavior in a structural system. A program to extend the tests to full size structures to determine the parameters which can not be evaluated otherwise would be most desirable and beneficial to both countries.

3. Industrial Buildings

Up to the present time research on buildings has been concentrated on the high rise type of residential and commercial types because of the hazards to the lives of the occupants. Very little attention has been given or devoted to other types of facilities which are equally unimportant to the welfare of the community. These are the industrial buildings which provide the economic base for the existence of the community. The amount of earthquake resistance in these buildings is dependent upon the design engineer of the building who may or may not have had experience with earthquake design criteria. In general, however, it appears that most industrial facilities have not been intentionally designed to resist seismic forces.

The National Science Foundation is currently funding several projects which are related to the industrial sphere of structures and buildings. Among these are: (a) the analysis and shake table tests of ground storage tanks with varying heights of liquids, (b) the seismic resistance of the major structural components of fossil fuel power plants, such as the boiler, the coal handling conveyor system, the stack, the cooling tower, the piping systems, and the related structures, (c) a study to determine the seismic vulnerability of the electrical distribution system will result in policy decisions for types of spare parts, readiness of the operational crew, and similar type operational decisions.

As one views the industrial complex of both countries, it is a simple matter to observe the many types of facilities which will require intensive study and research to develop economical design procedures which plant managers will be willing to accept. A joint U.S. - Japan program to investigate these industrial facilities will reduce the duplication of effort and shorten the period of implementing the research results.

Areas of further research which could be undertaken in consort or separately are:

- a. hydroelectric plants and all their appurtenances
- b. other components of fossil fuel power which are not already under study such as turbines, and other pieces of equipment.
- c. refineries
- d. chemical plants
- e. food processing plants
- f. warehouses, etc.

A plan to attack these problems with the greatest benefit to each country would be to assign certain projects to each nation and combine the results. Thereby, each nation would not duplicate the other and the total results would be obtained in much less time, than would otherwise be possible by each country doing all of the research alone.

4. Instrumentation at Foreign Sites

At any given site earthquakes are relatively rare events. This is fortunate for the possible affected populus, but leads to inherent difficulty in obtaining strong ground motion useful for extending our design practice. Both the United States and Japan have active instrumentation programs designed in part to instrument sites of likely activity to yield data on both ground design and building response. Both our programs are weak, however, in that we have not necessarily placed these instrumentation networks in the areas of the world where the data return is likely to be the highest. To date we have amassed a substantial data collection for low magnitude and intensity events. As intensity and magnitude increase, the recorded data falls off at least logarithmically; indeed data at damaging intensity levels for earthquakes with Richter magnitude above 6.5 are virtually non-existent. Yet our design considerations are dominated by this magnitude event. There is a definite world need for near field strong motion data for quakes of magnitude 7 and over. Since they are infrequent (particularly in the 8.0 range) we must place the networks where these magnitude events are most likely to occur. This involves the placement of networks outside of our respective countries. Since we both benefit from this data, we ought to pool our resources to design, place and maintain these systems.

To accomplish the goal of the timely collection of near field, large magnitude, strong motion data we propose the joint development of special arrays to be placed outside our respective countries through the following steps:

- Select regions of the world with sufficiently high seismic activity which are expeditious to develop in such arrays;

- Define the nature of the arrays which may be utilized effectively for this purpose;

- Evaluate the instrumentation needed to implement these arrays;

- Design specific arrays for several of the active areas selected in the first tasks;

- Jointly place and maintain the instrument sites;

- Regularly exchange data.

5. Land Use Planning/Site Planning

Averting or lessening the potential effects of many geophysical based disaster can be achieved by regulating the use to which land is put and the materials and methods employed in the design and construction of physical facilities. For the most part, seismic land use considerations in the U.S. have been either through the publication of seismic risk maps for state sized regions, or through the imposition of relatively vague legislative admonitions. In California's case, they have enacted a statute that requires the consideration of earthquake hazards in each communities master plan, although there is little agreement on what such an incorporation should entail as its technical content. Land use is a technique that offers the opportunity for control not only of earthquake related damage, (shaking, faulting, landslides, tsunami, etc) but also for other geobased hazards. Within the U.S.,

it is unlikely that land use criteria based solely on earthquake hazard can be widely adopted. When floods, landslide, earthquakes and allied hazards are considered, there is some likelihood for implementing technical land use criteria to reduce the public hazard exposure. Research in this area is embryonic in the U.S. and we conjecture that it is also in Japan. We propose that a binational working group be established under the auspices of the Panel to investigate the most appropriate objectives for joint activities and develop an integrated research/information exchange program to implement these objectives.

6. Structural Upgrading - Repair and Retrofitting

Most current structural research and that of the past years has concentrated on the behavior of materials components, structural and systems in order to develop techniques to improve new construction. Very little, if any research was devoted to the problem of retrofitting for strengthening purposes, or repair after an event. These were left to the judgment of the engineer or building official to decide how the building was to be repaired or strengthened. Their decision was usually based on past personal experience rather than research results and, in general, these professionals have performed well. However, because many large cities are in potentially high seismic risk zones, and have many old buildings which are subject to damage if an earthquake strikes, it is imperative that consideration be given to the problems of retrofitting and repair.

In recent experimental studies of structural components it has become the practice to test specimens up to a failure point, but not to total destruction. By this method repairs are made using epoxies, or grouts and the specimen is retested to determine the new load resistance capacity. Comparisons of the effectiveness of the repair techniques are made to determine the best possible method.

A specific project is underway to evaluate the resistance of structures up to four stories in height, typical of school buildings, and to determine the most cost-effective method of retrofitting the building. Various materials, such as steel and reinforced concrete with different framing systems are to be studied. The objective for the project is to develop a methodology for the evaluation of an existing building and to outline the various methods which may be used to retrofit the specific building.

No doubt, in both countries there are many buildings which could be retrofitted to a higher seismic resistance and consequently provide a greater degree of safety for the occupants.

A joint program outlining the types of buildings each country could study would certainly reduce the time and cost of obtaining this most useful information. A subcommittee of this panel could meet to decide the distribution of activities between countries which would lead to a common goal.

Conclusion

The time is ripe for our two countries to extend our cooperation in the earthquake area from one of information to one of joint endeavor. We propose to accomplish this through two actions. First to extend the participation in the Panel to all of the disciplines engaged in earthquake mitigation research and implementation. Second that the Panel foster a

series of focused research studies to be undertaken jointly. Obviously such undertakings will require both the commitment of time and personnel to develop the program and the allocation of resources to carry it out. We are prepared to act as the focal point for development of the U.S. participation in such a planning effort.

<u>INSTITUTION</u> <u>FY 75</u>	<u>PRINCIPAL</u> <u>INVESTIGATOR</u>	<u>TITLE</u>	<u>MONTHS</u>	<u>AMOUNT</u>
American Institute of Architects Research Corporation	John P. Eberhard	Architect's Role in Reducing Earthquake Damage to Buildings	7	\$ 84,100
University of Michigan	Subhash C. Goel	Inelastic Hysteresis Behavior of Structural Members Subjected to Combined Cyclic Bending and Axial Forces for use in Studying the Behavior of Braced Frame Structures During Earthquakes	24	125,800
University of Washington	Neil M. Hawkins	Seismic Resistance of Concrete Slab to Column and Wall Connections	12	115,300
University of Colorado	J. E. Haas	Socioeconomic and Political Consequences of Earthquake Prediction	7	114,100
C.M. Simonson & T.R. Simson Consulting Engineers	T. R. Simonson	Seismic Resistant Design of Mechanical and Electrical Systems	9	70,200
American Society for Engineering Education	Bernard Wobbeking	Summer Institute on Protective Design	10	18,300
University of Illinois	N. M. Newmark	Design for Protection Against Natural Hazards	12	476,500
Washington University	T. V. Galambos	Feasibility Study of Dynamic Tests on Full Scale Eleven Story Building-in Pruitt-IGOE Housing Project	3	20,000
University of California - Berkeley	Ray W. Clough	National Information Service in Earthquake Engineering	12	137,200

<u>INSTITUTION</u> <u>FY 75</u>	<u>PRINCIPAL</u> <u>INVESTIGATOR</u>	<u>TITLE</u>	<u>MONTHS</u>	<u>AMOUNT</u>
Massachusetts Institute of Technology	John M. Biggs	Evaluation of Seismic Safety of Buildings	24	\$236,500
U.S. Geological Survey	R. B. Matthiesen	Strong Motion Instrumentation Program	12	700,000
National Bureau of Standards	Samuel Kramer	Development of Comprehensive Seismic Design Provisions	20	415,000
California Institute of Technology	George Housner	Effects of Damage from Strong Earthquakes	24	436,800
McCue Boone Tomsick	Gerald M. McCue	Building Enclosure and Finish Systems: Their Interaction with the Primary Structure During Seismic Action	9	70,300
University of Illinois - Urbana	Mete A. Sozen	Effects of Earthquake Motions on Reinforced Concrete Buildings	24	316,100
University of California - Berkeley	A. K. Chopra	Earthquake Response of Dams Including Hydrodynamic and Foundation Interaction	24	89,400
California Institute of Technology	Ronald F. Scott	Feasibility Study: Dynamic Soil Testing by Centrifuge	12	82,200
J.H. Wiggins Company	John H. Wiggins	Cost-Benefit Risk Analysis of Research Budgeting for Selected Natural Hazards	9	81,000
University of California - Berkeley	Ray W. Clough	Energy Absorption Characteristics of Structural Systems Subjected to Earthquake Excitation	12	994,500
University of California -	Bruce A. Bolt	Design Earthquake Parameters	24	65,450

<u>INSTITUTION</u> <u>FY 75</u>	<u>PRINCIPAL</u> <u>INVESTIGATOR</u>	<u>TITLE</u>	<u>MONTHS</u>	<u>AMOUNT</u>
Cornell University	Richard N. White	Shear Transfer in Thick Walled Reinforced Concrete Structures under Seismic Loading	12	\$ 71,300
Polytechnic Institute of New York	R. F. Drenick	A Minimax Procedure for Specifying Earthquake Motions	24	32,500
California Institute of Technology	Fredric Raichlen	A Study of Tsunamis: Their Generation, Propagation and Coastal Effects (The Experimental Program)	18	108,600
National Bureau of Standards	Robert A. Crist	Workshop on Earthquake Resistant Masonry Construction	4	20,800
California Institute of Technology	T. Y. Wu	Theoretical Studies of Tsunamis: Their Generation, Propagation and Coastal Effects	18	92,500
Cornell University	D. A. Sangrey	Behavior of Fine Grained Soil Under Earthquake and Other Repeated Loading	24	97,400
University of California - San Diego	James Brune	Laboratory and Numerical Simulation of Near Field Earthquake Ground Motion	12	93,200
California Institute of Technology	Donald Hudson	National Information Service for Earthquake Engineering	12	<u>104,000</u>

HIGH WIND STUDY
IN THE
PHILIPPINES

by

Noel J. Raufaste
Federal Building Program Coordinator
Office of Federal Building Technology
Center for Building Technology
Institute for Applied Technology
National Bureau of Standards
Washington, D.C. 20234

ABSTRACT

A review of the National Bureau of Standards three-year high wind study in the Philippines is presented. Accomplishments during the first two years of the study are discussed. Principal accomplishments include 1) formation of a Philippine Advisory Committee to coordinate local wind research, 2) selection of three field test sites, 3) construction and instrumentation of six test buildings with wind recording equipment at the test sites, 4) instrumentation of the University of Philippines wind tunnel, and 5) participation in two international workshops on high winds in Manila.

Key Words: High winds, Philippines, field studies, instrumentation, wind tunnel test.

Introduction

The National Bureau of Standards (NBS) is developing improved design criteria for low-rise buildings to better resist the effect of extreme winds. The three-year project is sponsored by Agency for International Development (AID).

This research project originated from recognition of a need for additional research to supplement the limited amount of existing data concerning the effects of wind on low-rise buildings, especially in developing countries. Many existing criteria for wind loads design do not make provision for steady and fluctuating wind pressures along the edges of roofs and walls where flow separations occur. Yet wind pressures along these regions are one of the primary contributors to building damages. This research and the resultant development of suitable design criteria and methodologies will reduce losses of structures and lives in the countries where the criteria are applied.

The Philippines experience the highest worldwide annual frequency of intense tropical storms. Within the Philippines, the frequency of tropical storms is greatest in Luzon. Statistics indicate that between 1948 and 1971 the Philippines were exposed to 482 tropical storms, or an average of 20 per year. As such, these occurrences make the Philippines a natural laboratory to measure wind loads on buildings.

NBS's extreme wind study includes several components. It is based largely on field work (collection of wind loading data from seven field test buildings) and from wind tunnel testing of building scale models. The study also includes a review of climatological data from the weather bureaus of the Philippines and two other developing countries, Bangladesh and Jamaica. Socio-economic, architectural and structural data, from the Philippines and other developing countries will be included in the implementation aspects of this study. In addition, knowledge about wind effects on buildings obtained in other countries such as the United States, Japan, Australia and the United Kingdom will be used as required.

It should be noted that Dr. Richard Marshall, the principal investigator, is responsible for directing the wind research activities as discussed in this report. These activities are found on pages 3 - 10.

Background Information

The first step in performing this research was to identify interested organizations, agencies, universities and other groups within the Philippines, selected Bay of Bengal countries and several northern Caribbean islands to assess their degree of interest for possible in-country project participation. On April 27, 1973 the Philippine Advisory Committee was formed. Professionals from various building related fields were brought together. The response from the Philippine Government and the private sector numbered more than 30 scientists, engineers and researchers representing government entities, professional organizations and private groups. Also included were the USAID Mission to the Philippines and the U.S. National Bureau of Standards. The Philippine Advisory Committee serves as the focal point for coordinating project activities centering in the Philippines.

The committee is composed of the following organizations:

University of the Philippines

Philippine Atmospheric Geophysical and Astronomical Services Administration (PAGASA)

National Housing Corporation

Land and Housing Development Corporation

Peoples Homesite and Housing Corporation

Government Service Insurance System

Social Security System

Philippine Standards Association

A. R. Flores and Associates

National Building Code Committee

National Society for Seismology and Earthquake Engineering of the Philippines

Association of Structural Engineers of the Philippines

Philippine Institute of Civil Engineers

Bureau of Public Works

Philippine Civil Aeronautics Administration

National Science Development Board

USAID Mission to the Philippines

Bangladesh University of Engineering and Technology

CARE, Inc. - Bangladesh

Douet, Brown, Adams and Associates, Jamaica

U.S. National Bureau of Standards

In addition to NBS and AID support, principal members from the above groups donated their time and professional expertise, test buildings, land to construct test buildings, scientific facilities and funding for continuation of Philippine research activities.

In mid-1973 two individuals were selected, representing the Bay of Bengal and the northern Caribbean Island. These individuals contributed information about their respective geographic areas as inputs to the development of final design criteria. They will also transfer the project results to their respective geographic areas.

Wind Research Activities

Field Test Sites

Three field test sites are being operated under the full-scale phase of the test program. In order of selection and installation of equipment, they are as follows: (1) Science Garden at Quezon City, (2) Daet and (3) Laoag City. A number of factors were considered in selecting these test sites; the final choices required some compromise in the original selection criteria. The main factors in order of importance were as follows;

High frequency of extreme winds,
Accessibility,
Availability of commercial power,
Type of wind exposure, and
Security

The Science Garden site was an obvious choice since it is staffed with qualified PAGASA technicians. These technicians form the nucleus of a team trained by NBS in the installation, operation and maintenance of test equipment. It was thus possible for the NBS team members to transfer a significant portion of the installation work and associated responsibilities during the early stages of the program. Science Garden also serves, in conjunction with the University of the Philippines, as the center for reference standards, spare parts and service equipment.

Selection of the remaining sites was not so obvious. PAGASA weather stations were selected because of the security and personnel available to service the equipment. In addition, measurements of temperature and barometric pressure would be available, thus freeing data channels for additional pressure measurements. In discussions with the Philippine Advisory Committee, serious consideration was given to sites at Virac, Casiguran, Aparii, Baguio City, Daet and Laoag City. Virac and Baguio City were eliminated on the basis of unusual terrain features (mountain top locations) which are not typical of wind exposures for housing developments and would be extremely difficult to model in the wind tunnel. Casiguran was eliminated because of the difficulties of transporting equipment and personnel for periodic maintenance and calibration (boat service only). Aparii was eliminated because of plans to relocate the present PAGASA weather station site, and the lack of electrical power.

Daet and Laoag City were selected with some compromise on statistical independence and frequency of extreme winds. However, it is believed that other attributes of these sites (ease of transporting equipment and personnel, availability of electric power, non-unusual terrain features) more than offset these compromises.

Arrangements were made with the Philippine Advisory Committee to build test houses at the sites and, where possible or necessary, to use existing PAGASA structures. Test equipment was assembled, tested, calibrated and packaged at the NBS for shipment to the test sites.

Science Garden, Quezon City. The wind exposure at this site varies with wind direction, being relatively clear and flat from N to SE and slightly rough from SE to W due to construction of high-rise buildings some 500 metres away. The site is moderately rough from W to N due to local topographical features and other low-rise buildings on the test site. Three test houses are instrumented. Basic plan dimensions of the first two gable roof units are 7 x 8 metres. The third unit designed by CARE, Inc. in Bangladesh was shipped to Quezon City for full-scale testing. This building is barrel vaulted in end elevation and has plan dimensions of 5.4 x 2.5 metres. The data acquisition system is located in the PAGASA Instrumentation Building (adjacent to the first test house) which is air conditioned and relatively free from dust. A total of 21 pressure channels are available (an increase of 10 channels through use of an auxiliary signal conditioning system).

Dust Weather Station. The Daet site is approximately 230 km SE of Manila. It is located next to the city airport which borders the Pacific Ocean. The site has a very flat and clear exposure with the exception of a coconut grove running from NE to SE adjacent to the ocean. The main PAGASA Station Building was instrumented. This is the only building under

test which has a hip roof. The data acquisition system is installed in the main building's radar equipment room which is air conditioned. An emergency generating system is available at this site in the event that commercial power service is disrupted.

Laoag City Weather Station. This site is approximately 500 km north of Manila. As with Daet, the site is adjacent to the municipal airport and has a clear and flat exposure for all directions. Two test houses with plan dimensions identical to the test units at Science Garden (but with different roof slopes and eaves overhang) were constructed, one on the PAGASA station ground and one on CAA property. One of the two units is located in close proximity to two existing buildings which will allow the influence of neighboring structures to be evaluated.

Research Equipment

Full-Scale Test Equipment. Based on technical needs, some of the data acquisition equipment was specially developed at NBS while the balance was obtained from commercial sources. The data acquisition system used in the full-scale test program consist of five basic subsystems; (1) the sensors of transducers, (2) a logic section, (3) a signal conditioner, (4) a recorder, and (5) a power supply. The equipment was assembled, tested and packaged for shipment to the Philippines by the NBS project staff.

The system is designed to continuously monitor input signals and to go into a calibration and record sequence when the signal being monitored exceeds a preset level. When the recording period ends, the system enters a "hold" period during which no data are collected, regardless of the signal level on the channel being monitored. The "record" and "hold" periods are switch-selectable and are usually set at 20 and 30 minutes, respectively. The total recording time available on a reel of tape is approximately 6 hours. Thus, the total time period between changes in tape reels (assuming continuous high wind conditions) is approximately 12 hours which is considered to be sufficient for most typhoon passages.

Wind speed and direction are measured by a propeller-vane anemometer mounted on a 10-meter mast located far enough from the test buildings to register conditions in the undisturbed wind field. The anemometer is rated at 100 m/s and provides the signal which triggers the recording system. An ambient pressure probe is also mounted on the mast just below the anemometer and provides the differential pressure transducer with a standard reference pressure. The pressure transducers are mounted in low-profile housings which are designed to create a pressure intensity at their center equal to the pressure that would exist on the surface of the building without the housings installed. This obviates the problems involved with mounting the transducers flush with the wall or roof surfaces. The transducers are fitted with a solenoid valve which is activated by the logic system one minute before the generation of pressure records begins. This value places the transducer in a "closed-loop" configuration, thus allowing the subsequent record to be corrected for zero offset due to drift or loading of the transducer diaphragm with rainwater.

The logic portion of the data acquisition system normally operates in an automatic mode, but provisions exist for manual intervention for the purpose of calibration or periodic system checkout. The logic section also includes a time code generator which provides both digital and analog code of Greenwich Meridian Time (GMT) in days, hours, minutes and

seconds. The time code generator is set by radio countdown from PAGASA Headquarters in Quezon City and normally requires correction only two or three times a year.

Analog signals from the pressure transducers are converted to DC voltages (demodulation) and filtered by the signal conditioner prior to recording. The signals are also attenuated to match the range of the tape recorder, thus providing a better signal to noise ratio than would be possible by straight recording of the transducer outputs.

The recordings section consists of a 14-track analog tape unit with 26.7 cm reels containing 1100 metres of tape. Usual record speed is 4.8 cm/sec. The recorder is normally in a "powered down" mode and only operates on command from the logic section. As with the logic section, manual intervention is permitted for calibration, cleaning and rewinding tape. Recorded signals can be reproduced in the field to check recorder operation.

With the exception of the Laoag City test site, commercial power is used to operate the data acquisition systems. The Laoag City site is provided power by the CAA. To ensure availability of power under storm conditions, all three sites are equipped with a backup system of batteries. The batteries are continuously charged when external power is available and provide system power (115VAC) by means of an inverter. When commercial power is interrupted, the batteries automatically switch on and pick up the load to supply the data acquisition system for approximately 8 hours of continuous operation. The batteries are recharged automatically when service is restored.

Since typhoon winds can be expected to come from any direction, it is extremely difficult to determine a "best" configuration of pressure transducers. Because roof structures are known to be the most susceptible to wind damage, they received the highest priority in transducer allocations. Extreme pressures acting along ridge lines, eaves and roof corners are of interest as well as the average uplift pressures acting on the overall roof areas. The configuration of pressure transducers is arranged differently on each test building, thus providing the ability to measure a greater range of wind loadings. In all of the test buildings, transducers were installed inside the building to measure internal pressures which significantly influence the net roof uplift loads. An advantage of the test equipment used in this study is that the pressure transducer positions can be easily changed after a storm to study wind pressure distributions on other parts of the test houses, thereby enhancing the value of the data and reducing the amount of redundant information.

Wind Tunnel Test Equipment. Test equipment being used in the wind tunnel can be divided into three categories; (1) pressure transducers, (2) wind speed measuring equipment, and (3) signal conditioning and analysis equipment. The pressure transducers are quite similar to those being used in the full-scale tests except for the cylindrical transducer housings. Normally, four transducers are installed in the building model although six units are available.

Wind speeds are measured by pitot tubes when mean values are required. For measurement of wind speed fluctuations, hot-wire anemometers are used. The anemometers have an extremely high frequency response and are well suited to making measurement over the frequency range of interest (0 to 500 Hz). Two anemometer systems are used, permitting simultaneous measurements at two points in the tunnel for the determination of integral

scales (size of wind gusts). The second system also provides backup if a component should fail.

Wind Tunnel Modeling

The wind tunnel facility at the National Hydraulic Research Center (NHRC), University of the Philippines, is being used to carry out a series of tests on models of the full-scale test buildings. The cross section of this tunnel is 1.22 metres square and 3.70 metres long and produces a wind speed of approximately 30 metres per second. These model tests have aided in the interpretation of full-scale studies and have allowed design pressure coefficients to be determined in a systematic manner.

While it is not possible to exactly model atmospheric boundary layers in conventional wind tunnels, an acceptable degree of similitude is achieved by proper use of surface roughness elements and vortex generators. This modeling technique used in the NHRC tunnel was used in previous wind tunnel model studies and was perfected for this application in a slightly larger but quite similar wind tunnel at the Colorado State University (CSU). Tapered spires are placed at the entrance to the test section to produce a sheared flow of arbitrary turbulence intensity. The spires are followed by several rows of roughness elements located on the floor of the wind tunnel. The roughness elements generate a turbulent boundary layer which extends to almost the full height of the tunnel at the downstream end of the test section. Two combinations of spires and surface roughness elements were developed which produce turbulent boundary layers typical of smooth and moderately rough terrain, respectively. The model scale being used in these studies is 1:80. Ideally, this scale should be dictated by the integral scale of the turbulence, the effective surface roughness height and the length associated with the peak of the turbulent energy spectrum. Test results obtained in the CSU studies suggest a scale ratio of from 1:100 to 1:200. However, the physical size of the model precludes installation of pressure transducers at these small scales. Thus a compromise of 1:80 was used. Preliminary test results and results obtained in other wind tunnel model investigations suggest that scale matching is of secondary importance compared to intensity of turbulence and shape of the spectral density function.

Approximately 10 model configurations were investigated with roof slopes ranging from 0° to 30° and eaves overhangs ranging from 0 to 1.5 meters (full-scale). Two classes of surface roughness were used in these studies. Several low-rise building types were analyzed (houses, school buildings).

In addition to the wind tunnel modeling as described above, the NBS developed, specified, obtained and transported various items of test equipment for the UP wind tunnel facility. The equipment was installed in the wind tunnel and training sessions were conducted in the operation of equipment and the interpretation of test results. Major items of equipment transferred to the University of the Philippines include a signal correlator and probability analyzer, hot-wire anemometers, pressure transducers, electronic filters, signal amplifiers, x-y and stripchart recorders, voltmeters and an oscilloscope. This test equipment is housed in an air conditioned room built by the University. Computer programs

developed at the NBS for the analysis of random data were transferred to UP Computer Center. In addition, an extensive collection of documents dealing with the wind tunnel modeling of buildings and other engineering structures was placed in the UP Library.

Collection, Reduction and Analysis of Field Data

All data collected at the field test sites are recorded on analog magnetic tapes. Typically, these tapes contain one channel each of wind speed and direction data, 11 channels of pressure data and one channel of time code. Prior to the recording of data, a tape is assigned a site designation and tape identification number. This information, along with the time code, uniquely identifies the data.

The first step in the data reduction process is to record certain key channels, such as wind speed, wind direction and a representative pressure signal on a paper stripchart and subjectively classify the records by degree of stationarity. Records which contain redundant information are eliminated at this time. The remaining records are then viewed on an oscilloscope to determine the approximate maximum or minimum peak values and to verify that the recordings have an acceptable signal to noise ratio and are free of discontinuities. Once the records are determined to be of acceptable quality, they are converted to digital form for analysis.

Analog to digital conversion is accomplished by means of a computer-controlled data acquisition system which scans the analog channels in sequence and converts the voltage levels into binary equivalents. The data channels are multiplexed at a rate of 20,000 channels per second so that the time skew is negligible for the frequency range of interest. The scan rate can be varied but is typically 12 scans per second. Each channel is sampled 12,000 times, resulting in a record length of 1000 seconds (16 min - 40 sec). The multiplexing stage is followed by a programmable amplifier which allows best use of the digital representation (eleven binary bits plus sign). The digital data are entered on a 7-track magnetic tape for subsequent analysis in the NBS Computer Center. This tape also contains header information such as site and tape identification, the time of day when the original data were recorded, and the length of record.

Several programs were developed at the NBS for the analysis of random data. These include; Probability Density Function (PDF) which determines the peak values (either maximum or minimum) between zero crossings, calculates the mean and root mean square values and plots probability distribution functions; Correlation Analysis (CORREL) which calculates correlation functions and spectral density estimates; and a Summation Program (SUMP) which calculated the area-averaged surface pressures and the drag and uplift forces acting on a structure.

Data obtained from the wind tunnel are processed "on line" and are not recorded for future reduction or analysis. A hybrid computer allows the direct calculation of auto- and cross-correlation functions as well as probability density and distribution functions. A time domain analyzer is used to obtain direct measurements of mean and rms values. This system has the disadvantage of manual calculation of pressure coefficients, but this is insignificant when compared with the ability to quickly assess the test results and alter the model configuration without waiting for results from a central computer.

Development of Design Pressure Coefficients

The 1970 edition of the National Building Code of Canada (NBC) provides for risk of occurrence, terrain roughness, height above ground and building geometry in calculating wind pressures,

$$P = q C_e C_g C_p.$$

In this expression, q is a reference mean velocity pressure for a given mean recurrence interval, C_e is an exposure factor which varies with surface roughness and height above ground, C_g is a gust effect factor to provide for surface pressure fluctuations caused by turbulence and localized flow phenomena, and C_p is a conventional mean pressure coefficient. The proper values for C_e will be determined from existing data, full scale wind data and theoretical models of wind speed distributions in typhoons and hurricanes. The coefficients C_g and C_p must be determined experimentally. This is the primary output of the wind tunnel test program with the full-scale test results serving as a control on both the coefficients and final design criteria.

Assessment, Selection and Application of Climatological Data

A study of the available Philippine wind climate information with a view of assessing its adequacy from a structural engineering viewpoint will continue throughout the life of the project. Records of wind speeds, of typhoon observations and damages due to significant typhoons were collected by NBS through the courtesy of the PAGASA. Out of these records, data were selected which appear to be suitable for analysis. These will be used as input in computer programs available at NBS for predicting extreme winds corresponding to various mean recurrence intervals. A listing of the NBS programs was sent to the PAGASA Computer Center for adoption by the PAGASA as a calculation tool. NBS will provide appropriate assistance as required.

A parallel study of wind distributions, including the 1972 National Structural Code for Buildings of the Association of Structural Engineers of the Philippines and tropical cyclone frequency and intensity maps, reveals the area of northern Luzon, and perhaps parts of Western Luzon (including Manila) may need to be included in a more intense wind zone area. It is desirable that future editions of the building code differentiate between zones with different exposure (e.g. urban terrain vs. coastal sites). Results from this task will provide the appropriate Philippine code officials with much needed information for incorporation in a new building code. This information will serve as an input to the final report.

Information Transfer

In addition to advisory committee meetings, conferences and workshops provide a mechanism to transfer information to a larger body of individuals.

An International Workshop held in Manila, Philippines on November 14-17, 1973 addressed the state-of-the-art in mitigating building damages from winds. The workshop was jointly sponsored by AID, the Philippine Advisory Committee and the U.S. National Bureau of Standards.

Four themes covering climatology and aerodynamics, structural engineering, socio-economic and architectural considerations, and codes and standards were discussed.

The first two workshop days were devoted largely to presentations of technical papers. During the afternoon of the first day, a visit was scheduled to the field test site at the PAGASA Science Garden site, Quezon City.

Nine papers and five related reports were presented during the technical sessions with time reserved for discussions. The third day was devoted to subcommittee working sessions where 31 recommendations were developed. They were presented and discussed on the fourth day. Approximately 140 individuals from five countries (Jamaica, Bangladesh, the United Kingdom, the Philippines and the United States) attended the workshop.

The proceedings of the workshop was published as an NBS Building Science Series 56. This publication includes 14 recommendations (edited from 31) for improved building practices, the opening ceremonies, and the technical papers and reports.

On May 16-17, 1975 a regional conference was conducted in Manila, Philippines to discuss the draft project results to date. This meeting afforded the opportunity for members from wind-prone countries to further establish a dialogue for suggesting methods to better present the final results. A similar regional conference will be conducted in Kingston, Jamaica on November 6-7, 1975. The final report is expected to be published by the end of June 1976.

Conclusion

This paper describes the activities associated with developing improved design criteria for low-rise building to better resist the effects of extreme winds. It also discusses a very important element associated with developing technology--its transfer to the ultimate user. After completing the research a continuing effort by the Philippine Advisory Committee will be required to further the development of technology. This project is only one step in the process of improvement that will continue.

Acknowledgments

Parts of this paper were excerpted from NBSIR 74-567 FY 74 Progress Report on Design Criteria and Methodology for Construction of Low-Rise Buildings to Better Resist Typhoons and Hurricanes by Raufaste, N.S. and Marshall, R.D., Center for Building Technology, National Bureau of Standards, Washington, D.C. 20234.

References

1. "Climatology and Wind Related Problems in Philippines" by R.L. Kintanar, November 1973, Manila, Philippines (paper presented at a workshop in Manila, Philippines).

SURVEY ON SEISMOLOGY AND EARTHQUAKE
ENGINEERING IN INDIA, IRAN AND TURKEY

by

Makoto Watabe
International Institute of Seismology
and Earthquake Engineering

and

Hideo Tokuhira
Ministry of Construction

and

Masakazu Shinozuka
Japan International Cooperation Agency

ABSTRACT

A series of earthquake engineering courses have been held in Japan in cooperation with Iran, India and Turkey. This paper presents the details of these courses and the aid such courses have provided to the supporting countries.

Key Words: Earthquake engineering; Earthquakes; Education; India; Iran; Training; Turkey.

Summary

1) A training course was conducted at the International Earthquake Engineering Department of Building Research Institute, Ministry of Construction, which is greatly appreciated.

2) It is required to establish an advanced course for these ex-participants in order to provide an up-to-date knowledge and technique on earthquake engineering. In this connection, a 3 to 6 months' training course, is being organized.

3) Recruitment procedures for the training course should be made promptly (4 to 6 months prior to the commencement of the training course).

4) In regard to the follow-up of the ex-participants, it is necessary for a staff from either the Japanese Embassy or the JICA overseas office to keep close contact with their representatives. Such a successful case concerning this plan has been Turkey.

5) In addition to inviting a technical trainee, it is important to promote a visit from Japanese expert to the trainees country.

6) It is the intention of this program to strengthen our system so as to cope with the request from ex-participants, and to readily supply technical information and measuring instruments. Furthermore, an invitation of high ranking officials should be considered at the earliest date, in order to promote further technical cooperation in this field.

7) A follow-up team was well received in every country. It is required to accelerate this kind of service more positively, but more carefully in the future. If this follow up team is dispatched every three years and the selection of the participants for the advanced course is made at that time, the intensive training in Japan will be more beneficial.

Analysis of Questionnaire

1) Ex-participants' position in their countries are as follows; 86% of the ex-participants belong to the public or educational institution, and two thirds of them hold an important post. From this trend, it can be easily understood that their training in Japan was highly regarded and they were promising and selected researchers.

2) Evaluation of training

60% of the ex-participants or their senior officials highly praised their training in Japan.

3) Composition of the personnel at I.I.S.E.E. (International Institute of Seismology and Earthquake Engineering):

71% of the ex-participants are in favor of the present composition of our Insititute, while 15% of them expect an increase in the number of staff, and 4% hope that it will be enlarged. 19% of the ex-participants strongly wish to introduce lecturers from abroad, and 57% agree, while 24% think it necessary, or a matter of no consequence. As a conclusion, it can be interpreted that many of the ex-participants expect to have foreign lecturers added to the staff of the Institute.

4) Training System:

Each ex-participant enthusiastically hoped to be re-trained in a short period during the training course. In connection with the duration of training, 62% of the ex-partici-

pants hoped it would be less than 6 months, while 14% of them wanted a longer period. During this training, it is requested that more attention to the selection of applicants be paid, in order to allocate more time for special self-study, laboratory practice and an exchange of views on seismology and earthquake engineering.

5) Future follow-up service;

We have encountered numerous inquiries for catalogues of Japan-made measuring instruments and information on how to purchase these and if there is a sales agent in their country. Many of these engineers wanted a continuous supply of the research reports and the "Year Book" regularly published by the Institute, or the periodical "Technocrat". Furthermore, as the best means of follow-up, some engineers eagerly requested that Japanese experts be sent to their country.

Situation of Seismology and Earthquake Engineering in India, Iran and Turkey

1) India

The Japanese Ambassador has asked whether there are earthquakes or not in India. As such an event seldom occurs, people are quite indifferent to earthquakes. For that reason, it seems that the officials in charge of the technical cooperation at the Ministry of Finance in India will take a negative attitude toward allocating scholarships offered from Japan to this training course, although it is recognized that in the Meteorological Department of Roorkee University where there are many young researchers eager to study in England, United States, or Japan. Although the directors at the Meteorological Department have intended to send at least one researcher to our Institute every year, only one has come in the past 2 or 3 years to study in Japan. Due to the influence of England, seismology in India has advanced considerably as has earthquake engineering. In Roorkee University, located in about 200km north of New Delhi, Dr. J. Krishna and his excellent staff have established the Earthquake Engineering Center, and have invited young researchers from neighboring countries to study. However, Japan's follow up service has been badly evaluated in this country. For example, in regard to Japanese made measuring instruments, due to imperfection in the catalogue and specifications it is difficult to repair these instruments when they are out of order. Accordingly, the donation of experimental instruments should be made providing a service engineer be made available. On the other hand, the United States, because of the demand made when the instruments are out of order, replaced in a week through the diplomatic channels. Also relative to follow up service, Japan is far behind the United States.

2) Iran

It seems that Iran, favored with abundant oil, is seeking a well-balanced diplomatic policy toward the big powers and in part in the technical cooperation. Iranian people are in fear of earthquakes and thus the Government of Iran has given a considerable thought to this matter. In spite of active influence by the Ministry of Housing Development, a very limited number of participants have been conveyed to the Japanese Embassy, due to a difference in views with other organizations concerned with technical cooperation. Recently, a Building Research Center has been established by a joint project with UNESCO,

in Iran. Mr. Javdan, one of the ex-participants, has been engaged as director of this research work. His contribution toward the establishment of this organization is to be highly praised. This institution was formed for the purpose of providing leadership in the field of the earthquake engineering in the Middle and Near East. They disclosed a desire to purchase research equipment from Japan, nevertheless Mr. Pakdaman, Vice-Minister of the Housing Development expressed his regret to Japan because it took a long time and required sophisticated formalities in order to purchase such items. However, a feeling of satisfaction was obtained to see a dome-shaped housing complex with aseismatic structure, designed by the ex-participants which was constructed in the suburb of Gazvin city about 150km west of Tehran.

3) Turkey

It seems that an ideal type of technical cooperation between Japan and Turkey can be obtained. Ex-participants who studied in Japan are now taking initiative in this field and in particular research work relative to earthquake engineering. In addition, a close liaison among the ex-participants, both in the Earthquake Engineering and in Seismology, has been preserved at the same time, and there is constant contact with the Japanese Embassy. Success in this technical cooperation greatly owed to the prominent Japanese experts who made self-sacrificing efforts when in Turkey. It is assured that Japanese technology in the area of earthquake engineering and seismology will further help advance Turkey's technology.

Special Lecture

A follow up team made an attempt to present a special lecture on "Evaluation of Seismic Input Force" through a 16mm film of the earthquake engineering. To facilitate the understanding of the lecture, a series of color slides, and moreover a lecture notes were distributed to attendants. After 45 minutes of lecture, a short motion picture entitled "Vibration" was then shown, and a special lecture was then concluded with a question period. Because the actual lecture hall was not properly selected, some difficulty arose with respect to presentation of slides. However, the lectures were a success due to the kindness of the Japanese Embassy and the JICA overseas office. The special lecture was well received by attendants. The number of attendance in the respective countries were as follows;

India	160
Iran	70
Turkey	70
<hr/>	
Total	300

Contents of the lecture

- i) Stochastics on the history of earthquakes
- ii) Magnitude and intensity and the maximum acceleration
- iii) Evaluation of the intensity level of the earthquake in terms of return period
- iv) The earthquake damage and subsoil condition

- v) Aseismic regulations and response spectrum
- vi) International aseismic regulations

As for movie films

- i) Ship and wave
- ii) Earthquake and structure
- iii) Wind and suspension bridge
- iv) Air turbulence and air plane
- v) Road and automobile
- vi) Derailing and vibration of the train
- vii) Utilization of vibration

U.S. DEPT. OF COMM. BIBLIOGRAPHIC DATA SHEET		1. PUBLICATION OR REPORT NO. SP-470		2. Gov't Accession No.		3. Recipient's Accession No.	
4. TITLE AND SUBTITLE WIND AND SEISMIC EFFECTS (PROCEEDINGS OF THE SEVENTH JOINT PANEL CONFERENCE OF THE U.S.-JAPAN COOPERATIVE PROGRAM IN NATURAL RESOURCES)				5. Publication Date April 1977			
				6. Performing Organization Code			
7. AUTHOR(S) H. S. Lew, Editor				8. Performing Organ. Report No.			
9. PERFORMING ORGANIZATION NAME AND ADDRESS NATIONAL BUREAU OF STANDARDS DEPARTMENT OF COMMERCE WASHINGTON, D.C. 20234				10. Project/Task/Work Unit No.			
				11. Contract/Grant No.			
12. Sponsoring Organization Name and Complete Address (Street, City, State, ZIP) Same as Item # 9.				13. Type of Report & Period Covered			
				14. Sponsoring Agency Code			
15. SUPPLEMENTARY NOTES Library of Congress Catalog Card Number: 77-608015							
16. ABSTRACT (A 200-word or less factual summary of most significant information. If document includes a significant bibliography or literature survey, mention it here.) The Seventh Joint Meeting of the U.S.-Japan Panel on Wind and Seismic Effects was held in Tokyo, Japan on May 20-23, 1975. The proceedings of the Joint Meeting include the program, the formal resolutions, and the technical papers. The subject matter covered in the papers includes characteristics of strong wind; response of full-scale structures to wind action; geological distribution of seismic activity; maintenance of strong motion accelerographs and data processing; strong earthquake motions and ground failures; response of hydraulic and building structures to seismic forces; aseismic considerations for vessels; recent revisions of design standards on wind and seismic effects; joint research program utilizing large scale testing facilities; and technological assistance to developing countries.							
17. KEY WORDS (six to twelve entries; alphabetical order; capitalize only the first letter of the first key word unless a proper name; separated by semicolons) Accelerograph; bridges; buildings; codes; disaster; dynamic analysis; earthquakes; ground failures; hydraulic structures; seismicity; soils; standards; structural response; vessels and wind.							
18. AVAILABILITY <input type="checkbox"/> For Official Distribution. Do Not Release to NTIS <input checked="" type="checkbox"/> Order From Sup. of Doc., U.S. Government Printing Office Washington, D.C. 20402, SD Cat. No. C13.10:470 <input type="checkbox"/> Order From National Technical Information Service (NTIS) Springfield, Virginia 22151				19. SECURITY CLASS (THIS REPORT) UNCLASSIFIED		21. NO. OF PAGES 513	
				20. SECURITY CLASS (THIS PAGE) UNCLASSIFIED		22. Price \$5.60	

*There's
a new
look
to...*

DIMENSIONS

NBS

... the monthly magazine of the National Bureau of Standards. Still featured are special articles of general interest on current topics such as consumer product safety and building technology. In addition, new sections are designed to . . . PROVIDE SCIENTISTS with illustrated discussions of recent technical developments and work in progress . . . INFORM INDUSTRIAL MANAGERS of technology transfer activities in Federal and private labs. . . DESCRIBE TO MANUFACTURERS advances in the field of voluntary and mandatory standards. The new DIMENSIONS/NBS also carries complete listings of upcoming conferences to be held at NBS and reports on all the latest NBS publications, with information on how to order. Finally, each issue carries a page of News Briefs, aimed at keeping scientist and consumer alike up to date on major developments at the Nation's physical sciences and measurement laboratory.

(please detach here)

SUBSCRIPTION ORDER FORM

Enter my Subscription To DIMENSIONS/NBS at \$12.50. Add \$3.15 for foreign mailing. No additional postage is required for mailing within the United States or its possessions. Domestic remittances should be made either by postal money order, express money order, or check. Foreign remittances should be made either by international money order, draft on an American bank, or by UNESCO coupons.

Send Subscription to:

NAME-FIRST, LAST																			

COMPANY NAME OR ADDITIONAL ADDRESS LINE																			

STREET ADDRESS																			

CITY									

STATE	

ZIP CODE			

PLEASE PRINT

- ☐ Remittance Enclosed
(Make checks payable to Superintendent of Documents)
- ☐ Charge to my Departmental Account No.

MAIL ORDER FORM TO:
Superintendent of Documents
Government Printing Office
Washington, D.C. 20402

NBS TECHNICAL PUBLICATIONS

PERIODICALS

JOURNAL OF RESEARCH reports National Bureau of Standards research and development in physics, mathematics, and chemistry. It is published in two sections, available separately:

Physics and Chemistry (Section A)

Papers of interest primarily to scientists working in these fields. This section covers a broad range of physical and chemical research, with major emphasis on standards of physical measurement, fundamental constants, and properties of matter. Issued six times a year. Annual subscription: Domestic, \$17.00; Foreign, \$21.25.

Mathematical Sciences (Section B)

Studies and compilations designed mainly for the mathematician and theoretical physicist. Topics in mathematical statistics, theory of experiment design, numerical analysis, theoretical physics and chemistry, logical design and programming of computers and computer systems. Short numerical tables. Issued quarterly. Annual subscription: Domestic, \$9.00; Foreign, \$11.25.

DIMENSIONS/NBS (formerly Technical News Bulletin)—This monthly magazine is published to inform scientists, engineers, businessmen, industry, teachers, students, and consumers of the latest advances in science and technology, with primary emphasis on the work at NBS. The magazine highlights and reviews such issues as energy research, fire protection, building technology, metric conversion, pollution abatement, health and safety, and consumer product performance. In addition, it reports the results of Bureau programs in measurement standards and techniques, properties of matter and materials, engineering standards and services, instrumentation, and automatic data processing. Annual subscription: Domestic, \$12.50; Foreign, \$15.65.

NONPERIODICALS

Monographs—Major contributions to the technical literature on various subjects related to the Bureau's scientific and technical activities.

Handbooks—Recommended codes of engineering and industrial practice (including safety codes) developed in cooperation with interested industries, professional organizations, and regulatory bodies.

Special Publications—Include proceedings of conferences sponsored by NBS, NBS annual reports, and other special publications appropriate to this grouping such as wall charts, pocket cards, and bibliographies.

Applied Mathematics Series—Mathematical tables, manuals, and studies of special interest to physicists, engineers, chemists, biologists, mathematicians, computer programmers, and others engaged in scientific and technical work.

National Standard Reference Data Series—Provides quantitative data on the physical and chemical properties of materials, compiled from the world's literature and critically evaluated. Developed under a world-wide program coordinated by NBS. Program under authority of National Standard Data Act (Public Law 90-396).

NOTE: At present the principal publication outlet for these data is the Journal of Physical and Chemical Reference Data (JPCRD) published quarterly for NBS by the American Chemical Society (ACS) and the American Institute of Physics (AIP). Subscriptions, reprints, and supplements available from ACS, 1155 Sixteenth St. N.W., Wash. D. C. 20056.

Building Science Series—Disseminates technical information developed at the Bureau on building materials, components, systems, and whole structures. The series presents research results, test methods, and performance criteria related to the structural and environmental functions and the durability and safety characteristics of building elements and systems.

Technical Notes—Studies or reports which are complete in themselves but restrictive in their treatment of a subject. Analogous to monographs but not so comprehensive in scope or definitive in treatment of the subject area. Often serve as a vehicle for final reports of work performed at NBS under the sponsorship of other government agencies.

Voluntary Product Standards—Developed under procedures published by the Department of Commerce in Part 10, Title 15, of the Code of Federal Regulations. The purpose of the standards is to establish nationally recognized requirements for products, and to provide all concerned interests with a basis for common understanding of the characteristics of the products. NBS administers this program as a supplement to the activities of the private sector standardizing organizations.

Consumer Information Series—Practical information, based on NBS research and experience, covering areas of interest to the consumer. Easily understandable language and illustrations provide useful background knowledge for shopping in today's technological marketplace.

Order above NBS publications from: Superintendent of Documents, Government Printing Office, Washington, D.C. 20402.

Order following NBS publications—NBSIR's and FIPS from the National Technical Information Services, Springfield, Va. 22161.

Federal Information Processing Standards Publications (FIPS PUBS)—Publications in this series collectively constitute the Federal Information Processing Standards Register. Register serves as the official source of information in the Federal Government regarding standards issued by NBS pursuant to the Federal Property and Administrative Services Act of 1949 as amended, Public Law 89-306 (79 Stat. 1127), and as implemented by Executive Order 11717 (38 FR 12315, dated May 11, 1973) and Part 6 of Title 15 CFR (Code of Federal Regulations).

NBS Interagency Reports (NBSIR)—A special series of interim or final reports on work performed by NBS for outside sponsors (both government and non-government). In general, initial distribution is handled by the sponsor; public distribution is by the National Technical Information Services (Springfield, Va. 22161) in paper copy or microfiche form.

BIBLIOGRAPHIC SUBSCRIPTION SERVICES

The following current-awareness and literature-survey bibliographies are issued periodically by the Bureau:

Cryogenic Data Center Current Awareness Service. A literature survey issued biweekly. Annual subscription: Domestic, \$20.00; Foreign, \$25.00.

Liquefied Natural Gas. A literature survey issued quarterly. Annual subscription: \$20.00.

Superconducting Devices and Materials. A literature survey issued quarterly. Annual subscription: \$20.00. Send subscription orders and remittances for the preceding bibliographic services to National Bureau of Standards, Cryogenic Data Center (275.02) Boulder, Colorado 80302.

U.S. DEPARTMENT OF COMMERCE
National Bureau of Standards
Washington, O.C. 20234

OFFICIAL BUSINESS

Penalty for Private Use, \$300

POSTAGE AND FEES PAID
U.S. DEPARTMENT OF COMMERCE
COM-215



SPECIAL FOURTH-CLASS RATE
BOOK

